# Emissions of Potent Greenhouse Gases from Appliance and Building Waste in Landfills

Draft Final Report

CARB Agreement Number: 11-308

Principal Investigators:
Nazli Yesiller
James L. Hanson
Jean E. Bogner

Prepared for:
The California Air Resources Board and The California Environmental Protection Agency

Prepared by:
Nazli Yesiller
James L. Hanson
Global Waste Research Institute
California Polytechnic State University
One Grand Avenue
San Luis Obispo, CA 93407
(805) 756-2932

January 9, 2016

# DISCLAIMER

The statements and conclusions in this Report are those of the contractor and not necessarily those of the California Air Resources Board. The mention of commercial products, their source, or their use in connection with material reported herein is not to be construed as actual or implied endorsement of such products.

# ACKNOWLEDGEMENTS

The research team included Dr. Donald R. Blake of University of California-Irvine and Dr. Tracy L. Thatcher, and Dr. Yarrow M. Nelson from California Polytechnic State University. Dr. Simone Meinardi from University of California-Irvine assisted with analytical testing. Several students from California Polytechnic State University participated in the project. Mr. Derek C. Manheim assisted with literature review and materials flow analysis. Mr. Alexander H. Sohn assisted with literature review and the field testing program. Mr. Timothy Robison, Mr. Michael Onnen, Mr. Juan Alverez, Ms. Briana Byrne, Mr. Joshua Core, Mr. Cameron Lane, and Mr. Ryne Mettler assisted with the field test program. Dr. Amro El Badawy from California Polytechnic State University also assisted with the field test program. Waste Connections Inc. coordinated access to the landfill field site. Staff of Potrero Hills Landfill cooperated with the research team during all phases of the field analysis.

This Report was submitted in fulfillment of ARB Contract Number: 11-308 provided for the Project entitled “Emissions of Potent Greenhouse Gases from Appliance and Building Waste in Landfills” by the Global Waste Research Institute at California Polytechnic State University under the sponsorship of the California Air Resources Board. Work was completed as of January 8, 2016.

# TABLE OF CONTENTS

# List of Figures

# List of Tables

# Acronym List

| | |
|---|---|
| ADC | Alternative Daily Cover (on a landfill) |
| AIC | Alternative Intermediate Cover (on a landfill) |
| AF | Auto fluff (non-metallic waste remaining after auto and appliance shredding) |
| Ar | Argon |
| ARB | California Air Resources Board |
| ASHRAE | American Society of Heating, Refrigerating, and Air-Conditioning Engineers |
| ASTM | ASTM International (formerly American Society for Testing and Materials) |
| atm. | Atmosphere (of pressure) |
| BA | (foam) blowing agent |
| BDL | Below Detection Limit |
| BING | Federation of European Rigid Foam Manufacturers |
| BRE | Building Research Establishment |
| BSC | Building Science Corporation |
| C&D | Construction and Demolition (waste) |
| CalRecycle | California Department of Resources Recycling and Recovery (CalRecycle) (formerly California Integrated Waste Management Board) |
| CARB | California Air Resources Board |
| CDIAC | Carbon Dioxide Information Analysis Center |
| CFC | Chlorofluorocarbon |
| $CH_4$ | Methane |
| CIWMB | California Integrated Waste Management Board (now CalRecycle) |
| $CO_2$ | Carbon Dioxide |
| $CO_2$-eq | Carbon Dioxide Equivalent |
| COV | Coefficient of Variation |

| | |
|---|---|
| DRE | Destruction and Removal Efficiency |
| DTSC | California Department of Toxic Substances Control |
| ECD | Electron Capture Detector or Electron Capture Detection |
| ED | Extended Daily Soil Cover (on a landfill) |
| EPA | United States Environmental Protection Agency |
| EPS | Expanded Polystyrene (foam) |
| F-gas | Fluorinated Gas |
| FC | Final Cover (on a landfill) |
| FID | Flame Ionization Detection |
| FTIR | Fourier Transform Infrared Spectrometer |
| g | gram |
| GC | Gas Chromatograph or Gas Chromatography |
| GCL | Geosynthetic Clay Liner |
| Gg | gigagram |
| GHG | Greenhouse Gas |
| GW | Green Waste |
| GWP | Global Warming Potential |
| HCFC | Hydrochlorofluorocarbon |
| HFC | Hydrofluorocarbon |
| HP | Hewlett-Packard |
| HRPM | Horizontal Radial Plume Mapping |
| IC | Interim Cover (on a landfill) |
| IDW | Inverse Distance Weighting (also called “Kriging”) |
| IPCC | Intergovernmental Panel on Climate Change |
| ISC3 | Industrial Source Complex Model - a steady-state Gaussian plume model which can be used to assess pollutant concentrations from a wide variety of sources |
| kg | kilogram |

| | |
|---|---|
| kPa | kilopascals, a unit of pressure |
| K-value | A measure of thermal conductivity value |
| KWe | kilowatt electric power produced or consumed |
| L | liter |
| LFG | Landfill Gas |
| LOD | Limit of Detection |
| Log $K_{ow}$, Log $K_{oc}$ | Log $K_{ow}$ and log $K_{oc}$ are both equilibrium constants that provide an indication of constituent sorption onto soil or organic matter, respectively. |
| $m^2K/W$ | Ratio of square meters per degree Kelvin to Watts, which is the R-value, a measure of thermal insulation (resistance to conductivity). |
| MFA | Materials Flow Analysis |
| mg | milligram |
| mL | milliliter |
| mmHg | millimeters of mercury (unit of pressure) |
| $MMTCO_2$-eq | Million Metric Tons Carbon Dioxide equivalents |
| MOCLA-FOAM | Model used to determine the fate of continuously releasing blowing agent to the pore air space of the landfilled waste. |
| mol or mole | The amount of a substance that contains as many atoms, molecules, ions, or other elementary units as the number of atoms in 0.012 kilogram of carbon 12. The number is $6.0225 \times 10^{23}$, or Avogadro's number. Also called gram molecule. |
| MSD | Mass Spectrometric Detection |
| MSW | Municipal Solid Waste |
| $MTCO_2eq$ | Metric Tons Carbon Dioxide equivalents |
| mW/mK | ratio of milliwatts to the thermal conductivity factor, a unit of thermal conductivity |
| MWe | Megawatt electric power produced or consumed |
| $N_2$ | Nitrogen |
| $N_2O$ | Nitrous oxide |

| | |
|---|---|
| ND | not detected |
| NICNAS | National Industrial Chemicals Notification and Assessment Scheme |
| NMOC | Non-methane Organic Compounds |
| NOMHICE | Non-Methane Hydrocarbon Intercomparison Experiment |
| NRCA | National Roofing Contractors Association |
| $O_2$ | Oxygen |
| OCF | One-Component Foam |
| ODP | Ozone Depleting Potential |
| ODS | Ozone Depleting Substances |
| OP-FTIR | Open Path – Fourier Transform Infrared Spectrometer |
| ORS | Optical Remote Sensing |
| PCRF | Per-Carbon-Response-Factor |
| PDC | Path-determining Component |
| P | Precipitation |
| PE | Polyethylene (foam) |
| PET | Potential Evapotranspiration |
| PHL | Potrero Hills Landfill |
| PIR | Polyisocyanurate (foam) |
| ppb | parts per billion |
| ppbv | parts per billion by volume |
| ppm | parts per million |
| ppmv | parts per million by volume |
| ppt | parts per trillion |
| PUR | Polyurethane (foam) |
| PVC | Polyvinyl chloride |

| | |
|---|---|
| $R^2$ | A coefficient of determination, a number that indicates how well data fit a statistical model. $R^2$ can also be presented as a line or curve. An $R^2$ of 1 indicates that the regression line perfectly fits the data, while an $R^2$ of 0 indicates that the line does not fit the data at all. |
| R-value | A measure of thermal insulation value |
| RAPRA | RAPRA Technologies, Ltd. |
| RPM | Radial Plume Mapping |
| SCS | SCS Engineering |
| SEM | Surface Emission Monitoring |
| $SF_6$ | Sulfur hexafluoride |
| SoCAB | Southern California Air Basin |
| SRM | Standard Reference Material |
| TDL | Tunable Diode Laser Spectroscopy |
| TEAP | (United Nations) Technology and Economic Assessment Panel |
| TOC/TON | ratio of total organic carbon to total organic nitrogen |
| TRU | Transport Refrigerated Unit |
| UCI | University of California at Irvine |
| ug | microgram |
| UNEP | United Nations Environment Programme |
| USCS | Unified Soil Classification System |
| USDA | United States Department of Agriculture |
| USEPA | United States Environmental Protection Agency |
| UV DOAS | Ultraviolet Differential Optical Absorption Spectroscopy |
| VOC | Volatile Organic Compound |
| VRPM | Vertical Radial Plume Mapping |
| $W/m^2$ | Watts per meter squared, a unit of radiative forcing |
| WTE | Waste to Energy |
| XPS | Extruded Polystyrene |

# ABSTRACT

This investigation was conducted to provide detailed assessment of emissions of target (hydro)chlorofluorocarbons (also termed F-gases) (CFC-11, HCFC-141b HFC-134a, and HFC-245fa) used as blowing agents from end of life management of rigid waste foam materials using a three-part approach. Very limited field landfill emissions data for (hydro)chlorofluorocarbons were identified in the U.S. with no data for California. In materials flow analysis conducted for California, CFC-11 emissions were predicted to be high for current conditions, with high HCFC-141b, HFC-134a, and HFC-245fa emissions for future conditions. Finally, in extensive field testing conducted at a northern California landfill, baseline air quality, emissions from various types of cover systems, and destruction efficiency of the gas management system were measured. Tests were conducted in regions of the landfill with different waste ages and were repeated for wet and dry seasons. The minimum and maximum measured fluxes for CFC-11, HCFC-141b, HFC-134a, and HFC-245fa were $9.47x10^{-7}$ and $2.57x10^{-1}$ g/m$^{-2}$-day, $-5.59x10^{-6}$ and $2.99x10^{-1}$ g/m$^{2}$-day, $5.69x10^{-7}$ and $3.79x10^{-2}$ g/m$^{2}$-day, and $9.74x10^{-9}$ and $5.21x10^{-2}$ g/m$^{2}$-day, respectively. $CH_4$ and $CO_2$ emissions ranged from $-1.94x10^{-2}$ to $5.38x10^{+1}$ and $-2.36x10^{+1}$ to $7.47x10^{+2}$ g/m$^{2}$-day, respectively. The emissions decreased with the order daily, intermediate, and final covers; high to low permeability covers; and thin to thick covers. The destruction efficiency of the flare system was above 99%.

# EXECUTIVE SUMMARY

## Introduction

This investigation was conducted to provide detailed assessment of emissions of potent greenhouse gases (GHGs) from waste foam insulation (derived from discarded appliances and construction and demolition wastes) in landfills. The specific target gases were (hydro)chlorofluorocarbons (CFC-11, HCFC-141b HFC-134a, and HFC-245fa) used as blowing agents (BAs) in rigid foam insulation. The chemicals used as BAs have been modified over time (through sequential and increasingly rigorous regulations initiated with the Montreal Protocol). Even though outdated/prohibited BAs (e.g., CFC-11) are no longer used in manufacturing, significant quantities of such BAs remain in service as well as banked in landfills subsequent to disposal. Quantitative data is required to establish the context for regulating end-of-life management of foam wastes for foam-derived potent GHG emissions from landfills with respect to other phases of end-of-life management of foams and other sources of GHG emissions.

## Methods

The study consisted of three main phases: 1) a comprehensive literature review related to rigid foam blowing agents through end of life management of waste foams, 2) a California-specific materials flow analysis (MFA) for BAs in rigid foams, and 3) an extensive field testing program at a California landfill to measure baseline air quality at the site, emissions from various types of cover systems, and destruction efficiency of the gas management system. The literature review established the State of the Art for rigid foam blowing agents, fate of the BAs through end of life management of waste rigid foams, and emissions data for (hydro)chlorofluorocarbon BAs from landfills. The MFA was conducted to quantify emissions between end of life and the time of entry to landfill in detail. The MFA was used to estimate both the release of BAs and the quantity of BAs banked in foam materials entering the landfill. The analysis was conducted for two different time periods to account for differences in formulations of BAs with time. Separate MFAs were conducted for foams derived from: construction and demolition waste, domestic appliance waste, commercial appliance waste, transport refrigerated unit waste, and marine/other wastes. The field test program was conducted at Potrero Hills Landfill in northern California. The field program was conducted to determine baseline air quality and gas emissions as a function cover type and seasonal variations. Tests were conducted using static flux chambers. All cover systems, including daily cover, intermediate cover, and final cover, were tested. Tests were repeated in wet and dry seasons. The test locations included variable waste depth and variable waste age below the tested covers. Destruction efficiency was measured by comparing incoming and outgoing gas to the combustion system. For the field testing program, in addition to the 4 target F-gases, an additional 8 gases were analyzed to provide additional context for the analysis by including a broader range of constituents. Overall, the 14 chemicals analyzed in the investigation were: CFC-11, CFC-12, CFC-113, CFC-114, HCFC-21, HCFC-22, HCFC-141b, HCFC-142b, HCFC-151a, HFC-134a, HFC-152a, HFC-245fa, $CH_4$, and $CO_2$. For scaling flux results to represent total landfill emissions, the data obtained from the different cover types were assumed to be directly applicable to these specific cover types across the site.

## Results

Based on the literature review, very limited field landfill emissions data for (hydro)chlorofluorocarbons were identified in the U.S. with no data available for California. From the materials flow analysis, CFC-11 emissions were predicted to be high for current conditions, whereas HCFC-141b, HFC-134a, and HFC-245fa emissions were predicted to be high for future conditions. The amount of BAs remaining in waste foam at time of disposal in the landfill ranged from 31 to 94% of original BA content, depending on foam waste category and time period of interest. In the field testing program, high variability was observed for the measured ambient air concentrations as a function of constituent, season, and cover type. The overall variability of ambient concentrations (across all cover types and testing locations) ranged over 5 orders of magnitude for each season, and 6 orders of mangnitude annually. Measured F-gas ambient concentrations ranged from 0.4 to 598,000 pptv. For the target gases, higher ambient concentrations were observed for CFC-11 than HCFC-141b, HFC-134a, and HFC-245fa. For emissions, the ranges of measured fluxes (minimum to maximum) in the wet season for CFC-11, HCFC-141b, HFC-134a, and HFC-245fa were $2.27 \times 10^{-6}$ to $2.57 \times 10^{-1}$, $-5.59 \times 10^{-6}$ to $2.99 \times 10^{-1}$, $5.69 \times 10^{-7}$ to $3.79 \times 10^{-2}$, and $1.14 \times 10^{-7}$ to $5.21 \times 10^{-2}$ g/m$^2$-day, respectively. The ranges of measured fluxes (minimum to maximum) in the dry season for CFC-11, HCFC-141b, HFC-134a, and HFC-245fa were $9.47 \times 10^{-7}$ to $3.42 \times 10^{-2}$, $-5.01 \times 10^{-7}$ to $7.58 \times 10^{-3}$, $7.19 \times 10^{-7}$ to $5.07 \times 10^{-3}$, and $9.74 \times 10^{-9}$ to $8.77 \times 10^{-3}$ g/m$^2$-day, respectively. While the cover systems associated with minimum fluxes were either intermediate or final cover, all maximum fluxes (4 target constituents, both seasons) were measured for daily cover. The destruction efficiency data for the flare system was above 99.47% for all gases analyzed. The analysis to compare seasonal variations in emissions indicated high variablity depending on cover type, where flux through high permeability covers generally were higher in the wet season, whereas the flux through the low permeability covers were higher in the dry season.

## Conclusions

The emissions of potent GHGs (specifically F-gases) from landfills represent a contributing factor to climate change. Based on the field testing program, the $CO_2$ equivalents (100-year basis) for emissions of the summation of the 12 F-gases from the field test site ranged between 1010 and 3360 metric tonnes of $CO_2$ equivalents per year. Reported as fraction of total landfill emissions (F-gases + $CH_4$ + $CO_2$), these F-gas emissions were between 3.4 and 4.1%. The emission rates of F-gases reported as fraction of total landfill emissions (F-gases + $CH_4$ + $CO_2$) were variable by season, ranging between 5.1 and 23.3% for wet season and between 0.3 and 1.3% for dry season. Overall, contribution of F-gases to total GHG emissions from landflls is small yet not insignificant. Potent GHG emissions from landfills are a function of the following coupled mechanisms: waste conditions (waste age, depth of waste column beneath cover system), landfill cover configurations (material type, cover thickness, level of compaction), and climate (primarily wet versus dry season) and in general are highly complex from a mechanistic standpoint. Additional field data is required to make broad generalized statements related to specific mechanisms or correlations to variables.

# INTRODUCTION

This investigation was conducted to provide detailed assessment of emissions of target (hydro)chlorofluorocarbons (i.e., F-gases, CFC-11, HCFC-141b HFC-134a, and HFC-245fa) from end of life management of rigid waste foam materials. The three main components of the investigation included conducting an extensive literature search, conducting a California-specific materials flow analysis, and conducting an extensive field testing program at a typical California landfill. The results of the project are presented in three distinct sections within this report.

A summary of the literature review is presented in Part 1 of this report (full review included in Appendix 1). The review included fundamental information on properties and behavior of foam products and blowing agents of interest as well as atmospheric conditions in relation to the specific types of F-gases included in the study. End of life management practices for foam products were provided. Measurement and analysis methodologies applicable for investigating landfill gas emissions were reviewed. Available information was provided for emissions of the target F-gases during manufacture and use; during end of life management prior to final disposal; and from landfills. Data and analysis from laboratory and field experimental studies as well as modeling investigations were summarized.

The materials flow analysis is presented in Part 2 of this report. The system of waste foam material flows and stocks were quantified for waste foams for the period between the end of life and landfill disposal. Waste foam flows and stocks were estimated for conditions representative of foam use in California. Analysis included transportation of waste foams, storage/stockpiling, processing (e.g., shredding) of waste foams, as well as flows in a landfill facility exclusive of disposal (i.e., stockpiling and use as an alternative daily cover material). Estimates were provided for the relative proportions of remaining amount of blowing agents in end of life waste foams at the time of entry to the landfill with regard to initial amount of blowing agents present in new foam materials at the beginning of service life. Emissions between end of life and the time of disposal at the landfill were quantified in detail using the materials flow analysis.

The field test program is presented in Part 3 of this report. Emissions of a total of 14 gases (12 F-gases and $CO_2$ and $CH_4$) were provided for a typical landfill in California. Measurements were made using the static chamber flux technique at a total of seven locations representing four cover types (daily, extended daily, interim, and final). Data were obtained over the two predominant seasons (wet and dry) in California. Emissions of the 14 gases were determined in areas with different underlying waste ages. Effects of cover type and properties, waste age, operational conditions, and seasonal variations on emissions were assessed. Composite gas samples from the landfill gas extraction system were obtained to establish characteristics of source gas and to determine destruction/reduction of the target F-gases in gas collection and combustion systems and assess toxic combustion byproducts.

# PART 1 – LITERATURE REVIEW

## 1.1 Introduction

The annual municipal solid waste (MSW) generation in the U.S. has been on the order of 230 Mt since 2005, with 231 Mt of generation in 2013 (USEPA 2015a). Landfilling constitutes the main means of waste disposal in the U.S. with 122 Mt (53% of 231 Mt generated) disposed of in landfills in 2013. Signicanlty higher rates (on the order of 262 Mt) for landfill disposal also were reported (van Haaren et al. 2010, Powell et al. 2015). For California, the annual MSW disposal amount has been on the order of 27 Mt since 2009, with 28 Mt reported for 2014 (CalRecycle 2015). The number of landfills was reported to be 1,908 in the U.S. (USEPA 2015a) and 372 in California (Cascadia 2008).

Landfilling of municipal solid waste results in three main byproducts: landfill gas (LFG), leachate, and heat. Landfill gas is a biogas consisting of approximatey half methane ($CH_4$) and half carbon dioxide ($CO_2$) generated due to anaerobic microbial processes that occur in the landfill. LFG also includes minor amounts of oxygen and nitrogen from the atmosphere as well as a large number of trace components, which have been directly volatilized from the waste or generated by biotic or abiotic processes within the landfill. Scheutz et al. (2008) indicated that trace components were comprised of more than 200 species including alkanes, aromatics, alcohols, aldehydes, reduced S gases, and chlorinated and fluorinated hydrocarbons, with measured concentrations in the range of below detection limit to 1,780 ppmV. The gases of interest for this investigation consisted of halogenated hydrocarbons including chlorinated and fluorinated species chlorofluorocarbons (CFCs), hydrochlorofluorocarbons (HCFCs), and hydrofluorocarbons (HFCs). The specific gases investigated were CFC-11, HCFC-141b, HFC-134a, and HFC-245fa. These four gases collectively are referred to as target gases in this report.

## 1.2 General Background: CFCs, HCFCs, and HFCs

Chlorinated and fluorinated hydrocarbons commonly are used in refrigeration and insulation foam (Rettenberger and Stegmann 1996). Use as insulation materials is the most common application of chlorofluorocarbons due to the abilities of these compounds to absorb large amounts of heat upon vaporization (Vollhardt et al. 1999). The use of CFCs in insulation foams and refrigeration started in early 1930s (CARB 2008). After the Montreal Protocol banned the use of CFCs in 1993, CFCs were progressively replaced by HCFCs and HFCs. The most common waste products that emit these chlorinated and fluorinated gases are domestic, commercial, and industrial refrigeration and insulation foams used in appliances or buildings (Scheutz 2005). The most common gases present in these foams, including CFC-11, HCFC-141b, HFC-134a, and HFC-245fa, enter landfill facilities due to the disposal of waste foams. The waste materials with potential emissions are discards consisting of rigid foams. CFCs, HCFCs, and HFCs generally do not have significant health effects for humans however, are of primary concern due to their adverse environmental effects. The common CFCs, HCFCs, and HFCs are greenhouse gases that contribute to the depletion of the ozone layer and global climate change (Scheutz et al. 2007a). CFCs and HCFCs also are ozone-depleting substances (ODS) due to long atmospheric lifetimes, whereas ozone depletion impacts of the HCFCs are relatively small.

Chlorinated and fluorinated hydrocarbons are alkanes (long groups of single bonded carbon atoms) where all of the hydrogen atoms have been replaced by fluorine and chlorine atoms (Vollhardt et al. 1999). Physical and chemical properties of the target gases (CFC-11, HCFC-141b, HFC-134a, and HFC-245fa) are presented in Table 1.1 (from tests at 25°C and 1 atm pressure). Due to their relatively low boiling points (in the range of <0 to 100°C), CFCs, HCFCs, and HFCs are classified as volatile organic compounds (VOCs). In general, HFCs have higher volatility (higher vapor pressure, lower boiling point) and relatively lower solubility in water as compared to CFCs and HCFCs (Tsai 2005).

Table 1.1 – Physical and Chemical Properties of Target Gases
(from Scheutz et al. 2003a)

| Chemical Name | CFC-11 | HCFC-141b | HFC-134a | HFC-245fa |
|---|---|---|---|---|
| Synonyms | Trichlorofluoro-methane | 1,1-Dichloro-1-Fluoroethane | 1,1,1,2-Tetrafluoroethane | 1,1,1,3,3-Pentafluoro-propane |
| Structure | $CCl_3F$ | $CCl_2FCH_3$ | $CH_2FCF_3$ | $CF_3CH_2CHF_2$ |
| Molecular Weight (g/mol) | 137.37 | 116.95 | 102.03 | 134.05 |
| Boiling Point (°C) | 23.8 | 32 | -26.2 | 15.3 |
| Vapor Pressure (mmHg) | 798[2]-802.8[1] | 626[2]-707[1] | 430[1]-4,995[2] | 1,114[3]-1,139[2] |
| Water Solubility (mg/L) | 1,100[1,2] | 660[1]-2,632[2] | 67[1]-550[2] | 1,300[3]-1,900[3] |
| Log$K_{ow}$ | 2.53[1,2] | 2.04[2]-2.37[1] | 1.06-1.68[1] | 1.33-1.35[1] |
| Log$K_{oc}$ | 2.49[4] | 1.9-2.2[4] | 1.5[4] | 1.75-1.9[4] |
| Saturated Gas Concentration (g/L) | 5.62[1] | 4.78[1] | 4.17[1] | 5.48[1]-5.5[3] |

[1] Scheutz and Kjeldsen (2003a)
[2] Mackay et al. (2006)
[3] NICNAS (2004)
[4] Summarized from UNEP (1998, 2001), Balsiger et al. (2004), and ChemSpider (2013)

In general, the physical and chemical characteristics of CFCs, HCFCs, and HFCs favor the potential for accumulation in the atmosphere as opposed to the soil or groundwater, where accumulation depends on atmospheric retention times (higher for CFCs than HCFCs/HFCs). The current global atmospheric concentrations of selected GHGs are provided in Table 1.2. These data represent recent global averages over a 12-month period (ALE/GAGE/AGAGE Global Network Program 2013). Recent tropospheric concentrations of carbon dioxide are the highest of all GHGs analyzed at 390.5 ppm compared to approximately 1800 ppb of methane, 34 ppb ozone, 240 ppt CFC-11, 530 ppt CFC-12, 22 ppt HCFC-141b, and 63 ppt HFC-134a (CDIAC 2012, IPCC 2013).

Table 1.2 – Atmospheric Conditions for GHGs

| Gas | Recent Tropospheric Concentration (ppt)[1] | Recent Tropospheric Concentration (ppt)[4,5] | Atmospheric Lifetime (yrs)[1,2,3] | Global Warming Potential (100 yr)[1,2,3] | Ozone Depletion Potential[1,2] | Radiative Forcing ($W/m^2$)[1] |
|---|---|---|---|---|---|---|
| Carbon Dioxide | $3.91x10^8$ | N/A | 100 | 1 | 0 | 1.82 |
| Methane | $1.80x10^6$-$1.81x10^6$ | N/A | 9.1-12.4 | 25-28 | 0 | 0.48 |
| Nitrous Oxide | $3.24x10^5$ | N/A | 114-131 | 265-298 | 0 | 0.17 |
| Ozone[3] | $3.4x10^4$ | N/A | Hours-Days | N/A | N/A | 0.35 |
| CFC-11 | 237-239 | 259-301[4] | 45 | 3800-4660 | 1 | 0.06 |
| CFC-12 | 527-529 | 545-567[4] | 100 | 8100-10200 | 1 | 0.17 |
| CFC-113 | 74 | 79-90[4] | 85 | 5820-6130 | 0.8 | 0.022 |
| HCFC-141b | 21 | 16.4-20[5] | 9.2 | 700-782 | 0.1-0.12 | 0.0034 |
| HCFC-142b | 21 | 13.6-19[5] | 17.2-17.9 | 1800-1980 | 0.06-0.07 | 0.0040 |
| HCFC-22 | 213 | 220-295[5] | 11.9 | 1500-1780 | 0.05-0.055 | 0.045 |
| HFC-134a | 62-63 | 23-23.1[5] | 13.4-14 | 1300-1410 | 0 | 0.0100 |
| HFC-245fa | N/A | N/A | 6.6-7.7 | 858-1020 | 0 | |
| Halon 1211[3] | 4.1-4.3 | N/A | 16 | 1750-1890 | N/A | 0.001 |
| Halon 1301[3] | 3.2-3.3 | N/A | 65 | 6290-7140 | N/A | 0.001 |
| Carbon Tetrachloride | 85-86 | N/A | 26 | 1400-1730 | N/A | 0.015 |
| Sulfur Hexafluoride | 7.3 | N/A | 3200 | 22800-23500 | N/A | 0.0041 |
| Total Halocarbons[6] | Varies | N/A | Varies | Varies | N/A | 0.330 |

[1] IPCC 2013 summary of combined global ambient tropospheric concentrations in both rural and urban areas
[2] Ranges adapted from SAR (1995), TAR (2001), and TEAP (2009)
[3] CDIAC (2012)
[4] Barletta et al. (2006), global ambient tropospheric concentrations above 6 urban centers
[5] Barletta et al. (2002), global ambient tropospheric concentrations above 2 urban centers
[6] Also termed total "Montreal Protocol" gases (IPCC 2013)

## 1.3 Foam Materials

### 1.3.1 Background

Foams are used in refrigeration, building, and transportation industries as insulation, packaging, and cushioning (IPCC 2007). Based on crystallinity and melting temperatures, foams are classified as thermoset or thermoplastic. Most refrigeration and building insulation foam applications use thermoset materials due to high resistance to physical changes. A general classification of foams is provided in Figure 1.1 as a function of plasticity (thermoset/thermoplastic), stress-strain response (rigid/flexible), and density (high/low). The four main types of foam that are currently manufactured for building insulation and refrigeration applications include extruded polystyrene (XPS), expanded polystyrene (EPS), polyurethane (PUR), and polyisocyanurate (PIR) foams. PIR foams are a special class of PUR with high fire resistance (Schroer et al. 2011). The most common materials used in building insulation include low- and high-density rigid XPS panels (depending on roofing, flooring, or wall application) as well as rigid thermoset PUR/PIR panels, low density PUR spray insulation, PUR pipe in pipe sections, one component PUR foams (OCF), or PUR blocks (TEAP 2005). The most common materials used in appliances (both

commercial and domestic) include rigid PUR insulation foams poured in place during manufacturing (TEAP 2005). The majority of the foam materials used in the U.S. consist of PUR insulation (Throne 2004). For end of life management, thermoset foams generally cannot be readily reprocessed once the product is formed and thus are more difficult to recycle than thermoplastic foams, whereas thermoplastics can be broken down and recycled after use (Sivertsen 2007).

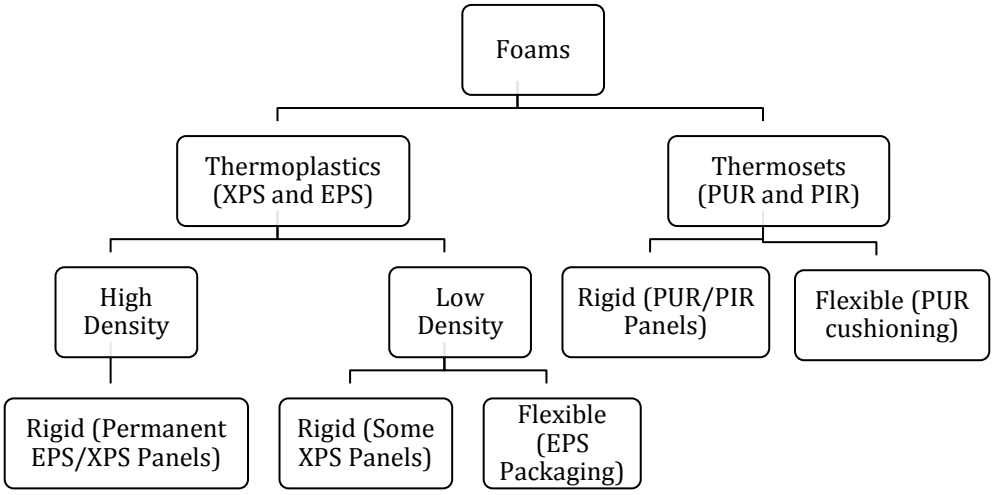


Figure 1.1. Classification of Foams (from Throne 2004)

Foams are composed of both a solid and a gas phase. The solid phase consists of a polymer matrix and the gas phase consists of a blowing agent (Landrock 1995). The polymer matrix is filled with the blowing agent (BA) to form the foam product. Ideal BAs for insulation applications have a high molecular weight, low thermal conductivity (achieved through BA type and cell formation), as well as a low diffusion coefficient, limiting the amount of BA released over the service life of the material (Colvin 2001). CFCs, HCFCs, and HFCs are common blowing agents used in the manufacture of foams. The chlorinated and fluorinated hydrocarbon BAs have higher insulation values (i.e. R-values) compared to non-halocarbon alternatives and lower diffusion rates than non-halocarbon alternatives (Dieckmann and Magid 1999). These combined effects lengthen the time the blowing agents are entrapped within the foam and thus result in long lifetimes (UNEP 1996). In addition, physical blowing agents such as CFC-11 are more thermally efficient in that they require less thickness to insulate the same area as compared to other blowing agents such as carbon dioxide or air. Low solubility can be achieved with chlorinated and fluorinated hydrocarbon BAs to create a solid foam structure with improved thermal and mechanical properties. Physical, chemical, and thermal properties of rigid foam influence the short and long term insulation performance, mechanical performance under loading, and relative short and long term release of blowing agents. A summary of physical and chemical properties of rigid PUR insulation foam obtained from end of life appliances is presented in Table 1.3. Foams blown with CFC-11 had higher cell gas content than foams blown with HFC-134a, which resulted in lower density. The PUR foam manufacturing process produces carbon dioxide considered a co-blowing agent along with the inserted chlorinated and

fluorinated hydrocarbon gas blowing agent. Carbon dioxide concentrations in PUR foams vary due to conditions during foam processing, blowing agent used, gas partial pressures, temperatures, and the presence of diffusion barriers such as bonded or adhered facers (Scheutz and Kjeldsen 2003a). The total BA content in foams varied between 7 and 13% as a function of the gas used. The PUR and PIR foam manufacturing process solubilizes the BA in the foam. The amount of BA dissolved in the PUR foam varied between 23 and 30% of the total BA content. Foams with CFC-11 had the highest sorbed fraction, whereas foams with HFC-134a contained the lowest sorbed fraction (Table 1.3).

Table 1.3 – Physical and Chemical Characteristics of four PUR Foam Refrigerator Insulation Panels (adapted from Scheutz and Kjeldsen (2003a))

| Parameter | Unit | CFC-11 | HCFC-141b | HFC-134a | HFC-245fa |
|---|---|---|---|---|---|
| Density (foam) | g/L | 24.6 | 32.2 | 39 | 30.7 |
| Porosity (calculated) | | 0.985 | 0.978 | 0.972 | 0.98 |
| Porosity (measured) | | 0.964 | 0.919 | 0.929 | 0.933 |
| Total Content of $CO_2$ | g/L | 0.14 | 0.75 | 1.5 | 0.48 |
| | % w/w | 0.58 | 2.34 | 3.86 | 1.61 |
| Fraction of $CO_2$ | % w/w | 3.9 | 16.6 | 35 | 11.6 |
| Total Content of BA | g/L | 3.43 | 3.77 | 2.78 | 3.66 |
| | % w/w | 13.3 | 11.6 | 7 | 11.6 |
| Content of BA in Polymer | g/L | 1.01 | 1.05 | 0.63 | 0.91 |
| Fraction Sorbed in PUR | % | 29.5 | 27.8 | 22.7 | 24.8 |
| Distribution Coefficient *K* | $m^3$ gas / $m^3$ PUR | 24.6 | 16.5 | 10.1 | 14.9 |

Foam applications include the use of either closed cell (rigid foams) or open cell (flexible foams). Rigid foams are used in thermal insulation of appliances (refrigeration), structures (buildings), and transportation units. Appliance foam uses include insulation of domestic refrigerators and freezers, commercial refrigerators and freezers, water heaters, and vending machines. Construction rigid foam uses consist of roof boards, lining boards, pipe sections, cold store panels, and spray systems. Transportation foam insulation applications include sandwich panels used for Reefer boxes and transport refrigerated units-TRUs (UNEP 1996). In addition, rigid foams are used in structural integrity and buoyancy applications in the marine industry, as well as for non-structural cold stores (commercial or industrial walk in freezers) (IPCC 2007). Flexible foams typically are used for packaging, transport, cushioning, and impact management purposes (IPCC 2007). Appliance applications only incorporate the use of PUR foam materials. Foams used in insulation applications for construction are composed of PUR/PIR, XPS, EPS, and Polyolefin foams. Transportation applications for insulation typically are limited to PUR and EPS foam materials.

Total rigid insulation foam consumption in California was estimated to be 3.5 million $m^3$/year (Caleb 2011). Variability in foam consumption with time or annual trends in foam consumption/manufacturing were not presented by Caleb (2011). Such data are

not readily accessible in the literature. Foam consumption by application for new foam was predominantly for construction of new buildings or refurbishment applications of existing building stock (up to 61%). Appliance foam was the next highest category for insulation foams at 36% of the total consumption, followed by marine, TRU, and cold store applications (Figure 1.2).

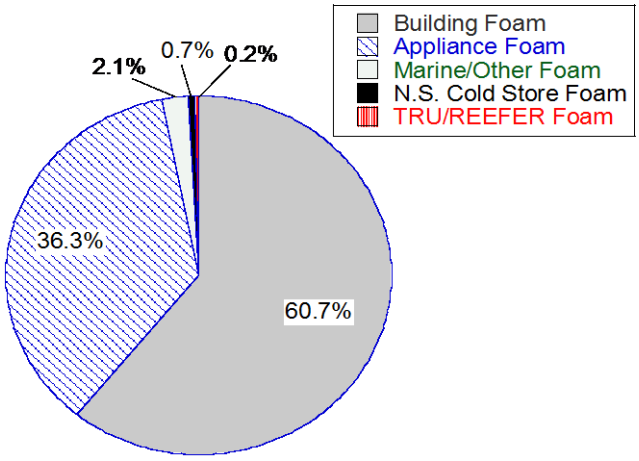


Figure 1.2. Foam Consumption in California by Application (from Caleb 2011)

Consumption trends for California by foam material indicated that approximately 55%, 29%, 10%, and 6% of building insulation consisted of PIR, XPS, PUR spray, and PUR panel, respectively (Figure 1.3). Assuming that appliance, marine, and TRU/Reefer foam is strictly PUR, total foam consumption can be estimated to include PIR, PUR, and XPS foam (EPS was not included by Caleb (2011)). Almost half of the rigid foam consumption was PUR based (49%), followed by PIR (33%), and XPS (18%) (Figure 1.4). Future growth in consumption was assumed to include a significant increase in PIR (10%/year) (Singh et al. 2005). Therefore, PUR/PIR foams comprise a significant portion of the current and future rigid insulation foam market in California, compared to polystyrene foams.

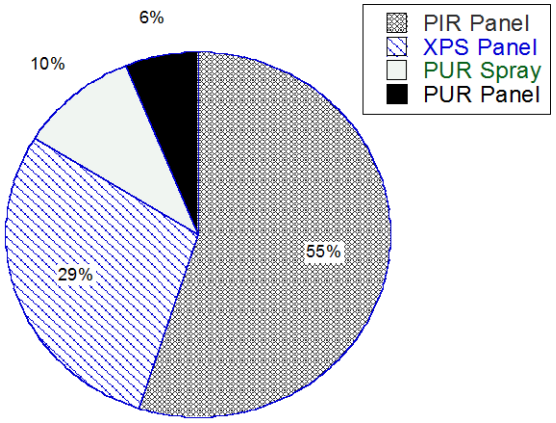


Figure 1.3. Building Foam Consumption in California (Caleb 2011)

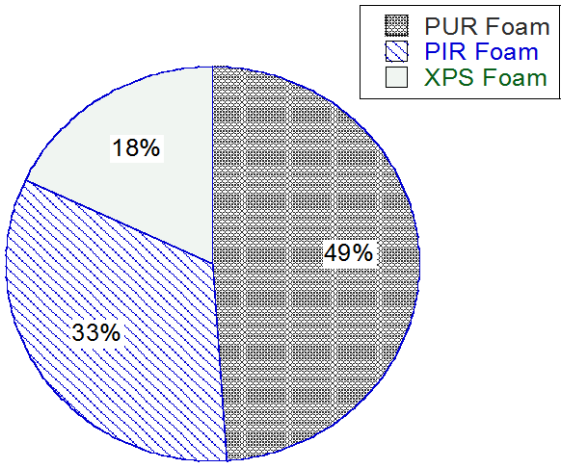


Figure 1.4. Estimated California Consumption of Rigid Foam Insulation (adapted from Caleb 2011)

### 1.3.2 Emissions of Blowing Agents from Foams

Emissions of blowing agents from foams may occur during three distinct phases: i) foam production and installation (regarded as first year losses), ii) losses from installed foam product during service, and iii) losses during decommissioning at end of life of a foam product (TEAP 2002, Godwin et al. 2003, TEAP 2005). The emissions before end of life (manufacturing through use) vary as a function of the application: building insulation, appliance insulation, and packaging, cushioning, and transportation insulation. For building insulation applications, significant variations were observed between application type and between foam materials used in a given application for first year release, time to total release, and total blowing agent remaining at decommissioning. The lowest first year releases were observed for appliance insulation (on the order of 5%), whereas highly variable and high magnitude (5 up to 100%) losses were reported for building insulation. The release rates subsequent to first year did not vary significantly between applications. Time to total release was highest for appliance foams indicating significant amount of banked BAs at end of life. PUR had significant BA banks with more than half of the initial BA amount remaining at end of life (Table 1.4).

The atmospheric emissions of blowing agents and formation of blowing agent banks depend on the extent of blowing agent release from the foam product during manufacturing and use. The specific factors that govern the release of blowing agents during use of foam products include: the type of foam (rigid or flexible), blowing agent used, partial pressure of the blowing agent within the foam, diffusion coefficient, whether a diffusion barrier (i.e., facer) exists, and temperature (Scheutz and Kjeldsen 2003a). For rigid foams, the type of BA used is the main factor that controls the total initial content of BA, the distribution of gas within the foam, as well as the diffusive properties of the gas itself. The partial pressure of the blowing agent, a result of the

manufacturing process, influences the diffusion of the BA out of the foam due to concentration gradients between the foam and the atmosphere. High partial pressures and low atmospheric barometric pressure result in a high diffusion of gas. Increasing the temperature also increases the rate of diffusion due to higher kinetic energy of the gas molecules. For flexible foams, the blowing agent used is expected to be released within a short timeframe, usually during manufacturing, or within the first year of use. This quick BA release is due to the open cell structure of flexible foams as compared to a closed cell structure for rigid insulation foams.

Data on BA content at different stages of life of rigid PUR, PIR, and XPS foams (panel, spray, and boardstock) used for building and appliance insulation applications are presented in Table 1.5 (generally testing at 25°C temperature and atmospheric pressure conditions). For EPS foams, most of the BA (up to 100%) was indicated to be lost by the time the materials reached end of life (Godwin et al. 2003). A greater difference between initial BA content and BA content at end of life was observed for PUR foam than XPS foam. BA content at end of life was a function of the gas used during manufacture. Foams with CFC-11 and HCFC-141b had somewhat higher BA at end of life than foams with HFC-134a and HFC-245fa. In general gaseous BA content at end of life was higher and solubilized BA content in foam polymer was lower for the HFCs than CFC-11 and HCFC-141b. Fredenslund et al. (2005) indicated that the BA contents were relatively similar before and after use for products with CFC-11 BA obtained from 8 refrigerator manufacturers prior to 1993. Kjeldsen and Jensen (2001) indicated that the closed cell diffusion of gaseous BAs during service from rigid appliance foams was expected to be very slow to negligible, compared to emissions at end of life. Losses of BA during service may result from losses of the fraction sorbed in the foam itself (Scheutz and Kjeldsen 2003a). Significant differences were present between the predicted/compiled data (Table 1.4) and experimental data (Table 1.5) for BA content at end of life of foams. These differences may have resulted from regional manufacturing and use practices as well as the assumptions inherent in the predictions provided in Table 1.4.

Table 1.4 – Stages of BA Emissions from Foams (data from TEAP 2002, Godwin et al. 2003,TEAP 2005)

| Foam Application | Foam Type | First Year Release (%) | Release Rate (%/year) | Time to Total Release (years) | Lifetime of Foam (years) | Total Remaining at Decommissioning (%) |
|---|---|---|---|---|---|---|
| Building Insulation (including Cold Store Insulation, Marine, and Other) | PUR Sandwich Panels | 40 | 2 | N/A | 25 | 10 |
| | PUR Continuous Panel | 5 | <0.5 | 190 | 50 | 70 |
| | PUR Discontinuous Panel | 6 | <0.5 | 188 | 50 | 69 |
| | PUR Continuous Block | 35 | 0.75 | 86 | 15 | 54 |
| | PUR Discontinuous Block | 40 | 0.75 | 80 | 15 | 49 |
| | Phen. Discontinuous Block | 40 | 0.75 | 80 | 15 | 49 |
| | PUR Boardstock | 6 | 0.5 to1 | 94 | 50 | 44 |
| | PIR Boardstock | 10 | 1.5 | N/A | 50 | 15 |
| | XPS Boardstock | 25 | 0.75 to 2.5 | 30 | 50 | 0 |
| | Phen. Boardstock | 6 | 0.25 to 1 | 94 | 50 | 44 |
| | PE Boardstock | 90 | 5 | 2 | 50 | 0 |
| | PUR Spray | 15 to 25 | 0.75 to 1.5 | 50 | 50 | 0 |
| | PUR OCF | 100 | N/A | 0 | 50 | 0 |
| | PUR Pipe in Pipe | 6 | 0.25 | 376 | 50 | 81.5 |
| | PE Pipe | 100 | N/A | 0 | 15 | 0 |
| Appliance Insulation | PUR Appliance | 4 | 0.25 | 384 | 15 | 92 |
| | PUR Com. Refrig | 6 | 0.25 | 376 | 15 | 90 |
| Cushioning, Packaging, Transportation Insulation | PUR Flexible | 100 | 0 | 0 | 0 | 0 |
| | PUR Integral Skin | 95 | 2.5 | 2 | 15 | 0 |
| | PUR Reefers/Trans | 4 to 6 | 0.5 | 188 | 15 | 86.5 |
| | Polyolefin | 95 | 2.5 | N/A | 2 | 0 |

N/A: Not applicable to study

Table 1.5 – Variation of BA Content in Rigid Insulation Foams

| Foam Type | Reference | Insulation Type and Configuration | Blowing Agent | Initial BA Content (%w/w) | BA Content at End of Life (%w/w) | Solubilized BA at End of Life (%) | Gaseous BA at End of Life[5] (%) |
|---|---|---|---|---|---|---|---|
| Rigid PUR/PIR | Khalil and Rasmussen (1986) | Building, Panel | CFC-11 | 15.1 | 10 | - | - |
| | Bomberg and Kumaran (1990) | Building, Spray | CFC-11 | - | 10 to 12 | 22 to 66 | 34 to 78 |
| | Pollack et al. (1993) | Building, Panel | CFC-11 | - | 5.4 to 12.8 | - | - |
| | Swanstrom and Ramnas (1996) | Building, Panel | CFC-11 | - | 5.2 to 7.9 | 46 to 52 | 48 to 54 |
| | Fyfe et al. (1996) | Building, Boardstock | HCFC-141b | - | - | 24 | 76 |
| | Hong and Duda (1998) | Building, Panel | CFC-11 | - | 4.1 to 12 | 13 to 16 | 84 to 87 |
| | | | HCFC-141b | - | 4 to 11.5 | 16 to 17 | 84 to 85 |
| | Singh et al. (1998) | Building, Panel | CFC-11 | - | 5.6 to 7.7 | 60 | 40 |
| | Hong et al. (2001) | Building, Panel | HFC-134a | - | 1.2 to 1.7 | 1.7 to 2 | 98 |
| | | | HFC-245fa | - | 5.4 | 9 | 91 |
| | Kjeldsen and Jensen (2001) | Appliance, Panel | CFC-11 | - | 11 to 15 | 41 to 44 | 56 to 59 |
| | Roe (2002)[1] | Building, Roof Panel | HCFC-141b | - | - | 9 | 91 |
| | | | HFC-245fa | - | - | 4 | 96 |
| | Scheutz and Kjeldsen (2003a) | Appliance, Panel | CFC-11 | - | 13.3 | 30 | 70 |
| | | | HCFC-141b | - | 11.6 | 28 | 72 |
| | | | HFC-134a | - | 7 | 23 | 77 |
| | | | HFC-245fa | - | 11.6 | 25 | 75 |
| | Fredenslund et al. (2005) and Scheutz et al. (2007a) | Appliance, Panel | CFC-11 | 14.0 to 16.4 | 13.0 to 15.4 | - | - |
| Rigid XPS | Fyfe et al. (1996) | Building, Boardstock | HCFC-142b | - | - | 13 | 87 |
| | Vo and Paquet (2004) | Building, Roof Panel | CFC-12 | 5 to 6.5 | 1.5 to 4 | - | - |
| | | | HCFC-142b | 8 to 8.4 | 1.5 to 6 | - | - |
| | | | HFC-134a | 6.5 to 7 | - | - | - |
| | Gendron et al. (2002) | Building, Boardstock | HCFC-142b | 11 to 15 | - | - | - |
| | | | HFC-134a | 6 to 8 | - | 0.8[2] | 99.2 |
| | Daigneault et al. (1998) | Building, Boardstock | HCFC-142b | - | - | 3(15)[3] | 97(85)[6] |
| | | | HFC-134a | - | - | 0.6(2)[3] | 99.4(98)[6] |
| | Gendron et al. (2006) | Building, Boardstock | HFC-134a | 6(8)[4] | - | - | - |

[1] PIR building insulation foams only
[2] BA solubility in polymer observed at 30°C
[3] Average and (maximum) solubility of BA observed at 40°C
[4] Average initial BA concentration and (maximum) initial concentration observed
[5] Assuming the foam at end of life is completely dry
[6] Calculated (maximum) BA in gaseous phase from (maximum) solubility in the previous column
- Omitted by the study

### 1.3.3 End of Life Management of Foams

Common management practices for end of life waste foam materials include reuse, recycling, and landfill disposal. In general, recycling operations include shredding of the foam wastes with or without recovery of foam BAs using two main processes (Scheutz et al. 2007a). The first process, termed general shredding, involves the shredding of foam waste in unsealed facilities (i.e. no gas recovered), recycling valuable materials (metals), and disposal of the shredder residue in a landfill. Most scrap recycling facilities in the U.S. operate under these conditions. The alternative process, termed recycling and recovery of ODS, recovers the CFCs, HCFCs and HFCs emitted during the shredding process of foam, treating the gases, while also recovering the reusable materials. The end of life management practices used for waste insulation foams in California vary as a function of the original foam application: construction and demolition, domestic refrigerator and freezer, commercial appliance (including water heaters and vending machines), transport foam (transport refrigerated units-TRUs), as well as marine and other foam wastes (including non-structural cold stores) (Caleb 2011). Approximately 92% of foam wastes from construction and demolition activities was estimated to be landfilled directly, whereas 8% of the foam wastes was shredded prior to landfilling. The reuse rate of domestic refrigerators/freezers was estimated to be 39%, the amount recycled with no foam recovery was 47%, and the amount of appliances with foam recovery/BA destruction (ODS processed) was 14%. For commercial appliances and vending machines, 100% of the devices were processed via shredder, degassed (refrigerant recovered), metals were recovered, and the remaining residue including foam was landfilled. For commercial water heaters, 100% of the devices were processed via shredder, metals were recovered, and the remaining residue including foam was landfilled. In transportation applications, 25% of TRUs and Reefers were estimated to be reused, whereas the remaining 75% were shredded, metals were recovered, and the remaining residue including foam was landfilled. For marine and other applications, 5% of leisure and recreational boats were exported and 95% were shredded and residue including foam was landfilled; 100% of canoes were shredded and residue including foam was landfilled; 100% of buoys and coolers were landfilled; and 100% of nonstructural cold storage units were landfilled.

An additional category of waste foam material is auto fluff, which is a combination of flexible foam products (seat cushioning) with an open celled structure, as well as rigid panel foam panel insulation (used on the outside frame of cars) (Scheutz et al. 2007c). Auto shredder residue waste is typically very heterogeneous (in both size and composition) and varies by both year and manufacturer of the car (Moakley et al. 2010). Plastics emanating from foams, textiles and carpets are typically the main component of the auto shredder residue (ASR) composition (Moakley et al. 2010). The Argonne National Laboratory evaluated auto shredder residue composition (ferrous and non-ferrous fractions) at a U.S. shredder facility (Duranceau and Spangenberger 2011). Non-ferrous fractions consisted of either <12 mm fine particles (2.5% w/w of the total feed entering the shredder) or coarse residue in the size range from 12 to 150 mm (17% w/w of the total feed entering the shredder) (Duranceau and Spangenberger 2011). For the fines category, mixed polymer concentrations were the highest among

the composition analyzed an average of 45% (w/w) of the total fine content). For the coarse fraction, oversized foam (flexible foam from seat cushioning) represented between 1 to 6% (w/w) of the total weight fraction. The BA in these products is expected to be emitted during manufacture and use with essentially no BA left in the foam at end of life (TEAP 2005). However, polymer concentrate ranged from 36 to 43% (w/w) that could contain small fractions of shredded foam residue, possibly from rigid panel insulation. The composition of polymer concentrate ranged from 4% (w/w) for polystyrene (present in XPS/EPS insulation), and 2-3% (w/w) polyurethane (present in PUR/PIR insulation), suggesting the presence of rigid foam insulation in the shredder residue. This range was consistent among manufactures and car types, but was observed to vary by age (Duranceau and Spangenberger 2011). These results agree with studies by Scheutz et al. (2007c, 2011a, and 2011b) that measured emissions of BAs and quantified foam present in auto shredder residue in Denmark. Scheutz et al. (2007c) attributed most of the small foam particles to rigid PUR insulation panels (blown with CFC-11, HCFC-141b, and HFC-134a). Detectable emissions of CFC-11 were quantified in laboratory lysimeter experiments using auto fluff sampled from the residue cells (Scheutz et al. 2007c, 2011a). In addition, small emissions of common BAs varied from CFC-11 and HFC-134a (Scheutz et al. 2011b) at different hotspot locations within the shredder residue cells. Thus, a combination of results from both laboratory and field experiments analyzing auto shredder residue imply that auto fluff may contribute to BA emissions within the landfill environment.

## 1.4 Foam Wastes in the Landfill Environment

### 1.4.1 CFCs, HCFCs, and HFCs Entering Landfills

The concentrations and amount of CFCs, HCFCs, and HFCs in rigid foam insulation wastes entering landfills are based on initial BA content and emissions of the BAs during manufacturing, use, and throughout end of life practices prior to disposal. Analyses of data from Caleb (2011) were used to estimate the amount and concentration of CFCs, HCFCs, and HFCs entering landfills and the amount of the BAs in landfills banked for recent conditions (1960-2010) and projected to be banked in the future (2011-2020). In addition, the report was used to estimate emissions from the banks identified. The Caleb (2011) report, developed for CARB, was the main available literature source identified by the research team. The total amount of foam waste generated in California was estimated to be 930,350 $m^3$/year for 2008 (Caleb 2011). Approximately 48% of the foam waste disposed was estimated to be building insulation foam compared to 34% domestic appliance foam waste with lower quantities associated with other categories of use as presented in Figure 1.5. The amount of BAs entering end of life processes was estimated using total amount of foam waste generation. Caleb (2011) provided timelines associated with historical use of the three BA types (i.e., CFCs, HCFCs, and HFCs) in California. These reported values for composition of BAs in different foam application categories were used to provide estimates for current and future conditions for foam wastes at end of life and foam wastes entering landfill facilities in Figures 1.6 and 1.7, respectively. Overall, significant decreases in CFCs and increases in HFCs are expected due to the BA substitutions in foams over time. Additional detailed analyses for lifetime

characteristics of rigid foams are provided in the Materials Flow Analysis section (Part 2) of this report.

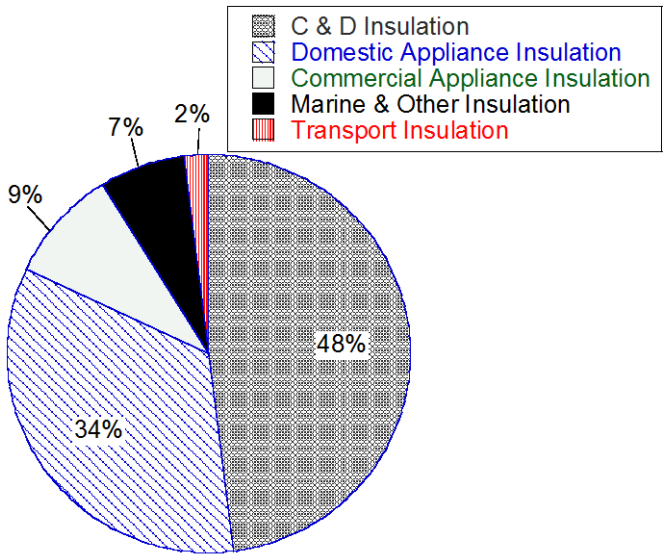


Figure 1.5. Sources of Foam Waste Generated in California (Caleb 2011)

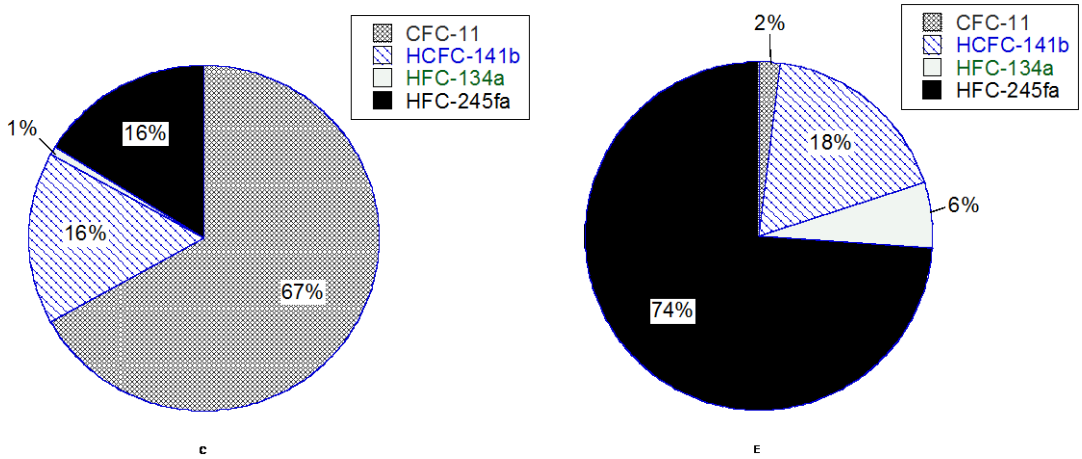


(a) Recent (2,705 tonnes BA/year) (b) Future (3,418 tonnes BA/year)

Figure 1.6. Foam Waste Insulation Materials Entering End of Life Management

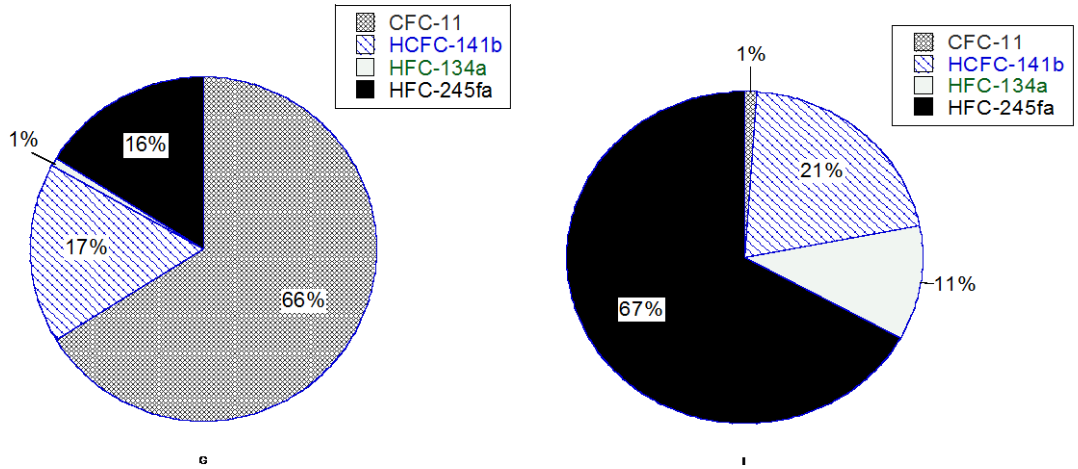


(a) Recent (1,784 tonnes BA/year) (b) Future (1,655 tonnes BA/year)

Figure 1.7. Foam Waste Insulation Materials Entering Landfills

In the future, the overall amount of foam wastes generated was predicted to increase, whereas the amount disposed of in landfills was predicted to decrease compared to current conditions (Figures 1.6 and 1.7). For current conditions, CFC-11 represented the highest amount of BA material to enter end of life management processes and to be disposed of in landfills. For future conditions, HFC-245fa represented the highest amount of BA material to enter end of life management and to be disposed of in landfills. The extent of reduction due to emissions of BA during end of life management practices prior to landfill disposal was more pronounced for HFC-245fa for future conditions (74 to 67%) than for CFC-11 for current conditions (67 to 66%). This difference resulted from the higher long-term diffusion and short term losses used for HFC-245fa than CFC-11.

### 1.4.2 Banks of CFCs, HCFCs, and HFCs in Landfills

Development of CFC, HCFC, and HFC banks from foam wastes in California was analyzed in Caleb (2011) for the period between 1996 and 2020 for total amount of foam wastes and foam wastes in landfills (Table 1.6). The total bank in California for each insulation category was a function of the total amount of CFCs, HCFCs, and HFCs in foams in current use and predicted in future use, emissions during manufacturing/use/end of life, as well as the amount of BAs in foams entering the waste stream (based on annual disposal rate) and previously accumulated in landfills. Highest BA banks were for buildings followed by appliances with smaller quantities associated with other application categories. The BA bank estimates declined from the 364 $MMTCO_2$-eq level in 1996 to 228 $MMTCO_2$-eq by 2020. The total amount of BAs in California landfills was estimated to be 50,000 tonnes in 2010 and projected to increase to 100,000 tonnes and 164 $MMTCO_2$-eq by 2020 (Caleb 2011). Highest BA banks in landfills resulted from building foam wastes followed by appliance foam

wastes with smaller quantities associated with other application categories (Table 1.7). The cumulative fraction of CFCs, HCFCs, and HFCs in landfill BA banks was 40% in 2010, which was predicted to increase to 72% in 2020 (Caleb 2011). The composition of the banked BAs in landfills was predicted to include large fractions of CFCs with low fractions of HCFCs and HFCs by 2020 (Figure 1.8). The majority of BAs entering landfills are from buildings that have long service lifetimes (50 years) and CFCs will continue to dominate the BA composition in landfill banks as old buildings with CFC BAs are decommissioned. The relative fraction of HCFCs and HFCs will increase in landfill banks as these BAs have become the main type of BAs used in foam applications, in particular with the entry of foams from appliances with relatively short lifetimes (20 years) into the waste stream. Thus, emissions from California landfill foam waste banks will primarily include CFC-11 with increases in emissions of HCFC-141b and HFC-245fa for the near future (Figure 1.8).

Table 1.6 – Summary of All Blowing Agent Banks ($MMTCO_2eq$)

| Year | Buildings | Appliances | Other Refrigeration | TRUs | Marine & Other | Total |
|---|---|---|---|---|---|---|
| 1996 | 286.31 | 41.28 | 6.08 | 15.01 | 15.01 | 363.69 |
| 2005 | 267.72 | 28.89 | 2.82 | 7.81 | 7.81 | 315.05 |
| 2010 | 244.97 | 25.15 | 1.59 | 3.65 | 3.65 | 279.01 |
| 2020 | 182.73 | 27.92 | 2.01 | 2.49 | 2.49 | 227.64 |

Table 1.7 – Summary of Blowing Agent Banks in Landfills ($MMTCO_2eq$)

| Year | Buildings | Appliances | Other Refrigeration | TRUs | Marine & Other | Total |
|---|---|---|---|---|---|---|
| 1996 | 14.7 | 10.21 | 1.80 | 1.91 | 9.07 | 37.7 |
| 2005 | 40.4 | 24.60 | 3.99 | 3.19 | 13.40 | 85.6 |
| 2010 | 58.7 | 29.77 | 4.43 | 3.92 | 16 | 112.8 |
| 2020 | 109.7 | 32.85 | 4 | 3.80 | 13.33 | 163.7 |

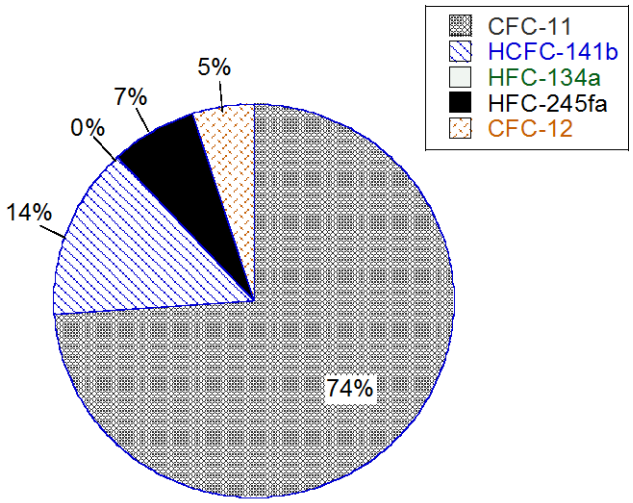


Figure 1.8. Composition of BAs Banked in California Landfills (2020 Projections)

### 1.4.3 Fate of BAs in the Landfill Environment

The fate of BAs in the landfill environment is highly dependent on the conversion processes (chemical and biological) in the landfill and is controlled in particular by anaerobic degradation within the waste mass and at great depth in the soil cover. In addition, oxidation of CFCs, HCFCs, and HFCs in the top portion of soil covers affects the fate of these chemicals. These two biological processes together (i.e., degradation and oxidation) govern the amount of BAs in the landfill environment as well as the amount and rate of emissions from landfills. Other chemical processes including sorption of the chemicals to the waste mass and dissolution in the leachate also contribute to the transport of the BAs within the waste mass and to the emissions of BAs from the landfill environment. The degradation and oxidation of insulation foam BAs disposed of in landfills were evaluated in laboratory investigations using waste microcosm tests and cover soil tests from multiple field sites (Scheutz et al. 2003a-c, 2008, 2009, 2011a). All of the landfill sites investigated were located in European countries.

Correlations were observed between soil cover characteristics (composition, depth, moisture content, TOC/TON) and measured BA oxidation/degradation rates. Oxidation rates of methane/HCFCs were typically higher for final covers compared to intermediate covers. In general, higher oxidation rates for HCFCs corresponded with soils sampled within the top 15-25 cm of final covers at high moisture contents. In the areas of high oxidation, a high TOC/TON level was measured from the production/accumulation of organic carbon/nutrients as a byproduct of cellular aerobic respiration. The presence of a gas extraction system or a geomembrane also affected oxidation/degradation of methane and BAs. Higher oxidation rates were observed for final covers and an active gas extraction system (without a geomembrane) due to the increased diffusion of air into the cover system moving the oxidation zone closer to the surface. The presence of a geomembrane limited the vertical diffusion of air/LFG into the top portions of the soil covers, thereby decreasing oxidation rates. Higher anaerobic degradation rates corresponded with soil sampled from well below 50 cm within the final soil covers, where moisture was available and oxygen was limited. Compost mixtures, in particular mixtures with woodchips, had higher oxidation and degradation efficiencies than sand and gravel cover soils, most likely due to the increased porosity/gas transport provided by the addition of wood chips. Tests also were conducted under aerobic conditions. Results of the tests indicated that the CFCs studied (CFC-11, CFC-12, CFC-113) did not degrade in the presence of oxygen, whereas degradation was observed under anaerobic conditions. The majority of the HCFCs studied (HCFC-21, HCFC-22, HCFC-31, HCFC-32) were oxidized in aerobic experiments and degraded in anaerobic experiments, where oxidation rates were generally higher than anaerobic degradation rates following both zero and first order kinetics. HCFC-141b did not undergo oxidation, with anaerobic degradation following zero order kinetics observed at low rates. Under anaerobic conditions, degradation was fastest for CFC-11 followed by HCFC-141b. HFC-41 was the only HFC that underwent aerobic oxidation and anaerobic degradation, where oxidation rates were generally higher than degradation rates. In general, HFC-134a and HFC-245fa did not undergo neither aerobic oxidation nor anaerobic degradation.

### 1.4.4 Emissions of BAs from Landfills

The release of blowing agents from foam insulation at end of life in landfills was determined to occur over three distinct phases: instantaneous release (on the order of minutes to hours), short-term release (on the order of hours to days), and long-term release (on the order of weeks to years) (Scheutz and Kjeldsen 2003a). Instantaneous release results from permanent damage to the cell from mechanical processes such as shredding, with a sudden large release of BAs. Short-term refers to BA release through small cracks in slightly damaged foam, while long-term release occurs due to slow diffusion across cell walls in essentially intact foam. Short-term and instantaneous releases were observed to be strongly dependent on particle size distribution of the shredded foam. Long-term release was governed by closed cell diffusion (i.e., concentration independent) and was modeled using diffusion coefficients obtained from short-term release experiments (Scheutz and Kjeldsen 2003a). A summary of durations for the three phases as obtained from experimental investigations and modeling studies (for long-term releases) is presented in Table 1.8. Based on the data in this table, instantaneous releases occur within 30 minutes up to 7 hours; short-term releases occur over 7 to 500 hours; and long-term releases start subsequent to 1000 hours and continue for tens to few hundreds of years.

Table 1.8 – Stages of End of Life BA Emissions

| Reference | Kjeldsen and Jensen (2001) | Scheutz et al. (2003a) | Scheutz and Kjeldsen (2003a) | Fredenslund et al. (2005) | Scheutz et al. 2007b | BRE UK (2010) |
|---|---|---|---|---|---|---|
| Instantaneous | - | 10 to 20 minutes | 10 to 30 minutes | - | 2 to 3 hours | Up to 7 hours |
| Short Term | 300 to 500 hours | 250 to 500 hours | 200 to 500 hours | - | - | 7 to 18 hours |
| Long Term | 9 to 300 years | 1,100 hours to 300 years | 1,100 hours to 300 years (Modeled to 50 years) | Modeled to 20 years | Modeled to 20 years | - |

Detailed results from landfill modeling studies with BA releases over the three distinct time periods are provided in Table 1.9. Emissions of BA from the landfill environment were determined to be a function of the initial, short-term, and the long-term releases. Initial (instantaneous) releases were dependent on the compaction process used within a landfill and the format of the foam panel (shredded, cut, full panel) arriving at the landfill. Initial releases were estimated to range between 5 and 15% of the initial BA content for shredded foam particles (Fredenslund et al. 2005). Information on the release of BA during compaction of foam insulation panels generally is not available in the literature. The instantaneous releases from compaction of full panels are expected to be higher than the releases from compaction of shredded foam as significant releases occur during shredding of the foams prior to arrival at a landfill site (Scheutz et al. 2007a). Short-term releases were defined as the releases occurring during the aerobic period as well as during the adjustment period from aerobic to complete anaerobic degradation within the landfill environment. The short-term releases were dependent on the blowing agent, operating conditions, climatic region, and in particular,

presence of anaerobic conditions. Model results indicated significant decreases in BA release when the foam wastes were amended with organic wastes to promote microbial activity and establishment of anaerobic conditions in the waste mass (Fredenslund et al. 2005, Scheutz et al. 2007b). The fractions of BA that were degraded by microbial activity, remained in the landfill, and released over the long term were a function of the BA type and operational conditions. Higher variation in releases was observed for CFCs than HCFCs and HFCs. The releases of HFCs were somewhat higher than the releases of CFCs and HCFCs. In addition, the total release of BA to the atmosphere was dependent on the presence of a gas extraction/combustion system, in which extraction/combustion systems operating at high collection/combustion efficiencies resulted in low BA releases (Scheutz et al. 2003a, 2007b, Fredenslund et al. 2005). It is important to note that none of these studies incorporated the effect of mechanical processes such as waste settlement. Additional releases of BAs may occur due to short- and long-term compression of the wastes associated with overburden stresses from the weight of overlying waste layers. Therefore, the modeling studies may have underestimated the BA released.

A summary BA emissions in the landfill environment based on data from Khalil and Rasmussen (1986, 1987), Kjeldsen and Jensen (2001), Scheutz and Kjeldsen (2003a), Scheutz et al. (2003a), Fredenslund et al. (2005), and Scheutz et al. 2007) is presented in Table 1.10. The values in the table represent studies that used modeling scenarios similar to those expected in a typical landfill operating in the U.S. (i.e., no waste amendment scenarios). Long- term BA release (from shredded foam particles only) studies included slow degradation rates (10% of laboratory determined values) and diffusion coefficients ranging from laboratory-determined values to ten times laboratory values (to cover potential variations in an average landfill) (Scheutz et al. 2003a, Fredenslund et al. 2005, Scheutz et al. 2007b). Limited data were available to predict long-term emissions of BAs from foam waste panels except from data from Khalil and Rasmussen (1986, 1987). These studies did not include emission predictions incorporating typical landfill conditions; therefore, long-term BA releases may be over or underestimated accordingly for foam waste insulation panels in the landfill environment. Similarly, limited data were available for predicting BA release over the nstantaneous and short release periods for both foam waste categories for landfill conditions. Overall, the average BA releases were generally higher for panel foam wastes than shredded foams. Less variation was observed for the shredded foams compared to foam waste panels. In general for the two foam waste types, the expected long-term emissions were higher than both instantaneous and short-term releases (Table 1.10, Figure 1.9).

Table 1.9 – Summary of Predicted BA Emissions from the Landfill Environment at End of Life

| Reference | Modeling Period (years) | Blowing Agent | Initial Release | Short-Term Release | Fraction Microbially Degraded (%)[4] | Fraction Remaining in Landfill (%) | Fraction of Long Term Release with LFG (%) | Fraction of Release with Leachate (%) | Fraction Released to Atmosphere (%)[1] | Fraction Released after Combustion by Gas System (%)[2] | Total Emissions from Landfill at End of Life (%) |
|---|---|---|---|---|---|---|---|---|---|---|---|
| | | | Compaction (%) | Microbial Inactive Period (%) | | | | | | | |
| Scheutz et al. (2003a) | 2 | CFC-11 | N/A | N/A | 0 to 99.7 | 0.3 to 68 | 0.2 to 32 | <0.01 to 0.08 | 0.05 to 8 | 0.01 to 1.4 | 0.06 to 9.4 |
| | 20 | | N/A | N/A | 0 to 99.7 | 0.1 to 8.8 | 0.2 to 91 | <0.01 to 0.24 | 0.05 to 23 | 0.01 to 4 | 0.06 to 27 |
| | 2 | HCFC-141b | N/A | N/A | 0 to 89.7 | 8 to 89 | 2.2 to 11 | 0.03 to 0.12 | 0.6 to 2.8 | 0.1 to 0.5 | 0.7 to 3.3 |
| | 20 | | N/A | N/A | 0 to 97 | 0.6 to 35.3 | 2.4 to 64 | 0.03 to 0.75 | 0.6 to 16.3 | 0.11 to 3 | 0.71 to 18.3 |
| Fredenslund et al. (2005) | 20 | CFC-11 | 15 | 3 to 39 | 7 to 36 | 5 to 21 | 0 to 2 | N/A | 0 to 0.5 | 0 to 0.1 | 0 to 55 |
| | 20 | | 5 | 0 | 40 to 60 | 10 to 29 | 1 to 4 | N/A | 0.25 to 1 | 0.05 to 0.2 | 5.7 to 6.3 |
| Scheutz et al. (2007) | 20 | CFC-11 | N/A | N/A | 94 to 99 | 0.5 to 1 | 0.5 to 5 | N/A | 0.13 to 1.25 | 0.02 to 0.23 | 0.15 to 1.5 |
| | | HCFC-141b | | | 48 to 92 | 2 to 33 | 6 to 29 | N/A | 1.5 to 7.25 | 0.3 to 1.3 | 2 to 9 |
| | | CFC-12 | | | 60 to 92 | 0 to 2 | 6 to 40 | N/A | 1.5 to 10 | 0.3 to 2 | 2 to 12 |
| | | HCFC-22 | | | 43 to 88 | 0 | 12 to 57 | N/A | 3 to 14.3 | 0.5 to 3 | 3.5 to 17.3 |
| ICF (2011)[3] | 1 | HCFC-141b | 19 | N/A | 48 | 23 | 29 | N/A | 3 | 2.35 | 5.35 |
| | | HFC-134a | | | 0 | 0 | 100 | N/A | 100 | 0 | 100 |
| | | HFC-245fa | | | 0 | 0 | 100 | N/A | 10 | 8.1 | 18.1 |

[1] Calculated from long term LFG release assuming a collection efficiency of 75% (SCS 2008)
[2] Calculated from long term LFG release assuming a destruction efficiency of 94% (Cianciarelli and Bourgeau 2002, Greer and Cianciarelli 2005)
[3] Study assumed a collection efficiency of 90%, and destruction efficiency of 91% (ICF 2011)
[4] Fraction microbially degraded includes the oxidation in the cover soil and anaerobic degradation in the waste layers
N/A: Not applicable to study

Table 1.10 – Summary of BA Emissions Predicted in the Landfill Environment

| Waste Type | Instantaneous Release | Short-Term Release | Long-Term Release with LFG |
|---|---|---|---|
| Shredded Insulation Foam Waste | 10 ± 5% | 14 ± 8% | 18 ± 18% |
| Panel Insulation Foam Waste (Non-processed) | 11 ± 11% | 19 ± 10% | 29 ± 29% |

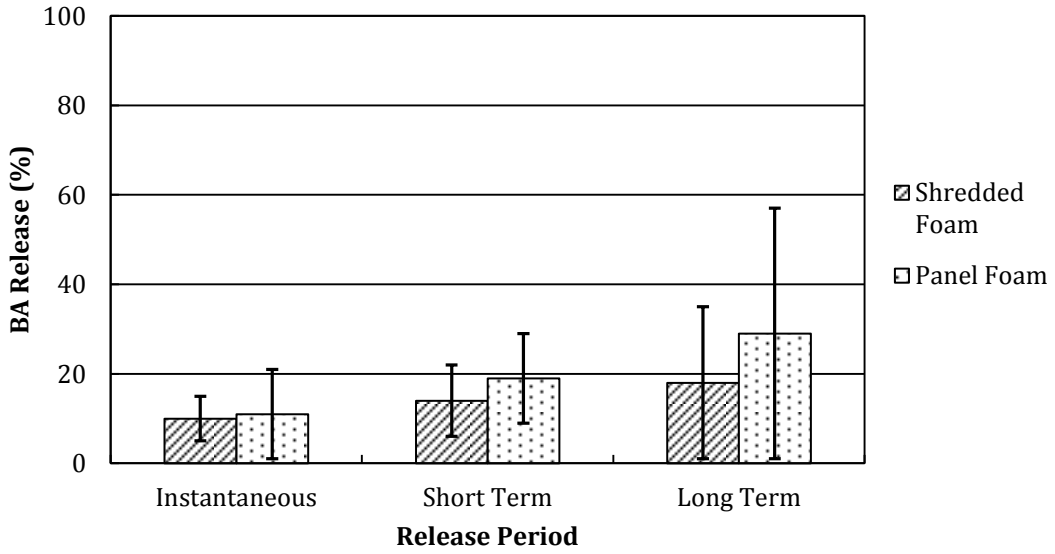


Figure 1.9. Summary of BA Release in the Landfill Environment

The field emissions of LFG are primarily driven by pressure differences (advection) or concentration differences (diffusion) between a landfill and the environment. Other possible processes include dilution (transport process), dissolution of landfill gas constituents in water, sorption to soil or waste particles, and oxidation (sink processes) (Rettenberger and Stegmann 1996). Migration of LFG within a landfill environment can be multidirectional, in the vertical or lateral directions. Gas migration is a complex process and is influenced by meteorological factors (barometric pressure, precipitation, temperature, and wind); waste factors such as the gas production rate, VOC release, presence of internal barriers or gas vents, the lengths of lateral or vertical migration pathways, and the tortuosity of the migration pathways; presence, type, and condition of bottom barriers; presence, type, and condition of cover systems; and subgrade soil and geological factors (cracks/fissures, permeability, diffusivity, porosity, water content, and organic matter content) (Rettenberger and Stegmann 1996).

Emissions of landfill gas typically occur in the vertical direction from the top of a landfill through the various cover systems. Downward and lateral migration and emissions are highly limited due to the presence of liner systems in modern landfills. Landfill gas

generation rates and associated emissions are highly variable due to cover conditions (daily, intermediate, permanent), inherent heterogeneity of wastes, site-specific operational conditions (waste placement density, waste placement sequence, type of daily cover materials), and site-specific climatic conditions (precipitation, temperature, humidity, atmospheric pressure, seasonal waste placement temperature). Landfill gas emissions typically decrease with the order daily, intermediate, and permanent covers; high permeability to low permeability covers; and thin to thick soil covers (Abichou et al. 2006a). Also, landfill gas emissions are highly variable both spatially and temporally within a given landfill as well as between landfills.

A great majority of the earlier field data on emissions of chlorinated and fluorinated hydrocarbons from MSW landfills have been obtained in Europe (Pruggmayer et al. 1982, Brooks and Young 1983, Arendt 1985, Rettenberger 1986, Dent et al. 1986, Schilling and Hinz 1987, Laugwitz et al. 1988, Deipser and Stegmann 1994, Allen et al. 1997). Data on emissions of chlorinated and fluorinated hydrocarbons from landfills in the U.S. are highly limited (Eklund et al. 1998). In particular, systematic investigations of landfill emissions of these gases are not available. These earlier studies conducted in the 1980s and 1990s may not contain highly relevant information due to the changing waste composition and introduction and use of new blowing agents in different foam materials. As an example, results were not provided for HCFC141b, HFC-134a, or HFC-245fa in these studies.

A review of studies from the last two decades that are expected to be more relevant for current waste and BA compositions is summarized in Table 1.11. Bogner et al. (2004) and Scheutz et al. (2003b, 2008) investigated emissions of methane and NMOCs at a landfill in France. Scheutz et al. (2003b), Scheutz and Kjeldsen (2003b), and Bogner et al. (2003) investigated emissions of methane and NMOCs at a second landfill in France. Barlaz et al. (2004) quantified CFC emissions from a landfill in the U.S. Maione et al. (2005) studied the concentrations and emissions of trace gas components from two landfills in Italy. The concentrations of CFC-11, CFC-12, and CFC-113 from MSW landfills in the U.S. and U.K. were evaluated by Hodson et al. (2010). Scheutz et al. (2011b) provided measurements of gas composition and net emissions from a shredder residue cell at a landfill in Denmark. A report by ARCADIS (2012) evaluated gas concentrations and surface emissions of ODS and high GWP trace gases present in LFG from three MSW landfills in the U.S. Emissions data were summarized for these studies and categorized into ranges of annual surface emissions and measured surface fluxes (Table 1.11). Annual emissions of the CFCs, HCFCs, and HFCs varied significantly across the landfill studied. Field investigations indicated that CFC-11 emissions (flux) varied between $-7.92 \times 10^{-5}$ and +0.002 g/m$^2$-day based on the studies conducted in different landfills (i.e., different waste ages, waste amounts, waste compositions, geographical locations, etc.). One of the few studies to analyze surface emissions in the U.S. indicated surface flux of HCFCs ranged between $10^{-5}$ to $10^{-3}$ g/m$^2$-day (Bogner et al. 1997a). Similarly, another study that analyzed CFC emissions in the U.S. reported fluxes ranging from $-8.8 \times 10^{-5}$ to $3.1 \times 10^{-4}$ g/m$^2$-day (Barlaz et al. 2004). These ranges (CFCs/HCFCs) are generally similar to the surface emissions obtained from the investigations in Europe. Measured surface

flux from several landfills ranged from $3.63x10^{-6}$ to $6.66x10^{-5}$ g/m$^2$-day and $-2.50x10^{-7}$ to $2.05x10^{-4}$ g/m$^2$-day, for HCFC-141b and HFC-134a, respectively (Table 1.11). Surface flux data for HFC-245fa was not available in the literature. Overall, the measured surface flux for CFCs, HCFCs, and HFCs generally ranged over one to three orders of magnitude. Variation in surface emissions within a specific landfill site were also reported to be high based on the large range in magnitude presented in individual studies (generally one to two orders of magnitude difference). Methane emissions from MSW landfills, for perspective, were reported to vary over seven orders of magnitude: from 0.0004 to 4,000 g/m$^2$-day (Bogner et al. 1997b). The variation in CFC, HCFC, and HFC emissions at individual landfill sites was attributed to several factors including the measurement location and seasonal variations. In addition, areas with higher methane emissions (especially around hotspots) were reported to demonstrate similar relatively high measured CFC, HCFC, and HFC emissions/concentrations.

The main factors that affected the surface emissions of CFCs, HCFCs, and HFCs were categorized into both operational/design practices at the landfills as well as the meteorological conditions/geographical locations of the landfills. Operational practices that affected surface emissions of CFCs, HCFCs, and HFCs included the operational time period (waste age), composition of waste (i.e., MSW as compared to shredder waste), amount of compaction/compression used (influenced by waste placement/waste density), the waste properties (i.e., moisture content, heterogeneity, etc.), and the amount of waste accumulated. Important design factors that influenced surface emissions of CFCs, HCFCs, and HFCs included the type/presence of a cover (i.e., final or intermediate), as well as the cover composition (i.e., presence of a geomembrane/barrier thickness, etc.), type/presence of a gas collection/combustion system, and type/presence of a bottom liner. Finally, meteorological conditions such as precipitation and barometric pressure (as a function of season and geographical location) influenced the biological/chemical processes within the waste mass and soil cover (including biodegradation/sorption processes of CFCs, HCFCs, and HFCs) as well as the gas transport properties of the soil cover used (i.e., the permeability of the soil or the diffusion gradient between the soil and the atmosphere). High variations in emissions occurred, for instance, between landfills with different final and intermediate covers, waste composition and age, as well as differing geographic locations (Cianciarelli and Bourgeau 2002, Greer and Cianciarelli 2005, Scheutz et al. 2003b, Scheutz and Kjeldsen 2003b, 2008, 2011a, 2011b, Bogner et al. 1997b, 2003, 2004, Maione et al. 2005, USEPA 2008, Hodson et al. 2010, ARCADIS 2012).

Table 1.11 – Summary of Emissions of Trace Components in LFG

| | Gas Component | Bogner et al. (2004), Scheutz et al. (2007a)[1, 2] | Scheutz et al. (2003b,c)[3] | Barlaz et al. (2004) | Maione et al. (2005)[4] | Hodson et al. (2010)[5] | Scheutz et al. (2011a,b)[6] | ARCADIS (2012)[4, 7] |
|---|---|---|---|---|---|---|---|---|
| Surface Flux ($g/m^2$-day) | CFC-11 | $7.94x10^{-8}$ to $3.73x10^{-5}$ | $-7.92x10^{-5}$ to $7.63x10^{-5}$ | $-8.8x10^{-5}$ to $4.2x10^{-5}$ | $6.85x10^{-6}$ to $3.24x10^{-5}$ | - | $2.0x10^{-3}$ | $1.97x10^{-7}$ to $1.20x10^{-6}$ |
| | CFC-12 | $-2.13x10^{-8}$ to $6.02x10^{-7}$ | $-1.68x10^{-5}$ to $2.56x10^{-5}$ | $-1.2x10^{-4}$ to $2.6x10^{-4}$ | $3.72x10^{-5}$ to $1.01x10^{-4}$ | - | - | $9.84x10^{-6}$ to $2.95x10^{-5}$ |
| | CFC-113 | $-9.98x10^{-9}$ to $1.01x10^{-7}$ | - | - | $1.28x10^{-7}$ to $1.66x10^{-5}$ | - | - | $9.84x10^{-8}$ to $1.98x10^{-5}$ |
| | CFC-114 | - | - | $-0.5x10^{-4}$ to $3.1x10^{-4}$ | $5.14x10^{-6}$ to $6.85x10^{-5}$ | - | - | $1.28x10^{-6}$ to $1.78x10^{-4}$ |
| | HCFC-141b | $3.63x10^{-6}$ to $6.66x10^{-5}$ | - | - | - | - | - | - |
| | HCFC-21 | - | - | - | - | - | | - |
| | HCFC-22 | $-6.10x10^{-8}$ to $9.07x10^{-6}$ | $-4.89x10^{-6}$ to $5.74x10^{-5}$ | - | $2.87x10^{-5}$ to $9.37x10^{-5}$ | - | $5.0x10^{-3}$ | - |
| | HCFC-31 | - | - | - | - | - | $6.0x10^{-3}$ | - |
| | HFC-142b | - | - | - | $6.58x10^{-6}$ to $1.46x10^{-4}$ | - | - | - |
| | HFC-134a | $-2.40x10^{-8}$ to $5.49x10^{-6}$ | - | - | $1.71x10^{-6}$ to $2.05x10^{-4}$ | - | - | - |
| | HFC-245fa | - | - | - | - | - | - | - |
| Total Surface Emissions (kg/year) | CFC-11 | $1.83x10^{-4}$ to $8.61x10^{-2}$ | - | - | 0.16 to 0.45 | 30,000 to 40,000 | 5.84 | 0.015 to 0.09 |
| | CFC-12 | $-4.92x10^{-5}$ to $1.40x10^{-3}$ | - | - | 0.87 to1.40 | 90,000 to 110,000 | - | 0.73 to 2.20 |
| | CFC-113 | $-2.30x10^{-5}$ to $2.33x10^{-4}$ | - | - | 0.003 to 0.23 | 6,000 | - | 0.007 to 1.50 |
| | CFC-114 | - | - | - | 0.12 to 0.95 | - | - | 0.09 to 15 |
| | HCFC-141b | $8.40x10^{-3}$ to 0.152 | - | - | - | - | - | - |
| | HCFC-21 | - | - | - | - | - | - | - |
| | HCFC-22 | $-1.41x10^{-4}$ to 0.021 | - | - | 0.67 to1.30 | - | 14.6 | - |
| | HCFC-31 | - | - | - | - | - | 17.5 | - |
| | HFC-142b | - | - | - | 0.16 to 2.03 | - | - | - |
| | HFC-134a | $-5.77x10^{-4}$ to 0.013 | - | - | 0.04 to 2.84 | - | - | - |
| | HFC-245fa | - | - | - | - | - | - | - |

[1]Total surface emissions were calculated by this study using the area of the landfill cell
[2]This study reported ranges from two landfill cells with different gas collection/combustion systems
[3]The range provided encompasses both the final cover and intermediate cover areas
[4]Surface flux was calculated using the given area of the landfill or cell
[5]Data were obtained from 16 landfill sites located in both the U.S. and U.K., no data on surface flux was provided
[6]This study provided a maximum emission at a landfill receiving shredder residue waste only
[6]This study reported ranges of values based on an average of three landfill sites for fall and spring seasons

# PART 2 – MATERIALS FLOW ANALYSIS

## 2.1 Introduction

Foam waste contains residual blowing agents, including CFCs, HCFCs, and HFCs, which are of concern for maintaining air quality because of their high global warming potential (GWP) (TEAP 2005). Variable estimates were provided for emissions of high GWP GHGs from foam in California: on the order of 12 million metric tons (MMT) of $CO_2$-eq per year based on scaling of data and analysis conducted by the USEPA for the entire U.S. for 2005 (Caleb 2011); slightly over 6 $MMTCO_2eq$ annually based on the analysis conducted by Caleb (2011); and on the order of 9 $MMTCO_2eq$ annually based on a study by CARB (2008). The emissions from foam materials alone accounted for 1.3 to 2.6% of the total GHG emissions in California, which were on the order of 459 $MMTCO_2eq$ in 2012 (CARB 2014) using the BA emissions provided above. The foam blowing agents are banked in waste foam as a result of the long lifetimes of buildings (on the order of 50 years) and domestic appliances (on the order of 20 years) coupled with the low diffusivities of blowing agents in building and domestic appliance foam insulation. Total quantities of these banked blowing agents including ozone depleting CFCs and HCFCs and high global warming potential HFCs were estimated to be slowly decreasing well into the future (past 2020), with a 25% decrease expected by 2020 (Caleb 2011). The individual quantities of BAs banked in landfills and emissions from these banks were not identified specifically In California, and have the potential to represent a large percentage of the banks and emissions identified.

This Materials Flow Analysis (MFA) was conducted to delineate the system of waste foam material flows and stocks quantitatively checking mass balance, sensitivities, and uncertainties from the end of life stage to entry to a landfill. Relative proportions of remaining amount of blowing agents in end of life waste foams at the time of entry to the landfill were estimated with regard to initial amount of blowing agents present in new foam materials at the beginning of service life. Emissions between end of life and the time of entry to landfill were quantified in detail using the MFA. Emissions from a typical landfill system from banked BAs in disposed foam were quantified using field measurements as described in detail in the next section (Part 3) of this report.

An MFA is a “systematic assessment of the flows and stocks of materials within a system defined in space and time” (Brunner and Rechberger 2004). The system selected for this study was the State of California, and a yearly mass flow basis was used. The space of this analysis included end of life processes from end of use by the consumer up to, but not including, time in the landfill. Data compiled from Caleb (2011) focusing on California-based foam banks were used to estimate the waste stream flows for different types of foam waste. The MFA was used to estimate both the release of BA and the quantity of BA banked in foam materials entering the landfill.

The analysis was conducted for two different time periods. The first period used was a “modern” disposal period which included foam waste disposed of between 1960 and 2010 (termed Scenario 1), and the second period was a “projected” disposal period that included foam waste disposed of between 1995 and 2050 (termed Scenario 2). CFC production began in the early 1960s and continued until manufacturing/use of

CFC-containing products was phased out in the U.S. at the end of 1995. The modern period (Scenario 1) was initiated at 1960 to capture the time period associated with high use of the early BAs. HCFC production and use began at the onset of the transitional period in 1993 until eventually declining by the year 2005 with the introduction of non-ODS HFCs (TEAP 2005). During the "modern" period (1960-2010), chlorofluorocarbons such as CFC-11 commonly were used as foam BAs, and consequently, foam waste banks were characterized with high CFC-11 quantities. During the projected period (1995-2050), fluorocarbon substitutes, including HFC-134a and HFC-245fa became more common, resulting in larger amounts in banked BAs than historical CFCs. The projected period (Scenario 2) was initiated in 1995 to include the transitional hydrofluorocarbon replacements (e.g., HCFC-141b) as a basis for comparison of the banked quantities to the modern time period (Scenario 1). The quantities of foam waste stocks in California were mainly obtained from Caleb (2011). Annual waste foam flows were calculated for a total of five major foam categories:

- Construction and demolition wastes
- Waste domestic appliances (including refrigerators/freezers)
- Commercial appliances (including water heaters, vending machines, and commercial refrigerators/freezers)
- Transport refrigerated units (TRUs)
- Marine and other foam products (including non-structural cold stores)

Defining the foam waste disposal and management practices and pathways for California was essential for conducting the MFA. The pathways included a combination of decommissioning, transport, storage, and processing (e.g., shredding) practices that were investigated separately for different types of waste foams. For example, a larger percentage of waste appliances at end of life may be shredded as compared to construction and demolition wastes (Caleb 2011). Other differences based on type of waste foam materials could be due to use of stockpiling for different applications for varying periods of time. Also, some waste foam is subject to reuse or permanent recovery and destruction.

Subsequent to identification of the foam waste management pathways, the emissions of each type of BA were estimated for each stage of the end of life management before entry into a landfill. Currently, published data and analysis are not available in the literature pertaining to the quantification of total loss of BA in waste foam materials from the point of end of life until entry into a landfill. To quantify pre-landfill-entry waste foam characteristics, references from the literature were used to estimate quantities of each foam waste stream, and the information obtained was used together with available data on rates of release of BAs during the various pre-landfilling processes. Data on time dependent foam BA release studies conducted by Scheutz and Kjeldsen (2003a), Scheutz et al. (2003a), Fredenslund et al. (2005), and Scheutz et al. (2007a), as well as by the Building Research Establishment (BRE) in the United Kingdom (2002) were used in the MFA analysis presented herein. An annual flow of BA from foam waste disposed of in California was estimated for each type of foam waste and total BA emissions were characterized from the end of life management process reviewed. In summary, the scope of the MFA consisted of 1) delineation of foam waste

stock and determination of annual volumetric/mass flow of foam waste material reaching end of life management per insulation foam application, 2) identification of foam waste end of life management pathways for each foam insulation application, and 3) evaluation of BA emissions during each step of the foam waste management pathway identified for each foam insulation application prior to landfill disposal.

### 2.2 Estimation of BA Release

The BA emissions during each step of the foam waste management pathways were estimated using release of the BAs from the foam products. Prior data and analyses are highly limited for release of blowing agents during storage, transport, and processing/recycling facility stages of the end of life management of waste foams. More data and analyses are available for the shredding stage compared to the other stages due to the high potential of BA releases during the shredding process. In general, shredding processes were used to varying degrees for all of the five foam applications included in this MFA.

The release of CFCs from foam insulation was subdivided into three stages as a function of time: initial instantaneous release (on the order of minutes), short-term release (on the order of hours to days), and long-term release (on the order of weeks to months to years) (Scheutz and Kjeldsen 2003a). Instantaneous and short-term releases were determined to be strongly dependent on particle size distribution of the foam. Long-term release was governed by closed cell diffusion and could be modeled using results from short-term release periods with diffusion coefficients obtained from the literature (Scheutz and Kjeldsen 2003a). For this study, it was assumed that instantaneous releases occurred for 30 minutes, followed by short-term releases of up to 5 days, and long term releases from 5 days onward based on data provided in literature (Scheutz and Kjeldsen 2003a, Scheutz et al. 2003a, Fredenslund et al. 2005). In addition to time, BA releases also were a factor of the type of foam material.

#### 2.2.1 Instantaneous BA Release

In general, the instantaneous release process was associated with the shredding of the waste foam. The instantaneous release of BA from shredding of foam was estimated based on the results of the study by Scheutz et al. (2007a). Loss of BA during the shredding process was determined to be governed by the particle size distribution of the shredded material (higher losses with smaller foam fractions). Post-shredding particle size distribution analysis of PUR appliance insulation panels indicated that the bulk of the foam (>81%) consisted of large particles retained on 32 mm and 16 mm screens (Scheutz et al. 2007a). Foam shredded to 32 mm had losses between 1.1 and 26.9% of BA compared to BA losses ranging from 57 to 61.3% for particles in the smallest size fraction (less than 8 mm). Overall, the larger particles had more influence on the weighted average BA release among the size fractions determined for the different shredding facilities used in the study. An average of 24.2±7.5% of the initial BA content was released as a result of the shredding process, determined using data obtained from three different facilities and for four different size fractions (Scheutz et al. 2007a). Large differences in BA release occurred due to the type of machinery and operation of the shredder facilities. Also, operational mode had

a significant effect on the release of BA (16.6 % release for wet mode compared to 34 % release for dry mode). For the present analysis, an average BA release of 24% was used as an estimate across all waste categories during the shredding process. Equal particle size distributions were assumed for all categories of foam applications after shredding.

### 2.2.2 Short-Term and Long-Term BA Release

The short-term and long-term BA releases were estimated using methodology similar to the approaches presented in Kjeldsen and Jensen (2001), Scheutz and Kjeldsen (2003a), and Scheutz et al. (2003a). The long-term diffusion of BA from the closed cell volume of foam (expressed as the change in concentration of the blowing agent over time) was assumed to follow Fick's law:

$$\frac{\partial C}{\partial t} = D_{eff} * \nabla C \tag{2.1}$$

where, $D_{eff}$ is the effective diffusion coefficient ($m^2/s$), and $\nabla C$ is the concentration gradient (mg/L). To solve this equation, Henry's law was used to describe the relationship of the concentration of the BA dissolved in the solid polymer fraction of the foam to the concentration in the void phase of the closed cell:

$$C_p = K * C_g \tag{2.2}$$

where $C_p$ is the concentration of BA sorbed in the polymer material (mol / $m^3$ polymer material), $C_g$ is the concentration of BA in the void (mol / $m^3$ gas), and $K$ is the distribution factor ($m^3$ gas / $m^3$ polymer material).

Multiple solutions to Fick's law (2.1) combined with Henry's law (2.2) were presented by Crank (1975) and Grathwohl (1998) and were adapted for various foam geometries including a sphere, cylinder, and slab. Solutions were categorized into two different groups for analysis of waste foam: *i*) the volume that the BA is released into is infinite (infinite bath scenario) or *ii)* the volume that the BA is released into is closed (bath of limited volume). The infinite bath scenario commonly was adopted in analysis of waste foam, where the BA was released into a very large volume with negligible change in BA concentration. The infinite bath solution was used to predict the release of BA into the atmosphere or the pores of soil cover in a landfill environment. The solution for sphere geometry is presented below for the infinite bath scenario:

$$\frac{M_t}{M_o} = 1 - \frac{6}{\pi^2} \sum_{n=0}^{\infty} \frac{1}{(n)^2} \exp\{-D(n)^2 \pi^2 t / a^2\} \tag{2.3}$$

where, $M_t$ is the BA content released from the foam, $M_o$ is the total BA content in the foam, $D$ is the diffusion coefficient ($m^2/s$), $t$ is time (s), and $a$ is the radius of the sphere (m).

The emission of BA from larger foam insulation panels (as opposed to small, shredded, spherical particles) also was estimated using Equation (2.3). For the large foam panels, a progressive volume conversion analysis was conducted to represent the volume of the panel in terms of an equivalent sphere and an equivalent radius (*a*) was calculated (Scheutz and Kjeldsen 2003a):

$$a = (\frac{3}{4} WT(\frac{H}{\rho} - T))^{1/3} \quad (2.4)$$

where, *W*, *T*, and *H* are the width, thickness, and height of the foam panel, all in units of (m). A compilation of common widths, thicknesses, and heights for various types of rigid insulation panel used for different applications is presented in Table 2.1. These data were obtained from an extensive search of data and specifications for rigid foam currently available in the U.S. market. The higher values were used, if a range of dimensions was provided by manufacturers for a conservative analysis. Data are presented in imperial units (as provided by the manufacturers) in Table 2.1 for information purposes. For marine, buoy, and cooler foam BA release predictions, data were provided by Caleb (2011) for foam mass (4 kg/unit for leisure boats, 0.45-180 kg/unit for buoys, and 2 kg/unit for coolers). These data were converted to volume per unit using a foam density of 30 kg/m$^3$ and the *a* value was back calculated assuming the unit was in the shape of a sphere or cylinder.

Table 2.1 – Common Panel Dimensions for Rigid Insulation Foam

| Insulation Type | Width (ft) | Thickness (in.) | Height (ft) |
|---|---|---|---|
| C&D Insulation Panels | 4 | 1 | 8 |
| Domestic Appliance Insulation Panels | 2 | 2.25 | 4.5 |
| Commercial Appliance Insulation Panels | 6 | 2.25 | 8 |
| Vending Machine Insulation Panels | 3 | 1.75 | 6 |
| Water Heater Insulation Panels | 2 | 1.5 | 5.5 |
| TRU/Reefer Insulation Panels | 8 | 5 | 31 |
| Walk In-Cold Store Insulation Panels | 8 | 4 | 15 |

Scheutz and Kjeldsen (2003a) used the double compartment model to estimate both short- and long-term diffusion coefficients in laboratory experiments. The double compartment model, as presented in Equation (2.5), described the BA content in foams during both the short term (effect of broken/damaged cells) and the long term (effect of long term diffusion of intact cells).

$$M_o = M_{o,1} + M_{o,2} \quad (2.5)$$

where $M_o$ is the total BA content, $M_{o,1}$ is the BA content in the broken/damaged cells, and $M_{o,2}$ is the BA content in the intact fraction of foam material. Graphing the mass (or flux) released over time ($M_t$) versus the square root of time ($t^{1/2}$) resulted in a bilinear relationship. The slopes of the individual segments were used to obtain diffusion coefficients $D_1$ and $D_2$ associated with short-term (from broken/damaged cells) and long-term (from intact cells) emissions, respectively. Scheutz and Kjeldsen (2003a) indicated that the diffusion coefficients that described the short-term release typically were higher (approximately two orders of magnitude) than the diffusion coefficients for long-term release.

In the current analysis, Equations (2.3) to (2.5) were used to predict the short and long-term BA releases by employing the calculated diffusion coefficients from literature, the time frame of interest, and the dimensions of the panel or shredded foam particle. To predict the BA releases, Equation (2.3) was iterated at least 60 times (n=60) (example calculation provided in Appendix 2). The short-term and long-term diffusion coefficients used for modeling BA releases in this MFA are presented in Table 2.2. The short-term release coefficients ($D_1$) varied more than long-term diffusion coefficients ($D_2$). High diffusion coefficients resulted in quick release of BA and high amounts of BA accumulating over the time frames modeled. BA releases were estimated for stockpiling/storage and transportation stages prior to entry into the landfill. Transportation processes were generally assumed to be short term (less than 5 days), while stockpiling/storage processes were a combination of short-term and long-term time frames (on the order of one month). Thus, modeling transportation processes required short-term release coefficients and modeling stockpiling processes required the use of both short and long-term diffusion coefficients. In modeling panel foam wastes (not shredded, for short-term release periods (i.e., transportation only), the foam panels were assumed to be damaged during removal/decommissioning of the insulation materials. The long-term release was assumed to be diffusion dependent (from closed cells) and did not include BA release from open cells in the foam structure caused by damage to the foam itself.

Table 2.2 – Short- and Long-Term Diffusion Coefficients for Foam Panel (Scheutz and Kjeldsen 2003a)

| BA Type | Short Term Release Coefficient (5 days or less) $D_1$ ($m^2/s$) | Long Term Diffusion Coefficient (Weeks to Months) $D_2$ ($m^2/s$) |
|---|---|---|
| CFC-11 | $4.1 \times 10^{-12}$ | $2.1 \times 10^{-14}$ |
| HCFC-141b | $1.5 \times 10^{-12}$ | $2.9 \times 10^{-14}$ |
| HFC-134a | $6 \times 10^{-12}$ | $2.1 \times 10^{-14}$ |
| HFC-245fa | $7.5 \times 10^{-12}$ | $1.9 \times 10^{-14}$ |

For modeling BA release from shredded foam particles, a constant particle size distribution was used across all foam categories (Table 2.3). The particle size distribution was derived from Scheutz et al. (2007a), and represented the average size distribution of post shredding waste foam particles at three U.S. shredder facilities. The radii (i.e., *a* values*)* were calculated for each particle size assuming that the particles were spherical and were used in Equation (2.3) to predict four levels of release as a function of particle size. These individual predicted BA releases were then summed to calculate total predicted release from the entire shredded foam mass. Similar to the analysis for panel materials, depending on whether the time frame assumed was short (on the order of days) or long (on the order of weeks to months), short- or long-term diffusion coefficients (or a combination of the two) were used to model the BA release from shredded foam particles during stockpiling or a combination of stockpiling/transportation processes post shredding.

Table 2.3 – Particle Size Distribution Used for Modeling Release of BA from Shredded Foam Waste

| Particle Size Range (mm) | Amount of Particles in Size Range (%) | Calculated *a* value (m) |
|---|---|---|
| <4 | 2.70 | 0.0144 |
| 4-12 | 9.70 | 0.0311 |
| 12-24 | 49 | 0.0476 |
| 24-48 | 38.6 | 0.0756 |

## 2.3 Construction and Demolition Foam Insulation Waste

### 2.3.1 Foam Waste Stock and Flows for Construction and Demolition Foam Insulation Waste

California's building stock (number of buildings), foam stock in the buildings, and foam waste flow from construction/demolition practices were estimated in Caleb (2011). In 2008, California's building stock was mostly single-family residential homes (56%), where over 16 million buildings existed with an estimated 30-year building life for both low-rise residential buildings as well as non-residential buildings. The use of insulation foams in building applications in California started in the early 1960s and expanded throughout the 1970s to 1980s (Caleb 2011). For the first time period examined (Scenario 1), the year 1960 was used as the first year of analysis. The types of foams used for building insulation mainly included polyisocyanurate (PIR) panels, extruded polystyrene (XPS) board stock, polyurethane (PUR) panels, and polyurethane (PUR) spray foam. Expanded polystyrene (EPS) boardstock also was used in building insulation applications, however, EPS was not covered in the scope of this report, as the foam blowing agent in EPS was reported to be emitted during the foam manufacturing process (TEAP 2005). The average foam use in buildings in California from 1960 to 2009 is summarized by type in Figure 2.1 (Caleb 2011). Foam volume from demolition of buildings presented in Caleb (2011) was used as the building foam waste stock in California (Table 2.4).

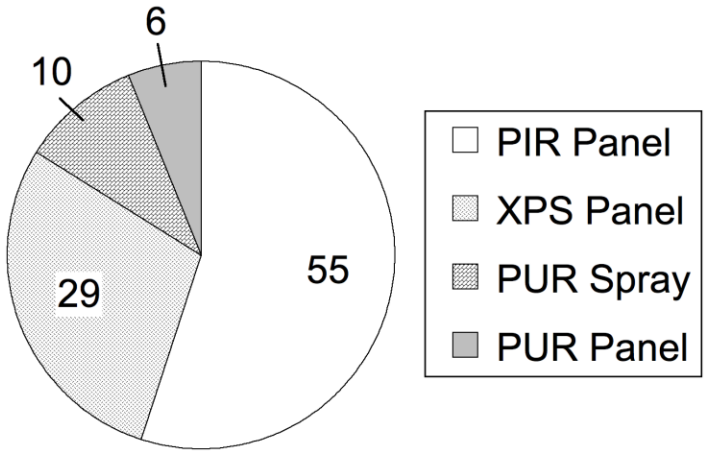


Figure 2.1 Average Building Insulation Foam Consumption in California by Material Fraction (Percentages) (1960-2009) (Caleb 2011)

Table 2.4 –Foam Volume in C&D Wastes (Caleb 2011)

| Building Use | Demolition Foam ($m^3$/yr) |
|---|---|
| Single Family Homes | 162,726 |
| Multi Family Homes | 161,976 |
| Commercial Buildings | 120,298 |
| Total | 445,000 |

To develop a detailed materials flow of C&D foam waste BAs in California, the type of BA used in each building application was considered. Historical BA substitution was reviewed for C&D foam to develop an accurate representation of the annual input of foam materials in the California waste stream. The percentage of BA type used for PIR, XPS, PUR panels, and PUR spray foam, as reported by Caleb (2011), are presented in Tables 2.5, 2.6, 2.7, and 2.8, respectively. These data represented the initial amount of BAs present in as-manufactured insulation panels made of different types of foams. Several BA substitutions were made over the years to reduce production of ODS, resulting in the different ratios of BAs included in these tables. For PIR and PUR foams, CFC-11 was assumed to be the only blowing agent in use from 1960 to 1992. For XPS foams, CFC-12 was used instead of CFC-11 during this same time period. Use of CFC-11 and CFC-12 were both phased out completely by 1996 in response to the Montreal Protocol. These CFCs were replaced by HCFCs, which were in turn replaced by HFCs in the early 2000s (Tables 2.5 to 2.8). Starting in early 2000s, building insulation manufacturers switched to a pentane formula for the replacement of high GWP BAs used for sandwich panels and board stock with reduced use or no use of the HCFCs and HFCs (Tables 2.5 to 2.7). For PUR spray, HFCs continue to be the main BA (Table 2.8).

Table 2.5 – Blowing Agents Used in PIR Building Foams (Caleb 2011)

| Year | CFC-11 | HCFC-141b | HFC-245fa | HC |
|---|---|---|---|---|
| 1992 | 100% | 0% | 0% | 0% |
| 1993 | 75% | 25% | 0% | 0% |
| 1994 | 50% | 50% | 0% | 0% |
| 1995 | 25% | 75% | 0% | 0% |
| 1996 | 0% | 100% | 0% | 0% |
| 1997 | 0% | 100% | 0% | 0% |
| 1998 | 0% | 100% | 0% | 0% |
| 1999 | 0% | 100% | 0% | 0% |
| 2000 | 0% | 95% | 5% | 0% |
| 2001 | 0% | 80% | 20% | 10% |
| 2002 | 0% | 70% | 10% | 10% |
| 2003 | 0% | 30% | 5% | 60% |
| 2004 | 0% | 15% | 5% | 80% |
| 2005 | 0% | 0% | 5% | 95% |
| 2006 | 0% | 0% | 5% | 95% |
| 2007 | 0% | 0% | 5% | 95% |
| 2008 | 0% | 0% | 5% | 95% |
| 2009 | 0% | 0% | 5% | 95% |
| 2010 | 0% | 0% | 5% | 95% |

Table 2.6 – Blowing Agents Used in XPS Building Foams (Caleb 2011)

| Year | CFC-12 | HCFC-142b | HFC-22 | HFC-134a |
|---|---|---|---|---|
| 1992 | 100% | 0% | 0% | 0% |
| 1993 | 75% | 16% | 9% | 0% |
| 1994 | 50% | 33% | 26% | 0% |
| 1995 | 25% | 49% | 35% | 0% |
| 1996 | 0% | 65% | 35% | 0% |
| 1997 | 0% | 65% | 35% | 0% |
| 1998 | 0% | 65% | 35% | 0% |
| 1999 | 0% | 65% | 35% | 0% |
| 2000 | 0% | 65% | 35% | 0% |
| 2001 | 0% | 65% | 35% | 0% |
| 2002 | 0% | 65% | 35% | 0% |
| 2003 | 0% | 65% | 35% | 0% |
| 2004 | 0% | 65% | 35% | 0% |
| 2005 | 0% | 65% | 35% | 0% |
| 2006 | 0% | 65% | 35% | 0% |
| 2007 | 0% | 65% | 35% | 0% |
| 2008 | 0% | 49% | 26% | 25% |
| 2009 | 0% | 16% | 9% | 75% |
| 2010 | 0% | 0% | 5% | 100% |

Table 2.7 – Blowing Agents Used in PUR Panel Building Foams (Caleb 2011)

| Year | CFC-11 | HCFC-141b | HFC-245fa | HC |
|---|---|---|---|---|
| 1992 | 100% | 0% | 0% | 0% |
| 1993 | 75% | 25% | 0% | 0% |
| 1994 | 50% | 50% | 0% | 0% |
| 1995 | 25% | 75% | 0% | 0% |
| 1996 | 0% | 100% | 0% | 0% |
| 1997 | 0% | 100% | 0% | 0% |
| 1998 | 0% | 100% | 0% | 0% |
| 1999 | 0% | 100% | 0% | 0% |
| 2000 | 0% | 95% | 5% | 0% |
| 2001 | 0% | 80% | 15% | 5% |
| 2002 | 0% | 70% | 20% | 10% |
| 2003 | 0% | 30% | 40% | 30% |
| 2004 | 0% | 15% | 45% | 40% |
| 2005 | 0% | 0% | 50% | 50% |
| 2006 | 0% | 0% | 50% | 50% |
| 2007 | 0% | 0% | 50% | 50% |
| 2008 | 0% | 0% | 50% | 50% |
| 2009 | 0% | 0% | 50% | 50% |
| 2010 | 0% | 0% | 50% | 50% |

Table 2.8 – Blowing Agents Used in PUR Spray Building Foams (Caleb 2011)

| Year | CFC-11 | HCFC-141b | HFC-245fa | HC |
|---|---|---|---|---|
| 1992 | 100% | 0% | 0% | 0% |
| 1993 | 75% | 25% | 0% | 0% |
| 1994 | 50% | 50% | 0% | 0% |
| 1995 | 25% | 75% | 0% | 0% |
| 1996 | 0% | 100% | 0% | 0% |
| 1997 | 0% | 100% | 0% | 0% |
| 1998 | 0% | 100% | 0% | 0% |
| 1999 | 0% | 100% | 0% | 0% |
| 2000 | 0% | 95% | 5% | 0% |
| 2001 | 0% | 80% | 20% | 0% |
| 2002 | 0% | 70% | 30% | 0% |
| 2003 | 0% | 30% | 70% | 0% |
| 2004 | 0% | 15% | 85% | 0% |
| 2005 | 0% | 0% | 100% | 0% |
| 2006 | 0% | 0% | 100% | 0% |
| 2007 | 0% | 0% | 100% | 0% |
| 2008 | 0% | 0% | 100% | 0% |
| 2009 | 0% | 0% | 100% | 0% |
| 2010 | 0% | 0% | 100% | 0% |

The volumetric flow rate of each foam type (i.e., PIR, XPS, PUR Panel and PUR Spray) was determined using the percentages in Figure 2.1 for building foam material type and the estimated total foam disposal rate of 445,000 $m^3$/year (Table 2.4). The analysis resulted in volumetric annual flow of foam material by type in C&D waste as presented in Table 2.9.

Table 2.9 – Volumetric Flow of Foam Material Type in C&D Waste

| Foam Material Type | Flow of Foam Material ($m^3$/yr) |
|---|---|
| PIR | 244,750 |
| XPS | 129,050 |
| PUR Panel | 26,700 |
| PUR Spray | 44,500 |

Next, the flow per year of each foam material was classified according to blowing agent type to determine a yearly mass flow of foam containing the different BAs. While most of the analysis in this report was focused on the four target BAs, other gases (such as the CFC-12 in this section) also were included the analysis when significant quantities of these additional gases were used in the foam materials bring investigated. It was assumed that all disposed foam waste had an equal probability of being generated from materials constructed in any given year. Thus, Tables 2.5 to 2.8 were used to determine the weighted fraction of each blowing agent used over the time period 1960 to 2010 (Scenario 1) and from 1995 to 2050 (Scenario 2). The weighted percentages included in Table 2.10a represent the fractions of each BA in each foam type averaged over the range of years associated with each scenario (example calculation provided in Appendix 2). The weighted fractions of CFC-11/CFC-12 in the foam waste were higher (67%) for all building foam in Scenario 1 compared to the projections in Scenario 2. The second highest BA banked in the foam for Scenario 1 was HCFC-141b, followed by HFC-245fa, and hydrocarbons (e.g., pentane). HFC-134a was only used in XPS foam for a short duration (Table 2.6), contributing to a small percentage (4%) for the XPS products. In Scenario 2, the main BAs were the HFCs (Table 2.10a). Estimates for the volumetric flow of the different BAs in each type of foam material are presented in Table 2.10b. For Scenario 2, it was assumed that the percent BA use in the projected time period from 2011 to 2050 was equivalent to that in 2010. Thus, the total volumetric flow of CFC-11, CFC-12, and HCFC-141b containing C&D insulation foam wastes was smaller for Scenario 2 as compared to Scenario 1 (Table 2.10b). In addition, due to the expected high consumption of alternative blowing agents in the future, larger volumetric flows of HFC-134a and HFC-245fa foams were determined for Scenario 2 compared to Scenario 1 (Table 2.10b).

Table 2.10a – Calculated BA Content in C&D Waste per Foam Material Type

| Foam Material | CFC-11 (%) | | CFC-12 (%) | | HCFC-141b (%) | | HFC-134a (%) | | HFC-245fa (%) | |
|---|---|---|---|---|---|---|---|---|---|---|
| Scenario Number | Sc.1 | Sc. 2 | Sc. 1 | Sc. 2 | Sc. 1 | Sc. 2 | Sc. 1 | Sc. 2 | Sc. 1 | Sc. 2 |
| PIR[1] | 67 | 0.5 | 0 | 0 | 17 | 14 | 0 | 0 | 2 | 5.2 |
| XPS[2] | 0 | 0 | 67 | 0 | 0 | 0 | 4 | 76 | 0 | 0 |
| PUR Panel[1] | 67 | 0.5 | 0 | 0 | 17 | 14 | 0 | 0 | 8.5 | 43 |
| PUR Spray | 67 | 0.5 | 0 | 0 | 16.8 | 14 | 0 | 0 | 16.2 | 86 |

[1]Remaining BA content consists of hydrocarbons
[2]1Remaining BA content consists of HCFC-142b and HFC-22

Table 2.10b – Annual Volumetric Flow of C&D Waste Foam Material

| Foam Material | CFC-11 ($m^3$/year) | | CFC-12 ($m^3$/year) | | HCFC-141b ($m^3$/year) | | HFC-134a ($m^3$/year) | | HFC-245fa ($m^3$/year) | |
|---|---|---|---|---|---|---|---|---|---|---|
| Scenario Number | Sc.1 | Sc. 2 | Sc. 1 | Sc. 2 | Sc.1 | Sc. 2 | Sc. 1 | Sc. 2 | Sc. 1 | Sc. 2 |
| PIR | 163,983 | 1,133 | 0 | 0 | 41,118 | 34,043 | 0 | 0 | 4,406 | 12,683 |
| XPS | 0 | 0 | 86,464 | 587 | 0 | 0 | 5,162 | 96,201 | 0 | 0 |
| PUR Panel | 17,889 | 121 | 0 | 0 | 4,486 | 3,714 | 0 | 0 | 2,270 | 11,530 |
| PUR Spray | 29,815 | 202 | 0 | 0 | 7,476 | 6,190 | 0 | 0 | 7,209 | 38,108 |
| Total Flow | 211,687 | 1,456 | 86,464 | 587 | 53,080 | 43,947 | 5,162 | 96,201 | 13,885 | 62,321 |

The results presented in Tables 2.10a and 2.10b (plus hydrocarbons, HCFC-142b, and HCFC-22 calculated separately), are presented graphically for Scenarios 1 and 2 in Figure 2.2. For the calculations, an equal probability of being demolished subsequent to a 30-year time period was assumed for all building types. In Scenario 1, CFC-11 and CFC-12 made up significant portions of the BAs in the end of life building foam stock (68%). HCFC-141b and 142b also made up a high portion (18%) of the BA banked in C&D foam waste under Scenario 1, while the HFCs were minimal in this time period. In Scenario 2, a larger amount of hydrocarbons (47%), HFC-245fa (14%), and HFC-134a (22%) were predicted to be present in the C&D foam insulation wastes.

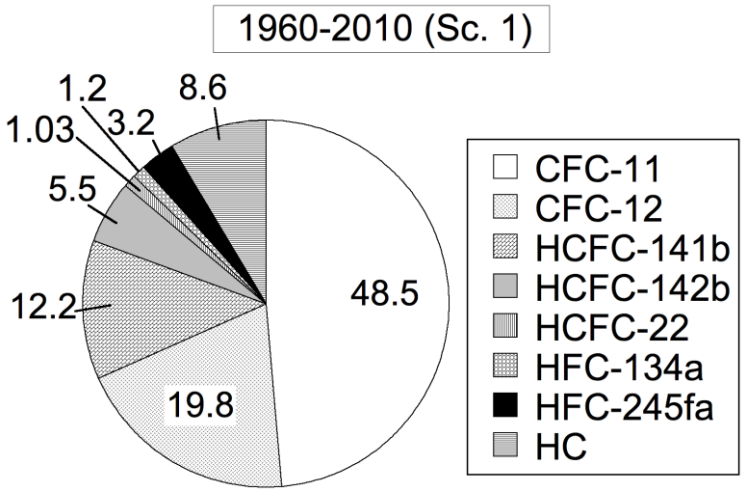


(a) Scenario 1

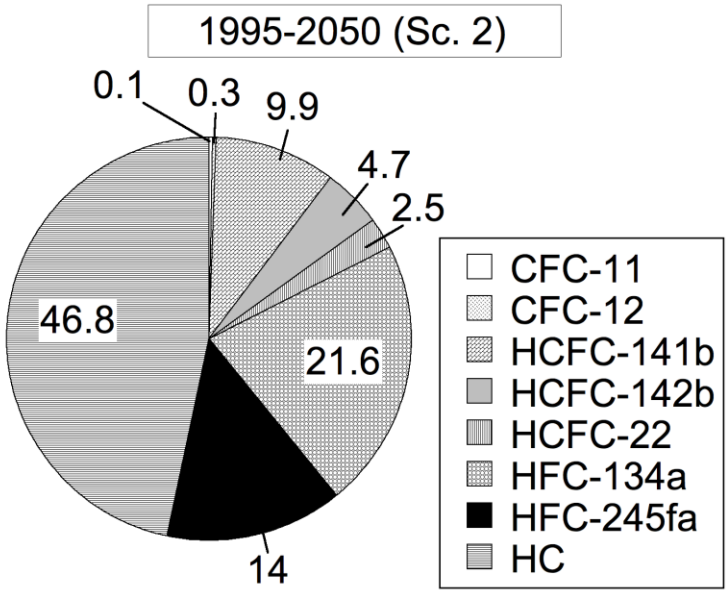


(b) Scenario 2

Figure 2.2. Estimated Volumetric Flows of C&D Waste Foam Containing Different BAs

The volumetric flows were then converted to mass flows and used throughout the calculations for establishing flows associated with the foam waste disposal pathways prior to landfilling. Mass-based analysis also allowed for estimating flow of blowing agents on a $MTCO_2eq$ basis. Initially, the volumetric flows presented in Table 9b were converted to mass flows using densities of the foams. The reported (Scheutz and Kjeldsen 2003a) densities of 24.6, 32.2, 39, and 30.7 g/L were used for foams containing CFC-11, HCFC-141b, HFC-134a, and HFC-245fa, respectively. These calculated BA masses represented the mass of BA in new building insulation foam and not end of life C&D wastes. To convert the initial amount of BAs in the foam panels to BAs remaining in the foams at end of life, data reported in literature for BAs remaining in foams at end of life were used. For PIR and PUR foams, end of life BA contents (%w/w) of 13.3, 11.6, 7, and 11.6% were reported for CFC-11, HCFC-141b, HFC-134a and HFC-245fa, respectively (Scheutz and Kjeldsen 2003a). These values were adopted for the MFA in this study. For XPS foams, measured end of life BA contents were not directly available. Use of BA content (w/w) on the order of 8% of HFC-134a during manufacture was reported for XPS foams (RAPRA 2001). BA release during initial use ($1^{st}$ year release) was estimated at 25% followed by a 0.75% release (per year) for building insulation foams (TEAP 2005). These release rates were adopted for the XPS in this study, and a remaining BA content of 5% was calculated at end of a 30-year lifetime for the XPS building foam.

The total average annual mass flows of the four target BAs are provided in Table 2.11 for Scenarios 1 and 2. The total amount of the blowing agents generated from C&D foam insulation waste was reduced by approximately 40% from the Scenario 1 time frame of analysis to the Scenario 2 timeline. Approximately 950 tonnes/year of BA were generated in Scenario 1, whereas the amount of BA generated was 579 tonnes/year in Scenario 2. CFC-11 comprised a significant quantity of the total blowing agent bank headed to end of life management for Scenario 1 (73%). Under Scenario 2, the mass flow was significantly lower for CFC-11 as compared to Scenario 1 (Table 2.11). Similar trends to volumetric flows (Table 2.10b) were observed for the mass flow of the other BAs (Table 2.11). The data in Table 2.11 were used as the input values for the materials flow diagrams developed below.

Table 2.11 – Annual Mass Flow of C&D Waste Foam Material

| Blowing Agent | CFC-11 | | HCFC-141b | | HFC-134a | | HFC-245fa | |
|---|---|---|---|---|---|---|---|---|
| Scenario Number | Sc. 1 | Sc.2 | Sc. 1 | Sc. 2 | Sc. 1 | Sc. 2 | Sc. 1 | Sc. 2 |
| Mass Flow of BA (tonnes/year) | 693 | 5 | 198 | 164 | 10 | 188 | 49 | 222 |

### 2.3.2 Disposal Pathways for Construction and Demolition Foam Insulation Waste

The pathway of C&D foam waste materials between end of life and landfilling varies among the categories of foam waste. During building demolition processes, foam waste materials were reported to be typically stripped and stored on site, in a process termed decommissioning (Caleb 2011). The foam material at this point was potentially

in a damaged state that could affect the outgassing of blowing agents during storage. The period assumed for this process was set at one month before transportation of the foam away from the C&D site based on the project team's insight on construction time periods. Subsequent to storage onsite, the transportation process was assumed to take one week and included processing at a materials recycling facility (MRF) to separate and/or recover materials. According to Caleb (2011) "the vast majority of foam waste material (92%) is sent directly to the landfill, while 8% is sent to a shredding facility first". Of the 92% foam waste sent directly to the landfill, 9% was reported to be stockpiled for use as an alternate daily cover in California (CalRecycle 2011a, Cascadia 2008). For the shredded foam material, stockpiling/transportation to the landfill was assumed to take one week after shredding similar to time periods reported by Wethje (2004). Higher BA releases occur from the shredded material prior to entry to the landfill than large panels (Scheutz et al. 2007a).

### 2.3.3 BA Release Estimates Prior to Landfilling for Construction and Demolition Foam Insulation Waste

For this study, BA releases were considered over four pathways prior to landfilling: 1) Decommissioning (including storage at demolition site), 2) Transportation, 3) Shredding, and 4) Stockpiling at the shredding facility or landfill. During demolition, CFCs are known to be released instantaneously if the material is crushed on-site. Multiple studies have indicated that the fraction of CFCs released from insulation materials during demolition, considered instantaneous releases, depends on the final particle size of the insulation foam (Kjeldsen 2010). At the current time, typical building demolition practices do not include standard approaches used to prevent the release of foam blowing agents. Current demolition technologies, such as the use of backhoe cranes and other heavy equipment, were considered not conducive for retaining BAs in the foam or for separating foam for recycling the foam. The release of BAs during decommissioning of buildings was reported to be dependent on the type of demolition practice (i.e., crane vs. manual) (Kjeldsen 2010). In particular, manual removal of the insulation foam prior to crane demolition was recognized to significantly reduce BA emissions by leaving the foam panels intact. In addition, these removed panels could be recycled or reused further reducing BA emissions directly or indirectly (Kjeldsen 2010). For the analysis presented herein, a combination of manual separation and machine removal was assumed. The insulation was not considered to be shredded during demolition, but rather that the demolition processes resulted in smaller pieces of foam compared to the full panels. This process of reducing foam size is akin to cutting the foam into small pieces. Such processes would result in an instantaneous release of BA (assumed to be 30 min.), followed by a short-term release (1 hour to 1 week), and a long-term release (1 week to several years) during storage onsite and transportation processes. The instantaneous release of BA from cutting foam insulation was studied by BRE (2002). The release of BA for a period of 15-30 minutes after manually cutting PUR foam refrigerator panels was investigated. On average 3% (w/w) of the BA in the PUR panels obtained from different foam manufacturers was released during the cutting process (BRE 2002). This average value was adopted for this study and it was assumed that the decommissioning process instantaneously released approximately 3% (w/w) of the BA remaining in the foam. Short and long-

term BA releases, subsequent to instantaneous release during the demolition process were defined and included under the transportation pathway.

A summary of the calculated BA fractional weighting factor transfer coefficient to quantify emissions during each step along the pathways to landfill disposal is presented in Table 2.12, and graphical representations of the mass-based materials flows for C&D waste foam are provided in Figures 2.3 and 2.4 for Scenarios 1 and 2, respectively. In these figures, the units used are tonnes of BA determined on an annual basis (average for the entire time-frame of the specific scenario). Results indicated that most of the BA was retained in the foam materials during end of life waste management, and approximately 92-94% of the BA present in the foam that reached end of life was banked in the landfill (Figures 2.3 and 2.4). These high BA retention values resulted from over 83% of the C&D waste foam materials sent directly to landfills without shredding or pre-processing. The main BAs entering the landfill during Scenario 1 (1960-2010) were determined to be CFC-11 (74%), followed by HCFC-141b (20%), HFC-245fa (5%), and HFC-134a (1%) (Figure 2.3). For the future disposal period in Scenario 2, higher fractions of HFC-245fa (38%) and HFC-134a (32%) were predicted compared to Scenario 1 for the banked foam material entering the landfill (Figure 2.4). Of the estimated 76.5 tonnes/yr of BA emitted during end of life processes for C&D foam wastes in Scenario 1, 74% of the emissions was from foam waste containing CFC-11, 20% from foam waste containing HCFC-141b, 1% from foam waste containing HFC-134a, and 5% from foam waste containing HFC-245fa. Of the smaller 44.2 tonnes of BA emitted annually from end of life management of C&D foam waste predicted under future disposal conditions (Scenario 2), a higher fraction of emissions resulted from HFC-245fa (40%) and HFC-134a (33%) (Figure 2.4). In general, the methodology used for C&D wastes was adopted for the foam wastes from other applications.

Table 2.12 – Summary of Calculated BA Release Fractions for C&D Foam Waste

| Disposal Stage | CFC-11 Release (%) | HCFC-141b Release (%) | HFC-134a Release (%) | HFC-245fa Release (%) |
|---|---|---|---|---|
| Decommissioning | 3 | 3 | 3 | 3 |
| Transportation | 2.6 | 2 | 2.3 | 2.4 |
| Shredding | 24 | 24 | 24 | 24 |
| Stockpiling at Shredding Facility | 8.8 | 6.6 | 10 | 10.8 |
| Stockpiling at Landfill for ADC | 2.5 | 2.1 | 2.9 | 2.75 |
| Total Release | 41 | 38 | 42 | 43 |
| Total Release Scaled[1] | 6-8 | 7-8 | 8 | 8 |

[1]The scaled value represents the quotient of the total release and the amount banked in landfill (values for both Scenario 1 and Scenario 2 provided).

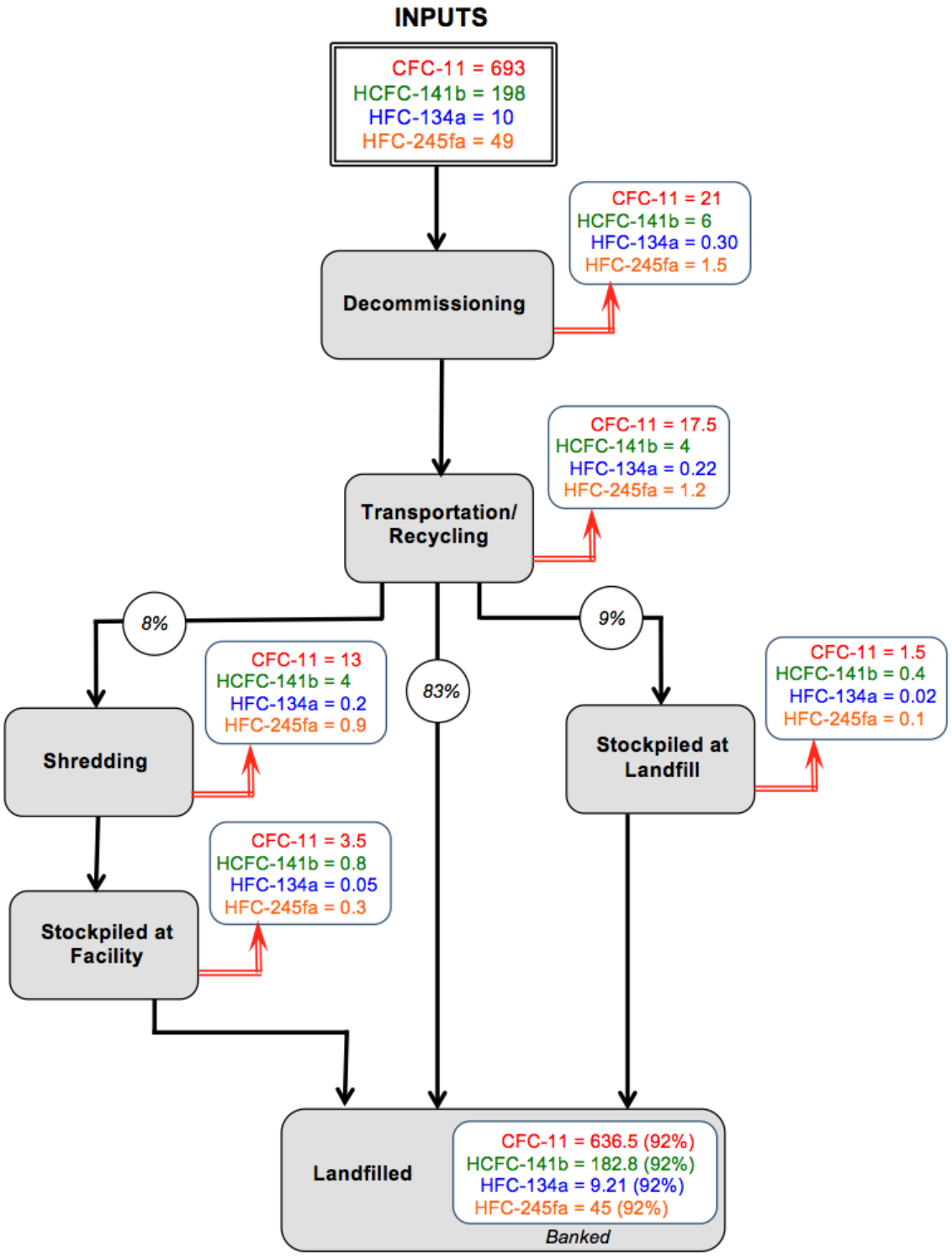


Figure 2.3. Pre-Landfill BA Losses from C&D Foam Wastes (Tonnes/year) (Scenario 1)

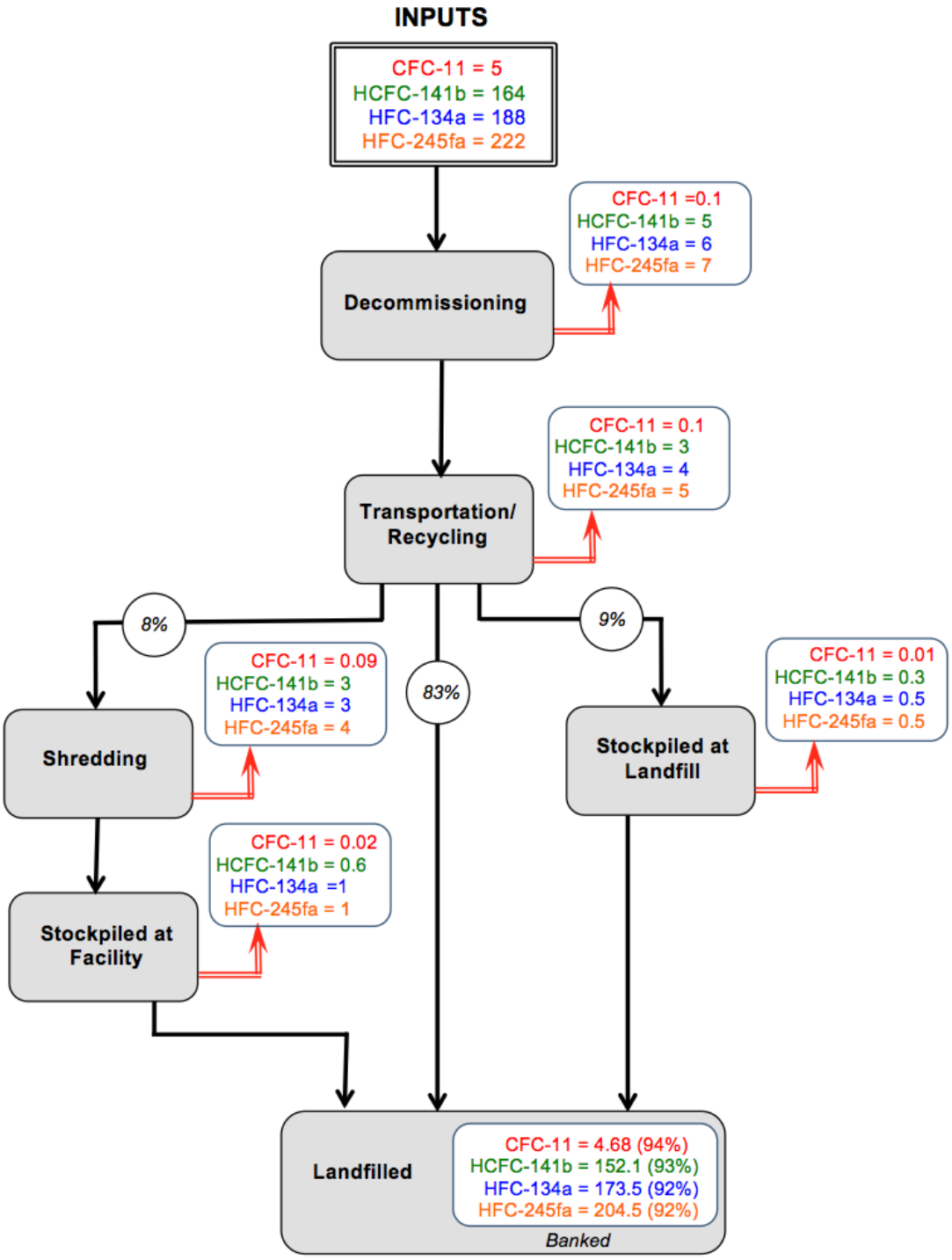


Figure 2.4. Pre-Landfill BA Losses from C&D Foam Wastes (Tonnes/year) (Scenario 2)

## 2.4 Domestic Appliance (Refrigerator/Freezer) Foam Insulation Waste

### 2.4.1 Foam Waste Stock and Flows for Domestic Appliance Foam Insulation Waste

Over one million refrigerators and freezers were reported to be disposed of annually in California (CARB 2008). This number was projected to grow by 50% by the year 2020 (Caleb 2011). The lifetime of most domestic refrigerators and freezers was indicated to be approximately 20 years (CARB 2008). Current management practices in California include recycling of end of life appliances, where metals are recovered, toxic substances including chlorofluorocarbons are removed, and remaining residual materials are shredded (DTSC 2002, 2007). The removal of toxics in the current practices only applies to refrigerants and does not cover insulation foam blowing agents. The insulation foam is included in the shredded residual materials, which are typically then landfilled. Some waste appliance foam is recovered in line with the USEPA's Responsible Appliance Disposal Program by manufacturers, municipalities, retailers, etc. (Caleb 2011). Estimates for 2008 and projections for 2020 were provided for volume of domestic appliance foam wastes in California (Caleb 2011). Generally, for both timeframes the amount of foam in refrigerators significantly exceeded the amount of foam in freezers with increases projected for both categories in 2020 compared to 2008 (Table 2.13).

Table 2.13 – Foam Volume in Domestic Appliance Wastes (Caleb 2011)

| Analysis Timeframe | Appliance Type | Decommissioned Foam ($m^3$/yr) |
|---|---|---|
| 2008 | Domestic Refrigerators | 205,441 |
| | Domestic Freezers | 108,169 |
| 2020 | Domestic Refrigerators | 830,564 |
| | Domestic Freezers | 307,757 |

PUR rigid insulation foam material was indicated to comprise 100% of the domestic appliance waste foam (Caleb 2011). Historical BA substitution was reviewed for appliance foam to develop an accurate representation of the annual input of foam materials in the California waste stream. A summary of historical BA use and the BA substitutions in domestic appliance rigid PUR insulation foams is presented in Table 2.14 based on data provided in Caleb (2011). Manufacturers of domestic refrigerators and freezers switched from using CFC-11 to HCFC-141b in 1993, and to HFC-245fa by 2003. For determining foam waste flows for time frames prior to 1992, domestic appliance foam insulation materials were assumed to have only CFC-11 BAs. For determining foam waste flows for time frames extending to 2050 (beyond the 2016 end date provided in Table 2.14), HC and HFC-245fa were assumed to remain in use at the 75%/25% ratio (HC/HFC-245fa) in domestic appliance insulation foams. The appliance lifetime assumed in this analysis was 20 years.

Table 2.14 – Blowing Agents Used in Domestic Appliances (Caleb 2011)

| Sales Year | Disposal Year | Percent of Units Disposed Annually by Blowing Agent | | | | |
|---|---|---|---|---|---|---|
| | | CFC-11 | HFC-134a | HCFC-141b | HFC-245fa | HC |
| 1992 | 2006 | 100% | 0% | 0% | 0 % | 0 % |
| 1993 | 2007 | 75% | 0 % | 25% | 0 % | 0 % |
| 1994 | 2008 | 50% | 0 % | 50% | 0 % | 0 % |
| 1995 | 2009 | 0% | 0 % | 100% | 0 % | 0 % |
| 1996 | 2010 | 0 % | 2% | 98% | 0% | 0% |
| 1997 | 2011 | 0 % | 3% | 97% | 0% | 0% |
| 1998 | 2012 | 0 % | 4% | 96% | 0% | 0% |
| 1999 | 2013 | 0 % | 5% | 95% | 0% | 0% |
| 2000 | 2014 | 0 % | 6% | 94% | 0% | 0% |
| 2001 | 2015 | 0 % | 7% | 75% | 18% | 0% |
| 2002 | 2016 | 0 % | 4% | 45% | 47% | 4% |
| 2003 | 2017 | 0 % | 0% | 21% | 70% | 9% |
| 2004 | 2018 | 0 % | 0% | 0% | 87% | 13% |
| 2005 | 2019 | 0 % | 0% | 0% | 83% | 17% |
| 2006 | 2020 | 0 % | 0% | 0% | 82% | 18% |
| 2007 | 2021 | 0 % | 0% | 0% | 82% | 18% |
| 2008 | 2022 | 0 % | 0% | 0% | 81% | 19% |
| 2009 | 2023 | 0 % | 0% | 0% | 80% | 20% |
| 2010 | 2024 | 0 % | 0% | 0% | 79% | 21% |
| 2011 | 2025 | 0 % | 0% | 0% | 79% | 21% |
| 2012 | 2026 | 0 % | 0% | 0% | 78% | 22% |
| 2013 | 2027 | 0 % | 0% | 0% | 77% | 23% |
| 2014 | 2028 | 0 % | 0% | 0% | 76% | 24% |
| 2015 | 2029 | 0 % | 0% | 0% | 76% | 24% |
| 2016 | 2030 | 0 % | 0% | 0% | 75% | 25% |

To calculate the domestic appliance foam waste volumetric flow, the disposal rates of refrigerators and freezers were assumed equivalent to the 2008 rates for the Scenario 1 timeframe (1960 to 2010). For Scenario 2, the 2008 rates were used for the time period between 1995 and 2010 and the 2020 projections were used for the years 2011 to 2050. With these assumptions, the fractions and volumetric flows of each type of BA in decommissioned appliances were calculated (Tables 2.15a and 2.15b). For Scenario 1, CFC-11 accounted for nearly 67% of the total BA content in foam waste material on a volumetric basis. HCFC-141b and HFC-245fa together constituted 30% of the total amount of BA in the decommissioned appliances (Figure 2.5), while HFC-134a and hydrocarbons demonstrated negligible contributions to BA banks in foam waste under Scenario 1 conditions. Scenario 2 flows included foam wastes with mostly HFC-245fa and HC. HCFC-141b and HFC-134a in domestic appliance foam wastes were similar for both Scenarios (Figure 2.5).

Table 2.15a – Calculated BA Content in Appliance Waste Foam

| Foam Material | CFC-11 (%) | | HCFC-141b (%) | | HFC-134a (%) | | HFC-245fa (%) | | HC (%) | |
|---|---|---|---|---|---|---|---|---|---|---|
| Scenario Number | Sc.1 | Sc. 2 | Sc. 1 | Sc. 2 | Sc. 1 | Sc. 2 | Sc. 1 | Sc. 2 | Sc. 1 | Sc. 2 |
| PUR Panel | 66.5 | 0 | 15.9 | 13.1 | 0.6 | 0.6 | 14.1 | 68.2 | 2.8 | 18.1 |

Table 2.15b – Annual Volumetric Flow of Appliance Waste Foam Material

| Foam Material | CFC-11 ($m^3$/year) | | HCFC-141b ($m^3$/year) | | HFC-134a ($m^3$/year) | | HFC-245fa ($m^3$/year) | | HC ($m^3$/year) | |
|---|---|---|---|---|---|---|---|---|---|---|
| Scenario Number | Sc.1 | Sc. 2 | Sc. 1 | Sc. 2 | Sc. 1 | Sc. 2 | Sc. 1 | Sc. 2 | Sc. 1 | Sc. 2 |
| PUR Panel | 208,551 | 0 | 49,927 | 99,334 | 1,944 | 4,271 | 44,470 | 516,924 | 8,718 | 137,222 |

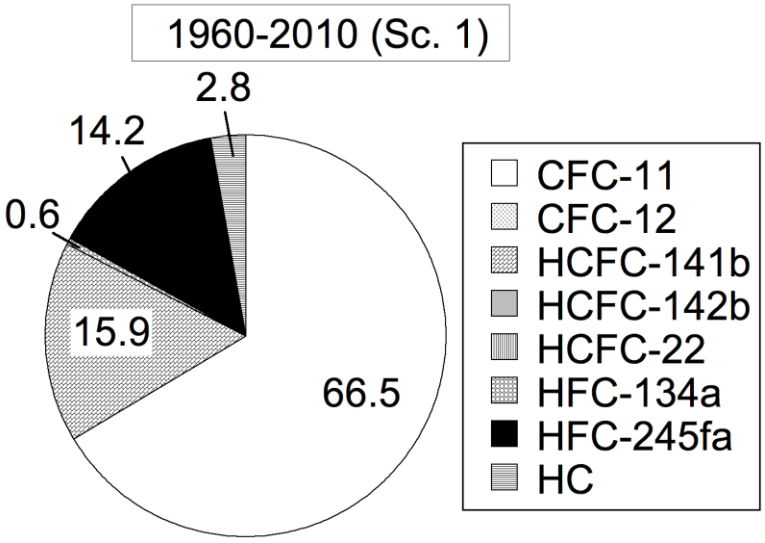


(a) Scenario 1

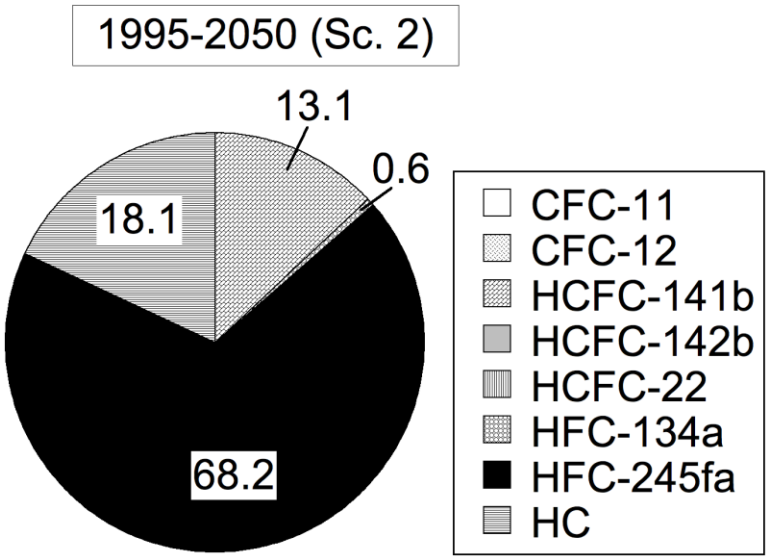


(b) Scenario 2

Figure 2.5. Estimated Volumetric Flows of Domestic Appliance Waste Foam Containing Different BAs (Percentages)

The volumetric flows were then converted to mass flows and used throughout the calculations for establishing flows associated with the foam waste disposal pathways prior to landfilling similar to the analysis conducted for C&D wastes. The volumetric flows presented in Table 2.15b were converted to mass flows using densities of: 24.6, 32.2, 39, and 30.7 g/L for foams containing CFC-11, HCFC-141b, HFC-134a, and HFC-245fa, respectively (Scheutz and Kjeldsen 2003a). The BAs remaining in the

PUR panel appliance foams were estimated using experimental data provided by (Scheutz and Kjeldsen 2003a): 13.3, 11.6, 7, and 11.6% were reported for CFC-11, HCFC-141b, HFC-134a and HFC-245fa, respectively. The total mass flows of the four target BAs are provided in Table 2.16. For Scenario 1, CFC-11 and HCFC-141b comprised the largest portion of the total insulation foam waste stream mass flows. For Scenario 2, mass flows of HFC-245fa increased significantly and constituted the majority of the mass-based annual insulation foam waste flow (Table 2.16).

Table 2.16 – Annual Mass Flow of Domestic Appliance Waste Foam Material

| Blowing Agent | CFC-11 | | HCFC-141b | | HFC-134a | | HFC-245fa | |
|---|---|---|---|---|---|---|---|---|
| Scenario Number | Sc. 1 | Sc. 2 | Sc. 1 | Sc. 2 | Sc. 1 | Sc. 2 | Sc. 1 | Sc. 2 |
| Mass Flow of BA (tonnes/year) | 682 | 0 | 186 | 371 | 5 | 12 | 158 | 1841 |

### 2.4.2 Disposal Pathways for Domestic Appliance Foam Insulation Waste

End of life management of domestic refrigerators and freezers included 39% reuse and 61% recycling. The appliances recycled with foam recovery and destruction accounted for 14% of the recycling stream, and those recycled with no foam recovery accounted for 47% (Caleb 2011). The 47% of the PUR foam insulation materials with no foam reuse or recovery were sent to recycling facilities for recovery of metals and hazardous materials from the refrigerants. The remaining components of the appliances were then shredded. At a given time, 5% of the shredded foam particles was reported to be stockpiled at the recycling facility prior to shipping to a landfill for approximately two weeks, and the remaining 95% was shipped within 24 hours of shredding to the landfill site (Wethje 2005). Wethje (2005) estimated further that 7% of the shredded appliance foam was used as an alternate daily cover in landfills with stockpiling for an estimated 1 week, and the remaining 93% was disposed of directly in the landfill without further stockpiling.

### 2.4.3 BA Release Estimates Prior to Landfilling for Domestic Appliance Foam Insulation Waste

The data and analyses of waste appliance foam stocks and disposal pathways both presented above were coupled to provide estimates for BA releases into the atmosphere. Results of the analysis are presented in Table 2.17 and in Figures 2.6 and 2.7 for Scenarios 1 and 2, respectively. No end of life release of BA was attributed to reuse applications, as the foam was assumed to be still in use. For the waste appliance foams recycled with foam recovery and destruction (14% of the total amount of end of life waste foam), a recovery and destruction rate of 96% was estimated based on data provided by Caleb (2011). Therefore, 4% BA release from waste PUR appliance foam was predicted for recycling with foam recovery and destruction activities.

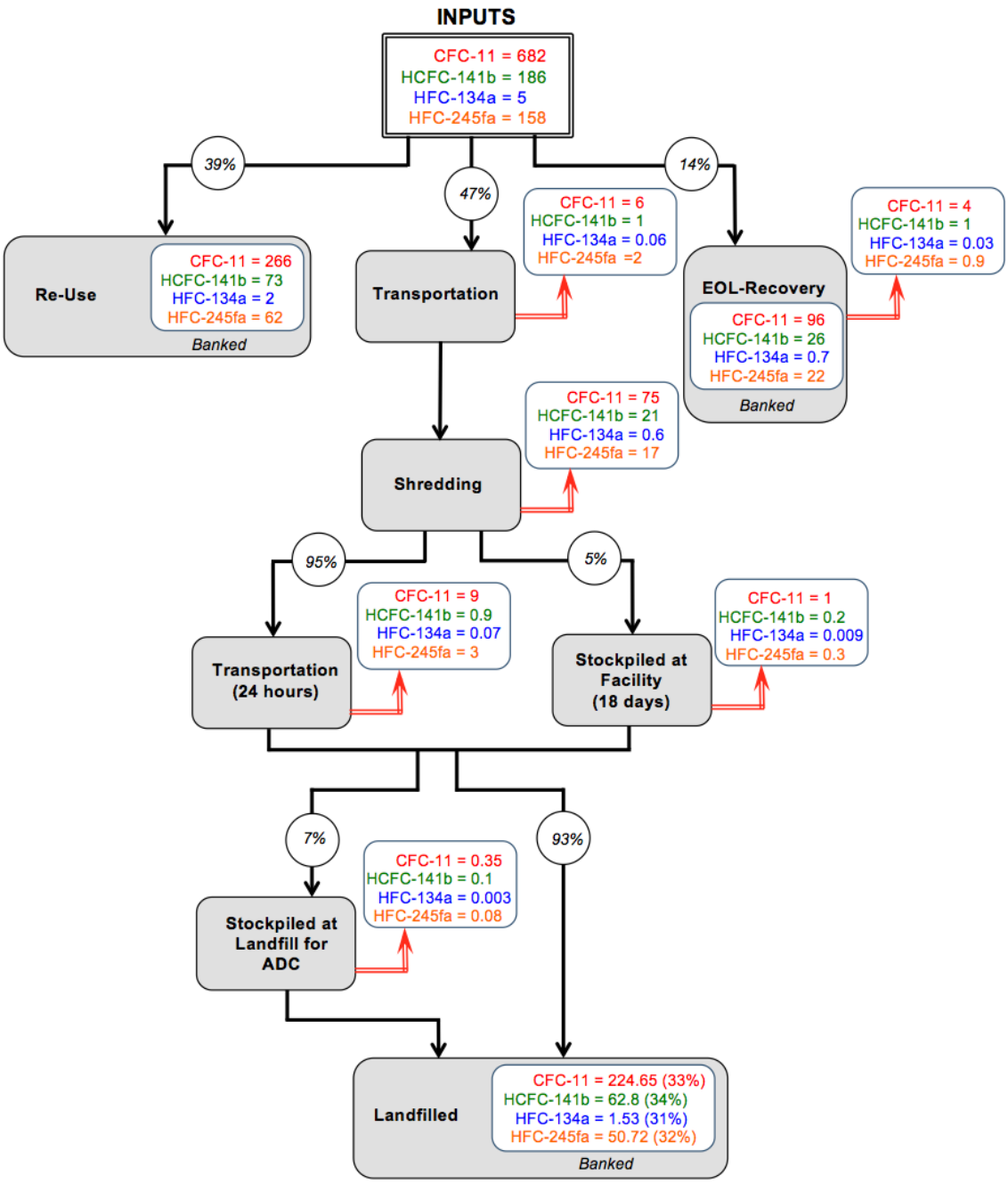


Figure 2.6. Pre-Landfill BA Losses from Domestic Appliance Foam Insulation Wastes (Tonnes/year) (Scenario 1)

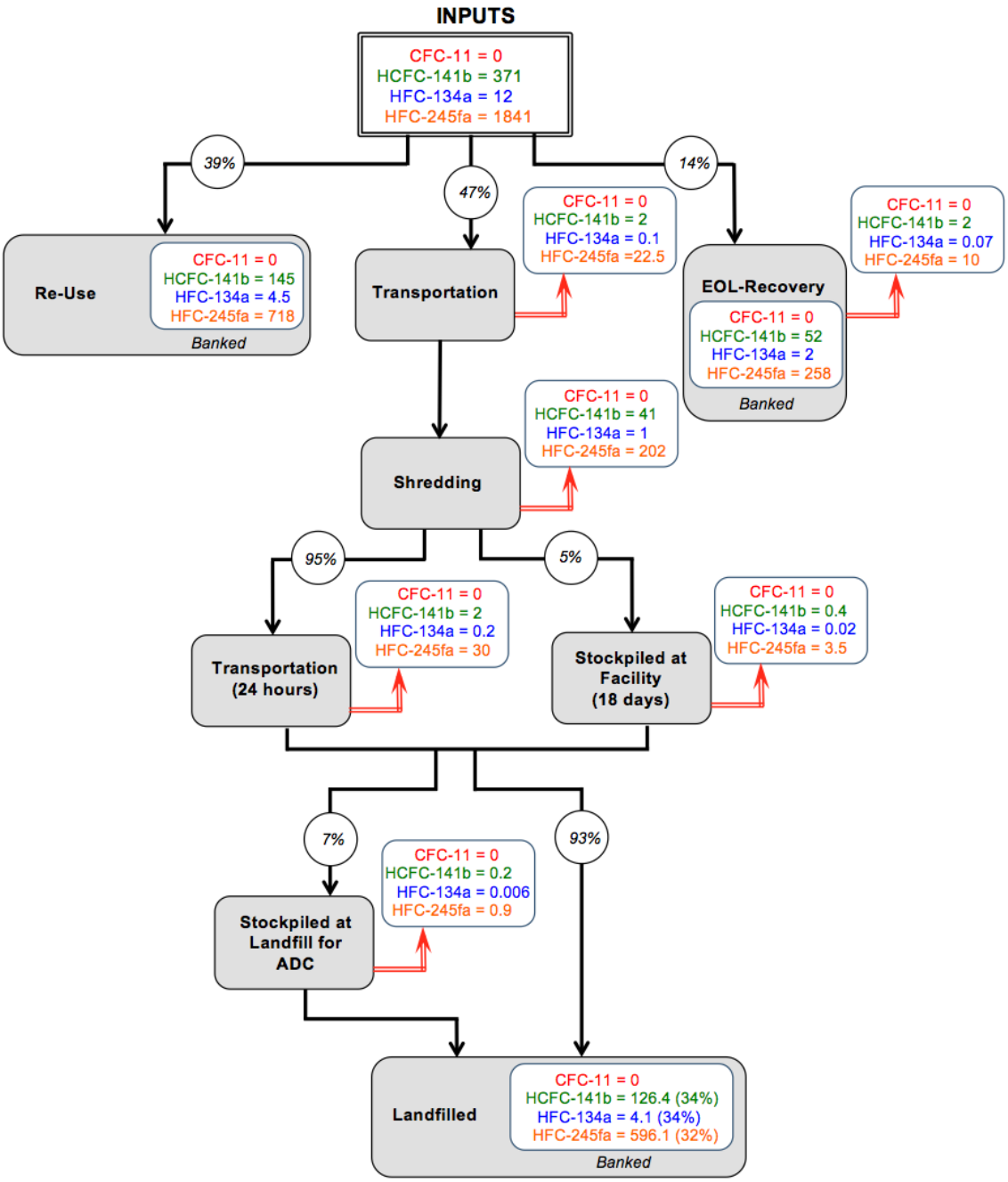


Figure 2.7. Pre-Landfill BA Losses from Domestic Appliance Foam Insulation Wastes (Tonnes/year) (Scenario 2)

Emissions of BAs during transportation to recycling facility and also to landfill from the recycling facility were based on the double compartment model and depended mostly on the short- and long-term diffusion coefficients and size of the insulation panels used in domestic appliances. Similar to the analysis for C&D waste, shredding was estimated to release approximately 24% of the initial BA content of the domestic appliance waste foam based on data from Scheutz et al. (2007a). Uniform size

fractions of processed foam were assumed to result from the shredding process, which governed the release of BA during stockpiling at the recycling facility. The shredding process at the recycling facility resulted in the highest fraction of the total BA releases. Stockpiling at the landfill for ADC had relatively low release since this step followed the short-term release during the transportation period and was subject to closed-cell diffusion of BA as opposed to release of BA from damaged cells during or immediately following shredding (Table 2.17).

For domestic appliance foam waste, results indicated 691.3 and 1497.4 tonnes of BA were emitted annually from end of life management of waste foams for Scenario 1 and Scenario 2, respectively. Overall, the amount of BA entering the landfill from appliance based foam insulation waste expressed as a percentage of the initial BA content of the foam at end of life ranged between 31% (HFC-134a, Scenario 1) and 34% (HCFC-141b, Scenario 1; HFC-134a and HCFC-141b, Scenario 2) (Figures 2.6 and 2.7). Reuse of foam and recovery and destruction of foams affected the amount of BA content entering the landfill. Shredding at the recycling facility and stockpiling thereafter under uncontrolled conditions (emissions were not captured at the recycling facility) resulted in the highest relative loss of BA among the various end of life waste management routes.

Table 2.17 – Summary of Calculated BA Release Fractions from Domestic Appliance Foam Waste

| Disposal Stage | CFC-11 Release (%) | HCFC-141b Release (%) | HFC-134a Release (%) | HFC-245fa Release (%) |
|---|---|---|---|---|
| Reuse | 0 | 0 | 0 | 0 |
| Foam Recovery and Destruction | 4 | 4 | 4 | 4 |
| Transportation | 2 | 1.3 | 2.3 | 2.6 |
| Shredding | 24 | 24 | 24 | 24 |
| Stockpiling at Recycling Facility | 8.8 | 6.6 | 10 | 10.8 |
| Transportation | 4 | 1.5 | 4 | 5 |
| Stockpiling at Landfill for ADC | 2.2 | 2.3 | 2.2 | 2.2 |
| Total Release | 45 | 40 | 47 | 49 |
| Total Release Scaled[1] | 67 | 66 | 66-69 | 68 |

[1]The scaled value represents the quotient of the total release and the amount banked in landfill (values for both Scenario 1 and Scenario 2 provided).

## 2.5 Commercial Appliance (Refrigerator/Freezer), Vending Machine, and Water Heater Foam Insulation Waste

### 2.5.1 Foam Waste Stock and Flows for Commercial Appliance, Vending Machine, and Water Heater Foam Insulation Waste

This section includes analysis of foam waste from commercial appliances including refrigerators and freezers (display cases and stand alone equipment) used primarily

within large grocery store chains and also refrigerated vending machines and water heaters. The foams used in commercial refrigeration, vending machine units, and water heaters were reported to consist of 100% PUR insulation panels, with typical densities ranging from 30-35 kg/$m^3$ (Caleb 2011). Estimates for 2008 and projections for 2020 were provided for volume of commercial appliance, vending machine, and water heater foam wastes in California (Caleb 2011). Generally, for both timeframes the amount of decommissioned foam in water heaters significantly exceeded the amount of foam in refrigerators/freezers and in particular the amount of foam in vending machines (Table 2.18). The projections included high increases for vending machines and water heaters and low increases for commercial appliances.

Table 2.18 – Waste Foam Volume in Commercial Appliances, Vending Machines, and Water Heaters (Caleb 2011)

| Analysis Timeframe | Appliance Type | Decommissioned Foam ($m^3$/yr) |
|---|---|---|
| 2008 | Commercial Appliances | 553,564 |
| | Refrigerated Vending Machines | 184,902 |
| | Water Heaters | 1,266,787 |
| 2020 | Commercial Appliances | 582,227 |
| | Refrigerated Vending Machines | 263,439 |
| | Water Heaters | 1,722,170 |

The historical trends in BAs used in commercial appliances, water heaters, and vending machine PUR insulation foams are presented in Tables 2.19 to 2.21. The tables were prepared using data in Caleb (2011). The composition of BAs present in waste foam insulation varied as a function of the type of appliance. Prior to 1994, all manufacturers of commercial appliances and vending machines were assumed to have used CFC-11 as the primary BA. By 1995, all manufacturers converted to HCFC-141b as the primary blowing agent. From 2003 onwards, all manufactures substituted HCFC-141b with a mixture of HFC-245fa and hydrocarbons. Commercial appliances and vending machines from the year 2005 onward were manufactured with HFC-245a as the primary BA. Water heaters were manufactured with HFC-245fa (10% of the total BA content) or hydrocarbons (90% of the total BA content) from the year 2005 onward.

Table 2.19 – Blowing Agents Used in Commercial Refrigerators and Freezers (Caleb 2011)

| Year | CFC 11 | HCFC 141b | HFC 245fa | HC |
|---|---|---|---|---|
| 1992 | 100% | 0% | 0% | 0% |
| 1993 | 75% | 25% | 0% | 0% |
| 1994 | 50% | 50% | 0% | 0% |
| 1995 | 0% | 100% | 0% | 0% |
| 1996 | 0% | 100% | 0% | 0% |
| 1997 | 0% | 100% | 0% | 0% |
| 1998 | 0% | 100% | 0% | 0% |
| 1999 | 0% | 100% | 0% | 0% |
| 2000 | 0% | 95% | 5% | 0% |
| 2001 | 0% | 80% | 20% | 0% |
| 2002 | 0% | 70% | 30% | 0% |
| 2003 | 0% | 30% | 70% | 0% |
| 2004 | 0% | 15% | 85% | 0% |
| 2005 | 0% | 0% | 100% | 0% |
| 2006 | 0% | 0% | 100% | 0% |
| 2007 | 0% | 0% | 100% | 0% |
| 2008 | 0% | 0% | 100% | 0% |
| 2009 | 0% | 0% | 100% | 0% |
| 2010 | 0% | 0% | 100% | 0% |
| 2011 | 0% | 0% | 100% | 0% |
| 2012 | 0% | 0% | 100% | 0% |
| 2013 | 0% | 0% | 100% | 0% |
| 2014 | 0% | 0% | 100% | 0% |
| 2015 | 0% | 0% | 100% | 0% |
| 2016 | 0% | 0% | 100% | 0% |
| 2017 | 0% | 0% | 100% | 0% |
| 2018 | 0% | 0% | 100% | 0% |
| 2019 | 0% | 0% | 100% | 0% |
| 2020 | 0% | 0% | 100% | 0% |

Table 2.20 – Blowing Agents Used in Vending Machines (from Caleb 2011)

| Year | CFC 11 | HCFC 141b | HFC 245fa | HC |
|---|---|---|---|---|
| 1992 | 100% | 0% | 0% | 0% |
| 1993 | 75% | 25% | 0% | 0% |
| 1994 | 50% | 50% | 0% | 0% |
| 1995 | 0% | 100% | 0% | 0% |
| 1996 | 0% | 100% | 0% | 0% |
| 1997 | 0% | 100% | 0% | 0% |
| 1998 | 0% | 100% | 0% | 0% |
| 1999 | 0% | 100% | 0% | 0% |
| 2000 | 0% | 95% | 5% | 0% |

| | | | | |
|---|---|---|---|---|
| 2001 | 0% | 80% | 20% | 0% |
| 2002 | 0% | 70% | 30% | 0% |
| 2003 | 0% | 30% | 70% | 0% |
| 2004 | 0% | 15% | 85% | 0% |
| 2005 | 0% | 0% | 100% | 0% |
| 2006 | 0% | 0% | 100% | 0% |
| 2007 | 0% | 0% | 100% | 0% |
| 2008 | 0% | 0% | 100% | 0% |
| 2009 | 0% | 0% | 100% | 0% |
| 2010 | 0% | 0% | 100% | 0% |
| 2011 | 0% | 0% | 100% | 0% |
| 2012 | 0% | 0% | 100% | 0% |
| 2013 | 0% | 0% | 100% | 0% |
| 2014 | 0% | 0% | 100% | 0% |
| 2015 | 0% | 0% | 100% | 0% |
| 2016 | 0% | 0% | 100% | 0% |
| 2017 | 0% | 0% | 100% | 0% |
| 2018 | 0% | 0% | 100% | 0% |
| 2019 | 0% | 0% | 100% | 0% |
| 2020 | 0% | 0% | 100% | 0% |

Table 2.21 – Blowing Agents Used for Water Heaters (Caleb 2011)

| Year | CFC 11 | HCFC 141b | HFC 245fa | HC |
|---|---|---|---|---|
| 1992 | 100% | 0% | 0% | 0% |
| 1993 | 75% | 25% | 0% | 0% |
| 1994 | 50% | 50% | 0% | 0% |
| 1995 | 0% | 100% | 0% | 0% |
| 1996 | 0% | 100% | 0% | 0% |
| 1997 | 0% | 100% | 0% | 0% |
| 1998 | 0% | 100% | 0% | 0% |
| 1999 | 0% | 100% | 0% | 0% |
| 2000 | 0% | 95% | 0% | 5% |
| 2001 | 0% | 80% | 5% | 15% |
| 2002 | 0% | 70% | 5% | 25% |
| 2003 | 0% | 30% | 10% | 60% |
| 2004 | 0% | 15% | 10% | 75% |
| 2005 | 0% | 0% | 10% | 90% |
| 2006 | 0% | 0% | 10% | 90% |
| 2007 | 0% | 0% | 10% | 90% |
| 2008 | 0% | 0% | 10% | 90% |
| 2009 | 0% | 0% | 10% | 90% |
| 2010 | 0% | 0% | 10% | 90% |
| 2011 | 0% | 0% | 10% | 90% |
| 2012 | 0% | 0% | 10% | 90% |
| 2013 | 0% | 0% | 10% | 90% |

| | | | | |
|---|---|---|---|---|
| 2014 | 0% | 0% | 10% | 90% |
| 2015 | 0% | 0% | 10% | 90% |
| 2016 | 0% | 0% | 10% | 90% |
| 2017 | 0% | 0% | 10% | 90% |
| 2018 | 0% | 0% | 10% | 90% |
| 2019 | 0% | 0% | 10% | 90% |
| 2020 | 0% | 0% | 10% | 90% |

The volumetric flow of commercial appliance, vending machine, and water heater foam insulation wastes was calculated using the BA substitution data provided (Tables 2.19 to 2.21) and the annual disposal rates provided for 2008 and 2020 (Table 2.18). The disposal rate estimated in 2008 was applied to the Scenario 1 time period (1960 to 2010) and assumed constant throughout these years. For Scenario 2, the 2008 rates were used for the time period between 1995 and 2010 and the 2020 projections were used for the years 2011 to 2050. The weighted fraction of BA for PUR materials (for both scenarios) was calculated using the BA substitution percentages in Tables 2.19 to 2.21 and presented in Table 2.22a. For the period 1960 to 2010 (Scenario 1), the weighted fraction and total annual volumetric flow of CFC-11 was higher compared to the other blowing agents (Tables 2.22a and 2.22b). For the period 1995 to 2050 (Scenario 2), the weighted fraction and total annual volumetric flow of HFC-245fa was higher than the other BAs (Tables 2.22a and 2.22b). A comparison of total annual volumetric flow rates of BA content of waste foams for commercial appliance, vending machine, and water heater insulation applications is presented in Figure 2.8 for the two scenarios. For Scenario 1, CFC-11 accounted for 67% of the total BA content, followed by HCFC-141b (17%), and HFC-245fa (9%). Scenario 2 resulted in a large fraction of HFC-245fa containing foam waste (44%) and hydrocarbon blowing agent mixtures (comprising 42% of the total volumetric flow). The larger projected volumetric flow of hydrocarbon containing insulation foam waste in Scenario 2 compared to Scenario 1 resulted from the increase of water heater manufactures substituting HCFC-141b with hydrocarbon BAs beginning in early 2001.

Table 2.22a – Calculated BA Content in Commercial Appliance, Vending Machine, and Water Heater Waste Foam

| Foam Material | CFC-11 (%) | | HCFC-141b (%) | | HFC-134a (%) | | HFC-245fa (%) | | HC (%) | |
|---|---|---|---|---|---|---|---|---|---|---|
| Scenario Number | Sc.1 | Sc. 2 | Sc. 1 | Sc. 2 | Sc. 1 | Sc. 2 | Sc. 1 | Sc. 2 | Sc. 1 | Sc. 2 |
| Commercial Appliance and Vending Machine PUR Panel | 66.5 | 0 | 17.3 | 14 | 0 | 0 | 16.2 | 86 | 0 | 0 |
| Water Heater PUR Panel | 66.5 | 0 | 17.3 | 14 | 0 | 0 | 3.6 | 21 | 12.6 | 65 |

Table 2.22b – Annual Volumetric Flow of Commercial Appliance, Vending Machine, and Water Heater Waste Foam

| Foam Material | CFC-11 ($m^3$/year) | | HCFC-141b ($m^3$/year) | | HFC-134a ($m^3$/year) | | HFC-245fa ($m^3$/year) | | HC ($m^3$/year) | |
|---|---|---|---|---|---|---|---|---|---|---|
| Scenario Number | Sc.1 | Sc. 2 | Sc. 1 | Sc. 2 | Sc. 1 | Sc. 2 | Sc. 1 | Sc. 2 | Sc. 1 | Sc. 2 |
| Total (Commercial Appliance, Vending Machine, and Water Heater) PUR Panel | 58,932 | 0 | 15,331 | 18,018 | 0 | 0 | 8,067 | 54,728 | 6,290 | 52,695 |

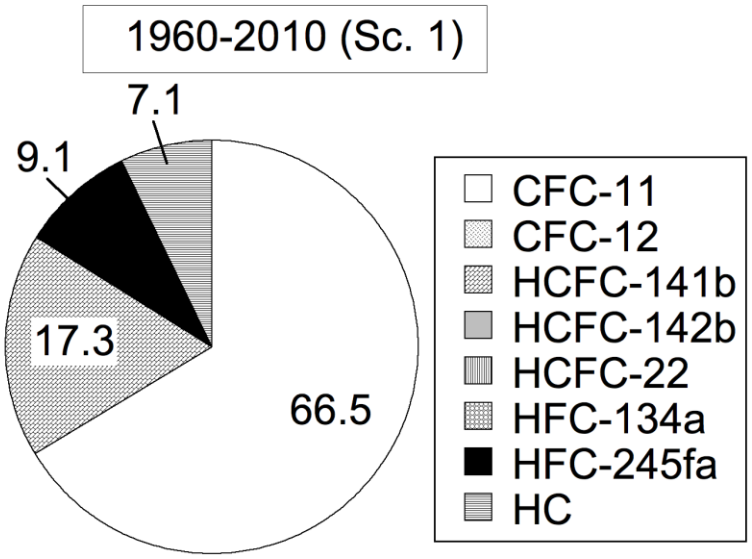


(a) Scenario 1

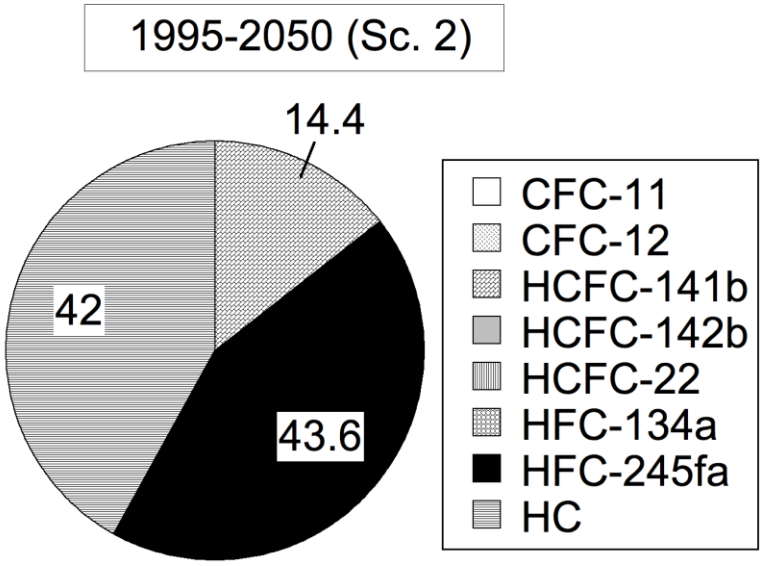


(b) Scenario 2

Figure 2.8 Estimated Volumetric Flows of Commercial Appliance, Vending Machine, and Water Heater Waste Foams Containing Different BAs

The volumetric flows were then converted to mass flows and used throughout the calculations for establishing flows associated with the foam waste disposal pathways prior to landfilling. The densities and BA contents used for the domestic appliance

foam waste also were used for the foam waste from commercial appliances, vending machines, and water heaters. The volumetric flows presented in Table 2.22b were converted to mass flows using densities of 24.6, 32.2, 39, and 30.7 g/L for foams containing CFC-11, HCFC-141b, HFC-134a, and HFC-245fa, respectively. The BAs remaining in the PUR panel appliance foams were estimated using the BA contents of 13.3, 11.6, 7, and 11.6% for CFC-11, HCFC-141b, HFC-134a and HFC-245fa, respectively. The total mass flows of the four target BAs are provided in Table 2.23. Mass flow calculations for Scenario 1 demonstrated that CFC-11 was the most dominant BA entering the waste stream (69% of total annual mass flow of BA), followed by HCFC-141b (20% of total annual mass flow of BA), and HFC-245fa (10% of total annual mass flow of BA). Scenario 2 results indicated large amounts of HFC-245fa (74% of total annual mass flow of BA) and HCFC-141b (26% of total annual mass flow of BA) BAs (Table 2.23).

Table 2.23 – Annual Mass Flow of Commercial Appliance, Vending Machine, and Water Heater Waste Foams

| Blowing Agent | CFC-11 | | HCFC-141b | | HFC-134a | | HFC-245fa | |
|---|---|---|---|---|---|---|---|---|
| Scenario Number | Sc. 1 | Sc. 2 | Sc. 1 | Sc. 2 | Sc. 1 | Sc. 2 | Sc. 1 | Sc. 2 |
| Mass Flow of BA (tonnes/year) | 193 | 0 | 57 | 67 | 0 | 0 | 29 | 195 |

### 2.5.2 Disposal Pathways for Commercial Appliance, Vending Machine, and Water Heater Foam Insulation Waste

End of life management pathways for commercial appliance, vending machine, and water heater insulation foams were indicated to include processing of all 100%) of the waste foams in a recycling center. The waste foams were shredded at these facilities and then sent directly to the landfill. Transportation time from the site of origin to the recycling facility was estimated to be 4 days based on data provided by Wethje (2005). Subsequent to shredding, the foam waste was assumed to be stockpiled for a short period prior to transportation to the landfill. The total combined time for stockpiling at the recycling facility and transportation to the landfill was estimated to be 5 days in line with the timeframes identified by Wethje (2005).

### 2.5.3 BA Release Estimates Prior to Landfilling for Commercial Appliance, Vending Machine, and Water Heater Foam Insulation Waste

The data and analyses of waste appliance foam stocks and disposal pathways both presented above were coupled to provide estimates for release of the BAs from the end of life management processes for commercial appliance, vending machine, and water heater foam insulation wastes. Results of the analysis are presented in Table 2.24 and in Figures 2.9 and 2.10 for Scenarios 1 and 2, respectively. Among the various steps in end of life management, shredding resulted in the highest release of BAs for both Scenarios 1 and 2, followed by stockpiling and transportation processes.

The relatively small magnitude of BA release during end of life management of commercial appliance, vending machine, and water heater foam wastes resulted in a high fraction of BA banked in the foams entering the landfill (over of 70% of the initial BA content remained). Total BA emissions prior to entry to the landfill were relatively similar and on the order of 80.3 and 75.8 tonnes/yr for Scenario 1 Scenario 2, respectively (Figures 2.9 and 2.10).

Table 2.24 – Summary of Calculated BA Release Fractions from Commercial Appliance, Vending Machine, and Water Heater Waste Foams

| Disposal Stage | CFC-11 Release (%) | HCFC-141b Release (%) | HFC-134a Release (%) | HFC-245fa Release (%) |
|---|---|---|---|---|
| Transportation | 1.63 | 1.2 | 1.9 | 2 |
| Shredding | 24 | 24 | 24 | 24 |
| Stockpiling at Recycling Facility | 4.4 | 4.4 | 4.5 | 5 |
| Total Release | 30 | 30 | 30 | 31 |
| Total Release Scaled[1] | 28 | 28-29 | 0 | 29-30 |

[1]The scaled value represents the quotient of the total release and the amount banked in landfill (values for both Scenario 1 and Scenario 2 provided).

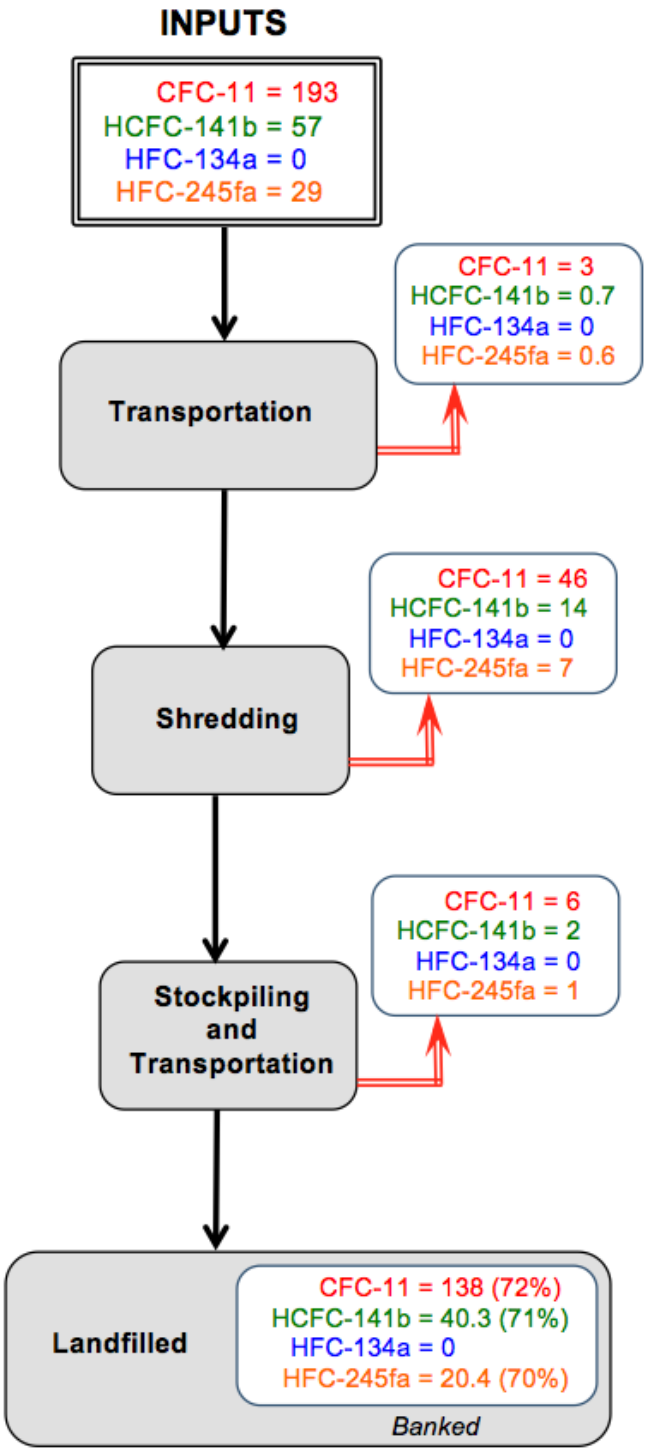


Figure 2.9. Pre-Landfill BA Losses from Commercial Appliance, Vending Machine, and Water Heater Foam Insulation Wastes (Tonnes/year) (Scenario 1)

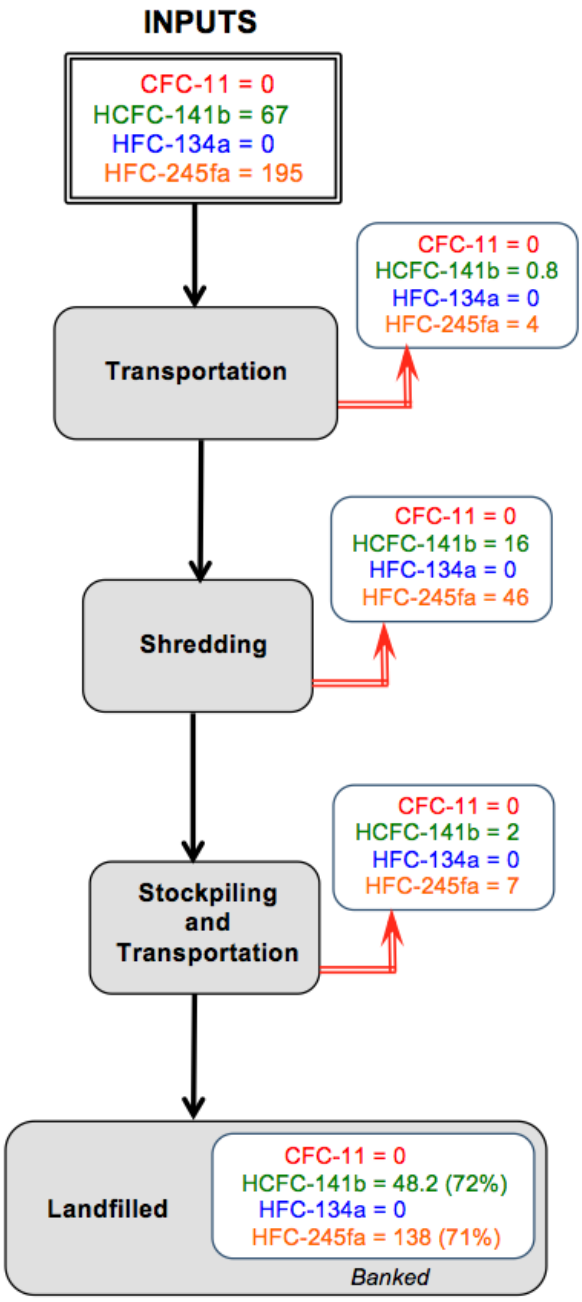


Figure 2.10. Pre-Landfill BA Losses from Commercial Appliance, Vending Machine, and Water Heater Foam Insulation Wastes (Tonnes/year) (Scenario 2)

## 2.6 Transport Refrigerated Unit (TRU) Foam Insulation Waste

### 2.6.1 Foam Waste Stock and Flows for TRU Foam Insulation Waste

Transport Refrigerated Units (TRU's) are used for transportation of perishable goods and include refrigerated trucks/vans, rail units, and ship Reefers (Caleb 2011). The total stock of TRUs in California was estimated to be on the order of 37,000 units in

2008. The great majority of the units were comprised of trucks and vans. A summary of estimates for volume of waste foam from TRUs for 2008 is presented in Table 2.25.

Table 2.25 – Waste Foam Volume in TRUs (Caleb 2011)

| TRU Type | Decommissioned Foam ($m^3$/yr) |
|---|---|
| Truck<br>Van | 14,164 |
| Rail | 1,256 |
| Sea/Reefers | 433 |
| Total | 15,853 |

Transport refrigerated units were reported to be constructed using entirely PUR rigid insulation foam panels (Caleb 2011). Historical BA substitution was used for TRU/Reefer foams to develop realistic representation of the annual input of these foams in the California waste stream (Table 2.26). From 1960 to 1993, 100% of the foam used in TRUs/Reefers was manufactured with CFC-11. HCFC-141b replaced CFC-11 beginning in 1994 and was the primary BA until 2000 when HFC-245fa was introduced. Since 2003, TRU foams have been manufactured with either HFC-245fa or hydrocarbon blends. The relative proportion of HC increased with respect to HFC-245fa with a higher fraction of insulation foams manufactured with hydrocarbons (60%) than HFC-245fa (40%) by 2010. An average lifetime of 15 years was used herein.

Table 2.26 – Blowing Agents Used in TRUs (Caleb 2011)

| Year | CFC 11 | HCFC 141b | HFC 245fa | HC |
|---|---|---|---|---|
| 1992 | 100% | 0% | 0% | 0% |
| 1993 | 100% | 0% | 0% | 0% |
| 1994 | 80% | 20% | 0% | 0% |
| 1995 | 60% | 40% | 0% | 0% |
| 1996 | 0% | 100% | 0% | 0% |
| 1997 | 0% | 100% | 0% | 0% |
| 1998 | 0% | 100% | 0% | 0% |
| 1999 | 0% | 100% | 0% | 0% |
| 2000 | 0% | 100% | 0% | 0% |
| 2001 | 0% | 80% | 20% | |
| 2002 | 0% | 40% | 60% | |
| 2003 | 0% | 0% | 80% | 20% |
| 2004 | 0% | 0% | 80% | 20% |
| 2005 | 0% | 0% | 80% | 20% |
| 2006 | 0% | 0% | 80% | 20% |
| 2007 | 0% | 0% | 70% | 30% |
| 2008 | 0% | 0% | 60% | 40% |
| 2009 | 0% | 0% | 50% | 50% |
| 2010 | 0% | 0% | 40% | 60% |

The volumetric flow rate of foam waste was determined using the BA substitutions provided for PUR insulation panels used for TRUs (Table 2.26) and the disposal rate provided (Table 2.25). The disposal rate (decommissioned foam volume estimate) was assumed constant during each time period and used for both Scenarios 1 and 2 (Tables 2.27a and 2.27b). For Scenario 1, CFC-11 was the BA with the highest calculated weighted percentage (68.8%) of total BA content in TRUs, whereas for Scenario 2, the most prominent BAs in the waste foams were hydrocarbons (47.3%) and HFC-245fa (39.6%) (Table 27a). A comparison of total annual volumetric flow rates of BA content of waste foams for TRU insulation applications is presented in Figure 2.11 for the two scenarios. Due to the BA substitutions the largely CFC-11 BAs in Scenario 1 were replaced with the hydrocarbons and HFC-245fa BAs in Scenario 2 (Table 2.27b and Figure 2.11).

Table 2.27a – Calculated BA Content in TRU Waste Foam

| Foam Material | CFC-11 (%) | | HCFC-141b (%) | | HFC-134a (%) | | HFC-245fa (%) | | HC (%) | |
|---|---|---|---|---|---|---|---|---|---|---|
| Scenario Number | Sc.1 | Sc. 2 | Sc. 1 | Sc. 2 | Sc. 1 | Sc. 2 | Sc. 1 | Sc. 2 | Sc. 1 | Sc. 2 |
| PUR Panel | 68.8 | 1.1 | 13.6 | 12 | 0 | 0 | 12.4 | 39.6 | 5.2 | 47.3 |

Table 2.27b – Annual Volumetric Flow of TRU Waste Foam

| Foam Material | CFC-11 ($m^3$/year) | | HCFC-141b ($m^3$/year) | | HFC-134a ($m^3$/year) | | HFC-245fa ($m^3$/year) | | HC ($m^3$/year) | |
|---|---|---|---|---|---|---|---|---|---|---|
| Scenario Number | Sc.1 | Sc. 2 | Sc. 1 | Sc. 2 | Sc. 1 | Sc. 2 | Sc. 1 | Sc. 2 | Sc. 1 | Sc. 2 |
| PUR Panel | 10,907 | 173 | 2,156 | 1,902 | 0 | 0 | 1,966 | 6,284 | 824 | 7,494 |

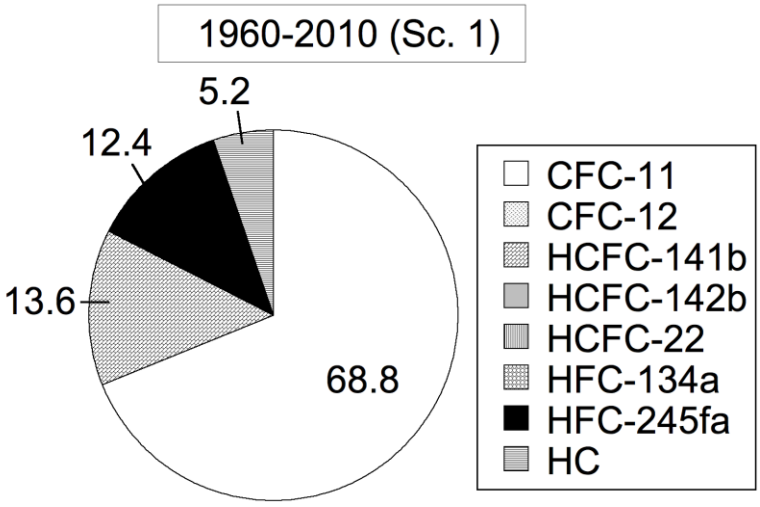


(a) Scenario 1

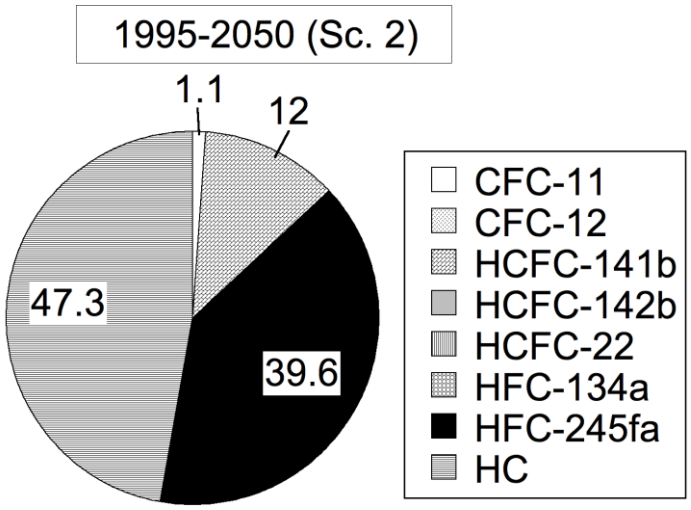


(b) Scenario 2

Figure 2.11. Estimated Volumetric Flows of TRU Waste Foams Containing Different BAs

The volumetric flows were then converted to mass flows and used throughout the calculations for establishing flows associated with the foam waste disposal pathways prior to landfilling. The densities and BA contents used for the previous foam applications also were used for the foam waste from TRUs. The volumetric flows presented in Table 27b were converted to mass flows using densities of 24.6, 32.2, 39, and 30.7 g/L for foams containing CFC-11, HCFC-141b, HFC-134a, and HFC-245fa, respectively. The BAs remaining in the PUR panel TRU foams were estimated using

the BA contents of 13.3, 11.6, 7, and 11.6% for CFC-11, HCFC-141b, HFC-134a and HFC-245fa, respectively. The total mass flows of the four target BAs are provided in Table 2.28. Mass flow calculations for Scenario 1 demonstrated that CFC-11 was the most dominant BA entering the waste stream (70.5% of total annual mass flow of BA), followed by HCFC-141b (15.7% of total annual mass flow of BA), and HFC-245fa (13.7% of total annual mass flow of BA). Scenario 2 results indicated large amount of HFC-245fa (74.3% of total annual mass flow of BA) BAs (Table 2.28).

Table 2.28 – Annual Mass Flow of TRU Waste Foams

| Blowing Agent | CFC-11 (tonnes/year) | | HCFC-141b (tonnes/year) | | HFC-134a (tonnes/year) | | HFC-245fa (tonnes/year) | |
|---|---|---|---|---|---|---|---|---|
| Scenario Number | Sc. 1 | Sc. 2 | Sc. 1 | Sc. 2 | Sc. 1 | Sc. 2 | Sc. 1 | Sc. 2 |
| Mass Flow of BA | 36 | 0.6 | 8 | 7 | 0 | 0 | 7 | 22 |

### 2.6.2 Disposal Pathways for TRU Foam Insulation Waste

End of life management pathways for TRU insulation foams were indicated to include reuse (approximately 25%) and processing at recycling facilities (75%). It was assumed that no BA release occurred in reuse applications. The remaining waste foams were shredded at the recycling facility and then sent directly to the landfill. Transportation time from the site of origin to the recycling facility was estimated to be 4 days based on data provided by Wethje (2005). Subsequent to shredding, the foam waste was assumed to be stockpiled for a short period prior to transportation to the landfill. The total combined time for stockpiling at the recycling facility and transportation to the landfill was estimated to be 5 days in line with the timeframes identified by Wethje (2005).

### 2.6.3 BA Release Estimates Prior to Landfilling for TRU Foam Insulation Waste

The data and analyses of waste appliance foam stocks and disposal pathways both presented above were coupled to provide estimates for release of the BAs from the end of life management processes for TRU insulation wastes. Results of the analysis are presented in Table 2.29 and in Figures 2.12 and 2.13 for Scenarios 1 and 2, respectively. The total release of BAs was relatively similar for the four target gases on the order of 29-30% (Table 2.29). Overall, the TRU waste foam insulation materials were predicted to release over half of the initial BA content (54 to 64%) at end of life due to current end of life management practices in California prior to entry to the landfill. Total BA emissions prior to entry to the landfill were relatively low compared to the other rigid foam applications and were on the order of 9.7 and 6.2 tonnes/yr for Scenario 1 Scenario 2, respectively (Figures 2.12 and 2.13).

Table 2.29 – Summary of Calculated BA Emissions from TRU Waste Foams

| Disposal Stage | CFC-11 Release (%) | HCFC-141b Release (%) | HFC-134a Release (%) | HFC-245fa Release (%) |
|---|---|---|---|---|
| Reuse | 0 | 0 | 0 | 0 |
| Transportation | 1 | 1 | 1 | 1 |
| Shredding | 24 | 24 | 24 | 24 |
| Stockpiling at Recycling Facility | 4.4 | 4.4 | 4.5 | 5 |
| Total Release | 29 | 29 | 30 | 30 |
| Total Release Scaled[1] | 36-45 | 41-46 | 0 | 46 |

[1]The scaled value represents the quotient of the total release and the amount banked in landfill (values for both Scenario 1 and Scenario 2 provided).

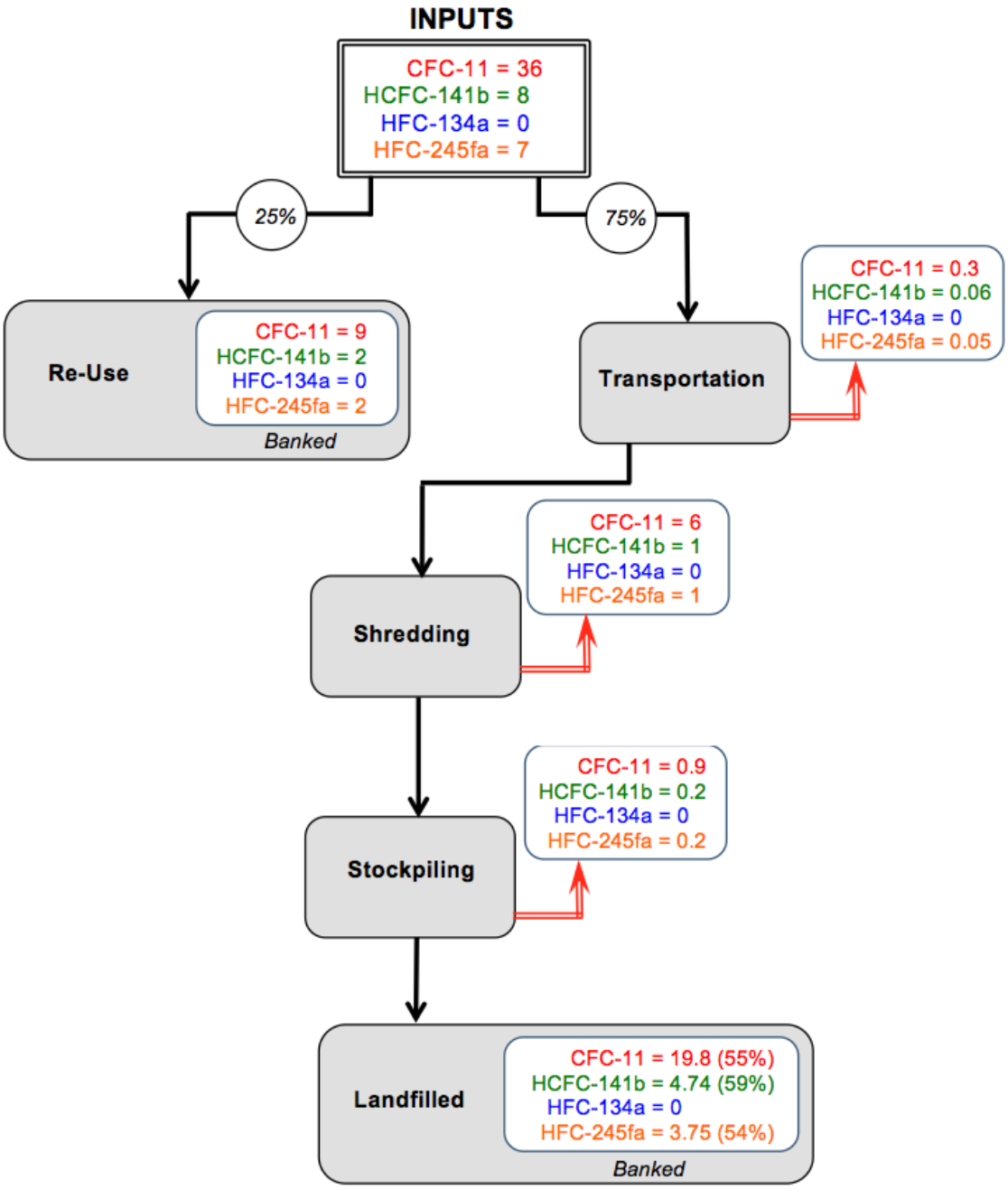


Figure 2.12. Pre-Landfill BA Losses from TRU Foam Insulation Wastes (Tonnes/year) (Scenario 1)

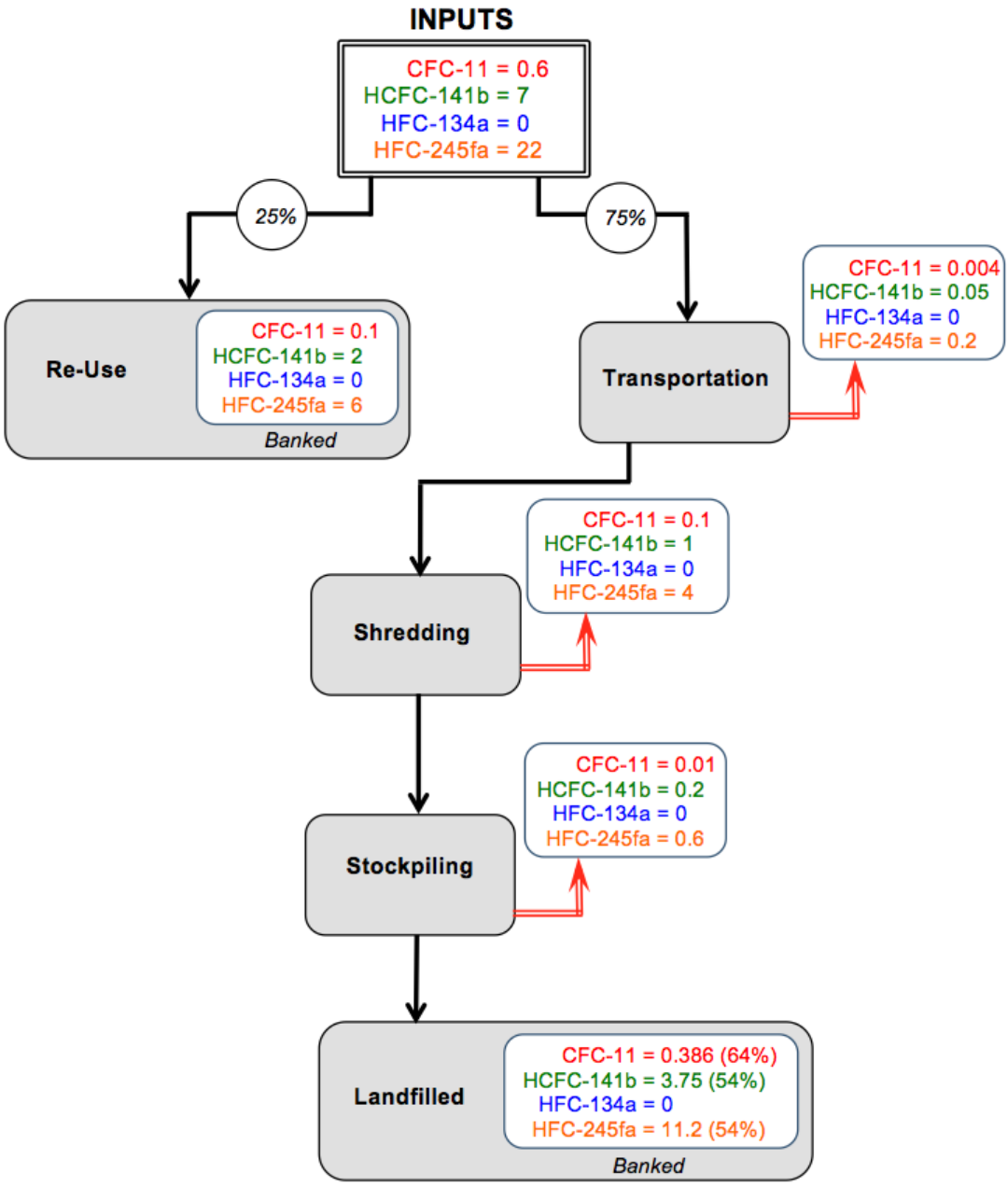


Figure 2.13. Pre-Landfill BA Losses from TRU Foam Insulation Wastes (Tonnes/year) (Scenario 2)

## 2.7 Marine and Other Foam Insulation Waste

### 2.7.1 Foam Waste Stock and Flows for Marine and Other Foam Insulation Waste

The final category of foam insulation wastes in California included in the materials flow analysis consisted of marine foam applications mainly associated with boats and canoes and cooler boxes or walk in cold store applications collectively termed other applications. A summary of the estimates for waste foam volume in marine and other

applications for 2008 based on data provided in Caleb (2011) is presented in Table 2.30. Of the 67,266 $m^3$ per year rigid foam volume disposed of in California from marine and other applications, 40% were from marine and 60% were from the other sources.

Table 2.30 – Waste Foam Volume from Marine and Other Applications (Caleb 2011)

| Application | | Decommissioned Foam ($m^3$/yr) |
|---|---|---|
| Marine | Boats | 25,664 |
| | Canoes | 1,300 |
| Other | Buoys, Cooler Boxes | 35,347 |
| | Walk in Cold Stores | 4,955 |
| Total | | 67,266 |

Foams used for the marine and other applications were reported to be 100% PUR based materials (Caleb 2011). Historical BA substitution was reviewed for marine/other foam products to develop an accurate representation of the yearly input of foam materials in the California waste stream (Table 2.31). BAs typically were HCFC-141b for boats, coolers, and cold stores and HFC-245fa/water and carbon dioxide for buoys (Caleb 2011). Between 1960 and 1993, CFC-11 was the primary blowing agent for all marine and other applications. HCFC-141b replaced CFC-11 beginning in 1993 with complete substitution by 1995. HFC-245fa was introduced in 2001 for most marine/other applications, followed by hydrocarbon substitutes beginning in 2003. From 2010 onwards, BAs consisted of either HFC-245fa or hydrocarbon blends with 40% and 60% use, respectively. An average lifetime of 15 years was used for a given TRU in this analysis.

Table 2.31 – Blowing Agents Used in Marine and Other Applications (Caleb 2011)

| Year | CFC 11 | HCFC 141b | HFC 245fa | HC |
|---|---|---|---|---|
| 1992 | 100% | 0% | 0% | 0% |
| 1993 | 100% | 0% | 0% | 0% |
| 1994 | 80% | 20% | 0% | 0% |
| 1995 | 60% | 40% | 0% | 0% |
| 1996 | 0% | 100% | 0% | 0% |
| 1997 | 0% | 100% | 0% | 0% |
| 1998 | 0% | 100% | 0% | 0% |
| 1999 | 0% | 100% | 0% | 0% |
| 2000 | 0% | 100% | 0% | 0% |
| 2001 | 0% | 80% | 20% | 0% |
| 2002 | 0% | 40% | 60% | 0% |
| 2003 | 0% | 0% | 80% | 20% |

| | | | | |
|---|---|---|---|---|
| 2004 | 0% | 0% | 80% | 20% |
| 2005 | 0% | 0% | 80% | 20% |
| 2006 | 0% | 0% | 80% | 20% |
| 2007 | 0% | 0% | 70% | 30% |
| 2008 | 0% | 0% | 60% | 40% |
| 2009 | 0% | 0% | 50% | 50% |
| 2010 | 0% | 0% | 40% | 60% |

The volumetric flow rate of foam waste was determined using the BA substitutions provided for PUR insulation materials used for marine and other applications (Table 2.31) and the disposal rate provided (Table 2.30). The disposal rate (decommissioned foam volume estimate) was assumed constant during each time period and used for both Scenarios 1 and 2 (Table 32). For Scenario 1, CFC-11 was the BA with the highest calculated weighted percentage (68.8%) of total BA content in marine/other applications (Table 2.32a), whereas for Scenario 2, the most prominent BAs in the waste foams were hydrocarbons (47.3%) and HFC-245fa (39.6%) (Table 2.32b). A comparison of total annual volumetric flow rates of BA content of waste foams for TRU insulation applications is presented in Figure 2.14 for the two scenarios. Due to the BA substitutions the largely CFC-11 BAs in Scenario 1 were replaced with the hydrocarbons and HFC-245fa BAs in Scenario 2.

Table 2.32a – Calculated BA Content in Marine and Other Waste Foam

| Foam Material | CFC-11 (%) | | HCFC-141b (%) | | HFC-134a (%) | | HFC-245fa (%) | | HC (%) | |
|---|---|---|---|---|---|---|---|---|---|---|
| Scenario Number | Sc.1 | Sc. 2 | Sc. 1 | Sc. 2 | Sc. 1 | Sc. 2 | Sc. 1 | Sc. 2 | Sc. 1 | Sc. 2 |
| PUR Panel | 68.8 | 1.1 | 13.6 | 12 | 0 | 0 | 12.4 | 39.6 | 5.2 | 47.3 |

Table 2.32b – Annual Volumetric Flow of Marine and Other Waste Foam

| Foam Material | CFC-11 ($m^3$/year) | | HCFC-141b ($m^3$/year) | | HFC-134a ($m^3$/year) | | HFC-245fa ($m^3$/year) | | HC ($m^3$/year) | |
|---|---|---|---|---|---|---|---|---|---|---|
| Scenario Number | Sc.1 | Sc. 2 | Sc. 1 | Sc. 2 | Sc. 1 | Sc. 2 | Sc. 1 | Sc. 2 | Sc. 1 | Sc. 2 |
| PUR Panel | 46,279 | 734 | 9,148 | 8,072 | 0 | 0 | 8,341 | 26,662 | 3,498 | 31,798 |

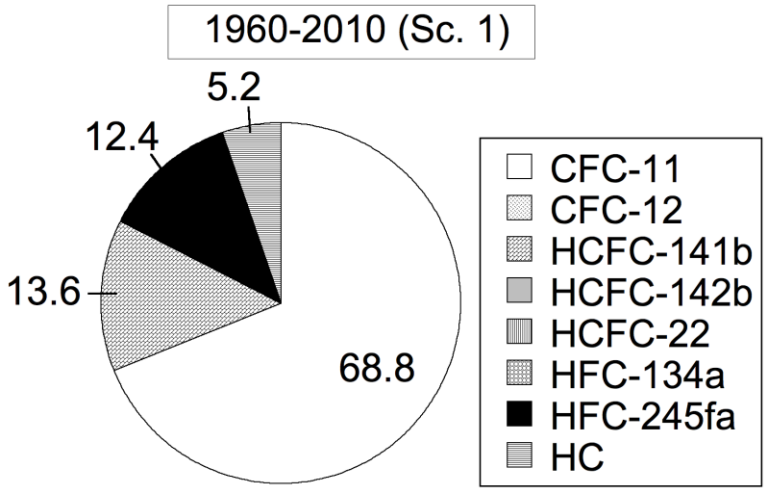


(a) Scenario 1

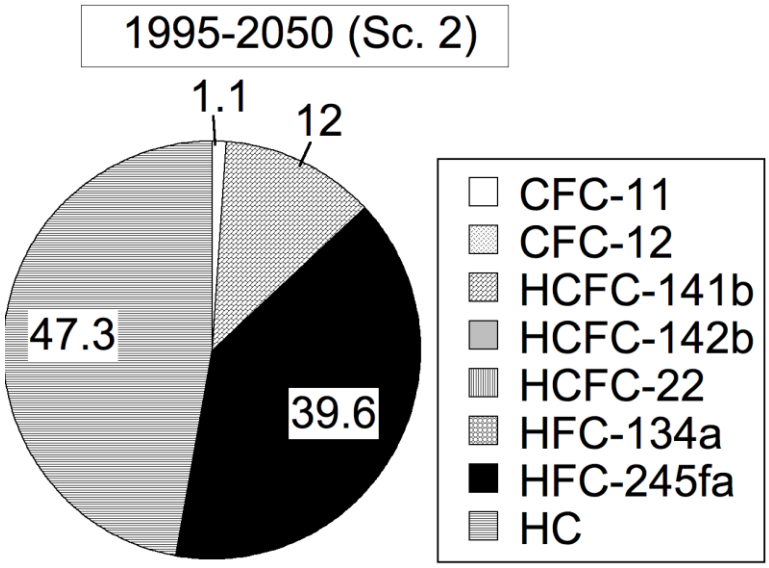


(b) Scenario 2

Figure 2.14. Estimated Volumetric Flows of Marine and Other Waste Foams Containing Different BAs

The volumetric flows were then converted to mass flows and used throughout the calculations for establishing flows associated with the foam waste disposal pathways prior to landfilling. The densities and BA contents used for the previous foam applications also were used for the foam waste from marine and other applications. The volumetric flows presented in Table 2.32b were converted to mass flows using densities of 24.6, 32.2, 39, and 30.7 g/L for foams containing CFC-11, HCFC-141b, HFC-134a, and HFC-245fa, respectively. The BAs remaining in the PUR panel TRU

foams were estimated using the BA contents of 13.3, 11.6, 7, and 11.6% for CFC-11, HCFC-141b, HFC-134a and HFC-245fa, respectively. The total mass flows of the four target BAs are provided in Table 2.33. Mass flow calculations for Scenario 1 demonstrated that CFC-11 was the most dominant BA entering the waste stream (70.2% of total annual mass flow of BA), followed by HCFC-141b (15.8% of total annual mass flow of BA), and HFC-245fa (14% of total annual mass flow of BA). Scenario 2 results indicated large amount of HFC-245fa (74.8% of total annual mass flow of BA) (Table 2.33).

Table 2.33 – Annual Mass Flow of Marine and Other Waste Foams

| Blowing Agent | CFC-11 | | HCFC-141b | | HFC-134a | | HFC-245fa | |
|---|---|---|---|---|---|---|---|---|
| Scenario Number | Sc. 1 | Sc. 2 | Sc. 1 | Sc. 2 | Sc. 1 | Sc. 2 | Sc. 1 | Sc. 2 |
| Mass Flow of BA (tonnes/year) | 151 | 2 | 34 | 30 | 0 | 0 | 30 | 95 |

### 2.7.2 Disposal Pathways for Marine and Other Foam Insulation Waste

First, the current recovery and disposal practices regarding marine/other foam applications assumed that boat hulls had an average 25-30 year life cycle, where the estimated hull retirement rate was 2.0% per year. Additional estimates included the prediction that 5% of canoes were discarded per year, 10% of coolers were discarded per year, and 5% of leisure boats were exported (Caleb 2011).

End of life management pathways for marine and other insulation foams included: 95% of end of life boats and 100% of end of life canoes processed at a facility prior to landfilling; 5% of end of life boats reused or exported; remaining end of life foams (from buoy, cooler, and cold store waste foams) landfilled directly based on data provided in Caleb (2011) and assumptions made by the research team. The pathways in processing facilities included shredding and stockpiling. Transportation time from the site of origin to the processing facility was estimated to be 4 days based on data provided by Wethje (2005). The total combined time for stockpiling at the processing facility and transportation to the landfill was estimated to be 5 days in line with the timeframes identified by Wethje (2005).

### 2.7.3 BA Release Estimates Prior to Landfilling for Marine and Other Foam Insulation Waste

The data and analyses of waste appliance foam stocks and disposal pathways both presented above were coupled to provide estimates for release of the BAs from the end of life management processes for marine and other insulation wastes. Results of the analysis are presented in Table 2.34 and in Figures 2.15 and 2.16 for Scenarios 1 and 2, respectively. The total release of BAs was similar for the four target gases at 30% (Table 2.34). The BA releases were relatively similar for marine/other waste foams containing CFC-11 (14-15%), HCFC-141b (13-14%), and HFC-245fa (14%)

with no releases of HFC-134a. Overall, relatively low percentage of the initial BA content of marine/other waste foam insulation materials were predicted to be released prior to entry to landfill due to the relatively low amount of processing of the end of life foams. High percentages (85-87%) of the initial BAs were banked in the foams entering the landfill for marine/other applications (Figures 2.15 and 2.16.) Total BA emissions prior to entry to the landfill were relatively and were on the order of 25.5 and 15 tonnes/yr for Scenario 1 Scenario 2, respectively (Figures 2.15 and 2.16).

Table 2.34 – Summary of Calculated BA Emissions from Marine and Other Waste Foams

| Disposal Stage | CFC-11 Release (%) | HCFC-141b Release (%) | HFC-134a Release (%) | HFC-245fa Release (%) |
|---|---|---|---|---|
| Reuse | 0 | 0 | 0 | 0 |
| Transportation | 1.2 | 1.1 | 1 | 1.1 |
| Shredding | 24 | 24 | 24 | 24 |
| Stockpiling at Processing Facility | 4.4 | 4.4 | 4.6 | 5 |
| Total Release | 30 | 30 | 30 | 30 |
| Total Release Scaled[1] | 14-15 | 13-14 | 0 | 14 |

[1]The scaled value represents the quotient of the total release and the amount banked in landfill (values for both Scenario 1 and Scenario 2 provided).

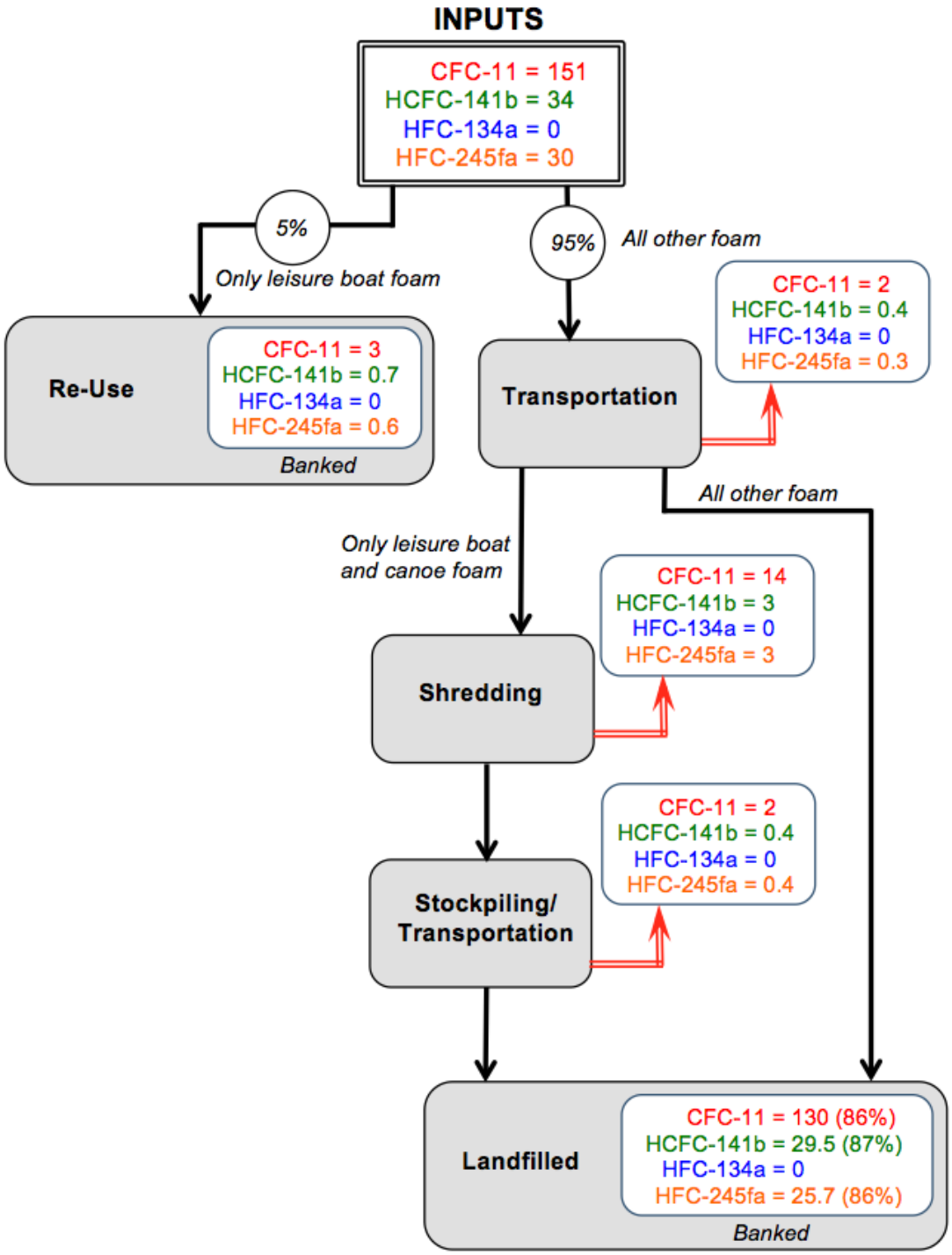


Figure 2.15. Pre-Landfill BA Losses from Marine and Other Foam Insulation Wastes (Tonnes/year) (Scenario 1)

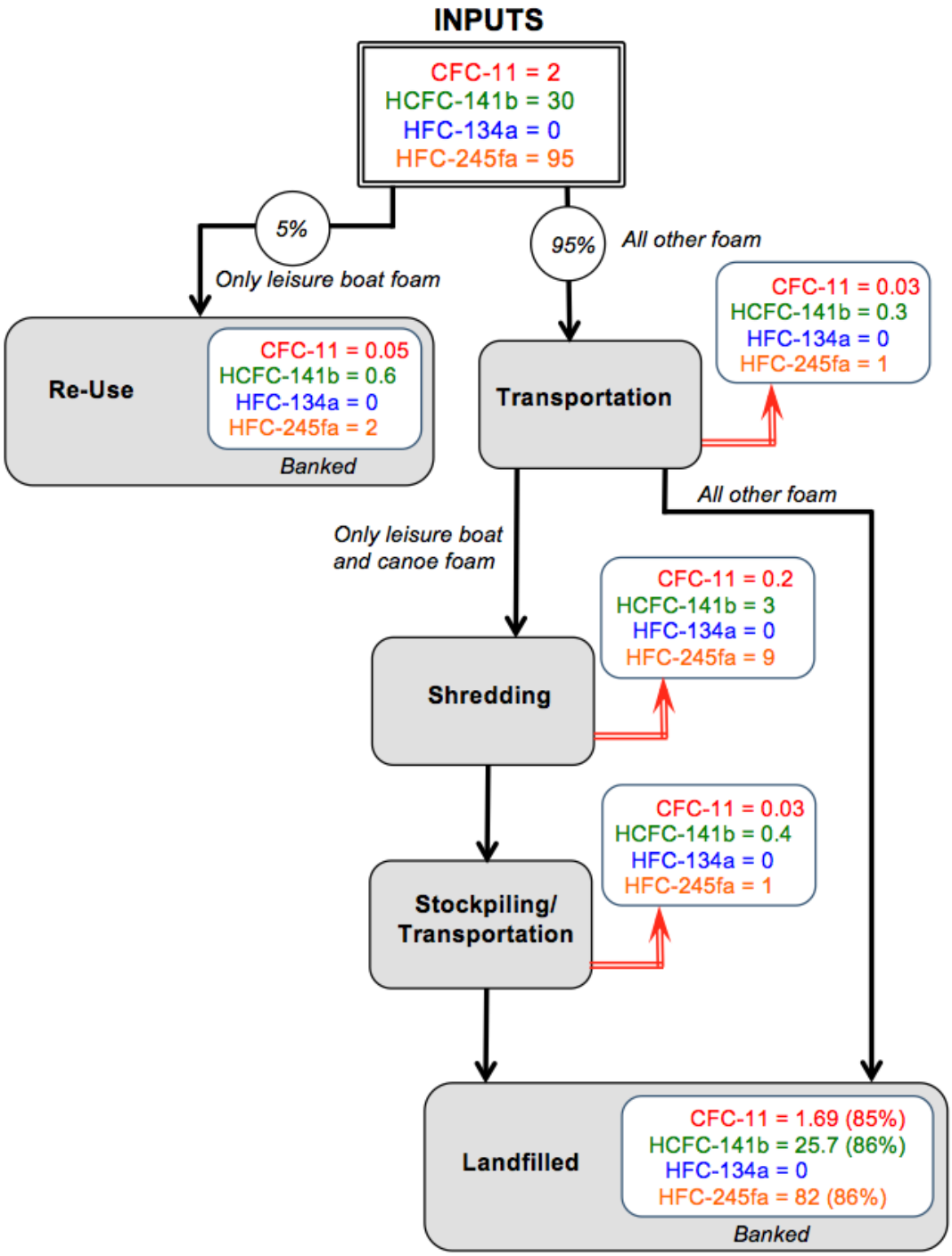


Figure 2.16. Pre-Landfill BA Losses from Marine and Other Foam Insulation Wastes (Tonnes/year) (Scenario 2)

## 2.8 Summary

A summary of the blowing agent flows for the five applications included in the materials flow analysis is provided in Table 2.35. The table includes inputs to the MFA, the amount of landfilled BAs, the BA amounts associated with reuse/recovery applications, and net emissions during the end of life processes prior to entry to landfill systems. In addition, emissions from the stage of the MFA with the highest relative contributions to emissions were identified and included in the table. The percentage contributions of the step with the highest amount of emissions also were provided in Table 2.35.

The inputs (i.e., amount of BAs from end of life waste foams) to the end of life stage of waste foams were high for C&D and appliance (domestic and commercial) wastes and low for TRU, marine, and other foam wastes (Table 2.35). Similarly, emissions from for C&D and appliance (domestic and commercial) wastes were higher than the TRU, marine, and other foam wastes. The emissions during the end of life ranged from 9.71 (TRU waste) to 143.6 (domestic appliance waste) tonnes/yr for Scenario 1 and from 6.16 (TRU waste) to 317.9 (domestic appliance waste) tonnes/yr for Scenario 2. The amount of landfilled BAs followed similar trends and were high for C&D and appliance (domestic and commercial) wastes and low for TRU, marine, and other foam wastes. The highest amount of BA emissions occurred during the shredding stage (77-83%) in the end of life management of rigid waste foams. Reuse and recovery practices used for domestic appliance, TRU, marine, and other foam wastes reduced both BA emissions and landfilled BA amounts. With the exception of domestic appliance waste, the inputs, emissions, and landfilled BA quantities were lower for Scenario 2 compared to Scenario 1 (Table 2.35).

A summary of the flows for each BA type (CFC-11, HCFC-141b, HFC-134a, HFC-245fa) is provided in Table 2.36. The table includes inputs to the MFA, the amount of landfilled BAs, the BA amounts associated with reuse/recovery applications, and net emissions during the end of life processes prior to entry to landfill systems. In addition, emissions from the shredding stage of the MFA were identified in the table.

The various categories in the MFA reflected the historical replacement of the specific BAs. The amount of CFC-11 was higher in Scenario 1 than Scenario 2, whereas the amounts of HCFC-141b, HFC-134a, and HFC-245fa were higher than CFC-11 in Scenario 2. The relative proportions of the BAs in Scenario 2 with respect to Scenario 1 increased as the BA replacements progressed from the HCFCs to the HFCs. The emissions during the end of life ranged from 1.56 (HFC-134a) to 232.05 (CFC-11) tonnes/yr for Scenario 1 and from 0.69 (CFC-11) to 359.2 (HFC-245fa) tonnes/yr for Scenario 2. The landfilled amount of BAs ranged from 10.74 (HFC-134a) to 1148.95 (CFC-11) tonnes/yr for Scenario 1 and from 6.77 (CFC-11) to 1031.8 (HFC-245fa) tonnes/yr for Scenario 2. I,n general, shredding resulted in the largest proportion of the emissions prior to landfilling.

Table 2.35 – Summary of MFA by Application

| Application for Waste Type | Inputs (tonnes/yr) | | Reuse/ Recovery (tonnes/yr) | | Landfilled (tonnes/yr) | | Emissions (tonnes/yr) | | Emissions Contribution (tonnes/yr) | |
|---|---|---|---|---|---|---|---|---|---|---|
| | Sc. 1 | Sc. 2 | Sc. 1 | Sc. 2 | Sc. 1 | Sc. 2 | Sc. 1 | Sc. 2 | Sc. 1 | Sc. 2 |
| C&D Waste | 950 | 579 | 0 | 0 | 873.51 | 534.78 | 76.49 | 44.22 | 28.8 (38%) Decommissioning | 18.1 (41%) Decommissioning |
| Domestic Appliance Waste | 1031 | 2224 | 547.7 | 1179.5 | 339.7 | 726.6 | 143.6 | 317.9 | 113.6 (79%) Shredding | 244 (77%) Shredding |
| Commercial Appliance Waste | 279 | 262 | 0 | 0 | 198.7 | 186.2 | 80.3 | 75.8 | 67 (83%) Shredding | 62 (82%) Shredding |
| TRU Waste | 51 | 29.6 | 13 | 8.1 | 28.29 | 15.34 | 9.71 | 6.16 | 8 (82%) Shredding | 5.1 (83%) Shredding |
| Marine and Other | 215 | 127 | 4.3 | 2.65 | 185.2 | 109.39 | 25.5 | 14.96 | 20 (78%) Shredding | 12.2 (82%) Shredding |
| Total | 2526 | 3221.6 | 565 | 1190.25 | 1625.4 | 1572.31 | 335.6 | 459.04 | 237.4 | 341.4 |

Table 2.36 – Summary of MFA by BA Type

| BA Type | Inputs (tonnes/yr) | | Reuse/ Recovery (tonnes/yr) | | Landfilled (tonnes/yr) | | Emissions (tonnes/yr) | | Shredding Contribution (tonnes/yr) | |
|---|---|---|---|---|---|---|---|---|---|---|
| | Sc. 1 | Sc. 2 | Sc. 1 | Sc. 2 | Sc. 1 | Sc. 2 | Sc. 1 | Sc. 2 | Sc. 1 | Sc. 2 |
| CFC-11 | 1755 | 7.6 | 374 | 0.15 | 1148.95 | 6.77 | 232.05 | 0.69 | 154 (66%) | 0.39 (56%) |
| HCFC-141b | 483 | 639 | 101.7 | 199.6 | 320.14 | 356.15 | 61.16 | 83.25 | 43 (70%) | 64 (77%) |
| HFC-134a | 15 | 200 | 2.7 | 6.5 | 10.74 | 177.6 | 1.56 | 15.9 | 0.8 (51%) | 4 (25%) |
| HFC-245fa | 273 | 2375 | 86.6 | 984 | 145.57 | 1031.8 | 40.83 | 359.2 | 28.9 (71%) | 265 (74%) |
| Total | 2526 | 3221.6 | 565 | 1190.25 | 1625.4 | 1572.32 | 335.6 | 459.04 | 226.7 | 333.39 |

# PART 3 – FIELD INVESTIGATION

## 3.1 Introduction

The main objective of the field investigation was to obtain detailed quantitative data on emissions of the four target (hydro)chlorofluorocarbon blowing agents, CFC-11, HCFC-141b, HFC-134a, and HFC-245fa, from a typical California landfill facility. The field testing program had additional objectives of collecting composite gas samples from the landfill gas extraction and control system to establish characteristics of source gas and to assess the destruction efficiency of the gas control system. The routine testing procedures at the Rowland-Blake Laboratory at the University of California-Irvine (UCI), where the analytical testing was conducted, included determination of concentrations of additional eight (hydro)chlorofluorocarbon gases. The research team decided to include data analysis and interpretation for these additional gases in the report expanding the scope of the investigation. Furthermore, data and analysis are provided for methane and carbon dioxide emissions and destruction efficiency at the test landfill. Methane and carbon dioxide are the main constituent components of landfill gas, whereas the remaining twelve gases analyzed in the project are trace components. Data for methane and carbon dioxide allowed for providing perspective on relative emissions of the trace (hydro)chlorofluorocarbons in relation to the main gases generated at the landfill.

A summary of the basic formulation, main uses, and substitution characteristics for the twelve F-gases included in the field testing program is provided in Table 3.1. While CFC-11, HCFC-141b, HFC-134a, and HFC-245fa are the main chemicals used as blowing agents in rigid foam materials, some of the additional eight gases analyzed also were used as foam blowing agents. A summary of atmospheric properties, concentrations, and atmospheric impact indicators for the fourteen gases included in the field analysis is provided in Table 3.2. The gases analyzed had atmospheric lifetimes varying between 1.5 and 190 years and tropospheric concentrations in the range of 2 ppt to $4x10^8$ ppt. The ozone depleting potential, radiative forcing, and global warming potential ranged from 0 to 1, 0.0003 to 1.66, and 1 to 10,200, respectively. The historical substitution of the old (hydro)chlorofluorocarbons, CFCs, first with transitional chemicals, HCFCs, and later with less harmful formulations, HFCs, all were aimed at reducing atmospheric impacts by moving away from the high global warming potential and ozone depleting materials to substances with low impact. The field test program was designed to quantify emissions and destruction efficiency for a wide variety of (hydro)chlorofluorocarbon compounds both from a historical use perspective as well as representing range of variability at a given time of use.

Overall, the field investigation was conducted to determine the surface emissions of (hydro)chlorofluorocarbons from a landfill system and the destruction efficiency of the landfill gas management system for these gases. To determine surface flux, static flux chamber tests were conducted at multiple locations throughout the site in consideration to different waste ages and cover types present on site. The locations tested had daily, intermediate, and final covers, which were constructed using a wide range of materials including various soils, auto fluff, and green waste. At each location, the static flux chamber tests were conducted at two times in winter/spring and the following summer over the course of a one-year period in order to capture the effects

of seasonal variations. Cover samples, subsurface gas samples, and cover temperature data also were obtained at each testing location to supplement interpretation of surface flux data.

Table 3.1 – (Hydro)chlorofluorocarbons Included in the Test Program

| Name | Chemical Name | Structural Formula | Principal Use[1,2,3,4] | Principal Current Substitute[1] |
|---|---|---|---|---|
| *Compounds already phased out under Montreal Protocol* | | | | |
| CFC-11 | Trichlorofluoromethane | $CCl_3F$ | Foam blowing agent | HCFC-141b |
| CFC-12 | Dichlorodifluoromethane | $CCl_2F_2$ | Refrigerant | HFC-134a |
| CFC-113 | 1,1,2-Trichlorotrifluoroethane | $C_2F_3Cl_3$ | Solvent | Other technology |
| CFC-114 | Dichlorotetrafluoroethane | $CF_3CFCl_2$ | Propellant | Hydrocarbons |
| *Compounds currently being phased out under Montreal Protocol* | | | | |
| HCFC-21 | Dichlorofluoromethane | $CH_2FCl_2$ | Refrigerant blends | HFC blends |
| HCFC-22 | Monochlorodifluoromethane | $CHF_2Cl$ | Refrigerant | HFC blends |
| HCFC-141b | Dichlorofluoroethane | $CH_3CFCl_2$ | Foam blowing agent | HFC-365mfc |
| HCFC-142b | Monochlorodifluoroethane | $CH_3CF_2Cl$ | Foam blowing agent | HFC-365mfc Formacel® TI |
| HCFC-151a | 1,1,-Chlorofluoroethane | $CH_3CHFCl$ | Refrigerant blends, Foams | NA |
| *Alternatives controlled under Kyoto Protocol* | | | | |
| HFC-134a | 1,1,1,2-Tetrafluoroethane | $CH_2FCF_3$ | Refrigerant blends, foams, fire suppressant, and propellant in metered-dose inhalers | NA |
| HFC-152a | Difluoroethane | $CH_3CHF_2$ | Refrigerant blends, foam blowing agent, and aerosol propellant | NA |
| HFC-245fa | 1,1,1,3,3-Pentafluoropropane | $CF_3CH_2CHF_2$ | Foam blowing agent and possible refrigerant in the future | NA |

[1]McCulloch (1999)
[2]USEPA (2010)
[3]UNEP (2006)
[4]USEPA (2014)
NA – Not Applicable

Table 3.2 – Atmospheric Properties and Concentrations of the 14 Study Gases

| Name | Boiling Point at 1 atm[1] (°C) | Atmospheric Lifetime (years)[2,3,4] | Tropospheric Concentration (ppt)[5,6] | ODP[2,3,4] | Radiative Forcing ($W/m^2$)[3] | GWP – 100 years[3] |
|---|---|---|---|---|---|---|
| Carbon Dioxide | -78 | 100 | $3.98 \times 10^{8}$ | 0 | 1.66 | 1 |
| Methane | -164 | 9.1 | $1.80 \times 10^{6}$ | 0 | 0.47 | 28 |
| CFC-11 | 23.8 | 45 | 233 | 1 | 0.07 | 4660 |
| CFC-12 | -29.8 | 100 | 524 | 1 | 0.17 | 10,200 |
| CFC-113 | 48 | 85 | 73 | 0.8 | NA | 5820 |
| CFC-114 | 3.8 | 190 | 16 | 1 | NA | 8590 |
| HCFC-21 | 8.9 | 1.7 | NA | 0.04 | NA | 148 |
| HCFC-22 | -40.6 | 11.9 | 226 | 0.055 | NA | 1760 |
| HCFC-141b | 32 | 9.2 | 23 | 0.11 | 0.04 | 782 |
| HCFC-142b | -9.2 | 17.2 | 22 | 0.065 | 0.003 | 1980 |
| HCFC-151 | 53.2 | NA | 6 | 0.004 | 0.003 | NA |
| HFC-134a | -26.5 | 13.4 | 74 | 0 | NA | 1120 |
| HFC-152a | -25 | 1.5 | NA | 0 | 0.01 | 138 |
| HFC-245fa | 15 | 7.7 | 2 | 0 | 0.0003 | 858 |

[1]ChemSpider (2015)
[2]WMO (2010)
[3]IPCC (2013)
[4]IPCC (2007)
[5]AGAGE (2014)
[6]NOAA (2014)
NA – Not Applicable

### 3.2 Field Test Site

The field test program was conducted at Potrero Hills Landfill (PHL) in Suisun City approximately 60 km northeast of San Francisco and 60 km southwest of Sacramento in Solano County, California (38.21188 Latitude, -121.981 Longitude) (Figure 3.1). The landfill is located in a temperate climate zone that has dry and hot summer (Csa) based on the Koppen-Geiger Climate Classification System (Peel et al. 2007). The field campaigns for the project were conducted in 2013 and 2014. The average daily high temperature, average daily low temperature, and average daily temperature were 23.6, 9.2 and 16.4°C, respectively, at the site during 2013 and 2014 (Wunderground 2015). The average daily precipitation was 1.0 and 1.54 mm for 2013 and 2014, respectively at the site (Wunderground 2015).

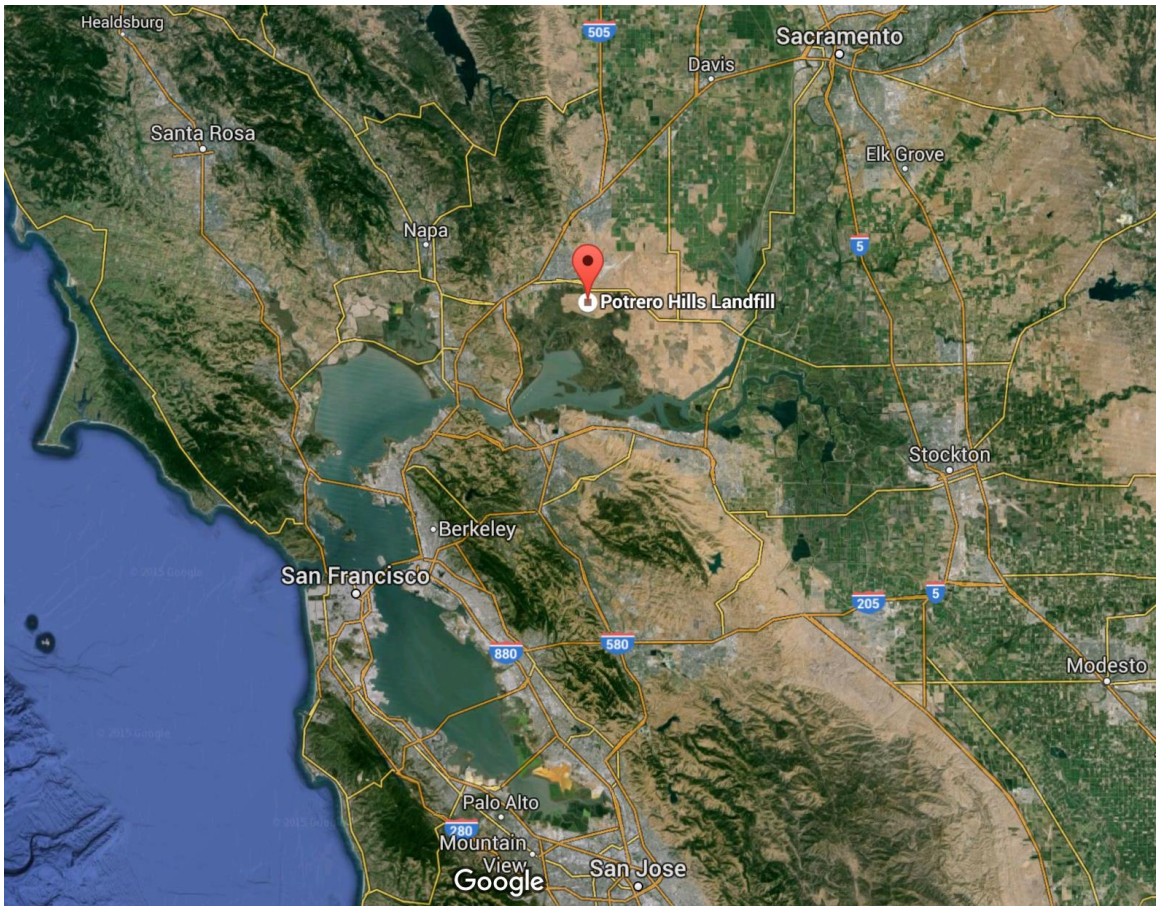


Figure 3.1. Location of Potrero Hills Landfill (Google Earth 2015)

Potrero Hills Landfill (CalRecycle Designation 48-AA-0075) has been in operation since 1987 and is classified as a Class III disposal facility. The site is permitted to accept nonhazardous solid wastes. PHL accepts residential, commercial, construction and demolition, industrial, and agricultural wastes as part of the MSW operations. The landfill also accepts materials that follow special waste handling procedures, which

include ash, septage, sewage sludge, drilling muds, contaminated soils, tires, treated wood waste, auto shred, appliances, and electronic wastes.

The Potrero Hills Landfill site covers 213 hectares in total and the current permitted disposal area is 138 hectares. The facility has a design capacity of 64 million $m^3$ with a maximum elevation limit above existing grade of 105 m and maximum depth limit below existing grade of 39 m. As of April 2014, the volume of waste in place at the site was 19 million $m^3$. The estimated closure date for the facility is 2045. The site has an average daily waste intake of 3,080 tonnes with a maximum permitted throughput of 3,900 tonnes per day. The wastes were either disposed of directly or used as alternative daily covers. In 2013, PHL received approximately 920,000 tonnes of waste, which corresponds to approximately 3% of wastes landfilled in California. The details regarding the type of materials received and breakdown between disposal and daily cover use are provided in Table 3.3. The Potrero Hills Landfill site was selected for this investigation due to several considerations: *i*) medium-high daily disposal capacity, *ii*) substantial amount of C&D wastes received, *iii*) high amount of alternative daily cover (ADC) use, including use of C&D waste and auto fluff, *iv*) presence of appliance waste (not inventoried for foam waste quantities), *v)* presence of different cover types and wastes with different ages, *vi*) operational LFG management system, *vii*) high level of cooperation and assistance from the site management and staff.

Table 3.3 – PHL Tonnage Report by Material for 2013

| Management Method | Material Type | Waste Received (Tonnes) | Relative Amount of Material Type (%) | % Total |
|---|---|---|---|---|
| Disposal | C&D Waste | 41,227 | 9 | 5 |
| | Soil | 22,771 | 5 | 2 |
| | Sewage Sludge | 16 | 0 | 0 |
| | Auto Fluff | 0 | 0 | 0 |
| | Green Waste | 5,170 | 1 | 1 |
| | MSW | 364,575 | 83 | 40 |
| | Miscellaneous | 4,750 | 1 | 1 |
| Total (Disposal Only) | | 438,509 | 100 | 48 |
| Cover | C&D Waste | 107,030 | 22 | 12 |
| | Soil | 253,817 | 53 | 28 |
| | Sewage Sludge | 58,901 | 12 | 6 |
| | Auto Fluff | 43,974 | 9 | 5 |
| | Green Waste | 13,379 | 3 | 1 |
| Total (Cover Only) | | 477,101 | 100 | 52 |
| Total Waste Received (Disposal and Cover) | | 915,610 | | 100 |

### 3.3 Field Test Program Design

The field test program was designed with three specific objectives to obtain representative emissions data from the test site as a function of the main factors that control gas emissions from landfill sites:

- Obtain data from all cover types including daily, interim, and final covers to assess effects of cover type on emissions
- Obtain data from locations underlain with wastes of varying ages to assess effects of waste age on emissions
- Obtain data over different seasons to assess effects of climatic conditions on emissions

A total of 7 locations with varying cover types and waste ages were selected for the field test program. The cover types consisted of daily cover (3 locations), interim cover (3 locations) and final cover (1 location). The daily covers included green waste (GW), auto fluff (AF), and extended daily cover (ED), which consisted of a soil material. All of the daily cover test locations were in Cell 12 at the site, which was the active waste disposal area during the field test program. The interim covers (ICs) tested were all constructed of soil. The interim cover test locations were in Cell 1 (IC-1), Cell 10 (IC-10), and Cell 15 (IC-15). The final cover (FC) location used for the test program was in Cell 1. The test locations were selected to include relatively flat areas in order to ensure proper installation of the measurement systems (i.e., static flux chambers). The selection of the specific test cells allowed for comparisons between the different materials used for a given cover type (e.g., materials used for daily cover) as well as between the different cover types (e.g., intermediate versus final cover). Gas extraction systems were installed at all of the cells that were included in the field test program. Details regarding the landfill cells included in the test program are provided in Table 3.4. The relative locations of the test cells at Potrero Hills Landfill are presented in Figure 3.2.

The tests were conducted in both wet and dry seasons to capture the main climatic conditions in California. The tests for wet season were conducted in February, March, and April 2014, whereas the tests for dry season were conducted in August 2014. The specific dates and detailed weather conditions, obtained from Wunderground (2015), during the field test program are provided in Table 3.5.

Table 3.4 – Landfill Cell Details

| Cell Number | Area Hectares (Acre) | Waste Height (m) | Average Waste Age (year)[1] | Description |
|---|---|---|---|---|
| 1 | 1.9 (4.6) | 17.7[2] / 18.1[3] | 22.6[2] / 21.5[3] | • Constructed prior to implementation of Subtitle D.<br>• Low permeability soil liner and leachate and collection system.<br>• Bottom liner construction completed in September 1985 and was last filled in 1997. |
| 10 | 3.6 (8.8) | 16.2 | 14.0 | • Constructed after implementation of Subtitle D<br>• Bottom liner construction completed in July 1995 and was last filled in 2006.<br>• Cell 10 is lined and has a leachate and gas collection system.<br>• Filling procedure started in September 1985 and was last filled in 1997. |
| 12-North | 2.4 (6.0) | 49.0[4] / 53.7[5] | 9.5[4] / 5.2[5] | • Constructed after implementation of Subtitle D<br>• Bottom liner construction completed in October 1998 and is currently active.<br>• Cell 12 is lined and has a leachate and gas collection system. |
| 15 | 4.5 (11.3) | 36.3 | 9.2 | • Constructed after implementation of Subtitle D<br>• Bottom liner construction completed in January 2005 and was last filled in 2011.<br>• Cell 15 is lined and has a leachate and gas collection system. |

[1]The waste age was determined using historic annual topographic survey files provided by PHL
[2]The waste height and age for the intermediate cover location in Cell 1
[3]The waste height and age for the final cover location in Cell 1
[4]The waste height and age where GW cover was tested during wet season in Cell 12
[5]The waste height and age where AF and ED covers were tested during wet season and AF, GW, and ED covers were tested over dry season

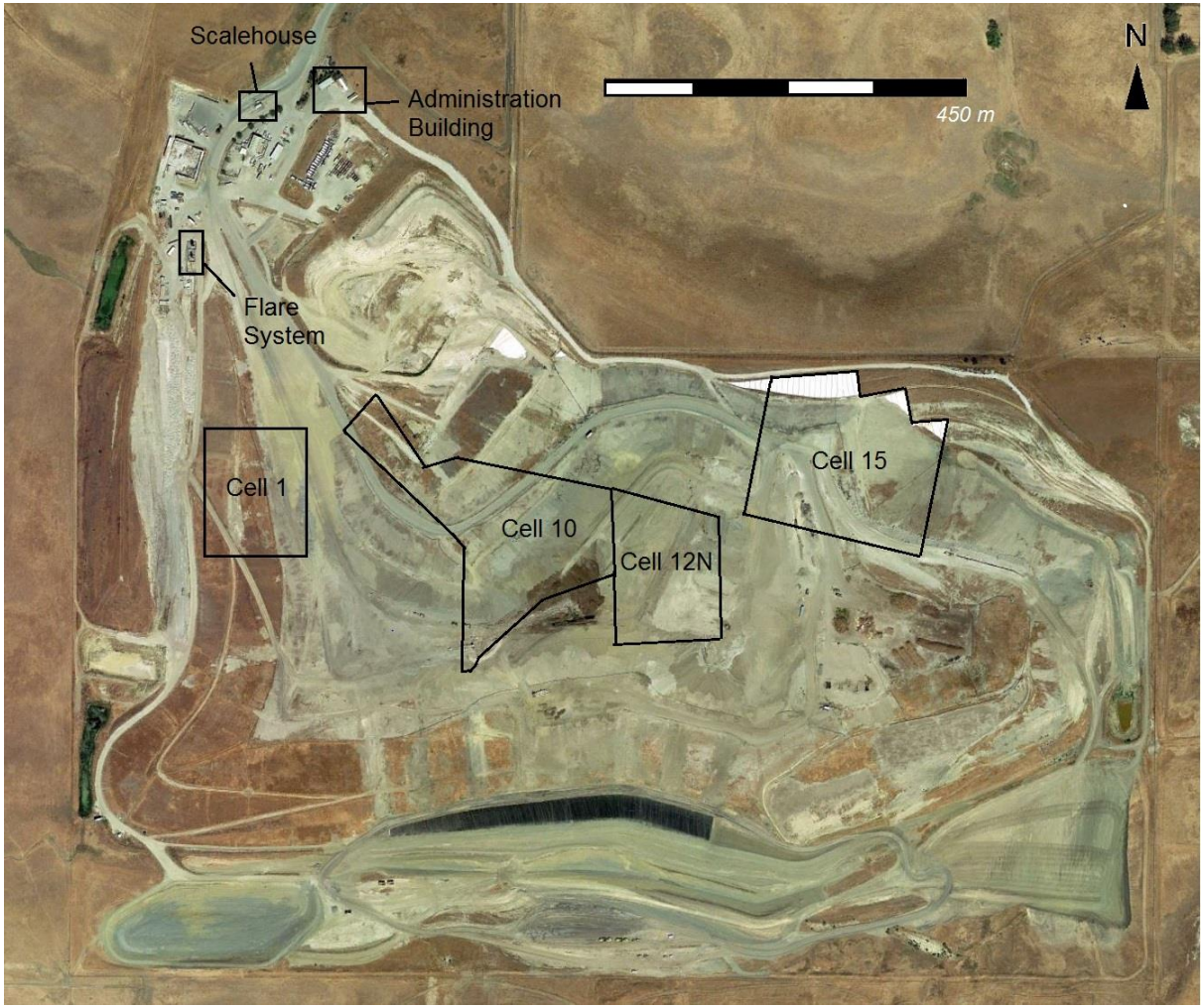


Figure 3. 2. Test Cell Locations at the Potrero Hills Landfill (Google Earth 2015)

Table 3.5 – Test Dates and Climatic Data

| Date | Season | Cover Type Tested | Barometric Pressure (hPa) | Min/Max Temperature (°C) | Average Temperature (°C) | Precipitation (mm) | Total Precipitation during Previous 7 days (mm) | Average Wind Speed (kph) and Direction |
|---|---|---|---|---|---|---|---|---|
| February 7, 2014 | Wet | GW | 1017 | 7.8 / 11.7 | 10.0 | 19.3 | 37.6 | 19.3 (SE) |
| March 28, 2014 | Wet | IC-10, IC-15 | 1020 | 10.0 / 16.7 | 13.3 | 18.0 | 19.3 | 14.5 (SW) |
| March 29, 2014 | Wet | IC-1 | 1017 | 9.4 / 14.4 | 13.3 | 11.7 | 1.22 | 16.1 (SSW) |
| March 30, 2014 | Wet | FC | 1019 | 6.1 / 16.7 | 11.1 | 0 | 1.22 | 17.7 (SW) |
| April 18, 2014 | Wet | AF, ED | 1012 | 10.6 / 23.3 | 16.7 | 0 | 0 | 19.3 (SW) |
| August 8, 2014 | Dry | AF, GW, ED | 1012 | 14.4 / 32.2 | 22.8 | 0 | 0.25 | 32.2 (SW) |
| August 9, 2014 | Dry | IC-10, IC-15 | 1012 | 13.9 / 26.7 | 20.6 | 0 | 0.25 | 38.6 (SW) |
| August 10, 2014 | Dry | IC-1, FC | 1013 | 13.9 / 27.8 | 20.6 | 0 | 0.25 | 35.4 (WSW) |

In the field test program, two different sampling intervals were used as presented in Tables 3.6 and 3.7. At a given location, a total of four static flux chambers were used for testing. The four chambers were designated A through D in the test program. Sampling intervals outlined in Table 3.6 were used for the first two field visits (February and March, 2014). Based on the analysis of the concentration data obtained from the February 2014 tests, the sampling intervals were modified as presented in Table 3.7 for the remainder of the field test program. The modification allowed for obtaining two additional reliable flux values, since the data from Chambers C and D were previously included only two points. At each test location, a total of 16 gas samples were obtained from the Chambers A through D. In addition, a subsurface gas sample was obtained subsequent to emissions data collection from each chamber location. Therefore, in total, 20 gas samples were obtained at each test location in a given season. Overall, a total of 280 gas samples were obtained from the static flux chambers over the duration of the field investigation for the two testing seasons.

Table 3.6 – Field Test Schedule During Wet Season with the Exception of Data Collection from AF and ED Covers

| Chamber | Elapsed Time (min) | | | | | | | |
|---|---|---|---|---|---|---|---|---|
| A | 0 | 7 | 15 | 30 | 60 | - | 120 | - |
| B | 0 | - | - | 30 | 60 | 90 | 120 | 150 |
| C | 0 | - | - | - | 60 | - | - | - |
| D | 0 | - | - | - | - | - | 120 | - |

- No data collection

Table 3.7 – Field Test Schedule During Dry Season and for AF and ED Covers in Wet Season

| Chamber | Elapsed Time (min) | | | | | | |
|---|---|---|---|---|---|---|---|
| A | 0 | 7 | 15 | 30 | 60 | - | - |
| B | 0 | - | - | 30 | 60 | 90 | 120 |
| C | 0 | - | - | 30 | 60 | - | - |
| D | 0 | - | - | - | 60 | - | 120 |

- No data collection

### 3.4 Field Test Methods

The field measurements conducted at PHL to obtain emissions and destruction efficiency data for the fourteen gases included static flux chamber tests and direct gas sampling. The flux chamber tests were conducted on the surface of the landfill cells capped with different cover materials. The direct gas sampling was conducted up and downstream of the gas management system at the site. The gas samples were analyzed at UCI to determine gas concentrations. In addition, extensive supplemental

laboratory testing was conducted to evaluate properties of the cover materials used at the site to support mechanistic explanations of the observed gas emissions behavior.

### 3.4.1 Static Flux Chamber Method

The field emission measurements at PHL were obtained using the static flux chamber method. Surface gas emissions from landfills can be determined using small to large-scale direct and indirect measurement approaches applied on a continuous or discrete basis. Point, line, and areal measurements can be made. The test methods can be used to estimate flux and/or concentration of target gases. The majority of the testing techniques provide concentration data and require the use of analytical or numerical models to estimate flux. The only method that can be used to directly determine flux (negative or positive) is the flux chamber method. This method was selected for the project to obtain representative estimates of the gas emissions from PHL.

The static chamber technique is based on establishing a sealed volume above the measurement surface where gas is emitted through (or gas is absorbed through) such that the gas cannot escape and its accumulation (or depletion) in the volume can be monitored. The large-scale flux chambers used in the test program were constructed of stainless steel square collars and square lids. The nominal dimensions of the collar were 1 m x 1 m with a measurement area of 1 $m^2$. For conducting a measurement: first the collar was inserted into the landfill surface to a depth of approximately 50 mm; then a bentonite-water paste was applied around the perimeter of the collar at the soil-collar interface to seal the interface against gas leakage; next the lid was placed and secured over the collar to form an air-tight seal; and finally a fan installed on the underside of the lid (i.e., inside the sealed chamber) was turned on to start mixing the gas accumulating in the chamber. A generator, which was placed 30 m downwind from the chambers, was used to power the fans. A photograph of an assembled flux chamber is presented in Figure 3.3.

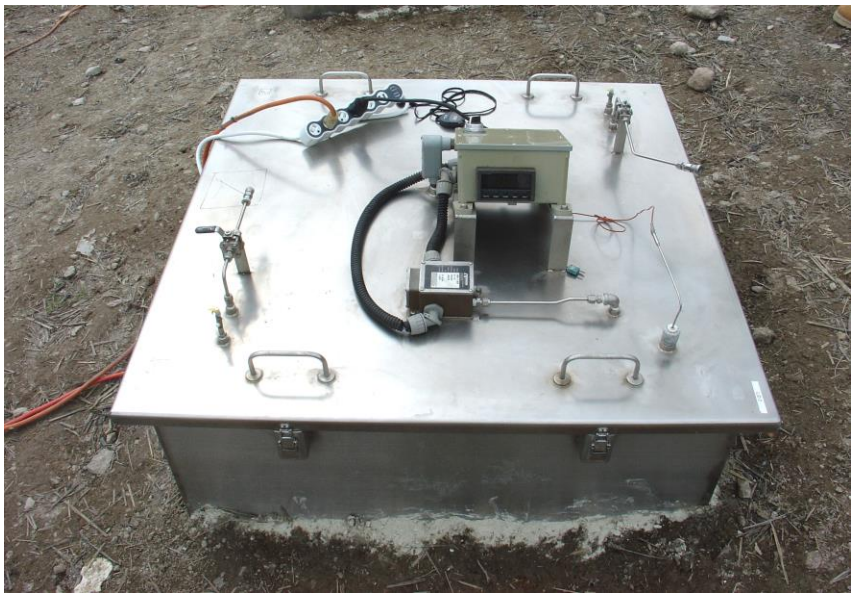

Figure 3.3. Static Flux Chambers Used in the Field Test Program

Gas samples were obtained from the chamber during a sampling event by connecting gas canisters to sampling ports installed on the lid of the chambers (Figure 3.4). The gas samples were obtained using 2-L evacuated stainless steel canisters equipped with bellow valves. The sampling ports consisted of ball valves, stainless steel tubing, and a Swagelok stainless steel Ultra-Torr vacuum fitting. For sampling, the valves were opened in the following order: the ball valve then the bellow valve. The valves were left open for approximately 10 seconds until the canister was full. Then, the valves were closed in the reverse order they were opened. This order was followed for opening and closing the valves to minimize contamination of the gas samples. The canister was then removed from the sampling port and was stored in a weather-proof box. The gas samples were collected using the pre-established schedule of sampling intervals (Tables 3.6 and 3.7). The start time of an individual sampling event was established as the time of the sealing of the lid/starting of the fan on the lid. A total of four flux chambers were used in the test program to obtain four measurements at each test location (Figure 3.5).


a) Gas being Sampled using 2-L Canister

b) Swagelok Gas Sampling Port

Figure 3.4. Gas Sampling

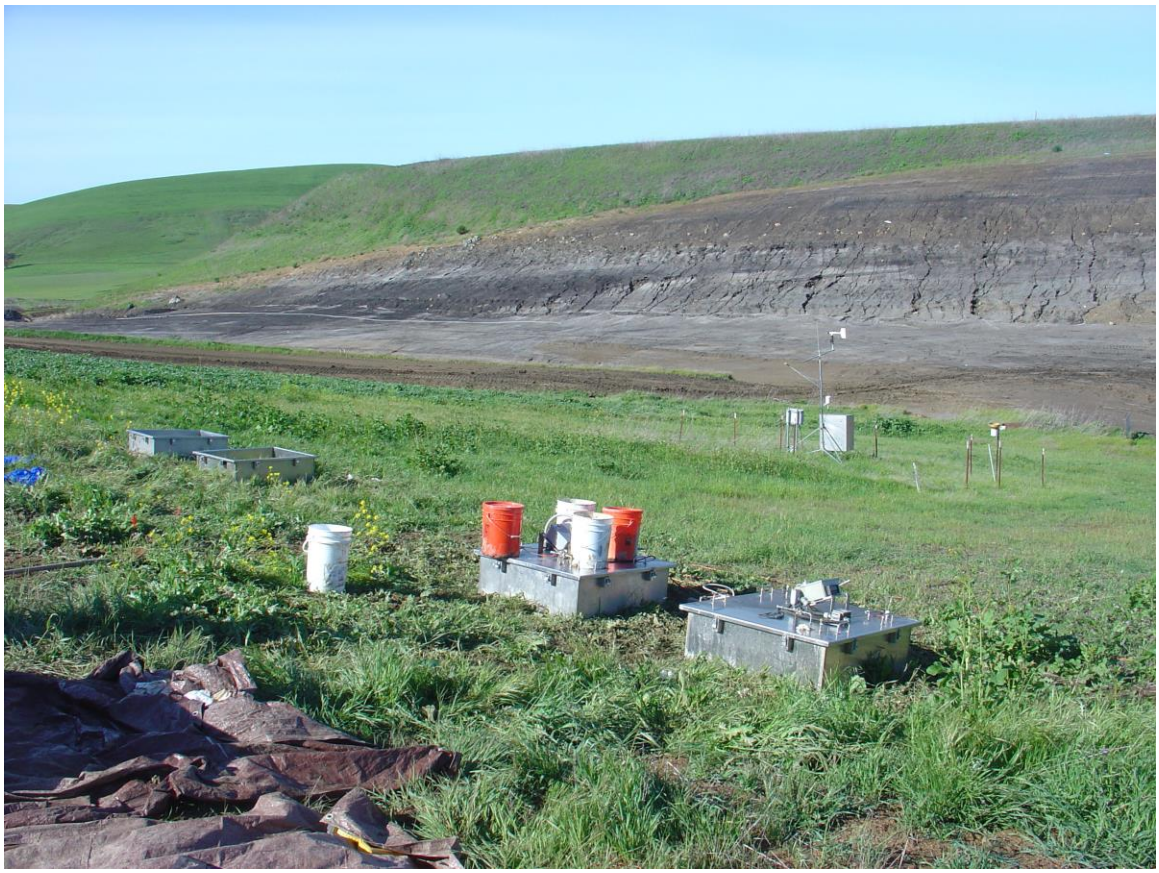

Figure 3.5. Four Flux Chambers at a Given Measurement Location

### 3.4.2 Landfill Gas Management System Sampling

The gas management system at Potrero Hills Landfill consists of a gas collection system and a flare. The gas collection system includes a network of vertical gas extraction wells and horizontal gas conveyance pipes. The LFG collected is transported to a high-temperature flare, where the gas is combusted. The flare operates at a temperature of approximately 930°C and combusts LFG with methane content ranging from approximately 40 to 60% (% v/v) throughout the year. The flare has a height of 12 m and a diameter of 3 m.

Raw gas (i.e., inflow) and post-combustion (i.e., outflow) samples were obtained from the flare to assess the destruction efficiency of the system. Raw LFG samples were obtained from the flare header at a location 10 m away from the inlet to the flare system. A Swagelok stainless steel Ultra-Torr tee vacuum fitting with a 0.3-m-long stainless steel tube was used to connect the stainless steel sampling canister (2-L capacity) to the sampling port as presented in Figure 3.6. The sampling port attached to the header consisted of a ball valve and a flexible PVC tube. The PVC extension from the Swagelok fitting was attached to the PVC tube prior to opening the bellow valve on the stainless steel canister. When all the connections were secured, the ball valve on the sampling port was opened to purge any ambient air present in the sampling connection. Subsequently, the bellow valve on the canister was opened for

approximately 10 seconds until the canister was full. A total of six raw LFG samples was taken during the field investigation.

Figure 3.6. Raw Gas Sampling

The post-combustion gas samples were obtained from a sampling port located at a height of 10.5 m (1.5 m below the top of the flare). The sampling port was accessed using a boom lift (Figure 3.7). The gas was sampled from a point 0.65 m radially inward from the outer wall using a 1.5-mm inner-diameter stainless steel tubing. The tubing was coiled and then passed through an ice bath to decrease the volume of the gas Figure 3.8a. The stainless steel tubing exiting the ice bath was connected to a 0.3-m-long stainless steel tube with a Swagelok stainless steel Ultra-Torr tee vacuum fitting. A stainless steel canister with 2-L capacity was attached to one end of the tee fitting while the other end was connected to a 0.3-m long stainless steel tube and a flexible PVC tube extension to a 60-mL syringe. The fully assembled sampling connection is presented in Figure 3.8b. The syringe was used to remove any ambient air present in the stainless steel coil prior to the sampling. Two full draws of the syringe were applied to the coil prior to beginning of sampling. Subsequently, the bellow valve on the canister was opened for 20 to 30 seconds until the canister was full. A total of three post-combustion gas samples were obtained.

Figure 3.7. Flare Sampling

(a) Ice Bath

(b) Sampling Assembly

Figure 3.8. Details of Flare Sampling

### 3.4.3 Additional Field Tests

Field tests, in addition to emission and destruction efficiency analysis, were conducted to supplement interpretation of the main test program. These additional tests included subsurface gas sampling, determination of cover temperatures, determination of in-situ cover properties, and collection of cover material samples for laboratory analysis. After the last scheduled sample was retrieved from a given chamber, the lid was removed and a 6-mm-diameter, 0.3-m-long stainless steel tube was inserted to an approximate depth of 0.1 m in the cover material. Moist bentonite was applied around the tube to prevent leakage. A gas canister was connected to the tube and a gas sample was collected from each chamber. Also, the height of the collars was measured at midpoint along each side for use in calculation of the chamber volume. In addition, the temperature of the tested cover material was measured at three different points within the perimeter of the chamber using a rigid thermocouple probe that was inserted approximately 50 mm into the cover material. Furthermore, sand cone tests in accordance with ASTM D1556 were conducted at each chamber location to determine density of the cover materials (Figure 3.9). Finally, cover samples were obtained from each chamber location for laboratory analysis with the mass of samples ranging from 100 to 2000 g depending on the cover material.

Figure 3.9. Sand Cone Test

Temperatures at the time of flux chamber tests and long-term variation of cover temperatures were evaluated in further field tests. Temperature measurement arrays were installed within the intermediate cover in Cell 15 (at a position near the flux chamber test locations) and the intermediate cover in Cell 17. The temperatures were measured using Type K thermocouples. The arrays with multiple thermocouples extended to 0.65 and 0.80 m depths below the ground surface into the covers in Cells 15 and 17, respectively. Photographs of hand augering to install a temperature array and retrieval of temperature data from datalogger are presented in Figure 3.10.

a) Hand Augering b) Temperature Data Retrieval

Figure 3.10. Field Temperature Measurement

### 3.5 Analytical Testing

The gas samples obtained in the field tests were analyzed at Rowland-Blake Laboratory in the Chemistry Department at the University of California-Irvine (Figure 3.11). The laboratory has high-resolution analysis systems capable of identifying and quantifying over 100 non-methane hydrocarbons and halocarbons including the (hydro)chlorofluorocarbons investigated in the current study. The laboratory is equipped with two VOC analytical systems, each of which consists of 3 Agilent 6890 gas chromatographs that house 2 electron capture detectors, 3 flame ionization detectors, and a quadrupole mass spectrometer. This laboratory was selected for the project due to the unique analytical systems in quantifying air samples for concentrations in the parts per billion to parts per quadrillion range (Colman et al. 2001, Blake et al. 2003, Zhang et al. 2006, Barletta et al. 2006, 2011).

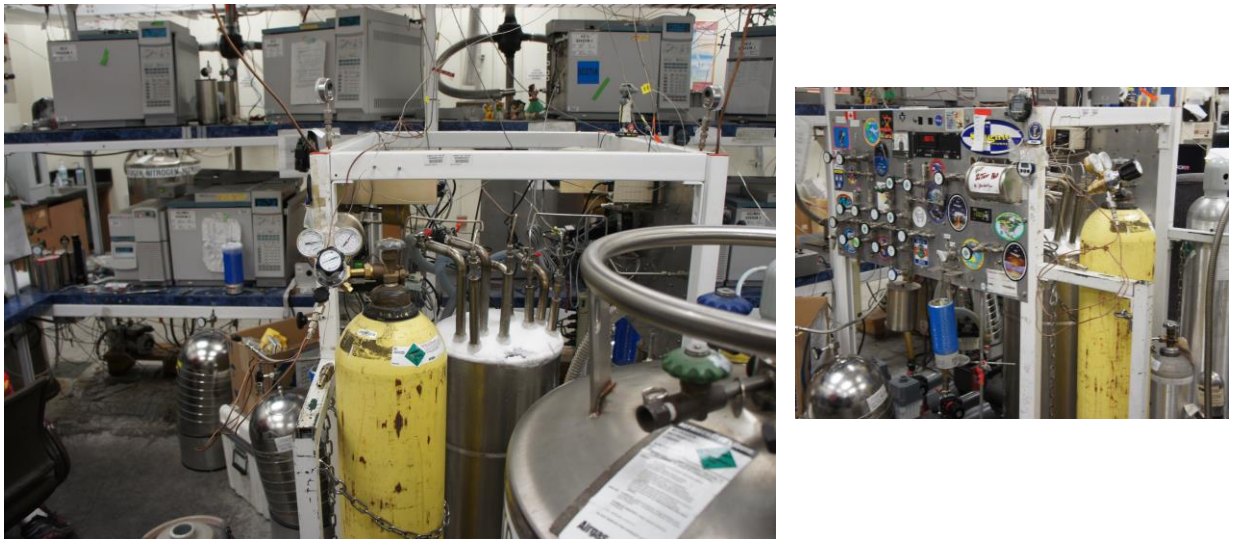

Figure 3.11. Analytical Testing Systems at University of California-Irvine

For analysis of the gas samples obtained in the study, the amount of gas trapped from the canisters ranged between 1100-1150 $cm^3$ (at standard temperature and pressure). This gas was introduced into the analytical system's manifold and then passed over glass beads contained in a loop and maintained at liquid nitrogen temperature. The flow was regulated by a Brooks Instrument mass flow controller (model 5850E), and was kept below 500 $cm^3$/min to ensure complete trapping of the relevant components. This procedure pre-concentrated the relatively less volatile components of the sample (such as halocarbons and hydrocarbons) while allowing more volatile components (such as $N_2$, $O_2$, and Ar) to be pumped away. The less volatile compounds were next re-volatilized by immersing the loop containing the beads in hot water (80°C), and then flushed into a helium carrier flow (head pressure 330 kPa). This sample flow was then split into six streams. Each stream was chromatographically separated on an individual column and sensed by a single detector. Three GCs (each HP 6890) form the core of the analytical system. The research group uses two ECDs (sensitive to halocarbons and alkyl nitrates), two FIDs (sensitive to hydrocarbons), and one quadrupole MSD (for unambiguous compound identification and selected ion monitoring). The output signal was captured using Dionex software. Each resulting chromatogram was inspected, and each peak shape individually checked. This type of quality control is very important for datasets of large sizes, because a slight change in retention time or peak shape can cause problems for automated quantification.

Calibration and measurement intercomparisons are conducted on a continuous basis. Calibration is an ongoing process, whereby new standards are referenced to older certified standards, with appropriate checks for stability, and also with occasional inter-laboratory comparisons. Multiple standards are employed, including working standards that are analyzed every four samples and absolute standards that are analyzed twice daily. The UCI research group regularly collects and calibrates pressurized cylinders of air from different environments for use as working standards. The primary reference standard for halocarbons was previously calibrated from static dilutions of standards prepared in the laboratory. Its absolute accuracy is tied to a manometer measurement and how accurately the appropriate volume ratios for the dilution line used are known. For hydrocarbons, the research group uses a National Bureau of Standards propane standard (SRM 1660A) to calculate a Per-Carbon-Response-Factor (PCRF) for the FIDs. This is compared to PCRFs calculated from more readily available commercial standards to check the absolute accuracy of the commercial standard, as well as the appropriateness of using the same PCRF for different compounds. The research group had cross-checked their calibration scheme against absolute standards from other groups for both hydrocarbons and halocarbons. In addition, the group has participated in the Non-Methane Hydrocarbon Intercomparison Experiment (NOMHICE). The results of this experiment demonstrate that the group's analytical procedures consistently yield accurate identification of a wide range of unknown hydrocarbons and produce excellent quantitative results. The typical absolute accuracy is estimated to be 2-10%, and up to 30% for some compounds, increasing as the detection limits are approached (Colman et al. 2001). The researchers impose a conservative limit of detection (LOD) of 3 pptv on the NMHCs. The halocarbon LOD varies by compound, from 0.01 pptv for chlorobrominated species (e.g., $CHBrCl_2$,

$CHBr_2Cl$, $CH_2BrCl$) to 10 pptv for CFC-12. Once the samples are assayed, the stored chromatograms are individually inspected and the reports from these are then summarized in spreadsheet format and checked for inconsistencies. The specific LODs for the chemicals included in the test program are presented in Table 3.8.

Table 3.8 – Limit of Detection for Chemicals Included in the Test Program

| Compound | LOD Range |
|---|---|
| CFC-11 | 5 - 20 pptv |
| CFC-12 | 5 - 20 pptv |
| CFC-113 | 5 - 20 pptv |
| CFC-114 | 5 pptv |
| HCFC-21 | 5 - 20 pptv |
| HCFC-22 | 5- 50 pptv |
| HCFC-141b | 5 - 10 pptv |
| HCFC-142b | 5 - 10 pptv |
| HCFC-151a | 5 - 20 pptv |
| HFC-134a | 5 - 60 pptv |
| HFC-152a | 5 - 10 pptv |
| HFC-245fa | 1 - 5 pptv |
| $CH_4$ | 10 - 100 ppbv |
| $CO_2$ | 3 - 100 ppmv |

**3.6 Laboratory Investigation**

Laboratory tests were conducted on samples of the different cover materials that were included in the field investigation. Geotechnical tests were conducted to determine moisture content, specific gravity, and particle size distribution of the cover materials to supplement the interpretation of the surface flux data.

The moisture content of the cover materials were determined using procedures described in ASTM D2216. For each material, samples with masses in the range of 200 to 600 g were used. Larger quantities of samples were required for materials with larger particle sizes to obtain representative measurements.

The specific gravity of the landfill cover samples were determined using ASTM D854 for the soil specimens. The standard procedure was modified for testing cover materials with relatively large particle sizes. The specific gravity test setup used for soils is presented in Figure 3.12a. For materials with large particle sizes, the method outlined in Yesiller et al. (2014) generally was followed. During the addition of the specimen to the 2000-mL Erlyenmeyer Flask, a screen was placed on top of the specimen to ensure full submersion of all the materials as presented in Figure 3.12b. The Erlenmeyer flask was calibrated with the screen to ensure representative measurements. In addition, the specimen was placed under vacuum for 3 hours with

periodic taps to the bottom of the Erlenmeyer flask at 10-minute intervals to ensure complete deairing of the specimen. After the mixture was fully deaired, the remaining headspace was filled with deaired, deionized water to the calibration line and the assembled setup was placed into a temperature controlled container to equilibrate for 24 hours. The mass of the volumetric flask and the temperature of the water inside were recorded after reaching equilibrium, which was used to determine the specific gravity using the methodology provided in ASTM D854.

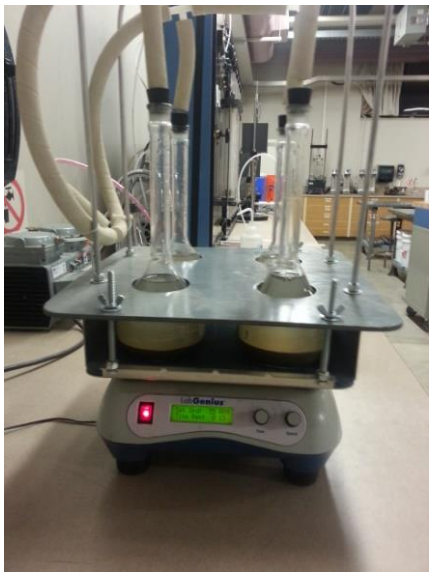

(a) Soil

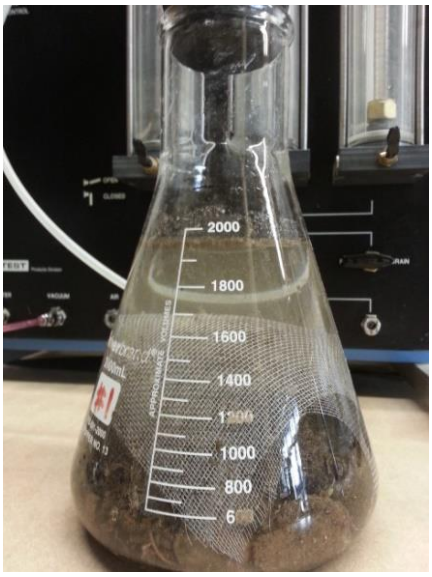


(b) Large Particle Size Materials

Figure 3.12. Specific Gravity Tests

Dry sieve analysis was performed to determine the particle size distribution of the soil specimens using ASTM D422. The particles size distribution of the fine fraction of the soil specimens were determined using hydrometer analysis in accordance with ASTM D422. The particle size distribution characteristics of the soils were used to classify the soils based on the Unified Soil Classification System (USCS) and the United States Department of Agriculture (USDA) soil classification system.

### 3.7 Field Test Location Details

The different types of covers used at the test site had variable thicknesses ranging from 26 to over 122 cm, with increasing thicknesses from daily to intermediate to final covers (Figure 3.13, Table 3.9). The cover soils ranged from coarse- to fine-grained soils (Figure 3.13, Table 3.10). The soil sample from ED location was classified as poorly-graded gravel with clay and sand with a high gravel fraction (54.3%). The soil samples from IC-10 and IC-15 were identified as clayey sand with gravel with high sand fraction (58.8% and 51.5%, respectively). The soil samples from IC-1 and FC were identified as fat clay with high fines fraction (99.6% for intermediate cover and 72.6% for final cover). The FC soil sample also had significant amount of gravel.

The geotechnical properties of the cover materials varied between the seven locations (Table 3.10). The auto fluff and green waste covers had relatively low specific gravity values, 1.48 and 1.42, respectively. In comparison, the specific gravities of the soil covers were considerably higher ranging from 2.62 to 2.77. The dry density also varied between the cover materials ranging from 266 to 1764 kg/m$^3$. The density of the green waste during the wet season could not be determined due to heavy precipitation during the sand cone test. The dry densities of the auto fluff and green waste covers were low ranging from 266 to 597 kg/m$^3$, whereas the dry densities of the soil covers ranged from 1076 to 1794 kg/m$^3$. The moisture contents and degrees of saturation of the cover materials were higher during the wet season than the dry season. In the wet season, the moisture contents varied between 9 and 24% with the exception of the green waste, which had a moisture content of 129%, whereas the moisture contents were lower than 13% in the dry season for all cover materials. Even though the degree of saturation values were higher in the wet season than the dry season, the cover materials remained unsaturated during the entire testing program. The porosity and void ratio increased with increasing fines content in the soil covers. These two parameters were high for the alternative daily covers, auto fluff and green waste. In general, the porosity and void ratio were not affected by season (Table 3.10).

Operational records and data at the test site were investigated to identify waste placement schedule at the site. A schematic presenting the thickness of waste layers and associated waste ages at the seven test locations at the site are provided in Figure 3.14. The daily covers and IC-15 were underlain by relatively young wastes (0 to 4 years), whereas IC-1 and FC were underlain by old waste (14 to 29 years). IC-10 was placed over wastes with intermediate ages (4 to 14 years).

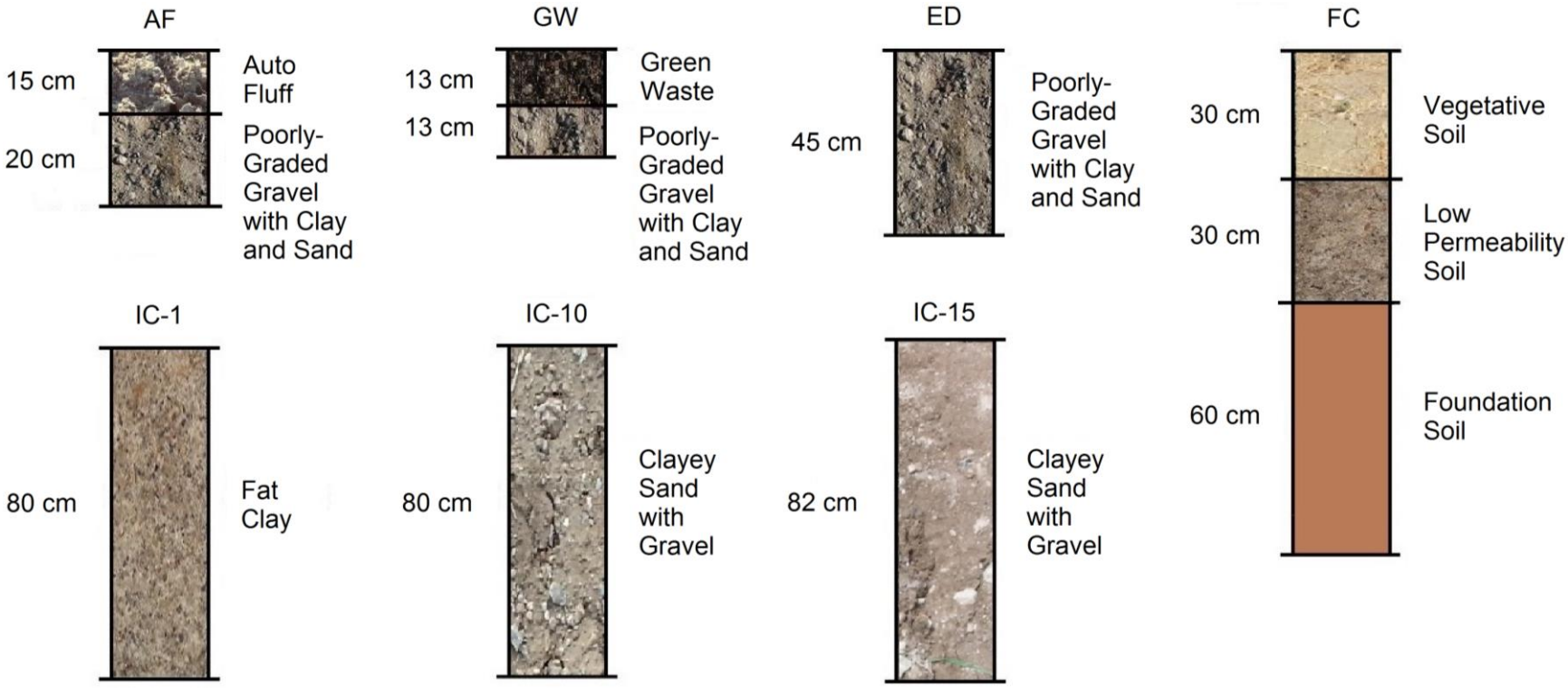


Figure 3.13. Cover Profiles at Potrero Hills Landfill

Table 3.9 – Cover Material Classification and Thickness

| Cover | Material | USCS Particle Size Distribution | | | Group Symbol | USCS Group Name | USDA Classification | Cover Thickness |
|---|---|---|---|---|---|---|---|---|
| | | Gravel (%) | Sand (%) | Fines (Silt and Clay) (%) | | | | |
| AF | Auto Fluff | N/A | N/A | N/A | N/A | N/A | N/A | 15 cm auto fluff and 20 cm soil |
| GW | Green Waste | N/A | N/A | N/A | N/A | N/A | N/A | 13 cm green waste and 13 cm soil |
| ED | Soil | 54.3 | 39.7 | 6.0 | GP-GC | Poorly-graded gravel with clay and sand | Loamy Sand | 45 cm |
| IC-1 | Soil | 0.0 | 0.4 | 99.6 | CH | Fat clay | Clay | 80 cm |
| IC-10 | Soil | 15.6 | 58.8 | 36.9 | SC | Clayey sand with gravel | Sandy Loam | 80 cm |
| IC-15 | Soil | 22.6 | 51.5 | 25.9 | SC | Clayey sand with gravel | Sandy Loam | 82 cm |
| FC | Soil | 18.8 | 9.6 | 72.6 | CH | Fat clay with gravel | Clay | 30 cm vegetative soil layer, 30 low permeability soil layer, and 60 cm foundation soil layer |

N/A – Not applicable

Table 3.10 – Baseline Geotechnical Properties of Cover Materials

| Location | $G_s$ | Wet Season | | | | | | Dry Season | | | | | |
|---|---|---|---|---|---|---|---|---|---|---|---|---|---|
| | | Moist Density ($kg/m^3$) | Dry Density ($kg/m^3$) | w (%) | S (%) | n | e | Moist Density ($kg/m^3$) | Dry Density ($kg/m^3$) | w (%) | S (%) | n | e |
| AF | 1.48 | 597 | 519 | 15 | 12 | 0.65 | 1.85 | 519 | 460 | 13 | 9 | 0.69 | 2.22 |
| GW | 1.42 | ND | ND | 129 | ND | ND | ND | 280 | 266 | 6 | 2 | 0.81 | 4.35 |
| ED | 2.66 | 1764 | 1605 | 9 | 36 | 0.40 | 0.66 | 2052 | 1893 | 8 | 52 | 0.29 | 0.41 |
| IC-1 | 2.77 | 1179 | 994 | 22 | 34 | 0.64 | 1.79 | 1246 | 1191 | 5 | 10 | 0.57 | 1.33 |
| IC-10 | 2.65 | 1349 | 1153 | 18 | 37 | 0.56 | 1.30 | 1243 | 1200 | 4 | 9 | 0.55 | 1.21 |
| IC-15 | 2.62 | 1589 | 1355 | 19 | 53 | 0.48 | 0.93 | 1439 | 1414 | 2 | 6 | 0.46 | 0.86 |
| FC | 2.67 | 1284 | 1035 | 24 | 41 | 0.61 | 1.58 | 1137 | 1076 | 6 | 11 | 0.60 | 1.48 |

ND – Not Determined

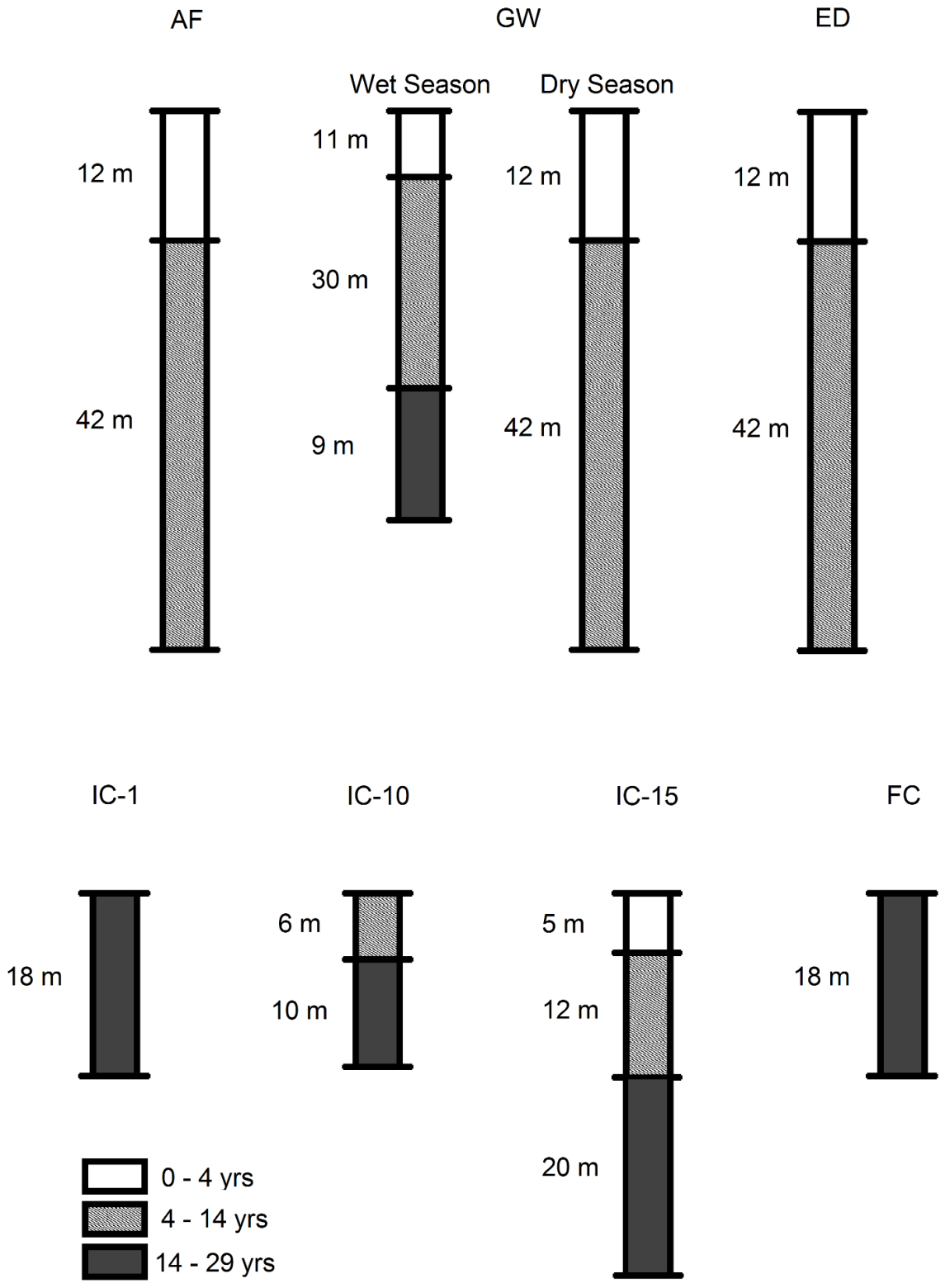


Figure 3.14. Waste Profiles at Measurement Locations

### 3.8 Emission Data Analysis Methodology

Analysis methodology for the data obtained in static flux chamber and gas management system tests are described in this section. The concentration data provided by the UCI research team were analyzed to calculate surface flux of the F-gases and the destruction efficiency of the LFG control system.

#### 3.8.1 Determination of Surface Flux

In order to quantify gas emissions from various landfill surfaces, surface flux specific to each location and constituent was determined. The surface flux was determined by converting concentration datasets obtained from the field investigation to surface flux using Equation 3.1.

$$F = \frac{dC}{dt}\left(\frac{V}{A}\right) \quad (3.1)$$

where, $F$ is the surface flux (expressed in units of mass per area-time.), $dC/dt$ is the concentration gradient, (the rate of change of concentration over time within the flux chamber), $V$ is the volume within the static flux chamber (units of volume), and $A$ is the area of the landfill surface enclosed by the chamber (units of area). To determine the concentration gradient, plots of the concentration versus sampling time were constructed for each location, constituent, and chamber (Chamber A, B, C, D). Prior to calculation of the surface flux, a linear regression analysis was performed to evaluate the fit of each concentration versus time dataset to obtain gradient data.

The fit of each linear regression model was evaluated using coefficient of determination ($R^2$), which indicates how well the regression models the data (Devore 2008). The analysis started with generating the concentration versus time data for each chamber measurement. $R^2$ acceptance and rejection criteria were used to determine the number of points that may need to be removed to potentially reach a predetermined threshold. Point removals were performed from data points obtained later in time to earlier points in order to give higher weight to the earlier points. The earlier data points were assigned higher weight in the analysis due to the potential decrease in the concentration gradient over the duration of the sampling event. The chemical accumulation that occurs after extended run time of the chamber can cause decreases in the concentration gradient.

The minimum number of points that could be removed from a dataset that contained more than two points was zero. The maximum number of points that could be removed from a dataset with 6 and 5 measurement points was established as 3 and 2 points, respectively, (linear regression loses its statistical significance for datasets with fewer than 3 points). The point removal methodology for 6-point dataset is presented in Figure 3.15. If the $R^2$ was greater than the threshold upon completion of the process presented in Figure 3.15, the dataset was accepted for surface flux calculation. An example of an accepted dataset is presented in Figure 3.16. If the $R^2$ was less than the threshold at the end of the point removal process, the dataset was rejected and surface flux was not calculated.

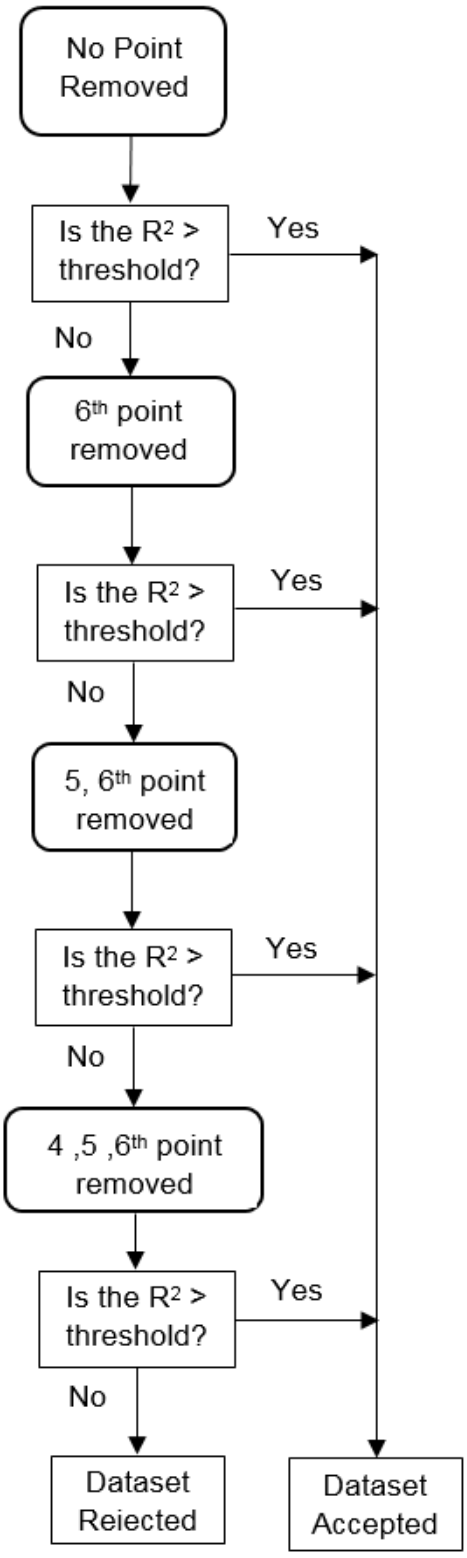


Figure 3.15. Surface Flux Analysis Scheme

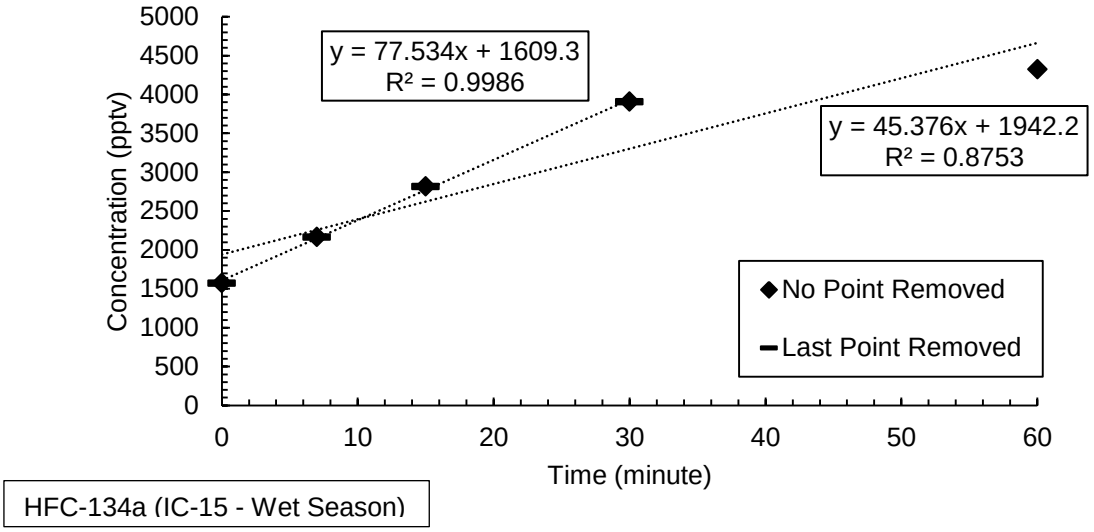


Figure 3.16. Accepted Dataset for Surface Flux Determination

The point removal process was automated using Visual Basic programming in MS Excel for the 12 F-gases, methane and carbon dioxide. In order to determine appropriate $R^2$ threshold, the point removal process was repeated with varying $R^2$ threshold values ranging from 0.65 to 0.90 in 0.05 increments. Subsequently, the percentages accepted with respect to number of points removed were calculated at each $R^2$ threshold. An $R^2$ of 0.9 was selected as the acceptance threshold.

In the next step of the analysis, the accepted datasets were used to determine the mass-based concentration gradients. Since the concentration gradients were measured in units of parts-per notation, the concentration gradients were converted to mass basis using the Ideal Gas Law (Equation 3.2):

$$\left(\frac{dC_{mass}}{dt}\right) = \frac{\left(\frac{dC_{pptv}}{dt}\right) P\, n}{R\, T} \qquad (3.2)$$

where, $C_{mass}$ is mass concentration (g/L), $C_{pptv}$ is volumetric concentration (pptv), $P$ is pressure (atm), $n$ is the molecular weight of the constituent (g/mole), $R$ is the ideal gas constant (0.8206 L-atm/mole-K), and $T$ is the soil cover temperature (K). With all the necessary parameters determined, the surface flux was calculated for each location, constituent, and chamber using Equation 3.1. The resulting units for flux values were g/m$^2$-day.

### 3.8.2 Determination of Destruction Efficiency

Destruction efficiencies for the 12 F-gases in the open flare system were determined using the raw and post-combustion concentration data collected during the field investigation. Since outlet concentration was diluted from addition of air during the combustion process, a dilution factor was calculated to determine the concentrations of the post-combustion gas prior to dilution using Equation 3.3. Methane, carbon

dioxide, and carbon monoxide have concentrations in units of parts-per notation. The numerator is the sum of the concentrations of methane, carbon dioxide, and carbon monoxide from the inlet of the flare while the denominator is the sum of the concentrations of methane, carbon dioxide, and carbon monoxide from the outlet of the flare. Use of the equation assumes that the carbons in the LFG primarily consist of methane, carbon dioxide, and carbon monoxide.

$$\text{Dilution Factor} = \frac{CH_{4\,in} + CO_{2\,in} + CO_{in}}{CH_{4\,out} + CO_{2\,out} + CO_{out}} \quad (3.3)$$

With the post-combustion gas concentrations prior to dilution determined, the destruction efficiencies of the flare system for the 12 F-gases were determined using Equation 3.4:

$$\text{Destruction Efficiency (\%)} = \frac{C_{in} - C_{out}}{C_{in}} \times 100\% \quad (3.4)$$

Where, *C* is chemical concentration of a chemical constituent expressed in parts-per notation.

### 3.9 Ambient Concentration Results

The results of the analysis of ambient concentration tests conducted using the static flux chamber method are presented in this section. The initial reading from the chamber (at time zero) is used to determine ambient concentration at the landfill surface. Data are presented for the 12 F-gases and methane and carbon dioxide. Results are presented for each test location (Tables 3.11 to 3.24). Data for all 14 gases are presented in each table. Results from Chambers A, B, C, and D are presented in the tables. First, wet season results are provided followed by dry season results.

Overall, the ambient concentrations were highly variable between constituents, between test locations, and between seasons. For constituents, at a given test location the ambient concentration varied by 2 to 5 orders of magnitude. for F-gases and by 7 to 9 orders of magnitude for all gases (incluiding $CH_4$ and $CO_2$). The $CH_4$ and $CO_2$ concentrations were considerably higher (between 4 and 9 orders of magnitude) than the concentrations of the trace components. Within the trace components, highest concentrations for the different test locations were observed for CFC-11, HCFC-21, and HCFC-141b (AF); CFC-11 and HCFC-141b (GW, dry season); CFC-11, CFC-12, HCFC-21, and HCFC-141b (ED); CFC-11, CFC-12, and HCFC-22 (IC-1); CFC-11, CFC-12, HCFC-22, and HFC-134a (IC-10); CFC-11, CFC-12, and HFC-134a (IC-15); and CFC-11, CFC-12, and HCFC-22 (FC). For GW in wet season and ED in dry season, all constituents were measured at high concentrations (all greater than 19 pptv). For test locations, the highest ambient concentrations across all constituents generally were associated with the AF and GW covers.

For seasonal variation, the difference at a given test location for a given constituent ranged from zero change to 5 orders of magnitude change (F-gases) and zero change to 9 orders of magnitude change (all gases) . Overall, the ambient concentrations were higher in wet season than dry season. Based on a comparison of individual chamber measurements, 54% of measured ambient concentrations were higher in wet season than dry season. The highest variation between seasons was observed for AF and GW covers. These covers were most sensitive to seasonal variability, where 100% (GW) and 72% (AF) of individual chamber measurements were greater in wet season than dry season. IC-10 cover also demonstrated higher ambient concentrations in wet season (for 61% of individual measurement locations). For ED, IC-1, IC-15, and FC, the ambient concentrations were higher in dry season than wet season (54%, 70%, 59%, and 72% of individual measurement locations, respectively). The greatest reduction in ambient concentration from wet to dry season (for a given test location) was 4 orders of magnitude (F-gases) and 9 orders of magnitude (all gases). The greatest increase in ambient concentration from wet to dry season (for a given test location) was 5 orders of magnitude (F-gases) and 9 orders of magnitude (all gases).

Table 3.11 **–** Ambient Concentration Data – AF (Wet Season)

| Constituent | Ambient Concentration (pptv) | | | |
|---|---|---|---|---|
| | Chamber A | Chamber B | Chamber C | Chamber D |
| CFC-11 | 2.02E+05 | 1.53E+05 | 4.19E+04 | 3.57E+04 |
| CFC-12 | 2.33E+03 | 2.06E+03 | 9.45E+02 | 8.08E+02 |
| CFC-113 | 9.00E+01 | 9.10E+01 | 7.70E+01 | 7.90E+01 |
| CFC-114 | 2.70E+01 | 3.00E+01 | 2.50E+01 | 2.60E+01 |
| HCFC-21 | 3.20E+05 | 2.87E+05 | 9.16E+04 | 8.92E+04 |
| HCFC-22 | 4.27E+00 | 4.46E+00 | 4.16E+00 | 4.90E+00 |
| HCFC-141b | 3.20E+05 | 2.87E+05 | 9.16E+04 | 8.92E+04 |
| HCFC-142b | 2.87E+00 | 2.97E+00 | 3.59E+00 | 3.65E+00 |
| HCFC-151a | 2.72E+03 | 2.82E+03 | 1.15E+03 | 3.12E+02 |
| HFC-134a | 1.77E+04 | 1.53E+04 | 4.72E+03 | 3.48E+03 |
| HFC-152a | 9.66E+03 | 8.44E+03 | 2.32E+03 | 2.32E+03 |
| HFC-245fa | 1.46E+04 | 1.55E+04 | 4.10E+03 | 4.14E+03 |
| $CH_4$ | 2.64E+08 | 1.65E+08 | 7.88E+07 | 3.23E+07 |
| $CO_2$ | 4.92E+08 | 4.94E+08 | 4.71E+08 | 4.36E+08 |

Table 3.12 – Ambient Concentration Data – GW (Wet Season)

| Constituent | Ambient Concentration (pptv) | | | |
|---|---|---|---|---|
| | Chamber A | Chamber B | Chamber C | Chamber D |
| CFC-11 | 2.98E+05 | 3.54E+04 | 3.84E+04 | 9.64E+03 |
| CFC-12 | 1.23E+04 | 3.10E+03 | 2.99E+03 | 1.02E+03 |
| CFC-113 | 2.11E+02 | 1.40E+02 | 1.22E+02 | 1.16E+02 |
| CFC-114 | 4.29E+02 | 1.64E+02 | 1.17E+02 | 2.72E+01 |
| HCFC-21 | 6.29E+03 | 1.69E+03 | 1.60E+03 | 2.89E+02 |
| HCFC-22 | 2.55E+04 | 5.55E+03 | 6.47E+03 | 1.28E+03 |
| HCFC-141b | 3.96E+05 | 7.72E+04 | 9.03E+04 | 1.80E+04 |
| HCFC-142b | 3.22E+04 | 7.25E+03 | 1.16E+04 | 1.74E+03 |
| HCFC-151a | 2.36E+04 | 1.10E+04 | 8.49E+03 | 1.53E+03 |
| HFC-134a | 4.75E+04 | 1.29E+04 | 8.55E+03 | 2.02E+03 |
| HFC-152a | 5.98E+05 | 7.62E+04 | 6.44E+04 | 2.07E+04 |
| HFC-245fa | 3.17E+04 | 8.82E+03 | 6.38E+03 | 1.40E+03 |
| $CH_4$ | 1.89E+08 | 1.62E+08 | 9.86E+07 | 5.31E+07 |
| $CO_2$ | 5.27E+09 | 3.39E+09 | 3.05E+09 | 7.68E+09 |

Table 3.13 – Ambient Concentration Data – ED (Wet Season)

| Constituent | Ambient Concentration (pptv) | | | |
|---|---|---|---|---|
| | Chamber A | Chamber B | Chamber C | Chamber D |
| CFC-11 | 3.40E+03 | 5.67E+03 | 6.47E+02 | 9.64E+03 |
| CFC-12 | 4.98E+02 | 5.98E+02 | 4.84E+02 | 5.14E+02 |
| CFC-113 | 6.90E+01 | 7.50E+01 | 7.00E+01 | 7.40E+01 |
| CFC-114 | 1.70E+01 | 2.00E+01 | 1.80E+01 | 1.80E+01 |
| HCFC-21 | 7.77E+03 | 1.50E+04 | 7.73E+03 | 9.75E+03 |
| HCFC-22 | 3.48E+00 | 3.97E+00 | 3.59E+00 | 4.72E+00 |
| HCFC-141b | 7.77E+03 | 1.50E+04 | 7.73E+03 | 9.75E+03 |
| HCFC-142b | 2.98E+00 | 4.03E+00 | 3.54E+00 | 3.44E+00 |
| HCFC-151a | 8.82E+02 | 7.48E+02 | 6.77E+02 | 7.02E+02 |
| HFC-134a | 9.78E+02 | 1.87E+03 | 1.45E+03 | 8.80E+02 |
| HFC-152a | 4.42E+02 | 8.75E+02 | 4.41E+02 | 4.37E+02 |
| HFC-245fa | 3.24E+02 | 9.57E+02 | 2.72E+02 | 3.29E+02 |
| $CH_4$ | 4.60E+07 | 4.80E+07 | 5.35E+07 | 3.86E+07 |
| $CO_2$ | 4.92E+08 | 6.58E+08 | 5.40E+08 | 4.70E+08 |

Table 3.14 – Ambient Concentration Data – IC-1 (Wet Season)

| Constituent | Ambient Concentration (pptv) | | | |
|---|---|---|---|---|
| | Chamber A | Chamber B | Chamber C | Chamber D |
| CFC-11 | 2.34E+02 | 2.22E+02 | 2.47E+02 | 2.07E+02 |
| CFC-12 | 5.09E+02 | 4.53E+02 | 5.28E+02 | 4.53E+02 |
| CFC-113 | 6.30E+01 | 6.40E+01 | 7.50E+01 | 6.40E+01 |
| CFC-114 | 1.50E+01 | 1.40E+01 | 1.50E+01 | 1.50E+01 |
| HCFC-21 | BDL | BDL | BDL | BDL |
| HCFC-22 | 2.17E+02 | 2.22E+02 | 2.63E+02 | 2.23E+02 |
| HCFC-141b | 7.20E+01 | 4.40E+01 | 3.20E+01 | 2.30E+01 |
| HCFC-142b | 2.40E+01 | 2.20E+01 | 2.30E+01 | 2.20E+01 |
| HCFC-151a | BDL | BDL | BDL | BDL |
| HFC-134a | 6.20E+01 | 6.30E+01 | 7.70E+01 | 7.60E+01 |
| HFC-152a | 3.30E+01 | 2.40E+01 | 2.00E+01 | 1.60E+01 |
| HFC-245fa | 3.10E+00 | 1.80E+00 | BDL | BDL |
| $CH_4$ | 2.00E+06 | 4.00E+06 | 2.30E+06 | 2.10E+06 |
| $CO_2$ | 5.17E+08 | 4.71E+08 | 4.33E+08 | 4.18E+08 |

Table 3.15 – Ambient Concentration Data – IC-10 (Wet Season)

| Constituent | Ambient Concentration (pptv) | | | |
|---|---|---|---|---|
| | Chamber A | Chamber B | Chamber C | Chamber D |
| CFC-11 | 2.22E+02 | 2.72E+02 | 2.60E+02 | 2.28E+02 |
| CFC-12 | 5.15E+02 | 7.42E+02 | 4.83E+02 | 4.87E+02 |
| CFC-113 | 6.40E+01 | 1.06E+02 | 7.20E+01 | 6.50E+01 |
| CFC-114 | 1.90E+01 | 2.60E+01 | 1.60E+01 | 1.90E+01 |
| HCFC-21 | BDL | BDL | BDL | BDL |
| HCFC-22 | 2.59E+02 | 4.21E+02 | 2.76E+02 | 2.64E+02 |
| HCFC-141b | 5.70E+01 | 1.17E+02 | 8.20E+01 | 6.50E+01 |
| HCFC-142b | 2.40E+01 | 3.50E+01 | 2.50E+01 | 2.40E+01 |
| HCFC-151a | BDL | BDL | BDL | BDL |
| HFC-134a | 1.07E+02 | 2.74E+02 | 1.31E+02 | 1.29E+02 |
| HFC-152a | 2.20E+01 | 3.50E+01 | 2.40E+01 | 2.50E+01 |
| HFC-245fa | 1.00E+00 | 6.50E+00 | 4.50E+00 | 3.50E+00 |
| $CH_4$ | 3.20E+07 | 2.70E+07 | 1.80E+07 | 1.77E+07 |
| $CO_2$ | 5.20E+08 | 4.51E+08 | 5.77E+08 | 4.31E+08 |

Table 3.16 – Ambient Concentration Data – IC-15 (Wet Season)

| Constituent | Ambient Concentration (pptv) | | | |
|---|---|---|---|---|
| | Chamber A | Chamber B | Chamber C | Chamber D |
| CFC-11 | 2.80E+02 | 3.60E+02 | 2.40E+02 | 4.97E+02 |
| CFC-12 | 5.07E+02 | 5.38E+02 | 5.08E+02 | 5.55E+02 |
| CFC-113 | 7.10E+01 | 7.20E+01 | 7.10E+01 | 7.40E+01 |
| CFC-114 | 2.40E+01 | 1.90E+01 | 2.70E+01 | 2.40E+01 |
| HCFC-21 | BDL | BDL | BDL | BDL |
| HCFC-22 | 2.75E+02 | 3.14E+02 | 2.88E+02 | 3.56E+02 |
| HCFC-141b | 1.47E+02 | 1.38E+02 | 9.80E+01 | 3.76E+02 |
| HCFC-142b | 3.40E+01 | 3.20E+01 | 3.30E+01 | 6.50E+01 |
| HCFC-151a | 5.50E+01 | BDL | 8.60E+01 | 5.90E+01 |
| HFC-134a | 2.44E+02 | 2.02E+02 | 4.88E+02 | 7.40E+02 |
| HFC-152a | 8.30E+01 | 2.30E+01 | 1.59E+02 | 1.10E+02 |
| HFC-245fa | 1.49E+01 | 1.00E+01 | 2.02E+01 | 6.03E+01 |
| $CH_4$ | 1.20E+08 | 1.50E+07 | 3.02E+08 | 1.90E+07 |
| $CO_2$ | 5.25E+08 | 4.31E+08 | 2.72E+08 | 3.14E+07 |

Table 3.17 – Ambient Concentration Data – FC (Wet Season)

| Constituent | Ambient Concentration (pptv) | | | |
|---|---|---|---|---|
| | Chamber A | Chamber B | Chamber C | Chamber D |
| CFC-11 | 2.54E+02 | 2.25E+02 | 2.12E+02 | 2.89E+02 |
| CFC-12 | 5.34E+02 | 4.63E+02 | 4.45E+02 | 6.15E+02 |
| CFC-113 | 7.50E+01 | 6.60E+01 | 6.70E+01 | 9.10E+01 |
| CFC-114 | 1.60E+01 | 1.60E+01 | 1.40E+01 | 1.90E+01 |
| HCFC-21 | BDL | BDL | BDL | BDL |
| HCFC-22 | 2.60E+02 | 2.33E+02 | 2.19E+02 | 2.81E+02 |
| HCFC-141b | 4.50E+01 | 3.90E+01 | 2.60E+01 | 3.50E+01 |
| HCFC-142b | 2.20E+01 | 2.20E+01 | 2.10E+01 | 2.30E+01 |
| HCFC-151a | BDL | BDL | BDL | BDL |
| HFC-134a | 7.60E+01 | 7.60E+01 | 6.80E+01 | 7.40E+01 |
| HFC-152a | 1.80E+01 | 1.70E+01 | 1.60E+01 | 2.10E+01 |
| HFC-245fa | BDL | BDL | BDL | BDL |
| $CH_4$ | 2.00E+06 | 2.00E+06 | 1.90E+06 | 2.00E+06 |
| $CO_2$ | 4.11E+08 | 3.96E+08 | 4.14E+08 | 4.04E+08 |

Table 3.18 **–** Ambient Concentration Data – AF (Dry Season)

| Constituent | Ambient Concentration (pptv) | | | |
|---|---|---|---|---|
| | Chamber A | Chamber B | Chamber C | Chamber D |
| CFC-11 | 3.15E+04 | 3.54E+04 | 2.12E+04 | 2.46E+04 |
| CFC-12 | 9.96E+02 | 8.07E+02 | 9.31E+02 | 8.46E+02 |
| CFC-113 | 9.80E+01 | 8.80E+01 | 8.50E+01 | 9.70E+01 |
| CFC-114 | 2.30E+01 | 2.20E+01 | 2.00E+01 | 2.10E+01 |
| HCFC-21 | 2.33E+02 | 1.54E+02 | 1.18E+02 | 1.19E+02 |
| HCFC-22 | 2.02E+03 | 1.28E+03 | 1.08E+03 | 1.46E+03 |
| HCFC-141b | 3.35E+04 | 4.43E+04 | 9.57E+03 | 3.37E+04 |
| HCFC-142b | 8.35E+02 | 5.70E+02 | 5.87E+02 | 3.97E+02 |
| HCFC-151a | 1.40E+03 | 7.40E+02 | 7.12E+02 | 6.14E+02 |
| HFC-134a | 4.13E+03 | 2.67E+03 | 3.08E+03 | 1.97E+03 |
| HFC-152a | 7.06E+03 | 1.29E+03 | 8.52E+02 | 2.17E+03 |
| HFC-245fa | 2.45E+03 | 1.90E+03 | 2.94E+03 | 1.37E+03 |
| $CH_4$ | 3.20E+08 | 7.90E+07 | 1.01E+08 | 1.65E+09 |
| $CO_2$ | 4.92E+08 | 4.36E+08 | 4.20E+08 | 4.27E+08 |

Table 3.19 **–** Ambient Concentration Data – GW (Dry Season)

| Constituent | Ambient Concentration (pptv) | | | |
|---|---|---|---|---|
| | Chamber A | Chamber B | Chamber C | Chamber D |
| CFC-11 | 6.88E+03 | 4.17E+03 | 1.64E+03 | 1.73E+03 |
| CFC-12 | 8.42E+02 | 5.99E+02 | 6.14E+02 | 6.05E+02 |
| CFC-113 | 1.03E+02 | 7.60E+01 | 1.40E+02 | 8.40E+01 |
| CFC-114 | 3.70E+01 | 1.90E+01 | 2.70E+01 | 2.70E+01 |
| HCFC-21 | 2.50E+02 | 4.60E+01 | 6.60E+01 | 8.90E+01 |
| HCFC-22 | 6.95E+02 | 3.59E+02 | 4.18E+02 | 4.47E+02 |
| HCFC-141b | 2.44E+04 | 5.50E+03 | 2.50E+03 | 3.98E+03 |
| HCFC-142b | 2.09E+02 | 8.00E+01 | 5.50E+01 | 6.00E+01 |
| HCFC-151a | 1.25E+03 | 2.02E+02 | 5.84E+02 | 8.96E+02 |
| HFC-134a | 9.00E+02 | 5.73E+02 | 8.30E+02 | 1.20E+03 |
| HFC-152a | 8.02E+02 | 4.23E+02 | 5.48E+02 | 1.01E+03 |
| HFC-245fa | 4.27E+02 | 1.87E+02 | 5.80E+01 | 7.20E+01 |
| $CH_4$ | 6.20E+07 | 3.30E+07 | 6.42E+07 | 7.85E+07 |
| $CO_2$ | 6.73E+08 | 5.31E+08 | 5.30E+08 | 5.17E+08 |

Table 3.20 **–** Ambient Concentration Data – ED (Dry Season)

| Constituent | Ambient Concentration (pptv) | | | |
|---|---|---|---|---|
| | Chamber A | Chamber B | Chamber C | Chamber D |
| CFC-11 | 3.33E+03 | 1.30E+03 | 3.41E+03 | 8.42E+03 |
| CFC-12 | 8.95E+02 | 6.64E+02 | 9.34E+02 | 1.56E+03 |
| CFC-113 | 8.30E+01 | 7.70E+01 | 7.90E+01 | 8.80E+01 |
| CFC-114 | 2.30E+01 | 1.90E+01 | 2.40E+01 | 2.10E+01 |
| HCFC-21 | 1.29E+02 | 4.30E+01 | 9.90E+01 | 1.37E+02 |
| HCFC-22 | 5.00E+02 | 3.38E+02 | 5.27E+02 | 1.03E+03 |
| HCFC-141b | 3.19E+03 | 1.36E+03 | 2.37E+03 | 1.12E+04 |
| HCFC-142b | 1.44E+02 | 6.10E+01 | 1.11E+02 | 9.77E+02 |
| HCFC-151a | 5.41E+02 | 1.85E+02 | 4.84E+02 | 8.13E+02 |
| HFC-134a | 1.02E+03 | 5.03E+02 | 1.03E+03 | 3.12E+03 |
| HFC-152a | 1.60E+03 | 5.42E+02 | 1.43E+03 | 1.24E+04 |
| HFC-245fa | 1.40E+02 | 7.90E+01 | 1.02E+02 | 7.48E+02 |
| $CH_4$ | 1.74E+08 | 7.80E+07 | 1.12E+07 | 1.08E+08 |
| $CO_2$ | 4.34E+08 | 4.07E+08 | 4.35E+08 | 4.30E+07 |

Table 3.21 **–** Ambient Concentration Data – IC-1 (Dry Season)

| Constituent | Ambient Concentration (pptv) | | | |
|---|---|---|---|---|
| | Chamber A | Chamber B | Chamber C | Chamber D |
| CFC-11 | 2.43E+02 | 2.38E+02 | 2.39E+02 | 2.37E+02 |
| CFC-12 | 5.38E+02 | 5.32E+02 | 5.42E+02 | 5.51E+02 |
| CFC-113 | 7.40E+01 | 7.90E+01 | 7.40E+01 | 9.40E+01 |
| CFC-114 | 1.60E+01 | 1.60E+01 | 1.60E+01 | 1.70E+01 |
| HCFC-21 | BDL | BDL | BDL | BDL |
| HCFC-22 | 2.29E+02 | 2.40E+02 | 2.49E+02 | 2.80E+02 |
| HCFC-141b | 2.40E+01 | 2.40E+01 | 2.40E+01 | 2.30E+01 |
| HCFC-142b | 2.40E+01 | 2.70E+01 | 2.40E+01 | 2.40E+01 |
| HCFC-151a | BDL | 7.00E+01 | BDL | BDL |
| HFC-134a | 7.80E+01 | 8.30E+01 | 8.50E+01 | 8.60E+01 |
| HFC-152a | 2.40E+01 | 1.80E+01 | 2.10E+01 | 3.70E+01 |
| HFC-245fa | 5.00E-01 | 1.10E+00 | 6.00E-01 | 6.00E-01 |
| $CH_4$ | 2.00E+06 | 2.00E+06 | 1.90E+06 | 2.60E+06 |
| $CO_2$ | 4.10E+08 | 3.78E+08 | 3.81E+08 | 3.93E+08 |

Table 3.22 **–** Ambient Concentration Data – IC-10 (Dry Season)

| Constituent | Ambient Concentration (pptv) | | | |
|---|---|---|---|---|
| | Chamber A | Chamber B | Chamber C | Chamber D |
| CFC-11 | 2.43E+02 | 2.38E+02 | 2.39E+02 | 2.37E+02 |
| CFC-12 | 5.38E+02 | 5.32E+02 | 5.42E+02 | 5.51E+02 |
| CFC-113 | 7.40E+01 | 7.90E+01 | 7.40E+01 | 9.40E+01 |
| CFC-114 | 1.60E+01 | 1.60E+01 | 1.60E+01 | 1.70E+01 |
| HCFC-21 | BDL | BDL | BDL | BDL |
| HCFC-22 | 2.29E+02 | 2.40E+02 | 2.49E+02 | 2.80E+02 |
| HCFC-141b | 2.40E+01 | 2.40E+01 | 2.40E+01 | 2.30E+01 |
| HCFC-142b | 2.40E+01 | 2.70E+01 | 2.40E+01 | 2.40E+01 |
| HCFC-151a | BDL | 7.00E+01 | BDL | BDL |
| HFC-134a | 7.80E+01 | 8.30E+01 | 8.50E+01 | 8.60E+01 |
| HFC-152a | 2.40E+01 | 1.80E+01 | 2.10E+01 | 3.70E+01 |
| HFC-245fa | 1.00E+00 | 1.00E+00 | 1.00E+00 | 1.00E+00 |
| $CH_4$ | 2.00E+06 | 2.00E+06 | 1.90E+06 | 2.60E+06 |
| $CO_2$ | 4.10E+08 | 3.78E+08 | 3.81E+08 | 3.93E+08 |

Table 3.23 **–** Ambient Concentration Data – IC-15 (Dry Season)

| Constituent | Ambient Concentration (pptv) | | | |
|---|---|---|---|---|
| | Chamber A | Chamber B | Chamber C | Chamber D |
| CFC-11 | 3.09E+03 | 3.57E+02 | 2.76E+02 | 2.85E+02 |
| CFC-12 | 6.09E+02 | 5.58E+02 | 6.07E+02 | 5.37E+02 |
| CFC-113 | 8.80E+01 | 7.80E+01 | 8.20E+01 | 8.00E+01 |
| CFC-114 | 2.10E+01 | 1.80E+01 | 1.90E+01 | 2.20E+01 |
| HCFC-21 | BDL | BDL | BDL | BDL |
| HCFC-22 | 3.80E+02 | 2.63E+02 | 3.01E+02 | 2.59E+02 |
| HCFC-141b | 2.69E+03 | 1.00E+01 | 9.80E+01 | 2.70E+01 |
| HCFC-142b | 1.47E+02 | 2.80E+01 | 2.50E+01 | 3.10E+01 |
| HCFC-151a | 1.60E+02 | 6.60E+01 | 7.20E+01 | 5.00E+01 |
| HFC-134a | 1.58E+03 | 2.69E+02 | 5.78E+01 | 5.50E+01 |
| HFC-152a | 3.44E+03 | 3.08E+02 | 1.70E+02 | 1.11E+02 |
| HFC-245fa | 1.27E+02 | 2.10E+01 | 8.00E+00 | 8.00E+00 |
| $CH_4$ | 1.00E+08 | 4.20E+07 | 2.35E+07 | 4.14E+07 |
| $CO_2$ | 5.31E+08 | 4.88E+08 | 4.80E+08 | 4.59E+08 |

Table 3.24 – Ambient Concentration Data – FC (Dry Season)

| Constituent | Ambient Concentration (pptv) | | | |
|---|---|---|---|---|
| | Chamber A | Chamber B | Chamber C | Chamber D |
| CFC-11 | 2.45E+02 | 2.50E+02 | 2.35E+02 | 2.37E+02 |
| CFC-12 | 5.42E+02 | 5.49E+02 | 5.33E+02 | 5.35E+02 |
| CFC-113 | 7.90E+01 | 7.90E+01 | 7.80E+01 | 8.20E+01 |
| CFC-114 | 1.70E+01 | 1.60E+01 | 1.80E+01 | 1.90E+01 |
| HCFC-21 | BDL | BDL | BDL | BDL |
| HCFC-22 | 2.33E+02 | 2.33E+02 | 2.40E+02 | 2.56E+02 |
| HCFC-141b | 2.70E+01 | 2.30E+01 | 2.30E+01 | 2.40E+01 |
| HCFC-142b | 2.40E+01 | 2.40E+01 | 2.30E+01 | 2.40E+01 |
| HCFC-151a | BDL | BDL | BDL | BDL |
| HFC-134a | 7.90E+01 | 8.20E+01 | 8.00E+01 | 8.30E+01 |
| HFC-152a | 1.50E+01 | 2.70E+01 | 3.50E+01 | 3.60E+01 |
| HFC-245fa | BDL | 5.00E-01 | 5.00E-01 | 4.00E-01 |
| $CH_4$ | 1.87E+06 | 1.88E+06 | 2.03E+06 | 1.89E+06 |
| $CO_2$ | 4.14E+08 | 3.94E+08 | 4.44E+08 | 4.22E+08 |

For F-gases, the overall variability of ambient concentrations (across all cover types and testing locations) ranged over 5 orders of magnitude (wet season), 5 orders of magnitude (dry season), and 6 orders of magnitude (over both seasons). For all gases, the overall variability of ambient concentrations (across all cover types and testing locations) ranged over 9 orders of magnitude (wet season), 10 orders of magnitude (dry season), and 10 orders of magnitude (over both seasons).

### 3.10 Surface Flux Results

The results of the analysis of surface emission tests conducted using the static flux chamber method are presented in this section. Data are presented for the 12 F-gases and methane and carbon dioxide. Initially, results are presented for each test location (Tables 3.25 to 3.38). Data for all 14 gases are presented in each table. Results from Chambers A, B, C, and D are presented in the tables. First, wet season results are provided followed by dry season results. Significant variations were observed in the flux values between the measurement locations. Variations on the order of six orders of magnitude were present in the data. For the four target gases, the lowest and highest fluxes were $9.47x10^{-7}$ and $2.57x10^{-1}$ g/m$^{-2}$-day, $-5.59x10^{-6}$ and $2.99x10^{-1}$ g/m$^2$-day, $5.69x10^{-7}$ and $3.79x10^{-2}$ g/m$^2$-day, and $9.74x10^{-9}$ and $5.21x10^{-2}$ g/m$^2$-day for CFC-11, HCFC 141b, HFC-134a, and HFC-245fa, respectively. For the F-gases overall, the lowest flux was $-5.59x10^{-6}$ and the highest flux was $2.99x10^{-1}$ g/m$^{-2}$-day. The methane and carbon dioxide emissions generally were higher than the trace gas components. The methane emissions ranged from $-1.94x10^{-2}$ to $5.38x10^{+1}$ g/m$^2$-day. The carbon dioxide emissions ranged from $-2.36x10^{+1}$ to $7.47x10^{+2}$ g/m$^2$-day. The variations in flux values were lower at a given location than between locations. The variations at a given

location were less than two orders of magnitude and for the majority of the cases flux was within the same order of magnitude. Exceptions were observed for methane and carbon dioxide when negative fluxes occurred through the cover systems in a low number of measurements. The rejected datasets typically were associated with low measured concentrations indicating that the minimum values provided above represent conservative conditions.

Table 3.25 – Wet Season Surface Flux Results for AF Location

| Compound | Chamber A ($g\ m^{-2}\ day^{-1}$) | Chamber B ($g\ m^{-2}\ day^{-1}$) | Chamber C ($g\ m^{-2}\ day^{-1}$) | Chamber D ($g\ m^{-2}\ day^{-1}$) | Min ($g\ m^{-2}\ day^{-1}$) | Max ($g\ m^{-2}\ day^{-1}$) |
|---|---|---|---|---|---|---|
| CFC-11 | 1.74E-01 | 2.57E-01 | - | 6.66E-02 | 6.66E-02 | 2.57E-01 |
| CFC-12 | 1.39E-03 | 4.48E-03 | - | 5.54E-04 | 5.54E-04 | 4.48E-03 |
| CFC-113 | 1.95E-05 | 6.31E-05 | - | - | 1.95E-05 | 6.31E-05 |
| CFC-114 | 1.12E-05 | 2.07E-05 | 5.59E-07 | - | 5.59E-07 | 2.07E-05 |
| HCFC-21 | 2.63E-01 | - | - | 1.20E-01 | 1.20E-01 | 2.63E-01 |
| HCFC-22 | - | 5.92E-07 | - | - | 5.92E-07 | 5.92E-07 |
| HCFC-141b | 2.99E-01 | - | - | 1.36E-01 | 1.36E-01 | 2.99E-01 |
| HCFC-142b | - | 1.46E-07 | 1.50E-08 | - | 1.50E-08 | 1.46E-07 |
| HCFC-151a | 1.11E-03 | 3.40E-03 | - | 1.53E-05 | 1.53E-05 | 3.40E-03 |
| HFC-134a | 1.00E-02 | 3.79E-02 | - | 6.46E-03 | 6.46E-03 | 3.79E-02 |
| HFC-152a | 5.35E-03 | 1.31E-02 | - | 3.15E-03 | 3.15E-03 | 1.31E-02 |
| HFC-245fa | 1.34E-02 | 5.21E-02 | - | 8.73E-03 | 8.73E-03 | 5.21E-02 |
| $CH_4$ | 2.00E+01 | 1.80E+01 | - | 7.41E-02 | 7.41E-02 | 2.00E+01 |
| $CO_2$ | -2.36E+01 | - | - | - | -2.36E+01 | -2.36E+01 |

(-) represents rejected dataset (i.e., flux value not calculated)

Table 3.26 – Wet Season Surface Flux Results for GW Location

| Compound | Chamber A ($g\ m^{-2}\ day^{-1}$) | Chamber B ($g\ m^{-2}\ day^{-1}$) | Min ($g\ m^{-2}\ day^{-1}$) | Max ($g\ m^{-2}\ day^{-1}$) |
|---|---|---|---|---|
| CFC-11 | 7.36E-02 | 3.12E-02 | 3.12E-02 | 7.36E-02 |
| CFC-12 | 1.95E-03 | 1.74E-03 | 1.74E-03 | 1.95E-03 |
| CFC-113 | 1.57E-05 | 9.67E-06 | 9.67E-06 | 1.57E-05 |
| CFC-114 | 5.59E-05 | 1.10E-04 | 5.59E-05 | 1.10E-04 |
| HCFC-21 | 1.65E-03 | 2.22E-01 | 1.65E-03 | 2.22E-01 |
| HCFC-22 | 3.43E-03 | 2.23E-03 | 2.23E-03 | 3.43E-03 |
| HCFC-141b | 8.70E-02 | 5.22E-02 | 5.22E-02 | 8.70E-02 |
| HCFC-142b | 4.93E-03 | 4.54E-03 | 4.54E-03 | 4.93E-03 |
| HCFC-151a | 3.73E-03 | 5.67E-03 | 3.73E-03 | 5.67E-03 |
| HFC-134a | 7.08E-03 | 7.13E-03 | 7.08E-03 | 7.13E-03 |
| HFC-152a | 6.76E-02 | 2.09E-02 | 2.09E-02 | 6.76E-02 |
| HFC-245fa | 7.44E-03 | 7.55E-03 | 7.44E-03 | 7.55E-03 |
| $CH_4$ | 9.16E+00 | 1.26E+01 | 9.16E+00 | 1.26E+01 |
| $CO_2$ | 7.47E+02 | 6.31E+02 | 6.31E+02 | 7.47E+02 |

Table 3.27 – Wet Season Surface Flux Results for ED Location

| Compound | Chamber A ($g\ m^{-2}\ day^{-1}$) | Chamber B ($g\ m^{-2}\ day^{-1}$) | Chamber C ($g\ m^{-2}\ day^{-1}$) | Chamber D ($g\ m^{-2}\ day^{-1}$) | Min ($g\ m^{-2}\ day^{-1}$) | Max ($g\ m^{-2}\ day^{-1}$) |
|---|---|---|---|---|---|---|
| CFC-11 | 5.78E-04 | 2.34E-03 | 5.50E-04 | - | 5.50E-04 | 2.34E-03 |
| CFC-12 | 2.32E-05 | 8.26E-05 | 5.99E-05 | - | 2.32E-05 | 8.26E-05 |
| CFC-113 | - | - | 1.57E-06 | - | 1.57E-06 | 1.57E-06 |
| CFC-114 | - | 1.59E-06 | 2.68E-06 | - | 1.59E-06 | 2.68E-06 |
| HCFC-21 | 5.42E-04 | 4.08E-03 | 7.08E-03 | - | 5.42E-04 | 7.08E-03 |
| HCFC-22 | 3.09E-08 | 4.22E-08 | 6.09E-08 | - | 3.09E-08 | 6.09E-08 |
| HCFC-141b | 6.16E-04 | 4.63E-03 | 8.04E-03 | - | 6.16E-04 | 8.04E-03 |
| HCFC-142b | 7.30E-08 | - | 6.67E-08 | - | 6.67E-08 | 7.30E-08 |
| HCFC-151a | - | 2.71E-04 | 4.67E-04 | - | 2.71E-04 | 4.67E-04 |
| HFC-134a | 1.17E-04 | 1.04E-03 | 1.42E-03 | - | 1.17E-04 | 1.42E-03 |
| HFC-152a | 2.06E-05 | 1.44E-04 | 1.48E-04 | - | 2.06E-05 | 1.48E-04 |
| HFC-245fa | 1.05E-04 | 5.71E-04 | 3.96E-04 | - | 1.05E-04 | 5.71E-04 |
| $CH_4$ | 2.68E-01 | 5.03E+00 | 6.18E+00 | 1.32E+01 | 2.68E-01 | 1.32E+01 |
| $CO_2$ | 4.60E+00 | - | 2.23E+01 | 4.54E+01 | 4.60E+00 | 4.54E+01 |

(-) represents rejected dataset (i.e., flux value not calculated)

Table 3.28 – Wet Season Surface Flux Results for IC-1 Location

| Compound | Chamber A ($g\ m^{-2}\ day^{-1}$) | Chamber B ($g\ m^{-2}\ day^{-1}$) | Min ($g\ m^{-2}\ day^{-1}$) | Max ($g\ m^{-2}\ day^{-1}$) |
|---|---|---|---|---|
| CFC-11 | 2.27E-06 | - | 2.27E-06 | 2.27E-06 |
| CFC-12 | - | - | - | - |
| CFC-113 | 2.06E-06 | - | 2.06E-06 | 2.06E-06 |
| CFC-114 | 3.05E-07 | - | 3.05E-07 | 3.05E-07 |
| HCFC-21 | BDL | BDL | ND | ND |
| HCFC-22 | 2.26E-06 | - | 2.26E-06 | 2.26E-06 |
| HCFC-141b | -5.59E-06 | 1.04E-06 | -5.59E-06 | 1.04E-06 |
| HCFC-142b | 1.78E-07 | - | 1.78E-07 | 1.78E-07 |
| HCFC-151a | BDL | BDL | ND | ND |
| HFC-134a | - | - | - | - |
| HFC-152a | 5.06E-06 | 4.92E-06 | 4.92E-06 | 5.06E-06 |
| HFC-245fa | BDL | BDL | ND | ND |
| $CH_4$ | - | - | - | - |
| $CO_2$ | 2.30E+01 | 2.16E+01 | 2.16E+01 | 2.30E+01 |

(-) represents rejected dataset (i.e., flux value not calculated)
BDL – below detection limit
ND – not determined

Table 3.29 – Wet Season Surface Flux Results for IC-10 Location

| Compound | Chamber A ($g\ m^{-2}\ day^{-1}$) | Chamber B ($g\ m^{-2}\ day^{-1}$) | Min ($g\ m^{-2}\ day^{-1}$) | Max ($g\ m^{-2}\ day^{-1}$) |
|---|---|---|---|---|
| CFC-11 | 5.19E-06 | 8.93E-06 | 5.19E-06 | 8.93E-06 |
| CFC-12 | 5.67E-05 | - | 5.67E-05 | 5.67E-05 |
| CFC-113 | 2.59E-06 | - | 2.59E-06 | 2.59E-06 |
| CFC-114 | 8.99E-06 | - | 8.99E-06 | 8.99E-06 |
| HCFC-21 | BDL | BDL | ND | ND |
| HCFC-22 | 7.07E-05 | - | 7.07E-05 | 7.07E-05 |
| HCFC-141b | 3.65E-05 | 7.99E-06 | 7.99E-06 | 3.65E-05 |
| HCFC-142b | 2.13E-06 | -3.50E-07 | -3.50E-07 | 2.13E-06 |
| HCFC-151a | 4.47E-06 | - | 4.47E-06 | 4.47E-06 |
| HFC-134a | 1.48E-05 | - | 1.48E-05 | 1.48E-05 |
| HFC-152a | 5.24E-06 | 1.40E-06 | 1.40E-06 | 5.24E-06 |
| HFC-245fa | 1.14E-07 | - | 1.14E-07 | 1.14E-07 |
| $CH_4$ | 6.29E+00 | -1.94E-02 | -1.94E-02 | 6.29E+00 |
| $CO_2$ | 6.40E+01 | 1.85E+01 | 1.85E+01 | 6.40E+01 |

(-) represents rejected dataset (i.e., flux value not calculated)
BDL – below detection limit
ND – not determined

Table 3.30 – Wet Season Surface Flux Results for IC-15 Location

| Compound | Chamber A ($g\ m^{-2}\ day^{-1}$) | Chamber B ($g\ m^{-2}\ day^{-1}$) | Min ($g\ m^{-2}\ day^{-1}$) | Max ($g\ m^{-2}\ day^{-1}$) |
|---|---|---|---|---|
| CFC-11 | 9.92E-06 | 7.93E-06 | 7.93E-06 | 9.92E-06 |
| CFC-12 | 1.16E-05 | -3.41E-06 | -3.41E-06 | 1.16E-05 |
| CFC-113 | - | -5.22E-07 | -5.22E-07 | -5.22E-07 |
| CFC-114 | 3.72E-05 | - | 3.72E-05 | 3.72E-05 |
| HCFC-21 | 1.47E-06 | BDL | 1.47E-06 | 1.47E-06 |
| HCFC-22 | 2.30E-05 | -1.60E-06 | -1.60E-06 | 2.30E-05 |
| HCFC-141b | 9.80E-05 | 1.02E-05 | 1.02E-05 | 9.80E-05 |
| HCFC-142b | 5.90E-06 | - | 5.90E-06 | 5.90E-06 |
| HCFC-151a | 1.22E-04 | - | 1.22E-04 | 1.22E-04 |
| HFC-134a | 3.29E-04 | - | 3.29E-04 | 3.29E-04 |
| HFC-152a | 1.18E-04 | 4.00E-07 | 4.00E-07 | 1.18E-04 |
| HFC-245fa | 2.31E-05 | 3.75E-07 | 3.75E-07 | 2.31E-05 |
| $CH_4$ | 3.60E+01 | -9.65E-03 | -9.65E-03 | 3.60E+01 |
| $CO_2$ | 1.07E+02 | 7.43E+00 | 7.43E+00 | 1.07E+02 |

(-) represents rejected dataset (i.e., flux value not calculated)
BDL – below detection limit

Table 3.31 – Wet Season Surface Flux Results for FC Location

| Compound | Chamber A ($g\ m^{-2}\ day^{-1}$) | Chamber B ($g\ m^{-2}\ day^{-1}$) | Min ($g\ m^{-2}\ day^{-1}$) | Max ($g\ m^{-2}\ day^{-1}$) |
|---|---|---|---|---|
| CFC-11 | - | - | - | - |
| CFC-12 | - | - | - | - |
| CFC-113 | - | - | - | - |
| CFC-114 | 1.30E-06 | 1.11E-05 | 1.30E-06 | 1.11E-05 |
| HCFC-21 | BDL | BDL | ND | ND |
| HCFC-22 | - | 1.55E-05 | 1.55E-05 | 1.55E-05 |
| HCFC-141b | - | - | - | - |
| HCFC-142b | - | 6.60E-07 | 6.60E-07 | 6.60E-07 |
| HCFC-151a | BDL | BDL | ND | ND |
| HFC-134a | - | 5.69E-07 | 5.69E-07 | 5.69E-07 |
| HFC-152a | 9.79E-07 | 5.89E-07 | 5.89E-07 | 9.79E-07 |
| HFC-245fa | BDL | BDL | ND | ND |
| $CH_4$ | -1.07E-03 | - | -1.07E-03 | -1.07E-03 |
| $CO_2$ | 1.86E+01 | 2.18E+01 | 1.86E+01 | 2.18E+01 |

(-) represents rejected dataset (i.e., flux value not calculated)
BDL – below detection limit
ND – not determined

Table 3.32 – Dry Season Surface Flux Results for AF Location

| Compound | Chamber A ($g\ m^{-2}\ day^{-1}$) | Chamber B ($g\ m^{-2}\ day^{-1}$) | Chamber C ($g\ m^{-2}\ day^{-1}$) | Chamber D ($g\ m^{-2}\ day^{-1}$) | Min ($g\ m^{-2}\ day^{-1}$) | Max ($g\ m^{-2}\ day^{-1}$) |
|---|---|---|---|---|---|---|
| CFC-11 | 1.72E-02 | 7.10E-03 | 3.42E-02 | 2.31E-02 | 7.10E-03 | 3.42E-02 |
| CFC-12 | 2.76E-04 | 2.84E-04 | 9.14E-04 | - | 2.76E-04 | 9.14E-04 |
| CFC-113 | - | 6.63E-06 | - | 6.37E-06 | 6.37E-06 | 6.63E-06 |
| CFC-114 | - | - | 7.15E-07 | - | 7.15E-07 | 7.15E-07 |
| HCFC-21 | 8.41E-05 | 8.83E-05 | 1.54E-04 | - | 8.41E-05 | 1.54E-04 |
| HCFC-22 | 1.03E-03 | 5.54E-04 | 1.46E-03 | - | 5.54E-04 | 1.46E-03 |
| HCFC-141b | 7.58E-03 | - | 3.09E-03 | - | 3.09E-03 | 7.58E-03 |
| HCFC-142b | 3.95E-04 | 3.32E-04 | 9.68E-04 | - | 3.32E-04 | 9.68E-04 |
| HCFC-151a | 3.07E-04 | 1.36E-04 | 3.78E-04 | - | 1.36E-04 | 3.78E-04 |
| HFC-134a | 1.79E-03 | 1.21E-03 | 5.07E-03 | - | 1.21E-03 | 5.07E-03 |
| HFC-152a | 2.98E-04 | 2.18E-04 | 3.56E-04 | - | 2.18E-04 | 3.56E-04 |
| HFC-245fa | 2.05E-03 | 1.68E-03 | 8.77E-03 | - | 1.68E-03 | 8.77E-03 |
| $CH_4$ | 3.05E+01 | 3.82E+00 | 1.51E+01 | - | 3.82E+00 | 3.05E+01 |
| $CO_2$ | -1.54E+00 | - | - | - | -1.54E+00 | -1.54E+00 |

(-) represents rejected dataset (i.e., flux value not calculated)

Table 3.33 – Dry Season Surface Flux Results for GW Location

| Compound | Chamber A ($g\ m^{-2}\ day^{-1}$) | Chamber B ($g\ m^{-2}\ day^{-1}$) | Chamber C ($g\ m^{-2}\ day^{-1}$) | Chamber D ($g\ m^{-2}\ day^{-1}$) | Min ($g\ m^{-2}\ day^{-1}$) | Max ($g\ m^{-2}\ day^{-1}$) |
|---|---|---|---|---|---|---|
| CFC-11 | - | - | - | 2.71E-04 | 2.71E-04 | 2.71E-04 |
| CFC-12 | | 1.46E-05 | 1.95E-05 | 1.24E-05 | 1.24E-05 | 1.95E-05 |
| CFC-113 | - | 5.79E-07 | - | 6.91E-07 | 5.79E-07 | 6.91E-07 |
| CFC-114 | - | - | - | 8.07E-06 | 8.07E-06 | 8.07E-06 |
| HCFC-21 | - | - | - | - | - | - |
| HCFC-22 | - | 1.58E-05 | - | 1.22E-05 | 1.22E-05 | 1.58E-05 |
| HCFC-141b | - | - | - | - | - | - |
| HCFC-142b | - | - | - | - | - | - |
| HCFC-151a | 9.40E-04 | 7.80E-05 | - | - | 7.80E-05 | 9.40E-04 |
| HFC-134a | - | - | - | 2.34E-04 | 2.34E-04 | 2.34E-04 |
| HFC-152a | - | 5.50E-05 | 5.04E-05 | 9.44E-05 | 5.04E-05 | 9.44E-05 |
| HFC-245fa | 2.83E-04 | - | - | - | 2.83E-04 | 2.83E-04 |
| $CH_4$ | - | 1.96E+00 | 2.11E+00 | 2.99E+00 | 1.96E+00 | 2.99E+00 |
| $CO_2$ | - | - | 3.27E+01 | 1.32E+01 | 1.32E+01 | 3.27E+01 |

(-) represents rejected dataset (i.e., flux value not calculated)

Table 3.34 – Dry Season Surface Flux Results for ED Location

| Compound | Chamber A ($g\ m^{-2}\ day^{-1}$) | Chamber B ($g\ m^{-2}\ day^{-1}$) | Chamber C ($g\ m^{-2}\ day^{-1}$) | Chamber D ($g\ m^{-2}\ day^{-1}$) | Min ($g\ m^{-2}\ day^{-1}$) | Max ($g\ m^{-2}\ day^{-1}$) |
|---|---|---|---|---|---|---|
| CFC-11 | 8.13E-03 | 1.35E-03 | - | 5.28E-03 | 1.35E-03 | 8.13E-03 |
| CFC-12 | 1.12E-03 | 2.14E-04 | 8.69E-04 | 1.03E-03 | 2.14E-04 | 1.12E-03 |
| CFC-113 | - | - | 4.94E-06 | 9.05E-06 | 4.94E-06 | 9.05E-06 |
| CFC-114 | 3.34E-06 | 6.34E-07 | 3.33E-06 | 4.03E-06 | 6.34E-07 | 4.03E-06 |
| HCFC-21 | 2.18E-04 | 1.59E-05 | 2.75E-04 | 2.24E-04 | 1.59E-05 | 2.75E-04 |
| HCFC-22 | 3.51E-04 | 5.94E-05 | 2.90E-04 | 4.48E-04 | 5.94E-05 | 4.48E-04 |
| HCFC-141b | 7.22E-03 | 5.68E-04 | - | 1.82E-03 | 5.68E-04 | 7.22E-03 |
| HCFC-142b | 1.21E-04 | 2.01E-05 | 6.82E-05 | 1.23E-04 | 2.01E-05 | 1.23E-04 |
| HCFC-151a | 3.19E-04 | 5.32E-05 | 5.13E-04 | 8.62E-04 | 5.32E-05 | 8.62E-04 |
| HFC-134a | 1.21E-03 | 1.85E-04 | - | 1.47E-03 | 1.85E-04 | 1.47E-03 |
| HFC-152a | 1.07E-03 | 1.94E-04 | 9.66E-04 | 1.27E-03 | 1.94E-04 | 1.27E-03 |
| HFC-245fa | 7.55E-05 | 1.72E-05 | 1.14E-04 | 1.78E-04 | 1.72E-05 | 1.78E-04 |
| $CH_4$ | 5.38E+01 | 1.47E+01 | 3.49E+01 | - | 1.47E+01 | 5.38E+01 |
| $CO_2$ | -1.96E+01 | - | - | -2.55E-01 | -1.96E+01 | -2.55E-01 |

(-) represents rejected dataset (i.e., flux value not calculated)

Table 3.35 – Dry Season Surface Flux Results for IC-1 Location

| Compound | Chamber A ($g\ m^{-2}\ day^{-1}$) | Chamber B ($g\ m^{-2}\ day^{-1}$) | Chamber C ($g\ m^{-2}\ day^{-1}$) | Chamber D ($g\ m^{-2}\ day^{-1}$) | Min ($g\ m^{-2}\ day^{-1}$) | Max ($g\ m^{-2}\ day^{-1}$) |
|---|---|---|---|---|---|---|
| CFC-11 | - | - | - | 9.47E-07 | 9.47E-07 | 9.47E-07 |
| CFC-12 | - | 1.63E-06 | - | - | 1.63E-06 | 1.63E-06 |
| CFC-113 | 5.31E-07 | - | - | -5.96E-07 | -5.96E-07 | 5.31E-07 |
| CFC-114 | 6.56E-07 | - | - | - | 6.56E-07 | 6.56E-07 |
| HCFC-21 | BDL | BDL | BDL | BDL | ND | ND |
| HCFC-22 | 4.50E-06 | - | - | -1.07E-07 | -1.07E-07 | 4.50E-06 |
| HCFC-141b | 4.79E-06 | - | - | - | 4.79E-06 | 4.79E-06 |
| HCFC-142b | 3.84E-06 | - | - | - | 3.84E-06 | 3.84E-06 |
| HCFC-151a | BDL | BDL | BDL | BDL | ND | ND |
| HFC-134a | 1.31E-05 | 7.19E-07 | - | - | 7.19E-07 | 1.31E-05 |
| HFC-152a | - | - | 1.83E-06 | - | 1.83E-06 | 1.83E-06 |
| HFC-245fa | - | - | 2.35E-08 | - | 2.35E-08 | 2.35E-08 |
| $CH_4$ | - | - | - | - | - | - |
| $CO_2$ | 3.69E+01 | 2.29E+00 | 2.90E+00 | - | 2.29E+00 | 3.69E+01 |

(-) represents rejected dataset (i.e., flux value not calculated)
BDL – below detection limit
ND – not determined

Table 3.36 – Dry Season Surface Flux Results for IC-10 Location

| Compound | Chamber A ($g\ m^{-2}\ day^{-1}$) | Chamber B ($g\ m^{-2}\ day^{-1}$) | Chamber C ($g\ m^{-2}\ day^{-1}$) | Chamber D ($g\ m^{-2}\ day^{-1}$) | Min ($g\ m^{-2}\ day^{-1}$) | Max ($g\ m^{-2}\ day^{-1}$) |
|---|---|---|---|---|---|---|
| CFC-11 | - | 1.57E-05 | 3.91E-06 | 9.12E-06 | 3.91E-06 | 1.57E-05 |
| CFC-12 | - | - | - | - | - | - |
| CFC-113 | - | - | - | 5.46E-07 | 5.46E-07 | 5.46E-07 |
| CFC-114 | 5.59E-07 | 6.33E-07 | 6.56E-07 | 1.06E-07 | 1.06E-07 | 6.56E-07 |
| HCFC-21 | BDL | BDL | BDL | BDL | ND | ND |
| HCFC-22 | - | -2.30E-06 | 9.22E-07 | -1.33E-07 | -2.30E-06 | 9.22E-07 |
| HCFC-141b | - | 2.07E-05 | 5.19E-06 | - | 5.19E-06 | 2.07E-05 |
| HCFC-142b | - | -7.04E-08 | 3.57E-07 | - | -7.04E-08 | 3.57E-07 |
| HCFC-151a | BDL | BDL | BDL | BDL | ND | ND |
| HFC-134a | - | - | 9.06E-07 | - | 9.06E-07 | 9.06E-07 |
| HFC-152a | - | - | - | - | - | - |
| HFC-245fa | - | 4.51E-08 | - | 3.68E-08 | 3.68E-08 | 4.51E-08 |
| $CH_4$ | - | - | -6.06E-03 | 1.17E-03 | -6.06E-03 | 1.17E-03 |
| $CO_2$ | 9.32E+00 | 1.63E+01 | 8.15E+00 | 3.90E+00 | 3.90E+00 | 1.63E+01 |

(-) represents rejected dataset (i.e., flux value not calculated)
BDL – below detection limit
ND – not determined

Table 3.37 – Dry Season Surface Flux Results for IC-15 Location

| Compound | Chamber A ($g\ m^{-2}\ day^{-1}$) | Chamber B ($g\ m^{-2}\ day^{-1}$) | Chamber C ($g\ m^{-2}\ day^{-1}$) | Chamber D ($g\ m^{-2}\ day^{-1}$) | Min ($g\ m^{-2}\ day^{-1}$) | Max ($g\ m^{-2}\ day^{-1}$) |
|---|---|---|---|---|---|---|
| CFC-11 | - | - | - | 4.81E-06 | 4.81E-06 | 4.81E-06 |
| CFC-12 | - | 3.27E-06 | - | - | 3.27E-06 | 3.27E-06 |
| CFC-113 | - | 8.29E-07 | - | 4.46E-07 | 4.46E-07 | 8.29E-07 |
| CFC-114 | 3.23E-05 | 3.14E-05 | 1.18E-05 | 6.85E-06 | 6.85E-06 | 3.23E-05 |
| HCFC-21 | - | 7.21E-07 | BDL | BDL | 7.21E-07 | 7.21E-07 |
| HCFC-22 | 1.80E-05 | 8.90E-06 | 7.23E-06 | 9.57E-06 | 7.23E-06 | 1.80E-05 |
| HCFC-141b | - | - | 1.93E-05 | - | 1.93E-05 | 1.93E-05 |
| HCFC-142b | 3.08E-06 | 4.78E-06 | 2.19E-06 | 2.49E-06 | 2.19E-06 | 4.78E-06 |
| HCFC-151a | 9.29E-05 | 6.14E-05 | 4.74E-05 | 5.66E-05 | 4.74E-05 | 9.29E-05 |
| HFC-134a | 1.82E-04 | 1.95E-04 | 1.24E-04 | 1.24E-04 | 1.24E-04 | 1.95E-04 |
| HFC-152a | - | 1.86E-04 | 2.94E-05 | 1.22E-05 | 1.22E-05 | 1.86E-04 |
| HFC-245fa | 2.30E-05 | 1.22E-05 | 7.56E-06 | 1.03E-05 | 7.56E-06 | 2.30E-05 |
| $CH_4$ | 1.73E+01 | 9.33E+00 | 1.36E+01 | 1.22E+01 | 9.33E+00 | 1.73E+01 |
| $CO_2$ | 1.13E+02 | 1.25E+02 | 7.96E+01 | 6.21E+01 | 6.21E+01 | 1.25E+02 |

(-) represents rejected dataset (i.e., flux value not calculated)
BDL – below detection limit

Table 3.38 – Dry Season Surface Flux Results for FC Location

| Compound | Chamber A ($g\ m^{-2}\ day^{-1}$) | Chamber B ($g\ m^{-2}\ day^{-1}$) | Chamber C ($g\ m^{-2}\ day^{-1}$) | Chamber D ($g\ m^{-2}\ day^{-1}$) | Min ($g\ m^{-2}\ day^{-1}$) | Max ($g\ m^{-2}\ day^{-1}$) |
|---|---|---|---|---|---|---|
| CFC-11 | - | - | - | - | - | - |
| CFC-12 | - | - | - | - | - | - |
| CFC-113 | - | - | - | -6.81E-08 | -6.81E-08 | -6.81E-08 |
| CFC-114 | - | - | - | - | 1.54E-06 | 1.54E-06 |
| HCFC-21 | BDL | BDL | BDL | BDL | ND | ND |
| HCFC-22 | - | - | - | - | - | - |
| HCFC-141b | -5.01E-07 | - | - | - | -5.01E-07 | -5.01E-07 |
| HCFC-142b | - | - | - | - | - | - |
| HCFC-151a | BDL | BDL | BDL | BDL | ND | ND |
| HFC-134a | - | - | - | - | - | - |
| HFC-152a | 1.70E-06 | - | - | - | 1.70E-06 | 1.70E-06 |
| HFC-245fa | - | 9.89E-09 | - | 9.74E-09 | 9.74E-09 | 9.89E-09 |
| $CH_4$ | - | - | - | 2.94E-04 | 2.94E-04 | 2.94E-04 |
| $CO_2$ | 1.27E+01 | 1.95E+00 | 1.85E+01 | - | 1.95E+00 | 1.85E+01 |

(-) represents rejected dataset (i.e., flux value not calculated)
BDL – below detection limit
ND – not determined

Flux data are presented for individual chemicals in Figures 3.17 to 3.30. Data are presented for all seven test locations for each chemical in the figures. Results obtained for wet and dry seasons are presented in each figure. In general, the flux decreased from the daily covers to intermediate covers to the final cover. Negative fluxes were measured during both wet and dry seasons. Negative fluxes were measured in all cover types except GW. For wet season, 3.6% of all flux tests resulted in negative flux. For wet season, 2.8% of all flux tests resulted in negative flux. The maximum flux values typically occurred through the auto fluff daily cover. The minimum flux typically was through the final cover or in some cases through IC-1. Based on the type of the cover materials (Table 3.8), the daily covers are expected to have high permeability; the intermediate covers, IC-10 and IC-15, to have moderate permeability; and the intermediate cover IC-1 and the final cover to have low permeability. While placement of the intermediate covers at the site did not follow strict compaction QA and QC procedures, the presence of the high-plasticity fat clay in Intermediate Cover 1 is expected to have contributed to the low permeability and resulting low emissions from this cover. The final cover was constructed using strict engineering controls and the construction practices together with the presence of the fat clay is expected to have resulted in low permeability and associated low flux values. In addition, the thicknesses of the cover systems (Figure 3.13, Table 3.8) increased from daily to intermediate to final covers contributing to the flux that decreased in the same order. These observations agreed with data provided in literature, where landfill gas emissions were reported to typically decrease with the order daily, intermediate, and permanent covers; high permeability to low permeability covers; and thin to thick soil covers (e.g., Abichou et al. 2006a).

The data obtained in the investigation was compared to emissions data presented in the literature (Table 1.11). Comparisons were made only to data obtained from MSW and using static flux chamber measurements (first three columns in Table 1.11). Also, comparisons were made for three of the four target F-gases, as data had not been previously reported for HFC-245fa in the literature. For CFC-11, the measured range in this study ($9.47x10^{-7}$ to $2.57x10^{-1}$ g/m$^2$-day) was higher than the range reported in the literature ($-8.8x10^{-5}$ to $7.63x10^{-5}$ g/m$^2$-day). For HCFC-141b, the measured range ($-5.59x10^{-6}$ to $2.99x10^{-1}$ g/m$^2$-day) was higher than the range in the literature $3.63x10^{-6}$ to $6.66x10^{-5}$ g/m$^2$-day). Similarly, for HFC-134a, the range measured in this study ($5.69x10^{-7}$ to $3.79x10^{-2}$ g/m$^2$-day) was higher than the range reported in the literature ($-2.50x10^{-7}$ to $2.05x10^{-4}$ g/m$^2$-day). The higher values in this test program resulted from the data obtained from the three daily cover locations. None of the previous studies included testing of daily covers. When only intermediate and final covers are considered, the data obtained in this test program indicated that the CFC-11 emissions were approximately one order of magnitude lower; HCFC-141b emissions were generally in line with; and HFC 134a emissions were up to two orders of magnitude higher than the emissions reported in the literature. The data in the literature had been obtained approximately between early and mid 2000s. The current study, which was conducted approximately a decade after the studies reported in the literature, likely captured the historic replacement trends for (hydro)chlorofluorocarbons in waste products.

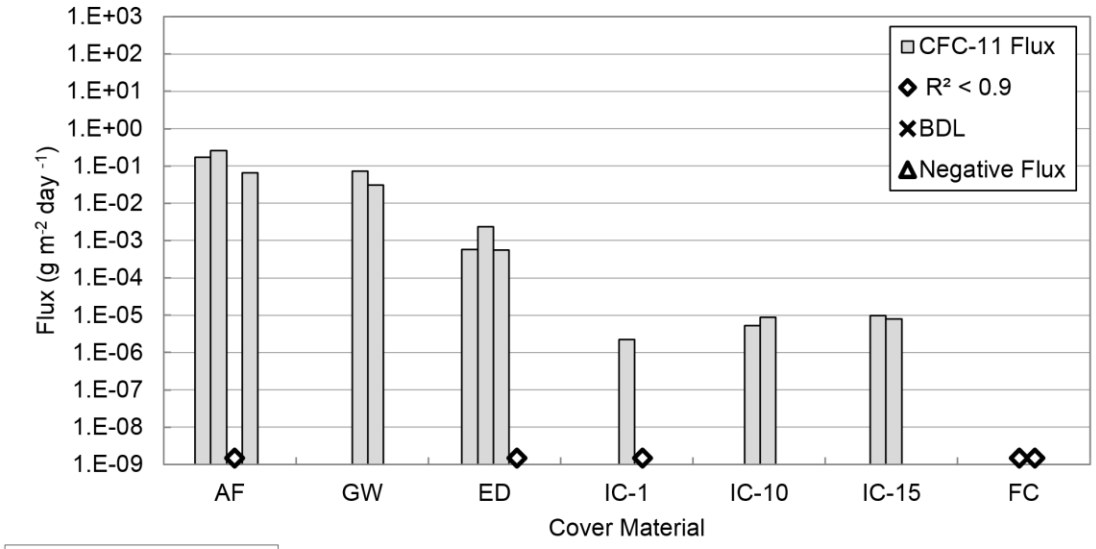


CFC-11 (Wet Season)

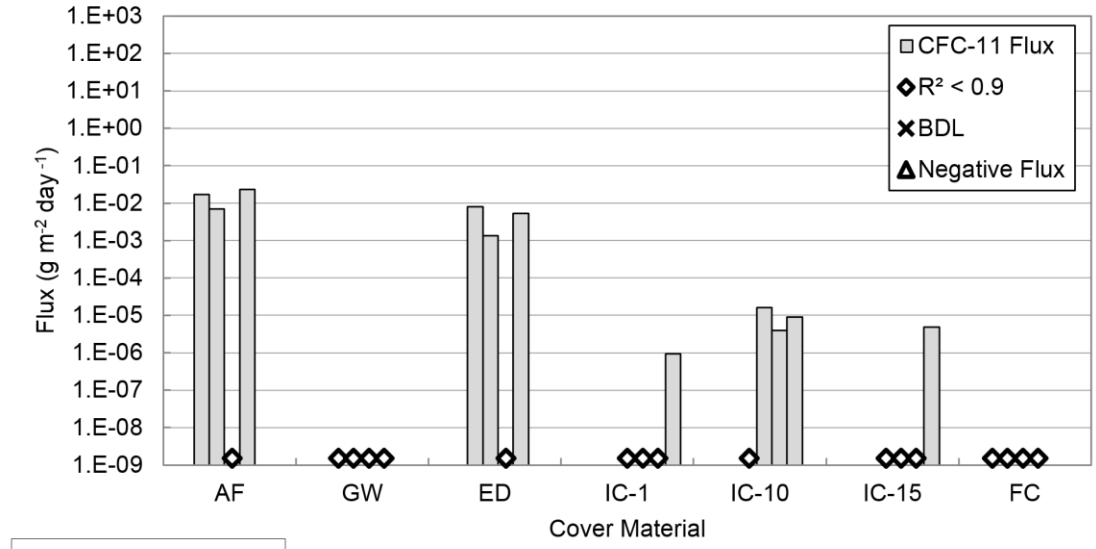


CFC-11 (Dry Season)

Figure 3.17. Measured Surface Flux of CFC-11 at the Test Site

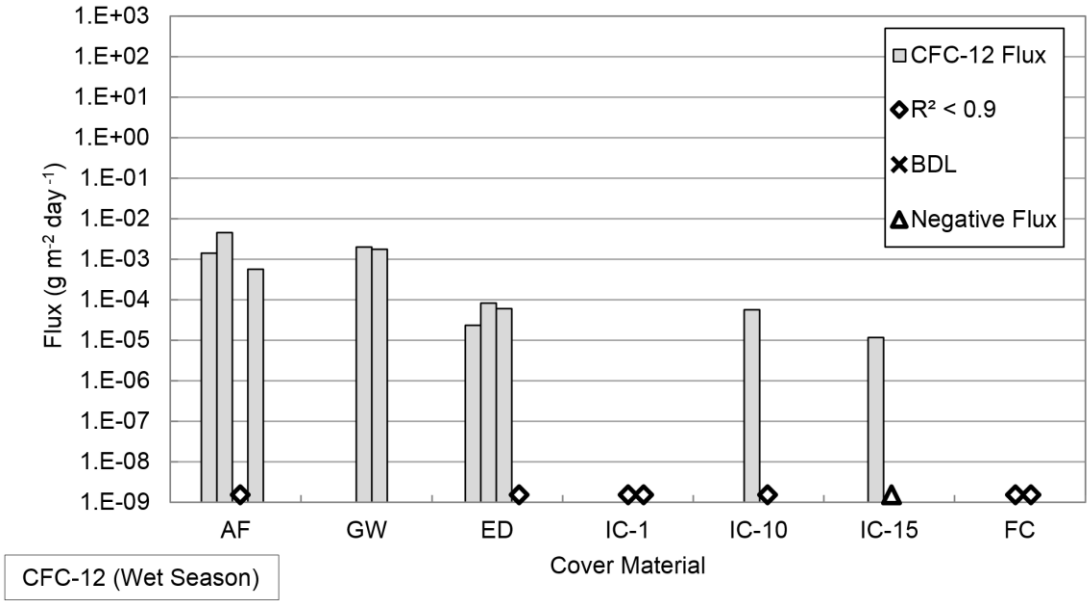


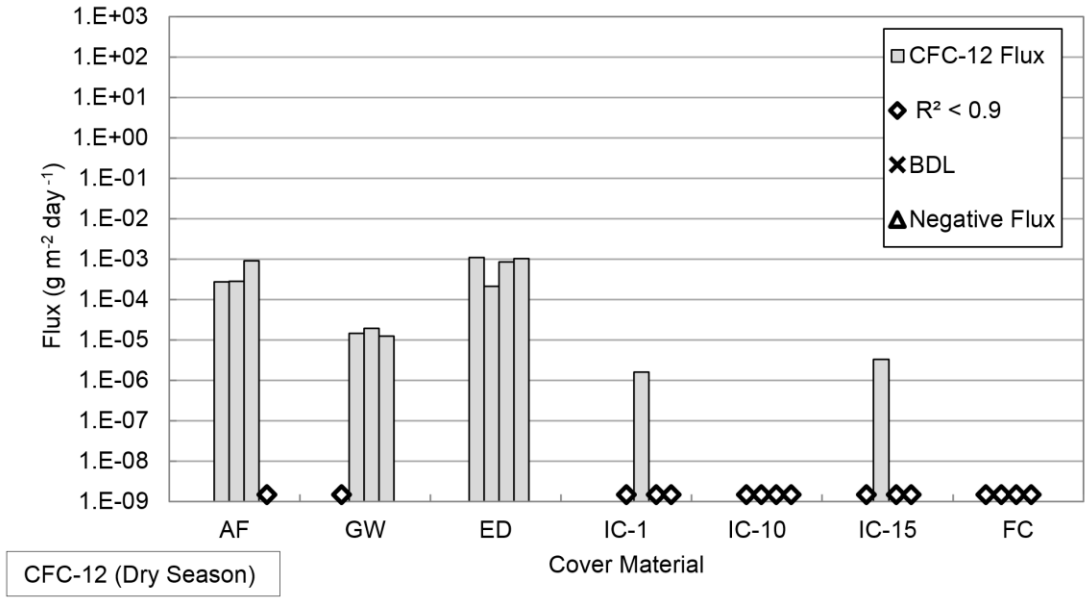


Figure 3.18. Measured Surface Flux of CFC-12 at the Test Site

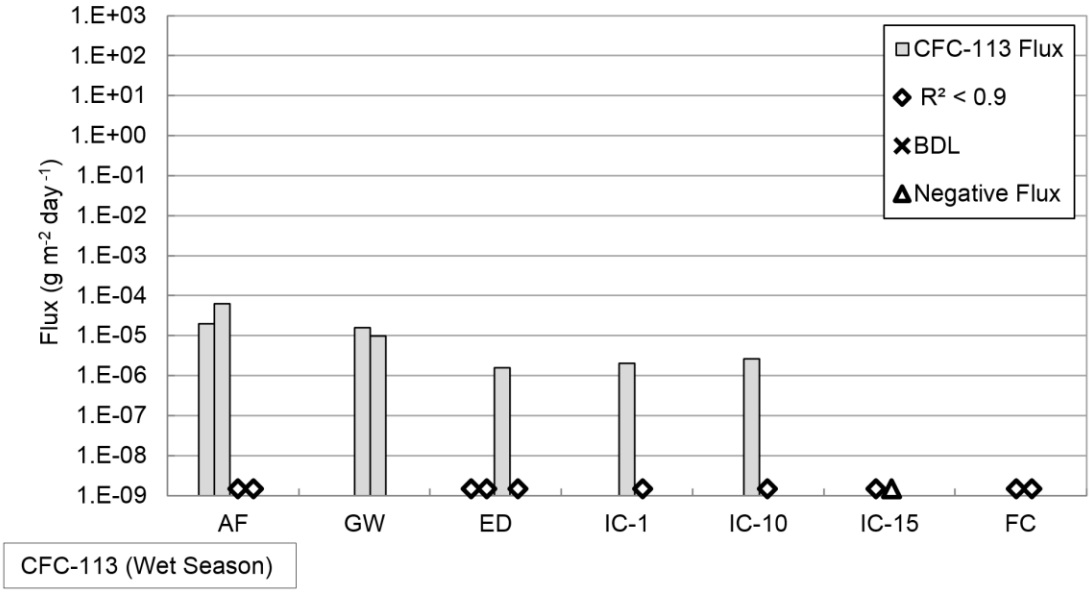


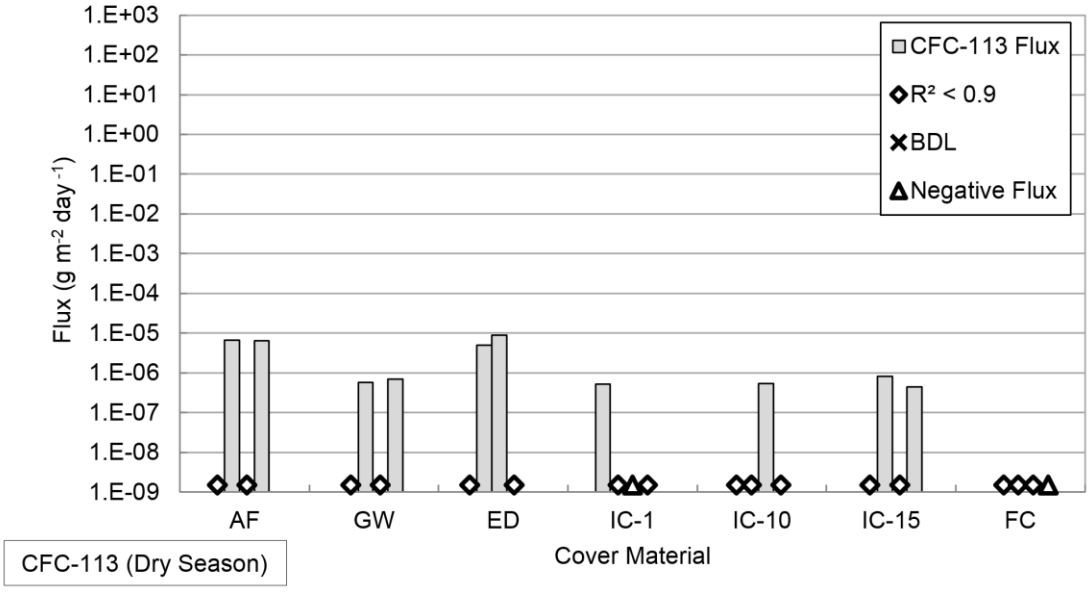


Figure 3.19. Measured Surface Flux of CFC-113 at the Test Site

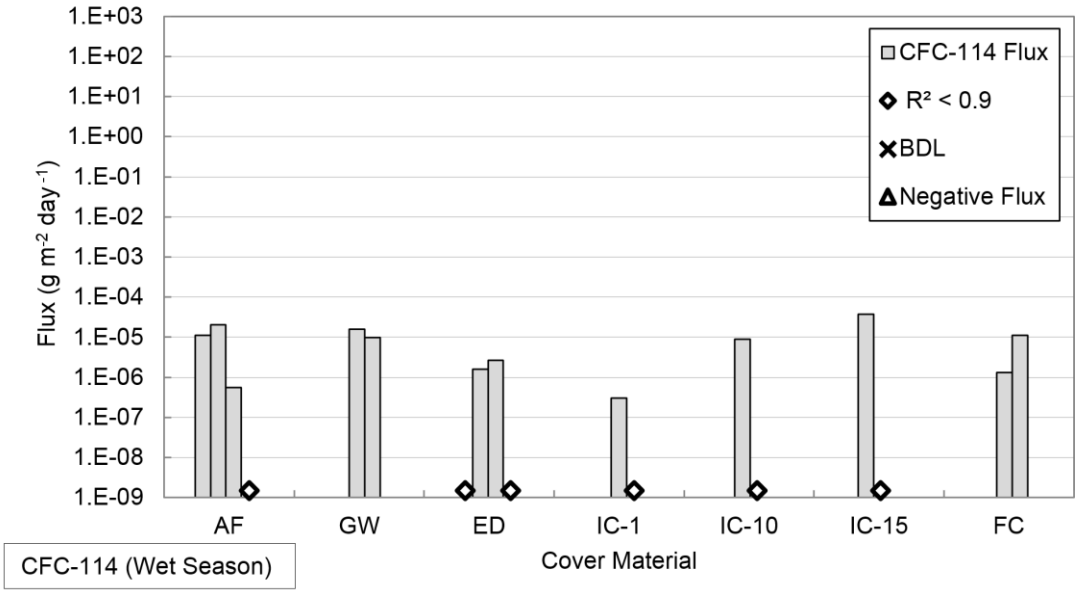


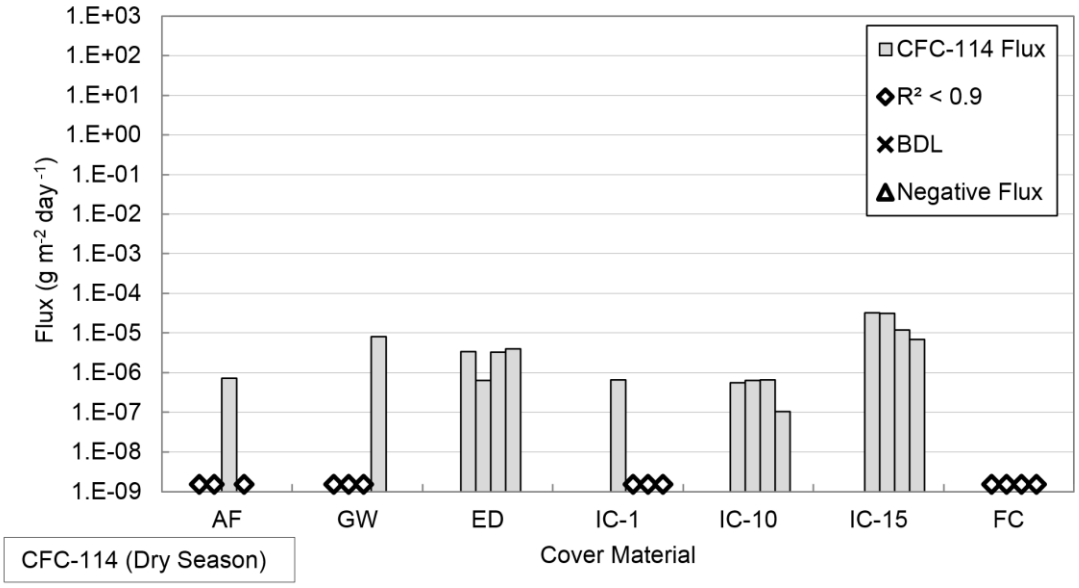


Figure 3.20. Measured Surface Flux of CFC-114 at the Test Site

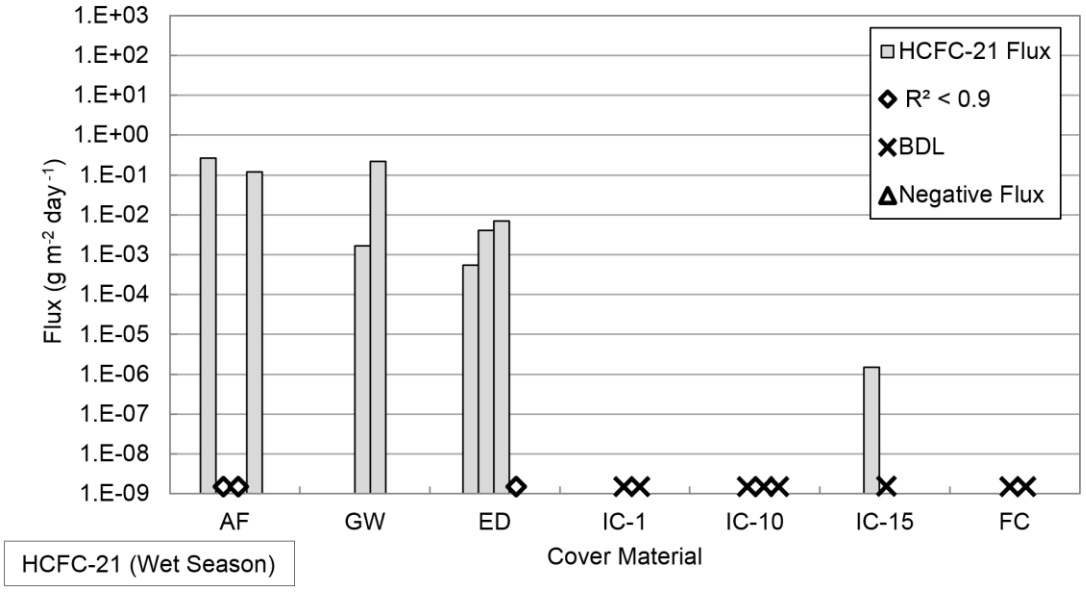


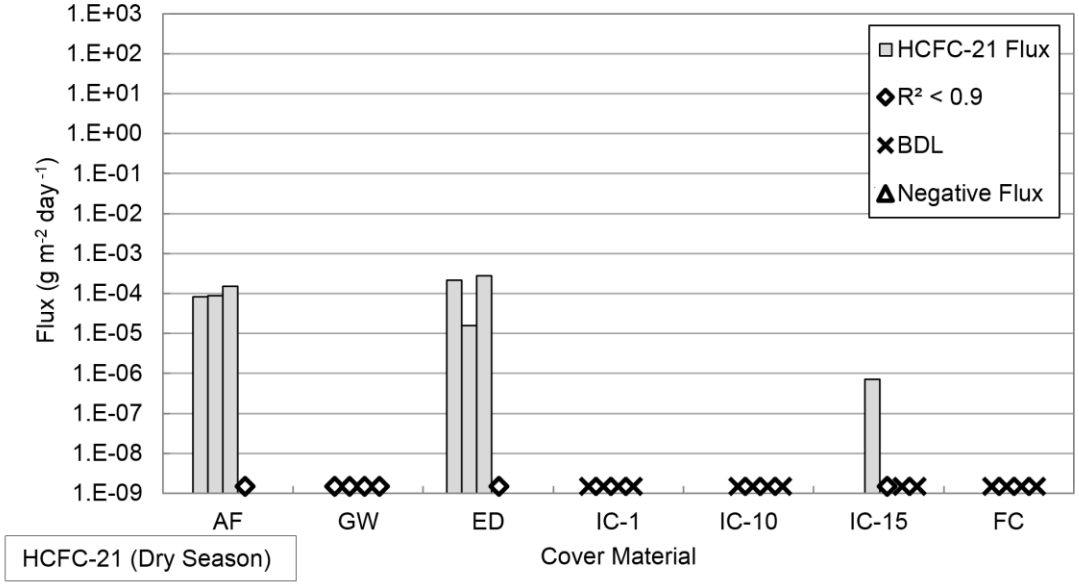


Figure 3.21. Measured Surface Flux of HCFC-21 at the Test Site

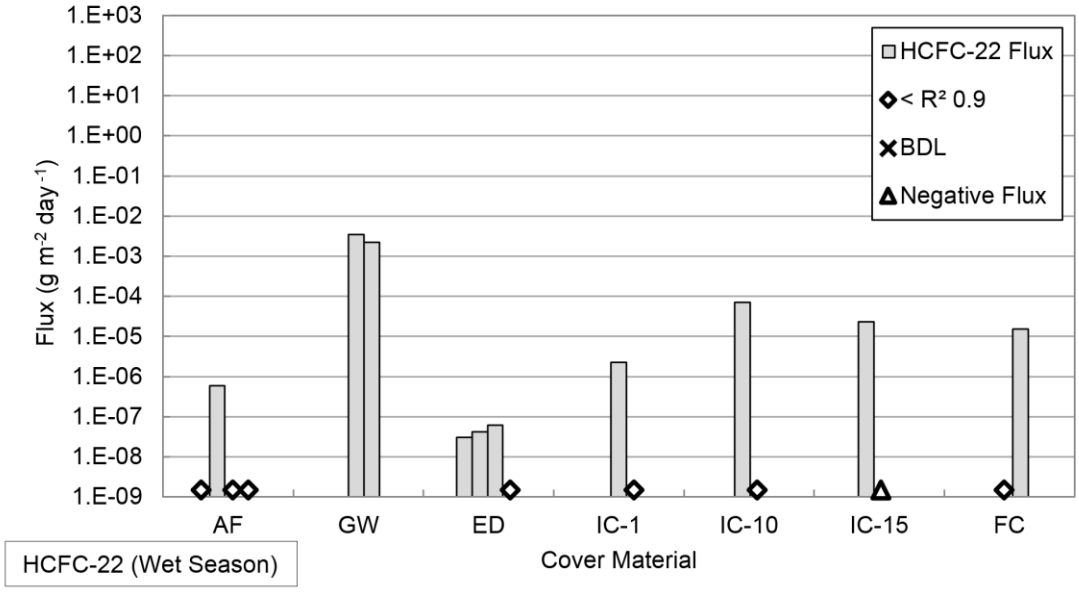


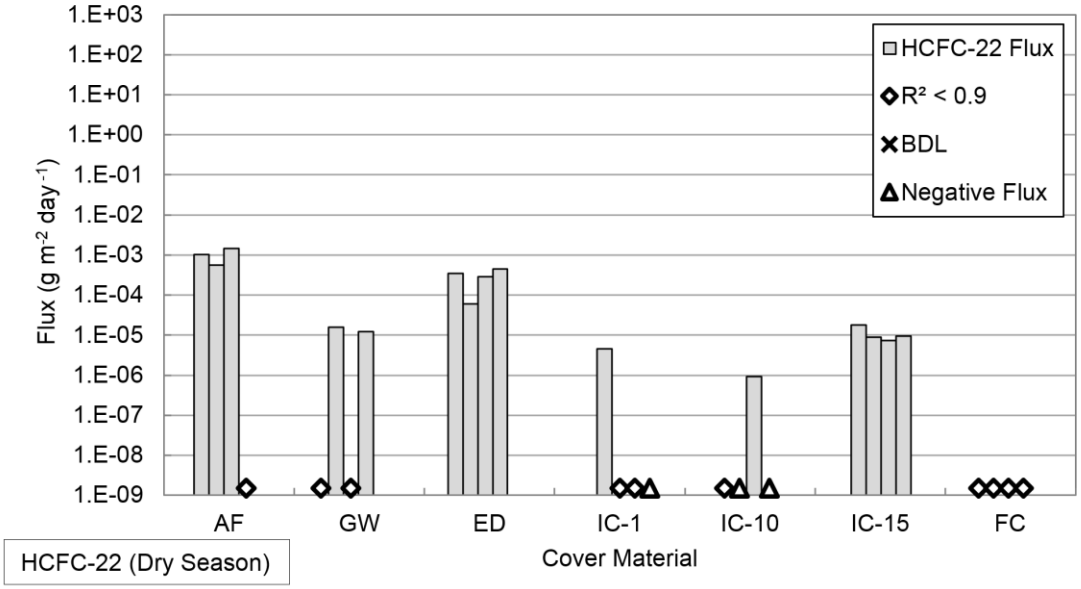


Figure 3.22. Measured Surface Flux of HCFC-22 at the Test Site

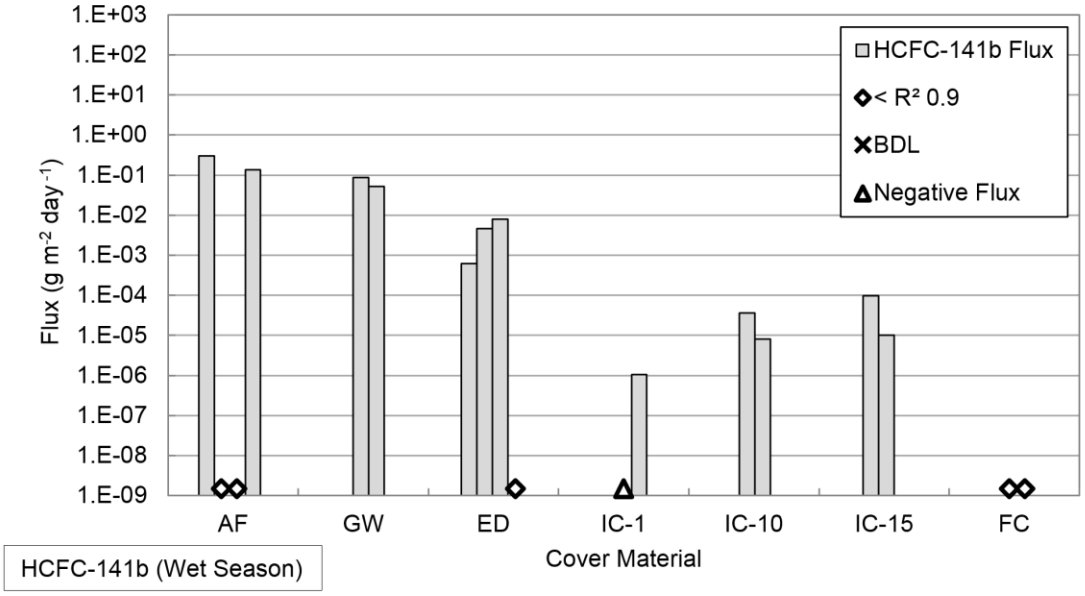


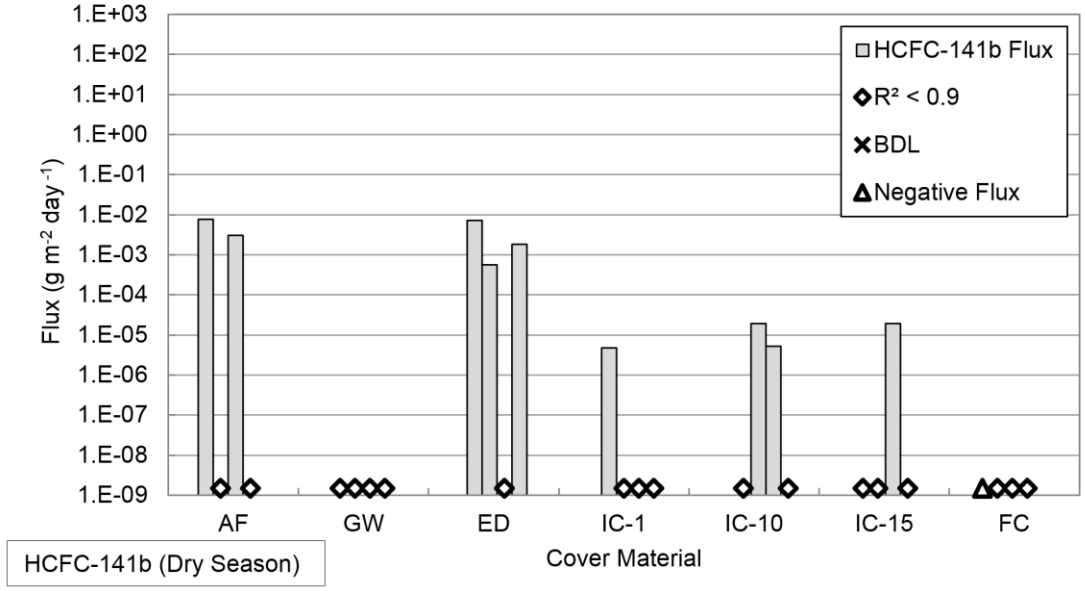


Figure 3.23. Measured Surface Flux of HCFC-141b at the Test Site

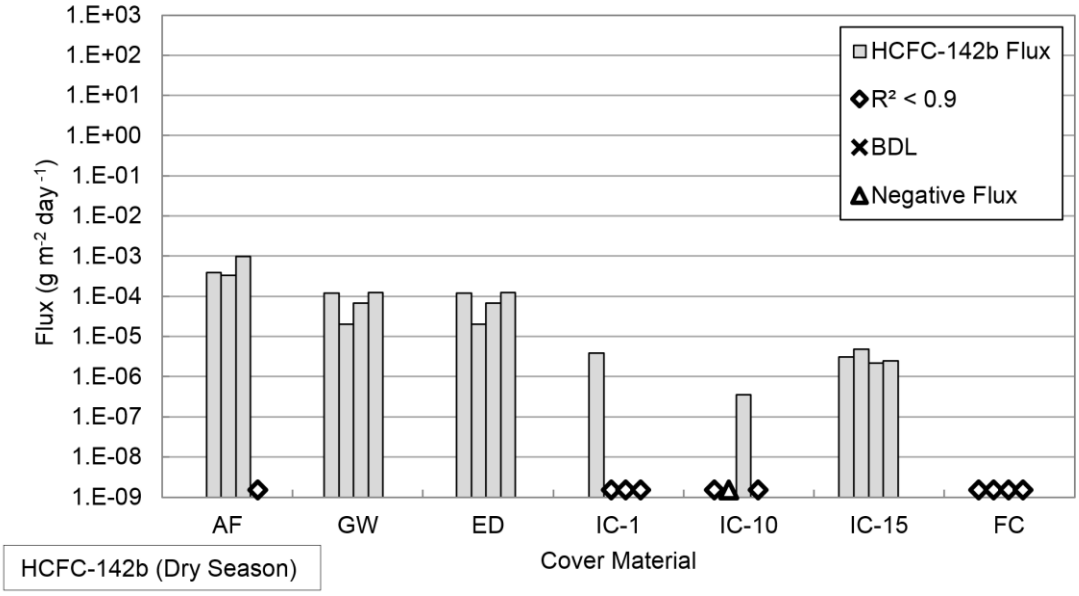


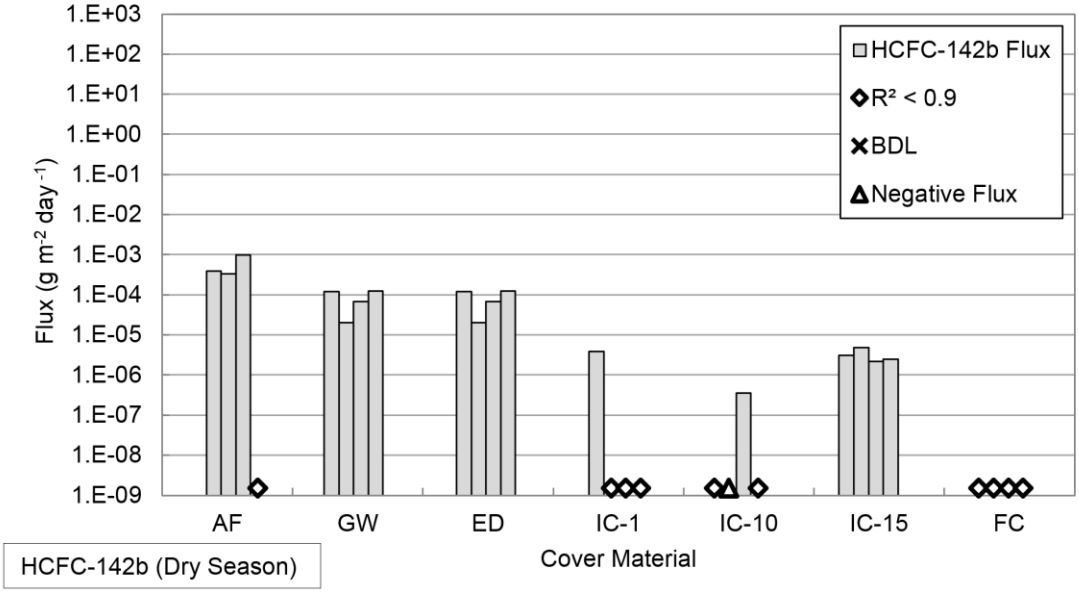


Figure 3.24. Measured Surface Flux of HCFC-142b at the Test Site

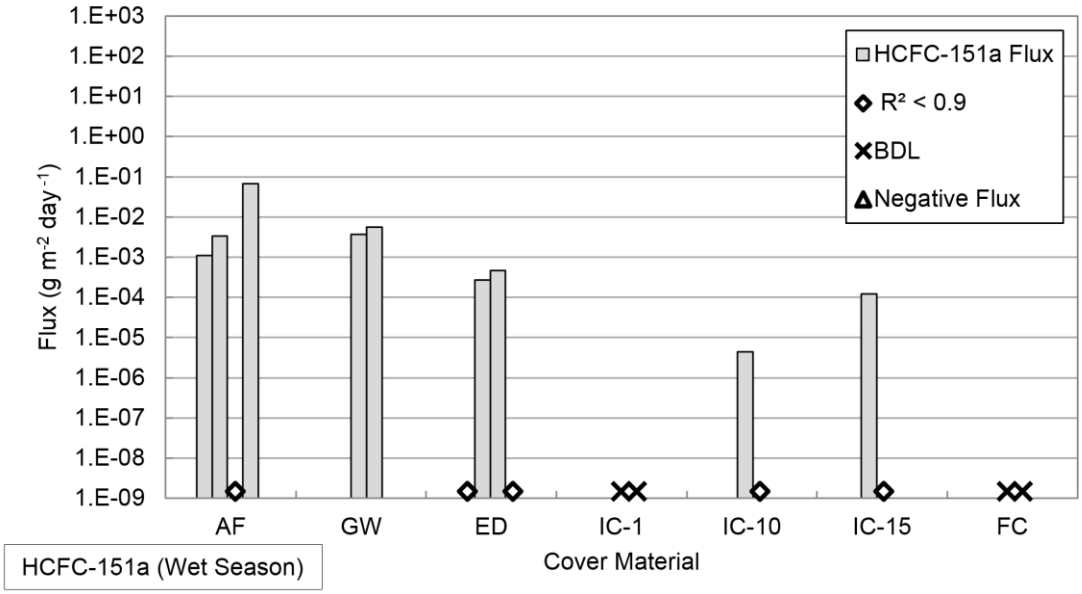


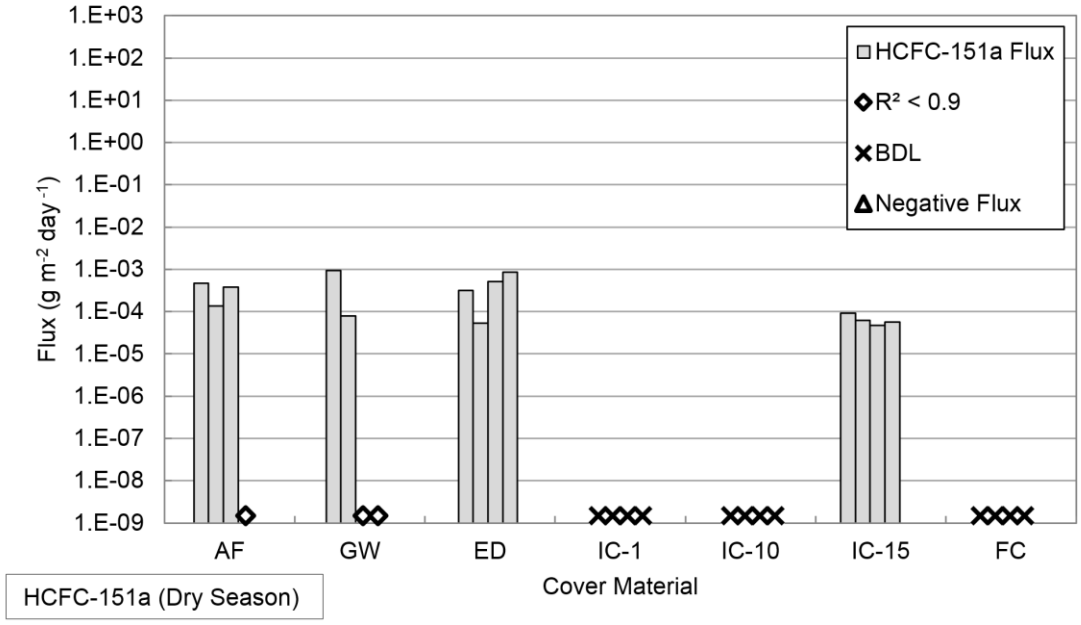


Figure 3.25. Measured Surface Flux of HCFC-151a at the Test Site

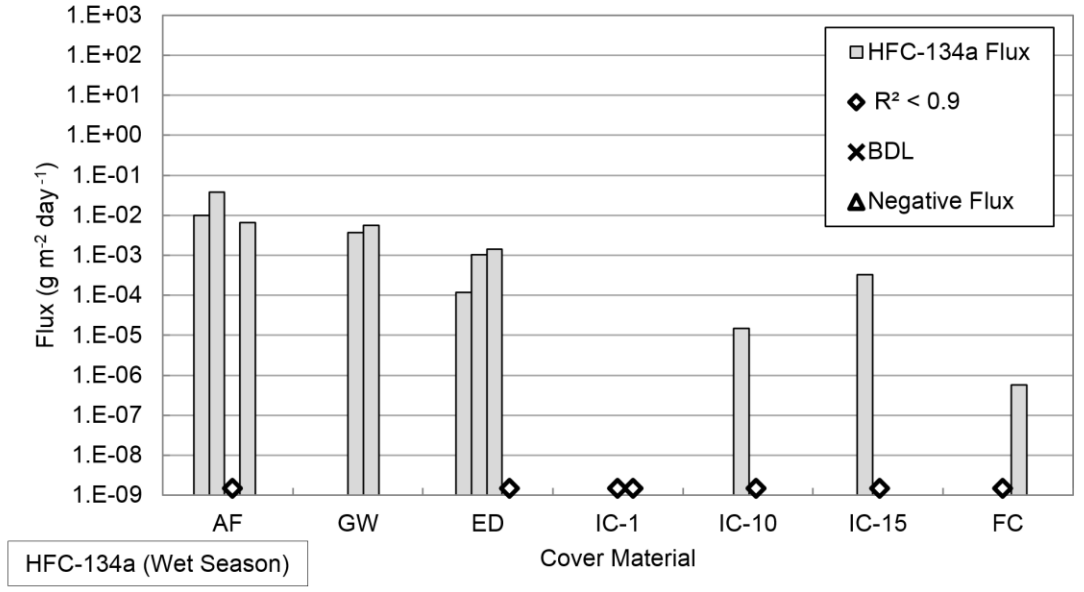


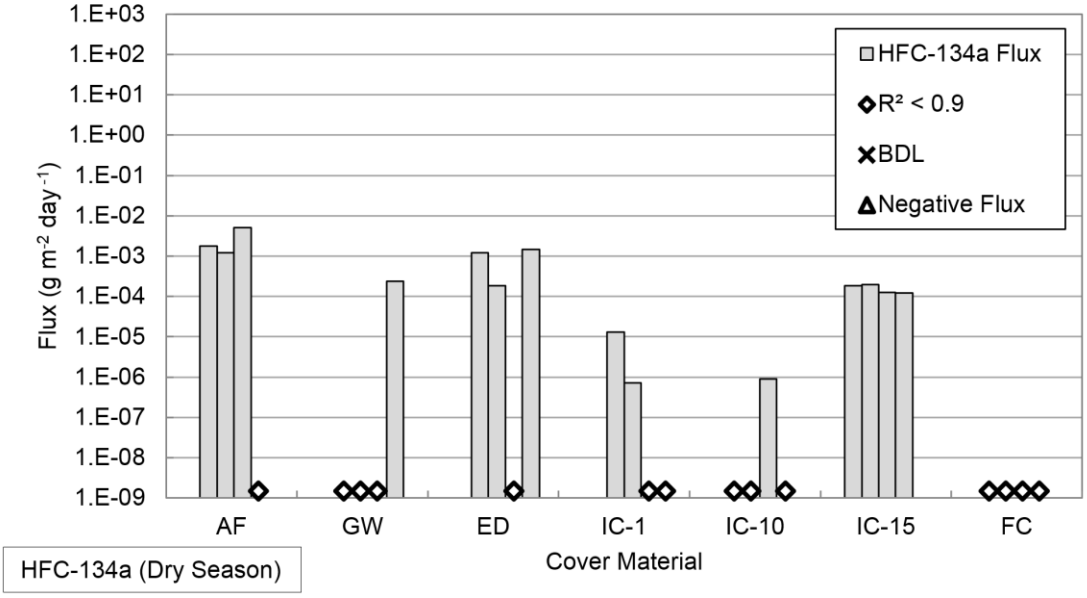


Figure 3.26. Measured Surface Flux of HFC-134a at the Test Site

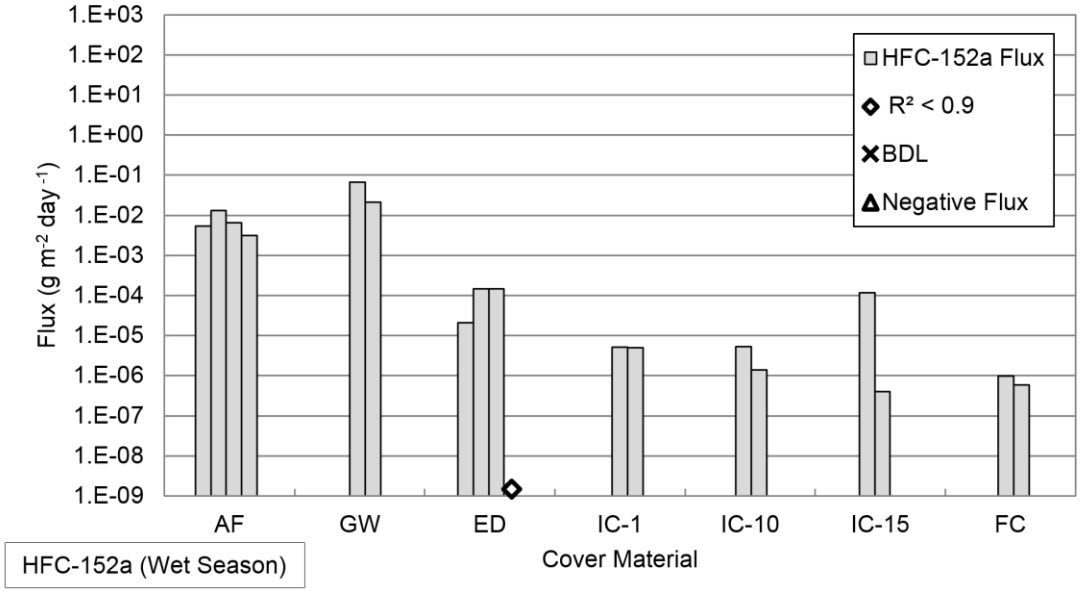


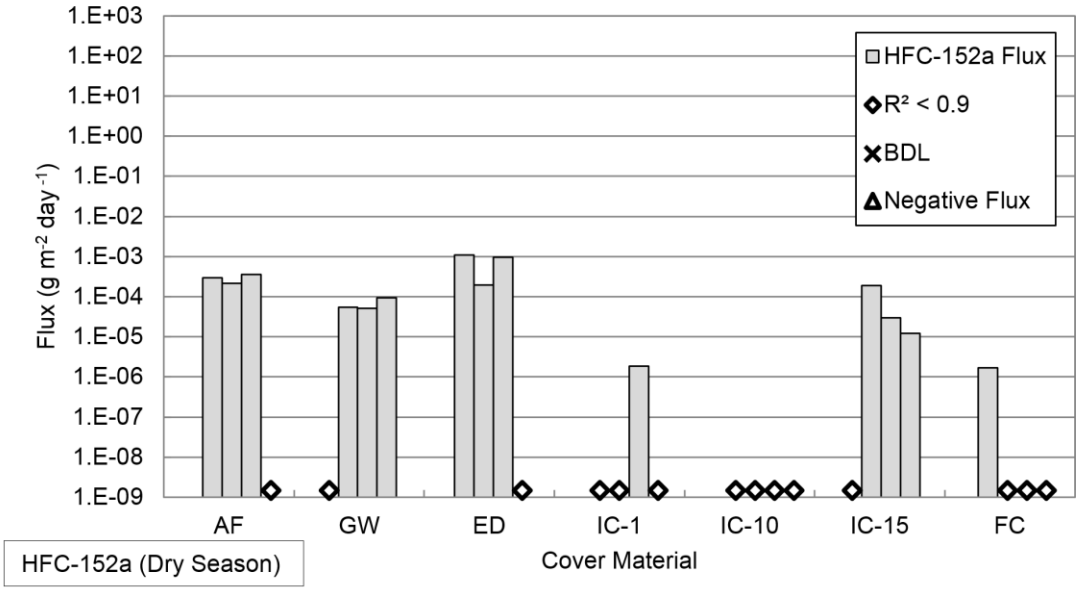


Figure 3.27. Measured Surface Flux of HFC-152a at the Test Site

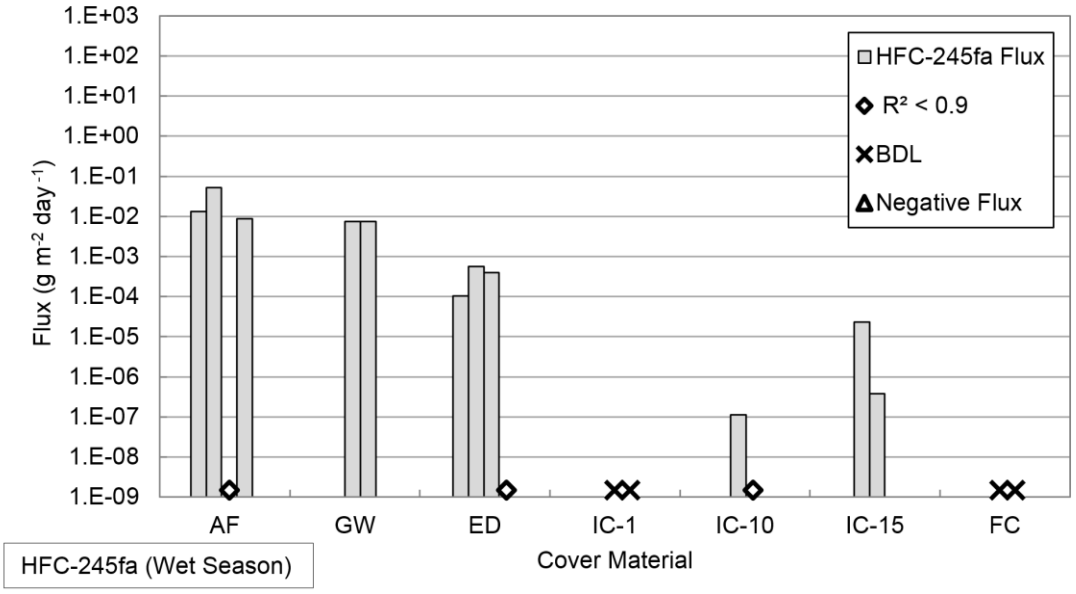


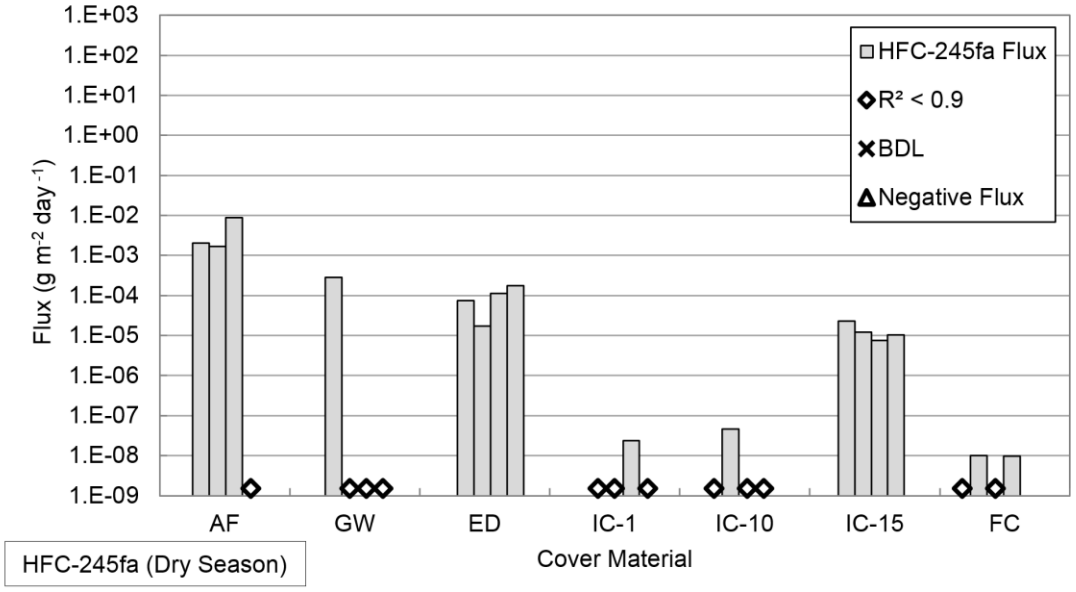


Figure 3.28. Measured Surface Flux of HFC-245fa at the Test Site

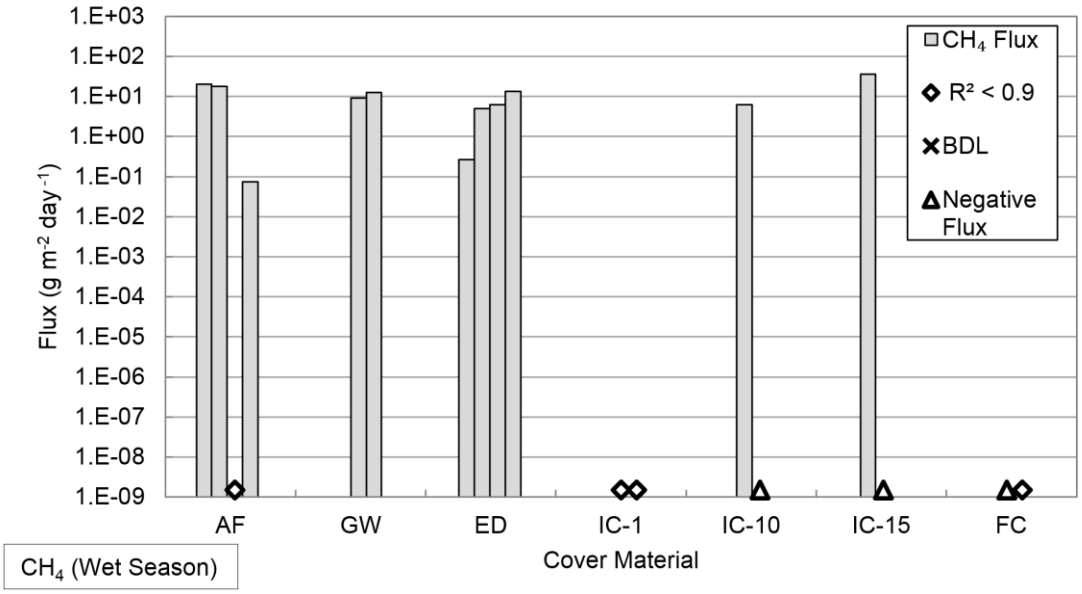


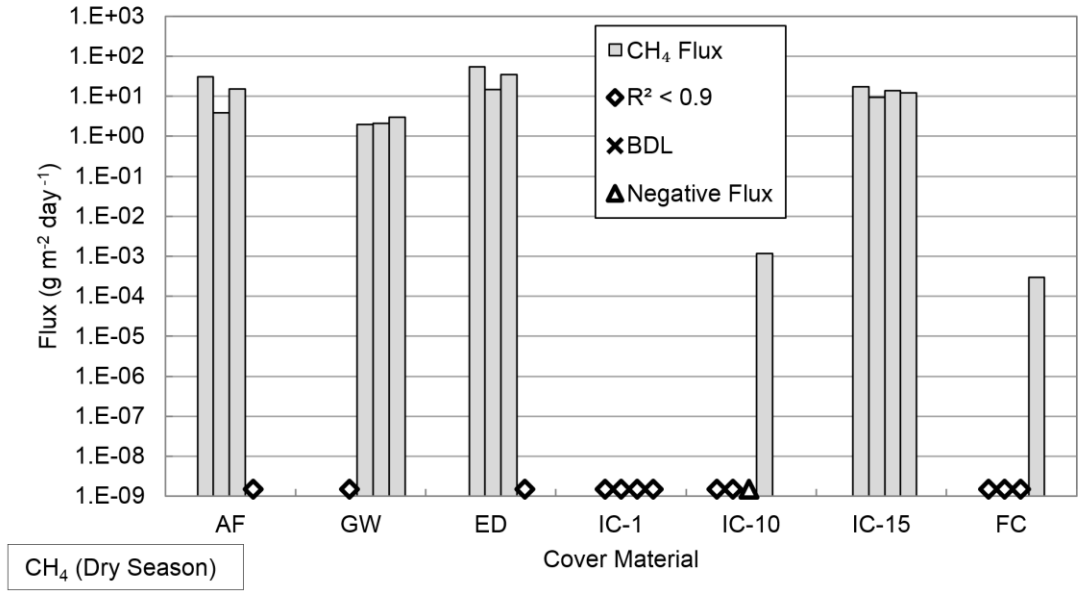


Figure 3.29. Measured Surface Flux of Methane at the Test Site

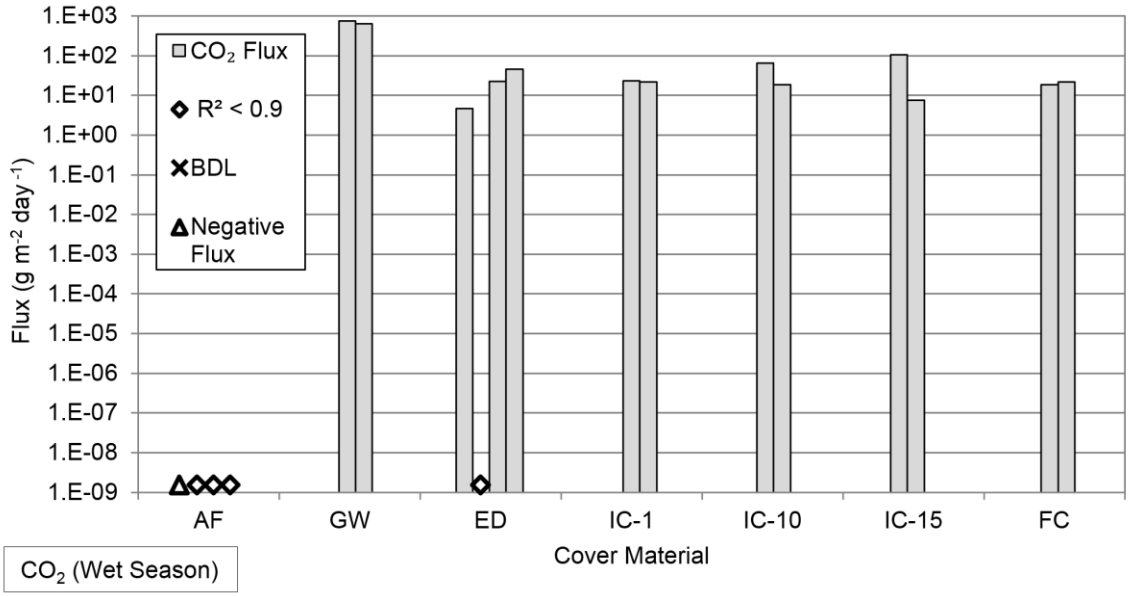


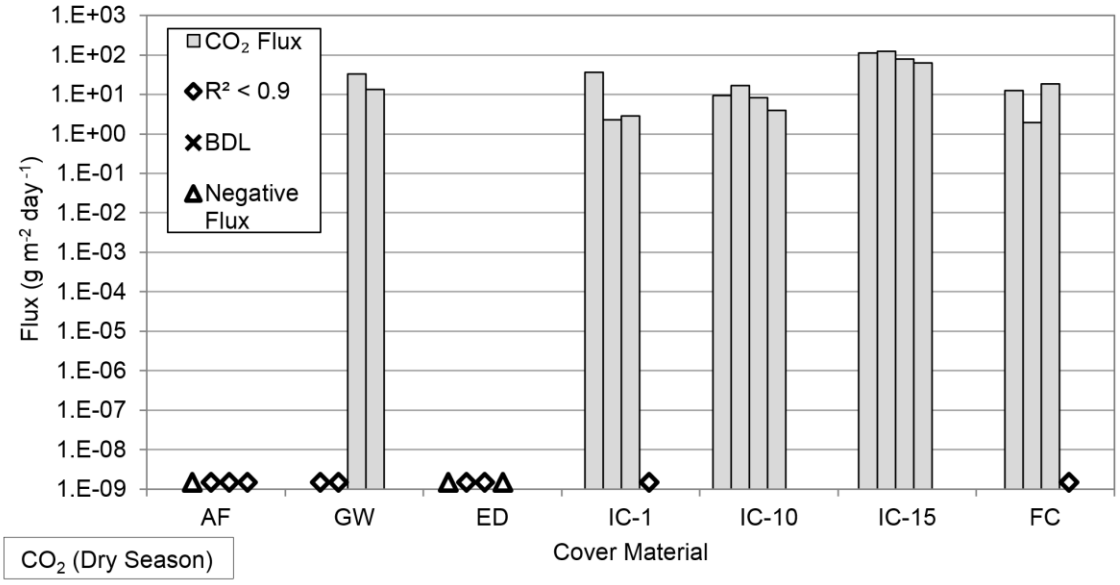


Figure 3.30. Measured Surface Flux of Carbon Dioxide at the Test Site

Based on the flux data obtained in the test program, in the wet season, the minimum and maximum fluxes for CFC-11, HCFC-141b, HFC-134a, and HFC-245fa were $2.27x10^{-6}$ and $2.57x10^{-1}$ g/m$^{-2}$-day, $-5.59x10^{-6}$ and $2.99x10^{-1}$ g/m$^{-2}$-day, $5.69x10^{-7}$ and $3.79x10^{-2}$ g/m$^{-2}$-day, and $1.14x10^{-7}$ and $5.21x10^{-2}$ g/m$^{-2}$-day, respectively. In the dry season, the minimum and maximum fluxes for CFC-11, HCFC-141b, HFC-134a, and HFC-245fa were $9.47x10^{-7}$ and $3.42x10^{-2}$ g/m$^{-2}$-day, $-5.01x10^{-7}$ and $7.58x10^{-3}$ g/m$^{-2}$-day, $7.19x10^{-7}$ and $5.07x10^{-3}$ g/m$^{-2}$-day, and $9.74x10^{-9}$ and $8.77x10^{-3}$ g/m$^{-2}$-day, respectively. The wet season fluxes were generally higher than the dry season fluxes. A detailed summary of the analysis of seasonally variable data obtained in the test program is provided in Table 3.39. The seasonal variations were affected by the type of the cover material with opposite effects observed for low permeability versus medium/high permeability covers. The data indicated that in general, for the low permeability materials (ED, IC-1, and FC), the emissions were higher in the dry season than the wet season. For the medium/high permeability materials (AF, GW, IC-10, IC-15), the opposite trend was observed with higher emissions in the wet season than the dry season.

Table 3.39 – Comparison of Seasonal Flux Values

| Cover Type | Material Type | # of Constituents Compared | # of Constituents Greater in | | % of Constituents Greater in | |
|---|---|---|---|---|---|---|
| | | | Wet | Dry | Wet | Dry |
| Daily | Auto Fluff (AF) | 14 | 10 | 4 | 71 | 29 |
| Daily | Green Waste (GW) | 14 | 11 | 3 | 79 | 21 |
| Extended Daily | Poorly-Graded Gravel with Clay and Sand (ED) | 14 | 4 | 10 | 29 | 71 |
| Intermediate | Fat Clay (IC-1) | 8 | 3 | 5 | 38 | 63 |
| Intermediate | Clayey Sand with Gravel (IC-10) | 10 | 9 | 1 | 90 | 10 |
| Intermediate | Clayey Sand with Gravel (IC-15) | 14 | 11 | 3 | 79 | 21 |
| Final | Fat Clay with Gravel (FC) | 3 | 1 | 2 | 33 | 67 |

The degree of saturation (i.e., the fraction of pore volume occupied by water) in the cover materials was higher in the wet season than the dry season with the exception of the ED cover. Both the air (Table 3.5) and cover system (Figure 3.31) temperatures were lower in the wet than the dry season. Combined high degree of saturation and low temperatures impede flux of gases due to decreased air/gas filled pore spaces and increased tortuosity of the gas flow path as well as the decreased biological/biochemical degradation processes, respectively. These mechanisms likely

controlled the response of the low permeability materials. Even though in the wet season the sites available for sorption of the gases on the surface of the cover materials were expected to have been selectively occupied by water allowing for easier transport of gases, this process was likely not the controlling mechanism for the low permeability covers. The potentially increased biological/biochemical degradation processes as well as the high amount of sites on the cover material surfaces available for sorption likely controlled the response of the high/medium permeability materials, as these cover systems had low emissions in the dry season. The degree of saturation was low during the dry measurement periods, yet the increased pore space available for flow did not result in high flow. The dominant mechanisms controlling the response of the materials with the different permeabilites were different demonstrating the complexity of the emission processes.

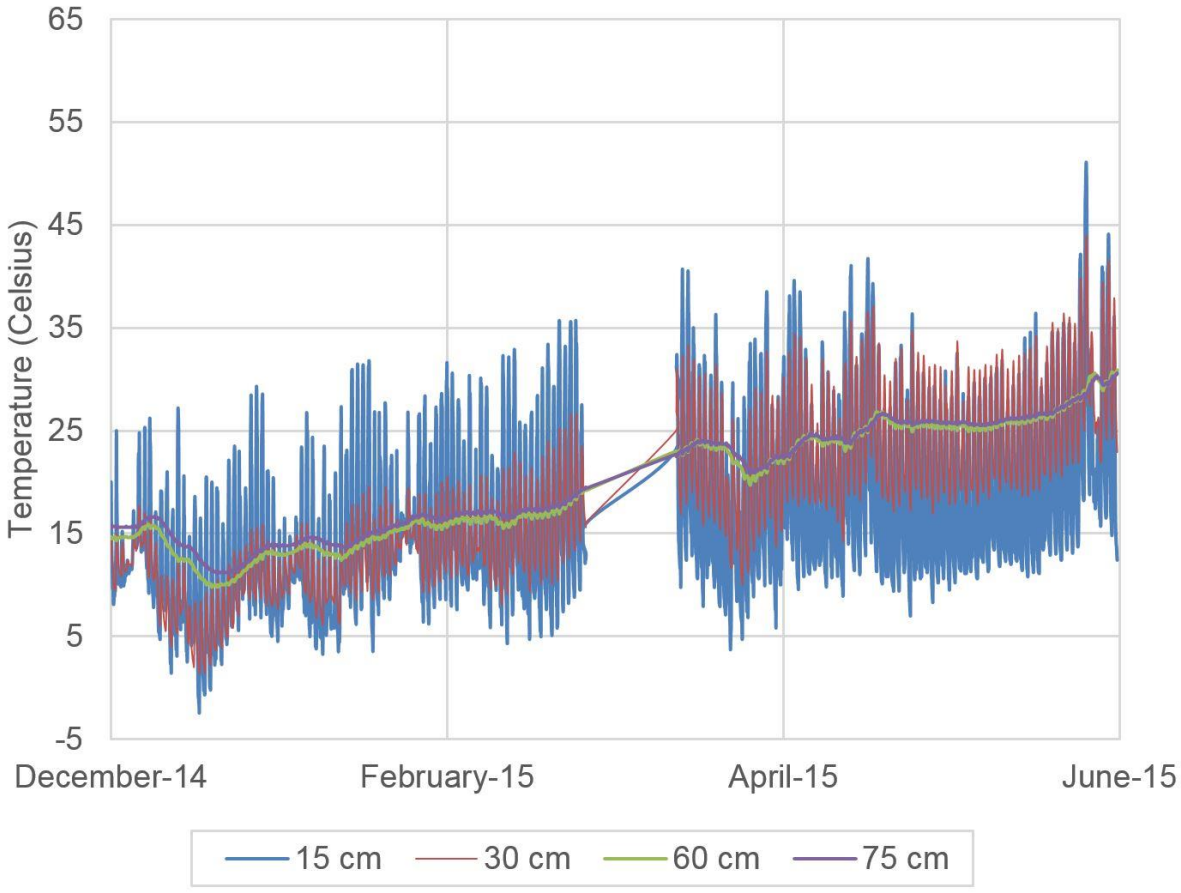


Figure 3.31. Cover Temperatures at Cell 15

Finally, data are presented in Figure 3.32 for flux of the four target gases as a function of waste age. This analysis was conducted using only intermediate covers as wastes with variable ages were present only at locations overlain by the intermediate covers at the site. In general, the maximum flux values decreased as the waste age increased (Figure 3.32).

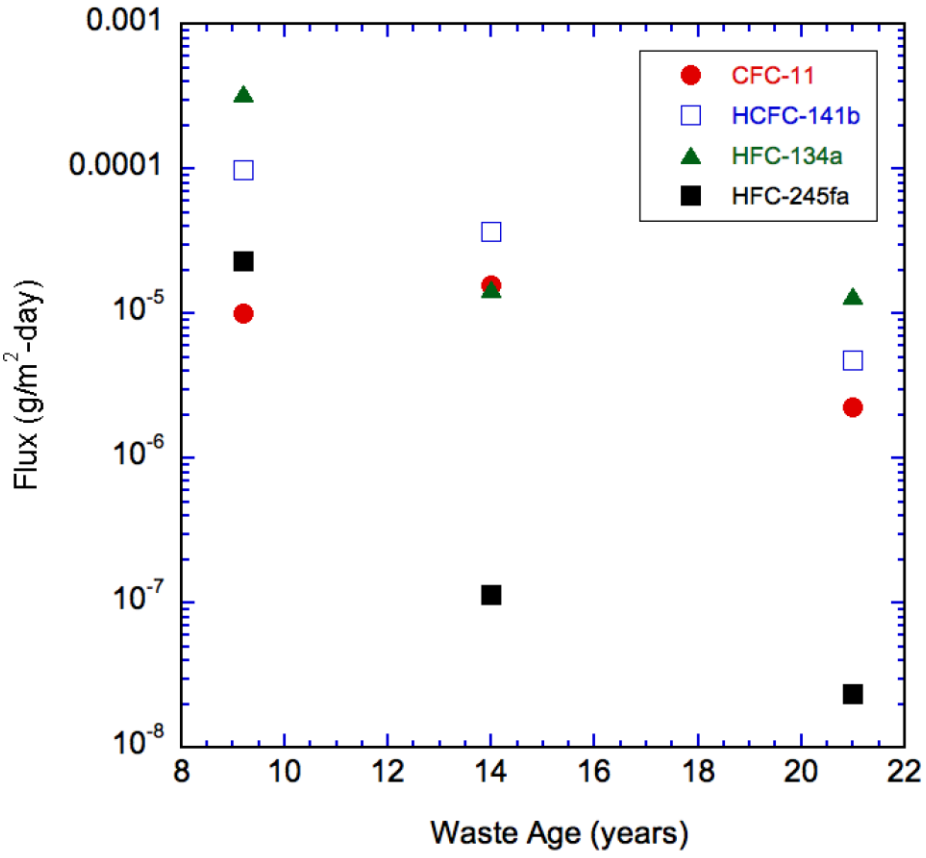


Figure 3.32. Maximum Flux versus Waste Age

### 3.11 Flare System Destruction Data

The destruction efficiency data for the flare system used at Potrero Hills Landfill for the fourteen gases analyzed in the investigation are presented in Table 3.40. The data indicated that the destruction efficiency was above 99% for all gases and was 100% for CFC-113.

Table 3.40 – Destruction Efficiency of the High-Temperature Flare

| Compounds | Average Inlet Concentration (pptv) | Average Outlet Concentration (pptv) | | Destruction Efficiency (%) |
|---|---|---|---|---|
| | | Actual | With Correction for Air Dilution | |
| CFC-11 | 6.69E+04 | 1.18E+01 | 7.64E+01 | 99.89% |
| CFC-12 | 1.21E+06 | 9.94E+02 | 6.43E+03 | 99.47% |
| CFC-113 | 3.15E+03 | 0.00E+00 | 0.00E+00 | 100.00% |
| CFC-114 | 1.08E+05 | 3.95E+01 | 2.56E+02 | 99.76% |
| HCFC-21 | 2.74E+04 | 5.00E+00 | 3.24E+01 | 99.88% |
| HCFC-22 | 1.94E+06 | 5.00E+00 | 3.24E+01 | 99.99% |
| HCFC-141b | 8.28E+05 | 5.00E+00 | 3.24E+01 | 99.99% |
| HCFC-142b | 1.23E+05 | 5.00E+00 | 3.24E+01 | 99.97% |
| HCFC-151a | 1.34E+05 | 5.00E+00 | 3.24E+01 | 99.98% |
| HFC-134a | 2.16E+06 | 6.88E+01 | 4.45E+02 | 99.98% |
| HFC-152a | 1.21E+06 | 5.00E+00 | 3.24E+01 | 99.99% |
| HFC-245fa | 2.60E+04 | 5.00E+00 | 3.24E+01 | 99.88% |
| $CH_4$ | 4.39E+11 | 7.47E+06 | 4.84E+07 | 99.99% |
| $CO_2$ | 1.56E+11 | 4.67E+10 | 3.02E+11 | N/A |

### 3.12 Scaled Emissions

Further analysis was conducted to scale the measured emissions to the entire site and for converting the emissions of the various gases to $CO_2$ equivalents to provide extended California-specific data. The minimum and maximum emissions of each gas by season were scaled for the entire site using relative areas occupied by each cover type used at the site and tested in the field program (Table 3.41). The relative areas of the different cover systems at PHL were determined using site records to be: daily covers 3% (AF 1%, GW 1%, ED 1%); intermediate covers 84% (IC-1 28%, IC-10 28%, IC-15 28%) and final cover 13%. For the four target gases, in the wet season, the CFC-11 and HCFC-141b emissions were on the order of $10^{-4}$ to $10^{-3}$ g/m$^2$-day, whereas the emissions were lower and on the order of $10^{-4}$ g/m$^2$-day for HFC-134a and HFC-245fa. For the four target gases, in the dry season, the emissions were lower and were somewhat less variable compared to the wet season. CFC-11, HCFC-141b, and HFC-134a emissions were on the order of $10^{-5}$ to $10^{-4}$ g/m$^2$-day and the emissions were on the order of $10^{-5}$ g/m$^2$-day for HFC-245fa. The methane emissions were more variable in the wet season (between $10^{-2}$ to $10^{+1}$ g/m$^2$-day) than the dry season, where

the emissions were on the order of $10^0$ g/m$^2$-day. The carbon dioxide emissions were on the order of $10^{+1}$ g/m$^2$-day for both seasons.

Table 3.41 – Scaled Emissions of the Test Gases for the Landfill

| Compound | Wet Season | | Dry Season | |
|---|---|---|---|---|
| | Minimum (g/m$^2$-day) | Maximum (g/m$^2$-day) | Minimum (g/m$^2$-day) | Maximum (g/m$^2$-day) |
| CFC-11 | 9.88E-04 | 3.34E-03 | 8.99E-05 | 4.32E-04 |
| CFC-12 | 3.81E-05 | 8.43E-05 | 6.40E-06 | 2.19E-05 |
| CFC-113 | 1.46E-06 | 1.96E-06 | 2.21E-07 | 6.89E-07 |
| CFC-114 | 1.38E-05 | 1.58E-05 | 2.23E-06 | 9.55E-06 |
| HCFC-21 | 1.22E-03 | 4.92E-03 | 1.20E-06 | 4.49E-06 |
| HCFC-22 | 4.43E-05 | 6.32E-05 | 7.61E-06 | 2.58E-05 |
| HCFC-141b | 1.89E-03 | 3.98E-03 | 4.47E-05 | 1.60E-04 |
| HCFC-142b | 4.71E-05 | 5.17E-05 | 5.19E-06 | 1.34E-05 |
| HCFC-151a | 7.56E-05 | 1.31E-04 | 1.59E-05 | 4.87E-05 |
| HFC-134a | 2.33E-04 | 5.61E-04 | 5.14E-05 | 1.26E-04 |
| HFC-152a | 2.43E-04 | 8.45E-04 | 8.77E-06 | 7.02E-05 |
| HFC-245fa | 1.63E-04 | 6.09E-04 | 2.19E-05 | 9.87E-05 |
| $CH_4$ | 8.68E-02 | 1.23E+01 | 2.82E+00 | 5.72E+00 |
| $CO_2$ | 2.18E+01 | 6.48E+01 | 1.93E+01 | 5.27E+01 |

The scaled emissions that were presented above in Table 3.41 were converted to total emissions from the site. The data were converted using the molecular masses of the gases and the areas occupied by the different cover types at the site. In this analysis, emissions measured during the field campaigns were assumed to be applicable to the specific cover types throughout the entire site. The results are presented in Tables 3.42 and 3.43 for the wet and dry seasons, respectively. The emissions of the F-gases were observed to be lower in the dry season than the wet season. For methane, maximum emissions were higher in the wet than the dry season, with the opposite trend for the minimum emissions. The emissions of carbon dioxide were not significantly affected by seasonal variations. The maximum emissions typically were one order of magnitude higher than the minimum emissions. The total emissions were generally on the order of $10^{+4}$ Tonnes/year range, whereas the cumulative F-gas emissions were in the $10^0$ Tonnes/year range in the wet season and varied between $10^{-2}$ and $10^{-1}$ Tonnes/year in the dry season. The CFC-11 emissions were higher than the emissions of most of the other (hydro)chlorofluorocarbons. The HCFC-141b emissions were in line with CFC-11 emissions and higher than HFC-134a and HFC-245fa emissions in the wet season. The HCFC-141b, HFC-134a, and HFC-245fa emissions were generally in line and lower than CFC-11 emissions in the dry season.

Table 3.42 – Total Emission Rates of the Test Gases (Wet Season)

| Compound | Surface Emissions (Tonnes/year) | | | |
|---|---|---|---|---|
| | Minimum | % | Maximum | % |
| CFC-11 | 2.16E-01 | 0.00 | 7.29E-01 | 0.00 |
| CFC-12 | 8.33E-03 | 0.00 | 1.84E-02 | 0.00 |
| CFC-113 | 3.20E-04 | 0.00 | 4.28E-04 | 0.00 |
| CFC-114 | 3.01E-03 | 0.00 | 3.45E-03 | 0.00 |
| HCFC-21 | 2.67E-01 | 0.01 | 1.08E+00 | 0.00 |
| HCFC-22 | 9.69E-03 | 0.00 | 1.38E-02 | 0.00 |
| HCFC-141b | 4.13E-01 | 0.01 | 8.70E-01 | 0.00 |
| HCFC-142b | 1.03E-02 | 0.00 | 1.13E-02 | 0.00 |
| HCFC-151a | N/A | N/A | N/A | N/A |
| HFC-134a | 5.09E-02 | 0.00 | 1.23E-01 | 0.00 |
| HFC-152a | 5.30E-02 | 0.00 | 1.85E-01 | 0.00 |
| HFC-245fa | 3.56E-02 | 0.00 | 1.33E-01 | 0.00 |
| Total F-Gas Emissions | 1.07E+00 | 0.02 | 3.16E+00 | 0.00 |
| $CH_4$ | 1.90E+01 | 0.40 | 7.53E+04 | 84.15 |
| $CO_2$ | 4.78E+03 | 99.58 | 1.42E+04 | 15.85 |
| Total Surface Emissions (F-Gases + $CH_4$ + $CO_2$) | 4.80E+03 | 100.00 | 8.94E+04 | 100.00 |

Table 3.43 – Total Emission Rates of the Test Gases (Dry Season)

| Compound | Surface Emissions (Tonnes/year) | | | |
|---|---|---|---|---|
| | Minimum | % | Maximum | % |
| CFC-11 | 1.96E-02 | 0.00 | 2.17E-01 | 0.00 |
| CFC-12 | 1.40E-03 | 0.00 | 1.10E-02 | 0.00 |
| CFC-113 | 4.83E-05 | 0.00 | 3.46E-04 | 0.00 |
| CFC-114 | 4.86E-04 | 0.00 | 4.79E-03 | 0.00 |
| HCFC-21 | 2.63E-04 | 0.00 | 2.26E-03 | 0.00 |
| HCFC-22 | 1.66E-03 | 0.00 | 1.29E-02 | 0.00 |
| HCFC-141b | 9.78E-03 | 0.00 | 8.06E-02 | 0.00 |
| HCFC-142b | 1.13E-03 | 0.00 | 6.74E-03 | 0.00 |
| HCFC-151a | 3.49E-03 | N/A | 2.44E-02 | N/A |
| HFC-134a | 1.12E-02 | 0.00 | 6.34E-02 | 0.00 |
| HFC-152a | 1.92E-03 | 0.00 | 3.52E-02 | 0.00 |
| HFC-245fa | 4.80E-03 | 0.00 | 4.96E-02 | 0.00 |
| Total F-Gas Emissions | 5.58E-02 | 0.00 | 5.08E-01 | 0.00 |
| $CH_4$ | 1.41E+03 | 12.73 | 2.87E+03 | 9.79 |
| $CO_2$ | 9.70E+03 | 87.27 | 2.65E+04 | 90.21 |
| Total Surface Emissions (F-Gases + $CH_4$ + $CO_2$) | 1.11E+04 | 100.00 | 2.93E+04 | 100.00 |

Finally, estimates for the fluxes of the 14 gases in terms of equivalent $CO_2$ emission rates are provided in Table 3.44 for the wet season and in Table 3.45 for the dry season. The maximum emissions were on average one order of magnitude higher than the minimum emissions (varied from same order to two orders of magnitude difference). The $CO_2$ equivalent total emissions were higher by one order of magnitude in the dry than the wet season. For F-gases alone, the differences between the wet and dry seasons were low with the total F-gas emissions in general in the $10^{+3}$ Tonnes/year range. While the total gas emissions were higher in the dry than the wet season, the relative contributions of F-gases to the total emissions and most of the individual F-gas emissions were higher in the wet season than the dry season. The $CO_2$ equivalent CFC-11 emissions were higher than the emissions of all of the other (hydro)chlorofluorocarbons. The HCFC-141b emissions were higher than those for HFC-134a and HFC-245fa in the wet season. The HFC-134a emissions were higher than the HCFC-141b and HFC-245fa emissions in the dry season. Reported as fraction of total landfill emissions (F-gases + $CH_4$ + $CO_2$), the F-gas emissions were between 5.1 and 23.3% for wet season and between 0.3 and 1.3% for dry season. Overall, the magnitude and relative contributions of F-gas emissions were exacerbated when the emissions were converted to $CO_2$ equivalent values due to the high atmospheric impacts of these chemicals.

Table 3.44 – Total $CO_2$ Equivalent Emission Rates of the Test Gases (Wet Season)

| Compound | Surface Emissions ($CO_2$eq Tonnes/year) | | | |
|---|---|---|---|---|
| | Minimum | % | Maximum | % |
| CFC-11 | 1.01E+03 | 14.54 | 3.40E+03 | 3.61 |
| CFC-12 | 8.49E+01 | 1.23 | 1.88E+02 | 0.20 |
| CFC-113 | 1.86E+00 | 0.03 | 2.49E+00 | 0.00 |
| CFC-114 | 2.59E+01 | 0.37 | 2.97E+01 | 0.03 |
| HCFC-21 | 3.95E+01 | 0.57 | 1.59E+02 | 0.17 |
| HCFC-22 | 1.70E+01 | 0.25 | 2.43E+01 | 0.03 |
| HCFC-141b | 3.23E+02 | 4.67 | 6.80E+02 | 0.72 |
| HCFC-142b | 2.04E+01 | 0.29 | 2.24E+01 | 0.02 |
| HCFC-151a | N/A | N/A | N/A | N/A |
| HFC-134a | 5.70E+01 | 0.82 | 1.37E+02 | 0.15 |
| HFC-152a | 7.32E+00 | 0.11 | 2.55E+01 | 0.03 |
| HFC-245fa | 3.06E+01 | 0.44 | 1.14E+02 | 0.12 |
| Total F-Gas Emissions | 1.61E+03 | 23.32 | 4.78E+03 | 5.07 |
| $CH_4$ | 5.31E+02 | 7.67 | 7.53E+04 | 79.88 |
| $CO_2$ | 4.78E+03 | 69.01 | 1.42E+04 | 15.04 |
| Total Surface Emissions (F-Gases + $CH_4$ + $CO_2$) | 6.92E+03 | 100.00 | 9.42E+04 | 100.00 |

Table 3.45 – Total $CO_2$ Equivalent Emission Rates of the Test Gases (Dry Season)

| Compound | Surface Emissions ($CO_2$eq Tonnes/year) | | | |
|---|---|---|---|---|
| | Minimum | % | Maximum | % |
| CFC-11 | 9.15E+01 | 0.19 | 1.01E+03 | 0.93 |
| CFC-12 | 1.43E+01 | 0.03 | 1.12E+02 | 0.10 |
| CFC-113 | 2.81E-01 | 0.00 | 2.01E+00 | 0.00 |
| CFC-114 | 4.18E+00 | 0.01 | 4.12E+01 | 0.04 |
| HCFC-21 | 3.89E-02 | 0.00 | 3.34E-01 | 0.00 |
| HCFC-22 | 2.93E+00 | 0.01 | 2.28E+01 | 0.02 |
| HCFC-141b | 7.64E+00 | 0.02 | 6.30E+01 | 0.06 |
| HCFC-142b | 2.25E+00 | 0.00 | 1.33E+01 | 0.01 |
| HCFC-151a | N/A | N/A | N/A | N/A |
| HFC-134a | 2.89E+01 | 0.06 | 7.10E+01 | 0.07 |
| HFC-152a | 6.08E-01 | 0.00 | 4.86E+00 | 0.00 |
| HFC-245fa | 9.45E+00 | 0.02 | 4.25E+01 | 0.04 |
| Total F-Gas Emissions | 1.62E+02 | 0.33 | 1.38E+03 | 1.28 |
| $CH_4$ | 3.96E+04 | 80.07 | 8.04E+04 | 74.28 |
| $CO_2$ | 9.70E+03 | 19.61 | 2.65E+04 | 24.44 |
| Total Surface Emissions (F-Gases + $CH_4$ + $CO_2$) | 4.95E+04 | 100.00 | 1.08E+05 | 100.00 |

### 3.13 Summary and Conclusions

The field test program was conducted to provide detailed in situ emissions data for selected landfill gases. In particular, baseline background concentrations and flux of the gases were determined as a function of cover type and seasonal variations. The field investigation was conducted at a landfill located in northern California using large-scale (1 m x 1 m area) static flux chambers. All cover systems used at the site, including daily cover, intermediate cover, and final cover, were tested. Tests were repeated in wet and dry seasons. The locations selected for testing included variable waste depth and variable waste age below the tested covers. In addition, destruction efficiency of the gas flare system at the site was measured by comparing incoming and outgoing gas to the combustion system. Measurements were made for 4 target F-gases (CFC-11, HCFC-141b, HFC-134a, and HFC-245fa). Also, data were provided for 8 other F-gases (CFC-12, CFC-113, CFC-114, HCFC-21, HCFC-22, HCFC-142b, HCFC-151a, and HFC-152a) and $CH_4$ and $CO_2$ to provide additional context for the analysis by including a broader range of constituents. The field test program provided emissions data for daily covers and HFC-245fa, which had not been previously reported in the literature. In addition, emissions from multiple types of daily covers and interim covers were investigated at a single site, which had not been previously reported. Furthermore, all data were obtained using the large-scale flux chambers. Overall, the field test program represented the most comprehensive and systematic investigation of landfill F-gas emissions conducted to date.

The ranges of ambient air concentrations at the test site (minimum to maximum) for CFC-11, HCFC-141b, HFC-134a, and HFC-245fa were 2.07 x $10^2$ to 2.98 x $10^5$, 1.00 x $10^1$ to 3.96 x $10^5$, 5.50 x $10^1$ to 4.75 x $10^4$, and BDL to 3.17 x $10^4$ pptv, respectively. Maximum ambient concentrations for all 4 target F-gases were measured at the GW cover in wet season. For context, the ambient concentrations for $CH_4$ and $CO_2$ at the site ranged from approximately 2 x $10^6$ to 2 x $10^9$ and from 3 x $10^7$ to 8 x $10^9$ pptv, respectively.

The average concentrations from raw gas samples (taken at the inlet of the flare system) for CFC-11, HCFC-141b, HFC-134a, and HFC-245fa were 6.69 x $10^4$, 8.28 x $10^5$, 2.16 x $10^6$, and 2.60 x $10^4$ pptv, respectively. The destruction efficiency for the gas flare system was above 99.88% for the 4 target gases and was above 99.47% for all gases analyzed.

In the wet season, the ranges of measured fluxes (minimum to maximum) for CFC-11, HCFC-141b, HFC-134a, and HFC-245fa were 2.27 x $10^{-6}$ to 2.57 x $10^{-1}$, -5.59 x $10^{-6}$ to 2.99 x $10^{-1}$, 5.69 x $10^{-7}$ to 3.79 x $10^{-2}$, and 1.14 x $10^{-7}$ to 5.21 x $10^{-2}$ g/$m^2$-day, respectively. In the dry season, the ranges of measured fluxes (minimum to maximum) for CFC-11, HCFC-141b, HFC-134a, and HFC-245fa were 9.47 x $10^{-7}$ to 3.42 x $10^{-2}$, -5.01 x $10^{-7}$ to 7.58 x $10^{-3}$, 7.19 x $10^{-7}$ to 5.07 x $10^{-3}$, and 9.74 x $10^{-9}$ to 8.77 x $10^{-3}$ g/$m^2$-day, respectively. While the cover systems associated with minimum fluxes were either intermediate or final covers, all maximum fluxes (4 target constituents, both seasons) were measured for daily cover materials. Emissions of CFC-11 were lower, HCFC-141 were generally in line with, and HFC 134a were higher than the emissions reported in literature. The current study, which was conducted approximately a decade after the studies reported in the literature, likely captured the historic replacement trends for (hydro)chlorofluorocarbons in waste products.

The measured minimum and maximum surface emissions with location are summarized in Tables 3.46, 3.47, and 3.48. For the F-gases, flux values varied from negative values up to approximately 3x$10^{-1}$ g/$m^2$-day. The positive flux values varied by seven orders of magnitude (Table 3.46). For methane, flux varied from negative values up to 5.38x$10^{+1}$ g/$m^2$-day. Negative fluxes generally occurred in the wet season and through the intermediate and final covers. The positive fluxes varied by over an order of magnitude (Table 3.47). For carbon dioxide, flux varied from negative values up to 7.47x$10^{+2}$ g/$m^2$-day. Negative fluxes generally occurred in the wet season and through the intermediate and final covers. The positive fluxes varied by over an order of magnitude (Table 3.48). In general, for all of the gases, the fluxes were higher through the daily covers than the intermediate and final covers. Overall, flux decreased with decreasing hydraulic conductivity and increasing cover thickness. These observations agreed with data provided in literature, where landfill gas emissions were reported to typically decrease with the order daily, intermediate, and final covers as well as decreasing conductivity and increasing thickness.

Table 3.46 – Surface Flux of the Twelve F-Gases by Location

| Location | Minimum ($g/m^2$-day) | | Maximum ($g/m^2$-day) | |
|---|---|---|---|---|
| | Wet | Dry | Wet | Dry |
| AF | 1.50E-08 | 7.15E-07 | 2.99E-01 | 3.42E-02 |
| GW | 9.67E-06 | 5.79E-07 | 2.22E-01 | 9.40E-04 |
| ED | 3.09E-08 | 6.34E-07 | 8.04E-03 | 7.22E-03 |
| IC-1 | -5.59E-06 | -5.96E-07 | 5.06E-06 | 1.31E-05 |
| IC-10 | -3.50E-07 | -2.30E-06 | 7.07E-05 | 2.07E-05 |
| IC-15 | -3.41E-06 | 4.46E-07 | 3.29E-04 | 1.95E-04 |
| FC | 5.69E-07 | -5.01E-07 | 1.55E-05 | 1.70E-06 |

Table 3.47 – Surface Flux of Methane by Location

| Location | Minimum ($g/m^2$-day) | | Maximum ($g/m^2$-day) | |
|---|---|---|---|---|
| | Wet | Dry | Wet | Dry |
| AF | 7.41E-02 | 3.82E+00 | 2.00E+01 | 3.05E+01 |
| GW | 9.16E+00 | 1.96E+00 | 1.26E+01 | 2.99E+00 |
| ED | 2.68E-01 | 1.47E+01 | 1.32E+01 | 5.38E+01 |
| IC-1 | - | - | - | - |
| IC-10 | -1.94E-02 | -6.06E-03 | 6.29E+00 | 1.17E-03 |
| IC-15 | -9.65E-03 | 9.33E+00 | 3.60E+01 | 1.73E+01 |
| FC | -1.07E-03 | 2.94E-04 | -1.07E-03 | 2.94E-04 |

- methane flux did not meet the 0.9 $R^2$ criteria

Table 3.48 – Surface Flux of Carbon Dioxide by Location

| Location | Minimum ($g/m^2$-day) | | Maximum ($g/m^2$-day) | |
|---|---|---|---|---|
| | Wet | Dry | Wet | Dry |
| AF | -2.36E+01 | -1.54E+00 | -2.36E+01 | -1.54E+00 |
| GW | 6.31E+02 | 1.32E+01 | 7.47E+02 | 3.27E+01 |
| ED | 4.60E+00 | 6.34E-07 | 4.54E+01 | 7.22E-03 |
| IC-1 | 2.16E+01 | 2.29E+00 | 2.30E+01 | 3.69E+01 |
| IC-10 | 1.85E+01 | 3.90E+00 | 6.40E+01 | 1.63E+01 |
| IC-15 | 7.43E+00 | 6.21E+01 | 1.07E+02 | 1.25E+02 |
| FC | 1.86E+01 | 1.95E+00 | 2.18E+01 | 1.85E+01 |

Reported as fraction of total landfill emissions (F-gases + $CH_4$ + $CO_2$), the F-gas emission rates were between 5.1 and 23.3% for wet season and between 0.3 and 1.3% for dry season. For further analysis, the estimated $CO_2$ equivalent emissions

were converted to a 1-year period (Table 3.49). The values were obtained using rates for wet and dry seasons (Tables 3.44 and 3.45) for associated annual fractions of wet (58%, November through May) and dry (42%, June through October) seasons for the test site. When converted to annual $CO_2$ equivalent emissions, the F-gas emissions as a fraction of total landfill emissions (F-gases + $CH_4$ + $CO_2$) were between 3.4 to 4.1%. The total annual emissions for F-gases ranged from 1010 to 3360 $CO_2$eq Tonnes. Overall, contribution of F-gases to total GHG emissions from landflls is small yet not insignificant.

Table 3.49 – Total $CO_2$ Equivalent Emissions of the Test Gases (Annual)

| Compound | Surface Emissions ($CO_2$eq Tonnes) | | | |
|---|---|---|---|---|
| | Minimum | % | Maximum | % |
| CFC-11 | 6.23E+02 | 2.52 | 2.40E+03 | 2.40 |
| CFC-12 | 5.53E+01 | 0.22 | 1.56E+02 | 0.16 |
| CFC-113 | 1.20E+00 | 0.00 | 2.29E+00 | 0.00 |
| CFC-114 | 1.68E+01 | 0.07 | 3.45E+01 | 0.03 |
| HCFC-21 | 2.30E+01 | 0.09 | 9.26E+01 | 0.09 |
| HCFC-22 | 1.11E+01 | 0.04 | 2.37E+01 | 0.02 |
| HCFC-141b | 1.91E+02 | 0.77 | 4.21E+02 | 0.42 |
| HCFC-142b | 1.28E+01 | 0.05 | 1.86E+01 | 0.02 |
| HCFC-151a | N/A | N/A | N/A | N/A |
| HFC-134a | 4.52E+01 | 0.18 | 1.10E+02 | 0.11 |
| HFC-152a | 4.51E+00 | 0.02 | 1.68E+01 | 0.02 |
| HFC-245fa | 2.17E+01 | 0.09 | 8.41E+01 | 0.08 |
| Total F-Gas Emissions | 1.01E+03 | 4.06 | 3.36E+03 | 3.35 |
| $CH_4$ | 1.69E+04 | 68.31 | 7.74E+04 | 77.34 |
| $CO_2$ | 6.84E+03 | 27.63 | 1.93E+04 | 19.30 |
| Total Surface Emissions (F-Gases + $CH_4$ + $CO_2$) | 2.47E+04 | 100.00 | 1.00E+05 | 100.00 |

The values for emissions reported herein are highly variable representing different cover conditions, different underlying waste conditions (age and depth), and different seasons. Emssions of F-gases are expected to vary by landfill location (including effects of both climatic and operational conditions). In addition, the emissions are expected to vary with time to account for waste stream effects (i.,e., relative fraction of specific compounds in foam wastes).

## References


Abichou, T., Chanton, J., Powelson, D., Fleiger, J., Escoriaza, S., Lei, Y., and Stern, J., (2006a), "Methane Flux and Oxidation at Two Types of Intermediate Landfill Covers," *Waste Management*, Vol. 26, 1305-1312.

Abichou, T., Chanton, J., and Powelson, D., (2006b), "Field Performance of Biocells, Biocovers, and Biofilters to Mitigate Greenhouse Gas Emissions from Landfills," Final Report, Prepared for Florida Center for Solid and Hazardous Waste Management.

Abichou, T., Powelson, D., Chanton, J., Escoriaza, S., and Stern, J., (2006c), "Characterization of Methane Flux and Oxidation at a Solid Waste Landfill," *Journal of Environmental Engineering*, Vol. 132(2), 1305-1312.

Allen, M., Braithwaite, A., and Hills, C. H., (1997), "Trace Organic Compounds in Landfill Gas at Seven UK Waste Disposal Sites," *Environmental Science & Technology*, Vol. 31, 1054-1061.

ARCADIS U.S., Inc., (2012), "Quantifying Methane Abatement Efficiency at Three Municipal Solid Waste Landfills," Final Report Prepared for the USEPA, #RN990271.0007.

Arendt, G., (1985), "Untersuchung von Spurenstoffen im Deponiegas hinsichtlich technischer Nutzungskonzeptionen." *Umweltbundesamt,* (ed.) Deponiegasnutzung: Dokumentation einer Fachtagung, Berlin, 5-11.

ASHRAE, (2013), "ASHRAE Refrigerant Designations," https://www.ashrae.org/standards-research--technology/standards--guidelines/standards-activities/ashrae-refrigerant-designations#mo, last accessed March 23, 2013.

Balsiger, C., (2004), "Fate of Volatile Fluorinated Compounds in the Subsurface," http://www.kobo.ch/balsiger/cv/publications/fvfcs/these_3025_christian_balsiger.pdf, last accessed May 2, 2013.

Bareither, C., Benson, C., and Edil, T., (2012), "Compression of Municipal Solid Waste in Bioreactor Landfills: Mechanical Creep and Biocompression," *Journal of Geotechnical and Geoenvironmental Engineering,* ASCE.

Barlaz, M. A., Green, R. B., Chanton, J. P., Goldsmith, C. D., and Hater, G. R., (2004), "Evaluation of a Biologically Active Cover for Mitigation of Landfill Gas Emissions," *Environmental Science and Technology*, Vol. 38, 4891-4899.

Barletta, B., Meinardi, S., Simpson, I. J., Haider, A. K., Blake, D., and Rowland, F. S., (2002), "Mixing Ratios of Volatile Organic Compounds (VOCs) in the Atmosphere of Karachi, Pakistan," *Atmospheric Environment,* Vol. 36, 3429-3443.

Barletta, B., Meinardi, S., Simpson, I. J., Rowland, F. S., Chan, C. Y., Wang, X., Zou, S., Chan, L. Y., and Blake, D. R., (2006), "Ambient Halocarbon Mixing Ratios in 45 Chinese Cities," *Atmospheric Environment*, Vol. 40, 7706-7719.

Barletta, B., Nissenson, P., Meinardi, S., Dabdub, D., Rowland, F. S., VanCuren, R. A., Pederson, J., Diskin, G. S., and Blake, D. R., (2011), "HFC-152a and HFC-134a Emission Estimates and Characterization of CFCs, CFC Replacements, and other Halogenated Solvents Measured during the 2008 ARCTAS Campaign (CARB phase) over the South Coast Air Basin of California," *Atmospheric Chemistry and Physics*, 11(6), 2655-2669.

Barletta, B., Sospedra, M.C., Cohan, A., Nissenson, P., Dabdub, D., Meinardi, S., Atlas, E., Lueb, R., Holloway, J.S., Ryerson, T. B., Pederson, J., VanCuren, R. A., Blake, D. R., (2013), "Emission Estimates of HCFCs, and HFCs in California from the 2010 CalNex Study," *Journal of Geophysical Research: Atmospheres,* Vol. 118 (4), 2019-2030.

Bellucci F., Bogner J., and Sturchio N. C., (2012), "Greenhouse Gas Emissions at the Urban Scale," *Elements*, Special Issue on Urban Geochemistry, Vol. 8, 445-450.

Bender, M., & Conrad, R., (1993), "Kinetics of Methane Oxidation in Oxic Soils," *Chemosphere*, Vol. 26(1), 687-696.

Benner, R. L. and Lamb, B., (1985), "A fast response continuous analyzer for halogenated atmospheric tracers," *Journal of Atmospheric and Oceanic Technology*, American Meteorological Society, 2(4), 582–589.

BING, (2006), "Thermal Insulation Materials Made of Rigid Polyurethane Foam (PUR/PIR): Properties and Manufacture," http://www.excellence-in-insulation.eu/site/fileadmin/user_upload/PDF/Thermal_insulation_materials_made_of_rigid_polyurethane_foam.pdf, last accessed February 24, 2013.

Bjarngard, A. and Edgers, L., (1990), "Settlement of Municipal Solid Waste Landfills," *Proceedings of the 13th Annual Madison Waste Conference, Madison, Wisconsin*, 192-205.

Blake, N. J., Blake, D. R., Simpson, I., Meinardi, S., Swanson, A. L., Lopez, J. P., Katzenstein, A. S., Barletta, B., Shirai, T., Atlas, E., Sachse, G., Avery, M., Vay, S., Fuelberg, H. E., Kiley, C. M., Kita, K., and Rowland, F. S., (2003), "NMHCs and Halocarbons in Asian Continental Outflow during the Transport and Chemical Evolution over the Pacific (TRACE-P) Field Campaign: Comparison With PEM-West B," *Journal of Geophysical Research*, Vol. 108.

Boeckx, P. and Van Cleemput, O., (1996), “Methane Oxidation in a Neutral Landfill Cover Soil: Influence of Moisture Content, Temperature, and Nitrogen-Turnover,” *Journal of Environmental Quality*, Vol. 25(1), 178-183.

Boeckx, P., Cleemput, O. V., and Villaralvo, I. D. A., (1996), “Methane Emission from a Landfill and the Methane Oxidizing Capacity of its Covering Soil,” *Soil Biology and Biochemistry*, Vol. 28(10), 1397-1405.

Bogner, J. E., Spokas, K., Burton, E., Sweeney, R., and Corona, V., (1995), “Landfills as Atmospheric Sources and Sinks,” *Chemosphere*, Permagon, 31(9), 4119-4130.

Bogner, J., Spokas, K., Niemann, M., Niemann, L., Baker, J., (1997a), “Emissions of Non-Methane Organic Compounds at the Greene Valley Landfill, Dupage County, Illinois, Preliminary Field Measurements,” *Proceedings Sardinia, 97 International Landfill Symposium*, Christensen, T.H., Cossu, R., Stegmann, R. (Eds.), Vol. IV. CISA-Environmental Sanitary Engineering Center, Cagliari, Italy, pp. 127–138.

Bogner, J., Meadows, M., and Czepiel, P. (1997b). “Fluxes of Methane between Landfills and the Atmosphere: Natural and Engineered Controls,” *Soil Use and Management*, Wiley Interscience, 13, 268-277.

Bogner, J., Spokas, K. A., and Burton, E. A., (1997c), “Kinetics of Methane Oxidation in a Landfill Cover Soil: Temporal Variations, a Whole Landfill Oxidation Experiment, and Modeling of Net $CH_4$ Emissions,” *Environmental Science & Technology*, American Chemical Society, 31, 2504-2514.

Bogner, J. E., Scheutz, C., Chanton, J., Blake, D., Morcet, M., Aran, C., and Kjeldsen, P., (2003), “Field Measurement of Non-Methane Organic Compound Emissions from Landfill Cover Soils,” *Proceedings of the Ninth International Waste Management and Landfill Symposium*, CISA, S. Margherita di Pula, Cagliari, Italy.

Bogner, J., Scheutz, C., Chanton, J., Blake, D., Morcet, M., Aran, C., and Kjeldsen, P., (2004), “Field Measurements of Speciated HAP [Hazardous Air Pollutants] Emissions from Landfill Cover Soils,” *Proceedings of the SWANA 27$^{th}$ International Landfill Gas Symposium*, Published by Solid Waste Association of North America, Silver Spring, MD.

Bogner, J., Pipatti, R., Hasimoto, S., Diaz, C., Mareckova, K., Diaz, L., Kjeldsen, P., Monni, S., Faaij, A., Gao, Q., Zhang, T., Ahmed, M. A., Sutamihardja, R.T.M., and Gregory R., (2007), “Mitigation of Greenhouse Gas Emissions from Waste: Conclusions and Strategies from the Intergovernmental Panel on Climate Change (IPCC) Fourth Assessment Report: Working Group III (Mitigation),” *Waste Management Research*, 26, 11-32.

Bogner, J., Chanton, J., Blake, D., Abichou, T., and Powelson, D., (2010), "Effectiveness of a Florida Landfill Biocover for Reduction of $CH_4$ and NMHC Emissions," *Environ. Science and Technology*, 44, 1197-1203.

Bogner, J., and Spokas, K., (2010), "Chapter 11: Landfills", in *Methane and Climate Change*, D. Reay, P. Smith and A. van Amstel, eds., Earthscan Publishers, UK.

Bogner, J., Spokas, K., and Chanton, J., (2011), "Seasonal Greenhouse Gas Emissions (Methane, Carob dioxide, Nitrous oxide) from Engineered Landfills: Daily, Intermediate, and Final California Landfill Cover Soils," *Journal of Environmental Quality,* Vol. 140, 1010-1020.

Bomberg, M.T., and Kumaran, M.K., (1990), "Thermal Performance of Sprayed Polyurethane Foam Insulation with Alternative Blowing Agents," *Journal of Thermal Insulation,* Vol. 14, 43-57.

Börjesson, G. and Svensson, B. H., (1997), "Seasonal and Diurnal Methane Emissions from a Landfill and their Regulation by Methane Oxidation," *Waste Management and Research,* Vol. 15, 33-54.

Börjesson, G., Sundh, I., Tunlid, A., & Svensson, B. H., (1998), "Methane Oxidation in Landfill Cover Soils, as Revealed by Potential Oxidation Measurements and Phospholipid Fatty Acid Analyses," *Soil Biology and Biochemistry*, Vol. 30(10-11), 1423-1433.

Börjesson, G., Danielsson, A., and Svensson, B. H., (2000), "Methane Fluxes from a Swedish Landfill Determined by Geostatistical Treatment of Static Chamber Measurements," *Environmental Science & Technology*, American Chemical Society, Vol. 34(18), 4044-4050.

Building Science Corporation (BSC), 2007, "Guide to Insulating Sheathing," http://www.buildingscience.com/documents/guides-and-manuals/gm-guide-insulating-sheathing, last accessed March 28, 2013.

Burns, S.B., Singh, S.N., Bowers, J.D., (1998), "The Influence of Temperature on Compressive Properties and Dimensional Stability of Rigid Polyurethane Foams Used in Construction," *Journal of Cellular Plastics*, Vol. 34(1), 18-38.

Burrough, P. A. and McDonnell, R. A., (1998), "Optimal Interpolation Using Geostatistics." *Principles of Geographical Information Systems.* Burrough, P.A. and McDonnell, R.A., ed. Oxford University Press: Oxford. 132-161.

Brookes, B. I. and Young, P. J., (1983), "The Development of Sampling and Gas Chromatography-Mass Spectrometry Analytical Procedures to Identify and Determine the Minor Organic Components of Landfill Gas," *Talanta*, Vol. 30(9), 665-676.

Caleb Management Services, Ltd., (2004), “Determination of Comparative HCFC and HFC Emission Profiles for the Foam and Refrigeration Sectors Until 2015 (Foam Projections) Part 2,” U.S. EPA, Washington D.C.

Caleb Management Services Ltd., (2011), “Developing a California Inventory for Ozone Depleting Substances (ODS) and Hydrofluorocarbon (HFC) Foam Banks and Emissions from Foams,” Final Report to the California Air Resources Board and the California Environmental Protection Agency.

California Air Resources Board, (2008), "Draft Concept Paper Foam Recovery and Destruction Program," http://www.arb.ca.gov/cc/hgwpss/meetings/021508/Foam_Recovery_Destruction_Program_Draft_Concept_Paper.pdf, last acessed May 13, 2013.

California Air Resources Board, (2011), “California Waste Disposal and ADC/AIC Amounts Supporting Data.”

CalRecycle, (2006), “Targeted Statewide Waste Characterization Study: Detailed Characterization of Construction and Demolition Waste,” Report to California Environmental Protection Agency Integrated Waste Management Board.

CalRecycle, (2011a), CalRecycle Disposal Reporting System, State-wide Alternative Daily Cover by Material Type 1995-2011, at: http://www.calrecycle.ca.gov/lgcentral/Reports/DRS/Statewide/ADCMatlTyp.aspx , last accessed November 8th, 2011.

CalRecycle, (2011b), Solid Waste Information System (SWIS), Site/Facility Listing, http://www.calrecycle.ca.gov/SWFacilities/Directory/SearchList/List?FAC=Disposal&OPSTATUS=Active&REGSTATUS=Permitted, last accessed November 10, 2011.

CalRecycle, (2011c), Solid Waste Information System (SWIS), 2010 Landfill Summary Tonnage Report, http://www.calrecycle.ca.gov/SWFacilities/Landfills/Tonnages, last accessed November 8, 2011.

CalRecycle, (2011d), Solid Waste Information System (SWIS), “Landfills that Accept C and D Waste,” http://www.calrecycle.ca.gov/SWFacilities/Landfills, last accessed November 10th, 2011.

CalRecycle, (2015), “Local Government Central, Statewide Diversion and Per Capita Disposal Rate Statistics,” http://www.calrecycle.ca.gov/LGCentral/GoalMeasure/DisposalRate/default.htm, last accessed September 28th, 2015.

Cambaliza, M. O., Shepson, P. B., Bogner, J., Daulton, D., Stirm, B., Sweeney, C., Montzka, S., Gurney, K., Spokas, K., Salmon, O., Lavoie, T., Hendricks, A., Mays, K., Turnbull, J., Miller, B., Lauvaux, T., Davis, K., Karion, A., Moser, B., Miller, C.,

Obermeyer, C., Whetstone, J., Prasad, K., Crosson, E., Miles, N., and Richardson, S., (2015), “Quantification and Source Apportionment of the Methane Emission Flux from the City of Indianapolis,” *Elementa: Science of the Anthropocene*, 3:000037, doi: 10.12952/journal.elementa.000037, 1-18.

Cardellini, C., Chiodini, G., Frondini, F., Granieri, D., Lewicki, J., and Peruzzi, L., (2003), “Accumulation Chamber Measurements of Methane Fluxes: Application to Volcanic-Geothermal Areas and Landfills,” *Applied Geochemistry,* Vol. 18(1), 45–54.

Carusa, C. and Quarta, F., (1998), “Interpolation Methods Comparison,” *Computers & Mathematics with Applications,* Vol. 35 (12), 109–126.

Cascadia Consulting Group, (2008), “California 2008 Statewide Waste Characterization Study,” Report to California Environmental Protection Agency Integrated Waste Management Board.

CDIAC, (2012), "Current Greenhouse Gas Concentrations," http://cdiac.ornl.gov/pns/current_ghg.html, last accessed April 1, 2013.

Cecchi, F., Pavan, P., Musacco, A., Mata-Alvarez, J., and Vallini, G. (1993). “Digesting the Organic Fraction of Municipal Solid Waste: Moving from Mesophilic (37°C) to Thermophilic (55°C) Condition*s,” Waste Management* & *Research,* Vol. 11, 403–414.

Chemspider, (2013), “Trichlorofluormethane (CFC-11) Data Sheet,” http://www.chemspider.com/Chemical-Structure.6149.html, last accessed March 20, 2013.

Christophersen, M., Kjeldsen, P., Holst, H., and Chanton, J., (2001), “Lateral Gas Transport in Soil Adjacent to an Old Landfill: Factors Governing Emissions and Methane Oxidation,” *Waste Management & Research*, Vol. 19(6), 595-612.

Cianciarelli, D. and Borgeau, S., (2002), “Characterization of Emissions from a 1 MWe Reciprocating Engine Fired with Landfill Gas,” *Environment Canada,* Report ERMD 2001-03.

Colman, J. J., Swanson, A. L., Meinardi, S., Sive, B. C., Blake, D. R., and Rowland, F. S., (2001), “Description of the Analysis of a Wide Range of Volatile Organic Compounds in Whole Air Samples Collected during PEM-Tropics A and B”, *Analytical Chemistry*, Vol. 73(15), 3723-3731.

Colvin, B. G., (2001), “New Blowing Agents for Insulated Panels,” *Blowing Agents and Foaming Processes Conference Proceedings,* RAPRA Technology, LTD., March 13-14, Frankfurt, Germany, 1-8.

Cregut, M., Bedas, M., Assaf, A., Durand-Thouand, M. J., and Thouand, G., (2013), "Applying Raman Spectroscopy to the Assessment of the Biodegradation of Industrial Polyurethane Wastes," *Environmental Science and Pollution Research*, 1-7.

Crosson, E. R., (2008), "A Cavity Ring-Down Analyzer for Measuring Atmospheric Levels of Methane, Carbon Dioxide, and Water Vapor," *Applied Physics B: Lasers and Optics*, Vol. 92, 403-408.

Czepiel, P. M., Mosher, B., Crill, P.M., and Harris, R. C., (1996a), "Quantifying the Effect of Oxidation on Landfill Methane Emissions," *Journal of Geophysical Research*, 101(D11), 16,721-166,729.

Czepiel, P. M., Mosher, B., Harris, R. C., Shorter, J. H., McManus, J. B., Kolb, C. E., Allwine, E., and Lamb, B. K., (1996b), "Landfill Methane Emission Measured by Enclosure and Atmospheric Tracer Methods," *Journal of Geophysical Research*, American Geophysical Union, 101(D11), 16711-16719.

Czepiel, P.M., Shorter, J.H., Mosher, B., Allwine, E., McManus, J.B., Harriss, R.C., Kolb, C.E., and Lamb, B.K., (2003), "The Influence of Atmospheric Pressure on Landfill Methane Emissions," *Waste Management*, Vol. 23(7), 593-598.

Daigneault, L.E., Handa, Y.P., Wong, B., and Caron, L.M., (1998), "Solubility of Blowing Agents HCFC-142b, HFC-134a, HFC-125, and Isopropanol in Polystyrene," *Journal of Cellular Plastics,* Vol. 34(3), 219-230.

Deipser, A. and Stegmann, R, (1994), "The Origin and Fate of Volatile Trace Components in Municipal Solid Waste Landfills," *Waste Management & Researc*h, Vol. 12(2), 129-139.

Delgado, A.H., Mukhopadhyaya, P., Normandin, N., Paroli, R.M., (2005), "Characteristics of Membranes and Insulations Used for Low Slope Roofs," *IRC Building Science Insight Seminar Series*, 1-14.

Dent, C. G., Scott, P., and Baldwin, G., (1986), "Study of Landfill Gas Composition at Three UK Domestic Waste Disposal Sites," *Proceedings of Energy from Landfill Gas Conference*, Department of the Environment, Solihull, England, October 28-31, 1986, 130-149.

Desjarlais, A. O., and Tye, R. P., (1987), "Experimental Methods for Determining the Thermal Performance of Cellular Plastic Insulation Material Used in Roofs," *Proceedings of the 8th Conference on Roofing Technology*, National Bureau of Standards/National Roofing Contractors Association, April 1987, 12-22.

DeWalle, F. B., Chian, E. S. K., and Hammerberg, E., (1978), "Gas Production from Solid Waste in Landfills," *Journal of the Environmental Engineering Division,* ASCE, Vol. 104, (EE3), 415–432.

Dieckmann, J. and Magid, H., (1999), “Global Comparative Analysis of HFC and Alternative Technologies for Refrigeration, Air Conditioning, Foam, Solvent, Aerosol Propellant, and Fire Protection Applications,” Final Report to the Alliance for Responsible Atmospheric Policy, http://unfccc.int/files/methods_and_science/other_methodological_issues/interactions_with_ozone_layer/application/pdf/adlittle.pdf, last accessed May 1, 2013.

Duranceau, C. and Spangenberger, J., (2011), “All Auto Shredding: Evaluation of Automotive Shredder Residue Generated by Shredding Only Vehicles,” Report from the Argonne National Laboratory, http://www.es.anl.gov/energy_systems/crada_team/publications/all_auto_report.pdf, last accessed May 14, 2013.

Dvorchak, M.J., (1985), “Use of Phenolic Foam in Low-Slope Roofing,” *Proceedings of the 2nd International Symposium on Roofing Technology*, NRCA, 360-367.

Edil, T. B., Ranguette, V.J., and Wuellner, W.W., (1990), “Settlement of Municipal Refuse.” *Geotechnics of Waste Fills-Theory and Practice. ASTM STP 1070,* ASTM, West Conshohocken, PA, 225-239.

Eklund, B., Anderson, E., Walker, B., Burrows, D., (1998), “Characterization of Landfill Gas Composition at the Fresh Kills Municipal Solid-Waste Landfill,” *Environmental Science & Technology*, 2233-2237.

Environment Agency, (2004), “Guidance on monitoring landfill gas surface emissions,” *UK Environment Agency*, http://www.environment-agency.gov.uk/static/documents/Business/lftgn07_surface_936575.pdf, last accessed December 19, 2008.

Figueroa, R. A., (1993), “Methane Oxidation in Landfill Top Soils,” *Proceedings of the 4th International Landfill Symposium,* Vol. 1, CISA, Cagkiari, Italy, 701-716.

Fourie, A. B and Morris, J. W. F., (2004), “Measured Gas Emissions from Four Landfills in South Africa and Some Implications for Landfill Design and Methane Recovery in Semi-Arid Climates,” *Waste Management & Research*, Vol. *22*(6), 440-453.

Fredenslund, A. M., Scheutz, C., and Kjeldsen, P., (2005), “Disposal of Refrigerators - Freezers in the US: State of the Practice 2. Determination of Content of Blowing Agent in Pre-And Post-Shredded Foam and Modeling,” Environment & Resources DTU, Technical University of Denmark, Kgs. Lyngby. 1-26.

Fyfe, C. A., Mei, Z., and Grondey, H., (1996), “Investigation of Fluorocarbon Blowing Agents in Insulating Polymer Foams by FNMR Imaging,” *Magnetic Resonance Imaging,* Vol. 14(7), 887-889.

Gaddy, G. D., Cullen, W. C., Barbari, T. A., Rossiter, W. J., (2005), “Impact of Exposure Conditions on the Mechanical Properties of Polyisocyanurate Foam Insulations,” *Proceedings of the 10th Conference on Roofing Technology,* Gaithersburg, Maryland, April 22-23, 64-71.

Galle, B., Samuelsson, J., Svensson, B. H., and Borjesson, G., (2001), “Measurements of methane emissions from landfills using a time correlation tracer method based on FTIR absorption spectroscopy,” *Environmental Science & Technology*, American Chemical Society, 35, 21-25.

Gautam, R., Bassi, A. S., and Yanful, E. K., (2007), “A Review of Biodegradation of Synthetic Plastic and Foams,” *Applied Biochemistry and Biotechnology,* Vol. 141, 85-108.

Geankoplis, C. J., (2009). *Transport Processes and Separation Principles.* 4th ed. Prentice Hall.

Gendron, R., Huneault, M., Tatibouet, J., and Vachon, C., (2002), “Foam Extrusion of Polystyrene Blown with HFC-134a,” *Cellular Polymers*, Vol. 21(5), 315-342.

Gendron, R., Champagne, M. F., Delaviz, Y., and Polasky, M. E., (2006), “Foaming Polystyrene with a Mixture of Carbon Dioxide and Ethanol,” *Journal of Cellular Plastics,* Vol. 42(2), 127-138.

Gentner, D. R., Miller, A. M., and Goldstein, A. H., (2010), “Seasonal Variability in Anthropogenic Halocarbon Emissions,” *Environmental Science and Technology,* Vol. 44, 5377-5382.

Gerilowski, K., Krautwurst, S., Kolyer, R. W., Thompson, D. R., Jonsson, H., Krings, T., Horstjann, M., Leifer, I., Eastwood, M., Green, R. O., Vigil, S., Schüttemeyer, D., Fladeland, M. M., Burrows, J. P., Bovensmann, H., (2015), “Airborne Passive Remote Sensing of Large-Scale Methane Emissions from Oil Fields in California's San Joaquin Valley and Validation by Airborne In-Situ Measurements - Initial Results from COMEX,” EGU General Assembly 2015, 12-17 April, 2015 in Vienna, Austria. id.14545.

Godwin, D. S., Van Pelt, M. M., Peterson, K., (2003), “Modeling Emissions of High Global Warming Potential Gases,” US EPA, http://www.epa.gov/ttnchie1/conference/ei12/green/godwin.pdf, last accessed March 5, 2013.

Greer, A. and Cianciarelli, D., (2005), “Characterization of Emissions from a 26$kW_e$ Micro Turbine Fired with Landfill Gas at Shepard Landfill: Calgary, Alberta,” *Environment Canada,* Report ERMD 2004-02.

Hanson, J. L., Yesiller, N., and Kendall, L. A., (2005), “Integrated Temperature and Gas Analysis at a Municipal Solid Waste Landfill,” *Proceedings of the 16th International Conference on Soil Mechanics and Geotechnical Engineering, Geotechnology in Harmony with the Global Environment*, Osaka, Japan, Millpress Science Publishers, Rotterdam, the Netherlands, Vol. 4, 2265-2268.

Hanson, J. L., Yesiller, N., Howard, K. A., Liu, W. L., and Cooper, S. P., (2006), “Effects of Placement Conditions on Decomposition of Municipal Solid Wastes in Cold Regions,” *Current Practices in Cold Regions Engineering - Proceedings of the 13th International Conference on Cold Regions Engineering*, M. Davies and J. E. Zufelt, Eds., ASCE, p. 1-11.

Hanson, J. L., Yesiller, N., Von Stockhausen, S. A., and Wong, W. W., (2010), “Compaction Characteristics of Municipal Solid Waste,” *Journal of Geotechnical and Geoenvironmental Engineering*, ASCE, Vol. 136(8), 1095-1102.

Harper, M., (2000), "Sorbent Trapping of Volatile Organic Compound from Air," *Journal of Chromatography,* 129-151.

Hartman, B., (2003), “How to Collect Reliable Soil-Gas Data for Upward Risk Assessments,” http://www.handpmg.com/articles/lustline44-flux-chambers-part-2.html, last accessed February 10, 2013.

Hartz, K. E., Klink, R. E., and Ham, R. K., (1982), “Temperature Effects: Methane Generation from Landfill Samples,*” Journal of the Environmental. Engineering Division*, ASCE, Vol. 108(4), 629–638.

Harvey, D., (2007), "Net Climatic Impact of Solid Foam Insulation Produced with Halocarbon and Non-halocarbon Blowing Agents," *Building and Environment,* Vol. 42, 2860-2879.

Hashmonay, R. A., Varma, R. M., Kagann, R. H., Segall, R. R., Sullivan, P. D., (2008), "Radial Plume Mapping: A US EPA Test Method for Area and Fugitive Source Emission Monitoring Using Optical Remote Sensing," *Advanced Environmental Monitoring,* Vol. 2, 26-31.

Heinemeyer, A., and McNamara, N., (2011), "Comparing the Closed Static Versus the Closed Dynamic Chamber Flux Methodology: Implications for Soil Respiration Studies," *Plant Soil*, 145-151.

Hodson, E. L., Martin, D., and Prinn, R. G., (2010), “The Municipal Solid Waste Landfill as a Source of Ozone-Depleting Substances in the United States and the United Kingdom,” *Atmospheric Chemistry and Physics*, 10, 1899-1910.

Hong, S. U., and Duda, L. J., (1998), “Diffusion of CFC-11 and Hydrofluorocarbons in Polyurethane,” *Journal of Applied Science*, Vol. 70, 2069-2073.

Hong, S. U., Albouy, A., and Duda, L. J., (2001), “Transport of Blowing Agents in Polyurethane,” *Journal of Applied Polymer Science,* Vol. 79(4), 696-702.

Hossain, M. S. and Gabr, M. A., (2005), “Prediction of Municipal Solid Waste Landfill Settlement with Leachate Recirculation,” *Waste Containment and Remediation*, ASCE, 1-14.

Howard, T., Lamb, B., and Zimmerman, P., (1992). “Measurement of VOC emission fluxes from waste treatment and disposal systems using an atmospheric tracer flux,” *Journal of the Air & Waste Management Association*, Air and Waste Management Association, 42, 1336–1344.

Hsu, Y. K., VanCuren, T., Park, S., Jakover, C., Herner, J., FitzBibbon, M., Blake, D. R., and Parrish, D. D., (2010), “Methane Emissions Inventory Verification in Southern California,” *Atmospheric Environment*, 44, 1, 1-7, DOI: 10.1016/j.atmosenv.2009.10.002.

Hurst, D. F., Lin, J. C., Romashkin, P. A., Daube, B. C., Gerbig, C., Matross, D. M., Wofsy, S. C., Hall, B. D., and Elkins, J. W, (2006), “Continuing Global Significance of Emissions of Montreal Protocol-Restricted Halocarbons in the United States and Canada,” *Journal of Geophysical Research-Atmospheres,* Vol. 111, 1-15.

ICF, (2011), “Lifecycle Analysis of High-Global Warming Potential Greenhouse Gas Destruction,” Final Report to the California Air Resources Board.

Intergovernmental Panel on Climate Change (IPCC), (1995), “IPCC Second Assessment Report on Global Climate Change (SAR),” http://www.ipcc.ch/pdf/climate-changes-1995/ipcc-2nd-assessment/2nd-assessment-en.pdf, last accessed January 1, 2013.

Intergovernmental Panel on Climate Change (IPCC), (2001), “IPCC Third Assessment Report on Global Climate Change (TAR): Synthesis Report,” http://www.grida.no/publications/other/ipcc%5Ftar/?src=/climate/ipcc_tar/, last accessed January 5, 2013.

Intergovernmental Panel on Climate Change (IPCC), (2005), “Safeguarding the Ozone Layer and the Global Climate System: Issues Related to Hydrofluorocarbons and and Perfluorocarbons: Annex V: Major Chemical Formulae and Nomenclature,” http://www.ipcc.ch/pdf/special-reports/sroc/sroc_a5.pdf, last accessed March 20, 2013.

Intergovernmental Panel on Climate Change (IPCC), (2006), “2006 IPCC Guidelines for National Greenhouse Gas Inventories, Vol. 5: Waste,” *http://www.ipcc-nggip.iges.or.jp/public/2006gl/vol5.html*, last accessed January 1, 2016.

Intergovernmental Panel on Climate Change (IPCC), (2007), “Special Report:

Safeguarding the Ozone Layer and the Global Climate System: Chapter 7: Foams," http://www.ipcc.ch/pdf/special-reports/sroc/sroc07.pdf, last accessed May 2, 2013.

Intergovernmental Panel on Climate Change (IPCC), (2013), "Climate Change 2013: The Physical Science Basis," http://www.climatechange2013.org/images/uploads/WGIAR5_WGI-12Doc2b_FinalDraft_All.pdf, last accessed December 19, 2015.

Ishigaki, T., Masato, Y., Masanao, N., Yusaku, O., and Yuzo, I., (2005), "Estimation of Methane Emission from Whole Waste Landfill Site Using Correlation Between Flux and Ground Temperature," *Journal of Environmental Geology,* Vol. 48, 845-853.

Jones, H. A. and Nedwell, D. B., (1993), "Methane Emission and Methane Oxidation in Landfill Cover Soil," *FEMS Microbiology Ecology,* Vol. 102, 185-195.

Jeong, S., Hsu, Y. K., Andrew, A. E., Bianco, L., Vaca, P., Wilczak, J. M., Fischer, M. L., (2013), "A Multitower Measurement Network Estimate of California's Methane Emissions," *Journal of Geophysical Research: Atmospheres*, Vol. 118, 11339-11351.

Kaplan, D. L., Hartenstein, R., and Sutter, J., (1979), "Biodegradation of Polystyrene, Poly(methyl methacrylate), and Phenol Formaldehyde," *Applied and Environmental Microbiology*, Vol. 38(3), 551-553.

Khalil, M. A. K., and Rasmussen, R. A., (1986), "The Release of Trichlorofluoromethane from Rigid Polyurethane Foams," *Journal of the Air Pollution Control Association,* Vol. 36(2), 159-163.

Khalil, M. A. K. and Rasmussen, R. A., (1987), "The Residence Time of Trichlorofluoromethane in Polyurethane Foams: Variability, Trends, and Effects of Ambient Temperature," *Chemosphere,* Vol. 16(4), 759-775.

Kitanidis, P. K. and Kuo-Fen, S., (1996), "Geostatistical Interpolation of Chemical Concentration," *Advances in Water Resources,* Vol. 19 (6), 369– 378.

Kjeldsen, P. and Jensen, M. H., (2001), "Release of CFC-11 from Disposal of Polyurethane from Waste," *Environmental Science and Technology*, 35, 3055-3063.

Kjeldsen, P., (2010), "Construction and Demolition waste – a Source to Ozone Depletion and Global Warming?," *Proceedings* of the *Global Waste Management Symposium*, 1-7.

Lamb, B., McManus, B., Shorter, J., Kolb, C., Mosher, B., Harriss, R., Allwine, E., Blaha, D., Howard, T., Guenther, A., Lott, R., Siverson, R., and Westberg, H., (1995), "Development of atmospheric tracer methods to measure methane emissions from natural gas facilities and urban areas," *Environmental Science & Technology*, American Chemical Society, 29(6), 1468–1479.

Lamothe, D., and Edgers, L., (1994), “The Effects of Environmental Pa- rameters on the Laboratory Compression of Refuse,” *Proceedings of the 17th International Madison Waste Conference*, Department of Engineering Professional Development, University of Wisconsin, Madison, Wisconsin, 592–604.

Landrock, A. H., (1995). *Handbook of Plastic Foams: Types, Properties, Manufacture, and Applications.* Noyes Publications, New Jersey.

Laugwitz, G., Poller, T., and Stegmann, R., (1988), “Entstehen und Verhalten von Spurstoffen im Deponiegas sowie umweltrelevante Auswirkungen von Deponiegasemissionen,” *Deponiegasnutzung.* Dokumentation einer Fachtagung: Hamburg. p 153- 163.

Leonard, M. L. and Floom, K. J., (2003), “Estimating Method and Use of Settlement,” *SCS Engineers*, www.scsengineers.com/SCS_papers.html, last accessed March 31, 2013.

Li, J., Cunnold, D. M., Wang, H. J., Weiss, R. F., Miller, B. R., Harth, C., Salameh, P., Harris, J. M., (2005), “Halocarbon Emissions Estimated from Advanced Global Atmospheric Gases Experiment Measured Pollution Events at Trinidad Head, California,” *Journal of Geophysical Research: Atmospheres,* Vol. 110(D14,27).

Ling, H. I., Leshchinsky, D., Mohri, Y., and Kawabata, T., (1998), “Estimation of Municipal Solid Waste Landfill Settlement,” *Journal of Geotechnical and Geoenvironmental Engineering,* ASCE, 21-28.

Liptak, B.G., (2003). *Instrument Engineers Handbook: Process Measurement and Analysis.* CRC press. 4th ed.

Livingston, G. P. and Hutchinson, G. L., (1995), “Enclosure-Based Measurement of Trace Gas Exchange: Applications and Sources of Error.” *Biogenic Trace Gases: Measuring Emissions from Soil and Water.* Matson, P.A. and Harriss, R.C. Eds. Blackwell Scientific Publications: Oxford, 14–51.

Mackay, D., Shiu, W. Y., Ma, K. C., and Lee, S. C., (2006). *Handbook of Physical-Chemical Properties and Environmental Fate for Organic Chemicals: Volume II Halogenated Hydrocarbons.* 2nd Ed. Boca Raton: Taylor and Francis Group.

Maione, M., Arduini, J., Rinaldi, M., Mangani, F., and Capaccioni, B., (2005), “Emission of Non $CO_2$ Greenhouse Gases from Landfills of Different Age Located in Central Italy,” *Environmental Sciences,* 167-176.

Mata-Alvarez, J., and Martinez-Viturtia, A., (1986), “Laboratory Simula- tion of Municipal Solid Waste Fermentation with Leachate Recycle.” *Journal of Chemical Technology and Biotechnology*, Vol. 36(12), 547–556.

Martin, L. and Kerfoot, B., (1988), "Soil-Gas Surveying Techniques," *Environmental Science & Technology,* Vol. *22*, 741.

McElroy, D. L., Courville, J. E., Christian, R. S., and Linkous, R. L., (1991), “Thermal Properties of Polyisocyanurate Foam Board Roof Insulation Blown with CFC-11 Substitutes,” *Proceedings of the 3rd Internal Symposium on Roofing Technology*, Gaithersburg, Maryland, April 17-19, 1991, 133-141.

Merz, R. C., (1964), “Investigation to Determine the Quantity and Quality of Gases Produced During Refuse Decomposition,” Final Report to the California Water Quality Control Board, University of Southern California, (#99-10).

Mihlayanlar, E., Dilmac, S., Guner, A., (2008), "Analysis of the Effect of Production Process Parameters and Density of Expanded Polystyrene Insulation Boards on Mechanical Properties and Thermal Conductivity," *Materials and Design,* Vol. 29, 344-352.

Millet, D. B., Atlas, E. L., Blake, D. R., Blake, N. J., Diskin, G. S., Holloway, J. S., Hudman, R. C., Meinardi, S., Ryerson, T. B., and Sachse, G. W, (2009), “Halocarbon Emissions from the United States and Mexico and Their Global Warming Potential,” *Environmental Science & Technology*, Vol. 43, 1055–1060.

Moakley, J., Weller, M., and Zelic, M., (2010), “Alternative Methods to Landfilling Auto Shredding Residue in Compliance with the Strict Environmental Quota by the European Union,” Final Report by the Worcester Polytechnic Institute, http://www.wpi.edu/Pubs/E-project/Available/E-project-051110-050238/unrestricted/Final_Report.pdf, last accessed May 14, 2013.

Modesti, M., Lorenzetti, A., and Dall’Acqua, C., (2005), “Long-Term Performance of Environmentally-Friendly Blown Polyurethane Foams,” *Polymer Engineering and Science,* 260-270.

Moon, S., Nam, K., Kim, J. Y., Hwan, S. K., Chung, M., (2008), “Effectiveness of Compacted Soil Liner as a Gas Barrier Layer in the Landfill Final Cover System,” *Waste Management*, Vol. 28, 1909-1914.

Morris, D. and Woods, C., (1990), “Setlement and Engineering Considerations in Landfill and Final Cover Design,” *Geotechnics of Waste Fills-Theory and Practice. ASTM STP 1070,* ASTM, West Conshohocken, PA, 9-21.

Mosher, B. W., Czepiel, P. C., Shorter, J., Allwine, E., Harriss, R. C., Kolb, C., and Lamb, B., (1996), “Mitigation of Methane Emissions at Landfill Sites in New England, USA,” *Energy Conversion and Management*, Vol. 37(6), 1093-1098.

Mosher, B., Czepiel, P., Shorter, J., McManus, B., Kolb, C., Allwine, E., Lamb, B., and

Harriss, R., (1999), “Measurements of Methane Emissions from 9 Landfills in the Northeast United States,” *Environmental Science & Technology*, American Chemical Society, Vol. 33(12), 2088-2094.

Mukhopadhyaya, P., and Kumaran, M. K., (2008), “Long-Term Thermal Resistance of Closed-Cell Foam Insulation: Research Update from Canada,” *Proceedings of the 3rd Global Insulation Conference and Exhibition*, October 16-17th, 2008, Barcelona, Spain.

Muñoz, F. D., Anderson, B. A., Lopez, J. M., Andres, A. C., (2009), “Uncertainty in the Thermal Conductivity of Insulation Materials,” *Proceedings of the 11th International IBPSA Conference*, Glasgow, Scotland, July 27-30, 2009, 1008-1013.

National Industrial Chemicals Notification and Assessment Scheme (NICNAS), (2004), “Full Public Report: HFC-245fa,” http://www.nicnas.gov.au/publications/car/new/ex/exfullr/ex0000fr/ex53fr.pdf, last accessed May 1, 2013.

Otake, Y., Kobayashi, T., Asabe, H., Murakami, N., and Ono, K., (1995), “Biodegradation of Low-Density Polyethylene, Polystyrene, Polyvinyl Chloride, and Urea Formaldehyde Resin Buried Under Soil for Over 32 Years,” *Journal of Applied Polymer Science*, Vol. 56, 1789-1796.

Parker, T., Pointer, P., Rosevear, A., Braithwaite, P., and Stone, K., (2007), “A Different Gas Generating Regime within Low-Carbon Waste Landfills in the UK and Europe,” *Proceedings of the 11th International Waste Management and Landfill Symposium*, CISA, Margherita di Pula, Cagliari, Italy, October 1-5, 1-10.

Park, H. I. and Lee, S. R., (1997), “Long-term Settlement Behavior of Landfills with Refuse Decomposition,” *Journal of Resource Management Technology,* Vol. 24(2), 159-165.

Park, J. W. and Shin, H. C., (2001), “Surface Emission of Landfill Gas from Solid Waste Landfill,” *Atmospheric Environment*, Vol. 35(20), 3445-3451.

Peach, M. J. and Carr, W. G., (1986), “Air Sampling and Analysis for Gases and Vapors,” Center for Disease Control, http://www.cdc.gov/niosh/pdfs/86-102-c.pdf, last accessed April 22, 2013.

Peischl, J., Ryerson, T. B., Brioude, J., Aikin, K. C., Andrews, A. E., Atlas, E., Blake, D., Daube, B. C., de Gouw, J. A., Dlugokencky, E., Frost, G. J., Gentner, D. R., Gilman, J. B., Goldstein, A. H., Harley, R. A., Holloway, J. S., Kofler, J., Kuster, W. C., Lang, P. M., Novelli, P. C., Santoni, G. W., Trainer, M., Wofsy, S. C., 6 and Parrish, D. D., (2013), “Quantifying Sources of Methane Using Light Alkanes in the Los Angeles Basin, California,” *Journal of Geophysical Research: Atmospheres*, Vol. 118, 4974–4990.

Pellizzari, E. D., Gutknecht, W. F., Cooper, S., and Hardison, D., (1984), “Evaluation of Sampling Methods for Gaseous Atmospheric Samples,” Research Triangle Park NC: U.S. Environmental Protection Agency.

Peischl, J., Ryerson, T. B., Brioude, J., Aikin, K. C., Andrews, A. E., Atlas, E., Blake, D., Daube, B. C., de Gouw, J. A., Dlugokencky, E., Frost, G. J., Gentner, D. R., Gilman, J. B., Goldstein, A. H., Harley, R. A., Holloway, J. S., Kofler, J., Kuster, W. C., Lang, P. M., Novelli, P. C., Santoni, G. W., Trainer, M., Wofsy, S. C., Parrish, D. D., (2013), “Quantifying Sources of Methane Using Light Alkanes in the Los Angeles Basin, California,” *Journal of Geophysical Research: Atmospheres*, Vol. 118, 4974-4990.

Pollack, A. J., Holdren, M. W., Keigley, G. W., and Severance, R. A., (1993), “A Thermal Desorption Procedure for Determining Residual Blowing Agent (CFC-11) in Rigid Foam,” *Air and Waste,* Vol. 43(8), 1101-1105.

Powell, J. T., Townsend, T. G., and Zimmerman, J. B. (2015), “Estimates of Solid Waste Disposal Rates and Reduction Targets for Landfill Gas Emissions,” *Nature Climate Change*, Advance Online Publication, Macmillan Publishers Limited, doi: 10.1038/NCLMATE2804, 1-4.

Powelson, D. K., Chanton, J. P., and Abichou, T., (2007), “Methane Oxidation in Biofilters Measured by Mass-Balance and Stable Isotope Methods,” *Environmental Science and Technology,* Vol. 41(2), 620-625.

Pruggmayer, D., Arendt, G., Frische, R., and Klopffer, W., (1982), “Identifizierung chemischer Stoffe in Deponien, Bericht fur den Regierungsprasidenten Koln,” BF-R-64, 956-959.

Rachor, I., Streese-Kleeberg, J., and Gebert, J., (2009), “Spatial and Temporal Variability of Gas Emissions from Old Landfills,” *Proceedings of the 12th International Waste Management and Landfill Symposium*, CISA, S. Margherita di Pula, Cagliari, Italy, October 5-9, 1-9.

Ramaswamy, J. N., (1970), “Nutritional Effects of Acid and Gas Production in Sanitary Landfills.” Diss. University of West Virginia, Morgantown.

Rees, J. F., (1980a), “Optimization of Methane Production and Refuse De-composition in Landfills by Temperature Control,*” Journal of Chemical Technology and Biotechnology*, Society of Chemical Industry, Vol. 30(8), 458–465.

Rees, J. F., (1980b), “The Fate of Carbon Compounds in the Landfill Disposal of Organic Mat*ter,” Journal of Chemical Technology and Biotechnology*, Society of Chemical Industry, Vol. 30(4), 161–175.

Reinhart, D. R., Cooper, D. C., and Walker, B. L, (1992), “Flux Chamber Design and

Operation for the Measurement of Municipal Solid Waste Landfill Gas Emission Rates," *Journal of the Air & Waste Management Association*, Vol. 42(8), 1067-1070.

Rettenberger, G., (1986), "Spurenstoffe im Deponiegas. Auswirkungen auf dei Gasverwertung," *GIT Supplement,* Vol. 1(86), 53-57.

Rettenberger, G. and Stegmann, R., (1996), "Landfill Gas Components." *Landfilling of Waste: Biogas.* Ed. Christensen, T.H., Cossu, R., and Stegmann, R. London: E & FN Spoon, 1996. 51-59.

Rettenberger, G., Deipser, A., and Poller, T., (1996), "Emissions of Volatile Halogenated Hydrocarbons from Landfills." Ed. Christensen, T.H., Cossu, R., and Stegmann, R. London: E & FN Spoon, 1996. 59-73.

Ridha, M., (2007), "Mechanical and Failure Properties of Rigid Polyeurethane Foam Under Tension." Diss. Department of Mechanical Engineering, National University of Singapore.

Roe, R., (2002), "Polyiso Roof Insulation: Zero Ozone Depletion Potential, Long-Term Thermal Stability, and a Four Year Track Record," https://rci-online.org/interface/2002-08-roe.pdf, last accessed May 1, 2013.

Scheutz, C. and Kjeldsen, P., (2003a), "Determination of the Fraction of Blowing Agent Released from Refrigerator/Freezer Foam Decommissioning the Product," Final Report, Prepared for the Appliance Research Consortium by the Environment & Resources DTU.

Scheutz, C., and Kjeldsen, P., (2003b), "Capacity for Biodegradation of CFCs and HCFCs in a Methane Oxidative Counter-Gradient Laboratory System Simulating Landfill Soil Covers," *Environmental Science & Technology*, Vol. 37, 5143-5149.

Scheutz, C., Fredenslund, A., Kjeldsen, P., (2003a), "Attenuation of Alternative Blowing Agents in Landfills," Final Report, Prepared for the Appliance Research Consortium by Environment & Resources DTU.

Scheutz, C., Bogner, J., Morcet, M., and Kjeldsen, P., (2003b), "Aerobic Degradation of Non-Methane Organic Compounds in Landfill Cover Soils," *Proceedings of Ninth International Waste Management and Landfill Symposium*, CISA, October, S. Margherita di Pula, Cagliari, Italy, 1-10.

Scheutz, C., Bogner, J., Chanton, J., Blake, D., Morcet, M., Kjeldsen, P., (2003c), "Comparative Oxidation and Net Emissions of Methane and Selected Non-Methane Organic Compounds in Landfill Cover Soils," *Environmental Science & Technology*, Vol. 37, 5150-5158.

Scheutz, C., Mosbæk, H., and Kjeldsen, P., (2004), “Attenuation of Methane and Volatile Organic Compounds in Landfill Soil Covers,” *Journal of Environmental Quality*, Vol. 33(1), 61-71.

Scheutz, C., and Kjeldsen, P., (2004), “Environmental Factors Influencing Attenuation of Methane and Hydrochlorofluorocarbons in Landfill Cover Soils,” *Journal of Environmental Quality*, Vol. 33(1), 72-79.

Scheutz, C., (2005), “Attenuation of Methane and Trace Organics in Landfill Soil Covers.”Diss. Environment & Resources, Technical University of Denmark.

Scheutz, C., Fredenslund, A. M., Tant, M. and Kjeldsen, P., (2007a), “Release of Fluorocarbons from Insulation Foam in Home Appliances during Shredding,” *Journal of the Air & Waste Management Association*, 57, 1452-1460.

Scheutz, C., Dote, Y., Fredenslund, A. M., Mosbæk, H. and Kjeldsen, P., (2007b), “Attenuation of Fluorocarbons Released from Foam Insulation in Landfills,” *Environmental Science & Technology*, 41, 7714-7722.

Scheutz, C., Fredenslund, A. M., Lemming, G., and Kjeldsen, P., (2007c), “Investigation of Emissions from the AV Miljo Landfill-1. Gas Quantity, Quality, and Attenuation Properties,” Institute of Environment and Resources, Technical University of Denmark, http://www.er.dtu.dk/Publikationer.aspx, last accessed May 15, 2013.

Scheutz, C., Bogner, J., Chanton, J. P., Blake, D., Morcet, M., Aran, C., and Kjeldsen, P., (2008), “Atmospheric Emissions and Attenuation of Non-Methane Organic Compounds in Cover Soils at a French Landfill,” *Waste Management*, 28, 1892-1908.

Scheutz, C., Pedersen, G., Costa, G., and Kjeldsen, P., (2009), “Biodegradation of Methane and Halocarbons in Simulated Landfill Biocover Systems Containing Compost Materials,” *Journal of Environmental Quality*, 38, 1363-1371.

Scheutz, C., Fredenslund, M., Nedenskov, J., and Kjeldsen, P., (2011a), “Release and Fate of Fluorocarbons in a Shredder Residue Landfill Cell: 1. Laboratory Experiments,” *Waste Management*, 30, 2153-2162.

Scheutz, C., Fredenslund, M., Nedenskov, J., and Kjeldsen, P., (2011b), “Release and Fate of Fluorocarbons in a Shredder Residue Landfill Cell: 2. Field Investigations,” *Waste Management*, 30, 2163-2169.

Schroer, D. Hudack, M., Soderquist, M., Beulich, I., (2011), “Rigid Polymeric Foam Boardstock Techical Assessment,” Midland, United States: The Dow Chemical Company.

Schilling, H. and Hinz, W., (1987), “Konzeption der Gasreinigungsanlage für die Deponie Kapiteltal,” Firmenschrift Leybold.

SCS, (2008), “Current MSW Industry Position and State-of-the-Practice on LFG Collection Efficiency, Methane Oxidation, and Carbon Sequestration in Landfills,” Report prepared for Solid Waste Industry for Climate Solutions by SCS Engineers.

Shackelford, C. D., (2005), “Environmental Issues in Geotechnical Engineering,” *Proceedings of the 16th Conference on Soil Mechanics and Geotechnical Engineering*, 95-122.

Sharma, H. and Reddy, K., (2004). *Geoenvironmental Engineering: Site Remediation, Waste Containment, and Emerging Waste Management Technologies.* New York: Wiley. Print.

Singh, S. N., Randall, D., Karremans, M., and Biesmans, G., (1998), “Long Term Performance of Rigid Foams Blown with Non-CFC Blowing Agents,” *Journal of Cellular Plastics*, Vol. 34(4), 349-360.

Sivertsen, K., (2007), “Polymer Foams,” http://www.core.org.cn/NR/rdonlyres/BC5A6FD8-4841-4031-8795-5153AA5E3DAF/0/polymer_foams.pdf, last accessed March 19, 2013.

Smith, K. A., and Bogner, J. E., (1997), *Report of joint North American-European workshop on measurement and modeling of methane fluxes from landfills*, IGAC, Cambridge, Mass.

Sowers, G. F., (1973), “Settlement of Waste Disposal Fills,” *Proceedings of the 8th International Conference on Soil Mechanics and Foundations Engineering*, Moscow, 207-210.

Spokas, K., Graff, C., Morcet, M., and Aran, C., (2003), “Implications of the Spatial Variability of Gas Emission Rates on Geospatial Analysis,” *Waste Management*, Pergamon, Vol. 23, 599-607.

Spokas, K., Bogner, J., Chanton, J.P., Morcet, M., Aran, C., Graff, C., Moreeau-Le Golvan, Y., and Hebe, I., (2006), “Methane Mass Balance at Three Landfill Sites: What is the Efficiency of Capture by Gas Collection Systems?” *Waste Management*, Vol. 26(5), 516-525.

Spokas, K. A., and Bogner, J. E., (2011), “Limits and Dynamics of Methane Oxidation in Landfill Cover Soils,” *Waste Management*, 31, 823-832.

Spokas, K. A., Bogner, J., and Chanton, J. A., (2011), “A Process-Based Inventory Model for Landfill $CH_4$ Emissions Inclusive of Soil Microclimate and Seasonal Methane Oxidation,” *Journal of Geophysical Research –Biogeosciences*, Vol. 116, 1-19.

Spokas, K., Bogner, J., Corcoran, M., and Walker, S., (2015), “From California Dreaming to California Data: Challenging Historic Models for Landfill $CH_4$ Emissions,” *Elementa: Science of the Anthropocene*, 3: 000051, doi: 10.12952/ journal.elementa.000051, 1-16.

Stein, V. B. and Hettiaratchi, J. P. A., (2001), “Methane Oxidation in Three Alberta Soils: Influence of Soil Parameters and Methane Flux Rates,” *Environmental Technology*, Vol. 22(1), 101-111.

Stern, J.C., Chanton, J., Abichou, T., Powelson, D., Yuan, L., Escoriza, S., and Bogner, J., (2007), “Use of a Biologically Active Cover to Reduce Landfill Methane Emissions and Enhance Methane Oxidation,” *Waste Management*, Vol. 27(9), 1248-1258.

Streese-Kleeberg , J. and Stegmann, R., (2008), “Biofiltration of Landfill Gas Methane with Active Ventilation.” *Proceedings of the Global Waste Management Symposium*. Barlaz, M.A., Benson, C.H., and Cekander, G.C. ed.

Strzepek, W. R., (1990), “Overview of Physical Properties of Cellular Thermal Insulations.” *Insulation Materials, Testing, and Application.* Philadelphia: ASTM. 121-140.

Stull, R. B., (1988), *An Introduction to Boundary Layer Meteorology*, Kluwer Academic Publishers, Dordrecht, the Netherlands.

Swanstrom, M. and Ramnas, O., (1996), “Determination of the Blowing Agent Distribution in Rigid Polyurethane Foam,” *Journal of Cellular Plastics*, Vol. 32(2), 159-171.

Tchobanoglous, G., Theisen, H., Vigil, S., (1993). *Integrated Solid Waste Management: Engineering Principles and Management Issues.* New York: Irwin McGraw-Hill.

Technology and Economic Assessment Panel (TEAP), United Nations Environment Program (2005), “Report of the Task Force on Collection, Recovery, and Storage: Volume 3A,” http://ozone.unep.org/Assessment_Panels/TEAP/Reports/Other_Task_Force/TEAP02V3a.pdf, last accessed April 20, 2013.

Technology and Economic Assessment Panel (TEAP), United Nations Environmental Program, (2005), “Report of the Task Force on Foam End of Life Issues: Volume 3,” http://ozone.unep.org/teap/Reports/TEAP_Reports/TEAP-May-2005-Vol-2-Forms-End-of-Life.pdf, last accessed April 4, 2013.

Technology and Economic Assessment Panel (TEAP), United Nations Environment Program, (2009), “Task Force Decision XX/7 Interim Report: Environmentally Sound Management of Banks of Ozone Depleting Substances,”

http://ozone.unep.org/teap/Reports/TEAP_Reports/teap-october-2009-decisionXX-7-task-force-phase2-report.pdf, last accessed December 12, 2012.

Throne, J. L., (2004). *Thermoplastic Foam Extrusion: An Introduction*. Cincinnati: Hans Gardner Publishers. Print.

Tsai, W. "An Overview of Environmental Hazards and Exposure Risk of Hydrofluorocarbons." *Chemosphere 61* (2005): 1539-1547.
United Nations Environment Program (UNEP), (1996). *Sourcebook of Technologies for Protecting the Ozone Layer: Flexible and Rigid Foams Handbook.*

United Nations Environment Program (UNEP), (1996), "HFCs: A Critical Link in Protecting the Ozone Layer," A UNEP Synthesis Report, http://www.unep.org/dewa/Portals/67/pdf/HFC_report.pdf, last accessed October 30, 2013.

United Nations Environment Program (UNEP), (1998), "Concise International Chemical Assessment Document 11: 1,1,12-Tetrafluoroethane (HFC-134a)" http://www.who.int/ipcs/publications/cicad/en/cicad11.pdf, last accessed March 21, 2013.

United Nations Environment Program (UNEP), (2001), "1,1-DiChloro-1,Fluoroethane (HCFC-141b): SIDS Initial Assessment Report for 12th SIAM," http://www.inchem.org/documents/sids/sids/1717006.pdf, last accessed March 1, 2013.

Urgun-Demirtas, M., Singh, D., and Pagilla, K., (2007), "Laboratory Investigation of Biodegradability of a Polyurethane Foam Under Anaerobic Conditions," *Polymer Degradation and Stability*, Vol. 92, 1599-1610.

USEPA, (1993), "The Use of Alternative Materials for Daily Cover at Municipal Solid Waste Landfills," EPA Report # 68-C1-0018.

USEPA, (1995), "User's Guide for the Industrial Source (ISC3) Dispersion Models: Volume I-User Instructions," http://www.epa.gov/ttn/scram/userg/regmod/isc3v1.pdf, last accessed March 23rd, 2013.

USEPA, (2004), "Identification of Time-Integrated Sampling and Measurement Techniques to Support Human Exposure Studies," http://cfpub.epa.gov/si/si_public_record_report.cfm?dirEntryId=83797, last accessed January 15th, 2013.

USEPA, (2005), "Guidance For Evaluating Landfill Gas Emissions From Closed or Abandoned Facilities," http://nepis.epa.gov/Adobe/PDF/P1000BRN.PDF, last accessed May 15, 2013.

USEPA, (2006), “OTM 10, Optical Remote Sensing for Emission Characterization from Non-point Sources,” Final ORS Protocol, http://www.epa.gov/ttn/emc/prelim/otm10.pdf, last accessed December 18, 2012.

USEPA, (2007), “Evaluation of Fugitive Emissions Using Ground-Based Optical Remote Sensing Technology,” http://nepis.epa.gov/Exe/ZyPDF.cgi?Dockey=P100ADVE.PDF, last accessed March 31, 3013.

USEPA, (2008), “Background Information Document for Updating AP-42 Section 2.4 for Estimating Emissions from Municipal Solid Waste Landfills,” http://www.epa.gov/ttnchie1/ap42/ch02/draft/db02s04.pdf, last accessed May 2, 2013.

USEPA, (2009). “Definition of Volatile Organic Compounds (VOCs),” http://www.epa.gov/ttn/naaqs/ozone/ozonetech/def_voc.htm, last accessed May 1, 2013.

USEPA, (2010), “Responsible Appliance Disposal Program,” www.reginfo.gov/public/do/DownloadDocument?documentID2254ss02.doc, last accessed August 29th, 2012.

USEPA, (2011), “EPA Handbook: Optical Remote Sensing for Measurement and Monitoring Emission Flux,” http://www.epa.gov/ttnemc01/guidlnd/gd-052.pdf, last accessed February 15th, 2013.

USEPA, (2015a), “Advancing Sustainable Materials Management: Facts and Figures 2013,” http://www3.epa.gov/epawaste/nonhaz/municipal/pubs/2013_advncng_smm_rpt.pdf, last accessed September 28th, 2015.

USEPA, (2015b), “Landfill Methane Outreach Program, Basic Information,” http://www3.epa.gov/lmop/basic-info/index.html, last accessed September 28th, 2015.

van Haaren, R., Themelis, N., and Goldstein, N., (2010), “17th Nationwide Survey of MSW Management in the U.S.: The State of Garbage in America,“ *BioCycle: Advancing Composting, Organics Recycling and Renewable Energy,* JG Press, Inc., October, 2010, 16-23.

Vo, C. and Paquet, A., (2004), "An Evaluation of the Thermal Conductivity of Extruded Polystyrene Foam Blown with HFC-134a or HCFC-142b," *Cellular Plastic,* Vol 40, pgs. 205-228.

Vollhardt, K., Peter, C., Schore, N, (1999). *Organic Chemistry: Structure and Function*. New York: W.H. Freeman. Print.

Volmer, M. K., Miller, B. R., Rigby, M., Reimann, S., Muhle, J., Krummel, P. B., O'Doherty, S., Kim, J., Rhee, T. S., Weiss, R. F., Fraser, P. J., Simmonds, P. G., Salameh, P.K., Harth, C. M., Wang, R. H. J., Steele, L. P., Young, D., Lunder, C. R., Hermansen, O., Ivy, D., Arnold, T., Schimbauer, N., Kim, K. R., Greally, B. R., Hill, M., Leist, M., Wenger, A., Prinn, R., (2011), "Atmospheric Histories and Global Emissions of the Anthropogenic Hydrofluorocarbons HFC-365mfc, HFC-245fa, HFC-227ea, and HFC-236fa," *Journal of Geophysical Research,* Vol. 116, 1-16.

Wang, J. and Qi, F., (1998), "The Effect of Sampling Design on Spatial Structure Analysis of Contaminated Soil," *The Science of the Total Environment,* Vol. 224 (1-3), 29-41.

Wethje L. R., (2005), "Disposal of Refrigerators-Freezers in the US: State of the Practice," EPA Grant # CXA831729-01-0, *http://www.aham.org/industry/ht/a/GetDocumentAction/i/16317*, last accessed November 10, 2011.

Wilkes, K., Yarbrough, W.D., Nelson, G., (2003). *Aging of Polyurethane Foam Insulation in Simulated Refrigerator Panels - Four-Year Results with Third-Generation Blowing Agents*. Oak Ridge National Laboratory.

Whalen, S. C., Reeburgh, W. S., and Sandbeck, K. A, (1990), "Rapid Methane Oxidation in a Landfill Cover Soil," *Applied and Environmental Microbiology*, Vol. 56(11), 3405-3411.

Xu, L., Amen, J., Lin, X., and Welding, K., (2013), "The Impact of Changes in Barometric Pressure on Landfill Methane Emission," http://oldwastecon.swana.org/Portals/7/pdfs/2011Proceedings/Xu_Liukang_WC11_Paper.pdf, last accessed May 2, 2013.

Yesiller, N., Hanson, J. L., and Liu, W.L., (2005), "Heat Generation in Municipal Solid Waste Landfills," *Journal of Geotechnical and Geoenvironmental Engineering*, ASCE, Vol. 131(11), 1330-1344.

Yesiller, N., Hanson, J. L., and Abichou, T., (2008a), *Measurement and Estimation of Landfill Surface Gas Emissions*, Report to City of Vancouver.

Yesiller, N, Hanson, J. L., Oettle, N. K., and Liu, W. L., (2008b), "Thermal Analysis of Cover Systems in Municipal Solid Waste Landfills," *Journal of Geotechnical and Geoenvironmental Engineering*, Vol. 134(11), 1655-1664.

Yesiller, N., Wong, W. W., and Hanson, J. L., (2010), "Hydraulic Conductivity of Municipal Solid Waste as a Function of Placement Conditions," *Proceedings Sixth International Conference on Environmental Geotechnics*, New Delhi, India.

Yesiller, N. and Shackelford, C. D., (2011), “Geonenvironmental Engineering: Chapter 13.” *Geotechnical Engineering Handbook.* Das, B.M.. Ed. J Ross Publishing: Ft. Lauderdale, Florida, 1-61.

Young, A., (1992), “The Effect of Fluctuations in Atmospheric Pressure on Landfill Gas Migration and Composition,” *Water, Air and Soil Pollution,* Vol. 64, 601–616.

Young, P. J. and Heasman, L. A., (1985), “An Assessment of the Odor and Toxicity of the Trace Components of Landfill Gas,” *Proceedings of the 8th International Landfill Gas Symposium,* GRCDA, April, San Antonio, Texas, 93-114.

Yourd, R. A., (1996), “Compression Creep and Long-Term Dimensional Stability in Appliance Rigid Foam,” *Journal of Cellular Plastics*, Vol. 32(6), 601-616.

Yucel, K. T., Basyigit, C., Ozel, C., (1995), “Thermal Insulation Properties of Expanded Polystyrene as Construction and Insulating Materials,” http://zenonpanel.com.mk/al/wp-content/uploads/2009/06/Thermal-Insulation-properties.PDF, last accessed March 23, 1989.

Yu, C. W. F., Crump, D. R., and Gardiner, D., (1995), “CFC-Free Thermal Insulation Foams (Poster Presentation.” *Cellular Polymers III: 3rd International Conference.* ed. RAPRA Technology, LTD. U.K. 9-10. Print.

Zekkos, D., Bray, J.D., Riemer, M., Kavazanjian, E., and Athanasopoulos, G.A., (2007), “Response of Municipal Solid Waste from Tri-Cities landfill in Triaxial Compression,” *Proceedings of the 11th International Waste Management and Landfill Symposium*, CISA, S. Margherita di Pula, Cagliari, Italy, October 1-5, 1-10.

Zhang, F., Wang, X., Yi, Z., Li, L., Chan, C., Chan, L., and Blake, D. R., (2006), “Preliminary Investigation on Levels and Trends of Atmospheric Chlorodifuoromethane (HCFC-22) in the Pearl River Delta,” *Huanjing Kexue Xuebao*, Vol. 26, 987-991.

# APPENDIX 1 – LITERATURE REVIEW

## 1.1 Introduction

The annual municipal solid waste (MSW) generation in the U.S. has been on the order of 230 Mt since 2005, with 231 Mt of generation in 2013 based on latest data available from USEPA (2015a). Landfilling constitutes the main means of waste disposal in the U.S. with 122 Mt (53% of 231 Mt generated) disposed of in landfills in 2013. For California, the annual MSW disposal amount has been on the order of 27 Mt since 2009, with 28 Mt of generation reported for 2014 based on latest data available from CalRecycle (2015). The number of landfills was reported to be 1,908 in the U.S. (USEPA 2015a) and 372 in California (Cascadia 2008).

Landfilling of municipal solid waste results in three main byproducts: landfill gas (LFG), leachate, and heat. Landfill gas is generated mainly due to biochemical processes including biological decomposition and degradation and chemical reactions that occur within the waste mass. Gas generation also may occur to a lesser extent due to physical processes such as evaporation and volatilization and release of trapped gases from discarded materials due to mechanical processes (Tchobanoglous et al. 1993, Sharma and Reddy 2004). The main constituent components of landfill gas are methane ($CH_4$) and carbon dioxide ($CO_2$) with oxygen, nitrogen, hydrogen, and trace gases present at relatively low amounts (USEPA 2015b). The typical LFG composition on a volumetric basis is approximately 55-60% (v/v) methane and 40-45% (v/v) carbon dioxide under stable gas production conditions (Scheutz 2005). The oxygen, nitrogen, and hydrogen concentrations typically are less than 5% (v/v) in LFG (Rettenberger and Stegmann 1996).

The trace gases in LFG generally occur at fractions ≤1%. These gases are generated during anaerobic degradation or may be anthropogenic and present in the deposited waste (Rettenberger and Stegmann 1996). Rettenberger and Stegmann (1996) indicated that the degradation products included oxygen compounds, sulphur components, and terpene hydrocarbons, while the anthropogenic trace compounds mainly included aromatic and chlorinated hydrocarbons. The USEPA (2015b) indicated that the trace gases consisted of nonmethane organic compounds (NMOCs) and trace amounts of inorganic compounds. Scheutz et al. (2008) indicated that nonmethane organic compounds comprised more than 200 organic compounds including alkanes, aromatics, chlorinated and fluorinated hydrocarbons, and various volatile organic compounds with typical concentrations in the range of below detection limit to 1,780 ppmV. The gases of interest for this investigation consisted of halogenated hydrocarbons including chlorinated and fluorinated species chlorofluorocarbons (CFCs), hydrochlorofluorocarbons (HCFCs), and hydrofluorocarbons (HFCs). The specific gases investigated were CFC-11, HCFC-141b, HFC-134a, and HFC-245fa. These four gases collectively are referred to as target gases in the Literature Review section.

## 1.2 General Background: CFCs, HCFCs, and HFCs

Historically, liquid and gaseous CFCs were used in various applications ranging from cleaning products, to aerosol sprays, to adhesives and paint strippers, as well as

refrigerants, and insulation/cushioning foams (Rettenberger and Stegmann 1996). Chlorinated and fluorinated hydrocarbons commonly are used in refrigeration and insulation foam (Rettenberger and Stegmann 1996). Use as insulation materials is the most common application of chlorofluorocarbons due to the abilities of these compounds to absorb large amounts of heat upon vaporization (Vollhardt et al. 1999). The use of CFCs in insulation foams and refrigeration started in 1931 after the commercial development of chlorinated and fluorinated hydrocarbons by DuPont chemical company (CARB 2008). After the Montreal Protocol banned the use of CFCs in 1993, CFCs were progressively replaced by HCFCs and HFCs. The most common waste products that emit these chlorinated and fluorinated gases are domestic, commercial, and industrial refrigeration and insulation foams whether used originally in appliances or buildings alike (Scheutz 2005). The most common gases present in these foams, including CFC-11, HCFC-141b, HFC-134a, and HFC-245fa, enter landfill facilities due to the disposal of these waste foams. The waste materials with potential emissions are discards consisting of rigid foams. The wastes associated with soft, flexible non-insulation type foams used in automobile and other industries typically are not expected to contain high levels of chemicals at the time of disposal (TEAP 2005).

CFCs, HCFCs, and HFCs generally do not pose significant adverse health effects to humans, yet these compounds are of primary concern due to their adverse environmental effects. The common CFCs, HCFCs, and HFCs in manufactured foam materials are greenhouse gases. A greenhouse gas (GHG) is a gas that, due to its long retention time in the atmosphere, absorbs and emits radiation within the thermal infrared range (USEPA 2004). Although present in small concentrations, CFCs, HCFCs, and HFCs exhibit a disproportionate environmental burden in that these compounds actively contribute to the depletion of the ozone layer and global climate change (Scheutz et al. 2007a). CFCs and HCFCs are ozone-depleting substances (ODS) since they are chlorinated and have long lifetimes in the atmosphere, whereas ozone depletion impacts of the HCFCs are smaller compared to the impacts of CFCs. HFCs have high potential to absorb outgoing infrared radiation, a precursor to global climate change.

Due to the long lifetime of these compounds in insulation foams past the useful service life of both appliances and building materials, as well as relatively slow degradation processes encountered within a landfill environment, banks of CFCs, HCFCs, and HFCs are generated. Since these chemicals are banked in appliance and building insulation foam waste within landfills (up to 9 $MMTCO_2$ equivalents in California), predicting, measuring and quantifying emissions are critical for managing current and future sources of ozone depletion and global climate change (CARB 2008).

### 1.2.1 Basic Characteristics

Chlorinated and fluorinated hydrocarbons are alkanes (long groups of single bonded carbon atoms) where all of the hydrogen atoms have been replaced by fluorine and chlorine atoms (Vollhardt et al. 1999). In general, CFCs and HCFCs are alkanes with one carbon (methanes) and HFCs are alkanes with two to three carbons (ethanes and propanes). Classification, chemical names, and chemical formulations of common

chlorinated and fluorinated hydrocarbons are provided in Table 1. The atomic structures of CFC-11, HCFC-141b, HFC-134a, and HFC-245fa are presented in Figure 1.

Table 1 – Classification of Common CFCs, HCFCs, and HFCs

| Name | Classification[1] | Chemical[2] Name | Structural Formula |
|---|---|---|---|
| CFC-11 | R[3]-11 | Trichlorofluoromethane | $CCl_3F$ |
| CFC-12 | R-12 | Dichlorodifluoromethane | $CCl_2F_2$ |
| CFC-113 | R-113 | 1,1,2-Trichloro-1,2,2-Trifluoroethane | $CCl_2FCClF_2$ |
| CFC-114 | R-114 | 1,2-Dichlorotetrafluoroethane | $CClF_2CClF_2$ |
| HCFC-141b | R-141b | 1,1-Dichloro-1-Fluoroethane | $CH_3CFCl_2$ |
| HCFC-142b | R-142b | 1-Chloro-1,1-Difluoroethane | $CH_3CF_2Cl$ |
| HCFC-21 | R-21 | Dichlorofluoromethane | $CHCl_2F$ |
| HCFC-22 | R-22 | Chlorodifluoromethane | $CHClF_2$ |
| HCFC-31 | R-31 | Chlorofluoromethane | $CH_2ClF$ |
| HCFC-32 | R-32 | Difluoromethane | $CH_2F_2$ |
| HFC-134a | R-134a | 1,1,1,2-Tetrafluoroethane | $CH_2FCF_3$ |
| HFC-152a | R-152a | 1,1-Dichloroethane | $CH_3CHF_2$ |
| HFC-245fa | R-245fa | 1,1,1,3,3-Pentafluoropropane | $CF_3CH_2CHF_2$ |
| - | R-717 | Ammonia | $NH_3$ |
| - | R-744 | Carbon Dioxide | $CO_2$ |

[1] Based on ASHRAE (2013)
[2] Based on IPCC (2005) nomenclature
[3] R: Refrigerant

Physical and chemical properties of the target gases (CFC-11, HCFC-141b, HFC-134a, and HFC-245fa) are presented in Table 2. The parameters presented in the table are associated with testing conditions at 25°C and 1 atm pressure. Due to their relatively low boiling points (in the range of <0 to 100°C), CFCs, HCFCs, and HFCs are classified as volatile organic compounds (VOCs). These compounds evaporate (or volatilize) readily when exposed to the atmosphere (as presented in USEPA 2009). Even though the volatility of these compounds are acknowledged, the CFCs, HCFCs, and HFCs are unregulated due to their, “negligible photochemical reactivity” under the provision 40 CFR 5.100(s) (USEPA 2009). The volatility of the target gases are associated with the characteristically high vapor pressures (in the range of 430 to 5,000 mmHg) observed, compared to water (22.8 mmHg) at 1 atm and 25°C. In general, HFCs have higher volatility (higher vapor pressure, lower boiling point) and relatively lower solubility in water as compared to CFCs and HCFCs (Tsai 2005). HFC-134a has a higher variation in reported vapor pressure values among studies (due to differences in method of estimation or measurement) with overall high reported vapor pressures. The reported water solubility is lowest for HFC-134a and highest for HCFC-141b indicating a high affinity for the aqueous phase compared to the other three target gases (Table 2).

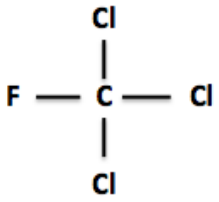


(a) CFC-11 (Trichlorofluoromethane)

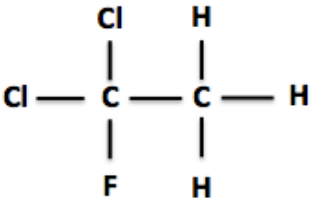


(b) HCFC-141b (1,1-Dichloro-1-Fluoroethane)

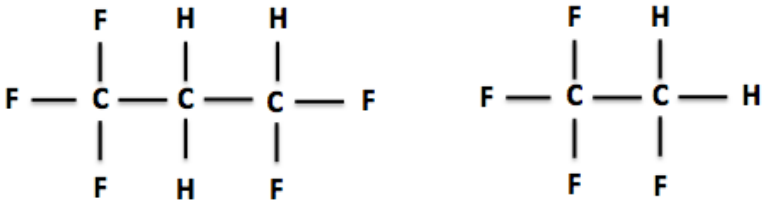


(c) HFC-245fa (1,1,3,3-pentafluoropropane) and HFC-134a (1,1,1,2-tetrafluoroethane)

Figure 1. Atomic Structure of Target Gases

Table 2 – Physical and Chemical Properties of Target Gases
(from Scheutz et al. 2003a)

| Chemical Name | CFC-11 | HCFC-141b | HFC-134a | HFC-245fa |
|---|---|---|---|---|
| Synonyms | Trichlorofluoromethane | 1,1-Dichloro-1-Fluoroethane | 1,1,1,2-Tetrafluoroethane | 1,1,1,3,3-Pentafluoropropane |
| Structure | $CCl_3F$ | $CCl_2FCH_3$ | $CH_2FCF_3$ | $CF_3CH_2CHF_2$ |
| Molecular Weight (g/mol) | 137.37 | 116.95 | 102.03 | 134.05 |
| Boiling Point (°C) | 23.8 | 32 | -26.2 | 15.3 |
| Vapor Pressure (mmHg) | 798[2]-802.8[1] | 626[2]-707[1] | 430[1]-4,995[2] | 1,114[3]-1,139[2] |
| Water Solubility (mg/L) | 1,100[1,2] | 660[1]-2,632[2] | 67[1]-550[2] | 1,300[3]-1,900[3] |
| Log$K_{ow}$ | 2.53[1,2] | 2.04[2]-2.37[1] | 1.06-1.68[1] | 1.33-1.35[1] |
| Log$K_{oc}$ | 2.49[4] | 1.9-2.2[4] | 1.5[4] | 1.75-1.9[4] |
| Saturated Gas Concentration (g/L) | 5.62[1] | 4.78[1] | 4.17[1] | 5.48[1]-5.5[3] |

[1] Scheutz and Kjeldsen (2003)
[2] Mackay et al. (2006)
[3] NICNAS (2004)
[4] Summarized from UNEP (1998, 2001), Balsiger et al. (2004), and ChemSpider (2013)

The overall gas to liquid phase partitioning of the target gases was further assessed using the dimensionless Henry's constant, calculated using Equation 1 below. The dimensionless Henry's law constant can be used to compare the affinity of the chemical for either the gas or aqueous phase according to (Eq. 2).

$$K_H = \frac{K}{RT} \quad (1)$$

where $K_H$ refers to the dimensionless Henry's law constant, $K$ is equivalent to the Henry's law constant ($m^3$ atm/mole), $R$ is the universal gas constant ($8.2057 \times 10^{-5}$ $m^3$ atm/mole °K), and $T$ is the temperature in which $H$ was measured (°K).

$$K_H = \frac{C_g}{C_s} \quad (2)$$

where $C_g$ is the concentration of VOC in gaseous phase ($\mu g/m^3$) and $C_s$ is the saturation concentration of VOC in liquid phase in equillibrium ($\mu g/m^3$) (Tchobanoglous et al. 1993).

The calculated values of $K_H$ for CFC-11, HCFC-141b, HFC-134a, and HFC-245fa were 3.97, 0.986, 2.27, and 0.924, respectively. The relatively high $K_H$ values for CFC-11 and HFC-134a indicated that these target gases were more likely to be in the gaseous phase than aqueous phase at atmospheric pressure and 25°C temperature. At higher

temperatures, such as the elevated temperatures at landfills, the Henry's constants would increase due to an expected increase in vapor pressure to result in higher concentration of volatilized gases in the waste mass.

The octanol-water partition coefficient ($K_{ow}$), and the organic carbon sorption coefficient ($K_{oc}$) were used to assess the adsorption/absorption capacity of the gases. $K_{ow}$ and $K_{oc}$ are calculated as:

$$K_{ow} = \frac{C_{octanol}}{C_{water}} \quad (3)$$

where $K_{ow}$ is the octanol-water partition coefficient, $C_{octanol}$ is the concentration of the chemical in octanol (mg/L), and $C_{water}$ is the concentration of the chemical in water (mg/L) when in equilibrium.

$$K_{oc} = \left(\frac{C_{soil}}{C_{water}}\right) * \frac{1}{f_{oc}} \quad (4)$$

where $K_{oc}$ is the partition (distribution) coefficient normalized to organic carbon content of a sorbent, $C_{soil}$ is the concentration adsorbed to the soil (mg/L) at equilibrium, $C_{water}$ is the concentration of the chemical in the aqueous phase (mg/L) at equilibrium, and $f_{oc}$ is the fraction of organic carbon (%).

The reported $K_{ow}$ values for CFCs and HCFCs are higher than those for HFCs (Table 2) indicating: i) lower potential for transport in water/leachates, ii) higher adsorption to soils/waste materials, and iii) lower bioaccumulation in living organisms. Predicted $K_{oc}$ values also were higher for CFCs and HCFCs (at neutral pH levels) than HFCs, indicating that CFCs and HCFCs have a higher potential for adsorption to soils/waste materials, even when normalized to the organic fraction content of the soil/waste materials.

In general, the physical and chemical characteristics of CFCs, HCFCs, and HFCs favor the potential for accumulation in the atmosphere as opposed to the soil or groundwater, where accumulation depends on atmospheric retention times (higher for CFCs than HCFCs/HFCs). For additional environmental and health effects, higher $K_{ow}$ values of CFC-11 and HCFC-141b indicate that these compounds are more likely to be bioaccumulated by animals in the environment, as compared to HFCs that have a low potential for bioaccumulation (Tsai 2005). Similarly, HFCs and HCFCs have a low eco-toxicity, with a generally low environmental impact (Tsai 2005).

### 1.2.2 Atmospheric Conditions

The current global atmospheric concentrations of GHGs, including common CFCs, HCFCs, and HFCs, are provided in Table 3. These data represent recent global averages over a 12-month period (ALE/GAGE/AGAGE Global Network Program 2013). The range in values presented in the table (third column from the right) is a compilation of results presented by Barletta et al. (2002, 2006), ranging from 6 cities across the world for all CFCs studied and 2 cities across the world for HFCs and

HCFCs respectively. The data presented in Table 3 provides the latest available values for the different compounds, the data may change in future to reflect new research developments from IPCC working group conventions. Recent tropospheric concentrations of carbon dioxide are the highest of all GHGs analyzed at 390.5 ppm compared to approximately 1800 ppb of methane, 34 ppb ozone, 240 ppt CFC-11, 530 ppt CFC-12, 22 ppt HCFC-141b, and 63 ppt HFC-134a (CDIAC 2012, IPCC 2013). The historic (pre-1750) concentrations of all chlorinated alkanes and HFCs were approximately zero with a large increase due to anthropogenic activities. Carbon dioxide, nitrous oxide, and ozone have increased 30%, 63%, and 26% from historic (pre 1750) concentrations, signifying a drastic imbalance of the global carbon cycle (CDIAC 2012). General global trends demonstrated higher concentrations of CFCs over urban areas, as compared to HFCs and HCFCs with opposite trends observed in rural areas.

Table 3 – Atmospheric Conditions for GHGs

| Gas | Recent Tropospheric Concentration (ppt)[1] | Recent Tropospheric Concentration (ppt)[4,5] | Atmospheric Lifetime (yrs)[1,2,3] | Global Warming Potential (100 yr)[1,2,3] | Ozone Depletion Potential[1,2] | Radiative Forcing ($W/m^2$)[1] |
|---|---|---|---|---|---|---|
| Carbon Dioxide | $3.91x10^8$ | N/A | 100 | 1 | 0 | 1.82 |
| Methane | $1.80x10^6$-$1.81x10^6$ | N/A | 9.1-12.4 | 25-28 | 0 | 0.48 |
| Nitrous Oxide | $3.24x10^5$ | N/A | 114-131 | 265-298 | 0 | 0.17 |
| Ozone[3] | $3.4x10^4$ | N/A | Hours-Days | N/A | N/A | 0.35 |
| CFC-11 | 237-239 | 259-301[4] | 45 | 3800-4660 | 1 | 0.06 |
| CFC-12 | 527-529 | 545-567[4] | 100 | 8100-10200 | 1 | 0.17 |
| CFC-113 | 74 | 79-90[4] | 85 | 5820-6130 | 0.8 | 0.022 |
| HCFC-141b | 21 | 16.4-20[5] | 9.2 | 700-782 | 0.1-0.12 | 0.0034 |
| HCFC-142b | 21 | 13.6-19[5] | 17.2-17.9 | 1800-1980 | 0.06-0.07 | 0.0040 |
| HCFC-22 | 213 | 220-295[5] | 11.9 | 1500-1780 | 0.05-0.055 | 0.045 |
| HFC-134a | 62-63 | 23-23.1[5] | 13.4-14 | 1300-1410 | 0 | 0.0100 |
| HFC-245fa | N/A | N/A | 6.6-7.7 | 858-1020 | 0 | |
| Halon 1211[3] | 4.1-4.3 | N/A | 16 | 1750-1890 | N/A | 0.001 |
| Halon 1301[3] | 3.2-3.3 | N/A | 65 | 6290-7140 | N/A | 0.001 |
| Carbon Tetrachloride | 85-86 | N/A | 26 | 1400-1730 | N/A | 0.015 |
| Sulfur Hexafluoride | 7.3 | N/A | 3200 | 22800-23500 | N/A | 0.0041 |
| Total Halocarbons[6] | Varies | N/A | Varies | Varies | N/A | 0.330 |

[1] IPCC 2013 summary of combined global ambient tropospheric concentrations in both rural and urban areas
[2] Ranges adapted from SAR (1995), TAR (2001), and TEAP (2009)
[3] CDIAC (2012)
[4] Barletta et al. (2006), global ambient tropospheric concentrations above 6 urban centers
[5] Barletta et al. (2002), global ambient tropospheric concentrations above 2 urban centers
[6] Also termed total "Montreal Protocol" gases by the latest IPCC working group report (2013)

The concentrations of these gases in the atmosphere depend on the emissions rate and how long they remain in the atmosphere, also known as the atmospheric lifetime. The atmospheric lifetime of a chemical can be defined as, "… the time it takes for 67%

of the concentration of a molecule to be removed from the atmosphere in the absence of emissions" (UNEP 2011). The atmospheric lifetimes of the chlorofluorocarbons range between 45 and 100 years (excluding HCFCs), whereas the atmospheric lifetimes of HFCs and HCFCs are shorter, between 7 and 18 years.

The threat posed by CFCs and HCFCs to ozone depletion is characterized quantitatively using the ozone depletion potential (ODP). The ozone depleting potential can be defined as a, "measure of the extent of ozone layer depletion by a given ozone depleting substance, relative to that depleted by CFC-11 (CFC-11 has an ODP of 1.0)" (UNEP 2011). The ODP values HCFCs are lower than those for CFCs, and HFCs pose no potential to damage the ozone layer (Table 3). Global warming potential is, "a relative index that enables comparison of the climate effect of emissions of greenhouse gases as reference to carbon dioxide" (UNEP 2011). Carbon dioxide was chosen as the reference (with a GWP value of 1.0) due to its high concentration in the atmosphere, and its relatively large radiative forcing on the atmosphere (UNEP 2011). Radiative forcing is defined as, "a measure of how a greenhouse gas influences the energy balance of the earth, in which a positive value indicates a net heat gain to the lower atmosphere, leading to a global temperature increase, while a negative value is indicative of a heat loss" (UNEP 2011). GWP values were presented in ranges from a combination of reports to reflect the variation in calculations over the past 15-20 years (SAR 1995, TAR 2001, TEAP 2009, IPCC 2013). The GWPs for the chlorinated and fluorinated hydrocarbons were higher than those for general GHGs (e.g., $CO_2$, $CH_4$, $NO_2$). CFCs (11, 12, and 113) were estimated to possess the highest GWP (100-year) ranging from 3,800-10,720 (Table 3). The predicted GWPs for HFCs were relatively lower than those for HCFCs (with the exception of HCFC-141b) in the range from 858 to 1,410 as compared to 1,500 to 2,270. CFC-12, with a high GWP and atmospheric lifetime, demonstrated the largest radiative forcing (0.17 $W/m^2$) out of all chlorinated and fluorinated hydrocarbons. Both the HCFCs and HFCs had relatively insignificant radiative forcing values as of 2013, but are expected to rise within the next 50 years (IPCC 2007, 2013).

In addition, current atmospheric concentrations and emission trends for CFCs, HCFCs, and HFCs were reviewed for California. Atmospheric concentrations and emission trends in California were measured or predicted in Li (2005), Gentner et al. (2010), Gorham et al. (2010), Hsu et al. (2010), Volmer et al. (2011), and Barletta et al. (2011, 2013). Emissions and atmospheric concentrations of these components around the Southern California Air Basin (SoCAB) were the focus of many of these studies. The SoCAB was determined to have high fugitive emissions ratio from landfills based on measured concentrations of atmospheric methane (Li et al. 2005, Hsu et al. 2010, Peischl et al. 2013, Jeong et al. 2013). According to Li et al. (2005), using air measurements from Mt. Wilson (Los Angeles), fugitive emissions of methane from landfills accounted for 66% of the total Los Angeles county methane emissions, as compared to 21% based on statewide emissions in California determined using all California landfills (adapted from CARB 2008). Results from Peischl et al. (2013) demonstrated good agreement between measured atmospheric data (NOAA P-3 flybys) and CARB (2008) GHG inventory data quantifying large (up to 38 Gg/yr)

methane emissions for two of the largest landfills in the SoCAB (Olinda Alpha and Puente Hills). However, potential problems are present with the existing CARB landfill methane emission methodology (IPCC 2006, Spokas et al. 2011, 2015). These include: lack of field validation for emissions and a primary depence on waste in place rather than composition, cover thickness, and site-specific methane oxidation rates, which vary with climate over an annual. Other air basins from California also were included in this review of concentrations and estimated emissions of CFCs, HCFCs, and HFCs as a comparison using Trinidad Head, California. A summary of all of these estimates is presented in Table 4. In general, CFC-11 concentrations were high with lower concentrations measured for HCFC-141b and HFC-134a (Barletta et al. 2011, 2013). Only one investigation included measurements of HFC-245fa with relatively low reported concentrations in Northern California. However, the estimated emissions for HFC-245fa were higher than the emissions for the other gases (Table 4). Incoming air from the Pacific Ocean carries high concentrations of several chemicals listed.

Emissions of CFCs, HCFCs, and HFCs combined in California are approximately 9 $MMTCO_2eq$ annually based on USEPA's vintaging model (Godwin et al. 2003) and scaled down to account for California's population (CARB 2008). These emissions were expected to decline and stabilize at 2.1 $MMTCO_2eq$ per year (25% of the initial emission level) due to substitution of CFCs/HCFCs with HFCs or other low GWP blowing agents (CARB 2008). Cumulative emissions spanning 50 years into the future from existing foam banks (not including new banks created) were predicted to result in approximately 236 $MMTCO_2eq$ (CARB 2008). Combining data from Li et al. (2005), Gentner et al. (2010), and Barletta et al. (2013), an estimate was made for emissions of CFCs, HCFCs, and HFCs in California. GWP values from the IPCC TAR (2001) report were used to convert from Gg (gigagrams) per year to million metric tonnes of $CO_2eq$ per year. The estimated annual emissions were 37 $MMTCO_2eq$, which is significantly higher than the CARB (2008) estimate of 9 $MMTCO_2eq$ per year (a 400% increase). This difference may have resulted from the assumptions inherent in the estimates and the variations in annual emission estimates as well as the total time periods associated with the different studies. Further differences may have resulted from the EPA model not accounting for naturally occurring degradation or generation processes within the atmosphere. For example, under certain conditions within the troposphere CFCs could degrade forming more HCFC-22 as a byproduct. Measured emissions values are required to increase the level of confidence in obtaining representative emissions of CFCs, HCFCs, and HFCs in California. Further field measurements are additionally required to obtain representative emissions of these gases as well as to validate estimates.

Table – 4 Summary of Atmospheric Concentrations and Emission Prediction Studies in California

| Trace Gas Component Measured | Measured Mean Atmospheric Concentration (ppt) | | | | | | | Emission (Gg/year) | | | | | |
|---|---|---|---|---|---|---|---|---|---|---|---|---|---|
| | Inflow (Pacific Ocean) | SoCAB | | | L.A. Area | Trinidad Head | | L.A. Area | SoCAB | | | Trinidad Head | |
| | Barletta et al. (2011) | Gentner et al. (2010) | Barletta et al. (2011) | Barletta et al. (2013) | Barletta et al. (2011) | Li et al. (2005) | Volmer at al. (2011) | Barletta et al. (2011) | Gentner et al. (2010) | Barletta et al. (2011) | Barletta et al. (2013) | Li et al. (2005) | Volmer et al. (2011) |
| CFC-11 | 245 | 275 | 259 | | 258 | 261 | | | 0.24 | | | 0.61 | |
| CFC-12 | 528 | | 541 | | 539 | 540 | | | | | | 1.82 | |
| CFC-113 | 76.3 | | 77.9 | | 78.1 | 99 | | | | | | 0.08 | |
| CFC-114 | 16.1 | | 16.3 | | 16.3 | | | | | | | | |
| HCFC-141b | 19.7 | 65 | 21.3 | 30.7 | 29.9 | | | | 0.18 | | 0.27 | | |
| HCFC-142b | 20.1 | | 95.9 | 22.9 | 59.4 | | | | | | 0.06 | | |
| HCFC-22 | 201 | | 107 | 310 | 276 | | | | | | 3.05 | | |
| HFC-134a | 45.9 | | 67.3 | 109 | 89.1 | | | 1.16-1.26 | | 1.29-2.12 | 1.89 | | |
| HFC-152a | 8.9 | | 61.1 | 91.2 | 42.5 | | | 0.72-0.82 | | 0.91-1.60 | 1.94 | | |
| HFC-245fa | | | | | | | 0.6-1 | | | | | | 6.1-6.77 |

A comparative summary of the data presented for the target gases in Section 1.2 is presented in Table 5. The summary includes physical and chemical properties of the gases as well as interactions between the gases and the environment and the effects of the gases on the atmosphere.

Table – 5 Summary of Characteristics of Target Gases

| Chemical | CFC-11 | HCFC-141b | HFC-134a | HFC-245fa |
|---|---|---|---|---|
| Volatility | Moderate | Low-Moderate | High | Moderate-High |
| Water Solubility | Low-Moderate | Moderate | Low | Low-Moderate |
| Toxicity (Toxicity to Humans) | Low | Low | Low | Low |
| Ecotoxicity (Toxicity to the Environment) | Low-Moderate | Low | Low | Low |
| Bioaccumulation | Moderate | Low-Moderate | Low | Low |
| Biodegradability | High | Moderate | Low | Low |
| ODP | High | Low-Moderate | None | None |
| GWP | Moderate-High | Low-Moderate | High | Moderate-High |
| Atmospheric Lifetime | Moderate-High | Low | Low-Moderate | Low |

## 1.3 Foam Basics

Foams, also known as cellular polymers or cellular plastics, have been used in refrigeration, building, automobile, and transportation industries including use as insulation, packaging, and cushioning (IPCC 2007). Foams are composed of both a solid and a gas phase. The solid phase consists of a polymer matrix and the gas phase consists of a blowing agent (Landrock 1995). The polymer matrix is filled with the blowing agent to form the foam product.

The polymers, defined as mixtures of compounds with repeating structural units, termed monomers, are formed through a process known as polymerization. Polymerization refers to the chemical reaction involved to form polymer chains from repeating monomers, thereby creating structured networks. The most common monomers used in foams include styrene and urethane that react through polymerization to form the polymers polystyrene and polyurethane (Landrock 1995).

The degree of structure formed during polymerization is categorized by crystallinity, which is a measure of packing order of monomers in the polymer structure (Throne 2001). The polymers are classified as amorphous, intermediate, and crystalline based on structure. Amorphous polymers tend to lack positional order on the molecular scale (no 3-D structure), whereas crystalline polymers are structured with regular 3-D packing arrays, with intermediate polymers having some degree of packing order. Crystalline polymers demonstrate a set temperature ($T_f$, true melting temperature) where the molecular arrangement breaks up and the polymer transitions from solid to liquid phase. Amorphous polymers do not exhibit specific melting temperatures and soften over a wide temperature range known as the glass transition range from $T_g$ to $T_f$, where $T_g$ is the glass transition temperature (Figure 2). Most flexible foams exhibit amorphous characteristics, in that they exhibit a defined glass transition phase, where

the extent of the transition phase (i.e. width of the transition temperature range) is controlled by the degree of structure (Landrock 1995). Rigid insulation foams, on the other hand, exhibit intermediate-crystalline characteristics, in that the glass transition phase is small (Landrock 1995).

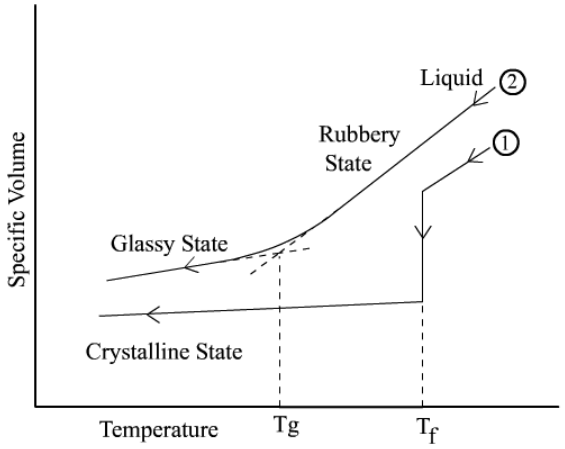


Figure 2. Melting Response of (1) Crystalline and (2) Amorphous Polymers (Landrock 1995)

Based on the differences in molecular order (i.e., crystallinity) and melting temperatures, foams are classified as either thermoset or thermoplastic. Thermoset foams consist of crosslinked polymers and demonstrate a high degree of crystallinity, whereas thermoplastic foams generally consist of amorphous, non crosslinked polymers with low degree of crystallinity (Throne 2001). Thermoset foams have specific melting temperatures, whereas thermoplastic foams melt over a wide temperature range demonstrating glass transition behavior (BSC 2007). Thermoset foams can be used in higher temperature applications and generally are more resistant to solvents and chemicals than thermoplastic foams (BSC 2007). Most refrigeration and building insulation foam applications involve the use of thermoset materials due to high resistance to physical changes such as the introduction of water or heat. For end of life management, thermoset foams generally cannot be readily reprocessed once the product is formed and thus are more difficult to recycle than thermoplastic foams (Sivertsen 2007). Thermoplastics can be broken down and recycled after use (Sivertsen 2007). Basic properties of thermoset foams render these materials more suitable for refrigeration and insulation applications, however, the basic molecular structure leading to the desirable performance characteristics also result in less recyclability than thermoplastic foams.

Manufacturing processes also lead to differences in stress-strain and density characteristics of foam products. Chemical composition, degree of crystallinity, and degree of crosslinking control stress-strain characteristics, where a high degree of crystallinity and crosslinking and high glass transition temperatures leads to rigid structures in foams (as compared to flexible foams) (Landrock 1995). In addition, rigid foams typically have closed-cell structures, whereas flexible foams are open celled, in

which the blowing agent is released during manufacturing (no bubbles or air pockets are formed). Rigid foams with closed cells are manufactured to retain the blowing agents and have improved thermal properties over flexible foams. Density of thermoplastic foams during manufacture can be varied for intended applications (i.e., high density for load bearing applications). Density of thermoset products typically varies over a narrow range (Throne 2001). High-density thermoplastic foams are used in permanent structure applications (most appliance/building insulation), while low-density foams are used in single use disposable products (some building insulation, mostly transportation insulation) (Throne 2001).

Foams are manufactured with blowing agents (also termed foaming agents) that influence structure and resulting thermal properties of foam materials (TEAP 2005). The blowing agent (BA) refers to the gas inserted into the polymer structure during manufacture. Two types of blowing agents are used including chemical and physical blowing agents (Throne 2001). Chemical foaming agents are pure chemicals inserted to the polymer foam structure that undergo chemical reactions to produce the blowing agents under a process known as heat induced decomposition (Throne 2001). The chemical blowing agents are prevalent in high-density foam materials and also may be used in conjunction with physical foaming agents for some low-density foam applications (Throne 2001). Physical blowing agents under pressure are inserted directly into the polymers without an accompanying chemical reaction. Physical blowing agents typically are used for low-density foam applications (Throne 2001). Insulation capability, cell control, solubility, viscosity, diffusion rate, exotherm control, and blowing efficiency of blowing agents affect manufacture and resulting long- and short-term properties of foams (UNEP 1996). Ideal blowing agents for insulation applications have a high molecular weight, low thermal conductivity (achieved through BA type and cell formation), as well as a low diffusion coefficient, limiting the amount of BA released over the service life of the material (Colvin 2001).

CFCs, HCFCs, and HFCs are common physical blowing agents used in the manufacture of foams. The chlorinated and fluorinated hydrocarbon BAs have higher insulation values (i.e. R-values) compared to non-halocarbon alternatives and lower diffusion rates than non-halocarbon alternatives (Dieckmann and Magid 1999). These combined effects lengthen the time the blowing agents are entrapped within the foam and thus result in longer lifetimes (UNEP 1996). In addition, physical blowing agents such as CFC-11 are more thermally efficient in that they require less thickness to insulate the same area as compared to other blowing agents such as carbon dioxide or air. Low solubility can be achieved with chlorinated and fluorinated hydrocarbon BAs to create a solid foam structure with improved thermal and mechanical properties of the foam material.

A general classification of polymer foams is provided in Figure 3 as a function of plasticity (thermoset/thermoplastic), stress-strain response (rigid/flexible), and density (high/low). The four main types of foam that are currently manufactured for use in building insulation and refrigeration applications include extruded polystyrene (XPS), expanded polystyrene (EPS), polyurethane (PUR), and polyisocyanurate (PIR) foams.

PIR foams are a special class of PUR based foams that exhibit high fire resistance (Schroer et al. 2011). The most common materials used in building insulation include low- and high-density rigid XPS panels (depending on intended roofing, flooring, or wall application) as well as rigid thermoset PUR/PIR panels, low density PUR spray insulation, PUR pipe in pipe sections, one component PUR foams (OCF), or PUR blocks (also known as slabstock) (TEAP 2005). The most common materials used in appliances (both commercial and domestic) include rigid PUR insulation foams that are poured in place during manufacturing (TEAP 2005). The majority of the foam materials used in the U.S. consist of PUR insulation (Throne 2001).

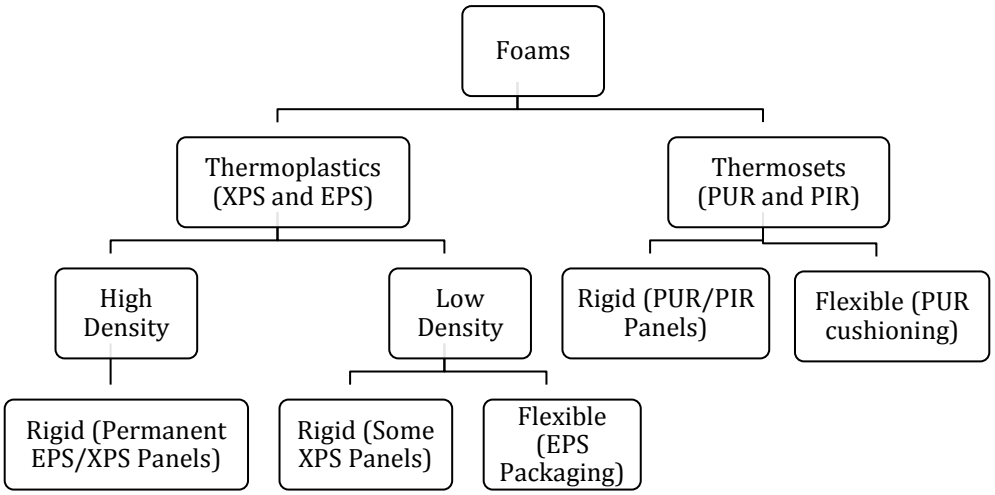


Figure 3. Classification of Foams (from Throne 2001)

Panel foams may have facers (gas and moisture barriers) placed on the outside surfaces. A foam facer can be either permeable or impermeable depending on the manufacturing process and the requirements for service use (BSC 2007). The permeability controls the amount of moisture intrusion, BA diffusion out, or air diffusion into the foam core. Rigid insulation boards with PUR/PIR materials are the most common materials that contain facers. Facer use is limited for XPS/EPS materials. Depending on the type of facer, the vertical diffusion of BA out of the foam and air into the foam becomes limited (Figure 4). However, the lateral diffusion of BA out of the foam core and air into the foam core material is not affected by the presence of the facer. Common facer types include aluminum foil facers, glass fiber reinforced cellulosic mats, and coated or uncoated polymer bonded glass-fiber mats. Facers are laminated (bonded or glued) or physically adhered to the foam core (NRCA 2006).

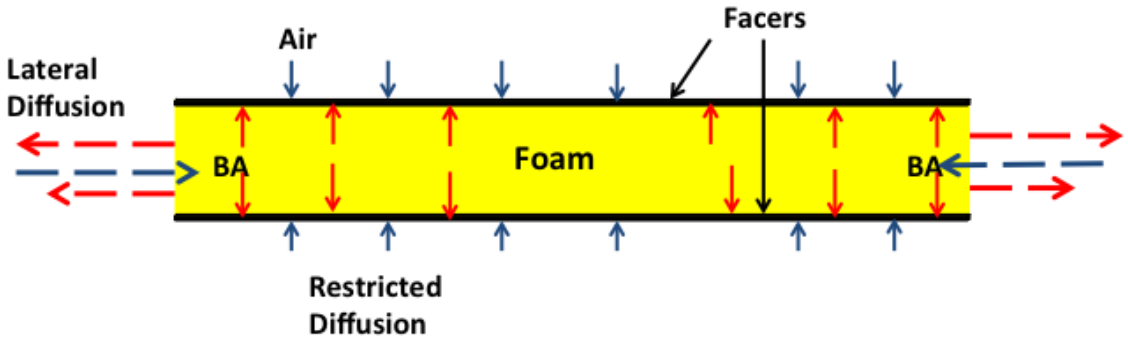


Figure 4. Facer for Closed Cell Insulation Foam
(adapted from Mukhopadhyaya and Kumaran 2008)

### 1.3.1 Foam Properties

Physical, chemical, and thermal properties of rigid foam influence the short and long term insulation performance, mechanical performance under loading, and relative short and long term release of respective blowing agents. Results of comprehensive investigations of physical and chemical properties of rigid PUR insulation foam obtained from end of life appliances are presented (Table 6). Density of the foam was determined to be consistent across manufacturers, ranging from 25 to 39 g/L in a laboratory experimental testing program (Scheutz and Kjeldsen 2003). This density range was similar to that measured by Fredenslund et al. (2005) and Scheutz et al. (2007b). These studies measured densities ranging between 24.8 to 30.4 g/L for 8 refrigerator foam panels obtained from different manufacturers. Foams blown with CFC-11 had higher cell gas content than foams blown with HFC-134a, which resulted in lower density.

Table 6 – Physical and Chemical Characteristics of four PUR Foam Refrigerator Insulation Panels (adapted from Scheutz and Kjeldsen 2003)

| Parameter | Unit | CFC-11 | HCFC-141b | HFC-134a | HFC-245fa |
|---|---|---|---|---|---|
| Density (foam) | g/L | 24.6 | 32.2 | 39 | 30.7 |
| Porosity (calculated) | | 0.985 | 0.978 | 0.972 | 0.98 |
| Porosity (measured) | | 0.964 | 0.919 | 0.929 | 0.933 |
| Total Content of $CO_2$ | g/L | 0.14 | 0.75 | 1.5 | 0.48 |
| | % w/w | 0.58 | 2.34 | 3.86 | 1.61 |
| Fraction of $CO_2$ | % w/w | 3.9 | 16.6 | 35 | 11.6 |
| Total Content of BA | g/L | 3.43 | 3.77 | 2.78 | 3.66 |
| | % w/w | 13.3 | 11.6 | 7 | 11.6 |
| Content of BA in Polymer | g/L | 1.01 | 1.05 | 0.63 | 0.91 |
| Fraction Sorbed in PUR | % | 29.5 | 27.8 | 22.7 | 24.8 |
| Distribution Coefficient *K* | $m^3$ gas / $m^3$ PUR | 24.6 | 16.5 | 10.1 | 14.9 |

The gas filled porosity was calculated using the density of solid PUR and the measured foam densities for each foam blown with a different BA. The equation used to calculate the gas filled porosity was (Scheutz and Kjeldsen 2003):

$$f_g = \frac{\rho_{foam} - \rho_{b,solidPUR}}{C_{BAO} - \rho_{b,solidPUR}} * MW_{BA} \quad (5)$$

where $f_g$ is the measured gas filled porosity (void volume fraction of the foam) in the material), $\rho_{foam}$ is the measured foam density (g/L), $\rho_{b,solidPUR}$ is the density of solid PUR (1240 g/L), $C_{BAO}$ is the concentration of BA in the void space (g/L, 1 atm and 25°C), and $MW_{BA}$ is the molecular weight (g/mol). The calculated porosities were compared to porosities measured using a compression test (Scheutz and Kjeldsen 2003). The gas filled porosities calculated were similar to the measured porosities, and indicative of a highly porous material (Table 6).

Since the PUR foam manufacturing process produces carbon dioxide, $CO_2$ is always considered a co-blowing agent along with the inserted chlorinated and fluorinated hydrocarbon gas blowing agent (Scheutz and Kjeldsen 2003). Analysis of carbon dioxide content in the PUR foam samples by Scheutz and Kjeldsen (2003) indicated a range in concentration of 0.14 to 1.5 g/L. Carbon dioxide diffuses out of the foam more rapidly than the hydrocarbon blowing agents due to its higher diffusion coefficient. Carbon dioxide concentrations in PUR foams vary due to conditions during foam processing, blowing agent used, gas partial pressures, temperatures, and the presence of diffusion barriers such as bonded or adhered facers (Scheutz and Kjeldsen 2003).

The total BA content in foams varied between 7 and 13% as a function of the gas used (Table 6). The PUR and PIR foam manufacturing process solubilizes the BA in the foam. During the heating process throughout manufacturing, BA enters the polymer matrix to reduce the cell gas pressure, preventing the foam from exploding (Scheutz and Kjeldsen 2003). The amount of BA that enters the polymer matrix of the foam depends on the solubility of the BA in the foam itself. Using a compression process, Scheutz and Kjeldsen (2003) determined that the amount of BA dissolved in the PUR foam refrigeration panels varied between 23 and 30% of the total BA content. The amount solubilized varied between blowing agents (Table 6). Foams with CFC-11 had the highest sorbed fraction, whereas foams with HFC-134a contained the lowest sorbed fraction.

The BA content in foam was further described on a volumetric basis using a distribution coefficient (*K*). The distribution coefficient, *K*, was defined as the volume of gas in the foam product divided by the volume of foam ($m^3$ blowing agent per $m^3$ of foam) by Scheutz and Kjeldsen (2003). The distribution coefficient was calculated as:

$$K = \frac{f_g M_f}{(1-f_g)(M_s - M_f)} \quad (6)$$

where, $f_g$ was the gas filled porosity (void volume fraction of the foam material), $M_f$ was the content of blowing agent in the compressed foam (g), and $M_s$ was the content of BA in the uncompressed foam (g). CFC-11 had the highest distribution coefficient, indicating more gas sorbed in the foam material with the CFC-11 than the foams containing other BAs. The distribution coefficient is an important characteristic to estimate environmental impact during use, and ultimately during end of life decommissioning of foam products containing the CFC-11, HCFC-141b, HFC-134a, and HFC-245fa blowing agents.

Physical and thermal properties of various building insulation foams are provided in Table 7. The physical, chemical, and thermal properties of foam influence the overall lifetime of a given product such as a refrigerator or freezer or structural component such as an insulated wall panel. The lifetime of products and structures affects the amount of foam waste generated. In addition, the thermal properties of a foam insulation material at end of life directly correspond to the amount of blowing agent still entrapped in the foam, where foam materials susceptible to aging have low BA at end of life. Therefore, knowledge of physical and thermal properties provides for establishing a better framework of the blowing agent content at end of life for various foam materials and material configurations and attributes. The properties in Table 7 are presented as a function of blowing agent/facer used. The thermal insulation value (R) refers to how much heat can be retained by the insulation product used. R is calculated as the quotient of the thickness of the foam material and the thermal conductivity of the foam. A higher R-value and a lower thermal conductivity value (k-value) are indicative of a better insulating material.

Densities for the foam insulation products ranged from 15 to 65 g/L (Table 7). In general, density of rigid building insulation PUR and PIR foam was between 30 and 45 g/L, with values up to 100 g/L reported for some roofing applications where strength performance was required (BING 2006). For XPS foam panels, densities were approximately between 25 and 65 g/L, whereas EPS panel densities were between 15 and 30 g/L.

The initial thermal properties are important for assessing the insulating performance of the material over time. The initial (i.e., prior to use) measured thermal properties of XPS did not vary significantly between blowing agents, whereas variation was present in the initial thermal properties of PUR between blowing agent and manufacturer (Table 7). EPS had a small range in insulation values with resistance (R-values) between 0.8 and 1.35 $m^2K/mW$ and exhibited relatively high thermal conductivity (up to 45 mW/mK) (Desjarlais and Tye 1987, Yu et al. 1995, Yucel et al. 1995, Strzepek 1990, and Mihlanyanlar et al. 2007). The initial thermal conductivity values of EPS foam generally were higher than those for PUR/PIR and XPS foams, signifying inferior initial insulation performance. PUR/PIR foam materials blown with CFC-11 had the largest R-value and low thermal conductivity (as low as 17 mW/mK) (Strzepek 1990, McElroy et al. 1991, Harvey 2007, Wilkes et al. 2008). In general, PUR solid foam (i.e., panels) had better initial insulation properties than the PUR spray foam. Results also are provided for less common foam materials, phenolic and polyolefin foams (Table 7).

Phenolic foams demonstrated relatively low initial insulation values. Polyolefin foams had high initial thermal conductivities. The presence of a facer and facer type also affected the initial thermal conductivities of PUR/PIR foams, where less permeable facers had lower conductivities (better insulation properties) (Desjarlais and Tye 1987, Strzepek 1990, and Muñoz et al. 2009).

Further investigation of the thermal properties of foams requires an analysis of the foam aging characteristics over time. Foam aging refers to how well a foam material will maintain its initial R-value over time. The physical and chemical properties of a foam such as cell size, initial BA content, composition of the cell gas (presence of carbon dioxide), diffusion rate are just some of the factors governing the reduction in heat trapping capabilities of a given foam material over time (Schroer et al. 2011). Additional factors include the thickness of foam material used as well as the exposure of the foam to varying extreme temperature ranges, moisture, or chemical environments that cause corrosion. Other parameters affecting foam aging include the density of the foam material, the manufacturing process, and the permeability of the surfaces (presence of foam facers) (Mukhopadhyaya and Kumaran 2008). The aging process is generally rapid after manufacturing (due to diffusion of air into the foam matrix) and during first year of service, slowing down with time, and ultimately reaching a state of very slow (almost negligible), closed cell diffusion of the blowing agent out of the foam (Mukhopadhyaya and Kumaran 2008).

In general, thermal resistance characteristics of EPS were more stable over time (based on average increases in thermal conductivity) than the characteristics of PUR/PIR and XPS materials (Table 7). Similarly, phenolic foams were observed to retain their insulating properties for a longer period as compared to PUR/PIR and XPS materials (Desjarlais and Tye 1987, Strzepek 1990, Schroer et al. 2011). The aging of XPS foam over a period of 50 years for various blowing agents was modeled using field and laboratory data collected by Vo and Paquet (2004). Vo and Paquet (2004) determined that the aging of XPS foam was a factor of blowing agent used and the thickness of the insulation panel. XPS foams manufactured with CFC-12, HCFC-142b or HFC-134a had high retention over 50 years due to slow diffusion rates of less than 1% per year, while thicker materials (regardless of BA), retained their insulating capabilities for longer periods than thinner materials.

Table 7 – Physical and Thermal Properties of Foams

| Foam Type | Reference | Density (g/L) | Blowing Agent / Facer Used | Initial Thermal Conductivity (mW/mK) | Initial R-Value ($m^2K/W$) | Long Term Thermal Conductivity (mW/mK) | Long Term R-Value ($m^2K/W$) | (%) R-value Lost between Initial and Long Term |
|---|---|---|---|---|---|---|---|---|
| PUR Spray Foam | Harvey 2007 | - | Water and $CO_2$ | N/A | N/A | 35 | N/A[1] | - |
| | | | HCFC-141b | N/A | N/A | 29 | N/A[1] | - |
| | | | HFC-365mfc | N/A | N/A | 30 | N/A[1] | - |
| | Bomberg and Kumaran (1990) | - | CFC-11 | 16 | 1.64 | 23.1 | 1.1 | 33% |
| | | | HCFC-141b | 18 | 1.43 | 24.6 | 1.03 | 28% |
| PUR/PIR Solid Panel | Harvey (2007) | - | Pentane | N/A | N/A | 24 | N/A[1] | - |
| | | | HFC-365mfc | N/A | N/A | 22 | N/A[1] | - |
| | | | HCFC-141b | N/A | N/A | 21 | N/A[1] | - |
| | Schroer et al. (2011) | 30 | Pentane | N/A | N/A | 23 | 1.1 | - |
| | Muñoz et al. (2009) | 27.2-114 | $CO_2$ | 29.1 | N/A[1] | N/A | N/A | - |
| | | 28.8-49.2 | Pentane | 29.5 | N/A[1] | N/A | N/A | - |
| | | 28.9-40 | Pentane / Foil faced | 28.7 | N/A[1] | N/A | N/A | - |
| | Yu et al. (1995) | - | CFC-11 | 17-21 | 2.4-2.9 | N/A | N/A | - |
| | | - | CFC-11 + $CO_2$ | 22-28 | 1.8-2.3 | N/A | N/A | - |
| | | - | $CO_2$ | 27-33 | 1.5-1.9 | N/A | N/A | - |
| | | - | HCFC-22 | 23-29 | 1.7-2.2 | N/A | N/A | - |
| | | - | HCFC-141b | 20-24 | 2.1-2.5 | N/A | N/A | - |
| | | - | HFC-134a | 24-26 | 1.9-2.1 | N/A | N/A | - |
| | | - | Pentane | 23-29 | 1.7-2.2 | N/A | N/A | - |
| | | - | CFC-12 | 25-35 | 1.43-2 | N/A | N/A | - |
| | Strzepek (1990) | 27-48 | CFC-11 / Low permeance facer | 18-22 | 1.18-1.35 | 20 | 1.27 | 6 |
| | | 27-48 | CFC-11 / High permeance facer | 18-32 | 0.985-1.35 | 24 | 1.04 | 23 |
| | Modesti et al. (2005) | 33-36 | HCFC-141b | 22.6 | N/A[1] | 30 | N/A[1] | 25 |
| | | 34-36 | HFC-134a | 26.5 | N/A[1] | 33.3 | N/A[1] | 20 |
| | | 34-36 | HFC-245fa | 26 | N/A[1] | 34 | N/A[1] | 24 |
| | Desjarlais and Tye (1987) | 37-43 | CFC-11 / Glass Faced | 21 | 1.80 | 28 | 1.37 | 24 |

| | | | | | | | | |
|---|---|---|---|---|---|---|---|---|
| | | 30 | CFC-11 / Foil Faced | 19 | 2.02 | 27 | 1.41 | 30 |
| | McElroy et al. (1991) | - | CFC-11 | 17.5 | 2.20 | 22.4 | 1.70 | 23 |
| | | | HCFC-141b | 19.1 | 1.90 | 25.4 | 1.50 | 21 |
| | | | CFC-11 | 18.2 | 2.10 | 24.5 | 1.55 | 26 |
| | | | HCFC-141b | 21 | 1.81 | 27.2 | 1.40 | 23 |
| | Wilkes et al. (2008)[2] | - | HCFC-141b | 19.2 | 0.53 | 26 | 0.39 | 26 |
| | | | HFC-134a | 23.1 | 0.44 | 30 | 0.34 | 23 |
| | | | HFC-245fa | 20 | 0.51 | 25.4 | 0.40 | 22 |
| | BING (2006) | - | Pentane | 22 | N/A[1] | 26 | N/A[1] | 15 |
| | | | | 22.7 | N/A[1] | 26.3 | N/A[1] | 14 |
| XPS Solid Panel | Harvey 2007[5] | 32 | CFC-12 | 22 | 2.27[4] | 29 | 1.72[4] | 24 |
| | | | HCFC-142b | 22 | 2.27[4] | 30 | 1.7[4] | 25 |
| | | | HCFC-142b[3] | 27 | 1.73[4] | 27.8 | 3.6[4] | 3 |
| | | | HFC-134a | 22 | 2.27[4] | 32.3 | 1.55[4] | 32 |
| | | | HFC-152a | 24 | 2.08[4] | 34 | 1.5[4] | 28 |
| | | | HCFC-22 | 24 | 2.08[4] | 34 | 1.5[4] | 28 |
| | | | $CO_2$ | 24 | 2.08[4] | 34 | 1.5[4] | 28 |
| | Schroer et al. (2011) | 25 | HFC-134a | N/A | N/A | 27 | 0.93 | - |
| | Muñoz et al. (2009) | 31-50.8 | $CO_2$ | 34 | N/A[1] | N/A | N/A | - |
| | Yu et al. (1995) | - | CFC-12 and $CO_2$ | 25-35 | 1.43-2 | N/A | N/A | - |
| | | - | HCFC-22 | 25-35 | 1.43-2 | N/A | N/A | - |
| | | - | HCFC-142b | 25-35 | 1.43-2 | N/A | N/A | - |
| | | - | Air | 33-41 | 1.2-1.5 | N/A | N/A | - |
| | Strzepek (1990) | 22-64 | N/A | 26 | 0.985-1.26 | 29 | 0.88 | 30 |
| | Desjarlais and Tye (1987) | 35 | CFC-12 | 27 | 1.43 | 28.4 | 1.34 | 6.3 |
| EPS Solid Panel | Mihlanyanlar et al. (2007) | 15 | Air | 39 | N/A[1] | N/A | N/A | - |
| | | 20 | | 33 | N/A[1] | N/A | N/A | - |
| | | 25 | | 36 | N/A[1] | N/A | N/A | - |
| | | 30 | | 35 | N/A[1] | N/A | N/A | - |
| | Yu et al. (1995) | - | Air | 37-45 | 1.11-1.35 | N/A | N/A | - |
| | Yucel et al. (1995) | 15 | Air | 36-38 | N/A | 46 | N/A | - |

| | | | | | | | | |
|---|---|---|---|---|---|---|---|---|
| | | 20 | | 34-36 | N/A | 39 | N/A | - |
| | | 28 | | 31-33 | N/A | 37 | N/A | - |
| | Strzepek (1990) | 16-32 | N/A | 33-29 | 0.77-0.88 | 33-29 | 0.77-0.88 | 0 |
| | Desjarlais and Tye (1987) | 25 | N/A | 37 | 1.02 | 39 | 0.9856 | 3.4 |
| Phenolic Solid Panel | Muñoz et al. (2009) | 19.2-45 | N/A | 28.7 | N/A | N/A | N/A | - |
| | Schroer et al. (2011) | 27 | Hydrocarbons | N/A | N/A | 21.14 | 1.84 | - |
| | | 37 | | N/A | N/A | 19 | 2.40 | - |
| | Strzepek (1990) | 32-48 | Closed Celled | 17 | 1.53 | 16.97 | 1.49 | 3 |
| | | | Open Celled | 29 | 0.88 | 29 | 0.88 | 0 |
| | Desjarlais and Tye (1987) | 58 | Closed Cell | 17 | 2.23 | 18 | 2.11 | 5 |
| Polyolefin Insulation Material (PO) | Yu et al. (1995) | - | Air | 36-38 | 1.3-1.4 | N/A | N/A | - |

[1] Panel thickness was not provided to calculate R-values
[2] For appliance insulation panels only
[3] Harvey (2007) study summarizing Vo and Paquet (2004) results
[4] Calculated R-values using a given panel thickness of 50 mm in the Harvey (2007) study
[5] Thickness of 100 mm instead of 50 mm
[N/A] Not applicable to the study
[-] Omitted by the Study

A summary comparison of relative physical, chemical, and thermal properties of foam insulation materials is provided in Table 8 based on information compiled from various sources (Desjarlais and Tye 1987, Strzepek 1990, McElroy et al. 1991, Burns et al. 1998, Vo and Paquet 2004, Modesti et al. 2005, BING 2006, Wilkes et al. 2008, Schroer et al. 2011). These properties are signficant to review for predicting BA release and content during end of life management (particularly in the landfill environment). The properties compared qualitatively in Table 8 include the initial thermal conductivity (up to one year in service), thermal conductivity after five years in service (as an indication of resistance to aging), moisture resistance (including both short and long term studies/retention of R-value over time), dimensional stability, corrosion resistance, and fire safety. Differences in thermal properties were observed when PUR/PIR foam products had either laminated or bonded facers. Facers improved the rated long-term thermal resistance, moisture resistance, dimensional stability, corrosion resistance, and fire safety performances of PUR/PIR foams. The initial thermal conductivities of PUR and PIR foams with facers were higher than those for XPS and EPS foams. Dimensional stability and corrosion resistance were better for XPS and EPS than PUR and PIR. Aging was less effective on PIR and PUR than XPS and EPS. Therefore, PIR and PUR products, depending on conditions during use, may have higher solubilized or gaseous blowing agents at end of life than other foam types. Also, facers can significantly encapsulate BAs at end of life if not shredded prior to entry into a landfill.

Table 8 – Summary of Physical and Thermal Properties of Building Foam Insulation Materials

| Property | PUR Spray | PUR Panel | | PIR Panel | | XPS Panel | EPS Panel | Phenolic Panel |
|---|---|---|---|---|---|---|---|---|
| | | Facer | No-Facer | Facer | No-Facer | | | |
| Initial Thermal Conductivity[1] | Moderate-High | High | Moderate-High | Moderate | High | Moderate-High | Moderate-High | High |
| Thermal Conductivity after Aging[2] | Moderate | Moderate-High | Moderate | High | High | Moderate | Moderate | High |
| Moisture Resistance[3] | N/A | Moderate-High | Moderate | Moderate-High | Moderate-High | High | Moderate | Low |
| Dimensional Stability | N/A | Moderate-High | Moderate | High | Moderate-High | High | Moderate | High |
| Corrosion Resistance | N/A | High | Moderate-High | High | High | High | Moderate-High | Low |
| Fire Safety | N/A | Moderate-High | Moderate | Moderate-High | High | Moderate-High | Moderate-High | High |

[1]Based on initial thermal conductivity values as stated by the manufacturer
[2]Based on thermal conductivity values after 5-years of use
[3]Including resistance to humidity, long term and short term moisture resistance testing

Mechanical properties of foams influence material behavior under applied stresses. Short-term compaction stresses during waste placement and long-term compression stresses from overlying wastes may lead to excessive deformation and failure of foam structure in a landfill environment at end of life. Foams also are subjected to mechanical stresses during decommissioning (at end of life) and landfilling. Emissions of foam blowing agents are directly influenced by the integrity of the foam structure. Data were compiled on compressive and tensile stress-strain response of foams. The stress-strain response in compression includes an initial generally linear elastic region followed by yielding and a stress plateau with limited change in stress with increasing strain, and finally foam crushing/structure failure with increasing stress with strain. The exact shape of the three regions on the stress-strain response is a function of foam type (Figure 5). While an initial linear elastic region is present in tension, the response of the materials vary as a function of foam type from linear elastic, to elasto-plastic, to elastic-brittle (Figure 6). A summary of mechanical property data from multiple studies is presented in Table 9.

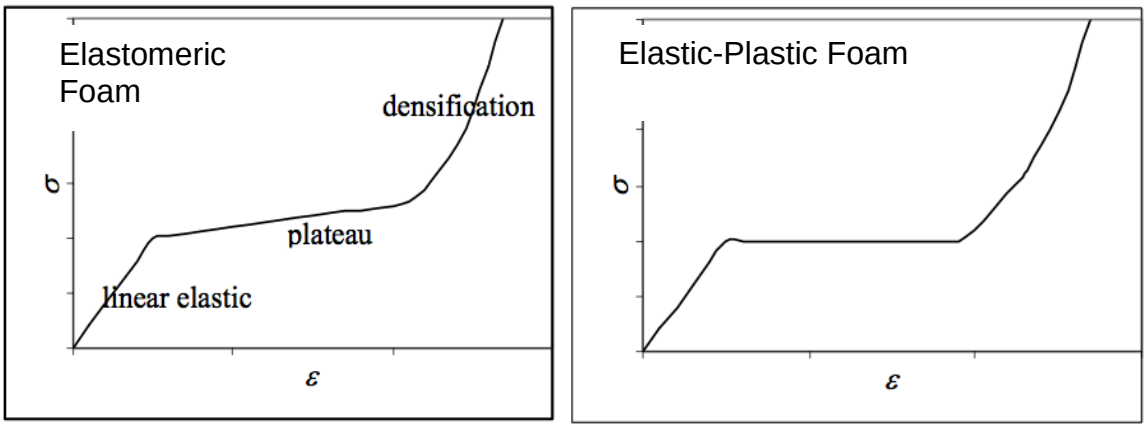


a. Flexible Foams

b. Flexible Foams

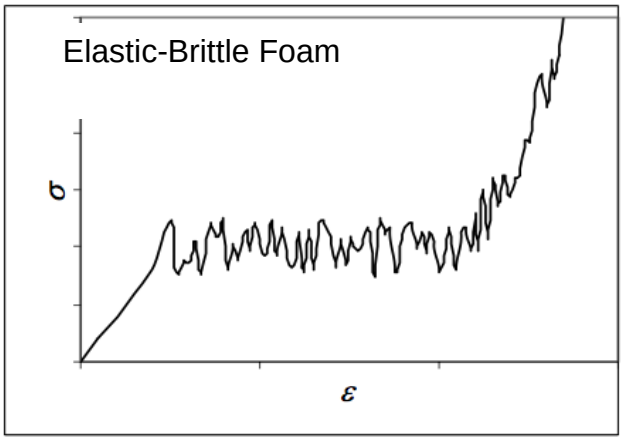


c. Rigid Foams

Figure 5. Stress-Strain Characteristics in Compression (from Ridha 2007)

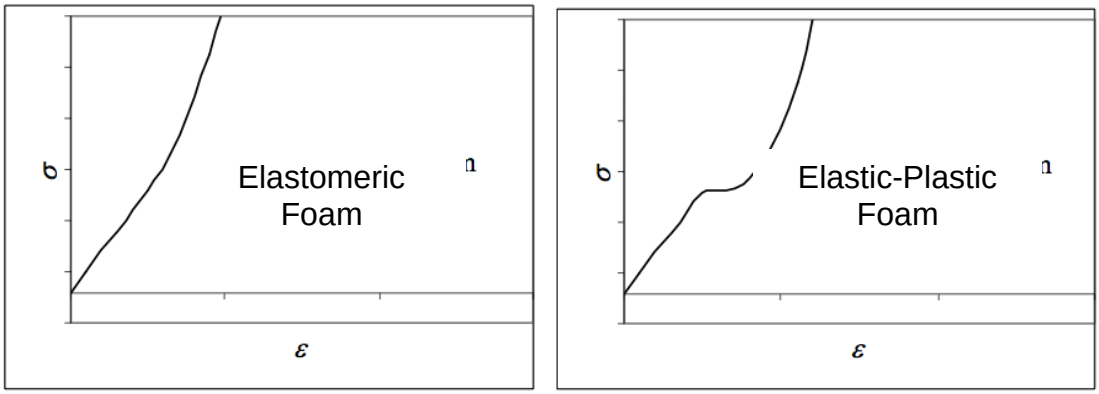


a. Flexible Foams b. Flexible Foams

c. Rigid Foams

Figure 6. Stress-Strain Characteristics in Tension (Ridha 2007)

For all foam materials, compressive strength, tensile strength, and tensile/compressive modulus were relatively similar at similar density as presented in Table 9. The strength and modulus generally increased with increasing foam density. Higher variation was observed in compressive and tensile strength/modulus between studies for EPS foams than PUR/PIR foams. The mechanical properties of the materials also were relatively similar for different types of blowing agents for all foam materials. A decrease in temperature improved the mechanical properties of PUR/PIR and XPS foams (except tensile strength), particularly for higher density foams (Strzepek 1990). This increase in mechanical response resulted from the stiffening of the polymers in the foam with decreasing temperatures causing the improved mechanical properties (Burns et al. 1998). Furthermore, all foams were determined to be anisotropic materials with generally the highest strengths and moduli in the foam rise direction (Strzepek 1990, Gaddy et al. 2005).

Compressive strengths were higher and compressive moduli were lower for PUR/PIR foams after exposure to simulated field-testing conditions (49 weeks of aging at ambient temperature/relative humidity) compared to new (unexposed) foams (Gaddy

et al. 2005). For used PUR/PIR foams, the mechanical properties were better (i.e., higher strength and higher modulus) for foams with adhered (laminated) facers than attached (glued or bonded) facers (Gaddy et al. 2005). For manufacture of PUR/PIR foam, the short-term compressive strengths are targeted to be 100 kPa. Creep strains are designed to be limited to a maximum of 2% over service life of 20 to 50 years at a load level of 40 kPa. Creep testing was conducted by Yourd (1996) for appliance insulation foams. PUR foams were loaded to 70-75% of compressive strengths (i.e., 40 to 100 kPa). Tests were terminated when strain reached 5% level. Differences were observed between BAs, where the duration associated with reaching the 5% strain level was longer for foams with CFC-11 than HCFC-141b. HCFC-141b was more soluble in the polymer matrix, which resulted in the weakening of the foam structure. For PUR/PIR foams, the maximum design tensile strength and shear strength were reported to be between 40 and 900 kPa (depending on density) and 120 and 450 kPa (depending on density), respectively. The flexural and maximum yielding strength of most PUR/PIR foams were between 250 and 1300 kPa depending on the density of the panel used (BING 2006). Table 10 provides a qualitative assessment of mechanical properties for foams. In general, XPS foams have the highest strengths and moduli followed by EPS, PUR/PIR, and Phenolic foam materials (Table 10).

Table 9 – Mechanical Properties of Foams

| Foam Material | Reference | Measured Thickness (mm) | Blowing Agent | Density ($kg/m^3$) | Compressive Strength (kPa) | Compressive Modulus (kPa) | Tensile Strength (kPa) | Tensile Modulus (kPa) | Flexural Strength (KPa) | Shear Strength ⊥ Rise (kPa) |
|---|---|---|---|---|---|---|---|---|---|---|
| PUR/ PIR | Gaddy et al. (2005)[1] | 25 | CFC-11 | 30[4] | 188 | 1188 | 204 | 1466 | - | - |
| | | | | 30[5] | 201 | 773 | 223 | 1485 | - | - |
| | | | | 30[6] | 217 | 711 | 187 | 1302 | - | - |
| | | 25 | HCFC-141b | 29.7[4] | 152 | 1269 | 239 | 1343 | - | - |
| | | | | 29.7[5] | 194 | 786 | 257 | 1379 | - | - |
| | | | | 29.7[6] | 181 | 740 | 152 | 1258 | - | - |
| | Shroer et al. (2011) | 25 | Hydrocarbons | 30[4] | 150 | N/A | N/A | N/A | - | - |
| | Dvorchak et al. (1985) | 50.8 | CFC-11 | 30.3[4] | 169 | 2620 | 24.8 | N/A | - | - |
| | Delgado et al. (2005) | N/A | HCFC-141b | 34-63[4] | 110-140 | - | - | - | 170-275 | - |
| | Strzepek (1990)[2] | N/A | CFC-11 | 32[4] | 172-241 | 6210 | 310 | 11040 | 345 | 138 |
| | | | | 96[4] | 690 | 17940 | 966 | 2600 | 1449 | 690 |
| | Strzepek (1990)[3] | N/A | CFC-11 | 32[4] | 276-345 | 13800 | 172 | 20700 | - | 138 |
| | | | | 96[4] | 1311 | 72450 | 1380 | 69000 | - | 1207 |
| | Colvin (2001) | N/A | HCFC-141b | 36.6[4] | 204 | 5100 | 355 | N/A | - | - |
| | | N/A | HFC-245fa | 38.2[4] | 244 | 5200 | 322 | N/A | - | - |
| | Dvorchak et al. (1985) | 50.8 | CFC-11 | 25.8[4] | 141 | 3606 | 256 | N/A | - | - |
| XPS | Shroer et al. (2011) | 25 | HFC-134a | 25[4] | 180 | N/A | N/A | N/A | - | - |
| | Strzepek (1990)[2] | N/A | CFC-12 | 22.4[4] | 103-172 | - | 172 | - | 276-483 | - |
| | | | | 32[4] | 172-345 | 8790 | 345 | 22080 | 345-690 | 241 |
| | | | | 64[4] | 793-862 | 20700 | 862 | 32430 | 690-966 | 483 |
| | Strzepek (1990)[3] | N/A | CFC-12 | 32[4] | 310-448 | 17250 | 172 | 28980 | - | 207 |
| EPS | Dvorchak et al. (1985) | 50.8 | Air | 15[4] | 78 | 2,089 | 58 | N/A | - | - |
| | Yucel et al. | N/A | Air | 15-28[4] | 70-260[1] | 160-3,100 | 150-520 | - | 160-500 | - |

| | | | | | | | | | | |
|---|---|---|---|---|---|---|---|---|---|---|
| | (2005) | | | | | | | | | |
| | Mihlayanlar et al. (2007) | 150 | Air | 15-40[4] | 82-287[1] | - | - | - | 139-405 | - |
| | | 50 | | 15-40[4] | 81-283[1] | - | - | - | 139-405 | - |
| | Delgado et al. (2005) | N/A | Air | 15[4] | 70-210 | - | - | - | 170-350 | - |
| | Strzepek (1990)[2] | N/A | Air | 16[4] | 69-97 | 1379 | 124 | 1380 | 172-207 | 138 |
| | | | | 32[4] | 172-227 | 3447 | 172 | 3450 | 345-517 | 241 |
| Phenolic | Shroer et al. (2011) | 20 mm | Hydrocarbons | 27.5[4] | 160 | N/A | N/A | N/A | - | - |
| | | 23 mm | Hydrocarbons | 37.5[4] | 170 | | | | - | - |
| | Dvorchak et al. (1985) | 50.8 mm | Hydrocarbons | 47[4] | 197 | 8904 | 71 | N/A | - | - |
| | Strzepek (1990)[2] | N/A | N/A | 32-48[4] | 69-241 | 6900 | 138 | 1380 | 172.5 | 83 |

[1]PIR materials only
[2]Measured at 24°C
[3]Measured at 75°K (-198°C)
[4]Foam panel/boardstock was measured under new (unexposed) conditions
[5]Foam panel/boardstock with facer was measured under exposed conditions (laboratory and field testing)
[6]Foam panel/boardstock with facer was measured under exposed conditions (laboratory and field testing)
[N/A] Not applicable to the study
[-] Omitted by the Study

Table 10 – Comparative Summary of Mechanical Properties of Foams

| Mechanical Property | PUR and PIR | XPS | EPS | Phenolic |
|---|---|---|---|---|
| Compressive Strength | Moderate-High | High | Moderate | Low-Moderate |
| Compressive Modulus | Moderate-High | Low-Moderate | High | Moderate |
| Flexural (Bending) Strength | Moderate | High | Moderate-High | Low-Moderate |
| Shear Strength | Moderate | Moderate-High | Moderate-High | Low-Moderate |
| Tensile Strength | Moderate-High | High | Moderate | Low-Moderate |
| Tensile Modulus | Moderate | Low-Moderate | Moderate-High | High |
| Overall | Moderate | Moderate-High | Moderate-High | Low |

### 1.3.2 Foam Applications

Foam applications include the use of either closed cell (rigid foams) or open cell (flexible foams). Rigid foams are used in thermal insulation of appliances (refrigeration), structures (buildings), and transportation units. Appliance foam uses include insulation of domestic refrigeration/freezers, water heaters, commercial refrigerators and freezers, and vending machines. Construction rigid foam uses consist of insulation based roof boards, lining boards, pipe sections, cold store panels, and spray systems. Transportation foam insulation applications include sandwich panels used for Reefer boxes and transport refrigerated units-TRUs (UNEP 1996). In addition, rigid foams are used in structural integrity and buoyancy applications in the marine industry, as well as for non-structural cold stores (commercial or industrial type walk in freezers) (IPCC 2007). Flexible foams typically are used for packaging, transport, cushioning, and impact management purposes (IPCC 2007). Foams used in insulation applications for construction are composed of PUR/PIR, XPS, EPS, and Polyolefin foams. Appliance applications only incorporate the use of PUR foam materials. Transportation applications for insulation typically are limited to PUR and EPS foam materials.

Total rigid insulation foam consumption in California was estimated to be 3.5 million $m^3$/year (Caleb 2011). Variability in foam consumption with time or annual trends in foam consumption/manufacturing were not presented by Caleb (2011). Such data were not readily accessible in the literature. Foam consumption by application for new foam was predominantly for construction of new buildings or refurbishment applications of existing building stock (up to 61%). Appliance foam was the next highest category for insulation foams at 36% of the total consumption, followed by marine, TRU, and cold store applications (Figure 7).

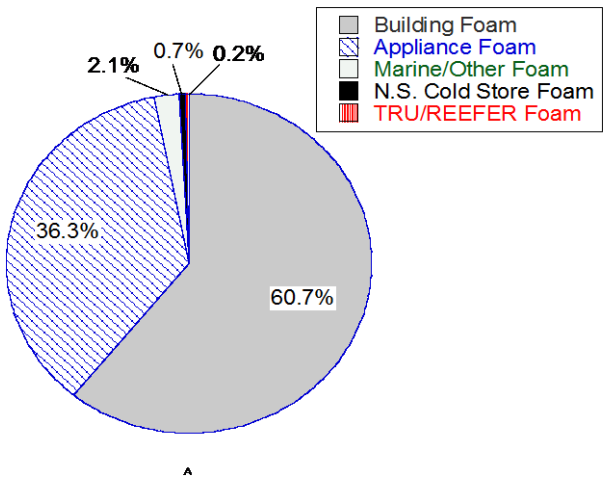


Figure 7. Foam Consumption in California by Application (from Caleb 2011)

Consumption trends for California by foam material also were presented (Caleb 2011). Approximately 55%, 29%, 10%, and 6% of California's consumption of building insulation consisted of PIR, XPS, PUR spray, and PUR panel products, respectively

(Figure 8). Assuming that appliance foam, marine, and TRU/Reefer foam is strictly PUR, total foam consumption can be estimated to include PIR, PUR, and XPS foam (EPS was not included by Caleb (2011)). Almost half of the rigid foam insulation consumption was estimated to be PUR based (49%), followed by PIR (33%), and XPS (18%) (Figure 9). This result is consistent with the U.S. insulation market (Figure 10), where 42% of the foam consumption was PUR based, followed by equal amounts of PIR and XPS (16%), with additional amounts associated with urea-formaldehyde (16%), and EPS (10%). Future growth for foam consumption in California was assumed to include a significant increase in PIR foam (10%/year) (Singh et al. 2005). Therefore, PUR/PIR insulation foams make up a significant portion of the current and future rigid insulation foam market in California, as compared to polystyrene foams.

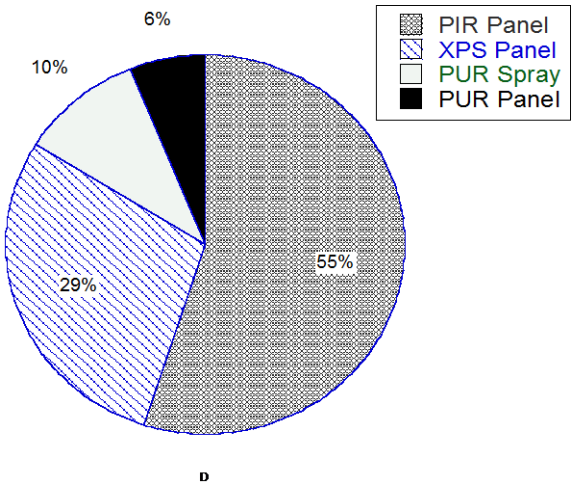


Figure 8. Building Foam Consumption in California (Caleb 2011)

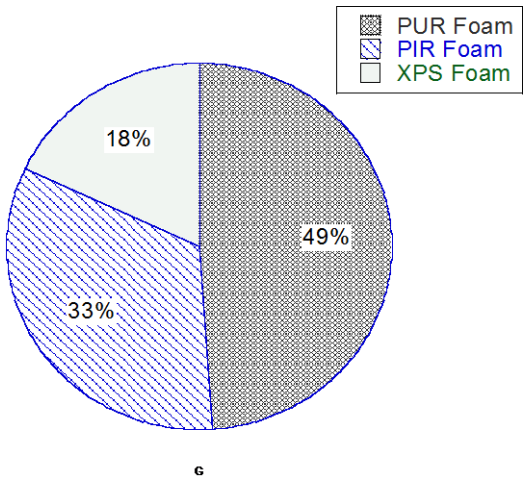


Figure 9. Estimated California Consumption of Rigid Foam Insulation (adapted from Caleb 2011)

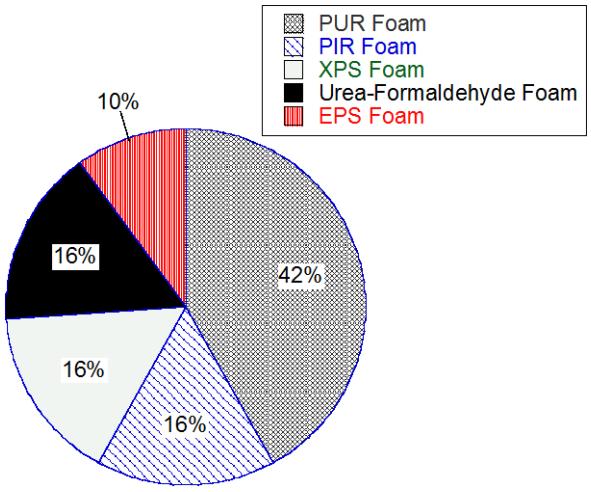


Figure 10. Foam Insulation Consumption in U.S. (adapted from Throne 2001)

### 1.3.3 Emissions of Blowing Agents from Foams

Emissions of blowing agents from foams may occur during three distinct phases: i) foam production and installation (regarded as first year losses), ii) losses from installed foam during service, and iii) losses during decommissioning at end of life of a foam product (TEAP 2002, Godwin et al. 2003, TEAP 2005). The emissions before end of life (manufacturing through use) vary as a function of the application: building insulation, appliance insulation, as well as packaging, cushioning, and transportation insulation (Table 11). The data in Table 11 were generated from a collaboration of the Task Force on Collection, Recovery, and Long Term Storage and the United Nations Foam Technical Options Committee as a compilation of emissions research conducted by the Japan Technical Center for Construction Materials, the Danish Technical University, and the American Alliance of Home Appliance Manufacturers. As such, these are averaged, often predicted values for different regions, are subject to variation due to different experiments/models, and are still developing as a work in progress (Caleb 2004). Results from the studies conducted by Danish Technical University (Scheutz and Kjeldsen 2003, Scheutz et al. 2003a, Fredenslund et al. 2005), in particular, were observed to conflict with the data presented in Table 11. However, these emissions data are significant, as they have been used extensively in Caleb (2011) in development of foam banks/emissions profiles for California.

For building insulation applications, significant variations were observed between application type and between foam materials used in a given application for first year release, time to total release, and total remaining at decommissioning (Table 11). The release rates subsequent to first year did not vary significantly between applications. The lowest first year releases were observed for appliance insulation (on the order of 5%), whereas highly variable and high magnitude (5 up to 100%) losses were reported for building insulation. Time to total release was highest for appliance foams (beyond service lifetime) indicating significant amount of banked BAs at end of life. PUR had significant BA banks with more than half of the initial BA amount remaining at end of life (Table 11).

Table 11 – Stages of BA Emissions from Foams (Data from TEAP 2002, Godwin et al. 2003,TEAP 2005)

| Foam Application | Foam Type | First Year Release (%) | Release Rate (%/year) | Time to Total Release (years) | Lifetime of Foam (years) | Total Remaining at Decommissioning (%) |
|---|---|---|---|---|---|---|
| Building Insulation (including Cold Store Insulation, Marine, and Other) | PUR Sandwich Panels | 40 | 2 | N/A | 25 | 10 |
| | PUR Continuous Panel | 5 | <0.5 | 190 | 50 | 70 |
| | PUR Discontinuous Panel | 6 | <0.5 | 188 | 50 | 69 |
| | PUR Continuous Block | 35 | 0.75 | 86 | 15 | 54 |
| | PUR Discontinuous Block | 40 | 0.75 | 80 | 15 | 49 |
| | Phen. Discontinuous Block | 40 | 0.75 | 80 | 15 | 49 |
| | PUR Boardstock | 6 | 0.5 to1 | 94 | 50 | 44 |
| | PIR Boardstock | 10 | 1.5 | N/A | 50 | 15 |
| | XPS Boardstock | 25 | 0.75 to 2.5 | 30 | 50 | 0 |
| | Phen. Boardstock | 6 | 0.25 to 1 | 94 | 50 | 44 |
| | PE Boardstock | 90 | 5 | 2 | 50 | 0 |
| | PUR Spray | 15 to 25 | 0.75 to 1.5 | 50 | 50 | 0 |
| | PUR OCF | 100 | N/A | 0 | 50 | 0 |
| | PUR Pipe in Pipe | 6 | 0.25 | 376 | 50 | 81.5 |
| | PE Pipe | 100 | N/A | 0 | 15 | 0 |
| Appliance Insulation | PUR Appliance | 4 | 0.25 | 384 | 15 | 92 |
| | PUR Com. Refrig | 6 | 0.25 | 376 | 15 | 90 |
| Cushioning, Packaging, Transportation Insulation | PUR Flexible | 100 | 0 | 0 | 0 | 0 |
| | PUR Integral Skin | 95 | 2.5 | 2 | 15 | 0 |
| | PUR Reefers/Trans | 4 to 6 | 0.5 | 188 | 15 | 86.5 |
| | Polyolefin | 95 | 2.5 | N/A | 2 | 0 |

N/A: Not applicable to study

The atmospheric emissions of blowing agents and formation of blowing agent banks from halocarbon containing foams typically depend on the pattern of use or consumption and extent of blowing agent release from the foam product during manufacturing and use. Various factors govern the release of blowing agents during use of foam products. The release of blowing agents from foam during the lifetime of the product depends on the type of foam (rigid or flexible), blowing agent used, partial pressure of the blowing agent within the foam, diffusion coefficient, whether a diffusion barrier (i.e., facer) exists, and temperature (Scheutz and Kjeldsen 2003). For rigid foams, the type of BA used is the main factor that controls the total initial content of BA, the distribution of gas within the foam, as well as the diffusive properties of the gas itself. The partial pressure of the blowing agent, a result of the manufacturing process, influences the diffusion of the BA out of the foam due to concentration gradients between the foam and the atmosphere. High partial pressures and low atmospheric barometric pressure result in a high diffusion of gas. Increasing the temperature also increases the rate of diffusion due to higher kinetic energy of the gas molecules. For flexible foams, the blowing agent used is expected to be released within a short timeframe, usually during manufacturing, or within the first year of use. This quick BA release is due to the open cell structure of flexible foams as compared to a closed cell structure for rigid insulation foams.

Data on BA content at different stages of life of rigid PUR, PIR, and XPS foams (panel, spray, and boardstock) used for building and appliance insulation applications are presented (Table 12). For EPS foam materials, most of the BA (up to 100%) was indicated to be lost by the time the materials reached end of life (Godwin et al. 2003). The majority of the data provided in Table 12 represents testing conditions at 25°C temperature and atmospheric pressure conditions (exceptions noted in the table). A greater difference between initial BA content and BA content at end of life was observed for PUR foam than XPS foam. BA content at end of life was a function of the gas used during manufacture. Foams with CFC-11 and HCFC-141b had somewhat higher BA at end of life than foams with HFC-134a and HFC-245fa. While variation was present between results reported in different studies, in general gaseous BA content at end of life was higher and solubilized BA content in foam polymer was lower for the HFCs as compared to CFC-11 and HCFC-141b. Fredenslund et al. (2005) indicated that the BA contents were relatively the same (largest loss in BA was 1%) before and after use among 8 different manufacturers of refrigerator foams produced prior to 1993 with CFC-11 BA. Kjeldsen and Jensen (2001) indicated that the closed cell diffusion of gaseous blowing agents during service from rigid appliance foams was expected to be very slow to negligible, compared to emissions at end of life. Losses of BA during service may result from losses of the fraction sorbed in the foam itself (Scheutz and Kjeldsen 2003). Significant differences were present between the predicted/compiled data (Table 11) and experimental data (Table 12) for BA content at end of life of foams. These differences may have resulted from regional manufacturing and use practices as well as the assumptions inherent in the predictions provided in Table 11.

Table 12 – Variation of BA Content in Rigid Insulation Foams

| Foam Type | Reference | Insulation Type and Configuration | Blowing Agent | Initial BA Content (%w/w) | BA Content at End of Life (%w/w) | Solubilized BA at End of Life (%) | Gaseous BA at End of Life[5] (%) |
|---|---|---|---|---|---|---|---|
| Rigid PUR/PIR | Khalil and Rasmussen (1986) | Building, Panel | CFC-11 | 15.1 | 10 | - | - |
| | Bomberg and Kumaran (1989) | Building, Spray | CFC-11 | - | 10 to 12 | 22 to 66 | 34 to 78 |
| | Pollack et al. (1993) | Building, Panel | CFC-11 | - | 5.4 to 12.8 | - | - |
| | Swanstrom and Ramnas (1996) | Building, Panel | CFC-11 | - | 5.2 to 7.9 | 46 to 52 | 48 to 54 |
| | Fyfe et al. (1996) | Building, Boardstock | HCFC-141b | - | - | 24 | 76 |
| | Hong and Duda (1998) | Building, Panel | CFC-11 | - | 4.1 to 12 | 13 to 16 | 84 to 87 |
| | | | HCFC-141b | - | 4 to 11.5 | 16 to 17 | 84 to 85 |
| | Singh et al. (1998) | Building, Panel | CFC-11 | - | 5.6 to 7.7 | 60 | 40 |
| | Hong et al. (2001) | Building, Panel | HFC-134a | - | 1.2 to 1.7 | 1.7 to 2 | 98 |
| | | | HFC-245fa | - | 5.4 | 9 | 91 |
| | Kjeldsen and Jensen (2001) | Appliance, Panel | CFC-11 | - | 11 to 15 | 41 to 44 | 56 to 59 |
| | Roe (2002)[1] | Building, Roof Panel | HCFC-141b | - | - | 9 | 91 |
| | | | HFC-245fa | - | - | 4 | 96 |
| | Scheutz and Kjeldsen (2003) | Appliance, Panel | CFC-11 | - | 13.3 | 30 | 70 |
| | | | HCFC-141b | - | 11.6 | 28 | 72 |
| | | | HFC-134a | - | 7 | 23 | 77 |
| | | | HFC-245fa | - | 11.6 | 25 | 75 |
| | Fredenslund et al. (2005) and Scheutz et al. (2007a) | Appliance, Panel | CFC-11 | 14.0 to 16.4 | 13.0 to 15.4 | - | - |
| Rigid XPS | Fyfe et al. (1996) | Building, Boardstock | HCFC-142b | - | - | 13 | 87 |
| | Vo and Paquet (2004) | Building, Roof Panel | CFC-12 | 5 to 6.5 | 1.5 to 4 | - | - |
| | | | HCFC-142b | 8 to 8.4 | 1.5 to 6 | - | - |
| | | | HFC-134a | 6.5 to 7 | - | - | - |
| | Gendron et al. (2002) | Building, Boardstock | HCFC-142b | 11 to 15 | - | - | - |
| | | | HFC-134a | 6 to 8 | - | 0.8[2] | 99.2 |
| | Daigneault et al. (1998) | Building, Boardstock | HCFC-142b | - | - | 3(15)[3] | 97(85)[6] |
| | | | HFC-134a | - | - | 0.6(2)[3] | 99.4(98)[6] |
| | Gendron et al. (2006) | Building, Boardstock | HFC-134a | 6(8)[4] | - | - | - |

[1] PIR building insulation foams only
[2] BA solubility in polymer observed at 30°C
[3] Average and (maximum) solubility of BA observed at 40°C
[4] Average initial BA concentration and (maximum) initial concentration observed
[5] Assuming the foam at end of life is completely dry
[6] Calculated (maximum) BA in gaseous phase from (maximum) solubility in the previous column
- Omitted by the study

### 1.3.4 End of Life Management of Foams

Common management practices for end of life waste foam materials include reuse, recycling, and landfill disposal. In general, recycling operations include shredding of the foam wastes with or without recovery of foam blowing agents using two main processes (Scheutz et al. 2007a). The first process, termed general shredding, involves the shredding of foam waste in unsealed facilities (i.e. no gas recovered), recycling valuable materials (metals), and disposal of the shredder residue in a landfill. Most scrap recycling facilities in the U.S. operate under these conditions. The alternative process, termed recycling and recovery of ODS, recovers the CFCs, HCFCs and HFCs emitted during the shredding process of foam, treating the gases (typically by incineration), while also recovering the reusable materials. The end of life management practices used for waste insulation foam materials in California vary by the category of original foam application: construction and demolition, domestic refrigerator and freezer, commercial appliance (including water heaters and vending machines), transport foam (from transport refrigerated units-TRUs), as well as marine and other foam wastes (including non-structural cold stores) (Caleb 2011).

Approximately 92% of foam wastes from construction and demolition activities was estimated to be landfilled directly, whereas 8% of the foam wastes was shredded prior to landfilling (Caleb 2011). The reuse rate of domestic refrigerators/freezers was estimated to be 39%, the amount recycled with no foam recovery was 47%, and the amount of appliances with foam recovery/BA destruction (ODS processed) was 14%. For commercial appliances and vending machines, 100% of the devices were processed via shredder, degassed (refrigerant recovered), metals were recovered, and the remaining residue including foam was landfilled. For commercial water heaters, 100% of the devices were processed via shredder, metals were recovered, and the remaining residue including foam was landfilled. In transportation applications, approximately 25% of TRUs and Reefers were estimated to be reused, whereas the remaining 75% were shredded, metals were recovered, and the remaining residue including foam was landfilled. For marine and other applications, 5% of leisure and recreational boats were exported and 95% were shredded and residue including foam was landfilled; 100% of canoes were shredded and residue including foam was landfilled; 100% of buoys and coolers were landfilled with possibly large buoys shredded first; and 100% of nonstructural cold storage units were landfilled with possibly large units shredded first.

An additional category of waste foam material is auto fluff, which is a combination of flexible foam products (seat cushioning) with an open celled structure, as well as rigid panel foam panel insulation (used on the outside frame of cars) (Scheutz et al. 2007c). Auto shredder residue waste is typically very heterogeneous (in both size and composition) and varies by both year and manufacturer of the car (Moakley et al. 2010). In general, the auto fluff composition and range of materials can be defined as a mixture of plastics (30-48%), fibers (4-26%), glass/ceramics (3-19%), metals (~3%), elastomers/rubbers (10-32%), as well as remaining minerals/residues (10-43%) (Moakley et al. 2010). Plastics emanating from foams, textiles and carpets are typically

the main component of the auto shredder residue (ASR) composition (Moakley et al. 2010).

In a recent field study conducted by the Argonne National Laboratory (Duranceau and Spangenberger 2011) at a shredder facility in Fort Myers, Florida, the auto shredder residue composition was evaluated in detail by shredding cars of various sizes, ages, and makes. The four categories evaluated by the shredding process included “Big” models (trucks and SUVs made from 2000 to 2005), “Normal/Domestic” models (sedans/smaller cars made in the U.S. pre-2000), “Transplant” models (all types built in the U.S. by foreign companies between 2000 and 2005), and “Import” models (all types built outside the U.S. between 2000 and 2005). After shredding, the residue was separated into ferrous and non-ferrous fractions. Non-ferrous fractions consisted of either <12 mm fine particles (2.5% w/w of the total feed entering the shredder) or coarse shredder residue classified in the size range from 12 to 150 mm (17% w/w of the total feed entering the shredder) (Duranceau and Spangenberger 2011).

For the fines category, mixed polymer concentrations were the highest among the composition analyzed, accounting for an average of 45% (w/w) of the total fine content. For the coarse fraction of residue (between 12 and 150 mm), oversized foam (flexible foam from seat cushioning) represented between 1 to 6% (w/w) of the total weight fraction of coarse particles (Duranceau and Spangenberger 2011). The BA in these products is emitted during manufacture and use with essentially no BA expected to be left in the foam at end of life (TEAP 2005). However, polymer concentrate ranged from 36 to 43% (w/w), which could contain smaller fractions of shredded foam residue, possibly from rigid panel insulation. The composition of polymer concentrate ranged from 4% (w/w) for polystyrene (present in XPS/EPS insulation), and 2-3% (w/w) polyurethane (present in PUR/PIR insulation), suggesting the presence of rigid foam insulation in the shredder residue. This range was fairly consistent among manufactures and car types, but was observed to vary by age (Duranceau and Spangenberger 2011). These results agree with studies by Scheutz et al. (2007c, 2011a, and 2011b) measuring emissions of blowing agents and quantities of foam present in auto shredder residue cells in Denmark. Specifically, Scheutz et al. (2007c) measured foam composition in auto shredder cells and attributed most of the smaller foam particles to rigid PUR insulation panels (blown with CFC-11, HCFC-141b, and HFC-134a). Further, detectable emission rates of CFC-11 were quantified in laboratory lysimeter experiments using auto fluff sampled from the residue cells (Scheutz et al. 2007c, 2011a). In addition, small emissions of common blowing agents varied from CFC-11 and HFC-134a (Scheutz et al. 2011b) at different hotspot locations within the shredder residue cells. Thus, a combination of results from both laboratory and field experiments analyzing auto shredder residue imply that auto fluff may contribute to BA emissions within the landfill environment.

### 1.4 Landfill Environment

The landfill environment is a complex system of waste conversion processes and pathways controlled by various physical, biochemical, and environmental factors (Tchobanoglous et al. 1993). The physical factors controlling the waste conversion

processes are associated with the design and operation of the landfill itself. These include the waste composition, compaction and compression processes, the use of daily, intermediate, and final covers as well as the presence and components of a liner system, a gas collection/combustion system, and a leachate collection and recirculation system. For example, installed liner systems limit the lateral and vertical diffusion or migration of landfill gas and leachate, while compaction and short or long term compression processes control the moisture content and unit weight of landfill wastes as well as fluid conductivity. Biochemical factors include the population, diversity, and characteristics of a diverse range of hydrolytic, fermentative, acetogenic, methanogenic, and methanotropic microorganisms.

Environmental factors include seasonal effects such as periods of precipitation, sunlight, and barometric pressure and also atmospheric concentration of carbon dioxide, methane, and trace gas components. Seasonal weather patterns influence the temperature of wastes at shallow depths and cover soils as well as the moisture content, in particular during periods of rain or drought. Temperature and precipitation also influence heat generation and resulting temperatures in the waste mass and liners in a landfill. At some sites, significant changes in barometric pressure have been observed to control the rate of landfill gas migration and flux to the atmosphere (Czepiel et al. 2003). Landfill gas can be emitted by diffusive fluxes (changes in the concentration gradient between the landfill and atmosphere or in the landfill cover soils), advection (flux due to pressure gradients-barometric), ebullition (bubbling flux through the liquid phase), as well as flux through vascular systems (plant-mediated) (Bogner and Spokas 2010). The chemical/biological factors are interdependent on both the physical and environmental factors. For instance, the presence of oxygen in specific waste layers, the organic fraction of the waste, and the temperature of the waste and many other factors govern the type, population, and activity of methanogens in these waste layers.

In the landfill environment, the primary waste conversion process is the anaerobic decomposition of organic waste by methanogenic bacteria, producing methane and carbon dioxide gas. Landfill methane makes up approximately 1.3% (0.6 Gt) of global anthropogenic GHG emissions as compared to total emissions across all sectors of 49 Gt $CO_2$eq per year (Bogner and Spokas 2010). Currently, landfills are the third largest source of anthropogenic methane in the U.S. after oil and gas leakages and ruminant animals. Although methane has a short atmospheric lifetime (approximately 13 years), it is a potent GHG due to its higher absorption efficiency of outgoing infrared radiation as compared to other GHGs (100-year GWP = 28). Therefore, since landfills can be significant sources of methane at the urban scale, mitigation of these emissions remains a high priority in many countries, including the U.S. (Belluci et al. 2012). Moreover, considering indirect effects of methane emissions inclusive of increased ozone and stratospheric water vapor, methane is responsible for approximately 40% of positive atmospheric forcing since the beginning of the industrial era (IPCC 2013). Other than methane, landfill gas is composed of trace components including CFCs, HCFCs, and HFCs. This produced LFG can be recovered by a gas extraction system, burned in a flare, or oxidized by methanotrophs in landfill cover soils (Figure 11). It is

important to note in Figure 11 that trace components such as CFCs, HCFCs, and HFCs also may be emitted with methane, degraded in the waste mass, oxidized in the cover soil, stored in the waste mass, or recovered by the gas extraction system. Some components of LFG, including CFCs, HCFCs, and HFCs, also can be sequestered in the landfill (i.e. adsorbed to the waste mass/cover soil) or solubilized in the leachate as a result in differences in physical/chemical properties and landfill operational/geographical conditions (not described in the figure).

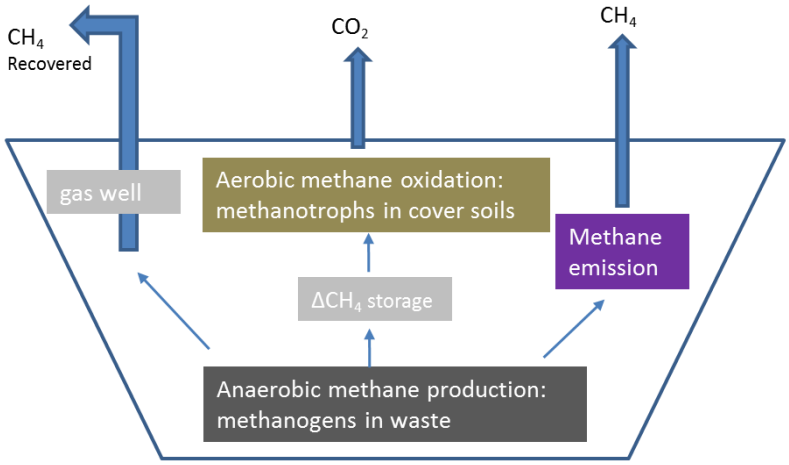


Figure 11. Methane Mass Balance in a Landfill Environment (modified from IPCC 2007)

### 1.4.1 Physical Factors

The composition of MSW affects all processes within a landfill, the most important being the anaerobic decomposition of waste and the production and properties of the primary landfilling byproducts of leachate, LFG, and heat. In general, the anaerobic degradation rate and the concentration of LFG increase with increasing fraction of organic material. Large-scale samples of MSW were characterized to identify the fraction (by weight) of constituent components of the waste stream in California in an investigation conducted in 2008 (Cascadia 2008). The data from this study are presented in Table 13. Foam wastes (insulation-rigid foam) were not included under any subcategory provided in the study. Assuming that foam wastes may have been classified under either “composite/remainder inerts and other” or “mixed residue”, up to 6.3% (w/w) of the California waste stream may have contained a mixture of rigid insulation foam wastes for a worst-case-scenario assessment (Table 13). An earlier investigation by CalRecycle (2006) on C&D waste loads entering waste disposal facilities identified approximately 6.4-8.8% (w/w) of foam insulation waste. The “inerts and other” category (29.1% of total waste) in Table 13 consists mainly of C&D materials with constituent component categories similar to those identified in CalRecycle (2006). Therefore, the 6.4-8.8% (7.6% average) range may be applied to

the “inerts and other” category in Table 13 to estimate a more representative amount of amount of foam waste than the worst-case-scenario conditions in California.

The total waste generation (Figure 12) in California peaked in 2007 and was reported to be 93 million tons; since then, waste generation has decreased slightly and was 86 million tons in 2012 (CalRecycle 2013). A larger relative change was observed in waste disposal amounts in California, decreasing from a peak of 39 million tons in 2007 to 29 million tons in 2012 (CalRecycle 2013) due in part to increased diversion rates. Based on the waste data provided for California by CalRecycle (2013) and the 6.3% maximum foam fraction, the total amount of foam wastes can be estimated to be on the order of 2.5 and 1.9 million tons for 2007 and 2012, respectively for worst-case-scenario conditions. For more representative conditions by using average 7.6% of “inerts and other” category in Table 13, the amount of foam wastes can be estimated at 0.86 and 0.64 million tons for 2007 and 2012, respectively. These values for foam waste are significantly higher than that predicted by Caleb (2011) of 0.031 million tons/year (using an average foam density of 30 g/L to convert volumetric data provided). The variations in the estimates for the amount of foam wastes generated in California indicate a need for better quantification of the amount of these materials in the waste stream.

Table 13 – California Waste Characteristics (Cascadia 2008)

| Material | Fraction | Tonnage | Material | Fraction | Tonnage |
|---|---|---|---|---|---|
| **Paper** | **17.3%** | **6,859,121** | Remainder/Composite Plastic | 2.8% | 1,104,719 |
| Uncoated Corrugated Cardboard | 4.8% | 1,905,897 | | | |
| Paper Bags | 0.4% | 155,848 | **Other Organic** | **32.4%** | **12,888,039** |
| Newspaper | 1.3% | 499,960 | Food | 15.5% | 6,158,120 |
| White Ledger Paper | 0.7% | 259,151 | Leaves and Grass | 3.8% | 1,512,832 |
| Other Office Paper | 1.2% | 472,147 | Prunings and Trimmings | 2.7% | 1,058,854 |
| Magazines and Catalogs | 0.7% | 283,069 | Branches and Stumps | 0.6% | 245,830 |
| Phone Books and Directionaries | 0.1% | 24,149 | Manures | 0.1% | 20,373 |
| Other Misc. Paper | 3.0% | 1,202,354 | Textiles | 2.2% | 886,814 |
| Remainder/Composite Paper | 5.2% | 2,056,546 | Carpet | 3.2% | 1,285,473 |
| | | | Remainder/Composite Organic | 4.3% | 1,719,743 |
| **Glass** | **1.4%** | **565,844** | | | |
| Clear Glass Bottles and Containers | 0.5% | 196,093 | **Inerts and Other** | **29.1%** | **11,577,768** |
| Green Glass Bottles and Containers | 0.2% | 79,491 | Concrete | 1.2% | 483,367 |
| Brown Glass Bottles and Containers | 0.3% | 108,953 | Asphalt Paving | 0.3% | 129,834 |
| Other Colored Glass Bottles and Containers | 0.1% | 40,570 | Asphalt Roofing | 2.8% | 1,121,945 |
| Flat Glass | 0.1% | 33,899 | Lumber | 14.5% | 5,765,482 |
| Remainder/Composite Glass | 0.3% | 106,838 | Gypsum Board | 1.6% | 642,511 |
| | | | Rock, Soil, and Fines | 3.2% | 1,259,308 |
| **Metal** | **4.6%** | **1,809,684** | Remainder/Composite Inerts and Other | 5.5% | 2,175,322 |
| Tin/Steel Cans | 0.6% | 236,405 | | | |
| Major Appliances | 0.0% | 17,120 | **Household Hazardous Waste (HHW)** | **0.3%** | **120,752** |
| Used Oil Filters | 0.0% | 3,610 | Paint | 0.1% | 48,025 |
| Other Ferrous | 2.0% | 801,704 | Vehicle and Equipment Fluids | 0.0% | 6,424 |
| Aluminum Cans | 0.1% | 47,829 | Used Oil | 0.0% | 3,348 |
| Other Non-Ferrous | 0.2% | 84,268 | Batteries | 0.0% | 19,082 |
| Remainder/Composite Metal | 1.6% | 618,747 | Remainder/Composite Household Hazardous | 0.1% | 43,873 |
| | | | | | |
| **Electronics** | **0.5%** | **216,297** | **Special Waste** | **3.9%** | **1,546,470** |
| Brown Goods | 0.2% | 76,725 | Ash | 0.1% | 40,736 |
| Computer-related Electronics | 0.1% | 32,932 | Treated Medical Waste | 0.0% | 0 |
| Other Small Consumer Electronics | 0.1% | 34,588 | Bulky Items | 3.5% | 1,393,091 |
| Video Display Devices | 0.2% | 72,053 | Tires | 0.2% | 60,180 |
| | | | Remainder/Composite Special Waste | 0.1% | 52,463 |
| **Plastic** | **9.6%** | **3,807,952** | | | |
| PETE Containers | 0.5% | 199,644 | **Mixed Residue** | **0.8%** | **330,891** |
| HDPE Containers | 0.4% | 157,779 | Mixed Residue | 0.8% | 330,891 |
| Misc. Plastic Containers | 0.4% | 163,008 | | | |
| Plastic Trash Bags | 0.9% | 361,997 | | | |
| Plastic Grocery and Other Merchandise Bags | 0.3% | 123,405 | | | |
| Non-Bag Commercial and Industrial Packaging Film | 0.5% | 194,863 | | | |
| Film Products | 0.3% | 113,566 | | | |
| Other Film | 1.4% | 554,002 | **Totals** | **100.0 %** | **39,722,818** |
| Durable Plastic Items | 2.1% | 834,970 | **Sample Count** | **751** | |

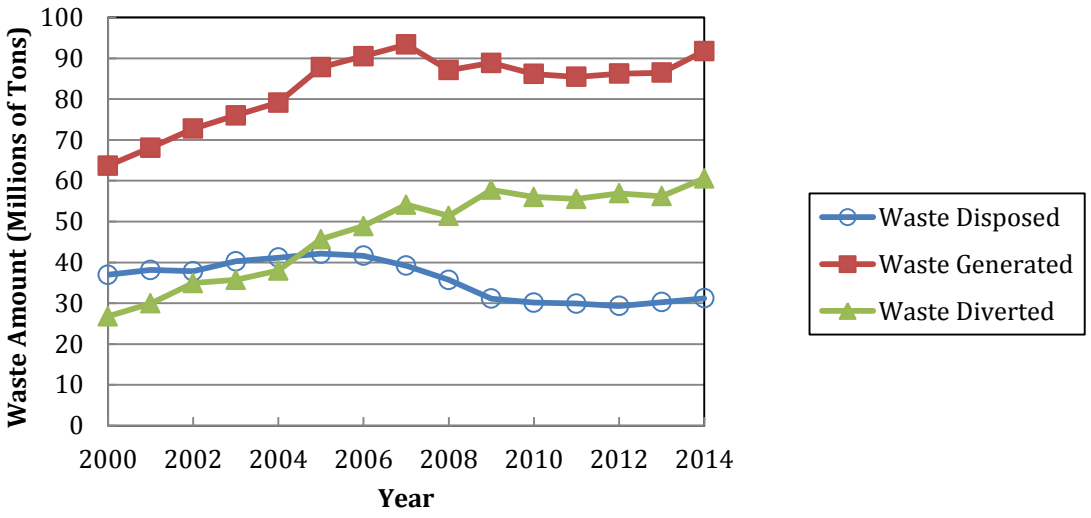


(a) Total Generation

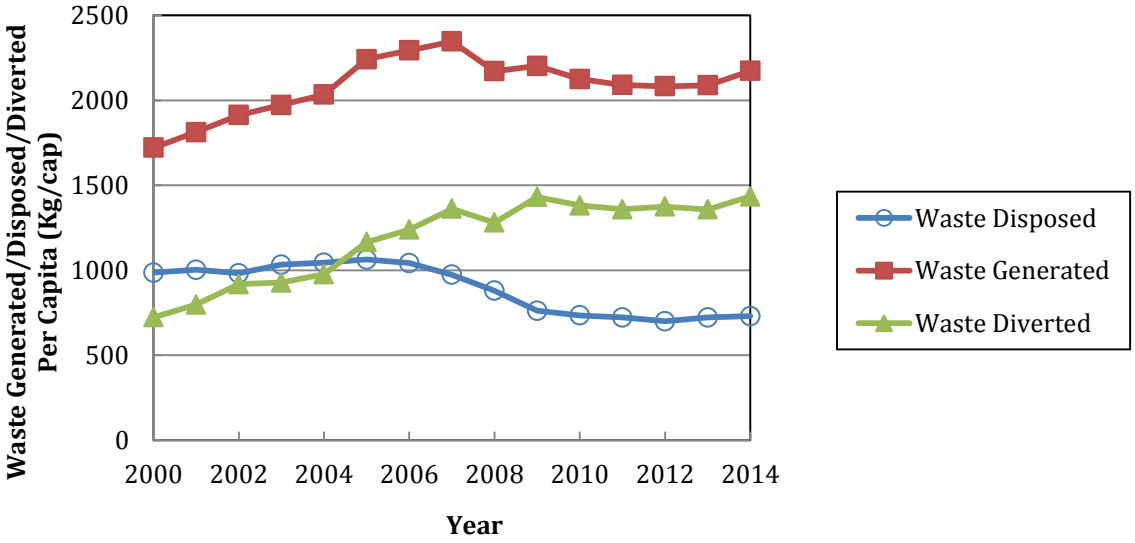


(b) Per Capita Generation

Figure12. California Waste Data (adapted from CalRecycle 2015)

Wastes are placed by compaction to densify the as-received waste materials. The densification process serves two purposes: to maximize the amount of wastes that can be disposed of in a given landfill volume and to ensure geomechanical stability of the disposed wastes. Conventional soil compaction theory is generally applicable to MSW in that the compaction properties of a waste mass are governed by the moisture content and compactive effort (Hanson et al. 2010). Shear strength increases and compressibility decreases due to compaction. Hydraulic conductivity of wastes decrease significantly as the moisture content increases from the dry of optimum

moisture content to the wet of optimum moisture content in similarity to cohesive soils (Yesiller et al. 2010). The air/gas conductivity of the wastes is expected to follow the same trends as hydraulic conductivity. Waste compaction equipment has evolved significantly over time and common compactors apply high compactive effort to wastes. The high compactive efforts and resulting high densities promote the formation of anaerobic conditions, as less space is available for oxygen migration within the highly compacted waste layers (Hanson et al. 2010). However, if wastes are highly compacted at high moisture contents, excess moisture may limit the both the transport and production of LFG. High compactive efforts may lead to high instantaneous release of BA from foam wastes. Determination of the full influence of compaction is complicated by competing effects through reduction in pore size, compaction moisture content, and influences on other engineering properties of wastes such as compressibility and hydraulic conductivity and should be established on a case-by-case basis (Yesiller et al. 2010).

Long-term compression and settlement processes affect the waste structure and thus the migration of air, moisture, and landfill gas within the compacted waste mass. Compression of waste has been described to occur due to four mechanisms: (1) mechanical: elastic compression, reorientation of structure (creep), (2) ravelling: migration of fines into larger voids, (3) physical-chemical effects: corrosion, oxidation, combustion, and (4) biodegradation: aerobic and anaerobic processes (Edil et al. 1990). High amounts of settlements occur in wastes with significant contribution of long-term secondary settlements. The long-term settlement of waste is primarily controlled by the biodegradation and creep mechanisms (Leonard et al. 2000). The compression of waste has been commonly compared to that of organic soil deposits because of the overall high compressibility and strong presence of secondary compression effects (Sowers 1973, Edil et al. 1990, Landva and Clark 1990, Stulgis et al. 1995).

Historically, mathematical relationships have been developed to predict long-term settlement of wastes based on analogies to soil mechanics, and based on empirical or rheological models (e.g., Sowers 1973, Yen and Scanlon 1975, Rao et al. 1977, Oweis and Khera 1986, Morris and Woods 1990, Edil et al. 1990, Bjarngard and Edgers 1990, Landva and Clark 1990, Fasset et al. 1994, Stulgis et al. 1995, Park and Lee 1997, Ling et al. 1998, El-Fadel and Al-Rashed 1998, Leonard and Floom 2003, Hossain and Gabr 2005, Bareither et al. 2012). Analysis of waste settlement data is complicated by the fact that separate long-term mechanisms occur simultaneously and may mask each other in the field (e.g., creep and biodegradation). The agreement between models and measured settlements appears successful as demonstrated by high values of correlation coefficients. However, limitations exist with model formulations due to simplifying assumptions. In general, the predictive significance of curve fitting methods (such as the hyperbolic method) is limited (Van Meerten et al. 1995). The fundamental understanding of the mechanisms of long-term compression of wastes also is limited.

Settlement is expected to affect the long-term release of BA from foam waste materials. The effects may occur through three distinct mechanisms: a) foam materials may fail under the applied stresses releasing blowing agents (quick releases), b) increased closed cell diffusion may occur under the applied stresses as diffusion increases with an increase in pressure due to applied stresses (Geankoplis 2009), and c) the densified waste subsequent to long-term compression will have different gas transport characteristics than the as-placed wastes. Experimental or modeling analyses for settlement induced BA release have not yet been reported.

Cover systems are another physical aspect of the landfill environment that affect the emission of LFG constituents. In general, landfill gas emission rates are correlated with the type of cover (i.e., daily, intermediate, or final), as well as the oxidation conditions developed in the cover itself (Yesiller et al. 2008a). Daily covers and intermediate soil covers are temporary and vary in composition. Daily covers can range from a thin layer of soil or non-putrescible wastes (15 to 30 cm) to alternative covers such as geosynthetics, spray-on foams, and various byproducts (USEPA 2013). Daily covers prevent the surface infiltration of moisture, eliminate any sources of disease vectors, reduce fugitive emissions of VOCs, and increase the aesthetic appeal of the landfill. Additional objectives of daily covers include prevention of windblown litter, migration of odors off site, and scavenging by birds or rodents, and reduction of fire hazards (USEPA 1993). The non-putrescible wastes used for alternative daily covers in California range from shredded C&D wastes to shredded auto fluff (USEPA 1993). Other covers used in California include tires, wood chips and green waste, compost, incinerator ash, contaminated sediments, wastewater treatment plant sludge, mixed waste, and other waste (CARB 2011). Intermediate covers differ in that they are expected to remain intact for an extended time period (generally over 1 year), educe infiltration of water, and prevent the release of leachate and LFG (USEPA 1993). Intermediate covers typically consist of soils and have thicknesses more than 30 cm, typically on the order of 60 up to 100 cm. Intermediate covers are placed over completed lifts in a given area of a landfill that has reached relatively final elevations to prevent LFG emissions and moisture infiltration. Depending on the time period, vegetation also may be allowed to grow to increase stability and prevent erosion (SCS 2008). Alternative intermediate covers (AICs, other than soil) allowed in California include green waste, shredded C&D waste, shredded auto fluff, contaminated sediments, compost, mixed waste, treatment plant sludge, tires, incinerator ash, and other wastes (CARB 2011). However, the use of these materials as AICs in California landfills is highly limited (CARB 2011).

Final cover systems are constructed when the waste heights reach final levels and the landfill facility is completely full. The overall objective is to minimize the amount of infiltrating water that may percolate through the cover into the underlying disposed waste as well as to facilitate management of LFG (i.e., limit emissions and enable collection). Cover systems are designed to resist infiltration while promoting high surface runoff and maintaining stability (against wind/water erosion and slope failure).

Common types of final cover systems include conventional covers and alternative covers. A typical conventional cover system consists of, from top to bottom: a vegetative soil layer, a protective soil layer, a blanket filter/drainage layer, and a barrier system (Yesiller and Shackelford 2011). A second blanket filter/drainage layer may be used beneath the barrier system. A protective/foundation soil layer is placed between the waste mass and the final cover (Figure 13). The vegetative soil layer supports plant growth and prevents erosion along the surface of the cover system. The protective soil layer provides a biotic barrier between the vegetative and the filter/drainage layer components against intrusion of plants from the vegetative layer as well as a barrier to animals from the ground surface. In cold climates, this layer also serves as a frost protection layer, where the components of the filter/drainage layer are placed below the local frost depth. The filter/drainage layer allows for collecting the water entering the cover system due to precipitation or from surface runoff from surrounding areas. The barrier system prevents infiltration of water into the waste mass, limits the transport of LFG, and also isolates the contained materials from the surrounding environment. Composite barriers with geomembrane components typically are required by regulation in the case where the bottom liner system includes a geomembrane liner. The second filter/drainage layer placed beneath the barrier system is used to facilitate collection and removal of the gas generated by wastes. The protective/foundation soil layer separates the cover from the wastes and provides a firm base over the wastes for the construction of the cover system. Typical final cover thicknesses range from 100 to 150 cm. The barrier layers are constructed using compacted clayey soils, geosynthetic clay liners (GCLs), and geomembranes. The filter/drainage layers are constructed using high hydraulic conductivity soils, geotextiles, geonets, and geotextile/geonet composites.

The primary design consideration for conventional covers is providing high resistance to infiltration of water and also high resistance to gas emissions (Figure 13). Low hydraulic conductivity is required in the barrier component of the cover system. The service conditions for cover systems include low applied effective stresses, low hydraulic gradients, and potentially high changes in moisture content and thus degree of saturation and hydraulic conductivity of earthen components. The cover systems also are subjected to high seasonal and diurnal temperature differentials and high thermal gradients, such that thermally driven moisture flow may occur in cover systems (Yesiller et al. 2008b). In general, gas conductivity is considered to follow similar trends and is affected by similar factors as hydraulic conductivity. However, the gas conductivity is expected to be higher than hydraulic conductivity. For example, Moon et al. (2008) determined that gas conductivity a compacted clay soil was 2 to 3 orders of magnitude higher than the hydraulic conductivity of the soil based on laboratory tests. Moon et al. (2008) indicated that such a compacted clay would not be sufficient to control gas emissions from a landfill. Both gas and hydraulic permeability are recognized to decrease dramatically for compacted clays wet of optimum moisture contents, decreasing gas/water transport through the cover system (Yesiller and Shackelford 2011). Opposite trends are observed at moisture contents dry of optimum moisture content.

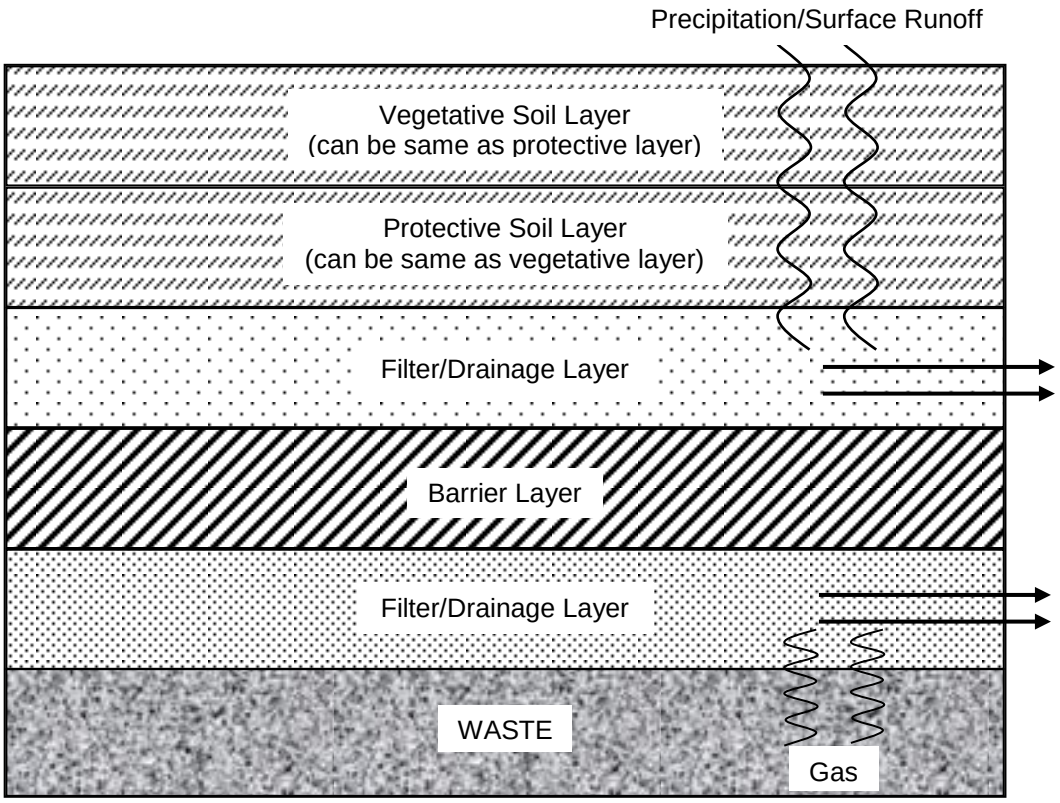


Figure 13. The Conventional Landfill Cover System
(Yesiller and Shackelford 2011)

Alternative covers are final covers that are designed and operated on the basis of the hydrologic water balance, where the amount of percolation is estimated using precipitation, surface runoff, intralayer flow, evapotranspiration, and soil-water storage (Yesiller and Shackelford 2011). The moisture loading by precipitation is counteracted by the remaining four mechanisms (surface runoff, intralayer flow, evapotranspiration, and soil-water storage) to obtain net percolation. Alternative covers typically have lower cost and expected greater durability than conventional covers. Common materials used for alternative covers include soils with low potential for desiccation cracking and frost damage, such as silty sands, silts, silty clayey sands, clayey silty sands, and similar materials. In general, this relatively wide range of soil types allows alternative covers to be constructed using locally available materials. The primary design consideration is to minimize percolation into the underlying wastes. Seasonal analyses are conducted to ensure sufficient water storage capacity to store infiltrating water with little or no drainage during periods of elevated precipitation and limited evaporation and transpiration (e.g., winter), followed by subsequent removal of the stored water during drier periods with greater evaporation and transpiration (e.g., summer). Alternative covers are particularly well suited for regions with arid or semiarid climates, where potential evapotranspiration (PET) far exceeds precipitation (P) (e.g., PET > 2P), such as some western regions of North America (Shackelford 2005).

The common two types of alternative covers are monolithic and capillary barrier covers (Shackelford 2005). Monolithic covers consist of a single layer of relatively fine-grained soil, whereas capillary barriers include a finer textured soil overlying a coarser textured soil. A capillary break forms between the two soil layers of the capillary barriers. At low degrees of saturation, the unsaturated hydraulic conductivity of the coarser layer is lower than that of the finer soil, which impedes the percolation into the coarser layer (and overall through the cover into the underlying wastes). The thicknesses of the alternative covers depend on climatic conditions and vegetation and typically range between on the order of 150 to over 300 cm. Research and practice in alternative covers have focused on hydrologic water balance and percolation of water with limited information on gas transport. As the hydraulic conductivity of the barrier layers used in alternative covers typically are higher than the conductivity of the barrier layers used in conventional covers, gas conductivity is expected to be higher for alternative covers than conventional covers.

An additional type of cover system is biocover (also termed biocell) that consists of a high gas permeability layer overlain by a high organic content compost or mulch amendment (Abichou et al. 2006b, Bogner et al. 2010). The high organic content layers serve to enhance methane oxidation in the covers. Use of biocovers is relatively new and less information is available for these covers than conventional or alternative covers. Results of experimental studies in the field indicated that effectiveness of the covers increased with increasing organic layer thickness and gas distribution layer (i.e., high gas permeability layer) thickness. Effectiveness of biocovers was significantly affected by seasonal moisture contents, where higher oxidation rates (and lower emissions) were observed in wet months than dry months. Biocovers also were demonstrated to be effective in mitigating emissions of most NMOCs, in particular aromatics, alkanes and lower chlorinated compounds (Abichou et al. 2006b). Decreases in emissions of CFCs up to 82% were observed in biocovers during spring months in comparison to control plots with no biocover in field experiments (Bogner et al. 2010). The control plots consisted of an interim cover 15 cm in depth with compacted sandy clay soil characteristics (Bogner et al. 2010). However, the CFC emissions increased in fall months compared to control plots indicating oxidation was not taking place. This variation in effectiveness of the biocover system in mitigating CFC emissions was most likely due to changes in optimum moisture content for oxidation within the biocovers tested (Bogner et al. 2010).

The effectiveness of the three main cover systems needs to be assessed on a case-by-case basis using realistic field service conditions with regard to competing performance requirements for low gas emissions and high gas oxidation in the cover system. Data and analyses are required for gas permeability of the varying cover designs.

A combination of conventional cover systems (incorporating compacted clay, GCL, and/or geomembrane barrier layers) and alternative cover systems complying with 27 CCR (12 in. loam/ 12 in. clay/ 24 in. silty clay loam) is expected across California landfills. Recently constructed final covers are expected to incorporate more

alternative cover designs, while older final covers include conventional cover designs. With these design approaches, not all landfill final cover systems in California incorporate a geomembrane, which has been demonstrated to significantly improve LFG collection and reduce fugitive LFG emissions (SCS 2008).

### 1.4.2 Biochemical Factors

The biochemical factors in the landfill environment include biological or chemical conversion or transformation processes. The most significant biological reactions include the anaerobic degradation of the organic fraction of waste resulting in production of carbon dioxide and methane as byproducts. Biological reactions also can take place under aerobic conditions, as in methane oxidation processes. Biological processes generate heat, as an additional byproduct to the gases. The general anaerobic transformation (gas production) involves the addition of organic matter, water, and nutrients to produce new bacterial cells, resistant organic matter, carbon dioxide, methane, ammonia, hydrogen sulfide, and heat. Chemical reactions include dissolution and suspension of landfill materials as well as the evaporation or volatilization of chemical compounds into the LFG, sorption of VOCs and semi-VOCs onto waste materials, or dehalogenation/ decomposition processes involving trace chemicals such as CFCs and HCFCs (Tchobanoglous et al. 1993).

The biological decomposition of the organic fraction of solid waste is affected by the landfill abiotic conditions and the landfill operating procedures (Rettenberger and Stegmann 1996). The landfill environment transforms from aerobic conditions to anaerobic conditions within weeks to several months subsequent to waste placement (Hanson et al. 2005). The anaerobic degradation of wastes is known to occur in three stages (Tchobanoglous et al. 1993). The first stage (hydrolysis) reduces higher molecular mass compounds into smaller compounds that provide sources of energy and cell tissue for the bacteria present. Thus, hydrolysis effectively solubilizes the larger solid organic matter and complex dissolved organic matter by cellular enzymes produced by fermentative bacteria (Rettenberger and Stegmann 1996). The next stage involves further reduction of the compounds in stage 1 to intermediate lower molecular mass compounds (acidogenesis). Acidogenesis involves acetogenic bacteria that use the fatty acids and alcohols produced by the fermentative bacteria hydrolysis to produce acetic acid, carbon dioxide, and hydrogen (Rettenberger and Stegmann 1996). The third stage (methanogenesis) comprises the bacterial conversion of the above intermediate compounds (acetatic acid and hydrogen) to form much simpler end products such as methane and carbon dioxide. Two types of methanogenic bacteria are responsible for the production of carbon dioxide and methane: the hydrogenophillic and the acetophillic. The hydrogenophillic require hydrogen and carbon dioxide to form methane, while the acetophillic convert acetic acid to methane and carbon dioxide (the most important reaction concerning methane formation) (Rettenberger and Stegmann 1996).

To carry out these processes (hydrolysis, acidogenesis, methanogenesis) in unison, both the nonmethanogenic and methanogenic bacteria populations must be in a state of dynamic equilibrium to form a syntrophic (i.e., mutually beneficial) relationship.

These processes depend on specific conditions within the landfill environment including the oxygen concentration, hydrogen concentration, pH and alkalinity, sulphate concentration, presence of nutrients or inhibitors, temperature, and water content (Rettenberger and Stegmann 1996). Oxygen concentrations must be limited (near-zero); hydrogen concentrations must be sufficient (for methanogens, the hydrogenophillic and the acetophillic bacteria); the environment must be free of inhibitory concentrations of free ammonia, heavy metal and sulfides; the pH should range from 6.5 to 7.5 and contain sufficient alkalinity to buffer low pH below 6.2 (1000 to 5000 mg/L); the absence of sulphates (to prevent competitive inhibition of substrates); the availability of nitrogen and phosphorus and micronutrients (sulphur, calcium, magnesium, potassium, iron, zinc, copper, cobalt, molybdenite and selenium); temperatures must be sufficiently high (30 to 40°C for mesophillic bacteria that favor moderate temperature ranges to survive and 50 to 60°C for thermophillic bacteria that favor more extreme temperature ranges to survive); and water content must be maintained at 25 to 60% (w/w wet) (Cecchi et al. 1993, Tchobanoglous et al. 1993, Rettenberger and Stegmann 1996). Long-term LFG production is significantly affected by moisture content as inadequate moisture results in incomplete anaerobic digestion (no peak of LFG production is observed). Recirculation of leachate enhances methane formation by an increase in moisture content, supply of nutrients/biomass, as well as a general dilution of high concentrations of inhibitors.

In addition to the conditions listed above, LFG generation rate is controlled by waste composition, atmospheric conditions, landfill cover, waste density, and waste age. These factors also contribute to the variation in gas production over time (Tchobanoglous et al. 1993). The rate of anaerobic degradation may reach a peak within the initial two-year period before slowly tapering off (for up to 20 to 25 years) in temperate climates. In cold and arid climatic zones, anaerobic conditions are established early in the landfill environment, however, the peak of LFG generation is significantly delayed (up to decades) due to low temperature and low moisture content (Hanson et al. 2006). Soil covers may positively affect anaerobic degradation processes by providing a buffer for avoiding low pH that inhibits methane formation. The variation in LFG produced is different between rapidly and slowly biodegradable wastes, with slowly biodegradable wastes peaking in production after an average of 10 years as compared to 5 years for rapidly degrading wastes. Waste composition affects the overall onset of anaerobic conditions and the duration of degradation with high organic waste composition increasing gas production rate and decreasing time to onset of LFG production. Compaction can influence LFG production by limiting the available pore spaces for movement of fluids in a landfill system.

For California, recent work (Spokas et al. 2015) using a database of all California landfills with engineered recovery (n=129) indicated that a relatively constant rate of biogas generation and recovery could be expected from each unit mass of landfilled waste. An extensive analysis was conducted to demonstrate that while biogas generation is primarily a function of waste mass in place at a given landfill (and statistically independent of waste age, landfill status – open or closed, size, or climatic regime), the gas emissions are strongly a function of both cover configuration and

climatic conditions. A linear empirical relationship was proposed between for California landfills between waste mass and landfill biogas recovery, with a value of 126 x $10^{-6}$ $Nm^3$ $CH_4$/hr-Mg waste (Spokas et al. 2015).

Biodegradation characteristics of foam materials directly influences the fate of foam wastes in the landfill environment. The biodegradability and long term integrity of a rigid PUR foam was tested under accelerated anaerobic conditions in controlled laboratory experiments simulating real world landfill conditions (Urgun-Demirtas et al. 2007). No changes in weight or tensile strength (mechanical properties) of the rigid PUR foam were observed after biological exposure. The results of accelerated, short-term experiments, which consisted of bioavailability assays, soil burial experiments, and accelerated bioreactor tests, indicated that rigid PUR foam was not likely to biodegrade under anaerobic conditions (Urgun-Demirtas et al. 2007). The type of polymer used (aromatic polyester and polyether PUR) and the highly cross-linked structure of the foam were significant factors slowing the decomposition process. However, Cregut et al. (2013) observed microbially mediated degradation of polyether based PUR (rigid foam similar to Urgun-Demirtas study) up to 27.5% over a month long biodegradation assay. Unlike the Urgun-Demirtas et al. (2007) study, Cregut et al. (2013) used a microbial inoculum isolated from an industrial site where PUR had been buried for 40 years, suggesting that PUR materials are biodegradable to some extent under similar environmental conditions. These favorable conditions generally are not expected to occur in younger, operating landfills and thus, biodegradation of PUR materials is expected to be low. The biodegradation potential of most polystyrene rigid foams was indicated to be very low (Kaplan et al. 1979, Otake et al. 1995). No definitive pathway has been identified for PS degradation (Gautam et al. 2007). As a result of microbial activity, little to no degradation or change in the structure of XPS/EPS foam is expected in the landfill environment.

Chemical processes mostly are associated with a given phase change or equilibrium conditions for a certain compound within a landfill. The compound of interest may volatilize, evaporate, or sorb onto different waste materials present. Other chemical transformations include dissolution, condensation, or microbially mediated dehalogenation or decomposition processes. Thus, the chemical transformation ultimately controls the transportation or sequestration of the chemical into or out of the landfill environment (Tchobanoglous et al. 1993).

Heat, in addition to gas and leachate, is a byproduct of biochemical processes that occur within the landfill environment (Yesiller et al. 2005). Heat generation is associated with the anaerobic decomposition of wastes as well as the chemical transformations occurring within the landfill environment. The elevated temperatures generated affect the ongoing biochemical processes, mechanical and hydraulic properties and behavior of the wastes, as well as the engineering properties of liners, covers, and surrounding subgrade soils. Temperature affects solid waste decomposition in two ways: short-term effects on reaction rates and longer-term effects on microbial population balance (Hartz et al. 1982). In general, decomposition of wastes increases with increasing temperatures up to limiting values. Optimum

temperature ranges for the growth of mesophilic and thermophilic bacteria were identified to be 30 to 40°C and 50 to 60°C, respectively, in laboratory studies (Cecchi et al. 1993, Tchobanoglous et al. 1993). Optimum temperature ranges for maximum gas production from waste decomposition were identified to range between 34 and 41°C in laboratory studies (Merz 1964 and Ramaswamy 1970 as reported in DeWalle 1978, Hartz et al. 1982, Mata-Alvarez and Martinez-Viturtia 1986). A temperature range of 40 to 45°C was identified as the optimum range for gas production at a landfill in England (Rees 1980a, b). In addition, engineering properties of wastes are affected by temperature. Settlements increased with increasing temperatures in a laboratory study (Lamothe and Edgers 1994). Increased settlements indicate a potential decrease in shear strength of wastes, which can affect stability of waste slopes. In analogy to soils, hydraulic properties and behavior of wastes also are expected to be affected by temperature.

Yesiller et al. (2005) and Hanson et al. (2010) studied heat generation in four landfill sites in North America in different climatic regions (Michigan, New Mexico, Alaska, and British Columbia) and with variable operational conditions. Waste ages investigated ranged from under 1 year to more than 38 years. Temperatures of wastes at shallow depths (up to 6 to 8 m depth) and near edges of cells (within approximately 20 m) conformed to seasonal variations, whereas steady elevated temperatures (25 to over 60°C) were reached at depth and at central locations. Temperatures decreased from the elevated levels near the base of landfills, yet remained higher than ground temperatures. The time-averaged waste temperatures were 1 to 33°C, 13 to 49°C, 15 to 56°C, and 21 to 34°C in Alaska, British Columbia, Michigan, and New Mexico, respectively. Thermal gradients were in the range of approximately –30 to +22°C/m with average absolute values typically less than 5°C/m. The highest values for heat generation, temperatures, gradients, and heat gain were observed for the Michigan site, followed by (in decreasing order): the British Columbia, Alaska, and New Mexico sites. The maximum heat gain in wastes was observed in Michigan due to coupled high precipitation/moisture conditions and high waste density, whereas the lowest differential was observed in New Mexico due to the dry climate and low waste density. The highest heat generation (i.e., energy) and fastest heat gain (i.e., rate of temperature change) was observed in British Columbia due to enhanced microbial activity associated with high precipitation and wet wastes. However, the highest heat gain (i.e., magnitude of temperature change) did not occur at this site due to the coupled comparatively high heat capacity and low dry density of these wet wastes. In British Columbia, temperature increases occurred for multiple years and then dissipated for tens of years. High waste moisture conditions resulted in rapid temperature increases. Longer periods of temperature increase were observed at the other sites, where temperatures continued to increase subsequent to approximately a decade since waste placement. Higher temperatures, temperature increases, and heat gain occurred during anaerobic decomposition of wastes than under aerobic conditions. Sustained high temperatures were measured in wastes under post-aerobic conditions that started within a few weeks to 3 months subsequent to waste placement.

Kinetics and volatile products of thermal degradation of the building insulation materials, XPS, EPS, and PUR, were investigated by Jiao et al. (2012). Thermal degradation was indicated to occur with the onset of the amorphous stage (glass transition temperature, $T_g$) for the polymers. The $T_g$ was reported to be 71, 228, and 377.4°C for PUR, XPS, and EPS, respectively. While some thermal degradation of the foam structure of the PUR materials and associated BA releases may be expected in the landfill environment due to the relatively low glass transition temperature, significant thermal effects are not likely for XPS and EPS foam wastes. Temperatures and heat generation in landfills will have indirect effects on BA releases due to the influence of temperatures on the structure of the waste mass through increased compressibility and reduced shear strength under prolonged elevated temperature conditions.

Net methane and trace gas emissions from landfills may be reduced due to microbial populations oxidizing the LFG components in landfill covers. This process occurs naturally in cover environments, particularly in soil covers and covers with high organic matter content such as compost and mulch. Oxidation in covers includes conversion of methane and other organics, oxygen, and nutrients to new bacterial cells, resistant organic matter, carbon dioxide, water vapor, ammonia, sulfate, and heat by aerobic methanotrophs (Scheutz 2005). Methane oxidation has been studied extensively as it affects the amount of methane released to the atmosphere from landfills (e.g., Bogner et al. 1997c, Börjesson et al. 2000, Abichou et al. 2006a, 2006c, Spokas et al. 2006, Powelson et al. 2007, Stern et al. 2007, Spokas and Bogner 2011). Scheutz (2005) identified two types of aerobic methanotrophs (Type I and Type II) with oxidation capabilities within landfill soil covers. The Type I methanotrophs facilitated conversion processes with low oxidation rates and favored low methane concentrations and high oxygen concentrations near the surface (within 0 to 15 cm). The Type II methanotrophs facilitated conversion processes with high oxidation rates and favored high methane concentrations and lower oxygen concentrations (usually 15 cm to 40 cm below the surface). In general, maximum oxidation activity was reported to occur within the top 15 to 20 cm of a soil cover profile with possible extension to 30 to 40 cm beneath the surface (sometimes to 60 to 70 cm depth) (Jones and Nedwell 1993, Czepiel et al. 1996a).

Oxidation in covers was reported to vary between landfill sites and cover soil conditions. The conditions necessary for the oxidation of methane and other LFG components included an environment with a stable pH, warm temperatures, oxygen availability and lack of carbon dioxide, sufficient amount and residence time of gas components in the cover, optimum moisture content, as well as the absence of inhibitory concentrations of metals, ammonia, sulfides, and toxic components (SCS 2008). Optimum temperatures for methane oxidation were identified to range between 20 and 30°C with 30°C identified as the optimum temperature in several studies (Whalen et al. 1990, Figueroa 1993, Bender and Conrad 1994, Boeckx et al. 1996, Boeckx and Van Cleemput 1996, Stein and Hettiaratchi 2001, Scheutz et al. 2004, Scheutz and Kjeldsen 2004, Streese-Kleeberg and Stegmann 2008, Spokas and Bogner 2011, Spokas et al. 2011). The optimum moisture content was determined to

generally vary between 15 and 25% with optimum moistures identified as low as 10% and over 30% (Whalen et al. 1990, Figueroa 1993, Bender and Conrad 1994, Boeckx et al. 1996, Boeckx and Van Cleemput 1996, Czepiel et al. 1996a, Börjesson 1997, Stein and Hettiaratchi, 2001, Scheutz et al. 2004, Scheutz and Kjeldsen 2004, Streese-Kleeberg and Stegmann 2008). An average oxidation rate of 35% was reported based on a summary of studies with different soil types, with high rates associated with sand soils (55%) and low rates with clay soils (22%) (SCS 2008). Methane oxidation rates overall varied from on the low end less than 1 $\mu$g $CH_4$ / g soil-day to over several hundred $\mu$g $CH_4$ / g soil-day. Methane oxidation rates also varied according to site specific operational conditions such as the presence of daily, intermediate, and final cover systems compared across three landfill sites in California (Bogner et al. 2011).

### 1.4.3 Environmental Factors

Common environmental factors that influence the landfill environment in relation to BA emissions include climatic conditions and seasonal weather patterns and ambient concentrations of halocarbons or greenhouse gases. Seasonal weather patterns affect moisture content of wastes, as well as heat generation, and temperature of wastes within a landfill and hence the anaerobic/aerobic degradation processes and the production and migration of LFG. Heat generation in landfills is directly influenced by waste placement temperatures with higher long-term waste temperatures resulting from higher temperatures at the time of waste placement (Yesiller et al. 2005, Hanson et al. 2005, Hanson et al. 2006). Waste temperature variations in tens of °C may occur as a function of initial waste temperatures in particular in areas with significant seasonal temperature variations. Landfill gas production is impeded at low waste temperatures. Heat generation also is significantly influenced by precipitation with maximum heat gain occurring in wastes in areas with average precipitation on the order of 2 mm/day (Yesiller et al. 2005). Waste moisture contents in the range of 50 to 60% (w/w wet) were indicted to be required for waste temperatures to reach 40 to 45°C (Rees 1980a).

In addition to anaerobic degradation/gas production, aerobic oxidation of methane and other trace gas components is influenced by seasonal weather patterns. Temperature and moisture content in covers have significant effects on gas emissions (Stern et al. 2007). Optimum ranges exist both for temperature and moisture content to achieve maximum gas oxidation rates. Cover temperatures at test sites in four climatic regions were investigated in detail (Yesiller et al. 2008b). Temperatures in the cover systems underwent seasonal variations similar to air temperatures and demonstrated amplitude decrement and phase lag with depth. Heat generation and elevated temperatures in the underlying wastes resulted in warmer temperatures and lower frost penetration in the covers compared to nearby subgrade soils. While seasonal air temperature fluctuations were predominant in controlling cover temperatures, the presence of underlying wastes at elevated temperatures also influenced cover temperatures and thermal properties. In general, maximum temperatures decreased and minimum temperatures increased with cover system depth, resulting in decreases in the ranges of measured temperatures with depth. Average temperatures generally increased with

depth at the sites. The ranges of measured temperatures ($T_{max}$−$T_{min}$) varied between 18.2 and 30.2°C and between 12.9 and 21.4°C at 1 and 2 m depths, respectively. The average temperatures varied between 12.9 and 17.5°C and between 14.3 and 23.3°C at 1 and 2 m depths, respectively. For soil and geosynthetic barrier materials around 1 m depth, the maximum and minimum temperatures were 22–25°C and 3–4°C, respectively. The prevailing direction of heat flow in the covers was upward (negative gradients) and the maximum and minimum cover gradients were 14 and −18°C/m, respectively, with average gradients in the range of −7 to 1°C/m. The gradients for barrier materials around 1 m depth varied between −11 and 9°C/m with an average of −2°C/m.

Variations in LFG flux were observed with season. Christophersen et al. (2001) reported larger fluxes of LFG during the summer months compared to winter and spring. Park and Shin (2001) observed similar seasonal trends of LFG flux, with fluxes ranging from 0.1584 to 0.8597 ($m^3/m^2$-hour) for winter and summer, respectively. Also, the composition of LFG varied with season with high carbon dioxide and low methane fluxes observed in summer (high oxidation) and low carbon dioxide and high methane fluxes (low oxidation) observed in winter (Börjesson et al. 2001, Christophersen et al. 2001). Hanson et al. (2005) reported that both methane and carbon dioxide concentrations of wastes at shallow depths near a landfill surface followed seasonal trends and varied with seasonal variations of waste temperatures at similar depths. In climates with low seasonal variations, ambient temperatures had low impact on methane production as compared to the effects of barometric pressure (Xu et al. 2013). In addition, soil moisture content near the surface affected LFG emissions, where emissions decreased with increasing moisture content due to reduced gas permeability (Börjesson and Svensson 1997, Christophersen et al. 2001). High precipitation coupled with a rapid drop in atmospheric pressure resulted in high advective flux of LFG into the atmosphere (Christophersen et al. 2001). These conditions also resulted in reduced oxidation and a larger fraction of methane in LFG. Jones and Nedwell (1993) indicated that the release of methane was higher in winter than summer due to higher precipitation and induced saturation of the pores of the soil cover and reduction in oxidation processes from this oversaturation (reduced gas transport). Therefore, increased precipitation rates may negatively affect the production, movement, transport, and composition of LFG.

Moisture content within a landfill, as affected by annual precipitation and the inherent moisture content of the disposed waste, affects the production of leachate, LFG, and heat. Moisture is required for the biological decomposition of wastes. Optimum waste moisture contents range from 50 to 60% (w/w wet basis) for maximum production of LFG (Tchobanoglous et al. 1993). A waste moisture content of 55% (w/w wet basis) resulted in high LFG production at a landfill site in a temperate climate (Rees 1980b). The moisture content of individual MSW components vary over a wide range with high values associated with organic wastes (approximately 80% for food waste) and low values associated with inorganic components (as low as 1-2% for metal and glass) (Tchobanoglous et al. 1993). Incoming MSW moisture contents vary with season and were reported to be approximately 30 and 50% for winter and summer, respectively at

a landfill located in a humid temperate climate (Hanson et al. 2010). Moisture contents also may vary with landfill depth. Higher moisture contents on the order of 20% at shallow depths and lower moisture contents on the order of 10% at great depths were reported at a landfill located in the Midwest (Zekkos et al. 2007). The organic contents at great depths at the landfill were low and were assumed to be associated with the low moisture contents. The amount of water entering through the cover materials depends on the hydraulic conductivity/field capacity and hydrologic balance parameters for conventional and alternative covers, respectively.

Both the concentration of atmospheric methane and trace gas components as well as the barometric pressure can further affect the emissions and transport of LFG components. Methane emissions were observed to be inversely related to atmospheric pressure (Young 1992, Czepiel et al. 1996a, and Christophersen et al. 2001, Czepiel et al. 2003, Xu et al. 2013). Methane emission quantities and rates were strongly dependent on atmospheric pressure changes, where rising atmospheric pressure suppressed the emission of LFG and falling atmospheric pressure enhanced emissions. Xu et al. (2013) cautioned that annual total gas emissions could not be accurately predicted from short-term emission rates without incorporating the effects of barometric pressure.

The concentration of atmospheric methane/trace gas components also can affect the diffusion processes within the landfill environment. Diffusion relies on the movement of gas from areas of high concentration to low concentration (Rettenberger and Stegmann 1996). Migration of LFG out of a landfill due to diffusion can be impeded, if the concentrations of methane or trace gas components are higher in the atmosphere than in the LFG (Rettenberger and Stegmann 1996). Landfills can act as both atmospheric sources and sinks for methane and trace NMOCs as a function of relative outflow or inflow (i.e., positive or negative fluxes) of gases from the landfill system (Bogner et al. 1995).

In summary, environmental conditions at landfills affect the extent of anaerobic or aerobic decomposition; heat generation within the waste mass; engineering properties of the waste mass and cover/bottom liner systems; waste and soil structure as well as the gas/water transport phenomena associated with each; as well as overall oxidation processes within the soil cover. All of these effects, as a result of environmental conditions (depending on geographic location) may significantly influence the emissions of target BAs from the landfill. Thus, emissions of BAs from landfills, and trace gas components in particular are site specific, and vary with environmental conditions associated with the respective landfill geographic location.

## 1.5 CFCs, HCFCs, and HFCs in Landfills

### 1.5.1 CFCs, HCFCs, and HFCs Entering Landfills

The concentrations and amount of CFCs, HCFCs, and HFCs in rigid foam insulation wastes entering landfills are based on initial BA content and emissions of these chemicals during manufacturing, use, and throughout end of life practices prior to

disposal. Analyses of data from Caleb (2011) were used to estimate the amount and concentration of CFCs, HCFCs, and HFCs entering landfills and the amount of the BAs in landfills banked at the current time and projected to be banked in the future. In addition, the report was used to estimate emissions from the banks identified. The Caleb (2011) report, developed for CARB, was the main available literature source identified by the research team. Data in the Caleb (2011) report were primarily obtained from surveys and interviews with limited detailed references and may not be entirely representative of full industry, rigid foam manufacturing, reuse, and disposal trends.

The total amount of foam waste generated in California was estimated to be 930,350 $m^3$/year for 2008 (Caleb 2011). Approximately 48% of the foam waste disposed was estimated to be building insulation foam compared to 34% domestic appliance foam waste with lower quantities associated with other categories of use as presented in Figure 14. The amount of blowing agents entering end of life processes was estimated using total amount of foam waste generation. Caleb (2011) provided timelines associated with historical use of the three different BA types (i.e., CFCs, HCFCs, and HFCs) in California. These reported values for composition of BAs in different categories of foam applications were used to provide estimates for current and future conditions for foam wastes at end of life and foam wastes entering landfill facilities in Figure 15 and Figure 16, respectively. Overall, significant decreases in CFCs and increases in HFCs are expected due to the BA substitutions in foams over time. Additional detailed analyses for lifetime characteristics of rigid foams are provided in the Materials Flow Analysis section (Part 2) of this report.

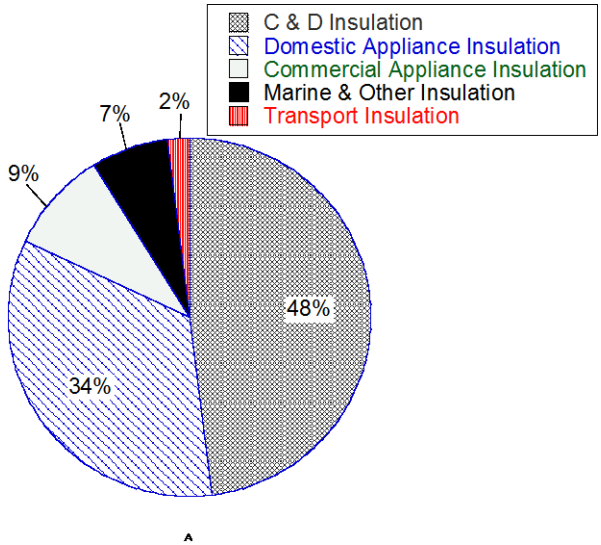


Figure 14. Sources of Foam Waste Generated in California (Caleb 2011)

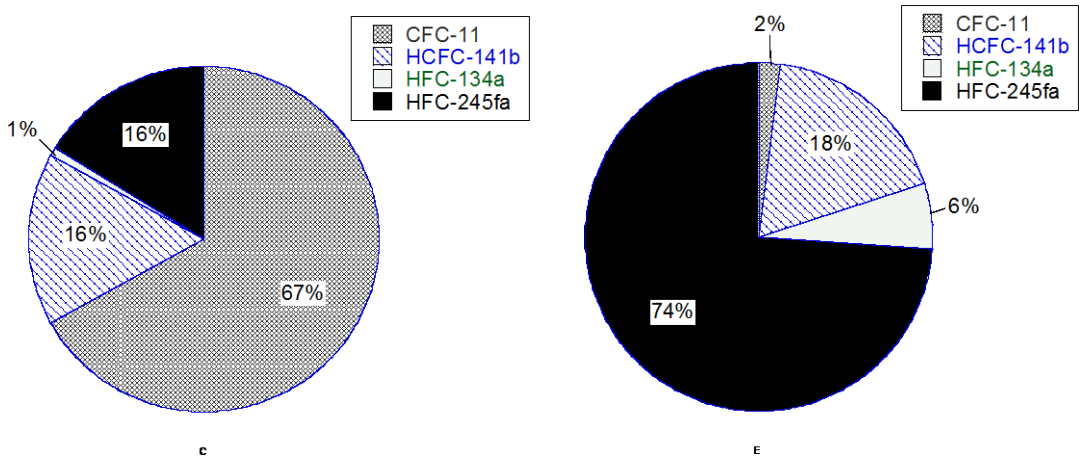


(a) Current (2,705 tonnes BA/year) (b) Future (3,418 tonnes BA/year)

Figure 15. Foam Waste Insulation Materials Entering End of Life Management

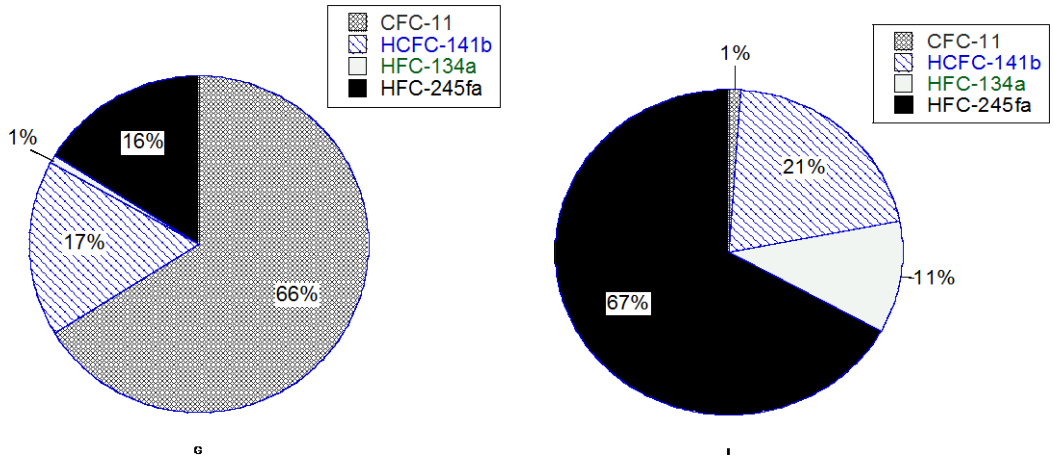


(a) Current (1,784 tonnes BA/year) (b) Future (1,655 tonnes BA/year)

Figure 16. Foam Waste Insulation Materials Entering Landfills

The overall amount of foam wastes generated in the future was predicted to increase, whereas the amount disposed of in landfills in the future was predicted to decrease from current conditions based on the data presented in Figures 15 and 16. For current conditions, CFC-11 represented the highest amount of BA material to enter end of life management processes and to be disposed of in landfills. For future conditions, HFC-245fa represented the highest amount of BA material to enter end of life management

processes and to be disposed of in landfills. The extent of reduction due to emissions of BA during end of life management practices prior to landfill disposal was more pronounced for HFC-245fa for future conditions (74 to 67%) than for CFC-11 for current conditions (67 to 66%). This difference resulted from the higher long-term diffusion and short term losses used HFC-245fa than CFC-11.

### 1.5.2 Banks of CFCs, HCFCs, and HFCs in Landfills

Development of CFC, HCFC, and HFC banks from foam wastes in California was analyzed in Caleb (2011). Data were generated for total amount of foam wastes and foam wastes in landfills for the time period between 1996 and 2020 (Tables 14 and 15). The total bank in California for each insulation category was a function of the total amount of CFCs, HCFCs, and HFCs in foams currently in use and predicted to be in use in the future, emissions during manufacturing/usage/at end of life, as well as the amount of BAs in foams entering the waste stream (correlated to the yearly disposal/demolition rate) and previously accumulated in landfills. Highest BA banks were associated with buildings followed by appliances with smaller quantities associated with other application categories. The BA bank estimates declined from the 364 $MMTCO_2$-eq level in 1996 to 227 $MMTCO_2$-eq by 2020 (Table 14). In contrast, the HFC bank was estimated to be increasing with a projected amount of 98.8 $MMTCO_2$-eq in 2020. The growth of the total HFC bank was largely determined to be due to the building sector foam insulation (Caleb 2011).

Table 14 – Summary of All Blowing Agent Banks ($MMTCO_2$-eq)

| Year | Buildings | Appliances | Other Refrigeration | TRUs | Marine & Other | Total |
|---|---|---|---|---|---|---|
| 1996 | 286.31 | 41.28 | 6.08 | 15.01 | 15.01 | 363.69 |
| 2005 | 267.72 | 28.89 | 2.82 | 7.81 | 7.81 | 315.05 |
| 2010 | 244.97 | 25.15 | 1.59 | 3.65 | 3.65 | 279.01 |
| 2020 | 182.73 | 27.92 | 2.01 | 2.49 | 2.49 | 227.64 |

Table 15 – Summary of HFC Blowing Agent Banks ($MMTCO_2$-eq)

| Year | Buildings | Appliances | Other Refrigeration | TRUs | Marine & Other | Total |
|---|---|---|---|---|---|---|
| 1996 | 0.00 | 0.04 | 0.00 | 0.00 | 0.00 | 0.04 |
| 2005 | 2.93 | 5.79 | 0.25 | 0.69 | 0.69 | 10.35 |
| 2010 | 9.99 | 17.27 | 0.89 | 1.72 | 1.72 | 31.59 |
| 2020 | 53.98 | 37.88 | 2.00 | 2.47 | 2.47 | 98.80 |

The total amount of BAs in California landfills was estimated to be 50,000 tonnes in 2010 and projected to increase to 100,000 tonnes and 164 $MMTCO_2$-eq by 2020 (Caleb 2011). Highest BA banks in landfills resulted from building foam wastes followed by appliance foam wastes with smaller quantities associated with other application categories (Table 16). The cumulative fraction of CFCs, HCFCs, and HFCs in landfill BA banks was 40% in 2010, which was predicted to expand to 72% in 2020 (Caleb 2011). The composition of the banked BAs in landfills was predicted to include large fractions of CFCs with low fractions of HCFCs and HFCs by 2020 (Figure 16). The majority of BAs entering landfills are associated with buildings that have long

service lifetimes (50 years). CFCs will continue to dominate the BA composition in landfill banks as old buildings with CFC BAs are decommissioned. The relative fraction of HCFCs and HFCs are expected to increase in landfill banks as these BAs have become the main type of BAs used in foam applications, in particular with the entry of foams from appliances with relatively short lifetimes (20 years) into the waste stream. Thus, emissions from California landfill foam waste banks are expected to primarily include CFC-11 with increases in emissions of HCFC-141b and HFC-245fa for the near future (Figure 17).

Table 16 – Summary of Blowing Agent Banks in Landfills ($MTCO_2$-eq)

| Year | Buildings | Appliances | Other Refrigeration | TRUs | Marine & Other | Total |
|---|---|---|---|---|---|---|
| 1996 | 14.7 | 10.21 | 1.80 | 1.91 | 9.07 | 37.7 |
| 2005 | 40.4 | 24.60 | 3.99 | 3.19 | 13.40 | 85.6 |
| 2010 | 58.7 | 29.77 | 4.43 | 3.92 | 16 | 112.8 |
| 2020 | 109.7 | 32.85 | 4 | 3.80 | 13.33 | 163.7 |

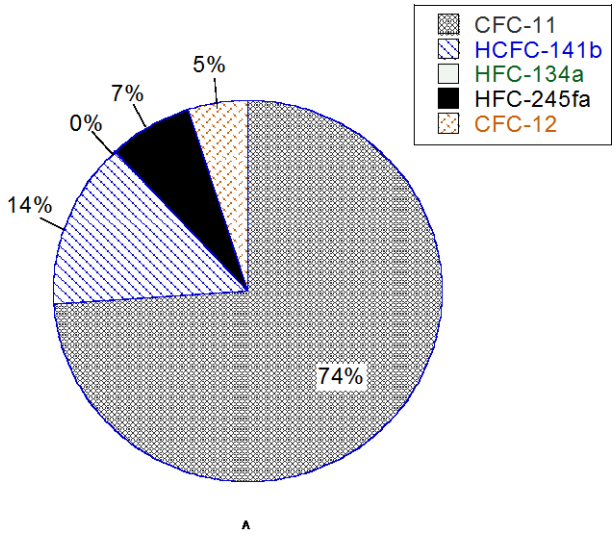


Figure 17. Composition of BAs Banked in California Landfills (2020 Projections)

### 1.5.3 Fate of BAs in the Landfill Environment

The fate of BAs in the landfill environment is highly dependent on the conversion processes in the landfill, both chemical and biological in nature. The fate of the BAs is controlled in particular by anaerobic degradation processes within the waste mass and at great depth in the soil cover. In addition, oxidation of CFCs, HCFCs, and HFCs in the top portion of soil covers affects the fate of these chemicals. These two biological processes together (i.e., degradation and oxidation) govern the amount of BAs in the landfill environment as well as the amount and rate of emissions from landfills. Other chemical processes including sorption of the chemicals to the waste mass and

dissolution in the leachate also contribute to the transport of the BAs within the waste mass and to the emissions of BAs from the landfill environment.

The degradation and oxidation of insulation foam BAs disposed of in landfills were evaluated in laboratory investigations using cover soil samples from multiple field sites. A summary of the landfill sites studied in the investigations included in this review and the characteristics of cover soils at each site is presented in Table 17. Laboratory experiments were conducted using both packed soil columns and microcosms containing wastes and soils sampled from landfill sites to determine oxidation levels and degradation rates of CFCs, HCFCs, and HFCs (Tables 18 and 19) (Scheutz et al. 2003a-d, 2008, 2009, 2011a). In addition, waste microcosm tests included investigation of anaerobic degradation of halogenated hydrocarbons in the presence of sampled MSW and landfill cover soil under simulated landfill conditions. All of the landfill sites investigated in soil column and microcosm tests were located in European countries and differed with respect to waste age, composition, operational conditions, and amount of waste received. In addition, the soil cover characteristics were compared, among the studies presented, based on depth sampled (from the top of the cover), total moisture content, total organic carbon content, as well as total nitrogen content.

The wastes used in waste microcosm laboratory experiments differed according to waste age, composition, and origin and was either: a) collected from Danish households directly; b) excavated from a U.S. landfill; or c) sampled from an experimental digester simulating landfill conditions (Table 20) (Scheutz et al. 2003a, 2007b). The Danish household waste was fresh and high in organic content, consisting of well-sorted fruits, bread, vegetables, rice, and corn. The U.S. waste was more mature and had a lower organic content, but more likely contained anaerobic bacteria preconditioned to BA degradation under anaerobic conditions present in the landfill environment. The digester waste was the most mature/decomposed of the three samples and was obtained from either a mesophilic biogas reactor (receiving agricultural waste) or from a biological sewage treatment plant (Scheutz et al. 2003a, 2007b).

Correlations were observed based on the reviewed studies between soil cover characteristics (i.e., composition, depth, soil moisture content, TOC/TON) and measured BA oxidation/degradation rates. Oxidation rates of methane/HCFCs were typically higher for final covers as compared to intermediate cover systems. In general, higher oxidation rates for HCFCs corresponded with soils sampled within the top 15-25 cm of final soil covers (loamy sands) at high moisture contents. In these areas of high oxidation, a high TOC/TON level was measured from the production/accumulation of organic carbon/nutrients as a byproduct of cellular aerobic respiration. The presence of a gas extraction system or a geomembrane also affected oxidation/degradation of methane and BAs. Higher oxidation rates were observed for final covers with an active gas extraction system (without a geomembrane) due to the increased diffusion of air into the cover system moving the oxidation zone closer to the surface. The presence of a geomembrane severely limited the vertical diffusion of air/LFG into the top

portions of the soil covers used, thereby decreasing oxidation rates. Higher anaerobic degradation rates corresponded with soil sampled from well below 50 cm within the final soil covers, where moisture was available and oxygen was limited.

Fate of methane and trace organic constituents in various cover materials were primarily investigated in laboratory packed soil column experiments simulating landfill cover conditions (Scheutz et al. 2003a, 2009, Scheutz and Kjeldsen 2003b). Artificial LFG with similar trace gas concentrations (containing CFCs, HCFCs, and HFCs of interest) was introduced from the bottom of the columns and allowed to flow through the height of the column. Aerobic conditions were established near the top of the columns, whereas anaerobic conditions were present near the bottom of the columns. A summary of the results for methane and CFC-11 (the only target gas studied) is presented in Table 18.

Compost mixtures, in particular mixtures with woodchips, had higher oxidation and degradation efficiencies than sand and gravel cover soils in the soil column experiments, most likely due to the increased porosity/gas transport provided by the addition of wood chips (Scheutz et al. 2009). Methane oxidation and CFC-11 degradation efficiencies decreased with increasing LFG flow rate and concentration of constituent components of interest in the LFG (Table 18). The decrease in removal of the gases was due to a smaller residence time of LFG within the soil column with a higher flow rate. As the oxidation zone moved upwards with increased flow rates, a larger anaerobic zone was created, sustaining the degradation of CFCs, but not HCFCs. Increasing the inlet concentration of CFC-11 at similar flow rates decreased the methane oxidation capacity, yet increased the CFC-11 degradation capacity/efficiency (Scheutz and Kjeldsen 2003b). Lower methane oxidation rates were observed for columns with higher concentrations of HCFCs, indicating competitive inhibition of oxidation with the methanotroph population present in the cover (Scheutz and Kjeldsen 2003b). However, no inhibition of methane oxidation was observed for columns with CFCs (higher chlorinated compounds) since these chemicals are not oxidized in aerobic environments (Scheutz and Kjeldsen 2003b). Degradation of the CFCs occurred within the anaerobic portions of the columns, while the HCFCs investigated degraded mainly in the aerobic zones in the columns (Scheutz et al. 2003a, 2009, Scheutz and Kjeldsen 2003b).

Methane oxidation and attenuation of halogenated/fluorinated hydrocarbons in the soil specimens also were evaluated under both aerobic and anaerobic conditions using laboratory soil microcosms simulating landfill conditions (Table 19). Soil microcosm experiments generally involved incubating a fixed amount of sampled cover soil at a given temperature and moisture content (simulating landfill conditions) with trace CFCs, HCFCs, and HFCs inserted in the headspace. The degradation or oxidation rates were determined by measuring the concentration of the CFCs, HCFCs, or HFCs remaining over time. Similar procedures were used for waste microcosm tests, but sampled waste was added in addition to the soil already present. Overall, for both soil and waste microcosm tests, oxidation rates were determined to follow zero order

kinetics, since the experiments were not methane limited (Table 19) and degradation was defined under either zero or first order kinetics (Tables 19 and 20).

Results for the soil microcosm tests indicated that the CFCs studied (CFC-11, CFC-12, CFC-113) did not degrade in the presence of oxygen in the soil microcosm experiments, whereas degradation was observed under anaerobic conditions (Table 19). The majority of the HCFCs studied (HCFC-21, HCFC-22, HCFC-31, HCFC-32) were oxidized in aerobic experiments and degraded in anaerobic experiments, where oxidation rates were generally higher than anaerobic degradation rates following both zero and first order kinetics (Table 19). However, HCFC-141b did not undergo oxidation, whereas anaerobic degradation following zero order kinetics was observed at slow rates (0.005 μg / g soil-day) (Table 19). Under anaerobic conditions, degradation was fastest for CFC-11 followed by HCFC-141b. HFC-41 was the only HFC that underwent aerobic oxidation and anaerobic degradation, where oxidation rates were generally higher than degradation rates (both zero and first order). In general, HFC-134a and HFC-245fa did not undergo neither aerobic oxidation nor anaerobic degradation in the soil microcosm experiments (Table 19).

Results of the waste microcosm tests indicated that the degradation coefficients for CFC-11 were higher than those for HCFC-141b, whereas degradation was not observed for the HFCs 134a and 245fa (Table 20). In general, the difference in degradation rates between CFC-11 and HCFC-141b was on the order of a magnitude. The degradation rates for fresh wastes were somewhat higher than the degradation rates for old wastes due potentially to higher amount of organic content and moisture content of fresh wastes compared to old wastes. Increasing the amount (mass) of fresh (organic) waste added to the microcosms slowed the first order anaerobic degradation rate of CFC-11, while the degradation rate of HCFC-141b was unaffected (Table 20). Increasing the amount (mass) of older disposed (less organic) waste increased the first order degradation rate of HCFC-141b, while the degradation rate of CFC-11 was unaffected (Table 20).

Table 17 – Soil Cover Studies - Summary of Landfill Characteristics and Soils Sampled

| Reference (Scheutz et al.) | Landfill Sites | Years of Landfill Operation | Waste Received (tonnes) | Waste Composition | Cover Soil Composition (Top to Bottom) | Depth of Soil Sample (cm) | Soil Moisture Content (%w/w wet) | Total Organic Carbon (%w/w) | Total Organic Nitrogen (mg/kg) | Landfill Characteristics |
|---|---|---|---|---|---|---|---|---|---|---|
| (2003a) (2003b) (Scheutz & Kjeldsen 2003b) | Skellingsted, Denmark | 19 (1971-1990) | 420,000 | 60% MSW, 40% Other[1] | Final Cover: 0-35 cm loamy sand, 35-70 cm sandy loam, 70-90 cm coarse sand/gravel | 15 to 20 | 27 to 33 | 3.2 to 3.7 | 3190 to 3500 | Active Gas Extraction System (vertical wells) |
| (2003b) (2003d) | Lapouyade, France | 2 (1996-1998 Phase I) | 310,000 | Household, Industrial, Construction | Final Cover: 40 cm coarse sand + 80 cm clayey silt topsoil (vegetated) | 50 | 10.7 | 2.1 | - | Active Gas Extraction System (vertical wells) |
| | | 13 (1998-2011 Phase II) | N/A | | Intermediate Cover: 40 cm coarse sand | 15 to 25 | - | - | - | No Gas Extraction System |
| (2003b) (2008) | Grand' Landes, France | 12 (1989-2001) | 2,220,000[2] | 100% MSW | Final Cover Cell A: Leveling Layer, compacted clay (70 cm) and topsoil vegetation (30 cm) | 5-10 | 14 | 1.86 | 1250 | Active Gas Extraction System (vertical wells) |
| | | | | | Final Cover Cell B: 70 cm compacted clay, 30 cm vegetated topsoil, underlain with a geotextile, 1.5 mm thick geomembrane, geotextile, geogrid, and 30 cm of gravel (gas collection layer) | 30 to 40 | 10 | 3.22 | 2440 | Innovative Gas Collection System (lateral HDPE perforated pipes) |
| (2011a) | AV-Miljo, Denmark | 10 (1990-2000) | 155,000 | Disposal of Shredder Waste[3] | Intermediate Cover: sparsely vegetated | 20 to 60 | - | - | - | No Gas Extraction System |

[1]Other consists of bulky waste, industrial waste, and sewage treatment sludge

[2]The two different waste cells each received 54,000 metric tons of waste per cell over the operation period indicated.

[3]The waste cell contained primarily auto and appliance shredder residue (mostly metallic waste, very little LFG production expected)

N/A: Not applicable to the study

-: Omitted by the study

Table 18 – Soil Column Experiments

| Reference (Scheutz et al.) | Cover Soil Composition | LFG Flowrate ($m^3/m^2$/day) | Inlet BA Concnetration (μg/L) | Methane Oxidation (Aerobic) | | CFC-11 Degradation (Anaerobic) | |
|---|---|---|---|---|---|---|---|
| | | | | Efficiency (%) | Capacity ($g/m^2$/day) | Efficiency (%) | Capacity ($g/m^2$/day) |
| (2003a) | Alluvial Sand and Gravel Sediments (Final Cover) | 0.86 | 86 | 92 | 240 | 38 | 0.03 |
| | | | 108 | 79 | 194 | 75 | 0.07 |
| (Scheutz and Kjeldsen 2003b) | Alluvial Sand and Gravel Sediments (Final Cover) | 0.24 | 15 | 88-97 | - | 98 | - |
| | | 0.76 | 15 | 81 | 210 | 90 | 0.01 |
| | | 4.1 | 15 | 24 | - | 86 | - |
| (2009) | Compost/ Woodchips (1:1) | 0.7 to 0.77 | 200 | 58 | 247 | 86 | - |
| | Compost/ Sand (1:1) | | | -10 | 116 | 77 | - |
| | Compost/ Sand (1:5) | | | 12 | 144 | 29 | |
| | Supermuld[1] | | | 48 | 202 | -1 | - |

[1] Supermuld is a Danish commercial compost product consisting of mature compost and sand
N.D.: Not detected by the study
N/A: Not applicable to the study
-: Omitted by the study

Table 19 – Soil Microcosm Tests: Zero Order Aerobic Oxidation/ Anaerobic Degradation Rates

| Reference (Scheutz et al.) | Methane (µg/g soil-day) | CFC-11 (µg/g soil-day) | CFC-12 (µg/g soil-day) | CFC-113 (µg/g soil-day) | HCFC-141b (µg/g soil-day) | HCFC-21 (µg/g soil-day) | HCFC-22 (µg/g soil-day) | HCFC-31 (µg/g soil-day) | HCFC-32 (µg/g soil-day) | HFC-134a (µg/g soil-day) | HFC-245fa (µg/g soil-day) | HFC-41 (µg/g soil-day) |
|---|---|---|---|---|---|---|---|---|---|---|---|---|
| (2003a) | 3,168 | N.D.[1] | - | - | N.D.[1] | - | - | - | - | N.D.[1] | N.D.[1] | - |
| | - | 0.02[2] | - | - | 0.005[2] | - | - | - | - | N.D.[2] | N.D.[2] | - |
| | | | | | | | | | | | | |
| (2003b) | 2688 | N.D.[1] | N.D.[1] | N.D.[1] | - | 12.2[1] | 8.2[1] | - | - | - | - | - |
| | 35 | N.D.[1] | N.D.[1] | N.D.[1] | - | 0.2[1] | 0.1[1] | - | - | - | - | - |
| | 674 | N.D.[1] | N.D.[1] | N.D.[1] | - | 3.7[1] | 2.2[1] | - | - | - | - | - |
| (Scheutz and Kjeldsen 2003b) | 2688 | N.D.[1] | N.D.[1] | - | - | 12.22[1] | 8.23[1] | - | - | - | - | - |
| | 480 | | | | | | | | | | | |
| | 6000 | | | | | | | | | | | |
| | 6000 | | | | | | | | | | | |
| | - | 0.21[2] | 0.0096[2] | - | - | 0.0312[2] | 0.0048[2] | - | - | - | - | - |
| (2003d) | 34 | N.D.[1] | N.D.[1] | N.D.[1] | - | 0.189[1] | 0.081[1] | - | - | - | - | - |
| | - | N.D.[1] | - | - | - | - | - | - | - | - | - | - |
| (2008) | 674 | N.D.[1] | N.D.[1] | N.D.[1] | N.D.[1] | 3.7[1] | 2.2[1] | - | - | N.D.[1] | - | - |
| | 28 | N.D.[1] | N.D.[1] | N.D.[1] | N.D.[1] | 0.2[1] | 0.1[1] | - | - | N.D.[1] | - | - |
| (2009) | - | N.D.[1] | - | - | - | 15.84[1] | - | 104.4[1] | - | - | - | 121[1] |
| | - | N.D.[1] | - | - | - | 1.1[1] | - | 5.4[1] | - | - | - | 5.8[1] |
| | - | 0.07[2] | - | - | - | 0.07[2] | - | - | - | - | - | - |
| | - | -[2] | - | - | - | - | - | - | - | - | - | - |
| (2011a) | - | -0.12[2] | -0.009[2] | - | -0.005[2] | -0.01[2] | -0.004[2] | -0.004[2] | N.D.[2] | N.D.[2] | - | N.D.[2] |
| | 410 | N.D.[1] | N.D.[1] | - | N.D.[1] | -0.007[1] | N.D.[1] | -0.006[1] | -0.005[1] | N.D.[1] | - | -0.067[1] |

[1]These experiments were primarily aerobic and consisted of batch soil microcosms with soil sampled from landfill covers: 20 g of soil was inoculated with a mixture of methane, oxygen, and the trace gas component. The headspace concentrations of all gases were measured over time to predict the oxidation rates.
[2]These experiments were primarily anaerobic and consisted of batch soil microcosms with soil sampled from landfill covers: 20 g of soil was inoculated with a mixture of methane, nitrogen, and the trace gas component. The headspace concentrations of all gases were measured over time to predict the degradation rates.
N.D.: Not detected (no measurable degradation) by the Study
- : Omitted by the Study

Table 20 – Waste Microcosm Tests: First Order Degradation Rates

| Reference | MSW Origin | Waste Composition | Methane Flux from Soil Sample Location (g $CH_4$ / g waste - day) | Type of Blowing Agent | Initial Concentration of BA (µg/L) | Amount of Waste Added (g) | Half Life, $T_{1/2}$ (Days) | Water Based First Order Degradation Coefficient, λ ($Day^{-1}$) | First Order Degradation Coefficient ($Day^{-1}$) | Methane Production (Days)[1] |
|---|---|---|---|---|---|---|---|---|---|---|
| Scheutz et al. (2003a) | A: Organic waste collected from Danish households | Organic material: fruits, vegetable, breads, rice | 0.014 | CFC-11 | 215 | 1 | 2.4 | - | 0.293 | - |
| | | | | | 215 | 5 | 3.2 | - | 0.22 | - |
| | | | | | 215 | 10 | 3.4 | - | 0.205 | - |
| | | | | HCFC-141b | 246 | 1 | 34 | - | 0.02 | - |
| | | | | | 246 | 5 | 34 | - | 0.02 | - |
| | | | | | 246 | 10 | 34 | - | 0.02 | - |
| | B: Older pre-disposed waste from a U.S. Landfill | N/A | 0.002 | CFC-11 | 589 | 1 | 2 | - | 0.355 | - |
| | | | | | 589 | 5 | 1.9 | - | 0.362 | - |
| | | | | | 589 | 10 | 2 | - | 0.349 | - |
| | | | | HCFC-141b | 202 | 1 | - | - | - | - |
| | | | | | 202 | 5 | 18.8 | - | 0.037 | - |
| | | | | | 202 | 10 | 7.2 | - | 0.096 | - |
| Scheutz et al. (2007b) | A: Organic waste collected from Danish households | Organic material: fruits, vegetable, breads, rice N/A | 0.014 | CFC-11 | 215 | 1 | 1.5 | 16.14 | 0.426 | 16 |
| | | | | CFC-12 | 225 | 1 | 23.9 | 2.9 | 0.029 | 15 |
| | | | | HCFC-141b | 246 | 1 | 26.7 | 0.36 | 0.026 | 12 |
| | | | | HCFC-21 | 210 | 1 | 24.1 | 0.14 | 0.029 | ND |
| | | | | HCFC-22 | 215 | 1 | 46.2 | 0.19 | 0.015 | 26 |
| | | | | HCFC-31 | 137 | 1 | 65.4 | 0.03 | 0.011 | ND |
| | | | | HFC-134a | 367 | 1 | - | - | - | 18 |
| | | | | HFC-245fa | 348 | 1 | - | - | - | 26 |
| | | | | HFC-41 | 164 | 1 | - | - | - | ND |
| | B: Older pre-disposed waste from a U.S. Landfill | N/A | 0.002 | CFC-11 | 589 | 1 | 2.7 | 9.81 | 0.259 | 26 |
| | | | | CFC-12 | 252 | 1 | 63 | 0.03 | 0.011 | 70 |
| | | | | HCFC-141b | 202 | 1 | 57.8 | 0.17 | 0.012 | 45 |
| | | | | HCFC-21 | 555 | 1 | 2.8 | 9.51 | 0.251 | 21 |
| | | | | HCFC-22 | 102 | 1 | - | - | - | 150 |
| | | | | HCFC-31 | 520 | 1 | 7.2 | 3.64 | 0.096 | ND |
| | | | | HFC-134a | 215 | 1 | - | - | - | 55 |
| | | | | HFC-245fa | 289 | 1 | - | - | - | 35 |
| | | | | HFC-41 | 420 | 1 | 28.9 | 0.12 | 0.024 | 92 |
| | C: Waste from a laboratory digester | N/A | 0.001 | CFC-11 | 210 | 1 | 2.3 | 11.29 | 0.298 | 25 |
| | | | | HCFC-141b | 197 | 1 | 69.3 | 0.14 | 0.01 | 50 |
| | | | | HFC-134a | 210 | 1 | - | - | - | 67 |
| | | | | HFC-245fa | 283 | 1 | - | - | - | 46 |

[1] Indicates the time period required (days) for the headspace in the soil microcosm to reach 20% (v/v) concentration of methane
N.D.: Not detected by the study, N/A: Not applicable to the study
-: Omitted by the study

Factors that affect methane oxidation and aerobic attenuation of trace gases in soil covers were studied by Scheutz and Kjeldsen (2004). The parameters investigated included temperature, soil moisture, pH, and ammonium as well as the presence of trace organic compounds themselves to determine the extent of competitive inhibition. The tests were conducted on methane and hydrochlorofluorocarbons HCFC-21 and HCFC-22. Temperature was determined to have a significant effect on the fate of the gases investigated. Maximum oxidation rates for both methane and HCFCs were reached at 30°C and inhibition of the process commenced at 50°C. Bacteria were observed to be active at temperatures as low as 2°C. Moisture content of the soil also had a large effect on the oxidation of methane and HCFCs, where the optimum moisture content for maximum oxidation of methane ranged from 18 to 24% (w/w wet) (Scheutz and Kjeldsen 2004). The optimum moisture contents for oxidation of HCFCs occurred over a broader range between 17 and 33% (w/w wet). The ideal pH for oxidation of methane and HCFCs was determined to be approximately neutral (6.5 to 7.5). Amendment of the test soils (original natural ammonium concentration of 2.3 mg/kg) with ammonium did not affect the oxidation rates of methane or HCFCs up to a concentration of 14 mg/kg. At higher concentrations, the oxidation rates were observed to decrease. Ammonium concentrations in a landfill may inhibit methane/HCFC oxidation if the cover soil is fertilized to promote plant growth. Also, covers that contain nitrogen rich wastes such as sewage sludge or compost may interfere with the oxidation rates within the cover soil. Inhibition of methane oxidation was observed with increasing concentrations of the HCFCs.

Increasing the HCFC concentration from 0 to 1600 µg/L reduced the methane oxidation rate by approximately 30%. However, typical concentrations of HCFCs in landfill soil covers were stated to be on the order of 250 µg/L and not expected to inhibit methane oxidation. Other trace gas components may have an inhibitory effect on methane oxidation based on their toxicity or toxic nature of the degradation end products. Similarly, HCFC oxidation was observed to decrease significantly with increasing methane concentrations. This inhibitory effect was observed when methane concentrations increased from 0 to 23%, which reduced the HCFC oxidation rate by over 90% (Scheutz and Kjeldsen 2004). Zones in the cover soil near the surface, where methane concentrations are limited, may promote the degradation of HCFCs.

### 1.6 Measurement and Monitoring of MSW Landfill Surface Gas Conditions

Landfill gas generation rates and associated emissions are highly variable due to cover conditions (daily, intermediate, permanent), inherent heterogeneity of wastes, site-specific operational conditions (waste placement density, waste placement sequence, daily cover materials), and site-specific climatic conditions (precipitation, temperature, humidity, atmospheric pressure, seasonal waste placement temperature). Also, landfill gas emissions are highly variable both spatially and temporally within a given landfill as well as between landfills.

Landfill gas surface emissions are best represented by heterogeneous emission patterns. High emissions occur from discrete locations with limited areas as opposed

to continuous large areas with low diffuse emissions (e.g., Czepiel et al. 1996). Correlations in emissions between nearby locations generally are low. Concentrated emissions ("hot spots") of LFG (including trace components) are common in landfill facilities.

Hotspots result either from soil-bound preferential pathways (high gas porosity or high gas permeability) due to cracking/hardening/clogging of the soil structure (as a result of meteorological/environmental conditions such as limited precipitation, etc.) or due to areas of increased gas production present in waste layers beneath the soil cover (Ranchor et al. 2009). Hot spot areas may indicate larger positive fluxes to the atmosphere as a result of the high concentration differences in methane below the surface of the cover system and atmospheric concentrations. In addition, hot spots have been known to vary across landfill surfaces both temporally (different emissions in different seasons) as well as spatially (different emissions measured in different hotspots along the landfill surface) (Ranchor et al. 2009). Hotspots can be detected using portable real time FID surface-screenings of a landfill to determine areas of elevated methane or trace compound concentrations (Ranchor et al. 2009) or may be visually identified in areas with macro features. Areas of the landfill surface not identified as hot spots may have either low positive or negative surface flux/measured and/or low LFG concentrations.

In attempt to estimate gas emissions from the surfaces of landfills, typically ambient air quality is monitored for target gaseous compounds. These measurements are made using small to large-scale direct and indirect approaches applied on a continuous or discrete basis. Point, line, and areal measurements can be obtained. The surface emission monitoring (SEM) technologies can be used to estimate flux and/or concentration. The only technology that can be used to directly determine flux is the stationery enclosure technique. All of the other technologies provide concentrations, which can be used to estimate flux indirectly via analytical or numerical models. Data collection and analysis can be conducted using the technologies in various settings and configurations.

Emissions of trace gases from MSW landfill sites can be determined using time-integrated and real-time monitoring. LFG can be sampled using grab sampling, real-time sampling, and time-integrated sampling including the stationary enclosure techniques. One or more sampling techniques and additional sensing technologies can be used to measure emissions. The measurement methodologies can be grouped under three categories: discrete point/area measurement methodologies that can be used to measure concentration and flux; tracer testing that can be used to measure concentration and estimate flux; and optical remote sensing that can be used to measure concentration and estimate flux (Yesiller et al. 2008a).

### 1.6.1 Sampling Techniques

#### 1.6.1.1 Grab Sampling

Grab sampling provides measurement of gas concentration at a single point in time. This method is used as a screening technique to identify contaminants and determine

approximate concentrations in a given test area (USEPA 2005). The main advantage of grab sampling is the low sampling cost and simple testing requirements. The disadvantages include obtaining only a concentration at a single point in time, low sample volume, and potential diffusion of gases in or out of samplers. Common devices used for grab sampling in landfill emissions analysis are specially-treated canisters, glass sampling bulbs, Tedlar bags, or solid sorbent tubes (USEPA 2005). Canisters are used commonly due to their ruggedness and ease of cleaning for reuse (Pellizari et al. 1984). For collection of trace gases from landfills or cover/surrounding soils, USEPA established method TO-14/TO-15 that requires specially-treated canisters to be used (USEPA 2005). The most common type of canister used for grab sampling is the Summa canister. Summa canisters refer to steel canisters that have internal surfaces deactivated using the Summa process. Tedlar bags also have been utilized as they provide simple, cost-effective means of collecting gas samples (Pellizari et al. 1984). The bags are used only for short-term sampling as the reliable storage time is limited to 24 hours or less unless bags are protected from potential contamination or leakage (Pellizari et al. 1984). Glass bulbs are another type collection medium used for grab sampling. Glass bulbs have higher long-term storage stability than Tedlar bags, yet are fragile, which limit their practical use (Pellizari et al. 1984). Solid sorbent tubes refer to a sampling medium that utilizes the principle of adsorption to extract contaminants from gas samples (Peach and Carr 1986). A known volume is drawn into the tube at a controlled flow rate where appropriate packing materials are present. For analyses, the contaminants are extracted from the sorbent by a liquid solvent or thermal desorption. The advantages are ease of sample management in the field and ease of transportation to the laboratory (Peach and Carr 1986). Sorbent tubes are more suited to sample polar compounds and low volatility compounds while canister samples are useful in sampling highly volatile and reactive compounds (Harper 2000).

#### 1.6.1.2 Real-Time Sampling

Real time sampling is a technique that provides instantaneous concentration values (USEPA 2005). Multiple measurements can be made over a short period of time, which allows for analysis and reporting of data nearly instantaneously. An advantage of this technique is that most portable real-time sampling devices are nonselective, meaning that entire class of compounds can be measured at one time. One disadvantage of real-time sampling is that the analytical system required for measurement is expensive. Also, the portable systems used are complex requiring highly trained field personnel, rigorous calibration procedures, and independent performance audits of routine monitoring and data handling operations (USEPA 2005).

Flame ionization detection (FID) is one of the most commonly used portable gas sampling techniques for real-time monitoring (USEPA 2005). As a pollutant enters the detector, it is mixed and then burned in a hydrogen flame to produce both ions and electrons (Liptak 2003). The electrons produced then enter an electrode gap, with decreasing gap resistance, to create a current. The flow of current then can be used to determine the pollutant concentration (USEPA 2005). A specific advantage of using FID is that it does not detect oxygen or water in the measurement process, which

eliminates possible disturbance from these compounds during measurement (Liptak 2003). The FID system measures the carbon atom that has been consumed during the combustion process (Liptak 2003). FID responds to a host of organic compounds and classes (USEPA 2005). A main disadvantage is that a mixture varying in composition can be difficult to calibrate due to different detector responses and lower explosive limits of concentration between components in the mixture (Liptak 2003). Typical detection limits for FID are approximately 100 ppbv (USEPA 2005).

#### 1.6.1.3 Time Integrated Sampling

Time integrated sampling includes measurement of gas concentration over a time period to provide a single, integrated value (USEPA 2005). The sampling period can vary from minutes to days to weeks. This technique is often used to detect very low concentrations since the sampling period can be varied to provide the analytical system sufficiently large samples to meet the detection limit (USEPA 2005). Various time-integrated sampling methods are available to collect compounds ranging from volatiles, semi volatiles, inorganics, organics, to particulate matter (USEPA 2005). Time integrated sampling can be conducted either using continuously or discontinuously operating devices. Continuous devices provide high time resolution but lack the sensitivity or selectivity to detect presence of specific classes or families of pollutants (USEPA 2004). Discontinuous techniques are favored due to the ability to detect low pollutant concentrations (USEPA 2004).

Time integrated sampling can be conducted using active or passive sampling techniques (USEPA 2005). Active sampling utilizes pumps to allow the gas of interest to accumulate in the collection medium such as specially-treated canisters, sorbent tubes, impingers, or treated filters containing liquid media. Passive sampling method, utilizes physical processes such as diffusion to collect samples in contrast to active sampling, which requires an active moving medium (USEPA 2005). Gas samples are collected on an adsorbent in containers such as tubes over extended sampling periods to allow the full diffusion of a certain compound from the air. Passive sampling has become more popular in recent years because it is simple, convenient, and inexpensive for obtaining time-integrated analysis, especially for the measurement of volatile organics (USEPA 2005). Passive sampling is unique in that specificity can be integrated into measurements by choosing an adsorbent substrate that can capture a specific compound of interest. Once the adsorbed chemical is captured in the sorbent tube, the chemical can be released by thermal desorption or chromatographic separation, and concentration/flux can be determined knowing the duration of sampling, the sampling area, and the mass of the chemical collected (USEPA 2005). Overall, time-integrated sampling has several advantages. The technique can be cost-effective and allow for detection of chemicals present at low concentrations. The main disadvantage of the technique is the lack of real-time data, which may be significant in cases with potential issues with acute exposure. In addition, sample integrity problems may occur during transport of sampled media to another location for analysis (USEPA 2005).

#### 1.6.1.4 Stationary Enclosure Measurement

A commonly used time-integrated sampling technique includes the measurement of trace gas emissions through stationary enclosure methods. Use of stationary enclosure methods has been the most common approach employed in the studies conducted to analyze emissions of chlorinated and fluorinated hydrocarbons from landfills and thus covered in detail in this section.

Two types of stationary enclosure measurement methods exist: static and dynamic chamber methods (Hartman 2003). Static chamber methods differ from dynamic chamber methods in that there is no continuous inflow and outflow of gases; thus, emanating gas from the surface is accumulated in a chamber over time (Hartman 2003). This makes operation of static flux chambers simpler and more cost-effective than dynamic chambers with no requirement for active equipment (Heinemeyer et al. 2011). One primary disadvantage of static chamber methods is that surface emission flux rate may decrease, if a sufficiently high concentration gradient accumulates within the flux chamber (Hartman 2003) and static flux chambers may underestimate emission rates (Martin and Kerfoot 1988). For dynamic chamber methods, a constant flow rate of clean air is introduced into the flux chamber, which mixes and transports the emitted gas from the surface (Reinhart et al. 1992). Next, continuous gas concentration measurements are made through the exit port (Reinhart et al. 1992). One significant advantage of using the continuous flow method is that it is unlikely to have any concentration buildup that may impede emissions (Hartman 2003). One disadvantage is that, due to active measurement process, operating procedures and calibration is more complex (Hartman 2003). Also, dynamic chambers require an analysis method with lower detection limits due to dilution of gases to be measured from inlet flows (Hartman 2003). Equipment associated with dynamic chamber methods is considerably more expensive compared to flux chambers due to equipment required for the continuous flow system (Heinemeyer et al. 2011).

The primary enclosure measurement technique that has been used for analysis of trace gas concentrations is the static flux chamber. Static chamber methods have been used extensively to quantify both methane and trace gas fluxes (such as CFCs, HCFCs, and HFCs) (Bogner et al. 1997a, 1997b, 2003, 2004, 2007, 2010, Scheutz et al. 2003d, 2007c, 2008, 2011b). The principle behind a static chamber technique is to establish a sealed volume above a surface where gas is emitted through or gas is absorbed through such that the gas cannot escape and the accumulation or depletion of the gas in the volume can be monitored (Abichou et al. 2006a, 2006b, 2006c). Surface flux as well as concentration are determined for the corresponding area of the chamber. A rigid frame (i.e., a collar) is inserted and sealed into the surface of the landfill to a depth of 5-20 cm. A cover is placed over the frame and secured in place to form a tight seal. The chamber is equipped with ports for collection of gas from the headspace above the landfill surface. A photograph of a static flux chamber is provided in Figure 18.

Figure 18. Static Flux Chamber Installed at a California Landfill

The dimensions of the chamber typically are on the order of several tens of cm in diameter (circular frame) or along the sides (rectilinear frame) and a few tens of cm in height. The areas of the chambers vary between 0.1 and 1 $m^2$ (Bogner et al. 1997b, Börjesson et al. 1998, Abichou et al. 2006a, 2006b, Spokas et al. 2006, Scheutz and Kjeldsen 2003b, Scheutz et al. 2008, Stern et al. 2007). Use of smaller chambers also has been reported (Mosher et al. 1996, Czepiel et al. 1996a, Börjesson et al. 2000). Chambers with large volume to area ratios and short deployment times are recommended for areas with high amount of emissions, whereas chambers with low volume to area ratios are recommended for locations with low emissions (Livingston and Hutchinson 1995 as reported by Fourie and Morris 2004). Large static flux chambers with areas on the order of 1 $m^2$ are well suited for methane and trace NMOC surface flux quantification (Bogner et al. 1997a, 1997b, Barlaz et al. 2004). Increasing the accumulation area provides a high number of sampling opportunities over a given time period, thereby allowing for improved time series analysis (Bogner et al. 1997a, 1997b, Barlaz et al. 2004).

A fan is used in the chamber to circulate the gas collected to ensure uniform distribution. The gas is sampled using gas-tight syringes and stored either in the syringes equipped for sample storage or transferred to sealed containers for storage (Mosher et al. 1996, Bogner et al. 1997b, Börjesson et al. 1998, Abichou et al. 2006a, 2006c, Stern et al. 2007). The gas samples are then analyzed using analytical techniques such as gas chromatography in the field or in the laboratory for determination of concentrations. An alternative method is provided by Spokas et al. (2006), where a pump is used to circulate the gas in the headspace to an outside loop. Gas concentrations are then measured using a portable gas chromatograph on site or in the laboratory if samples are collected.

In the static flux chamber method, methane or trace gas concentrations and mass flux are measured using the gas collected from the headspace of the chamber. A single sampling event provides concentration values, whereas repeated measurements over time allow for determination of flux. Concentrations are measured at intervals such as 5 minutes over total test durations of approximately 20 to over 60 minutes.

Concentration (*C* in ppmv) is plotted against time (*t* in minutes) and the surface flux is determined using concentration versus elapsed time data. The gas concentration within the chamber generally increases linearly and *dC/dt* represents the slope of the trend (typically a linear regression fit to the data). The change in volumetric concentration (*dC/dt*) is converted to a mass flux using the ideal gas law. The surface flux, F (g gas/$m^2$-d), is calculated as follows.

$$F = \frac{(P)(V)(M)(U)\left(\frac{dC}{dt}\right)}{(A)(T)(R)} \quad (7)$$

where *P* is pressure (atm), *V* is chamber volume (L), *M* is the molar mass of gas analyzed (g/mol), *U* is the unit conversion factor (0.00144 min / µL-d), $dC/dt$ is the change in concentration over time expressed in µL/min, *A* is the surface area covered by the chamber ($m^2$), *T* is chamber temperature (°K), and *R* is the ideal gas constant (0.08205 L-atm/(°K-mol)).

### 1.6.2 Measurement Methodologies

#### 1.6.2.1 Discrete Point/Area Measurements

Portable real-time sampling devices such as FID provide discrete point measurements of gas concentrations at a specific location. Measurements are made immediately above the surface (<50 to 75 mm) to capture localized emissions from a point on the surface of the landfill. Measurements can be made at higher elevations (1.5 to 2 m height) to distinguish emissions from the surface point location and incoming emissions from upwind locations. Large differences between near-surface and airborne readings indicate presence of emissions from the point source, whereas similar near-surface and airborne readings may indicate an upwind source (i.e., no appreciable emissions from the point) or high background readings at the site. Flux may be estimated by measuring gas flow at the locations of the concentration measurements using hot-wire anemometer, Pitot tubes, or micromanometer assemblies (Environment Agency 2004). Whereas surface concentrations can be further analyzed by models such as USEPA's (USEPA 1995) Industrial Source Complex (ISC3) model and other dispersion models are periodically applied to landfills, these models have not been comprehensively field-validated with respect to their projected ambient air concentrations. The stationary enclosure methods also provide discrete measurements over relatively small areas for determination of concentration and flux.

The number, location, and spacing of the data collection areas or points are important for discrete measurements. The location of the measurement points may be selected randomly or using a grid pattern. A two-step procedure may be used, where point measurements are conducted initially to obtain preliminary concentration data for a given site to determine baseline concentrations and potential hot spots or problematic areas. Including areas with surface fissures, gas or leachate collection protrusions, areas with stressed vegetation, and side slopes. Area measurements may then be conducted to determine flux from regions representative of different conditions. The discrete measurements obtained using area/point measurement techniques are

interpolated using geospatial analysis for a given site. Details of statistical approaches that may be used in landfill emission studies is presented in Section 3.2.

### 1.6.2.2 Tracer Tests

Tracer testing includes concurrent measurements of concentrations of a target LFG such as methane and an inert tracer gas released at a known rate at an upwind location from a landfill (Figure 19). The atmospheric tracer method can be used to calculate the total emission rate of the target gas such as methane from landfills (Czepiel et al. 1996b, Mosher et al. 1999). For methane measurements, pure sulphur hexafluoride ($SF_6$) was used as a tracer near the surface of the landfill and downwind from the landfill (Howard et al. 1992, Lamb et al. 1995, Czepiel et al. 2003, Spokas et al. 2003, Spokas et al. 2006). Nitrous oxide, $N_2O$, has also been used as the tracer gas as it has a lower greenhouse gas potential than $SF_6$ (Borjesson et al. 2000, Galle et al. 2001). In addition, use of acetylene recently has been reported in practice. Concentrations of the LFG and the tracer gas are measured along transects perpendicular to the prevailing wind direction.

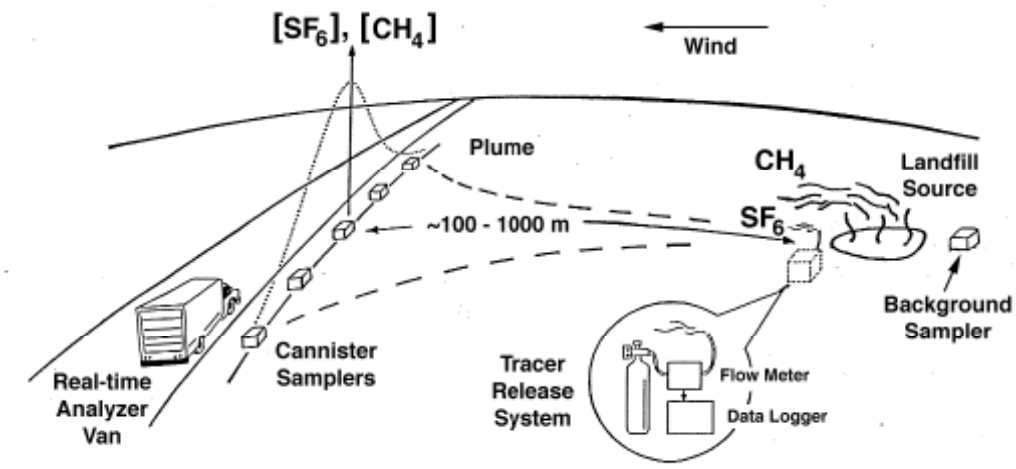


Figure 19. Tracer Testing (Czepiel et al. 2003)

When the released tracer gas is well mixed in the source plume (e.g., methane), then the $CH_4$ emission rate can be obtained directly by the ratio method as:

$$Q_m = Q_t\left(\frac{C_m}{C_t}\right) \tag{8}$$

where $Q_m$ is the $CH_4$ emission rate, $Q_t$ is the tracer release rate, $C_m$ is the measured $CH_4$ mixing ratio above background, and $C_t$ is the measured mixing ratio of the tracer. $CH_4$ and tracer release rates are expressed in units of volume per time. This method is restricted to cases when no interfering sources such as farms or other landfills are present in the area, a sufficient source signal is used to be measured against the background, and a suitably strong source is present to be measured far enough downwind to ensure adequate mixing with the tracer gas (Czepiel et al. 1996b, Smith and Bogner 1997). Molecular diffusion effects that result from differences in molecular

weight between the tracer (146 g mol¯1 for $SF_6$) and the target LFG such as methane (16 g mol¯1) have been analytically and experimentally demonstrated to be several orders of magnitude smaller than the effects of turbulence in the atmosphere (Stull 1988, Lamb et al. 1995).

Gas samples can be collected in the field and analyzed in the laboratory or can be continuously measured in the field. Benner and Lamb (1985) used a continuous $SF_6$ gas analyzer for real-time measurement of the tracer along with the measurement of $CH_4$. The instrument, developed by the Laboratory for Atmospheric Research at the Washington State University, uses an electron capture detector.

The LFG emission rate calculated using the tracer emission rate and mixing ratios for the tracer and LFG can be converted to mass flux using the source area for the LFG emission. However, exact footprint of the emission source area is difficult to estimate due to surface heterogeneities and potential sources of LFG components outside the landfill area as well as meteorological conditions. Eddy correlation and flux gradient methods (micrometeorological methods) can then be used to estimate the flux from the landfill. These methods are used to evaluate whole-landfill methane emissions, and because the systems are more automated, the methods are especially useful for the study of diurnal and seasonal flux variations. However, the methods require complex instrumentation and calculations, and also have surface constraints (requiring relatively level terrain) that may limit their application (Smith and Bogner 1997).

#### 1.6.2.3 Optical Remote Sensing

Optical remote sensing (ORS) describes integrated technologies and methodologies that can be used to determine gaseous emissions from non-point ground level area sources (i.e., OTM-10 described in USEPA 2006). The main goal of ORS is to identify hot spots and determine flux over whole landfill areas. ORS includes multiple measurement technologies and measurement protocols. The technologies used are mainly spectroscopy technologies including tunable diode laser spectroscopy (TDL), Fourier transform infrared spectroscopy (FTIR), and Ultraviolet differential optical absorption spectroscopy (UV DOAS) (USEPA 2007). The measurements are made in varied beam configurations along open paths using the varied technologies. The measurement protocol used is referred to as radial plume mapping (RPM), which describes the configuration of multiple-beams and scanning pathways used in ORS. RPM employs optical-remote sensors (ORS) coupled with a programmable aiming platform or scanner to make comprehensive measurements over large areas (USEPA 2011). Chemical concentrations of gas species of interest along each beam path are determined utilizing the measurement and analysis methods specific to the selected measurement technology to obtain path-integrated concentrations. Spectral data are obtained so that collection of physical samples is not required for ORS. Concentration data are converted to flux values using analytical/numerical modeling. The flux values are typically provided in units of mass/time. The flux is converted to mass/area-time by estimating the landfill surface area contributing to flux (ACF). The measurement protocols are categorized based on the beam configurations and commonly include horizontal radial plume mapping (HRPM) and vertical radial plume mapping (VRPM).

HRPM is used to determine gas concentrations over a horizontal plane (Figure 20). The HRPM algorithm provides horizontal distribution of path-integrated concentration data (USEPA 2005). The survey area is divided into rectangular areas termed pixels after determining size of the surveying area and the number of path-determining components (PDCs) (USEPA 2011). PDCs are positioned at the center of each pixel and then continuously scanned and measured using Open Path – Fourier Transform Infrared Spectrometer (OP-FTIR) over a designated sampling period. The total number of beam-paths is established such that at least one beam path terminates in each pixel. The concentration measurements at each pixel are then used to establish a path-integrated concentration map (USEPA 2011). To construct a RPM not limited to average concentration, triangle based cubic interpolation is used to determine a concentration that depicts the varying concentration gradient throughout the pixel (USEPA 2011).

VRPM is used to determine gas flux over a vertical plane, which is located downwind from an emission source. The VRPM algorithm provides a concentration profile along the vertical plane as a function of distance from the measurement equipment (USEPA 2011). Scanning along the vertical plane from the emission source provides the plume concentration profile along the vertical axis (USEPA 2005). Flux is then calculated by multiplying the downwind speed component by the vertical concentration profile (USEPA 2011). An example of the VRPM setup schematic used for vertical scanning is presented (Figure 21). A six beam configuration is depicted in Figure 21 where three PDCs (a, b, c) are aligned along ground level in crosswind direction and the additional two probes (e, f) are positioned in vertical direction. An example of the RPM output (i.e., contours of concentrations) is presented (Figure 22).

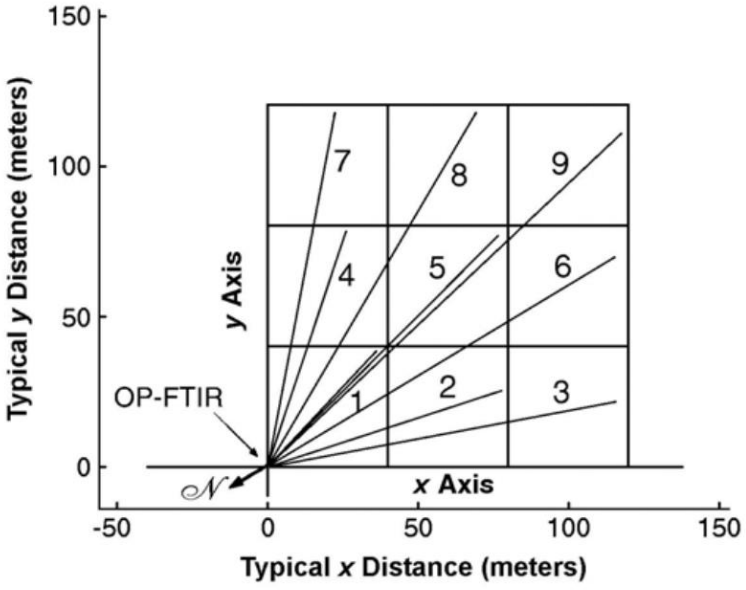


Figure 20. Horizontal RPM Setup (Hashmonay et al. 2008)

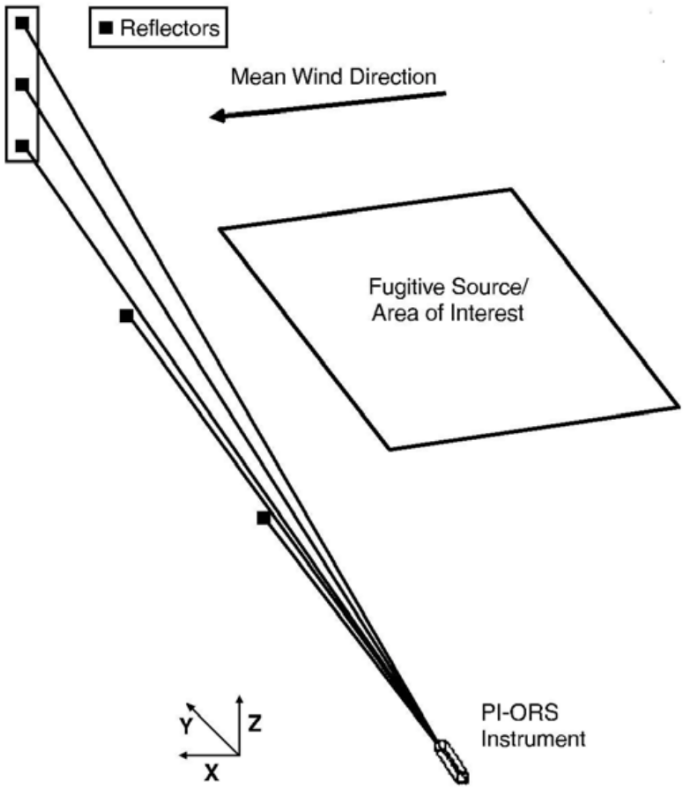


Figure 21. Vertical RPM setup (Hashmonay et al. 2008)

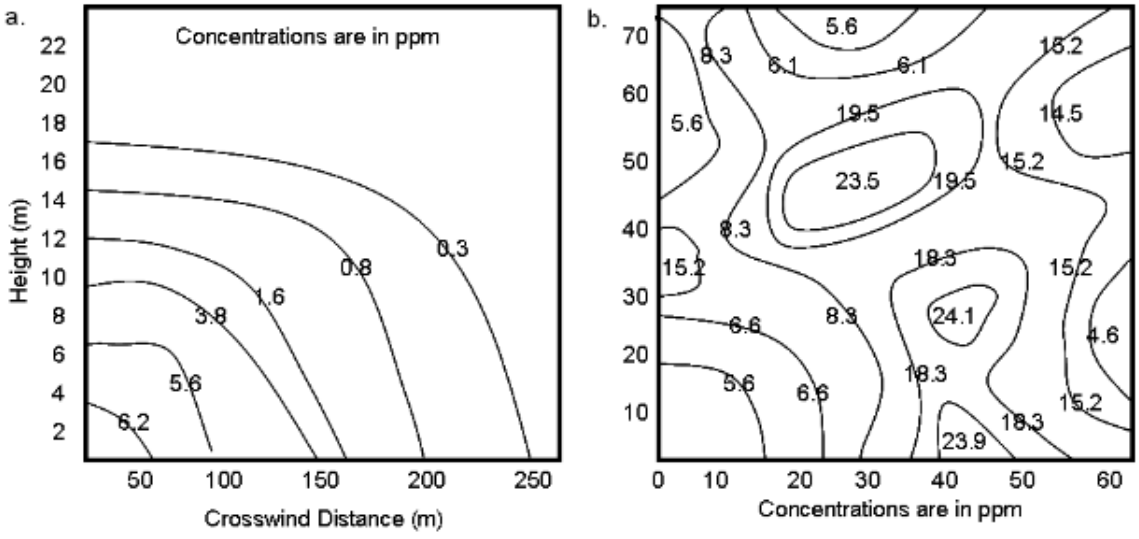


Figure 22. Example of RPM Output a) VRPM b) HRPM (Hashmonay et al. 2008)

#### 1.6.2.4 Aircraft-Based Mass Balance Methods

Recently, a new class of measurements utilizing aircraft-based mass balance methods has been developed (e.g., Crosson 2008, Cambaliza et al. 2015). In these methods, the flux is derived from vertical methane gradients and vertical wind speed gradients typically measured using a small plane equipped with a cavity ring down laser spectrometer instrument for methane. This method is now being widely deployed for fracking gas emissions, natural gas pumping station emissions, landfill emissions, dairy operation emissions, coalbed methane, and similar applications (e.g., Peischl et al. 2013, Gerilowski et al. 2015).

### 1.6.3 Comparison of Emission Measurement Techniques

A comparison of the emission monitoring systems including the static flux chamber, FID, tracer testing, and optical remote sensing either using TDL or FTIR is presented in Table 21 (Yesiller et al. 2008a). The technologies and methodologies currently available for monitoring emissions from landfills are evaluated with consideration to the factors listed below:

- Type of Technology
- Type of Methodology
- Data Obtained/Output: concentration, flux, source location, source homogeneity
- Meteorological Conditions
- Cover Conditions
- Landfill Operations
- Ease of Implementation
- Cost

While Optical Remote Sensing systems have potential for providing whole landfill emissions for a given site using sophisticated nondestructive testing equipment, the development of these methodologies have been complicated due to difficulties in providing representative emission estimates. Significant resources have been devoted for the development of these technologies, yet field applications have been limited. These systems were originally developed for applications where the source is well delineated, such as storage lagoons. The original formulation of path-integrated optical remote sensing (i.e., OTM-10 described in USEPA 2006) assumes that the source is small such that all of the emissions from the source are blown through the vertical plane of investigation. Furthermore, the source is assumed to be in an environment that does not contain any additional sources. These assumptions are the basis for the early development of the method and the associated mathematical approximations. Neither of these assumptions is valid when the method is extended to emissions from landfills. In landfills, the source of emissions is larger than the vertical plane, the surface emissions are highly variable with time and space, the topography tends to be variable, and multiple hot spots (i.e., sources) with large emissions may be present. These factors render the fitting process and interpretation complex leading to potential low reliability of these technologies.

Tracer-based methods involve the release of an inert tracer gas from points along the upwind edge of the emitting surface to simulate gas emission. If the released tracer gas is well mixed in a source plume and if the target gas concentration in the plume differs sufficiently from background atmospheric concentrations, then the emission rate can be obtained directly, using a ratio method as described by Czepiel et al. (1996b) and Mosher et al. (1999). Tracer methods can be used to evaluate the entire landfill and avoid the issue of spatial heterogeneity by integrating the whole area flux. However, the high cost, dependence on meteorological conditions, and potential for interference from other sources of gases limit the applicability of tracer methods. Overall, the disadvantages of ORS and tracer methods in estimation of flux such as sensitivity to micrometeorological conditions (including wind, rain, fog, and solar radiation), high cost, and uncertainties associated with the determination of area contributing to emissions, limit the applicability of these measurement and monitoring systems.

The stationary enclosure technique, static flux chamber, provides a viable alternative for determination of chlorinated and fluorinated hydrocarbons with direct measurement of both concentration and flux. The influence of landfill surface conditions and meteorological conditions are captured by repeated measurements. The discrete measurements can be extrapolated to large areas using statistical approaches as described in the next section.

Table 21 – Summary of Common Landfill Surface Emission Monitoring Systems (in part from Yesiller et al. 2008a)

| System | Description | Application | Advantages | Disadvantages | Cost |
|---|---|---|---|---|---|
| Static Flux Chamber | Gas accumulation in a relatively small sealed area above the surface of a landfill is monitored | Discrete measurements are obtained<br>Both concentration and flux are measured | Simple<br>Direct measurement of both concentration and flux<br>Multiple gases<br>Low cost | May miss hot spots<br>High number of measurements required for large areas<br>Uncertainty in extrapolation to whole area emissions | Moderate |
| Portable FID Gas Detector | Portable gas chromatography device transported around a site for conducting point measurements | Discrete measurements are obtained<br>Concentration is measured<br>Flux can be estimated using the contributing area | Simple<br>Fast<br>Highly sensitive<br>Multiple gases<br>Low Cost | May miss hot spots<br>High number of measurements required for large areas<br>Uncertainty in extrapolation to whole area emissions | Low |
| Tracer Testing Instantaneous: Infrared testing ($CH_4$, $CO_2$) Electron captor detectors ($SF_6$) Or GC after gas sample collection | A tracer gas is released from an upwind location and monitored together with landfill gases | Whole area measurements are obtained<br>Concentration is measured<br>Flux can be estimated using the area contributing to flux | Whole area emissions are determined<br>Large landfill areas are monitored over relatively short periods | High dependence on micrometeorological conditions<br>Affected by interfering sources<br>Uncertainty in determination of flux using the area contributing to flux | Low |
| Optical Remote Sensing Using Tunable Diode Laser Spectroscopy | Nondestructive spectroscopy tests used to measure emissions across near-surface vertical and horizontal planes | Whole area measurements are obtained<br>Concentration is measured<br>Flux can be estimated using the area contributing to flux | Whole area emissions are determined<br>Large landfill areas are monitored over relatively short periods | High dependence on micrometeorological conditions<br>Affected by interfering sources<br>High cost<br>Uncertainty in determination of flux using the contributing area<br>Single-species measured | High |
| Optical Remote Sensing Using Fourier Transform Infrared Spectroscopy | Nondestructive spectroscopy tests used to measure emissions across near surface vertical and horizontal planes | Whole area measurements are obtained<br>Concentration is measured<br>Flux can be estimated using the contributing area | Whole area emissions are determined<br>Large landfill areas are monitored over relatively short periods<br>Multiple species measured | High dependence on micrometeorological conditions<br>Affected by interfering sources<br>High cost<br>Uncertainty in determination of flux using the contributing area<br>Complicated measurements | High |
| Cavity Ring-Down Spectroscopy (CRDS) System | Aircraft-based measurement system for in-situ, real-time measurements | Combination of scanning large areas and collection of discrete air samples | Low-drift, high-precision GHG analyzer for multiple gases, no interference from other gases species | Variable winds with altitude complicate data interpretation | High |

### 1.7 Use of Statistical Methods in Landfill Emission Analysis

Statistical analysis and use of geostatistical methods (spatial interpolation) can be used to construct total area estimates from discrete gas emission measurements (Spokas et al. 2003). Spatial interpolation, including the use of geostatistical methods, can be defined as, "estimating data at unsampled locations using known, measured locations within the same area" (Burrough and McDonnell 1998). Geostatistics provides "a range of statistical techniques for determining the relationship between spatially distributed values, leading to the estimation of the property at unsampled locations" (Spokas et al. 2003). Kriging or Inverse Distance Weighing (IDW) are common techniques used to estimate a property at an unsampled location based on the spatially distributed relationships between sampled locations (Wang and Qi 1998).

Kriging can used to predict the value of a property (such as surface emissions) at an unsampled location, if sufficient spatial dependency and consistency is present within the data. Kriging (using a non-linear model) has been demonstrated to be effective for predicting average concentrations for highly skewed data sets (Kitanidis and Kuo-Fen 1996). Kriging optimizes the interpolation process given that spatial variation is divided into three components: deterministic variation, spatially autocorrelated variation, and uncorrelated noise. Estimates are generally made for unsampled locations with the determination of weights by assessing the distance between the measured data points and the underlying structure (i.e. spatial arrangement) of the data set. Spatially autocorrelated variation (autocorrelation) is graphically represented by a variogram and describes the variation in the measured data over a specified sampling distance (Burrough and McDonnell 1998). The ordinary kriging model/method used in the determination of net surface emissions of methane from landfills was derived using Equations (9-12). In particular, Equation 12 (the variogram function) describes the determination of the weights used in ordinary kriging geostatistical analysis. This equation, as the basis of the variogram plot (the most useful kriging tool), is important to predict the spatial correlation structure of the data, and is the main emphasis of kriging analysis used in the determination of net methane emissions from landfill surfaces (Börjesson et al. 2000, Spokas et al. 2003). The kriging analysis is conducted as follows:

$$Z(So) = \mu + \delta(s) \quad (9)$$

where $Z$ is the variable of interest (e.g., gas emissions) interpolated at locations in the vector $S_o$. The true population mean $\mu$ is estimated from the sample mean and assumed to be identical over the entire area except for the small-scale fluctuation $\delta(s)$, which depends on the spatial location in the sampling area (as cited in Börjesson et al. 2000).

$$Z(So) = \sum_{k=1}^{M} \mathcal{U}_K Z(s) \quad (10)$$

where the predictor $Z(S_o)$ can be described as a weighted average of observations of a variable within a neighborhood $M$ (as cited in Börjesson et al. 2000).

$$\sum_{K=1}^{M} \mathcal{U}_K = 1 \quad (11)$$

where the conditional weights $\mathcal{U}_K$ within a neighborhood *M* are unbiased (as cited in Börjesson et al. 2000).

$$\gamma(h) = \frac{1}{2N(h)} \sum_{p=1}^{N} [Z(Sp + h) - Z(Sp)]^2 \quad (12)$$

where *h* is the lag (the geographical distance between two observations, *N(h)* is the total amount of pairs at lag *h*, and *Z* is variable of interest as a function of the lag (*h*) and the location in the vector *Sp* (as cited in Börjesson et al. 2000).

Similar to the Kriging model described above, inverse distance weighting relies on a combination of weighted averages to determine the average of a highly skewed data set. This method can be applied when little spatial structure is present in a dataset (Spokas et al. 2003). The weighting calculation, however, is derived from the inverse distance from known measurements at nearby measurement locations (Burrough and McDonnell 1998). This process gives higher weighting to the nearest data points within a sampling area. In general, IDW takes an average of multiple interpolations of measured values using an inverse power of distance from a measurement at various sample locations (as cited in Spokas et al. 2003). Equation (13) describes the IDW formula for a certain unknown location within a sampling area (Caruso and Quarta 1998).

$$y^*(Zo) = \sum_{i=1}^{N} \lambda_i \, y(Z_i) \quad (13)$$

where $y^*(Zo)$ is the estimated value for the unknown location, N is the number of data points, $\lambda_i$ are the weights of the sample data points, and $y(Z_i)$ are the measured values for each data point (Caruso and Quarta 1998).

Several studies have investigated the use of kriging to predict total surface emissions of gases from landfill and volcanic sites (Czepiel et al. 1996b, Börjesson et al. 2000, Cardellini et al. 2003, Spokas et al. 2003, and Ishigaki et al. 2005). Czepiel et al. (1996b) examined methane emissions and spatial variability of flux measurements from a landfill in New Hampshire using a combination of static flux chambers and atmospheric tracer measurements. Over 139 flux chamber measurements were made over the 382,500 $m^2$ surface area of the landfill on a regular grid pattern with equal spacing on similar, consecutive days of meteorological conditions (Czepiel et al. 1996b). A total of 11 atmospheric tracer tests were conducted using sulfur hexafluoride. Overall, good agreement was achieved between both test methods for measurement of whole surface flux of methane from the landfill studied, with mean surface fluxes of 58 g $CH_4/m^2$-day and 44.1 g $CH_4/m^2$-day measured using the static flux chamber and atmospheric tracer tests, respectively (Czepiel et al. 1996b). A large spatial variability was observed at the landfill using kriging, with a coefficient of variation of 326% for flux chamber measurements (Czepiel et al. 1996b).

Börjesson et al. (2000) investigated three different kriging approaches to estimate whole landfill methane surface emissions from a Swedish landfill including kriging on logarithm transformed data, kriging with extremes excluded, and linear interpolation of measurements made using static flux chamber measurements. A total of 265 static flux chamber measurements were conducted across the surface of the landfill investigated over a one-year experimental period. During this one-year period, only three days were chosen for measurements (one day in May, July, and October), averaging 88 measurements on the surface per sampling day chosen (Borjesson et al. 2000). All kriging methods were determined to be unreliable for the static flux chamber measurements for the estimation of entire landfill surface flux of methane given that many more sampling areas were needed for each model to be effective (Börjesson et al. 2000). However, Börjesson et al. (2000) reported that the geostatistical analysis performed was important in that the analysis provided a qualitative representation of landfill surface emissions, and could be applied to map areas (with lower precision) of high and low surface emissions. In addition, error due to climatic factors such as temperature, rainfall, and barometric pressure was identified as an important aspect to be accounted for prior to making the kriging analysis (Börjesson et al. 2000).

Cardellini et al. (2003) applied both kriging and an in-depth stochastic simulation algorithm (sequential Gaussian simulation) to soil carbon dioxide gas flux from flux chamber measurement data collected from several volcanic/non-volcanic sites. In addition, the degassing areas studied were compared on the basis of the net carbon dioxide flux predicted/method used for prediction. Cardellini et al. (2003) concluded that an adequate number or range of samples were required for reliable predictions with the kriging method. An empirical relation was developed between the sample design (i.e. sampling density) and the uncertainty in the net carbon dioxide emission estimate made for each site. Moreover, if sufficient spatial dependency within a data set was not observed, inverse distance weighting (IDW) provided a more reliable representation of net carbon dioxide surface emissions (Cardellini et al. 2003). The stochastic simulation algorithm output for all data sets was well correlated with the outputs from the kriging analysis, in particular the histogram and variograms.

Flux measurements from static chambers were analyzed using both kriging and IDW to predict net methane surface emissions from Lapouyade landfill in France (Spokas et al. 2003). Spokas et al. (2003) indicated that the slope regions of the landfill contributed to 90% of the overall total landfill cell surface emissions. However, spatial discontinuities observed in measurement locations on the slope regions of the landfill led to an error in adequately applying the kriging method. Thus, it was determined that the spatial distribution of all measurements needed to be continuous for correctly applying the kriging (semi-variogram) method, a difficult requirement to meet (Spokas et al. 2003). The IDW representation provided a more accurate and precise approach for determining the net surface emission of methane from the landfill cell given that the IDW approach (due to the interpolation method) did not misrepresent any unknown, non-measurement areas and considered all data points in the analysis. Further, since there was a lack of spatial structure in the data set, the kriging method may have incorrectly smoothed or misrepresented the emissions at unknown measurement

locations. More importantly, Spokas et al. (2003) concluded that the incorporation of additional variables/properties inherent to soil systems such as soil moisture or temperature into the geostatistical treatment of flux chamber data might decrease the variability in net methane emission predictions from landfills.

Based on conclusions provided by Spokas et al. (2003), Ishigaki et al. (2005) improved the kriging estimation of net landfill surface emissions by presenting a correlation between net flux and soil temperature. This temperature-surrogated kriging method was used to determine the net emissions in the summer, fall, and winter months at a landfill in Japan (Ishigaki et al. 2005). Methane flux and ground temperature were observed to fluctuate both seasonally and spatially, where seasonal changes in methane emissions occurred. The locations of methane emission were postulated to change as a result of soil properties and condition such as porosity, hardness, soil moisture content, or cracking resulting from differences in meteorological conditions (precipitation, barometric pressure, etc.) (Ishigaki et al. 2005). Isolated zones of methane emissions were most likely a result of changing meteorological conditions and increased areas of poor soil conditions brought on by changes in seasons. An exponential relationship was developed between methane flux and ground temperature, where net methane flux was predicted using the kriging results of a series of ground temperature measurements (Ishigaki et al. 2005). The predictions for net methane flux from the kriging analysis of ground soil temperature were much smaller than predictions made by Börjesson et al. (2000) and Spokas et al. (2003), suggesting that the method provided by Ishigaki et al. (2005) was more accurate for estimation of net methane surface emissions from landfills (as the other studies may have been biased towards a high flux density most likely due to the kriging analysis used).

Most of the geostatistical analyses described above were conducted for methane; however, the analysis could be adapted to trace gases such as CFCs, HCFCs, and HFCs, since the measurement principles with the flux chamber method are similar. However, an in-depth kriging or IDW geostatistical analysis for CFCs, HCFCs, and HFCs may require numerous flux chamber measurement locations, which is both costly and labor intensive given the gaseous constituents measured are expected to have very low concentrations. The sampling locations need be designed to limit variability in the data (i.e., using a grid pattern instead of random sampling) and also provide an adequate representation of the net surface emission (avoid missing hotspots) (Czepiel et al. 1996b, Börjesson et al. 2000, Spokas et al. 2003, Ishigaki et al. 2005). Taking these above factors into consideration will allow for determination of representative of net surface emissions of CFCs, HCFCs, and HFCs from the landfill surface area under study using geostatistical treatment of the data collected.

## 1.8 Emissions of BAs from Landfills

### 1.8.1 Definition of BA Release Periods

The release of blowing agents from foam insulation at end of life (in landfills) was determined to occur over three distinct phases: instantaneous release (on the order of

minutes to hours), short-term release (on the order of hours to days), and long-term release (on the order of weeks to years) (Scheutz and Kjeldsen 2003). Instantaneous release results from permanent damage to the cell from mechanical processes such as shredding, resulting in a sudden large release of BAs. Short-term refers to BA release through small cracks in slightly damaged foam, while long-term release occurs due to slow diffusion across cell walls in essentially intact foam. Short-term and instantaneous releases were observed to be strongly dependent on particle size distribution of the shredded foam. Long-term release was governed by closed cell diffusion (i.e., concentration independent) and could be accurately modeled using diffusion coefficients obtained from short-term release experiments (Scheutz and Kjeldsen 2003). A summary of durations for the three phases as obtained from experimental investigations and modeling studies (for long-term releases) is presented in Table 22. Based on the data in this table, instantaneous releases occur within 30 minutes up to 7 hours; short-term releases occur over 7 to 500 hours; and long-term releases start subsequent to 1000 hours and continue for tens to few hundreds of years.

Table 22 – Stages of End of Life BA Emissions

| Reference | Kjeldsen and Jensen (2001) | Scheutz et al. (2003a) | Scheutz and Kjeldsen (2003) | Fredenslund et al. (2005) | Scheutz et al. 2007b | BRE UK (2010) |
|---|---|---|---|---|---|---|
| Instantaneous | - | 10 to 20 minutes | 10 to 30 minutes | - | 2 to 3 hours | Up to 7 hours |
| Short Term | 300 to 500 hours | 250 to 500 hours | 200 to 500 hours | - | - | 7 to 18 hours |
| Long Term | 9 to 300 years | 1,100 hours to 300 years | 1,100 hours to 300 years (Modeled to 50 years) | Modeled to 20 years | Modeled to 20 years | - |

### 1.8.2 Modeling and Laboratory Based BA Emissions Studies

Summaries of experimental and modeling studies on BA releases from foams during the three distinct phases are provided in Tables 23-25. Tests for instantaneous and short-term releases were conducted on PUR appliance insulation panels, whereas long-term studies included both appliance and building insulation foams. A great majority of the instantaneous and short-term release investigations (Tables 23 and 24) were conducted in the laboratory and the studies (laboratory or field) did not include investigation of such releases in a landfill environment. The studies focused on the releases from mechanical processing of foams and direct measurement, batch release, and infinite bath testing methods. In contrast, the majority of the modeling studies conducted for estimating long-term releases included consideration of the landfill environment. The results of the instantaneous release studies indicated that the releases varied with BA type. The releases of HCFC-141b and HFC-245fa generally were less than releases of CFC-11. Instantaneous release also was a function of particle size, with higher releases generally resulting from smaller size particles. Good correlation was observed between field and laboratory shredding experiments for

instantaneous releases. Cutting the appliance insulation foam, released a smaller weight fraction of CFC-11 compared to shredding (Table 23).

The results of the short-term release studies indicated that the releases varied with BA type. The releases of CFC-11 and HFC-134a generally were less than releases of HCFC-141b and HFC-245fa (Table 24). For CFC-11, the average emission was 13% within a range of 9 to 23%; the average emission for HCFC-141b was 17% over a range of 1% to 28%; the average emission of HFC-134a was 10% in a range of 3-15%; and the average short-term release of HFC-245fa was 21% in a range of 8-30%. Releases from field and laboratory experiments were on the same order. Some variation was observed in results as a function of manufacturer (Scheutz and Kjeldsen (2003), Table 24).

The results of the long-term release studies (Table 25) indicated that the release of BAs varied between modeling studies based on the end of life management practice (i.e., landfilling versus no landfilling). Khalil and Rasmussen (1986, 1987), Kjeldsen and Jensen (2001), and Scheutz and Kjeldsen (2003) modeled the long-term release of BAs to determine diffusion coefficients for PUR appliance/building insulation foam for no landfilling conditions (i.e., fate/release of BAs from stockpiled foam open to the atmosphere), which resulted in high release rates (up to 99% of BA content at end of life). Scheutz and Kjeldsen (2003) used three hypothetical scenarios for estimating the future releases of halocarbons from decommissioning used refrigerators/freezers in the U.S. Scenarios A, B, and C differed by the particle size distribution resulting from the decommissioning processes used (i.e. shredding versus cutting/compaction). Scenario A had the highest portion of small shredded particles (<16 mm), while Scenario C had the largest ratio of large shredded particles (>32 mm). Scenario B, was evenly distributed between Scenario's A and C, with most of the particle sizes falling between 16 and 32 mm. HFC-134a and HFC-245fa based foams released more BA over the long-term than HCFC-141b and CFC-11. Also, long-term emissions of BA were a function of particle size, where high releases occurred for small particle sizes (Table 16). Kjeldsen and Jensen (2001) determined that a long time period of up to 300 years was necessary for 98% of CFC-11 to be released from cut appliance foam waste, whereas the same amount of CFC-11 was released from shredded foam in 50 years (Table 25).

Long-term releases also were modeled using concentration dependent diffusion processes in the landfill environment (Scheutz et al. 2003a, Fredenslund et al. 2005, and Scheutz et al. 2007a). These models included the effects of adsorption, aerobic and anaerobic degradation, and absorption processes occurring throughout waste layers as well as the soil covers. Scheutz et al. (2003a) presented a preliminary model to predict the fate of BAs in landfills based on the degradation rates from laboratory batch microcosm experiments. The BA releases were a function of the first order degradation constant and the type of BA in the shredded foam material. For the 20-year modeling period (Scheutz et al. 2003a), up to 99.7% and 96.9% of the BA in the gas phase was predicted to be degraded resulting in 0.2 and 2.4% BA release for CFC-11 and HCFC-141b, respectively (Table 25). Releases of BA were higher (up to 91 to 64% for CFC-11 and HCFC-141b, respectively), when ten times lower and no

degradation conditions were assumed, sorption of the chemical to the waste was limited and the modeling period was long (Table 25). Several constraints such as the presence of anaerobic conditions and a high fraction of organics in the initial MSW composition were required for high degradation rates (Scheutz et al. 2003a). Even though modeling results indicated a large potential for anaerobic degradation in a landfill environment, uncertainty exists for whether anaerobic degradation occurs at a sufficiently fast rate to mitigate the immediate release of BA during initial compaction and short-term compression processes.

Fredenslund et al. (2005) evaluated the long-term emissions of BAs with the MOCLA FOAM model using two different foam waste management scenarios in landfills. The first scenario represented a typical foam waste disposal procedure in a landfill including a short period of foam stockpiling, volume reduction by a compactor, and a variation in the onset of anaerobic conditions. Scenario 1, unlike the Scheutz et al. (2003a) study, took the instantaneous BA emissions into account from compaction and also did not assume that anaerobic conditions were already present in the landfill. Scenario 2 included reduced instantaneous BA release from compaction (5% BA release as compared to 15% for Scenario 1). Degradation rates and diffusion coefficients were varied in the study by a factor of ten. The predicted total BA release was relatively similar for the different scenarios and foam characteristics (Table 25). The largest fraction of BA degraded was observed for the model with the ten times higher diffusion coefficient, likely due to the high amount of BA released to the waste pore space. High BA release occurred for low degradation rates. Anaerobic conditions and associated microbial activity promoted degradation of the BA in the waste mass. Similar to results in Scheutz et al. (2003a), modeling the fate of BAs indicated that a large fraction is degraded in the waste layers and limited amounts were released to the atmosphere. The operational conditions at a landfill such as degree of compaction and onset of anaerobic degradation influenced the overall release and degradation patterns. Overall, amending foam waste with aged waste prior to landfilling could mitigate up to 40% of CFC BA release during early stages of landfilling with limited microbial activity. These studies indicated the need to scale up modeling to combine results with measurements at landfills to achieve a better picture of the fate of BAs in a landfill environment.

Scheutz et al. (2007b) also investigated the sensitivity of the BA release to both the diffusion coefficient and the degradation rate using the MOCLA FOAM model. The main pathways for BA release were determined to be through LFG emission or degradation of the foam within the waste mass with negligible effects from leachate losses or diffusive losses through a soil cover. Increasing the diffusion coefficient had little effect on the fraction of BA released using the same degradation coefficient (Scheutz et al. 2007b). Similarly, increasing the release rate of LFG in the model did not have an effect on the fraction emitted or degraded, only the mass emitted over the twenty year period. Modeling results indicated that the extent of BA attenuation depended on the release rate of BA from the foam wastes as well as how fast degrading (i.e., anaerobic) conditions were established in the landfill. Uncertainties were present in the model due to lack of field measured data on initial and short-term release rates representing compaction process and early aerobic conditions at the

landfill, respectively. CFC-11 release rates were lower than the HCFC-141b release rates. Lower release rates were associated with higher degradation rates (Table 25).

Specific release rates and long-term releases of CFCs, HCFCs, and HFCs from shredder waste residue cells present in a landfill in Denmark were further measured by Scheutz et al. (2007c) in a series of laboratory experiments. The short-term release rates determined in the laboratory were further extrapolated to predict long-term emissions. Shredder waste was sampled from the AV Miljo landfill in Denmark from a shredder waste residue cell in three locations. The shredder waste primarily originated from the waste processing of automobiles and not appliances (Scheutz et al. 2007c). This section of the landfill covered a 7,200 $m^2$ area, with a total waste mass deposited of 47,000 tons, and a waste age of 10 years. The cell studied did not contain a permanent cover and was open to the atmosphere. Waste samples on the order of 75 to 88 kg were excavated from 1 to 1.5 m depth in the waste mass (where anaerobic conditions were assumed) and placed in 0.218 $m^3$ steel drums. The gas volume (headspace) within the steel drums also varied between the three sample areas from 0.071 to 0.120 $m^3$. To measure the release rates over time from the waste drums and ensure no degradation of CFC-11, CFC-12, or HCFC-141b, the experiments were conducted under aerobic conditions as air was circulated throughout the sampled waste mass during the test. Release rates were measured over the short-term period of 140 hours (6 days) by measuring headspace concentrations of CFC-11, HCFC-21, and HCFC-31.

A steady and continuous release of each compound was observed, with the highest release rate resulting from CFC-11 ranging from 0.04 to 0.78 µg CFC-11/kg waste-day (average of 0.35 µg CFC-11/kg waste-day). HCFC-21 and HCFC-31 demonstrated much smaller release rates, with average release rates of 0.17 and 0.03 µg HCFC-21/HCFC-31/kg waste-day, respectively (Scheutz et al. 2007c). The variation in release of CFC-11 was most likely a result of the varying amounts of foam in the waste samples as well as the variable CFC-11 content (%w/w) in the foam waste. Similarly, the variation in release rates observed with HCFC-21/HCFC-31 was a result of the different fractions sorbed on the waste samples and concentrations present (in the gas phase) due to varying anaerobic degradation rates of CFC-11 prior to waste sampling (Scheutz et al. 2007c).

A laboratory analysis of the amount of PUR foam in the waste samples and the BA content of the foam sampled confirmed the variation in release rates (Scheutz et al. 2007c). Variation in release rates for each area was confirmed to be a function of the varying foam contents sampled and the amount of blowing agent present in the foam (%w/w) (Scheutz et al. 2007c). Areas with higher release rates of a certain blowing agent were directly correlated with higher measured foam contents (%w/w) and higher measured blowing agent contents (%w/w) of the sampled foam. The release rates were then normalized to percent of CFC-11 emitted per day in the landfill environment using the average content of CFC-11 and the mass of foam in the sampled waste. The average percent CFC-11 emitted per day was 0.080% of the initial BA content of the shredded foam when placed in the landfill and the variation between areas sampled

was minimal. Assuming that this average release rate is valid for short term release (21 days) and long term release periods (1 year) of CFC-11 (settlement and degradation processes are neglected in the landfill), the total BA release for both short and long term periods can be extrapolated to 1% and 28% for each period respectively (Tables 24 and 25) (Scheutz et al. 2007c).

Table 23 – Summary of Instantaneous BA Release Studies

| Reference | BA Type | Experiment Type | Size Fraction | Total Initial Contents of BA (% w/w) | Relative Release of BA (% w/w) | Total BA Release (% w/w) | Average Total Release (% w/w) |
|---|---|---|---|---|---|---|---|
| Scheutz and Kjeldsen (2003) | CFC-11 | Laboratory Shredding | 16 to 32 | 13.3 | - | 9.4 | 24.9 |
| | | | 8 to16 | | - | 17.6 | |
| | | | 4 to 8 | | - | 33.8 | |
| | | | 2 to 4 | | - | 38.7 | |
| | HCFC-141b | Laboratory Shredding | 16 to 32 | 11.62 | - | 8.8 | 8.8 |
| | | | 8 to 16 | | - | - | |
| | | | 4 to 8 | | - | - | |
| | | | 2 to 4 | | - | - | |
| | HFC-245fa | Laboratory Shredding | 16 to 32 | 11.62 | - | 11.1 | 11.1 |
| | | | 8 to 16 | | - | - | |
| | | | 4 to 8 | | - | - | |
| | | | 2 to 4 | | - | - | |
| Scheutz et al. (2007a) | CFC-11 | Field Shredding | <32 | 15.4 | 16.0 ± 8.7 | 6.2 ± 3.7 | 24.2 ± 7.5 |
| | | | 16 to 32 | | 26.3 ± 8.1 | 12.9 ± 4.1 | |
| | | | 8 to16 | | 31.9 ± 8.1 | 3.1 ± 0.9 | |
| | | | <8 | | 61.1 ± 7.8 | 1.7 ± 0.3 | |
| BRE UK (2010) | CFC-11 | Laboratory Cutting | Refrigerator Panel | 13.3 | - | 3 | 2.8 |
| | | | Freezer Panel | | - | 3.9 | |
| | | | Chest Freezer Panel | | - | 1.4 | |

-:Omitted by the study

Table 24 – Summary of Short-Term BA Release Studies

| Reference | BA Type | Experiment Type | Duration of Experiment (Weeks) | Shredded | Size Fraction of Particles (mm) | Initial Content of BA (% w/w) | Total BA Release (% w/w) | Total Weight of the Foam Sample (g) |
|---|---|---|---|---|---|---|---|---|
| Kjeldsen and Jensen 2001 | CFC-11 | Laboratory[3] | 3 to 8 | Yes | 20 | 12 | 10 | - |
| | | | | | 10 | | 20 | |
| | CFC-11 | Laboratory[4] | 7 | No[8] | N/A | 11.4 | 23 | 0.036 [11] |
| Scheutz and Kjeldsen 2003 | CFC-11 | Laboratory[1] | 6 | No[8] | N/A | - | 20 | 13.6 |
| | CFC-11 | Field | 6 | Yes | 4 to 8 | 10.1 | 6.8 | - |
| | | | | | 6 to16 | 10.1 | 8.1 | |
| | CFC-11 | Laboratory[2] | 6 | Yes | 16 to 32 | 13 | 12.5 | - |
| | | | | | 8 to16 | | 8.5 | |
| | | | | | 4 to 8 | | 10.9 | |
| | CFC-11 | Laboratory[3] | 6 | No[9] | N/A | 11.4 | 17 | 0.019 [10] |
| | CFC-11 | Laboratory[5] | 17 | No[9] | N/A | 13.3 | 10 | 0.019 [10] |
| | CFC-11 | Laboratory[4] | 17 | No[9] | N/A | 13.3 | 17 | 0.019 [10] |
| | HFC-141b | Laboratory[3] | 6 | No[9] | N/A | 11.6 | 20 | 0.025 [12] |
| | HFC-141b | Laboratory[5] | 17 | No[9] | N/A | 11.6 | <1 | 0.025 [12] |
| | HFC-141b | Laboratory[4] | 17 | No[9] | N/A | 11.6 | 20 | 0.025 [12] |
| | HFC-141b | Laboratory[1] | 6 | No[8] | N/A | - | 28 | 16.2 |
| | HFC-245fa | Laboratory[3] | 6 | No[9] | N/A | 11.6 | 22 | 0.024 [13] |
| | HFC-245fa | Laboratory[4] | 17 | No[9] | N/A | 11.6 | 20 | 0.024 [13] |
| | HFC-245fa | Laboratory[5] | 17 | No[9] | N/A | 11.6 | 15 | 0.024 [13] |
| | HFC-245fa | Laboratory[6] | 6 | No[8] | N/A | 11.7 | 28 to 30 | 15.3 |
| | | | | | N/A | 13.7 | 7.60 | |
| | | | | | N/A | 18.2 | 9.5 | |
| | HFC-134a | Laboratory[5] | 17 | No[9] | N/A | 7 | 3 | 0.031 [14] |
| | HFC-134a | Laboratory[3] | 6 | No[9] | N/A | 7 | 10 | 0.031[14] |
| | HFC-134a | Laboratory[4] | 17 | No[9] | N/A | 7 | 10 | 0.031[14] |

| | | | | | | | | |
|---|---|---|---|---|---|---|---|---|
| | HFC-134a | Laboratory[6] | 6 | No[8] | N/A | 7 | 15 | - |
| | | | | | N/A | 8.6 | 7 | |
| | | | | | N/A | 7.5 | 13 | |
| Scheutz et al. 2003a | CFC-11 | Laboratory[7] | 14 | No[9] | N/A | 13.3 | 9 | 0.019 [10] |
| | HCFC-141b | Laboratory[7] | 14 | No[9] | N/A | 11.6 | 16 | 0.025 [12] |
| | HFC-134a | Laboratory[7] | 14 | No[9] | N/A | 7 | 9 | 0.031 [14] |
| | HFC-245fa | Laboratory[7] | 14 | No[9] | N/A | 12 | 19 | 0.024 [13] |
| Scheutz et al. 2007c | CFC-11 | Laboratory | 3 | Yes | - | - | 1 | 41,600 |

[1]Measured BA emissions with flux chambers
[2] Artificial shredding of foam in a glove box container
[3] Batch release experiment (Scheutz and Kjeldsen 2003)
[4] Infinite bath experiment, chemical extraction technique (Scheutz and Kjeldsen 2003)
[5] Infinite bath experiment, gravimetric extraction technique (Scheutz and Kjeldsen 2003)
[6] BA emissions measured with flux chambers on foam from different manufacturers
[7] Batch microcosm experiment with foam with organic waste and microbial inoculum (Scheutz et al. 2003)
[8]Foam specimens cut into foam cubes
[9]Foam specimens cut into foam cylinders
[10]Calculated value based on 1-cm-diameter, 1-cm-height cylinder with a foam density of 24.6 g/L
[11]Calculated value based on 1-cm-diameter, 1-cm-height cylinder with a foam density of 36 g/L
[12]Calculated value based on 1-cm-diameter, 1-cm-height cylinder with a foam density of 32.2 g/L
[13]Calculated value based on 1-cm-diameter, 1-cm-height cylinder with a foam density of 30.70 g/L
[14]Calculated value based on 1-cm-diameter, 1-cm-height cylinder with a foam density of 39 g/L
N/A: Not applicable to study
-: Omitted by the study

Table 25 – Summary of Long-Term BA Release Studies

| Reference | Type of BA | Landfill Environment | Duration of Simulation (Years) | Initial BA Content (% w/w) | Density (g/L) | Shape | Particle Size Range (mm) | Diffusion Coeff. Used (D)[6] | Degradation Coeff. Used ($K_1$)[7] | Predicted Total BA Release (%) |
|---|---|---|---|---|---|---|---|---|---|---|
| Khalil and Rasmussen (1986, 1987)[1] | CFC-11 | No | 1 | 10 | - | Panels (Unfaced) | - | D/50 | N/A | 0.6 |
| | | | 300 | | | | | | N/A | 7 |
| | | | 1 | | | Panels (Faced) | - | D/40-D/10 | N/A | 0.3-0.6 |
| | | | 300 | | | | | | N/A | 7.4-51 |
| Kjeldsen and Jensen (2001)[2] | CFC-11 | No | 1 | 11.8 to 14.5 | - | - | - | 100D-1000D | N/A | 0.05-10 |
| | | | 300 | | | | | | N/A | 40-98 |
| Scheutz and Kjeldsen (2003) | CFC-11[3] | No | 50 | 15.3 | 25 | Shredded Particles | 8 to 16 | D | N/A | 98 |
| | | | | | | | 16 to 32 | D | N/A | 89 |
| | | | | | | | > 32 | D | N/A | 74 |
| | CFC-11[4] | | 50 | 14.9 | 25 | | <4 | D | N/A | 0 |
| | | | | | | | 4 to 8 | D | N/A | 26 |
| | | | | | | | 8 to16 | D | N/A | 72 |
| | | | | | | | 16 to 32 | D | N/A | 86 |
| | | | | | | | >32 | D | N/A | 93 |
| Scheutz et al. (2003a)[5] | CFC-11 | Yes | 20 | 14.9 | 25 | Cubes | 50 | $3.5x10^8$D | $K_1$ | 0.2 |
| | | | | | | | | $3.5x10^8$D | $K_1$/10 | 2.6 |
| | | | | | | | | $3.5x10^8$D | $K_1$=0 | 91 |
| | HCFC-141b | | 20 | 14.9 | 32 | Cubes | 50 | $3.7x10^8$D | $K_1$ | 2.4 |
| | | | | | | | | $3.7x10^8$D | $K_1$/10 | 18.7 |
| | | | | | | | | $3.7x10^8$D | $K_1$=0 | 64.4 |
| Fredenslund et al. (2005)[5] | CFC-11 | Yes | 20 | 14.9 | 25 | Shredded Particles | 41 (>32) | D | $K_1$ | 1 |
| | | | | | | | 24 (16 to 32) | D | $K_1$/10 | 3 |
| | | | | | | | 12 (8 to 16) | 10D | $K_1$ | 0 |
| | | | | | | | 4 (<8) | 10D | $K_1$/10 | 2 |
| | HCFC-141b | | 20 | 14.9 | 25 | | 41 (>32) | D | $K_1$ | 1 |
| | | | | | | | 24 (16 to 32) | D | $K_1$/10 | 3 |
| | | | | | | | 12 (8 to 16) | 10D | $K_1$ | 1 |
| | | | | | | | 4 (<8) | 10D | $K_1$/10 | 4 |
| Scheutz et al. 2007b[5] | CFC-11 | Yes | 20 | 14.9 | 25 | Cubes | 50 | D | $K_1$ | 0.5 |
| | | | | | | | | | $K_1$/10 | 5 |
| | | | | | | | | 10D | $K_1$ | 0.5 |
| | | | | | | | | | $K_1$/10 | 5 |

| | | | | | | | | | | |
|---|---|---|---|---|---|---|---|---|---|---|
| | HCFC-141b | Yes | 20 | 14.9 | 32 | Cubes | 50 | D | $K_1$ | 6 |
| | | | | | | | | | $K_1/10$ | 29 |
| | | | | | | | | 10D | $K_1$ | 6 |
| | | | | | | | | | $K_1/10$ | 29 |
| | CFC-12 | Yes | 20 | 14.9 | Unknown | Cubes | 50 | D | $K_1$ | 6 |
| | | | | | | | | | $K_1/10$ | 40 |
| | | | | | | | | 10D | $K_1$ | 6 |
| | | | | | | | | | $K_1/10$ | 40 |
| | HCFC-22 | Yes | 20 | 14.9 | 25 | Cubes | 50 | D | $K_1$ | 12 |
| | | | | | | | | | $K_1/10$ | 57 |
| | | | | | | | | 10D | $K_1$ | 12 |
| | | | | | | | | | $K_1/10$ | 57 |
| Scheutz et al. 2007c | CFC-11 | Yes | 1 | - | - | Shredded Particles | <16 | D | - | 28 |

[1] Estimated results projected from 21 days (end of short term release) to 1 year (left column) and 300 years (right column) for faced and unfaced building insulation cut panels

[2] Extrapolated from Figure 5 in Kjeldsen and Jensen (2001) study from 0.1 (end of short term release) to 1 year (left column) and 300 years (right column)

[3] Long-term release time dependency study modeled by Scheutz and Kjeldsen (2003)

[4] Particle size range specific predictions modeled by Scheutz and Kjeldsen (2003)

[5] Long-term modeling study using the MOCLA-FOAM model. Model inputs and scenarios described in text.

[6] Assuming D ranges from $2.0 \times 10^{-14}$ to $5.1 \times 10^{-14}$ $m^2$/sec depending on the BA used (laboratory determined coefficients)

[7] Assuming K1 ranges from 0.4/day to 0.015/day depending on the BA used (laboratory determined rates)

N/A: Not applicable to study

-: Omitted by study

Detailed results from the modeling studies that incorporated landfill conditions for BA releases over the three distinct time periods are provided (Table 26). Emissions of BA from the landfill environment were determined to be a function of the initial, short-term, and the long-term releases occurring within the landfill (Table 26). Initial (instantaneous) releases were dependent on the compaction process used within a landfill and the format of the foam panel (shredded, cut, full panel) arriving at the landfill. Initial releases were estimated to range between 5 and 15% of the initial BA content for shredded foam particles (Fredenslund et al. 2005). Information on the release of BA during compaction of foam insulation panels generally is not available in the literature. The instantaneous releases from compaction of full panels are expected to be higher than the releases from compaction of shredded foam as significant releases occur during shredding of the foams prior to arrival at a landfill site (Scheutz et al. 2007a, Table 23). Short-term releases were defined as the releases occurring during the aerobic period as well as during the adjustment period from aerobic to complete anaerobic degradation within the landfill environment. The short-term releases were dependent on the blowing agent, operating conditions, climatic region, and in particular, presence of anaerobic conditions based on modeling studies. Model results indicated significant decreases in BA release when the foam wastes were amended with organic wastes to promote microbial activity and establishment of anaerobic conditions in the waste mass upon placement (Fredenslund et al. 2005, Scheutz et al. 2007b). The fractions of BA that were degraded by microbial activity, remained in the landfill, and released over the long term were a function of the BA type and operational conditions in a landfill. Higher variation in releases was obtained for CFCs compared to the HCFC and HFCs. The releases of HFCs were somewhat higher than the releases of CFCs and HCFCs. In addition, the total release of BA to the atmosphere was dependent on the presence of a gas extraction/combustion system, in which extraction/combustion systems operating at high collection/combustion efficiencies demonstrated low releases of BA (Scheutz et al. 2003, 2007b, Fredenslund et al. 2005). It is important to note that none of these studies incorporated the effect of mechanical processes such as waste settlement. Additional releases of BAs may occur due to short- and long-term compression of the wastes associated with overburden stresses from the weight of overlying waste layers. Therefore, the modeling studies may have underestimated the BA released.

A summary BA emissions in the landfill environment based on data from Khalil and Rasmussen (1986,1987, Kjeldsen and Jensen (2001), Scheutz and Kjeldsen (2003), Scheutz et al. (2003), Fredenslund et al. (2005), and Scheutz et al. 2007) is presented in Table 27. The values in the table represent averages of studies based on modeling scenarios similar to those expected in a typical landfill operating in the United States (i.e., no waste amendment scenarios were used). Results for long- term BA release (from shredded foam particles only) included studies with slow degradation rates (10% of laboratory determined values) and diffusion coefficients ranging from laboratory determined values to ten times laboratory values in order to gain a better representation of BA release scenarios from an average landfill (Scheutz et al. 2003a, Fredenslund et al. 2005, Scheutz et al. 2007b). Limited data were available to predict long-term emissions of BA from foam waste panels, and predictions using modeling

results from Khalil and Rasmussen (1986, 1987) were assumed to be adequate. However, these studies did not include emission predictions incorporating typical landfill conditions; therefore, long term BA release estimates may be over or underestimated accordingly for foam waste insulation panels in the landfill environment. Similarly, limited data were available predicting BA release over the short and instantaneous release periods for both foam waste categories assuming landfill conditions.

Emissions of BA during the various emission periods were similar between shredded foam and panel foam wastes. Over all release periods in the landfill environment, average BA releases were generally higher for foam waste panels as compared to shredded insulation particles. Less variation was observed for the shredded foams compared to foam waste panels given more studies focused on modeling the fate of shredded foam particles in the landfill environment. In general, expected long-term emissions within a landfill for the two foam waste types were higher than both instantaneous and short-term releases, where instantaneous and short-term releases were almost equivalent (Table 27, Figure 23).

Table 26 – Summary of Predicted BA Emissions from the Landfill Environment at End of Life

| Reference | Modeling Period (years) | Blowing Agent | Initial Release | Short-Term Release | Fraction Microbially Degraded (%)[4] | Fraction Remaining in Landfill (%) | Fraction of Long Term Release with LFG (%) | Fraction of Release with Leachate (%) | Fraction Released to Atmosphere (%)[1] | Fraction Released after Combustion by Gas System (%)[2] | Total Emissions from Landfill at End of Life (%) |
|---|---|---|---|---|---|---|---|---|---|---|---|
| | | | Compaction (%) | Microbial Inactive Period (%) | | | | | | | |
| Scheutz et al. (2003) | 2 | CFC-11 | N/A | N/A | 0 to 99.7 | 0.3 to 68 | 0.2 to 32 | <0.01 to 0.08 | 0.05 to 8 | 0.01 to 1.4 | 0.06 to 9.4 |
| | 20 | | N/A | N/A | 0 to 99.7 | 0.1 to 8.8 | 0.2 to 91 | <0.01 to 0.24 | 0.05 to 23 | 0.01 to 4 | 0.06 to 27 |
| | 2 | HCFC-141b | N/A | N/A | 0 to 89.7 | 8 to 89 | 2.2 to 11 | 0.03 to 0.12 | 0.6 to 2.8 | 0.1 to 0.5 | 0.7 to 3.3 |
| | 20 | | N/A | N/A | 0 to 97 | 0.6 to 35.3 | 2.4 to 64 | 0.03 to 0.75 | 0.6 to 16.3 | 0.11 to 3 | 0.71 to 18.3 |
| Fredenslund et al. (2005) | 20 | CFC-11 | 15 | 3 to 39 | 7 to 36 | 5 to 21 | 0 to 2 | N/A | 0 to 0.5 | 0 to 0.1 | 0 to 55 |
| | 20 | | 5 | 0 | 40 to 60 | 10 to 29 | 1 to 4 | N/A | 0.25 to 1 | 0.05 to 0.2 | 5.7 to 6.3 |
| Scheutz et al. (2007) | 20 | CFC-11 | N/A | N/A | 94 to 99 | 0.5 to 1 | 0.5 to 5 | N/A | 0.13 to 1.25 | 0.02 to 0.23 | 0.15 to 1.5 |
| | | HCFC-141b | | | 48 to 92 | 2 to 33 | 6 to 29 | N/A | 1.5 to 7.25 | 0.3 to 1.3 | 2 to 9 |
| | | CFC-12 | | | 60 to 92 | 0 to 2 | 6 to 40 | N/A | 1.5 to 10 | 0.3 to 2 | 2 to 12 |
| | | HCFC-22 | | | 43 to 88 | 0 | 12 to 57 | N/A | 3 to 14.3 | 0.5 to 3 | 3.5 to 17.3 |
| ICF (2011)[3] | 1 | HCFC-141b | 19 | N/A | 48 | 23 | 29 | N/A | 3 | 2.35 | 5.35 |
| | | HFC-134a | | | 0 | 0 | 100 | N/A | 100 | 0 | 100 |
| | | HFC-245fa | | | 0 | 0 | 100 | N/A | 10 | 8.1 | 18.1 |

[1] Calculated from long term LFG release assuming a collection efficiency of 75% (SCS 2008)
[2] Calculated from long term LFG release assuming a destruction efficiency of 94% (Cianciarelli and Bourgeau 2002, Greer and Cianciarelli 2005)
[3] Study assumed a collection efficiency of 90%, and destruction efficiency of 91% (ICF 2011)
[4] Fraction microbially degraded includes the oxidation in the cover soil and anaerobic degradation in the waste layers
N/A: Not applicable to study

Table 27 – Summary of BA Emissions Predicted in the Landfill Environment

| Waste Type | Instantaneous Release | Short-Term Release | Long-Term Release with LFG |
|---|---|---|---|
| Shredded Insulation Foam Waste | 10 ± 5% | 14 ± 8% | 18 ± 18% |
| Panel Insulation Foam Waste (Non-processed) | 11 ± 11% | 19 ± 10% | 29 ± 29% |

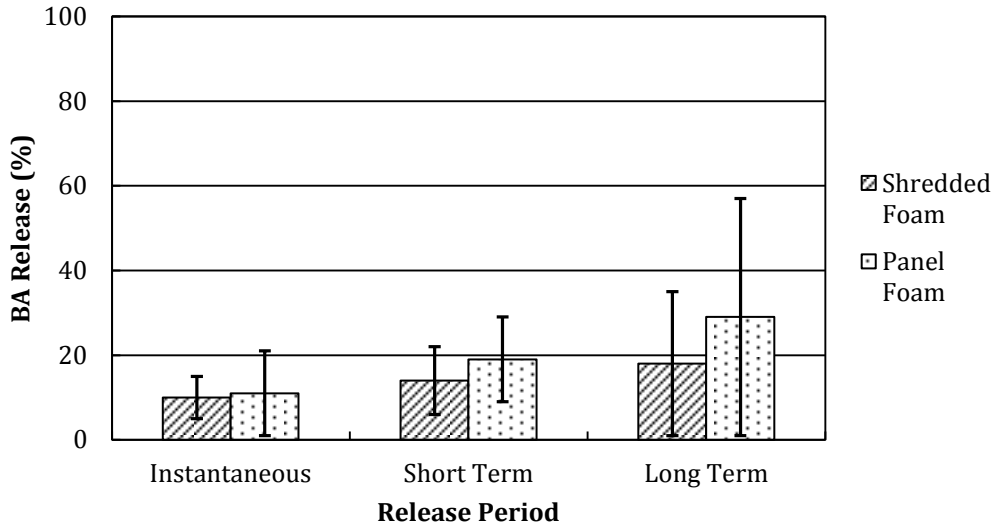


Figure 23. Summary of BA Release in the Landfill Environment

### 1.8.3 Field Based BA Emissions Studies

The emissions of LFG are either driven by pressure differences (advection) or concentration differences (diffusion) between a landfill and the environment. Other processes affecting the migration of LFG include dilution (transport process), dissolution of landfill gas constituents in water, sorption to soil or waste particles, and oxidation (sink processes) (Rettenberger and Stegmann 1996). Migration of LFG within a landfill environment can be multidirectional, generally in either the vertical or lateral directions. Diffusive movement of gases in either the vertical or lateral directions in the landfill environment is complex and depends on local concentration gradients within the waste mass, available pore space, moisture content, and temperature among many factors (Rettenberger and Stegmann 1996). The factors that influence gas migration are divided into meteorological factors (barometric pressure, precipitation, temperature, and wind); waste factors such as the gas production rate, VOC release, presence of internal barriers or gas vents, the lengths of lateral or vertical migration pathways, and the tortuosity of the migration pathways; presence, type, and condition of bottom barriers; presence, type, and condition of cover systems; and subgrade soil and geological factors (cracks/fissures, permeability, diffusivity,

porosity, water content, and organic matter content) (Rettenberger and Stegmann 1996).

Emissions of LFG components typically occur in the vertical direction from the top of a landfill through various cover systems including daily covers, intermediate covers, and final covers. Downward and lateral migration and emissions of LFG constituents from a landfill are highly limited due to the presence of liner systems in modern landfills. Landfill gas generation rates and associated emissions are highly variable due to cover conditions (daily, intermediate, permanent), inherent heterogeneity of wastes, site-specific operational conditions (waste placement density, waste placement sequence, daily cover materials), and site-specific climatic conditions (precipitation, temperature, humidity, atmospheric pressure, seasonal waste placement temperature). Landfill gas emissions typically decrease with the order daily, intermediate, and permanent covers; high permeability to low permeability covers; and thin to thick soil covers (Abichou et al. 2006a). Also, landfill gas emissions are highly variable both spatially and temporally within a given landfill as well as between landfills.

Properties and emissions of trace gas components including the target gases have been investigated in laboratory and field studies. A great majority of the field data on emissions of chlorinated and fluorinated hydrocarbons from MSW landfills have been obtained in Europe (Pruggmayer et al. 1982, Brooks and Young 1983, Arendt 1985, Rettenberger 1986, Dent et al. 1986, Schilling and Hinz 1987, Laugwitz et al. 1988, Deipser and Stegmann 1994, Allen et al. 1997). Data on emissions of chlorinated and fluorinated hydrocarbons from landfills in the U.S. are highly limited. In particular, systematic investigations of landfill emissions of these gases are not available.

Deipser and Stegmann (1994) provided data on halogenated hydrocarbons form laboratory lysimeter tests and analysis of landfill gas samples in an early investigation of trace gas components in LFG. Lysimeter tests included MSW obtained from a German landfill. The average concentrations measured in the laboratory were significantly higher than field samples for CFC11, CFC-12, and CFC-113, whereas the opposite trend was observed for CFC-114, HCFC-21, and HCFC-22. The field concentrations of CFC-11 in the LFG overall varied between 0.052 and 6.13 ppmV with an average concentration of 1.7 ppmV, while CFC-11 concentrations measured in the lysimeters ranged from 0.09 to 18.1 ppmV (Deipser and Stegmann 1994).

Rettenberger and Stegmann (1996) provided a summary comparison of seven studies that included the measurement of CFC and HCFC concentrations in landfill LFG (Table 28). The studies were conducted in Germany and the UK. Data were provided for concentrations with no flux information included. Measurement methods included mostly adsorbent tube grab sampling followed by thermal desorption and gas chromatography/mass spectrometry analysis for all studies. The areas where grab sampling measurements took place were limited in most of the German studies (Pruggmayer et al. 1982, Arendt 1985, Rettenberger 1986, Schilling and Hinz 1987, Laugwitz et al. 1988). However, the UK studies indicated that LFG concentration measurements were taken directly over the intermediate cover after the waste was

placed and up to a period ranging from 6 months to 3 years (Brookes and Young 1983, Young and Heasman 1985, Dent et al. 1986, Allen et al. 1997). Thus, concentration measurements were relatively higher for the UK based studies as compared to more current studies presented in the following paragraphs (with the exception of Scheutz et al. 2003b, 2007a). The concentrations were in the ppmV to ppbV range for most of the CFCs and HCFCs evaluated and the adsorbent tube sampling techniques were effective in measuring concentrations in this range (Table 28).

Allen et al. (1997) reviewed trace gas components at seven MSW landfill sites in the UK using point source measurements on gas samples collected using 500 mL grab samples collected from sorption tubes. The extracted gases were then analyzed using gas chromatography. The study sites included two landfills that were operational pre-1980 (since 1920 and 1965); three landfills operational from 1980 onward; and two landfills operating since 1990. The landfills also differed by construction and liner type, ranging from valley infills to quarry infills and former brick pits/clay extraction sites. The waste types varied from domestic waste to C & D and commercial wastes at varying heights between 15 and 30 m. Gas extraction systems were installed at all but one site (where large emissions have occurred), two sites used on-site extraction and flaring, and four of the sites had on-site combustion of the LFG for electricity generation. The concentration of CFC-11 (the only target gas included in the study) varied between <0.02 and 13 ppmV. Higher concentrations of HCFC-21 and HCFC-22 (up to 114 ppmV) were observed as compared to CFC-11 and CFC-12 (13 ppmV) as a result of reductive dechlorination occurring in most of the older landfills (Allen et al. 1997). The difference in magnitudes of measured CFCs and HCFCs across the 7 different sites was a result of the waste composition (age and compacted density) and more directly the efficiency of collection of the gas extraction/combustion systems present (Allen et al. 1997). Emissions of trace CFCs and HCFCs were also predicted using LFG collection data and gas composition measured for the four-landfill sites using collection systems. The emission rates were given in kg/year (not flux) assuming the landfill gas was not used for electricity generation. Total CFC emissions were estimated to be 1,435 kg/year based on measured concentrations.

Eklund et al. (1998) conducted an investigation on trace gases at the Fresh Kills MSW landfill in New York. Grab samples were collected using Tedlar bags and stainless steel canisters and also analyses were conducted using static flux chambers. Samples were collected at various locations including two areas of the final cover (one area without an impermeable PVC geomembrane in place), and the header and passive vents of the LFG collection system at the landfill for both LFG composition and surface concentration quantification. Laboratory analysis involved the use of gas chromatography to analyze the grab and static flux chamber samples. Results indicated that the concentrations of VOCs within the header were relatively constant with variability less than 10%. Samples taken from the passive vents indicated that approximately 60 VOCs were present in the LFG with little variation in the number and type of compounds. Flux chamber samples indicated the presence of more than 50 compounds with a large variation in concentrations across sampling locations. Concentrations of compounds determined using flux chambers were characterized as

spatially variable, where measured concentrations were higher over soil and clay surfaces (particularly in areas with cracks/fissures) as compared to areas with PVC covers. The only chlorinated or fluorinated compound detected was dichlorodifluoromethane (CFC-12) with an average concentration of 1.27 ppmV in the samples collected from the gas collection header system (Table 28). The volatile organic compound (VOC) to total non-methane organic compound (NMOC) ratio for CFC-12 was also compared across all sampling techniques with a higher percentage observed in the static flux chamber measurements as compared to the passive vent and gas collection samples (approximately 0.4% CFC-12 per total NMOC sampled).

These earlier studies conducted in the 1990s (e.g. Rettenberger and Stegmann 1996, Allen et al. 1997, Elklund et al. 1998) may not contain highly relevant information due to the changing waste composition and introduction and use of new blowing agents in different foam materials. As an example, results were not provided for HCFC141b, HFC-134a, or HFC-245fa in these studies. A review of studies from the last two decades that are expected to be more relevant with regard to current waste and BA compositions is provided in the following sections and is summarized in Tables 29-34.

Bogner et al. (2004) and Scheutz et al. (2003b, 2008) investigated emissions of methane and NMOCs at a landfill in Grand'Landes, France (Tables 29 and 30). Tests were conducted in two cells with different gas collection systems. The first cell included a conventional vertical gas collection system and cover design (Cell A). The cover system from top to bottom included a 30-cm-thick vegetated topsoil layer and a 70-cm-thick compacted clay layer. The second cell (Cell B) included what was described as an innovative gas collection system with two horizontal perforated pipes within a 30-cm-thick gravel gas collection layer (drainage layer) installed immediately beneath the cover system. The cover system from top to bottom included a 30-cm-thick vegetated topsoil layer, a 70-cm-thick compacted clay layer, a geotextile layer, a 1.5-mm-thick HDPE geomembrane, a protective geotextile, a geogrid layer, followed by the 30 cm granular drainage layer (Scheutz et al. 2008). The waste in the cells had an approximate age of 13 years. Field measurements included source gas sampling, flux and gas profile measurements, and soil sampling (Scheutz et al. 2008). Average source gas composition was determined using concentrated landfill gas samples taken from gas collection headers at both cells. Emission rates were determined using a series of static flux chamber measurements. Concentration measurements at header locations in the two cells and emission measurements using flux chambers at multiple test locations in the two cells are summarized in Table 30.

Landfill gas composition results indicated a large intrusion of atmospheric air into the soil covers of both cells, with ratios of nitrogen and oxygen of 32% and 7% (v/v), respectively in Cell A, and 42% nitrogen and 5% oxygen in Cell B. The air intrusion was deemed to occur due to the actively operating gas collection systems, which was drawing atmospheric air into the soil cover. The nitrogen oxygen ratio of Cell B was twice the atmospheric amount, indicating that oxygen depletion occurred in the soil cover, while the nitrogen oxygen ratio in Cell A was normal (Scheutz et al. 2008). Changes in the measured isotopic composition of methane and carbon dioxide

between samples from the header of the collection system as well as samples from deeper within the soil cover of the cells A and B indicated that methane oxidation was taking place in the LFG collection system. A total of 47 trace NMOCs were detected in the collection header samples. The concentrations presented were relatively similar between the cells (Table 30). Halogenated compounds were present at relatively elevated concentrations between 2-841 ppmV, with the exception of HCFC-141b measured at a concentration range of 4,354 ppmV in Cell A of and 11,625 ppmV in Cell B.

The cover soils in the cells were effective in mitigating the emission of methane and NMOC species. For Cell A, negative fluxes of methane were obtained at 6 out of the 12 chamber measurement locations, ranging from $-3x10^{-4}$ to $-2.5x10^{-3}$ g/m$^2$-day (Bogner et al. 2004, Scheutz et al. 2008). Positive rates were obtained at the remaining measurement locations ranging between 0.0001 to 29 g/m$^2$/day, with zero net flux measured at one location. Average fractional methane oxidation ranged from 0% to 54% and 7% to 68% for Cells A and B, respectively (even hot spots exhibited methane oxidation with lower percentages). For cell B, the surface soils acted as a sink for methane as all chamber measurements indicated net methane uptake with rates ranging from -0.0002 to -0.0022 g/m$^2$-day (Bogner et al. 2004, Scheutz et al. 2008). Background flux of methane was approximately 4.8 g/m$^2$/day, probably due to methanogenic activity in subsurface anaerobic zones of the control area tested (Scheutz et al. 2003b, 2008). NMOC fluxes in the covers were both positive and negative, on the order of $10^{-8}$ to $10^{-5}$ g/m$^2$-day for Cell A and $10^{-9}$ to $10^{-6}$ g/m$^2$-day for Cell B (Bogner et al. 2004, Scheutz et al. 2008). The highest fluxes of NMOCs occurred at hot spots, where higher chlorinated hydrocarbons (i.e. CFC-11 and HCFC-141b) demonstrated larger positive fluxes.

Scheutz et al. (2003b, 2003d) and Bogner et al. (2003) investigated emissions of methane and NMOCs at a second landfill in Lapouyade, France (Table 31). Waste placement at the landfill occurred over two phases of operation. Phase I included waste placement between 1996 and 1998, which totaled 310,000 tons of MSW (household waste, industrial waste, and bulky waste) (Scheutz et al. 2003b, 2003d). Phase II represented active operations at the landfill, which included waste placement since 1998. Active gas extraction systems at the site consisted of vertical wells and horizontal gas collectors. The Phase I Cell had a final cover, which consisted of, from top to bottom, an 80-cm-thick layer of loam with a vegetated surface and a 40-cm-thick coarse sand layer. The Phase II area had an intermediate cover, which consisted of 40 cm of coarse sand. Emission rates of methane and selected NMOCs were measured using the static flux chamber technique. Sampling techniques were identical to the study of Scheutz et al. (2008) for the measurement of both methane and NMOC fluxes. Concentration measurements at header locations in the area with the final cover and emission measurements using flux chambers at multiple test locations within the area with the final cover and within one area with the intermediate cover are summarized in Table 31.

The composition of landfill gas in the headers of the landfill gas extraction system included 49% methane (v/v), 15% nitrogen (v/v), 34% carbon dioxide (v/v), and 3% oxygen (v/v) (Scheutz et al. 2003d, Bogner et al. 2003). The presence of oxygen and nitrogen at elevated concentrations in the header suggested that air intrusion was occurring through the cover soil (similar to Grand'Landes landfill). In addition, minimal methane oxidation was detected in both sampled soil cover areas as a result of fractional analysis of stable carbon isotopes. Approximately 37 NMOCs were detected at the site. The concentrations of CFC-11, CFC-12, and HCFC-22 were 372, 1,178, and 236 ppmV, respectively (Table 31). Methane emissions from the final cover varied between -0.01 and 10 g/m$^2$-day. Average methane flux from the final cover was 1.97 ± 0.88 g/m$^2$-day (Scheutz et al. 2003b, 2003d). Results also indicated a high spatial variability in methane emissions from the final soil cover due to several hot spots with fluxes of methane ranging from 3.7 to 16.2 g/m$^2$-day (not included in Table 31). Negative fluxes also were observed in the final cover, suggesting methane oxidation was taking place. As compared to the final cover, the intermediate soil cover had a higher average net methane flux of 37.8 ± 14.4 g/m$^2$-day and a maximum flux of 49.9 g/m$^2$-day was observed in one hot spot. Using fractional analysis of stable carbon isotopes, an average of 40 and 3.8 % methane oxidation was measured in the final and intermediate soil covers, respectively (Scheutz et al. 2003b, 2003d). These results indicated that methane oxidation was more prominent in the final cover due to the thicker soil layer sustaining a large community of methanotrophs compared to the thinner intermediate cover with less organic material.

Final cover fluxes of NMOCs were minimal and varied between -7.92x10$^{-5}$ to 7.63x10$^{-5}$ g/m$^2$-day (Table 31). Negative fluxes were observed within the final cover for the following compounds: n-heptane, n-decane, ethyne, ethyl benzene, and methyl chloride. At the hot spot where maximum methane fluxes were observed, the flux of aromatics was negative, which was consistent with results from Bogner et al. (1997a). Larger fluxes of NMOCs were observed from the intermediate cover, which were positive and on the order of 10$^{-5}$ g/m$^2$-day (Bogner et al. 2003, Scheutz et al. 2003b, 2003d).

Scheutz et al. (2011b) provided measurements of net emissions and gas composition of a shredder residue cell at a landfill in Denmark. The fluorocarbons studied included CFC-11, CFC-12, HCFC-141b, HCFC-21, HCFC-21, HCFC-22, HCFC-31, HFC32, HFC41, HFC-134a and HFC 245fa. The results of the gas composition analysis are presented in Table 32. Based on the primary composition of 27% methane and 71% nitrogen, it was determined that methanogenisis was occurring in the landfill. However, small fractions of carbon dioxide were measured in the LFG, which was not expected given carbon dioxide is generally a byproduct of waste biodegradation, along with methane (Scheutz et al. 2011b). The lack of carbon dioxide was attributed to the corrosion of metal in shredder waste producing hydrogen under anaerobic conditions, which is used by hydrogenophilic bacteria present in the waste (Scheutz et al. 2011b). This phenomenon has been observed in other studies (Parker et al., 2007), more specifically when landfills have low contents of biodegradable carbon waste such as in shredder residue facilities. Also, elevated concentrations of nitrogen indicated a large

amount of air intrusion into the waste mass. The high gas porosity of the waste, the absence of a final cover, as well as the low LFG production rate was indicated to facilitate this intrusion (Scheutz et al. 2011b). Both HCFC-21 and HCFC-31 were measured at relatively high concentrations (7-16 ppmV, corrected concentration), which was postulated to be a result of sequential dechlorination of CFC-11. Only trace concentrations of CFC-12 (1.1-2.9 ppmV) and its sequential dechlorination byproducts were measured. The other BAs, including CFC-11 and HCFC-141b, were observed in small concentrations (between 0.4-1 ppmV) with the exception of HFC-134a with concentrations up to 6 ppmV. HFC-134a has been used to replace CFC-11 and HCFC-141b, yet still posses a high global warming potential. Laboratory investigations in a a parallel study (Scheutz et al. 2011a) measured significant amounts of released HCFC-141b and HFC-134a (when measured from shredder waste placed in lysimeters. The concentrations measured in the field (Scheutz et al. 2011b) were not as high, indicating that the release of these compounds is slower in the field than when stored under laboratory conditions. The anaerobic degradation of both CFCs and HCFCs taking place in the landfill environment presents another explanation for the smaller concentrations of CFCs, HCFCs, and HFCs achieved in the field as compared to the laboratory. Measured concentrations of CFCs, HCFCs, and HFCs in this study were generally lower than those observed in earlier studies as presented in Table 29, most likely due to the waste composition/age studied (i.e. younger, shredder waste). Scheutz et al. (2011b) also indicated that the landfill in the study did not accept refrigerator and freezer waste, which may have influenced both the type and concentration of BAs banked in the landfill.

Results of flux chamber measurements at the landfill cell are presented in Table 33. Chamber Locations 1, 3, and 5 demonstrated no measured methane emissions and several negative (uptake) areas of methane were observed. Both of the hot spots demonstrated high methane emissions between 23-78 g/m$^2$-day, indicating that the surface emissions were highly variable across the waste mass and confined to certain areas with significantly larger emissions (Scheutz et al. 2010b). The low average surface emissions were a result of a combination of the following three mechanisms: 1) a low gas generation rate (not enough organic material to degrade); 2) high oxidation potential in the upper soil cover; and 3) venting of the LFG through the leachate collection system (Scheutz et al. 2011b). Emissions of fluorocarbons based on the flux chamber measurements indicated the presence of a few hot spots where emissions of HCFC-21 and HCFC-31 were 0.005 and 0.006 g/m$^2$-day, respectively (Table 33). CFC-11 was detected only once at this hotspot at a flux of 0.002 g/m$^2$-day. The emissions of the other fluorocarbons were below the detection limit of (0.001 g/m$^2$/day). These results were consistent with the measured gas concentration from the soil probes, which indicated that both HCFC-21 and HCFC-31 were the most common fluorocarbons present. Measured emissions of HCFCs from the shredder waste landfill were similar to a study conducted by Bogner et al. (1997a) that measured HCFC fluxes on the magnitude of $10^{-5}$ to $10^{-3}$ g/m$^2$-day from a 45 cm thick intermediate soil cover (clay mixed with stone). Overall, the static flux chamber measurements indicated a few hot spots for the emissions of methane and fluorocarbons. Generally low surface emissions were a result of the upper layers of the

landfill serving as an oxidative zone (Scheutz et al. 2011b). This zone could be a result of a high air filled porosity of the shredder waste that enhanced oxygen and gas transport through the waste, allowing aerobic attenuation and oxidation to take place (Scheutz et al. 2011b). At the bottom of the landfill, anaerobic degradation of CFC-11 and CFC-12 contributed to higher production rates of lower chlorinated compounds such as HCFC-21 and HCFC-31, which were accumulated and oxidized near the surface of the cover soil (Scheutz et al. 2011b).

Maione et al. (2005) studied the emissions and concentrations of trace gas components from two landfill sites in Italy. The first landfill (Landfill 1) covered an area of 38,000 $m^2$, had a waste volume of 385,000 $m^3$, and was operated from 1976 to 2000 with an active gas collection system and a final cover. The second landfill (Landfill 2) covered an area of 64,000 $m^2$ surface with a waste volume of 430,000 $m^3$, had an active gas collection system, and had areas with intermediate covers and active, daily covers where waste was currently placed. The first landfill represented LFG from old wastes since the landfill was no longer in use and capped with a final cover, while the operational landfill site was representative of LFG from new wastes. Halocarbons were analyzed using sorption collection tubes and passive steel grab sampling canisters and analyzed using gas chromatography. Carbon dioxide was the only gas component measured using a static flux chamber technique.

Measured concentrations of halocarbons reached levels that were several orders of magnitude higher than background concentration levels (Maione et al. 2005). High variability was observed in measured halocarbon concentrations between the landfills with old and new wastes as well as between different locations within the same landfill (as observed with the large ranges in concentrations presented in Table 29). The LFG from older wastes had almost twice the concentration of halocarbon components as newer wastes for each active collection well sampled. CFC-12 and CFC-11 demonstrated large variations between landfills with higher concentrations at the older landfill (Table 29). In both landfills, CFC-12 was present in higher quantities than other trace gas constituents, suggesting that more domestic appliance foam waste blown with CFC-12 was banked in each landfill and that CFC-12 was more stable (less likely to be degraded) than CFC-11 in the landfill environments (Maione et al. 2005). A smaller variation was observed for CFC-113 and CFC-114 (Table 29). HFC-134a was measured in relatively high quantities at both landfills, but reached concentrations up to 400 ppmV at the younger landfill. In addition, higher concentrations of HCFC-142b were measured at the older landfill (1) of up to 370 ppmV. Across both landfills, higher measured concentrations of more recent BA substitutes for CFC-11/CFC-12 such as HFC-134a/HCFC-142b demonstrated that newly placed wastes (in landfills with varying waste ages) more frequently contributed to surface emissions. Within the same landfill (only Landfill 2), areas with younger (newly placed) waste had generally higher HCFC, and HFC concentrations as compared to the older (less recently covered) waste sections (Maione et al. 2005). Older areas of the same landfill were contrarily indicative of higher CFC concentrations (Maione et al. 2005). Net emissions of halocarbons were estimated from both landfills using measured concentrations and carbon dioxide flux-assuming it represents 50% of the total LFG. Fluxes were higher

for CFC-11, CFC-12, HCFC-22, HCFC-142b, and HCFC-134a for Landfill 1 (older landfill) as compared to Landfill 2 with the ranges 0.16-0.45 kg/year, 0.87-1.4 kg/year, 0.67-1.30 kg/year, 0.16-2.03 kg/year, and 0.04-2.84 kg/year, respectively. These fluxes were then normalized to a one-year period, where total flux of halocarbons from the first landfill with old wastes was on the order of 10 kg/year, whereas the flux of halocarbons from the second landfill with new wastes was 2 kg/year.

The USEPA recently revised the guidelines for LFG constituent concentrations and basic estimation of emissions gases from the concentrations for MSW landfills (USEPA 2008). The objective of Report AP-42 (EPA 2008) was to ensure the emissions factors were adequately up to date with changing landfill conditions, waste composition, and operations to improve estimation of LFG generation rates and efficiency of collection/combustion systems. The amount of speciated components reported in LFG detailed in this revision increased from 44 to 167. The methodology for determining suitable concentration levels of trace components in LFG for emissions factors involved collection of LFG samples from 62 gas collection headers and 22 punch probe tests, where LFG collected from the gas collection headers was considered a more representative composition than the punch probe testing (USEPA 2008). Punch probe tests included collection of samples 1 m beneath the cover. Both punch probe and header collection tests involved sampling LFG within evacuated stainless steel canisters followed by analysis by gas chromatography. The concentrations of the samples were then corrected for air infiltration using an equation developed by the USEPA. Results from this collection of measurements were compiled in the U.S. and categorized between pre-1992 and post-1992 landfill conditions. In general, reported results for concentrations of CFC-11/CFC-12 were relatively higher for pre-1992 landfills than the concentrations for post-1992 landfills and the values were generally lower than data provided in other studies (Table 29). CFC-12 was measured to have the highest concentration of the studied halocarbons (15.7 ppmV) in both pre-1992 and post-1992 landfills (USEPA 2008).

The Environment Canada studies (Cianciarelli and Bourgeau 2002, Greer and Cianciarelli 2005) evaluated the destruction efficiency (also defined as the DRE) of LFG combustion systems (microturbine and reciprocating engine) operating at different power outputs (26 KWe and 1 MWe) (Cianciarelli and Bourgeau 2002, Greer and Cianciarelli 2005). These studies were conducted to quantify the emissions of chlorinated and fluorinated hydrocarbons to the atmosphere during recovery and combustion of LFG. The Environment Canada (Cianciarelli and Bourgeau 2002) determined the destruction efficiencies of selected VOCs (including ozone depleting substances) with a modified Method 5 apparatus (USEPA TO-14) that was used to measure concentration and mass flow of inlet and outlet VOCs during typical combustion processes. Inlet mass flow rates from the gas collection system for CFC-11, CFC-12, CFC-113, CFC-114, and HCFC-22 were 7 g/day, 39.3 g/day, 2.4 g/day, 6 g/day, and 19.7 g/day, respectively. For the reciprocating engine, destruction efficiencies of 94% and 96% were observed for CFC-11, CFC-12, CFC-113, CFC-114, and HCFC-22. The total ODS destruction efficiency for all of the above compounds was 94.3% from the reciprocating 1 MWe engine, which was similar to the destruction

efficiency for the VOCs category of 93% (total averaged DRE for all VOCs detected) (Cianciarelli and Bourgeau 2002). Thus, approximately 6% emissions of chlorinated and fluorinated hydrocarbons can be expected from combustion systems using reciprocating engines (Cianciarelli and Bourgeau 2002). The Environment Canada study used the same sampling approach with the modified Method 5 sampling apparatus for the microturbine LFG combustion system (Greer and Cianciarelli 2005). The microturbine combustion system had a cleaner exhaust than the reciprocating engine, with an average DRE (destruction efficiency) for ODS of 99.01% (98%, 97.6%, 70%, 99%, and 99.5% for CFC-11, CFC-12, CFC-113, CFC-114, and HCFC-22, respectively). However, inlet ODS concentrations to the combustion unit (mass flow) were one order of magnitude smaller than directly concentrations measured directly from the LFG extraction system (due to air intrusion), which may have accounted for the higher destruction efficiency observed (Greer and Cianciarelli 2005). The overall VOC DRE was 99.41% for the microturbine system, indicating less than 1% of ODS emissions during combustion processes. Concentrations of the CFCs/HCFCs measured at the inlet of each combustion system are also provided (Table 29).

Hodson et al. (2010) evaluated the concentrations of CFC-11, CFC-12, and CFC-113 from MSW landfills in both the U.S. and U.K. Seven U.S. and nine U.K. MSW landfills receiving more than 50% of wastes from commercial and domestic sources (compared to industrial sources) were included in the analysis of emission (Table 29-range includes both U.S. and U.K. landfills). U.S. landfill sites used were characteristically older and contained less landfilled waste than the U.S. national average as compared to U.K. landfill sites, which were consistently younger and had much larger quantities of waste. All landfill sites maintained active gas collection systems. LFG samples were taken before the flare line or entrance into the waste to energy (WTE) plant over a one-year period. Overall, the U.S. and U.K. ODS emissions from landfills were observed to be insignificant (Hodson et al. 2010). Annual emissions of CFC-11, CFC-12, and CFC-113 from U.S. landfills were all less than 1% of total U.S. ODS emissions. Similarly, U.K. annual landfill emissions of CFC-11 were less than 1% of total U.K. ODS emissions. CFC-12 had higher emissions with 6.3% of the total annual U.K. ODS emission rate attributed to MSW landfills. Even though the 0.04 Gg/year emission rate for CFC-11 included the effect of gas collection systems and microbial oxidation of ODS in soil covers, emissions predicted using the EPA LandGem model (as presented as a comparison in Hodson et al. 2010) were much higher. Emission predictions studies by Li et al. (2005), Hurst et al. (2006), and Millet et al. (2009) for ODS emissions from U.S. landfills indicated higher emissions of CFC-11 and CFC-12 than the measured values in Hodson et al. (2010). Annual emission (by mass) rates predicted from these studies ranged an order of magnitude higher from 7 to 11 Gg/year for CFC-11 and 9 to 16 Gg/year for CFC-12.

A report by ARCADIS (2012) evaluated LFG concentrations and surface emissions of ODS and high GWP trace gases present in LFG from three MSW landfills in the U.S. to quantify methane collection efficiency from active gas collection systems. The first landfill site was one cell (129,500 $m^2$ area, waste volume not reported), and had operated in its last phase from 1997 to 2006. The first cell included an intermediate

soil cover (mixed soil). An active extraction system (reported to be inefficient) was additionally in place. To increase the efficiency of the collection system, 29 vertical wells were installed and horizontal trenches were constructed in 2009. The second site consisted of two cells, in which the first cell (352,077 $m^2$) contained 7.5 million tonnes of waste and stopped accepting waste in 2010 (with final cover/gas collection system indicated, but not described). The second cell (24,281 $m^2$) was in an operational portion of the landfill site and had been accepting waste for 3 months with no gas extraction system installed. The third landfill site had a 307,561 $m^2$ surface area, over 7.7 million tonnes of MSW, and was the oldest of the three sites (operating from 1972 to 2006). This landfill site was covered with a GCL, and the site had an active gas collection system installed. Both grab VOC and NMOC measurements were made from the main gas collection headers at the sites in conjunction with OTM-10 measurements. NMOC fluxes were estimated using the fraction of methane released, and not measured in the study (ARCADIS 2012).

Averaged results from the three landfill sites indicated small ranges in ODS concentrations compared to other studies (Table 29). The concentrations of the measured gases were below 1 ppmV and in the ppb range, indicating that possibly some dilution or air infiltration of the samples may have been occurring. Variations in patterns of release were observed for the ODSs analyzed, where concentrations of CFC-11 and CFC-113 were higher in spring, whereas the concentrations of CFC-12 and CFC-114 were higher in fall than other seasons. Fluxes also were estimated for CFC-11, CFC-12, CFC-113, and CFC-114 trace components based on the average concentrations measured. As compared to results from other current studies, emissions also were lower (Table 29). Surface emissions were predicted to range from 0.04 to 0.24 g/day for CFC-11, 2 to 6 g/day for CFC-12 (spring), 0.02 to 4.03 for CFC-113 (spring), and 0.26 to 36.2 g/day for CFC-114 (spring). A larger variation was present in predicted surface emissions for fall months than spring months, particularly for CFC-113 and 114. Thus, the net predicted surface emissions and concentrations measured varied across the three landfill sites as a function of landfill operation (i.e., waste age, composition, gas collection system, etc.) and season (change in meteorological conditions) (ARCADIS 2012).

Barlaz et al. (2004) quantified CFC emissions from a landfill in the U.S. (Louisville, Kentucky) while evaluating the effectiveness of a biocover system. The site operational conditions consisted of an active gas collection system with a final clay cover (1 m thick). The waste age was relatively young (3-5 years) and the waste was actively producing LFG. Surface emissions were measured over the course of one year and the experimental design incorporated an equivalent amount of sloped and flat areas within the landfill. An overall uptake of CFC-11 (average magnitude of $-2.3 \times 10^{-5}$ $g/m^2$-day) was observed for the conventional soil cover (no biocover in place). In addition, average CFC-12 and CFC-114 release rates ranged from $6.6 \times 10^{-5}$ to $1.3 \times 10^{-4}$ $g/m^2$-day, respectively. Standard deviations of the flux chamber measurements quantifying CFC emissions were generally high as implied by the high COV values extrapolated from the data presented (COV values above 100%). These CFC emission ranges were slightly higher than those presented in Table 34, suggesting that

surface emissions from landfills outside the U.S. may not be entirely representative for comparison of CFC, HCFC, and HFC emissions to landfills in the U.S. Moreover, the large variability in the collected measurements at the landfill site may imply that CFC emissions may vary significantly according to the measurement location and time of year (i.e., on a slope versus flat ground, or season).

Emissions data were summarized across all studies analyzed and categorized into ranges of yearly surface emissions and measured surface fluxes (Table 34). Yearly emissions of the CFCs, HCFCs, and HFCs per landfill studied were predicted to vary considerably across the landfill studied (Table 34). Field investigations indicated that CFC-11 emissions (flux) varied between $-7.92 \times 10^{-5}$ and +0.002 g/m$^2$-day across studies conducted in different landfills (i.e. different waste ages, waste amounts, waste compositions, geographical locations, etc.). One of the few studies to analyze surface emissions in the U.S. indicated surface flux of HCFCs ranged between $10^{-5}$ to $10^{-3}$ g/m$^2$-day (Bogner et al. 1997a). Similarly, another study that analyzed CFC emissions in the U.S. reported fluxes ranging from $-8.8 \times 10^{-5}$ to $3.1 \times 10^{-4}$ g/m$^2$-day (Barlaz et al. 2004). These ranges (CFCs/HCFCs) are similar to slightly different than ranges observed in surface emission investigations in Europe. Measured surface flux from several landfills ranged from $3.63 \times 10^{-6}$ to $6.66 \times 10^{-5}$ g/m$^2$-day and $-2.50 \times 10^{-7}$ to $2.05 \times 10^{-4}$ g/m$^2$-day, for HCFC-141b and HFC-134a, respectively (Table 34). Limited surface flux data for HFC-245fa was available in the literature. Overall variations among the measured surface flux taken at all landfills for CFCs, HCFCs, and HFCs studied generally ranged over 1-3 orders of magnitude. Variation in surface emissions within a specific landfill site were also reported to be high based on the large range in magnitude presented by individual studies (generally 1-2 orders of magnitude difference-Table 34). Methane emissions from MSW landfills, for perspective, were reported to vary over seven orders of magnitude: from 0.0004 to 4,000 g/m$^2$-day (Bogner et al. 1997b). In general, variation in CFC, HCFC, and HFC emissions at individual landfill sites was attributed to several factors including the measurement location (i.e. slope/flat areas) and seasonal fluctuation in emissions (due to change in temperature, etc.). In addition, areas with higher methane emissions (especially around hotspots) were reported to demonstrate similar relatively high measured CFC, HCFC, and HFC emissions/concentrations.

The main factors that affected the surface emissions of CFCs, HCFCs, and HFCs were categorized into both operational/design practices of landfills as well as the meteorological conditions/geographical locations of landfills. Operational practices affecting surface emissions of CFCs, HCFCs, and HFCs included the operational time period (waste age), composition of waste (i.e. MSW as compared to shredder waste), amount of compaction/compression experienced (influenced by waste placement/waste density), the waste properties (i.e., moisture content, heterogeneity etc.), and the amount of waste accumulated. Important design factors that influenced surface emissions of CFCs, HCFCs, and HFCs included the type/presence of a cover (i.e. final or intermediate), as well as the cover composition (i.e. presence of a geomembrane/barrier thickness, etc.), type/presence of a gas collection/combustion system, and type/presence of a bottom liner. Lastly, meteorological conditions such as

precipitation or barometric pressure (as a function of season and geographical location) influenced the biological/chemical processes within the waste mass and soil cover (including biodegradation/sorption processes of CFCs, HCFCs, and HFCs) as well as the gas transport properties of the soil cover used (i.e., the permeability of the soil or the diffusion gradient between the soil and atmosphere). High variations in emissions occurred, for instance, between landfills with different final and intermediate covers, waste composition and age, as well as differing geographic locations (Cianciarelli and Bourgeau 2002, Greer and Cianciarelli 2005, Scheutz et al. 2003b, 2003d, 2008, 2011a, 2011b, Bogner et al. 1997b, 2003, 2004, Maione et al. 2005, USEPA 2008, Hodson et al. 2010, ARCADIS 2012).

Table 28 – Concentrations of Selected Halocarbons from LFG Samples (from Landfilling of Waste: Biogas)

| | Reference | CFC-11 | CFC-12 | CFC-13 | CFC-113 | CFC-114 | HCFC-21 | HCFC-22 | HCFC-31 | HCFC-142b |
|---|---|---|---|---|---|---|---|---|---|---|
| Concentration ($mg/m^3$) | Pruggmayer et al. (1982) | - | 6.4 to 107 | - | - | - | - | - | - | - |
| | Brooks and Young (1983) | 20 | 10 | 0 to 10 | - | - | 5 | - | - | - |
| | Young and Heasman (1985) | 0.4 to 185 | 6 to 602 | - | - | - | - | 2 to 276 | 0.1 to 110 | - |
| | Arendt (1985) | 1 to 500 | 5 to 700 | - | 0.1 to 30 | - | - | - | - | - |
| | Rettenberger (1986) | 0.1 to 84 | 4 to 119 | 0 to 10 | - | - | 5 | | - | - |
| | Dent et al. (1986) | <0.1 to 185 | <0.1 to 486 | - | - | - | 0.1 to 602 | <0.1 to 276 | - | - |
| | Schilling and Hinz (1987) | 11 to 56 | 99 to 149 | - | - | - | - | - | - | - |
| | Laugwitz et al. (1988) | 0 to 220 | 4 to 145 | - | 0 to 6 | - | 0.4 to 14 | 3 to 28 | - | - |
| | Deipser and Stegmann (1994) | 0.3 to 35 | 10.3 to 111 | - | 0.07 to 1.7 | 2.3 to 8.9 | 0.7 to 28 | 1.9 to 30.7 | - | - |
| | Allen et al. (1997) | <0.11 to 73 | <0.49 to 114 | - | <0.77 to 6.1 | - | <0.42 to 231 | <0.35 to 403 | <0.6 to 95 | <0.41 to 33 |
| Concentration* (ppmV) | Pruggmayer et al. (1982) | | 1.3 to 21.3 | - | - | - | - | - | - | - |
| | Brooks and Young (1983) | 3.5 | 2 | 0 to 2.3 | - | - | 1.17 | - | - | - |
| | Young and Heasman (1985) | 0.1 to 32.4 | 1.2 to 120 | - | - | - | - | 0.6 to 77 | 0.035 to 39 | - |
| | Arendt (1985) | 0.2 to 88 | 1 to 139.3 | - | 0.13 to 4 | - | - | - | - | - |
| | Rettenberger (1986) | 0.2 to 15 | 0.8 to 24 | 0 to 2.3 | - | - | 1.17 | - | - | - |
| | Dent et al. (1986) | <0.02 to 33 | <0.02 to 90.1 | - | - | - | 0.02 to 143 | <0.03 to 78.1 | - | - |
| | Schilling and Hinz (1987) | 2 to 9.8 | 20 to 27 | - | - | - | - | - | - | - |
| | Laugwitz et al. (1988) | 0 to 39 | 0.8 to 29 | - | 0 to 0.77 | - | 0.1 to 3.3 | 0.8 to 8 | - | - |
| | Deipser and Stegmann (1994) | 0.05 to 6.13 | 2.1 to 22.1 | - | 0.01 to 0.218 | 0.32 to 1.25 | 0.16 to 6.5 | 0.53 to 8.5 | - | - |
| | Allen et al. (1997) | <0.02 to 13 | <0.1 to 23 | - | <0.1 to 0.8 | - | <0.1 to 55 | <0.1 to 114 | <0.2 to 34 | <0.1 to 8 |

*Conversion $mg/m^3$ to ppmV/ppbV: ppmv = (mg/m3)(273.15 + °C) / (12.187)(MW)
-: Omitted by the study

Table 29 – Concentrations of Trace Components in LFG (ppmV)

| Gas Component | Cianciarelli and Bourgeau 2002[1] | Bogner et al. 2004, Scheutz et al. 2008[2] | Bogner et al. 2003, Scheutz et al. 2003b, 2003d | Greer and Cianciarelli 2005[3] | Maione et al. (2005)[4] | EPA AP-42 Draft (2008) (Pre-1992 Landfills) | EPA AP-42 Draft (2008) (Post-1992 Landfills) | Hodson et al. (2010) | Scheutz et al. (2011 a and b)[5] | ARCADIS 2012 [6] |
|---|---|---|---|---|---|---|---|---|---|---|
| CFC-11 | 0.1 | 31 to 596 | 372 | 0.3 | 7.3 to 20.9 | 0.76 | 0.25 | 0.024 to 1.5 | 0.14 to 0.57 | 0.02 to 0.03 |
| CFC-12 | 0.6 | 114 to 841 | 1,178 | 1.5 | 148 to 231 | 15.7 | 1.2 | 0.02 to 2.80 | 0.14 to 0.34 | 0.06 to 0.50 |
| CFC-113 | 0.02 | 2 | - | 0.006 | 0.2 to1.55 | - | 0.067 | ND to 0.020 | - | 0.003 to 0.010 |
| CFC-114 | 0.06 | - | - | 0.11 | 12.4 to 12.8 | - | 0.11 | - | - | 0.040 to 0.060 |
| HCFC-141b | - | 4,354 to 11,625 | - | - | - | - | - | - | 0.31 to 0.52 | - |
| HCFC-21 | - | - | - | - | - | 2.62 | - | - | 4.1 to 8.7 | - |
| HCFC-22 | 0.4 | 340 to 503 | 236 | 4.2 | 134 to 237 | 2.52 | 0.80 | - | 0.45 to 0.67 | - |
| HCFC-31 | - | - | - | - | - | - | - | - | 4 to 10 | - |
| HFC-142b | - | - | - | - | 27 to 371 | - | - | - | - | - |
| HFC-134a | - | 369 to 626 | - | - | 200 to 453 | - | - | - | 1.2 to 3.6 | - |
| HFC-245fa | - | - | - | - | - | - | - | - | - | - |

[1]Caclulated as the average of 2 concentrations measured at the inlet to the combustion system
[2]This study reported ranges from two landfill cells with different gas collection/combustion systems
[3]Calculated using the inlet VOC mass flow and the average inlet flow of LFG to the combustion system
[4]This study used an average of 3 measurements per landfill and reported as a range for two different landfill sites
[5]This study provided a range based on an average of 14 samples over a one-year period at a landfill receiving shredder residue waste only
[6]This study reported ranges of values based on an average of three landfill sites for fall and spring seasons
-: Omitted by the study
N.D. : Not detected by the study

Table 30 – Trace Gas Concentration and Surface Emission from Grand'Landes Landfill at Different Area (Bogner et al. 2004, Scheutz et al. 2008)

| Area | Cell A Header | | Cell B Header | | Cell A Surface Emissions ($g/m^2$-day) | | | | | | Cell B Surface Emissions ($g/m^2$-day) | Control Surface Emissions ($g/m^2$-day) |
|---|---|---|---|---|---|---|---|---|---|---|---|---|
| Gas Constituent | LFG Conc. (ppmV) | LFG Conc. ($\mu g\ L^{-1}$) | LFG Conc. (ppmV) | LFG Conc. ($\mu g\ L^{-1}$) | Area 1 | Area 2 | Area 3 | Area 4 (Hotspot) | Area 5 (Hotspot) | Area 6 (Hotspot) | Area 1 | Area 1 |
| $CH_4$ | $3.70x10^5$ | $2.42x10^5$ | $2.90x10^5$ | $1.90x10^5$ | 0 | -0.0011 | 0.0001 | 29.03 | 24.03 | 1.45 | -0.002 | 4.78 |
| CFC-11 | 596 | 3.1 | 317 | 1.6 | $3.73x10^{-5}$ | $1.33x10^{-6}$ | $7.86x10^{-7}$ | $4.36x10^{-7}$ | $7.94x10^{-8}$ | $4.11x10^{-7}$ | $6.54x10^{-7}$ | $2.66x10^{-6}$ |
| CFC-12 | 114 | 0.7 | 841 | 4.9 | $-2.27x10^{-7}$ | $5.39x10^{-7}$ | $6.02x10^{-7}$ | $-2.13x10^{-8}$ | $-1.11x10^{-6}$ | $1.21x10^{-7}$ | $-2.16x10^{-7}$ | $-1.56x10^{-7}$ |
| CFC-113 | 2 | $1.0\cdot10^{-2}$ | 2 | $1.0\cdot10^{-2}$ | $-4.74x10^{-8}$ | $1.01x10^{-7}$ | $-7.81x10^{-8}$ | $4.26x10^{-8}$ | $-9.98x10^{-9}$ | $2.19x10^{-8}$ | $-2.06x10^{-8}$ | $4.16x10^{-8}$ |
| HCFC-141b | 4354 | 21.6 | 11,625 | 57.7 | $4.75x10^{-6}$ | $6.66x10^{-5}$ | $7.98x10^{-6}$ | $1.01x10^{-5}$ | $1.02x10^{-5}$ | $3.63x10^{-6}$ | $4.38x10^{-6}$ | $3.23x10^{-5}$ |
| HCFC-22 | 503 | 1.8 | 340 | 1.3 | $-6.10x10^{-8}$ | $1.85x10^{-7}$ | $-2.39x10^{-8}$ | $4.64x10^{-6}$ | $9.07x10^{-6}$ | $-3.14x10^{-8}$ | $-1.54x10^{-7}$ | $-5.20x10^{-8}$ |
| HFC-134a | 626 | 2.7 | 369 | 1.6 | $2.40x10^{-8}$ | $2.75x10^{-7}$ | $4.14x10^{-7}$ | $5.41x10^{-6}$ | $5.49x10^{-6}$ | $-2.50x10^{-7}$ | $-2.59x10^{-6}$ | $1.75x10^{-8}$ |
| H-1211 | 0.2 | $1.7\cdot10^{-3}$ | 0.1 | $8.1\cdot10^{-4}$ | $-3.89x10^{-9}$ | $4.61x10^{-9}$ | $-3.05x10^{-9}$ | $4.37x10^{-9}$ | $-1.09x10^{-8}$ | $-6.00x10^{-9}$ | $-8.44x10^{-9}$ | $2.84x10^{-9}$ |

Table 31 – Concentrations of LFG Components and Surface Emission at Lapouyade Landfill in Different Areas (Scheutz et al. 2003b, 2003d, Bogner et al. 2003)

| Chamber | LFG Concentration (ppmV) | LFG Concentration ($\mu g\ L^{-1}$) | Final Cover Surface Emissions ($g/m^2$-day) | | | | Intermediate Cover Surface Emissions ($g/m^2$-day) | Control Surface Emissions ($g/m^2$-day) |
|---|---|---|---|---|---|---|---|---|
| Location | N/A | N/A | Area 1 | Area 2 | Area 3 | Area 4 | Area 1 | Area 1 |
| Methane | $4.85x10^5$ | $3.17x10^5$ | 0.0084 | -0.0095 | -0.0104 | 10.0 | 49.9 | -0.0033 |
| Carbon Dioxide | $3.37x10^5$ | $5.70x10^5$ | 8.0 | 13.1 | 15.6 | 77.3 | 107.4 | 19.3 |
| CFC-11 | 372.036 | 2.0 | $-7.92x10^{-5}$ | $5.18x10^{-6}$ | $2.24x10^{-6}$ | $7.63x10^{-5}$ | $2.08x10^{-5}$ | $5.21x10^{-7}$ |
| CFC-12 | 1,177.675 | 5.7 | $-1.68x10^{-5}$ | $2.17x10^{-6}$ | $1.84x10^{-7}$ | $1.04x10^{-5}$ | $2.56x10^{-5}$ | $-7.86x10^{-8}$ |
| HCFC-22 | 235.695 | 0.8 | $-4.89x10^{-6}$ | $5.03x10^{-7}$ | $-4.06x10^{-6}$ | $2.26x10^{-5}$ | $5.74x10^{-5}$ | $-1.50x10^{-7}$ |

Table 32 – Average Gas Concentrations and Standard Deviation of Selected Landfill Gas Components in Waste Cells Receiving Shredder Waste (Scheutz et al. 2011b)

| Landfill Gas Constituent | Measured Gas Concentration (% v/v) | Measured Gas Concentration ($\mu g\ L^{-1}$) | Measured Gas Concentration (ppmV) | Corrected Measured Gas Concentration (% v/v) | Corrected Measured Gas Concentration ($\mu g\ L^{-1}$) | Corrected Measured Gas Concentration (ppmV) |
|---|---|---|---|---|---|---|
| $CH_4$ | 26 to 28 | - | | 49.852.2 | - | |
| $CO_2$ | -0.2 to 0.2 | - | - | -0.3 to 0.3 | - | - |
| $O_2$ | 0.9 to 1 | - | - | 1.8 to 2.2 | - | - |
| $N_2$ | 70 to 72 | - | - | 6 to 8 | - | - |
| CFC-11 | - | 0.8 to 3.2 | 0.14 to 0.57 | - | 2 to 5 | 0.36 to 0.89 |
| CFC-12 | - | 0.5 to 1.5 | 0.10 to 0.30 | - | 1.1 to 2.9 | 0.22 to 0.59 |
| HCFC-141b | - | 1.5 to 2.5 | 0.314 to 0.522 | - | 3.2 to 4.8 | 0.67 to 1 |
| HCFC-21 | - | 17 to 37 | 4.11 to 8.71 | - | 28.5 to 61.5 | 6.8 to 14.6 |
| HCFC-22 | - | 1.6 to 2.4 | 0.45 to 0.68 | - | 2.4 to 3.6 | 0.68 to 1 |
| HCFC-31 | - | 12 to 28 | 4.3 to 10 | - | 20.3 to 45.7 | 7.3 to16.3 |
| HFC-134a | - | 5 to15 | 1.18 to 3.62 | - | 8.2 to 25.8 | 1.97 to 6.2 |
| HFC-32 | - | -0.1 to 0.1 | -0.05 to 0.05 | - | -0.2 to 0.2 | -0.09 to 0.09 |
| HFC-41 | - | 0.7 to 1 | 0.5 to 0.93 | - | 1.5 to 2.5 | 1.1 to 1.8 |

Table 33 – Measured $CH_4$ and Select Halo/Fluorocarbon Flux Rates at the Five Locations at Shredder Residue Cell (Scheutz et al. 2011b)

| Location | Minimum $CH_4$ Flux ($g/m^2$-day) | Maximum $CH_4$ Flux ($g/m^2$-day) | Average $CH_4$ Flux ($g/m^2$-day) | Maximum Flux CFC-11 ($g/m^2$-day) | Maximum Flux HCFC-21 ($g/m^2$-day) | Maximum Flux HCFC-31 ($g/m^2$-day) |
|---|---|---|---|---|---|---|
| 1 (Hot Spot 1) | -1.9 | 78 | 17 ± 21 | 0.002 | 0.005 | 0.006 |
| 2 (Hot Spot 2) | b.d.l. | 23 | 6.6 ± 9.2 | b.d.l. | b.d.l. | b.d.l. |
| 3 (Random 1) | b.d.l. | 0.2 | * | b.d.l. | b.d.l. | b.d.l. |
| 4 (Random 2) | b.d.l. | b.d.l. | * | b.d.l. | b.d.l. | b.d.l. |
| 5 (Random 3) | b.d.l. | 0.3 | * | b.d.l. | b.d.l. | b.d.l. |

*: The $CH_4$ average flux could not be calculated since most measurements showed flux rates below the detection limit of this method (<0.1 $g/m^2$-d).
b.d.l.: Below detection limit.

Table 34 – Summary of Emissions of Trace Components in LFG

| | Gas Component | Bogner et al. (2004), Scheutz et al. (2008)[1, 2] | Scheutz et al. (2003b,d)[3] | Barlaz et al. (2004) | Maione et al. (2005)[4, 7] | Hodson et al. (2010)[4] | Scheutz et al. (2011a,b)[5] | ARCADIS (2012)[6, 7] |
|---|---|---|---|---|---|---|---|---|
| Surface Flux ($g/m^2$-day) | CFC-11 | $7.94x10^{-8}$ to $3.73x10^{-5}$ | $-7.92x10^{-5}$ to $7.63x10^{-5}$ | $-8.8x10^{-5}$ to $4.2x10^{-5}$ | $6.85x10^{-6}$ to $3.24x10^{-5}$ | - | $2.0x10^{-3}$ | $1.97x10^{-7}$ to $1.20x10^{-6}$ |
| | CFC-12 | $-2.13x10^{-8}$ to $6.02x10^{-7}$ | $-1.68x10^{-5}$ to $2.56x10^{-5}$ | $-1.2x10^{-4}$ to $2.6x10^{-4}$ | $3.72x10^{-5}$ to $1.01x10^{-4}$ | - | - | $9.84x10^{-6}$ to $2.95x10^{-5}$ |
| | CFC-113 | $-9.98x10^{-9}$ to $1.01x10^{-7}$ | - | - | $1.28x10^{-7}$ to $1.66x10^{-5}$ | - | - | $9.84x10^{-8}$ to $1.98x10^{-5}$ |
| | CFC-114 | - | - | $-0.5x10^{-4}$ to $3.1x10^{-4}$ | $5.14x10^{-6}$ to $6.85x10^{-5}$ | - | - | $1.28x10^{-6}$ to $1.78x10^{-4}$ |
| | HCFC-141b | $3.63x10^{-6}$ to $6.66x10^{-5}$ | - | - | - | - | - | - |
| | HCFC-21 | - | - | - | - | - | | - |
| | HCFC-22 | $-6.10x10^{-8}$ to $9.07x10^{-6}$ | $-4.89x10^{-6}$ to $5.74x10^{-5}$ | - | $2.87x10^{-5}$ to $9.37x10^{-5}$ | - | $5.0x10^{-3}$ | - |
| | HCFC-31 | - | - | - | - | - | $6.0x10^{-3}$ | - |
| | HFC-142b | - | - | - | $6.58x10^{-6}$ to $1.46x10^{-4}$ | - | - | - |
| | HFC-134a | $-2.50x10^{-7}$ to $5.49x10^{-6}$ | - | - | $1.71x10^{-6}$ to $2.05x10^{-4}$ | - | - | - |
| | HFC-245fa | - | - | - | - | - | - | - |
| Total Surface Emissions (kg/year) | CFC-11 | $1.83x10^{-4}$ to $8.61x10^{-2}$ | - | - | 0.16 to 0.45 | 30,000 to 40,000 | 5.84 | 0.015 to 0.09 |
| | CFC-12 | $-4.92x10^{-5}$ to $1.40x10^{-3}$ | - | - | 0.87 to1.40 | 90,000 to 110,000 | - | 0.73 to 2.20 |
| | CFC-113 | $-2.30x10^{-5}$ to $2.33x10^{-4}$ | - | - | 0.003 to 0.23 | 6,000 | - | 0.007 to 1.50 |
| | CFC-114 | - | - | - | 0.12 to 0.95 | - | - | 0.09 to 15 |
| | HCFC-141b | $8.40x10^{-3}$ to 0.152 | - | - | - | - | - | - |
| | HCFC-21 | - | - | - | - | - | - | - |
| | HCFC-22 | $-1.41x10^{-4}$ to 0.021 | - | - | 0.67 to 1.30 | - | 14.6 | - |
| | HCFC-31 | - | - | - | - | - | 17.5 | - |
| | HFC-142b | - | - | - | 0.16 to 2.03 | - | - | - |
| | HFC-134a | $-5.77x10^{-4}$ to 0.013 | - | - | 0.04 to 2.84 | - | - | - |
| | HFC-245fa | - | - | - | - | - | - | - |

[1]Total surface emissions were calculated by this study using the area of the landfill cell
[2]This study reported ranges from two landfill cells with different gas collection/combustion systems
[3]The range provided encompasses both the final cover and intermediate cover areas
[4]Data were obtained from 16 landfill sites located in both the U.S. and U.K., no data on surface flux was provided
[5]This study provided a maximum emission at a landfill receiving shredder residue waste only
[6]This study reported ranges of values based on an average of three landfill sites for fall and spring seasons
[7] Surface flux was calculated using the given area of the landfill or cell

# APPENDIX 2 – EXAMPLE MFA CALCULATION

a. <u>Calculating BA Release (%) Using *a* Value for Foam Panel (Short Term)</u>
Short term (5 days=432,000 seconds), panel calculated with dimensions described below, n=1 for this case, iterate 60 times, short term release coefficient (D) is $4.5x10^{-12}$ $m^2$/sec

Calculating *a* value for a foam panel (*a,* radius of equivalent sphere for panel)

For a PUR foam appliance panel

*Given:* Dimensions: 4.5' x 2' x 2.25'' (HxWxT)

$$a = \left(\frac{3}{4}WT\left(\frac{H}{\pi} - T\right)\right)^{1/3}$$

$$a = \left[\frac{3}{4}(2)(0.1875)\left(\frac{4.5}{\pi} - 0.1875\right)\right]^{1/3}$$

$$a = 0.705'$$

Calculating intial BA release

$$\frac{Mt}{Mo} = 1 - \frac{6}{\pi^2}\sum_{n=0}^{\infty}\frac{1}{(n)^2}\exp\{-D(n)^2\pi^2 t/a^2\}$$

$$\frac{Mt}{Mo} = 1 - \frac{6}{\pi^2}\sum_{n=0}^{60}\frac{1}{(1)^2}\exp\{-4.5x10^{-12}(1)^2\pi^2(432{,}000)/0.705^2\}$$

$$\frac{Mt}{Mo} = 1 - \frac{6}{\pi^2}\sum_{n=0}^{60}0.9999 + 0.249923 + \cdots$$

$$\frac{Mt}{Mo} = 0.014308 = 1.4\%\ Initial\ BA\ Released$$

b. Calculation of Weighted Fraction of BA-Containing Foam Waste
For C & D waste, PUR Panel, Scenario 1 (1960-2010), CFC-11 with the following CFC-11 BA composition:

| Year | CFC-11 |
|---|---|
| 1960-1991 | 100 |
| 1992 | 100 |
| 1993 | 75 |
| 1994 | 50 |
| 1995 | 25 |
| 1996 | - |
| 1997 | - |
| 1998 | - |
| 1999 | - |
| 2000 | - |
| 2001 | - |
| 2002 | - |
| 2003 | - |
| 2004 | - |
| 2005 | - |
| 2006 | - |
| 2007 | - |
| 2008 | - |
| 2009 | - |

$$Fraction = \frac{\left\{\left[\left(\frac{100}{100}\right) * 32\right] + \left[\left(\frac{100}{100}\right) * 1\right] + \left[\left(\frac{75}{100}\right) * 1\right] + \left[\left(\frac{50}{100}\right) * 1\right] + \left[\left(\frac{25}{100}\right) * 1\right]\right\}}{(50)}$$

*Fraction* = 0.69 = 69%